Petrogenesis of the Reversely Zoned Turtle Pluton, Southeastern California

by

Charlotte Mary Allen

Dissertation submitted to the Faculty of the

Virginia Polytechnic Institute and State University

in partial fulfillment of the requirements for the degree of

Doctor of Philosophy

in

Department of Geological Sciences

APPROVED:

A. Krishna Sinha, Chairman

Susan C. Eriksson

David A. Hewitt

Keith A. Howard

Carol Simpson

June, 1989

Blacksburg, Virginia

Petrogenesis of the Reversely Zoned Turtle Pluton,

Southeastern California

by

Charlotte Mary Allen

A. Krishna Sinha, Chairman

Department of Geological Sciences

(ABSTRACT)

Few plutons with a reversed geometry of a felsic rim and mafic core have been described in the geologic literature. The Turtle pluton of S.E. California is an intrusion composed of a granitic rim and granodioritic core and common microgranitoid enclaves. Field observations, mineral textures and chemistries, major and trace element geochemistry, and isotopic variability support a petrogenetic model of in situ, concomitant, magma mixing and fractional crystallization of rhyolitic magma progressively mixed with an increasing volume of andesitic magma, all without chemical contribution from entrained basaltic enclaves. Hornblende geobarometry indicates the Turtle pluton crystallized at about 3.5 kb. A crystallization sequence of biotite before hornblende (and lack of pyroxenes) suggests the initial granitic magma contained less than 4 wt% H_2O at temperatures less than 780°C. U-Pb, Pb-Pb, Rb-Sr and oxygen isotope studies indicate the terrane intruded by the Turtle pluton is 1.8 Ga, that the Turtle pluton crystallized at 130 Ma, that the Target Granite and garnet aplites are about 100 Ma, and that these intrusions were derived from different sources. Models based on isotopic data suggest the rhyolitic end member magma of the Turtle pluton was derived from mafic igneous rocks, and was not derived from sampled Proterozoic country rocks. Similarity of common Sr and Pb isotopic ratios of these rocks to other Mesozoic intrusions in the Colorado River Region suggest the Turtle pluton and Target Granite have affinities like rocks to the east, including the Whipple Mountains and plutons of western Arizona. P-T-t history of the southern Turtle Mountains implies uplift well into the upper crust by Late Cretaceous time so that the heating and deformation events of the Late Cretaceous and Tertiary observed in flanking ranges did not affect the study area.

Acknowledgements

First, I want to recognize those who encouraged my interest in science at an early age. My mother and father never lead me to believe that my abilities didn't meet the task. They have been generous beyond reason and love. My high school science teachers, , , and , pointed out my schizophrenic tendencies toward humanities and science, and awarded those tendencies and my knack for solving problems in an independent fashion. I doubt I have learned as much since.

This project was co-supported by my advisor, A.K. Sinha, and the U.S, Geological Survey, primarily through the Graduate Intern Program. I would like to thank those on the Virginia Tech faculty and staff who have helped my during my stay, especially my advisor and my committee here: Dave Hewitt, Sue Eriksson, and Carol Simpson. A.K. has contributed his valuable time and resources to this project. Dean Hefner and the people in the front office have been a tremendous morale booster just because of their positive outlooks. and were available to answer every kind of question. The technical staff have helped with this project in many ways. , , and made things, fixed things, and helped me along my way. and crew drafted some figures and kept the microprobe up and going. drafted my map and helped in the library.

At the USGS, my boss, , has put up with me and put out for me. His tremendous knowledge of the Mojave Desert and geology in general has been inspiring. supplied me with analyses, unpublished data, and conversations to match the quality of the data. allowed me access to his lab and to his knowledge of stable isotopes. My field assistants, and , were capable and entertaining, and made field work even more rewarding.

Other professionals that have helped with interpretations of my part of the world and with geology in general are: , , , and . A special thanks to for letting me collaborate on Klamath projects.

The perseverance to finish this task and most of the learning I have acquired at Virginia Tech have come from Lab Central and its cast of characters, , , , , , , , and , who have tolerated interruption for years. I especially want to thank for sharing his scientific knowledge and integrity.

The gains of the late eighties were the people. The 1804 crew will never be forgotten. The first fantastic and comical pairing of instantly made this place fun, and the fun continued with , , and . had the patience to watch me learn, and has shown me the care that all friendships deserve. , , and have directly contributed to my sanity. The unbegrudgingly opened their home to me whenever I needed their company, and the have been an inspiration in their relationship and lifestyle. Finally, has not so patiently spent the same percentage of her life in school as I. All of their friendships are very important to me.

Table of Contents

List of Illustrations

List of Tables

List of Appendices

Chapter 1

GEOLOGY OF THE TURTLE PLUTON AND ENVIRONS

Introduction

Aims of This Study

Concentrically zoned plutonic series occur in a range of geologic settings, and the majority have a mafic rim and a felsic core. Two thoroughly studied examples of zoned plutonic series are the Tuolumne Intrusive Series, California (Bateman and Chappell, 1979) and the Loch Doon pluton, Scotland (Tindle and Pierce, 1981). A progression of rock type from mafic (dioritic) to felsic (granitic) toward the core is shown in Figure 1, and this geometry is referred to as normal zonation which is most often attributed to crystal settling and marginal accretion (references above). Subordinate magma mixing and contamination have been proposed to account for isotopic and minor chemical heterogeneity in these and other normally zoned plutons (Kistler et al., 1986; Stephens and Halliday, 1980; Hill et al., 1988; Hill and Silver, 1988).

In contrast to the normally zoned intrusions, few plutons with the reverse geometry (mafic core and a felsic rim) have been described (Ayuso, 1982; Bourne and Danis, 1987; Nabelek et al., 1986; Wernicke, 1987; Figure 1). The overall change of composition as reflected by rock type is

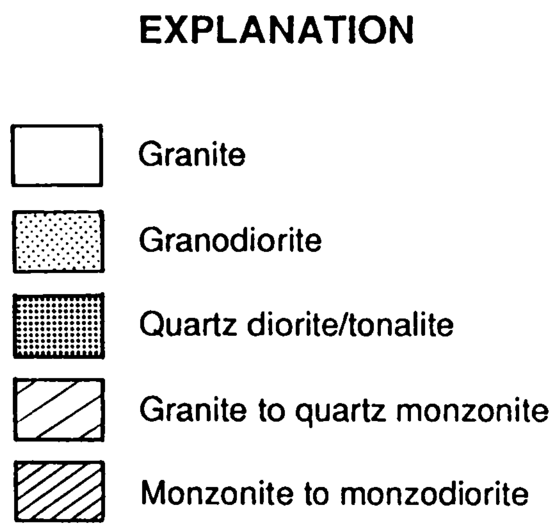

Figure 1. Distribution of rock types in concentrically zoned plutons: Rock types (given in the key, above) and subfacies (indicated by small letters) are defined by textural and/or mineralogical differences in the same rock type(s). Examples A and B are normally zoned plutons, ones with mafic rims. C-E are reversely zoned. A = Tuolumne Intrusive Series, California (Bateman and Chappell, 1979). B = Lock Doon pluton, Scotland (Tindle and Pierce, 1981). C = Bottle Lake Complex, Maine (Ayuso, 1984). D = El Topo pluton, Baja (Wernicke, 1987). E = Lacorne Complex, Canada (Bourne and Davis, 1987). Note that whereas normally zoned plutons have broad variations of rock type (granite to tonalite or quartz diorite), reversely zoned ones have more limited compositions, granite to granodiorite for example. Subfacies are A: cp = Cathedral Peak, jp = Johnson Porphyry, hde = Half Dome Equigranular, hdp = Half Dome Porphyritic. B: mg = microgranite, g = granite, t = tonalite, qd = quartz diorite. C: pr = Passadumkeag River pluton, heterogeneous, coarse-grained rim facies, pc = ditto, coarse-grained core facies with more mafic enclaves than the rim, wr = Whitney Cove pluton, coarse grained rim facies, wc = ditto, homogeneous, porphyritic core facies. E: i = inner facies, o = outer facies, lg = leucogranite.

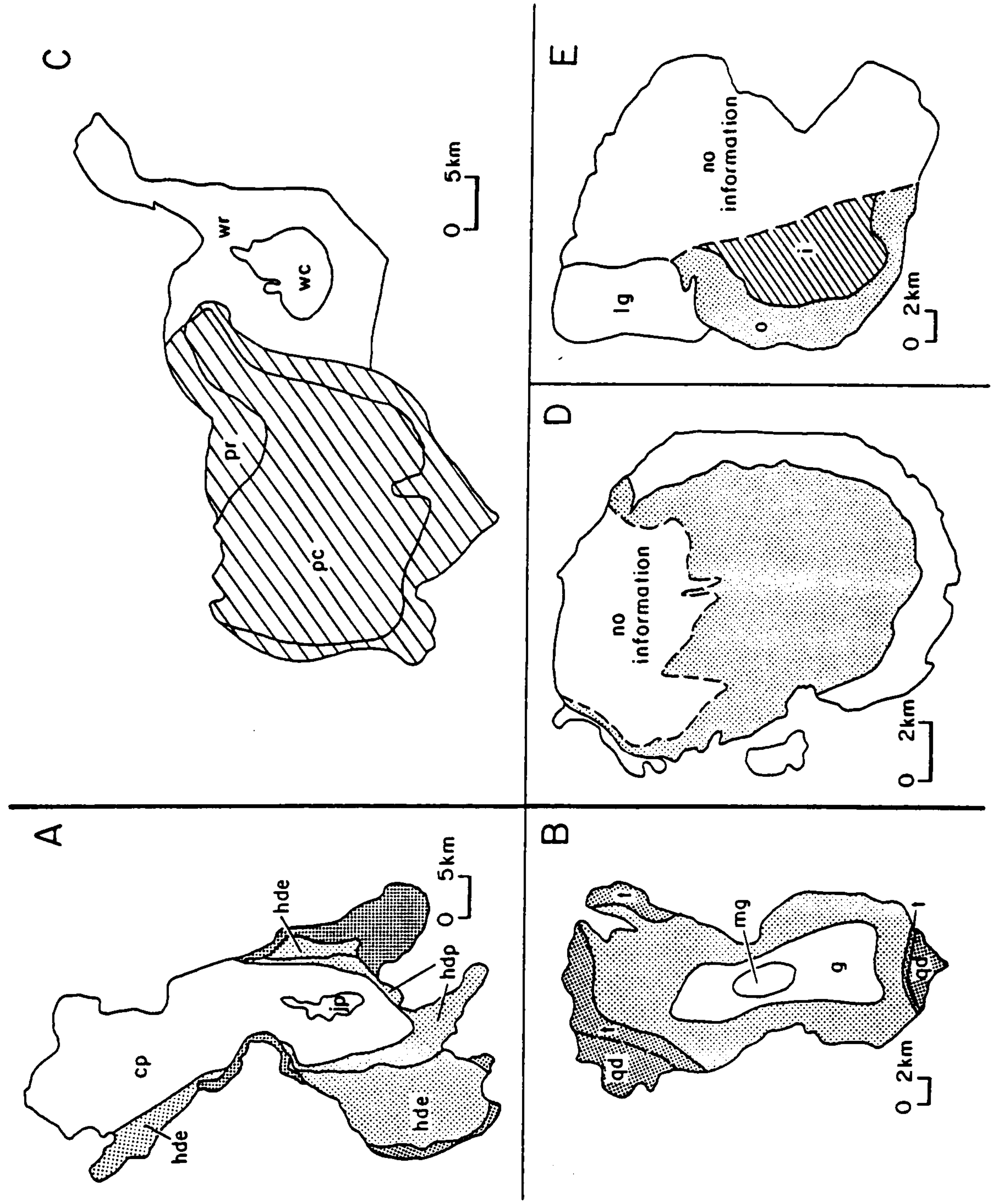
A
cp
jp
hde
hdp
hde
hde
0 5km
B
mg
g
qd
qd
0 2km
C
wr
wc
pr
pc
0 5km
D
no information
0 2km
E
no information
lg
o
i
0 2km

much less than that observed in normally zoned series. Some subvolcanic caldrons (Fridrich and Mahood, 1984), and volcanic ring dike complexes (Jacobson et al., 1958) also have felsic rims and mafic cores. Models for the origin of this reverse geometry include: (1) in situ differentiation from interior to exterior due to depression of the liquidus at the rim by addition of volatiles (Mutschler, 1980), (2) contamination by country rock (Ragland and Butler, 1972), (3) progressive partial melting (Hall, 1966), (4) restite unmixing such that the core contains a greater proportion of source material (Ayuso and Wones, 1980), (5) flow differentiation (Dostal, 1975), (6) intrusion of unrelated magmas (Ragland, et al., 1968), (7) intrusion of more mafic magma into an anatectic, crustal melt (Hutchinson, 1960), (8) rearrangement of a horizontally layered magma chamber (Fridrich and Mahood, 1984; Nabclek et al., 1986), (9) and sidewall crystallization and liquid fractionation proposed by Baker and McBirney (1985) and applied to the case of a reversely zoned pluton by Bourne and Danis (1987).

The Turtle pluton of southeastern California (Figure 2 and T in Figure 3) is an Early Cretaceous, reversely zoned intrusion. It has a granitic rim and granodioritic core, and contains numerous mafic, microgranitoid enclaves (inclusions). Field, chemical and isotopic studies from the Turtle pluton provide for a critical review of the mechanisms proposed for the origin of reversely zoned plutons. The data suggest the magmas that gave rise to the pluton evolved through magma mixing and fractional crystallization.

The Turtle Mountains (t in Figure 3) lie at the boundary of two tectonic provinces--the Tertiary to Cretaceous metamorphic core complexes to the east (including the Whipple Mountains = wh; Davis et al., 1980; Howard et al., 1982, and Chemehuevi Mountains = ch; John, 1986) and ranges underlain by Cretaceous nappes of metamorphosed Paleozoic sediments to the west (Old Woman Mountains = ow; Miller, et al., 1982 and south (Arica Mountains = a, Blatz, 1982; Big = bm and Little Maria Mountains = lm, Hamilton, 1982; Hoisch, 1987). K-Ar cooling ages and metamorphic assemblages suggest the Turtle Mountains did not experience the Late Cretaceous and/or Tertiary heating documented in these surrounding ranges (Howard et al., 1982; Hoisch et al., 1988; Martin et al., 1982). This suggests the Turtle Mountains experienced an unique history of intrusion, cooling, and perhaps uplift. Rb-Sr and U-Pb geochronology will be used to

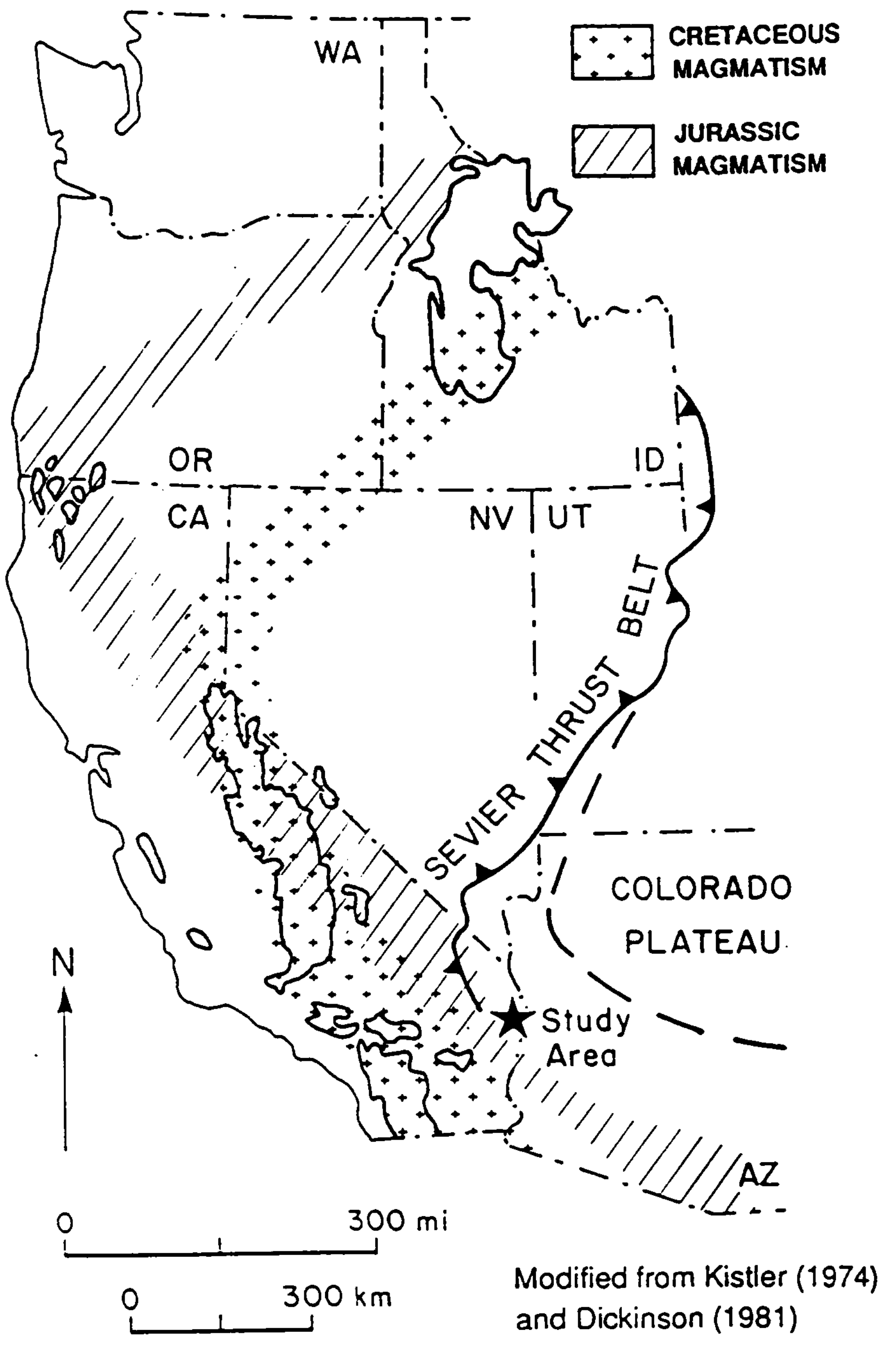

Figure 2. Location of the study area relative to major tectonic features: The study area (star) lies southwest of the Colorado Plateau, near the southern extension of the Sevier fold and thrust belt, and east of the major Mesozoic arcs (patterned) and batholiths (outlined), in a broad band of Cretaceous and Tertiary igneous rocks that extends from California to New Mexico.

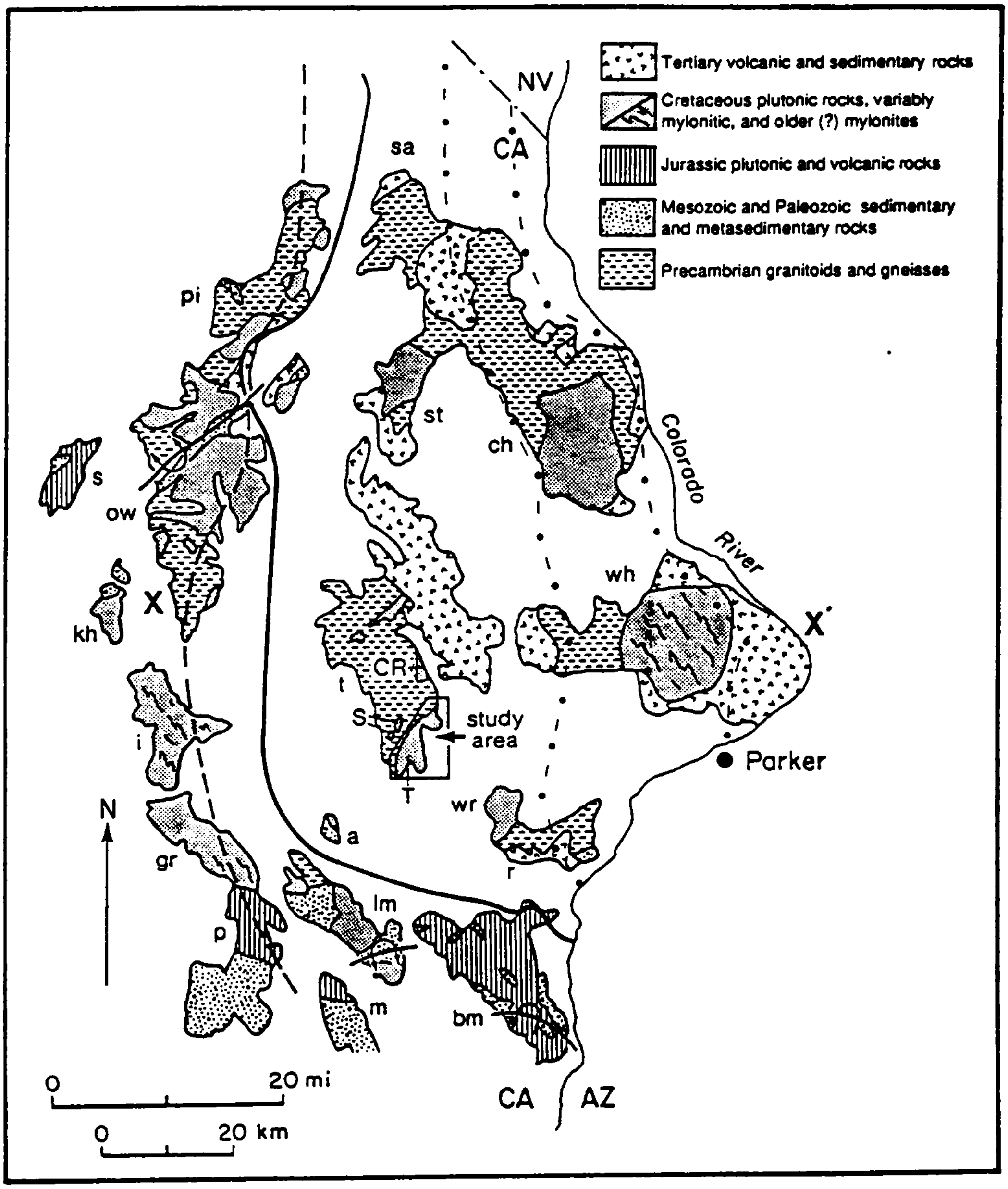

Figure 3. Geology of the Colorado River Region, S.E. California: This map shows bedrock and structural geology of the study region. Alluvium is unpatterned. Core complexes are outlined by dot-dash lines and the bold dashed and solid lines mark the western margin of the extensional corridor associated with metamorphic core complexes before and after erosion, respectively (from Howard and John, 1988). The Turtle Mountains (t) and the study area lie near the western edge of the extensional corridor, west of the core complexes, north and east of the Jurassic arc, and north and east of ranges containing large nappes (anticline and syncline symbols). T = Turtle pluton, S = satellite granodiorite, CR = Castle Rock pluton. a = Arica, bm = Big Maria, ch = Chemeheuvi, gr = Granite, i = Iron, lm = Little Maria, m = McCoy, ow = Old Woman, p = Palen, pi = Piute r = Riverside, s = Ship, sa = Sacramento, st = Stepladder, wh = Whipple Mountains, wr = West Riverside Mountains. kh = Kilbeck Hills.

constrain time of intrusion, source characteristics, and cooling paths. These results will be compared to modally similar plutonic rocks in the Turtle Mountains (Castle Rock pluton; CR in Figure 3) and in the West Riverside Mountains 25 km to the southeast (wr in Figure 3), and to well studied plutons of Late Cretaceous age in surrounding ranges (see ChapterS 5 and 6).

Location and Previous Work

The Turtle pluton lies at the southern tip of the Turtle Mountains, 45 km west of Parker, Arizona, 80 km south of Needles, California, and 4 km north of the settlement of Rice on California state highway 62 (Figure 3, and Figure 4). This region is the Basin and Range Province of the eastern Mojave Desert.

The southernmost Turtle Mountains were mapped as Precambrian rocks cut by Mesozoic granitoids and overlain by Tertiary volcanic and sedimentary rocks on the Needles 1° by 2° sheet (Bishop, 1963). K-Ar geochronology of the Turtle pluton and nearby intrusions indicated a Cretaceous cooling age of the Turtle pluton (Armstrong and Suppe, 1973). A geologic map of the field area produced as part of a power plant site examination (Woodward-McNeill and Associates, 1974) suggested several facies compose the Turtle pluton. Descriptions of rock types, additional K-Ar ages (Figure 5), and a regional model of Tertiary extension and uplift are given by Howard et al. (1982) and Howard and John (1988). U.S. Geological Survey Bulletin 1713-B (Howard et al., 1988) provides a map of the Turtle Mountains, descriptions of rock types, and a discussion of economic mineral potentials.

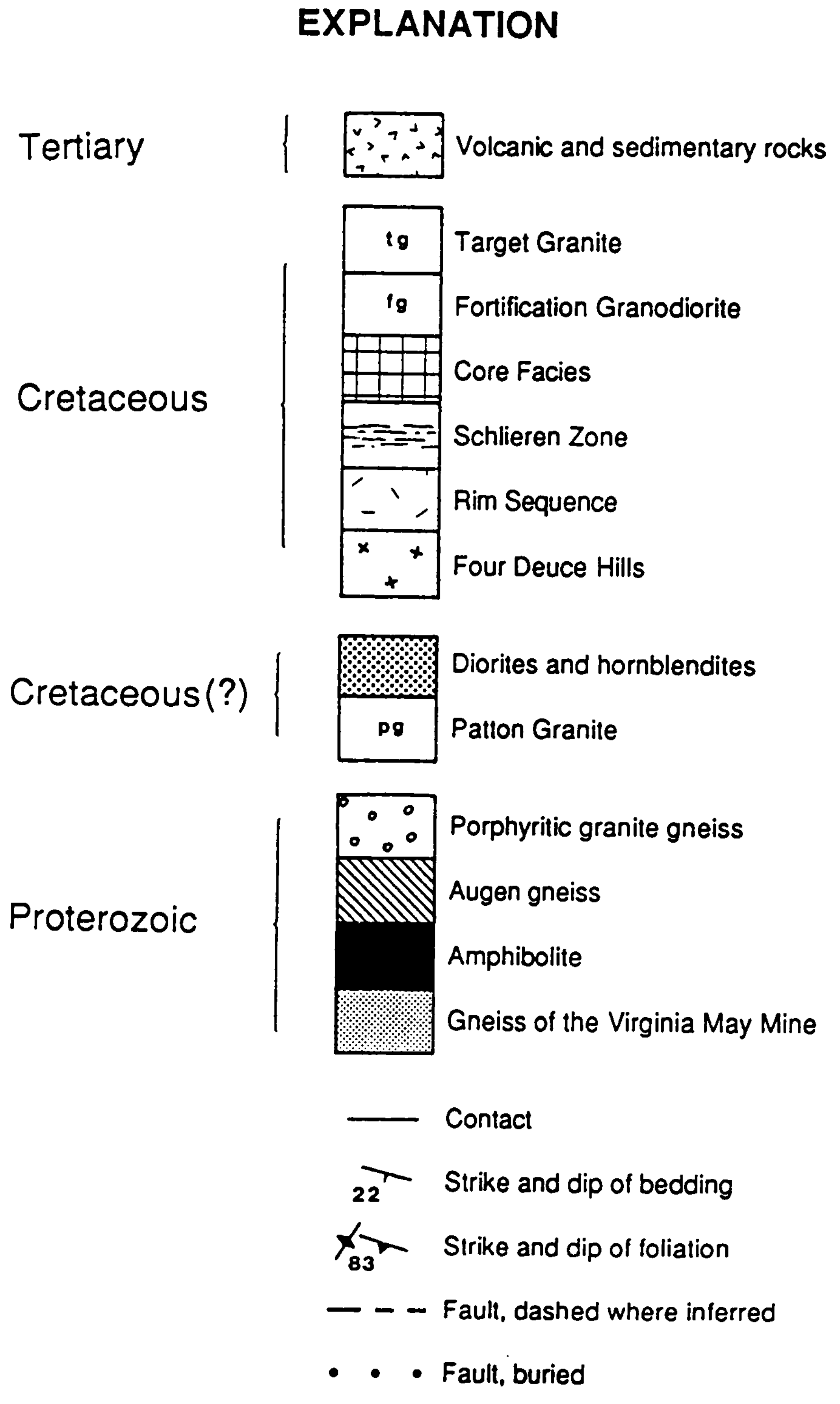

Figure 4. Generalized geologic map of the study area: This map shows the distribution of rock units, major faults, and strikes and dips of bedding in Tertiary volcanic rocks, and foliations in Precambrian gneisses.

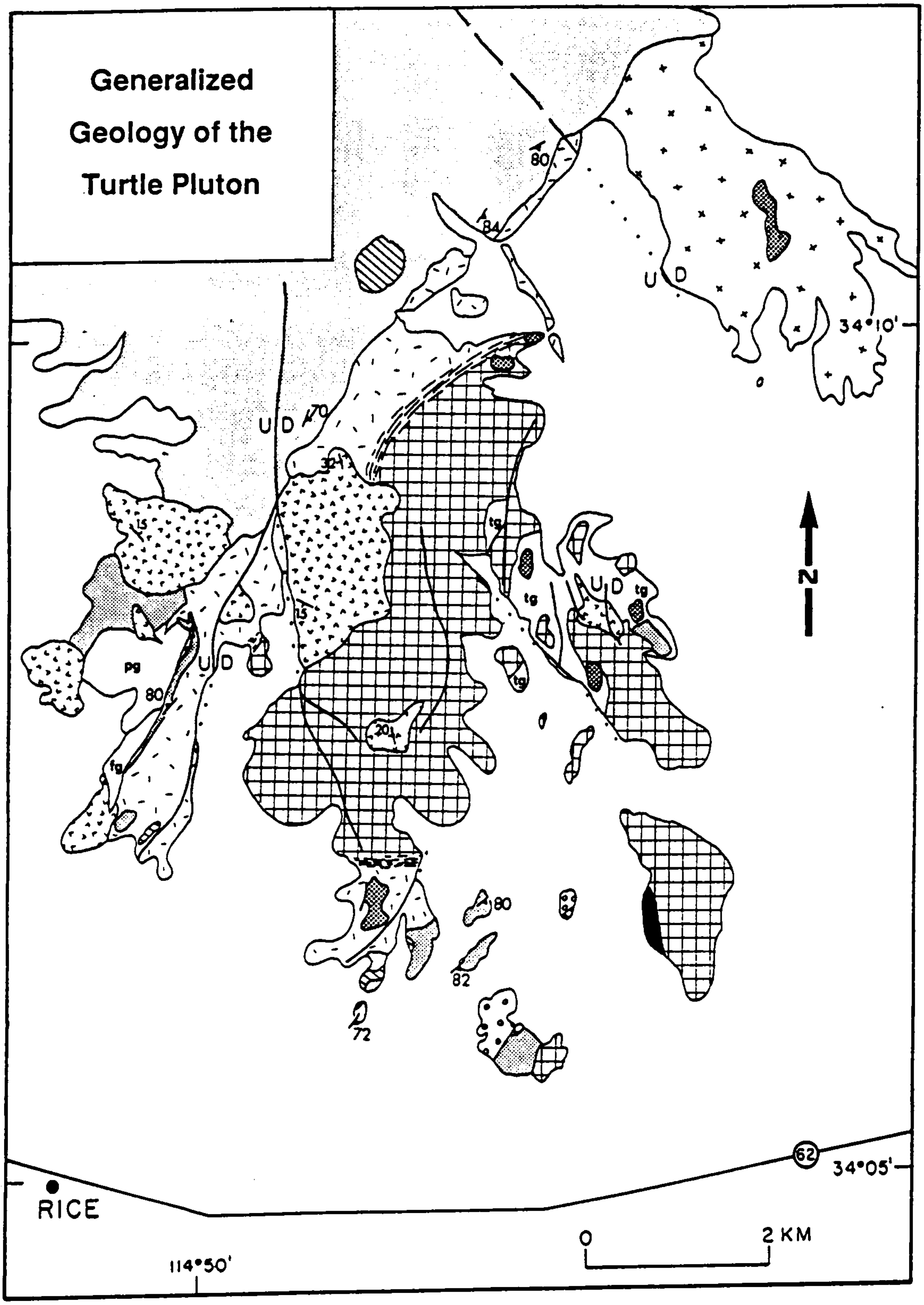
Generalized
Geology of the
Turtle Pluton
U D
70
80
84
34°10'
ts
pg
fg
tg
20
82
72
N
62
34°05'
RICE
0
2 KM
114°50'

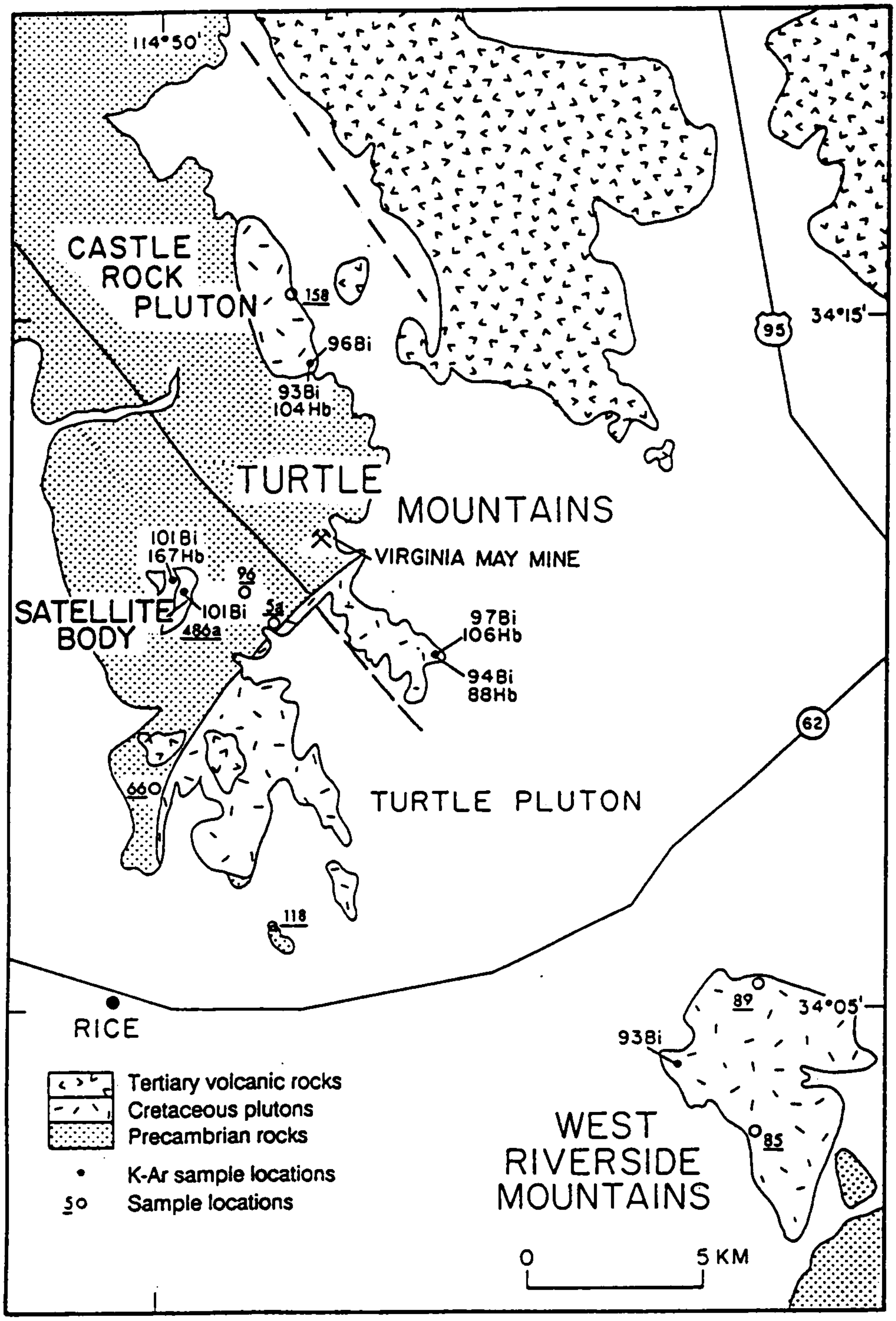

Figure 5. **K-Ar ages and locations of additional samples:** On this map are shown Cretaceous plutons in and near the the Turtle Mountains. Shown are K-Ar ages of Cretaceous plutons (dots; from Howard et al., 1982), and sample locations for modal and chemical analyses of Precambrian rocks and other plutons (circles). Additional samples of country rock are from the Virginia May Mine area (K.A. Howard, unpublished data).

Magmatic History of the Region

The Turtle pluton and crosscutting Target Granite lie east of the main Jurassic and Cretaceous magmatic arcs (Kistler, 1974; Dickenson, 1981; Figure 2) within a broad belt of Cretaceous and Tertiary plutonism that extends from the Sierra Nevada and Peninsula Ranges to New Mexico (Coney and Reynolds, 1977). Generally, across California and Arizona, pluton ages as defined by K-Ar and Rb-Sr geochronology decrease eastward, from about 130 to 40 Ma, and then change trend and decrease westward for Tertiary intrusions (Figure 6). This migration of igneous activity is interpreted to result from a shallowing subduction angle of the Farallon plate beneath the North American plate during the Cretaceous era, and then a steepening in the Tertiary Period (Coney and Reynolds, 1977). K-Ar ages for the Turtle pluton from Armstrong and Suppe (1973) and Howard et al. (1982) (Figure 5) fit the magmatic trend defined by Coney and Reynolds (1977) (Figure 6) moderately well though U-Pb and Rb-Sr geochronology of the Turtle pluton and plutonic rocks within a 40 km radius vary in age from 130 to 37 Ma (this study; Wright, et al., 1986).

Pre-Mesozoic rocks of the Turtle Mountains and surrounding ranges are Proterozoic (2.3 to 1.4 Ga) as deduced from regional correlations, from unpublished U-Pb geochronology on zircons (Wooden et al., 1988; J.L. Wooden, personal communication, 1989), from K-Ar geochronology on an undeformed dioritic stock in the central part of the range (1.35 Ga; Howard, et al., 1982), and from Rb-Sr geochronology on the gneisses in the southern Turtle Mountains (1.77 $\pm$ 0.04 Ga; Chapter 5).

After the Proterozoic, there is little evidence of igneous or metamorphic activity in the eastern Mojave Desert until the Jurassic Era, when a northwest-trending band of volcanic and plutonic rocks that range in age from 180 to 150 Ma were emplaced in southern California (Dickenson, 1981; Figure 2). At the latitude of the Turtle pluton, no known Jurassic intrusions occur east of the Ship Mountains for hundreds of kilometers (Howard and Shaw, 1981; s in Figure 3). Cretaceous plutons in the eastern-most Mojave shown in Figure 3 are voluminous (about 20 area%) and range

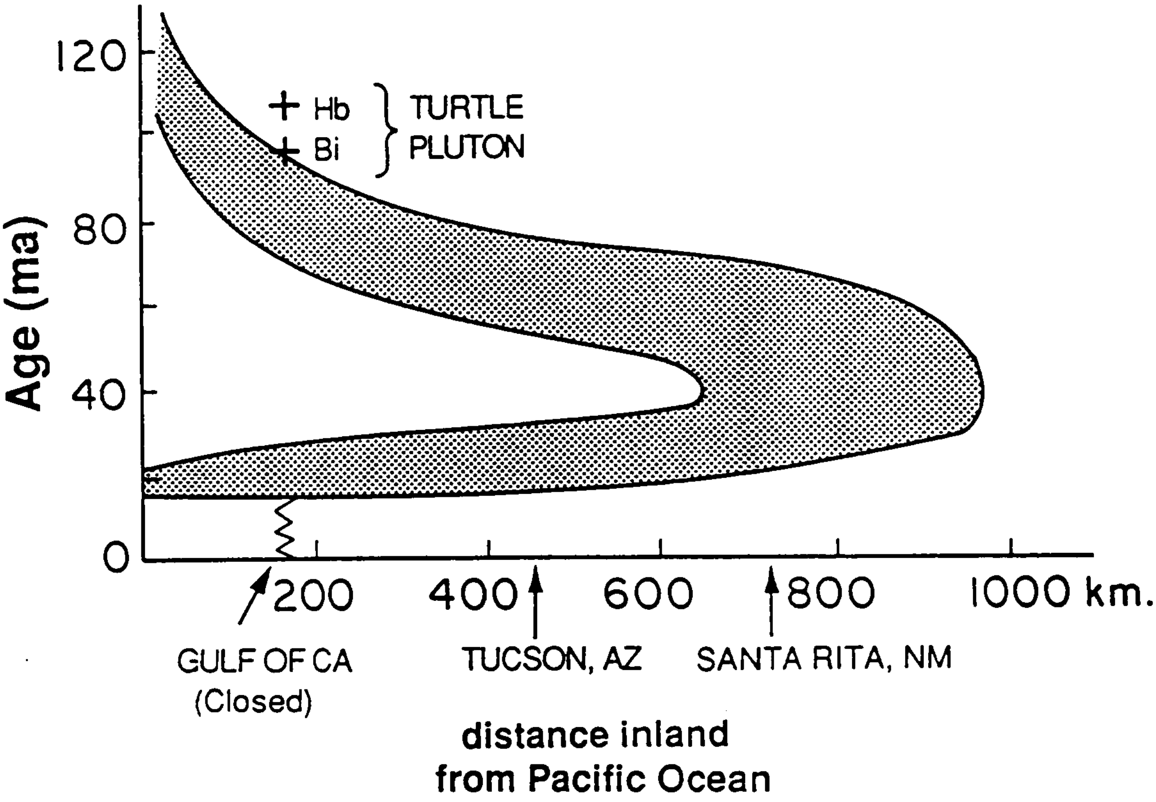

Modified from Coney and Reynolds (1977)

Figure 6. Migration of magmatism across the southwestern U.S.: The migration of magmatism across the southwestern U.S., as defined by K-Ar and Rb-Sr geochronology on plutonic and volcanic rocks, is thought to result from a varying angle of subduction with time. K-Ar ages on biotite and hornblende from the Turtle pluton (Howard et al., 1982) fit this trend moderately well though additional geochronology (U-Pb data) suggests plutons with ages from 130 Ma to 70 Ma and 37 Ma (this study, Wright et al., 1986) occur within a 40 km radius of the Turtle pluton.

in age from 130 to 65 Ma as determined by U-Pb geochronology on zircon and sphene or from K-Ar geochronology on biotite and hornblende in ranges near and including the Turtle Mountains (this study; Howard et al., 1982; Wright, et al. 1986). Recent, detailed U-Pb geochronology studies by Wright et al., 1986 (and personal communication, 1988) suggest 2 discrete Cretaceous magmatic pulses at 90 and 70 Ma in the Whipple and Old Woman Mountains. U-Pb geochronology of the Turtle pluton and Target Granite (this study) suggests an additional periods of magmatism at 130 Ma and 100 Ma, respectively. The oldest documented Cretaceous plutons in the area occur in the southern Turtle Mountains.

A large volume of Tertiary mafic and felsic volcanic rocks associated with Basin and Range extension were deposited in the area between 20 and 15 Ma ago (Howard et al., 1982; Hazlett, 1986).

Field Relations

Introduction

The Turtle pluton, informally named in Howard et al. (1982) is an Early Cretaceous body that concordantly intrudes steeply foliated Precambrian gneisses (Figure 4 and Plate A). The pluton comprises four facies: a gradational sequence of granite to granodiorite that forms the rim of the pluton, here informally called the Rim Sequence, a core of more mafic, granodiorite to quartz monzodiorite informally called the Core Facies, the contact zone between the Rim Sequence and Core Facies, and an eastern lobe of dominantly granodiorite called the Four Deuce Hills after an informal name given in a report by Woodward-McNeill and Associates, 1974) (Figure 7). The contact of the Rim Sequence and Core Facies, here informally called the Schlieren Zone, is a arcuate zone (a few tens of meters wide) of high strain defined by a strong vertical foliation in granodiorite. Mafic microgranitoid enclaves (< 3 m in length) and enclaves of hornblende diorite and hornblendite (a few to hundreds of meters in greatest dimension) are found in all parts of the pluton. Discussion of abundances, distributions, mineralogies and textures of these mafic rocks are given in Chapter 2.

The Early Cretaceous Turtle pluton is intruded by several units (Figure 7). The Core Facies is stoped by a leucogranite informally called the Target Granite in reference to war games held in the area under the command of General Patton during World War II. In the east, the Rim Sequence is cut by the Fortification Granodiorite, named after an informal reference to the nearby canyon in the report by Woodward-McNeill and Associates (1974). Pegmatites and aplites intrude all of the Cretaceous plutonic rocks. These Cretaceous units are overlain by erosional remnants of Tertiary volcanic and sedimentary rocks that generally dip 10 to 35 ° to the south and southwest (Figure 8). Tertiary (?) fine-grained dikes that range in composition from basalt to rhyolite intrude the Cretaceous rocks.

The host rocks of the Turtle pluton are Proterozoic metamorphic and igneous rocks except for the coarse-grained, undeformed granite, here called informally the Patton Granite, at the eastern margin of the Turtle pluton, (Figure 7 and Plate A) which, given its undeformed nature, is suspected to be Early Cretaceous. The most abundant country rock type is biotite quartzofeldspathic gneiss. Other rock types include in decreasing abundances) potassium feldspar augen gneiss, amphibolite, granite gneiss, and hornblende diabase (Figure 4 and Plate A).

A description of the plutonic units and their host rocks in terms of mineralogy, grain size, fabric, inclusion types, and association with aplites and pegmatites is given below. In Table 1 on page 19are given abbreviations for rock units and mineral species used in tables and appendices. For the purposes of this study the terms very coarse-, coarse-, medium-, and fine-grained denote average grain sizes of greater than 3.0 cm, between 3.0 and 0.5 cm, between 0.5 and 0.1 cm, and smaller than 0.1 cm, respectively (Bates and Jackson, 1980). In reference to mineral shape, acicular, tabular and prismatic, and equidimensional denote length/width ratios of > 3/1, < 3/1 but > 1/1, and 1/1, respectively (Bates and Jackson, 1980). Plutonic rock names were obtained by point

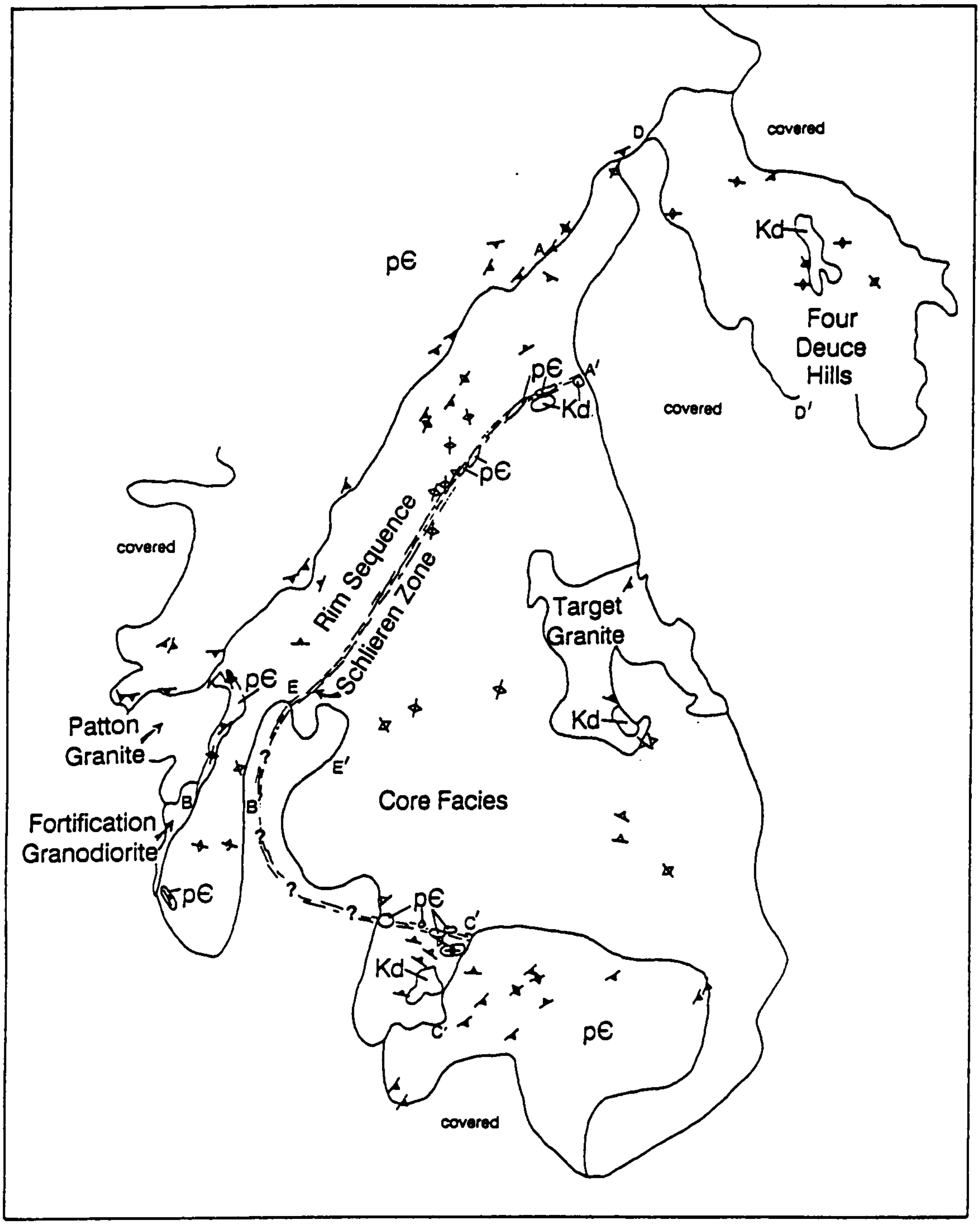

Figure 7. **Bedrock map showning plutonic units:** The Turtle pluton comprises four units: the Rim Sequence, Schlieren Zone, Core Facies, and Four Deuce Hills. The Core Facies is stoped by the Target Granite and the Rim Sequence is intruded by the Fortification Granodiorite. The Patton Granite is older than all other plutonic units.

Figure 8. **Field photographs of the Turtle pluton:** a. View of the Turtle pluton from the south showing tectonically tilted Tertiary volcanic flows (upper right) that overlie the pluton. Approximate contact marked by white dashes. b. Typical outcrop of Rim Sequence granodiorite along traverse A-A′ showing an enclave swarm. View about 2.5 meters across. c. Aligned potassium feldspar crystals in porphyritic Rim Sequence granodiorite with maximum crystal length of about 12 cm. Pencil is 14 cm long. d. View of the Schlieren Zone showing schlieren, microgranitoid enclaves, and aplite dikes. Pen is 13.5 cm long.

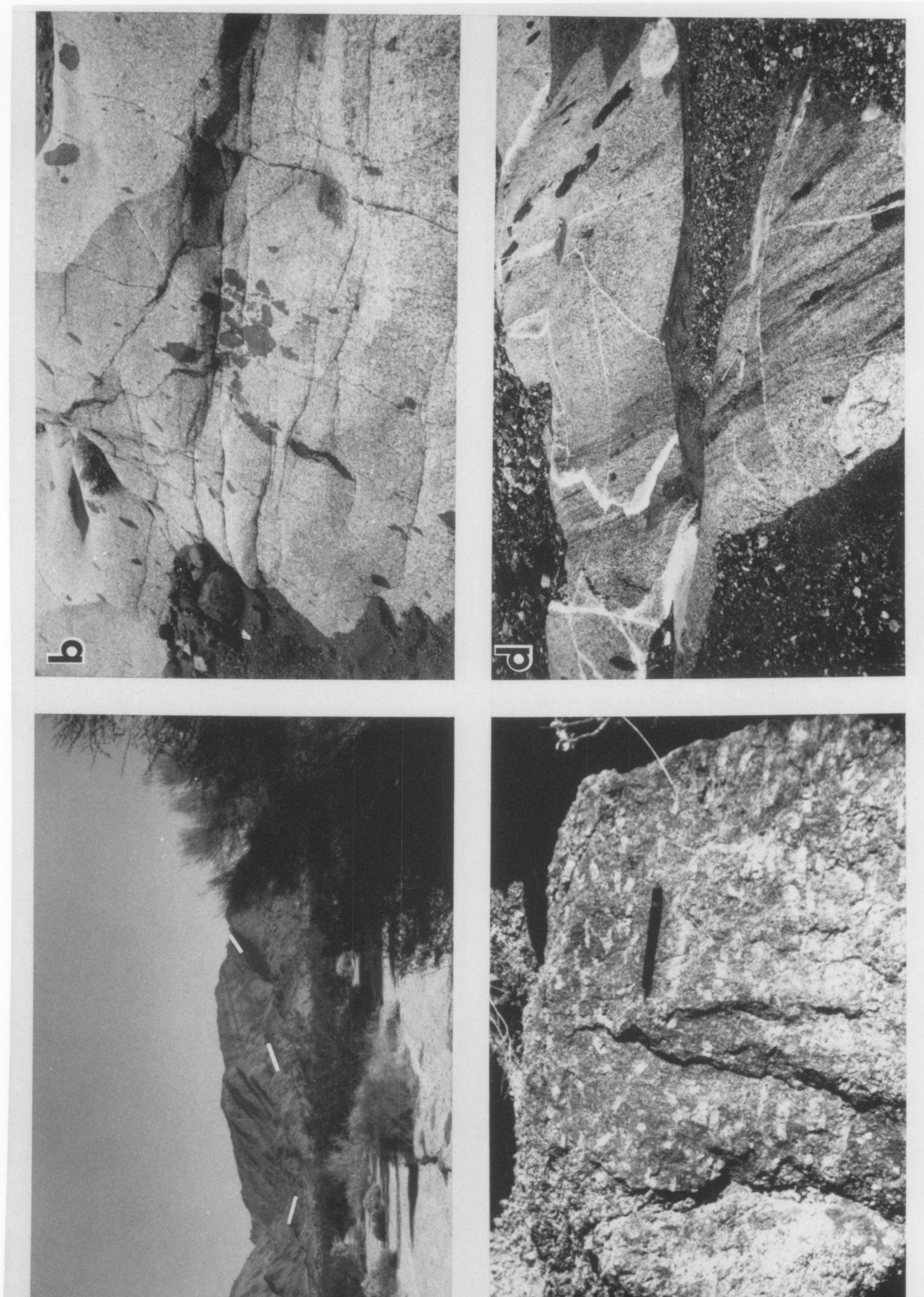
a
b
c
d

counts of stained slabs or thin sections (APPENDIX 1) using the classification of Streckeisen (1973).

Regional Structural Geology and Geometry of the Turtle Pluton

In a regional structural model presented by Howard and John (1988), the Turtle Mountains are thought to lie at the western edge of an extensional corridor which includes the metamorphic core complexes of southeastern California and western Arizona (Figure 3). The structure of the corridor is dominated by rotated crustal blocks which are divided by normal faults, and which lie on a low angle, normal (detachment) fault (Figure 9). Extension has rotated blocks above the detachment fault such that Tertiary strata in these blocks are tilted toward the west or southwest, more and more, from the Turtle Mountains to the core complexes. The subvertical normal faults that cut the southern Turtle Mountains (see Plate A), and the low tectonic dips of Tertiary volcanic flows (10 to 35° SW pictured in Figure 8) suggest minor rotation and horizontal transport of the Turtle Mountains above a detachment fault at depth, i.e. the Turtle Mountains are approximately autochthonous (Howard et al., 1982; Howard and John, 1988). Seismic reflections below the Turtle Mountains have been interpreted as an extension of the Whipple Mountain detachment fault (Frost and Okaya, 1986).

Minor normal faults are common throughout the study area and mimic both the high angle faults, and the low angle detachment fault inferred at depth. Mappable low angle faults include a west dipping structure in the central part of the field area of unknown offset, and an east dipping fault zone along the west edge of the Four Deuce Hills. Figure 10b shows an east facing view in this fault zone where a mafic dike is offset on faults with tops transported to the northeast. Total offset on this fault zone is unknown. The offset on high angle normal faults across the field area, on the order of a few hundred meters (see Plate A, cross section), is insignificant to a petrologic study.

Table 1. Abbreviations used in tables and appendixes.

Commonly Used:	AVG	= average
	STD DEV	= standard deviation
	STD	= standard deviation
	n	= number of observations
Rock Type:	gr	= granite
	gd	= granodiorite
	qmd	= quartz monzodiorite
	gap	= garnet aplite
	m encl	= microgranitoid enclave
	cg encl	= coarse grained enclave
	m dike	= mafic dike
	gn	= gneiss
Rock Unit:	RS	= Rim Sequence
	CF	= Core Facies
	FDH	= Four Deuce Hills
	TG	= Target Granite
	FGD	= Fortification Granodiorite
	SAT	= Satellite body
	CR	= Castle Rock pluton
	WR	= West Riverside Mts.
	Xvm	= Virginia May gneiss
	Xgg	= granite gneiss
	Xag	= augen gneiss
	Xa	= amphibolite
Chemistry:	A/CNK	= molec. Al/(Ca+Na+K)
	Fe#	= molec. Fe/(Fe+Mg)
	Al4	= tetrahedral Al
	Al6	= octahedral Al
	Sr_i	= initial $^{87}Sr/^{86}Sr$

Combinations of rock unit and rock type abbreviations are used to identify samples in figures, tables, and appendices.

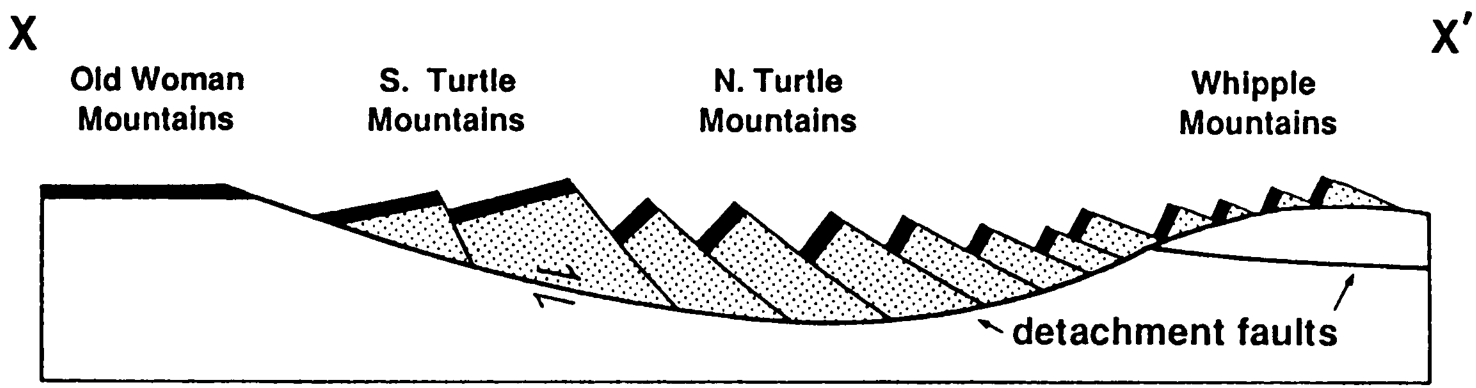

Figure 9. Schematic cross section of the Colorado River Region: This east-west cross section modified from Howard and John (1988) (see X-X', Figure 3) shows the fault style of the extensional corridor associated with metamorphic core complexes. The southern Turtle Mountains lie at the western edge of the corridor and are cut by high angle normal faults, have been rotated 10 to 30° to the west and southwest, and are thought to lie above a low angle normal (detachement) fault.

Figure 10. **Field photographs of the Turtle pluton and host rocks:** a. Vertically foliated Virginia May gneiss with folded and boudinaged felsic dikes north of the Turtle pluton (25 meters north of point A of traverse A-A′ in Figure 13 on page 32). Hammer handle 43 cm long. b. Mafic dike (CA85-4) with textures like micrograniloid enclaves in granodiorite of the Four Deuce Hills, along traverse D-D′ (Figure 19 on page 45). Dike is offset along low angle normal faults with transport top to the northeast. Hammer handle 43 cm long. c. Dike of Core Facies granodiorite with flattened mafic enclaves (right) in K-feldspar porphyritic Rim Sequence granodiorite at C′ of traverse C-C′ (Figure 13). Arrow points to contact. Notebook 23 cm long. d. Xenolithic screen of vertically foliated Virginia May gneiss in the Schlieren Zone. Xenolith is about two meters wide and tens of meters long (continues in background, arrows). White end of pen (13 cm long) points to the contact.

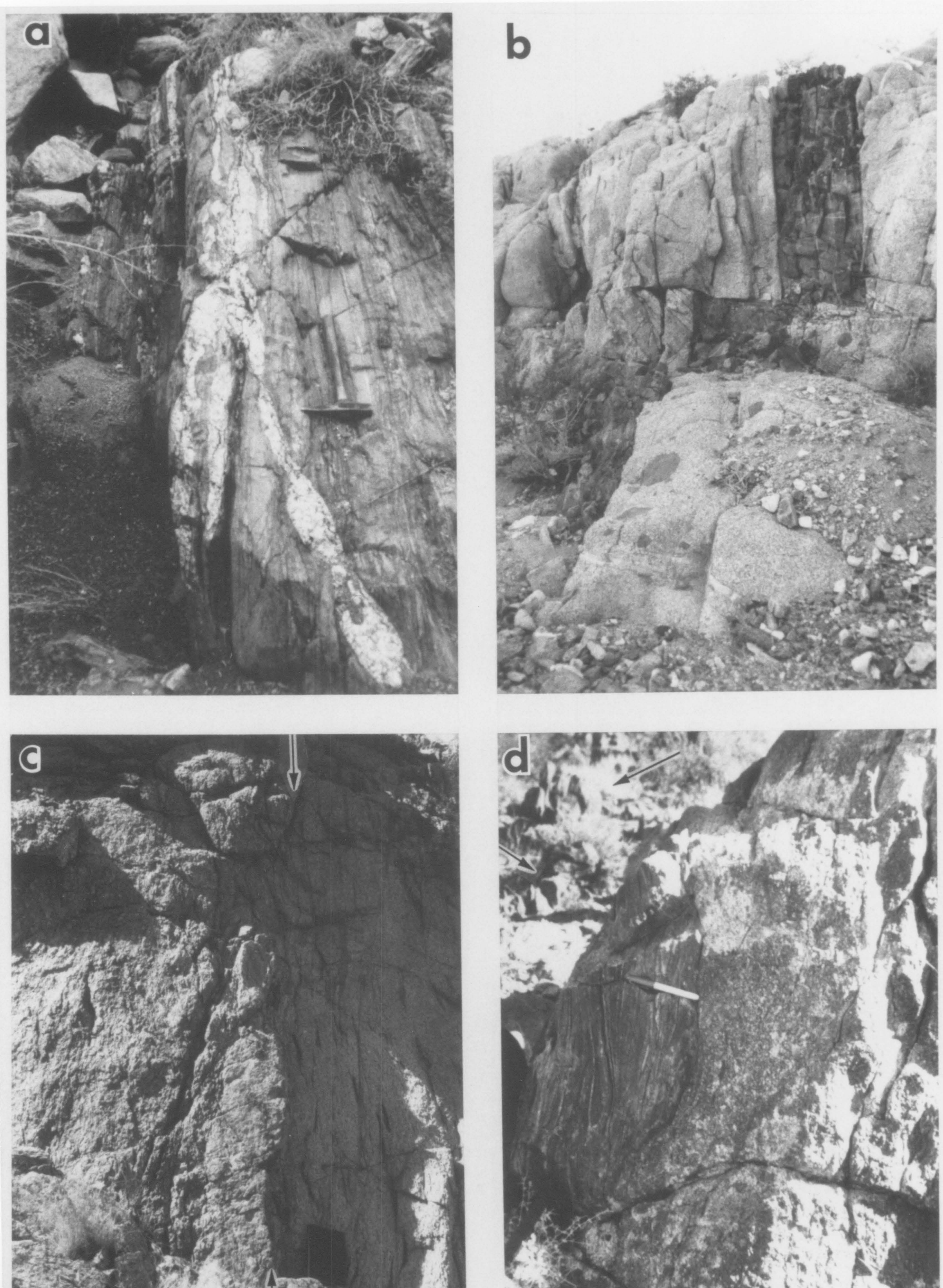
a
b
c
d

The Turtle pluton concordantly intrudes steeply foliated Precambrian schists and gneisses. This contact is generally sharp and there is no discernible contact metamorphism. This intrusive style suggests the Turtle pluton is mesozonal and was emplaced at depths of 8 to 14 kilometers, or about 2 to 4 kilobars (Buddington, 1959).

The three dimensional shape of the pluton is inferred from field measurements of Precambrian rocks surrounding the pluton (Figure 4 on page 8 and Plate A). Gneisses along the northern and southern contacts have northeast trending foliations and steep southerly dips, and along the western margin they have north-south foliations and subvertical dips. These data suggest a cylindrical structure with a steep southeastward plunge. A compilation of measurements for the internal contact of the Rim Sequence and Core Facies along the Schlieren Zone suggests an internal igneous fabric concentric with the host rock/pluton contact.

Country Rocks of the Turtle Pluton

Introduction

The dominant Proterozoic country rock type of the southern Turtle Mountains is a biotite quartzofeldspathic gneiss. It is deformed with some amphibolites and is crosscut by potassium feldspar augen gneiss, other amphibolites, porphyritic granite gneiss, and hornblende diabase. The areal distribution of these units is shown in Figure 4 on page 8 and Plate A, and field relations among units are shown schematically in Figure 11. These rock types will be discussed in order of their apparent age as determined from field relations.

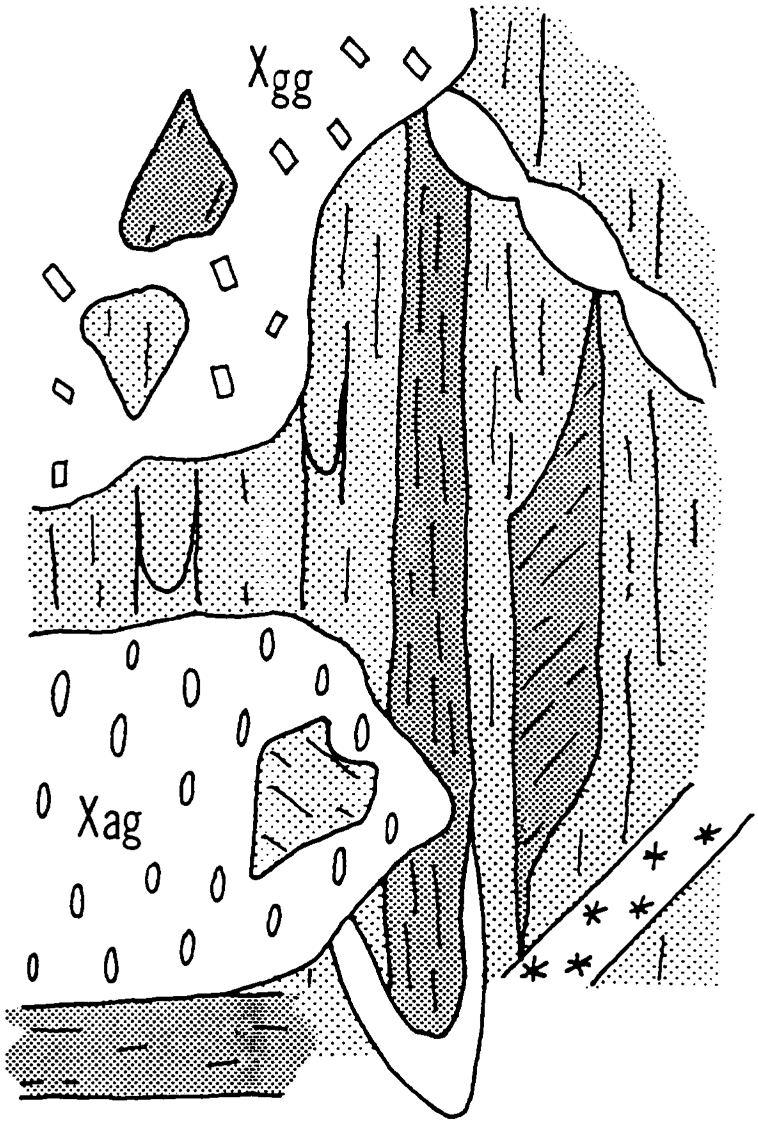

Figure 11. Field relationships among Precambrian rock types: This sketch shows the intrusive and structural relationships among host rocks of the Turtle pluton. Virginia May gneiss (light shading) is a multiply-deformed biotite quartzofeldspathic gneiss associated with leucocratic dikes (unpatterned) that are folded and boudinaged. There is more than one generation of amphibolite (dark shading): some generations have foliations partially or fully transposed parallel to that of the Virginia May gneiss; another generation of amphibolite truncates the foliation of an augen gneiss (Xag; similar to the augen gneiss of Johnsons Well, Howard et al., 1982) that crosscuts Virginia May gniess and other amphibolites. A gneissic granite (Xgg) also intruded the Virginia May gneiss and amphibolites, and its relationship to the augen gneiss is unknown. Hornblende diabase (stars) that lacks penetrative fabric intrudes Virginia May gneiss and amphibolites.

Virginia May Gneiss

The host rock for the Turtle pluton along most of its contact is a light to dark gray, fine-grained, biotite quartzofeldspathic gneiss that is associated with discordant, folded leucocratic dikes (Figure 10). This rock type is called the granite gneiss of Virginia May Mine (Howard, et al., 1982; Howard et al., 1988) after an occurrence at the Virginia May Mine located a few kilometers northeast of the Turtle Pluton (see Figure 5 on page 10 and north central section of Plate A). The informal name Virginia May gneiss is employed here. This fine-grained gneiss contains two feldspars + quartz + biotite ± muscovite ± accessory phases. Associated leucocratic dikes are medium to coarse-grained and contain two feldspars + quartz ± muscovite ± garnet.

In the map area, the Virginia May gneiss is generally steeply foliated with a northeasterly trend (average about N35E70S; see Plate A) and contains steeply plunging lineations as well as some shallower, folded lineations which indicate a poly-phase deformational history. Leucocratic dikes are folded and boudinaged, and therefore participated in at least one folding event (Figure 11).

Within this map unit of Virginia May gneiss occur amphibolite, augen gneiss, and hornblende diabase that are mapped as discrete units where ever they occur in sufficient size (map scale 1:24,000).

Amphibolite

A range of textures, mineralogies and crosscutting relationships suggest that more than one generation of amphibolite occurs in the map area (outcrop area about 0.1 km^2). Rock type varies from medium- to fine-grained, centimeter-scale, banded amphibolite with black hornblendite layers and white feldspar ± quartz layers, to more massive, medium- to fine-grained gray rocks composed of hornblende + plagioclase ± biotite ± chlorite ± epidote ± quartz (see modes, APPENDIX 1). One area of centimeter-scale, banded amphibolite with northeasterly strikes and variable dips is concordantly intruded by the Core Facies of the Turtle pluton with no discernible contact effects (southeastern portion of the study area, Figure 4; section 9 of Plate A).

Within the Virginia May gneiss, massive, meter-scale, gray, amphibolite layers are concordant with the foliation of their surrounding quartzofeldspathic gneiss, and have internal foliation either concordant or discordant to that of the Virginia May gneiss (Figure 11). Blocks of gray amphibolite within a porphyritic granite gneiss (see below) have foliations discordant to its host gneiss and this suggests these amphibolites are xenoliths within the granite gneiss. In another instance, a relatively massive amphibolite about two meters wide truncates the foliation of an augen gneiss (see below) which suggests deformation of the augen gneiss preceded emplacement of the amphibolite. These field relations suggest multiple generations of amphibolite.

Augen Gneiss

In the north, south, and southwestern portions of the map area, biotite potassium feldspar augen gneiss (Xag) underlies an outcrop area of about 0.4 km^2. This gneiss is composed of biotite ± hornblende, potassium feldspar augen, plagioclase, and quartz (see modes, APPENDIX 1). Pale pink augen that reach 4 cm in length are weakly to strongly aligned, and are prominently lineated in some areas (80SE42, 42SE58, 32SE62, for examples). This unit is very similar to the augen gneiss of Johnsons Well located in the west, central Turtle Mountains (Howard et al., 1982). The augen gneiss crosscuts the Virginia May gneiss, leucocratic dikes associated with the gneiss, and some amphibolite layers, but is crosscut by an amphibolite.

Granite Gneiss

A gneissic granite (Xgg) called the granite porphyry of southern Turtle Mountains (Howard et al., 1982) crops out in a 0.13 km^2 area in the southern part of the map area. Here it is referred to as simply granite gneiss. This rock type contains aligned tabular potassium feldspar phenocrysts to 2.5 cm in length, biotite that is altered to chlorite and hematite, minor muscovite, and accessory phases of allanite, zircon, sphene and apatite (APPENDIX 1). The rock has a weak to strong foliation primarily defined by ductilely deformed and recrystallized quartz and brittlely deformed feldspars. Enclaves of quartzofeldspathic gneiss and amphibolite with foliations at angles to that of their host were observed in this porphyritic granite gneiss, therefore the granite gneiss is assumed to have intruded the previously deformed gneisses, and subsequently was deformed itself.

Hornblende Diabase

Outcrops of hornblende diabase (similar to dikes described in the central and northern Turtle Mountains by Howard et al., 1982) occur in Virginia May gneiss. Sprays of plagioclase which reach 1 cm in length compose about 60 percent of the diabase, and hornblende plus pyroxene (partially replaced by hornblende) make up most of the remainder along with epidote, opaques and very sparse biotite. These rocks lack penetrative fabrics but tectonic disruption is suggested by discontinuous outcrops concordant with the foliation of the enclosing Virginia May gneiss. In the central part of the Turtle Mountains, K-Ar geochronology on hornblende from the diabases yields an age of 439 Ma which is interpreted as partially reset from a Proterozoic age (Howard et al., 1982).

Patton Granite

An undeformed, equigranular, medium-grained granite, here called the Patton Granite, intrudes Virginia May gneiss in the western part of the field area (Plate A) and is itself intruded by the Turtle pluton and Fortification Granodiorite (Figure 7 on page 15). The Patton Granite underlies an area of 0.8 km^2, is pink in outcrop and has a color index of 5 to 10. Estimated average grain sizes for the felsic phases are 1 cm for potassium feldspar and 0.5 cm for white plagioclase and gray quartz. In hand specimen, chloritized biotite books to 0.4 cm and much less abundant hornblende to 0.5 cm may be seen. The rock type contains very sparse enclaves; those observed were microgranitoid, fine-grained with a color index of about 30, and were less than 10 cm in length.

The lack of deformational fabric suggests that the Patton Granite post-dates deformation of the Proterozoic units it intrudes. It is intruded by the Rim Sequence of the Turtle pluton and therefore is constrained to be Proterozoic to Early Cretaceous in age.

Turtle Pluton

The four facies of the Turtle pluton are described below. Aplite and pegmatite dikes intrude all units of the Turtle pluton and a specific type of aplite readily identifiable in the field, that bearing garnets, was investigated petrographically and chemically. Mafic enclaves with microgranitoid and dioritic texture are found in all facies of the Turtle pluton and are discussed in Chapter 2.

Rim Sequence

The Rim Sequence of the Turtle pluton (areal extent of 4.5 km^2) is a gradational, 0.8 to 0.4 km wide suite of granite and granodiorite that systematically changes mineralogy and texture (see Figures 13 through 17) from biotite + ilmenite ± magnetite ± muscovite (ilmenite assemblage) to biotite + magnetite + sphene, to hornblende + biotite + magnetite + sphene (magnetite assemblage). It is intruded by the Core Facies at one location marked X on Figure 13 (and pictured in Figure 10). Mineralogic and textural changes in the Rim Sequence are documented by field observations throughout the unit and on a detailed traverse from north to south (A-A′ on Figure 13) that was undertaken in order to quantify the distribution of mafic enclaves, and the changes of granitoid texture and composition with position in the pluton. Mineral changes across traverse A-A′ are detailed below. Classification of rock types, cumulative modes, and a schematic diagram of changes in crystal size are given in Figure 14, Figure 15, and Figure 16.

Traverse A-A′ of the Rim Sequence

The detailed geology of a single north-south traverse of the Rim Sequence in a well-exposed wash is consistent with observations along other traverses and with field checks throughout the unit. The geology of this traverse is treated as a type section for the Rim Sequence and differences of other traverses will be compared to the type section.

Along traverse A-A′ from the host rock contact at A and southward to the Core Facies at A′, the Rim Sequence changes texture and rock type from an equigranular biotite granite, to a potassium feldspar porphyritic hornblende biotite granodiorite, to a nonporphyritic, biotite hornblende granodiorite. A suite of eight samples was collected, and their approximate locations from point A are shown in Figure 15 with sample numbers.

Potassium Feldspar

Potassium feldspar changes dramatically in size and abundance across the Rim Sequence (Figure 15 and Figure 16) though it is consistently pink throughout. Inclusions of plagioclase and biotite commonly decorate concentric growth zones in phenocrystic K-feldspar in all porphyritic granodiorite. Five meters from the country rock contact (A on Figure 13) potassium feldspar grains in equigranular granite are equidimensional to tabular (length/width = 2/1) and have a maximum length of 8 mm. Twenty meters from the contact, the phenocrysts are porphyritic, more elongate (3/1), and have a maximum length is about 20 mm. One hundred meters from the contact the rock is clearly porphyritic. K-feldspar phenocrysts (3/1) are tabular and a maximum length of about 30 mm. In this rock there is also a groundmass or interstitial potassium feldspar which composes roughly 20% of the total potassium feldspar. Two hundred to 300 meters from the contact, the granodiorite is coarsely porphyritic with potassium feldspar phenocrysts that reach 120x10x10 mm (Figure 8) but average 30x20x10 mm (field estimate). These phenocrysts are

Figure 12. Textural and mineralogical variation in the Rim Sequence: These photographs of stained slabs show grain size and mineralogic variation as well as the increase in foliation across the Rim Sequence from country rock contact (a) into the pluton (f). Yellow- stained potassium feldspar appears light gray. Example phenocrysts are labelled "k". Samples BW84-20, -18, -19, -22, -23, and -25 are labelled a-f, respectively.

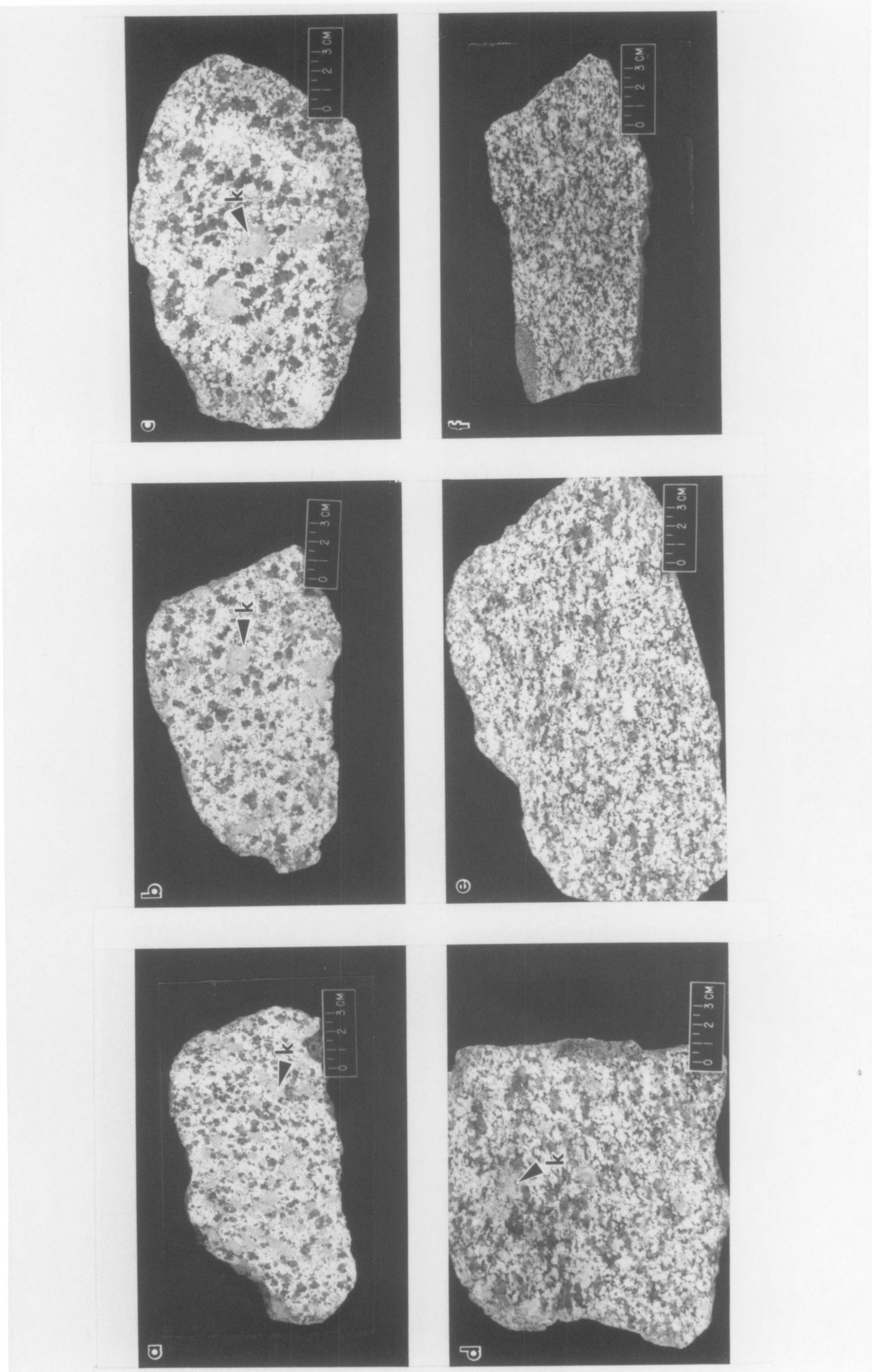
a
b
c
d
e
f
k
0 1 2 3 CM

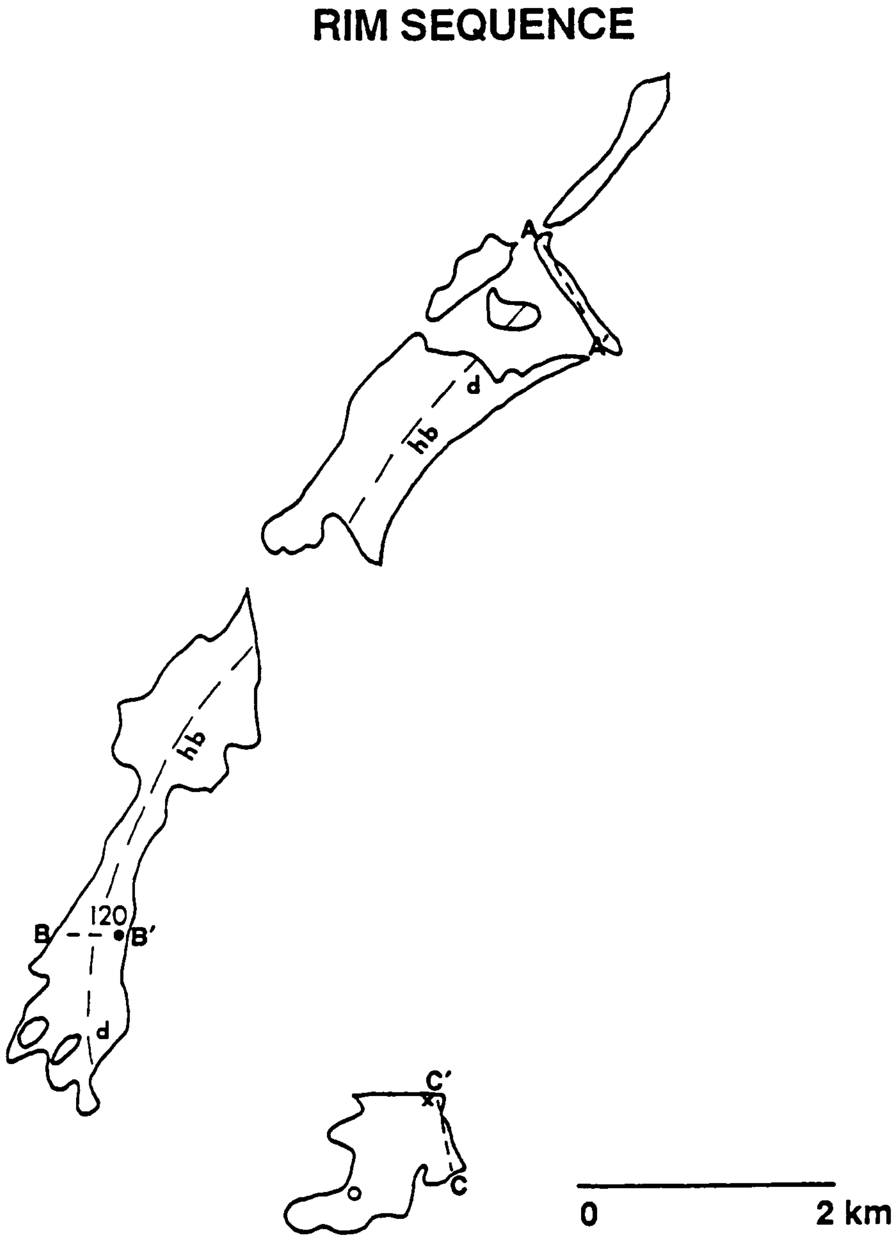

Figure 13. **Outline map of the Rim Sequence:** On this map of the Rim Sequence are given sample locations for modal (circle) and chemical analyses (dot with sample number), the approximate limit of hornblende-bearing rocks (hb), and the locations of detailed traverses, A-A′, B-B′, and C-C′. Eight samples (not marked) from traverse A-A′ are described in detail in the text. Also given are locations where the Rim Sequence are intruded by the Core Facies (X), and by mafic dikes with textures like microgranitoid enclaves (d).

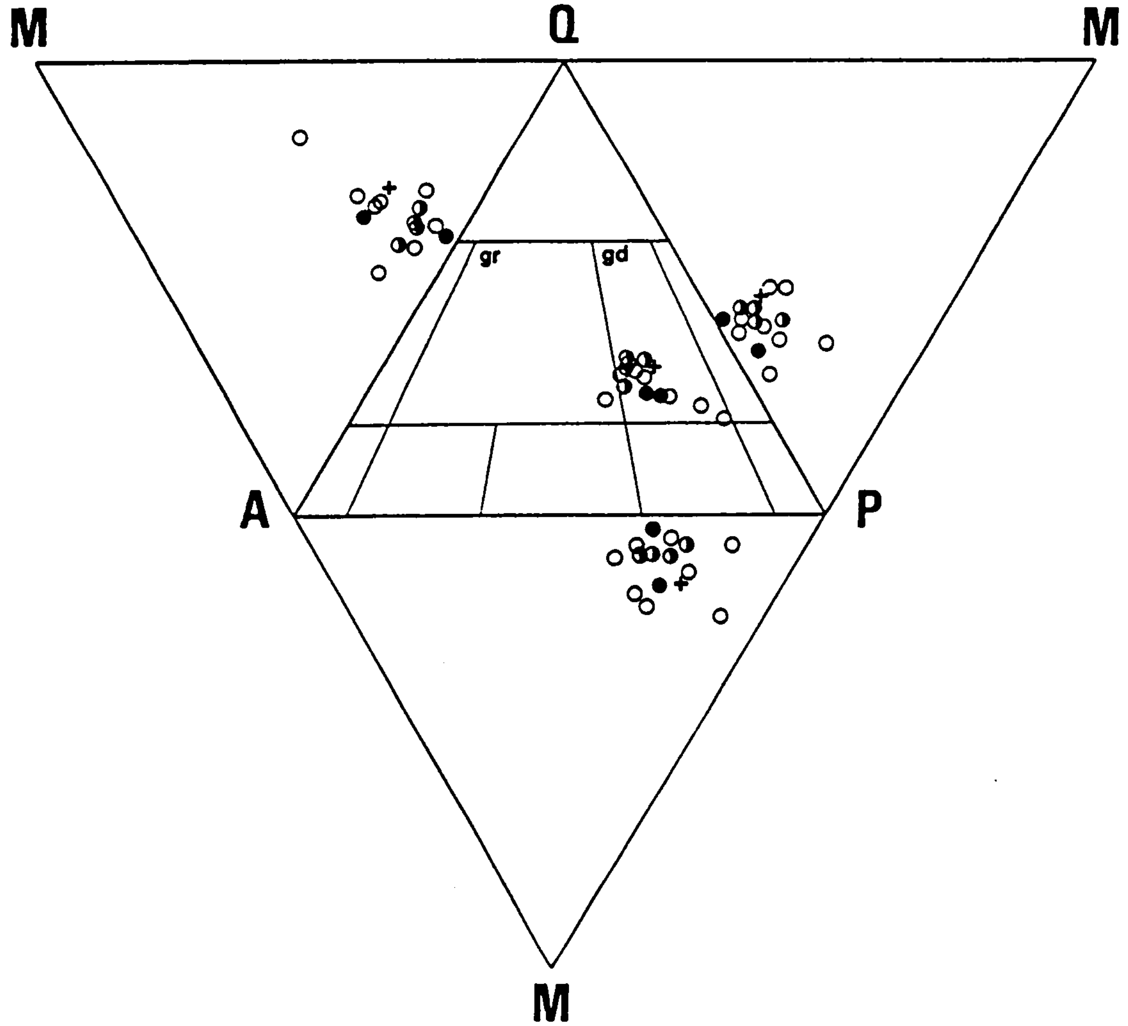

Figure 14. Modal composition of the Rim Sequence and Four Deuce Hills: The four modal components illustrated are potassium feldspar (A), plagioclase (P), quartz (Q), and the sum of all mafic minerals (M). Rock type varies from granite to granodiorite. Rim Sequence traverse (A-A') = circles, other Rim Sequence samples = dots, Four Deuce Hills = half filled circles. Composition of a sample from the Castle Rock pluton (cross) is given for comparison. Rock classification scheme after Streckeisen (1973).

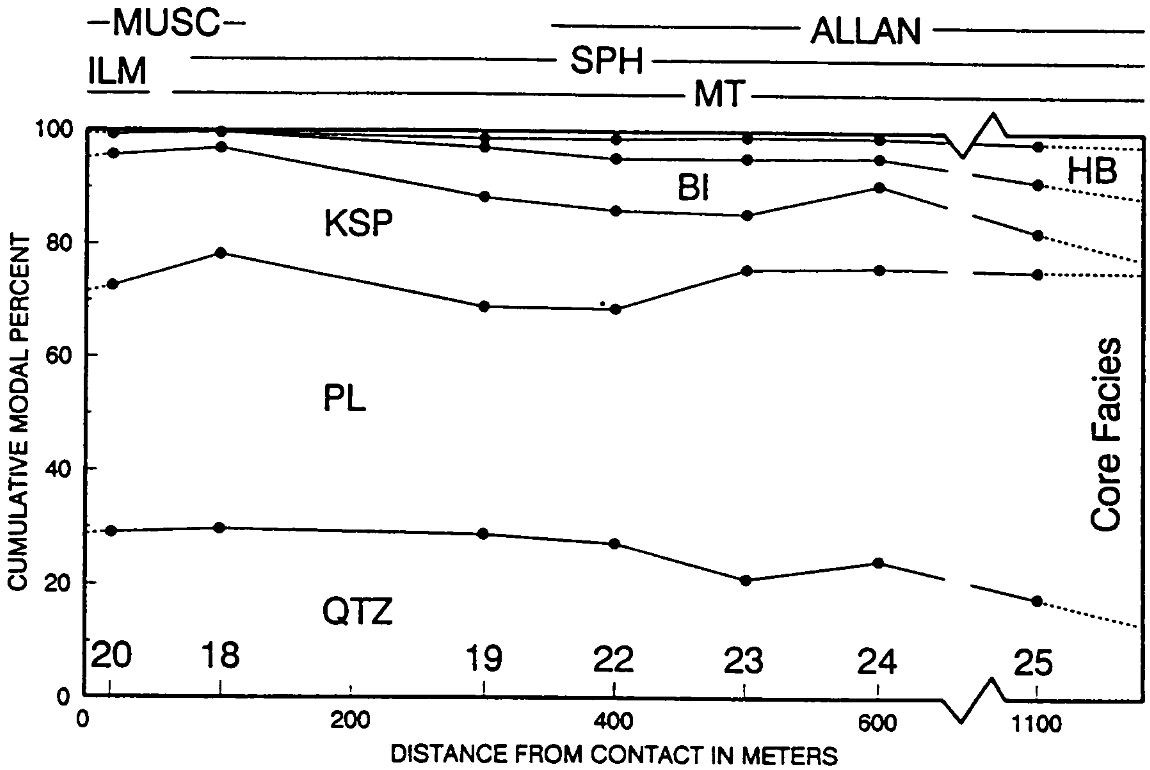

Figure 15. **Modal variations across the Rim Sequence:** Modal variations along traverse A-A' are described by seven samples (BW84-18 through 25, locations given along the horizontal axis) collected at various distances from the wall rock contact. Changes of mineralogy include dissappearence of ilmenite and muscovite, and appearence of hornblende, magnetite, sphene, and allanite.

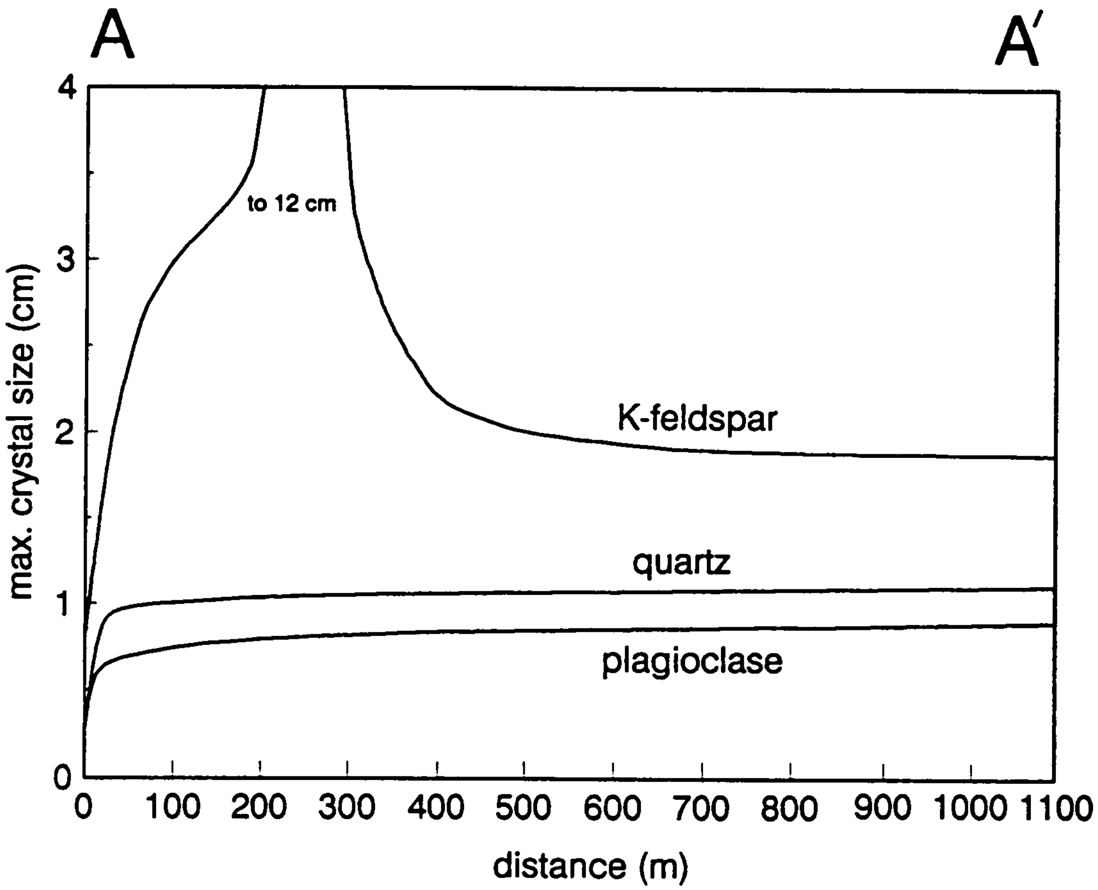

Figure 16. Maximum mineral sizes in rocks of the Rim Sequence: The approximate maximum sizes of felsic minerals in rocks collected along traverse A-A′ from the wall rock contact and into the pluton vary greatly, especially near the wall rock contact. The area within 50 meters of the wall rock could be interpreted as a "chilled margin". Potassium feldspar phenocrysts reach maximum length about 250 meters into the pluton (to 12 cm).

aligned parallel to the steep igneous foliation (N47E 78S, for example) defined by mafic minerals and mafic enclaves, and are also steeply lineated (40SE75, for example). The interstitial component remains about 20% of all potassium feldspar in the rock. Rocks at 400 meters from the contact contain smaller phenocrysts (maximum about 20x20x10 mm) and the proportion of interstitial K-feldspar is about 50%. Six hundred meters along the traverse to A′ (1100 meters), almost all potassium feldspar is interstitial though sparse phenocrysts (to 20x10x10 mm) were observed. The proportion of modal K-feldspar drops from 25 to 5% along the traverse, and the proportion of interstitial feldspar increases monotonically.

Plagioclase

Plagioclase feldspar (oligoclase to andesine), which is light gray in color, is seriate throughout the Rim Sequence, and has a size range of a millimeter to several millimeters. Grains are equidimensional to tabular. The greatest change of average grain size occurs within 20 m of the country rock contact (A on Figure 13; Figure 16). The maximum crystal length of plagioclase increase toward the interior of the pluton, from about 4 mm at 5 meters, 6 mm at 20 meters, and 8 mm at 500 to 1100 meters. Thus its maximum grain size is attained at a position further from the country rock than that for potassium feldspar.

Plagioclase composes about 40% of granite and granodiorite in the first 500 m of the traverse, and about 60% in granodiorite from 500 m to A′.

Quartz

Throughout the Rim Sequence, quartz is medium gray and seriate. The maximum crystal size is about 3 mm at a distance of 5 meters from the country rock contact, about 10 mm at 20 meters and beyond.

Quartz content decreases monotonically from about 30 to 20 % inward from the country rock contact (Figure 15).

Biotite

Biotite occurs as subhedral to euhedral flakes that define a steep, south dipping foliation in most rocks of the traverse. Grain size varies from about 1 to 3 mm in granite and 1 to 5 mm in granodiorite. Biotite composes about 5 modal% of all granitoids.

Hornblende

Hornblende occurs only beyond 100 meters from the contact in all granodioritic rocks except for magnetite biotite granodiorite (BW84-18, 100 m south of A). A sample (BW84-19) collected 300 meters from the contact contains two modal percent tabular hornblende which is less than 1 mm in length. At about 400 meters into the sequence, hornblende composes 4% of the rock and has a maximum length of 3 mm, and at 500 m, hornblende laths are conspicuous in hand sample, attain a maximum length of about 8 mm, and composes about 6 modal % of the rock.

Fe-Ti Oxides

Opaque phases compose less than 1 percent of all rocks and are less than 0.5 mm in length. Microprobe and EDAX analyses indicate that granite samples within 20 meters of the country rock contain Mn-rich ilmenite with lesser magnetite, here called the ilmenite assemblage. All other rocks of the traverse (granodiorite and a magnetite-biotite granite, BW84-18) contain only magnetite and are here called the magnetite assemblage.

Muscovite

Less than 1 modal % of the granite is muscovite which may be primary in some instances (see Petrography; CA85-5 and BW84-20).

Accessory Minerals

Observed trace phases are apatite, zircon, sphene and allanite and their distribution is shown in Figure 15. Apatite and zircon are ubiquitious. Apple green sphene and dark brown allanite occur in all hornblende-bearing rocks and in BW84-18, a magnetite biotite granodiorite.

Fabric and Enclaves

The Rim Sequence along traverse A-A′ displays a range of foliation styles, from absent to well-developed (Figure 12). Fabric is absent in granite near the country rock contact. Where present in granodiorite, this fabric is defined by aligned biotite, hornblende (where present), plagioclase, potassium feldspar phenocrysts elongate, partially recrystallized recrystallized quartz aggregates, and mafic enclaves. The foliation is generally concordant with contacts, either with the foliated country rock or with the Schlieren Zone (see Plate A) and is vertical or dips southward to southeastward. Locally, K-feldspar phenocrysts and enclaves define a lineation which is subvertical to south plunging (Figure 8).

Microgranitoid enclaves which occur throughout the unit are discoid to ellipsoid in shape and parallel the foliation and lineation of the granitoids. Foliation and degree of flattening of enclaves are most pronounced near the Schlieren Zone (see Chapter 2).

The fabrics in the pluton are considered to be the result of igneous flow phenomena based on their concordant and arcuate pattern, and on the steep lineations of potassium feldspar phenocrysts which display mineral decorations on igneous growth zones within the crystals. There is no mineralogic, mineral chemical, textural or chemical evidence of wholesale metamorphism of the pluton, or of growth of potassium feldspar phenocrysts in the solid state.

Four rock types are found in the Rim Sequence granitoids: microgranitoid enclaves, coarse-grained dioritic enclaves, and mafic dikes (all discussed at length in Chapter 2), and sparse xenoliths of quartzofeldspathic gneiss. Gneiss screens were observed within a few tens of meters of the country rock contact at A, and in the Schlieren zone at A′. No country rock xenoliths were observed in the Rim Sequence except at these contacts.

Other Traverses

Field observations where the Rim Sequence is fully exposed along the northwestern and western portions of the pluton suggest a similar sequence to that described for A-A′. The rocks along a west to east traverse (B-B′, Figure 13) are similar to those along traverse A-A′ but the entire section is not exposed. A fully exposed sequence along C-C′, however, displays some difference. At C, along the contact of the Rim Sequence with Virginia May gneiss, the rocks are equigranular, ilmenite biotite granite like rocks observed at A. The progression of rock types to the Schlieren Zone (at C) culminates in a potassium feldspar porphyritic hornblende biotite granodiorite similar to a rock from the intermediate portion of traverse A-A′. In other words, the section described for the interior half of traverse A-A′ (nonporphyrytic biotite hornblende granodiorite) was not observed along C-C′.

Schlieren Zone

An arcuate zone of high strain with abundant mafic rocks, schlieren and screens of quartzofeldspathic gneiss is present along the 3.5 km of exposed contact of the Rim Sequence and Core Facies (Figure 4; Plate A). This Schlieren Zone is generally tens of meters wide, and except for the southern portion of the boundary (C′ of traverse C-C′), does not occur at a modal or chemical discontinuity within the pluton (see Chemistry, Chapter 4). This zone of high strain has a steeply dipping igneous foliation defined by aligned mafic silicates in granodiorite, by ellipsoidal microgranitoid and dioritic enclaves, and by screens of gneiss. The foliation is concentric with the pluton-country rock contact. Dips are vertical to 65° toward the Core Facies. Concordant gneiss screens of mappable dimensions (2 to 10 m wide and tens of meters long) strike northeasterly along the northern exposures of the Schlieren Zone, and east-west along southern ones (Plate A). The pronounced steep foliation of the Schlieren Zone is shown in Figure 12 on page 30 no page.d. A steeply dipping screen of quartzofeldspathic gneiss like wall rocks of the Turtle pluton (background) parallels elongate, mafic enclaves and mafic silicates in the granodiorite (foreground). This internal contact is generally concentric with the pluton-country rock contact and both suggest a cylindrical geometry.

Lineations in the Schlieren Zone, as defined by elongate mafic enclaves and aligned hornblende crystals, are steep and plunge toward the Core Facies. Lineations in gneiss screens are also steep and this is the most common orientation observed in the Virginia May gneiss surrounding the Turtle pluton.

Core Facies

The core of the Turtle pluton comprises medium-grained, equigranular granodiorite and quartz monzodiorite that underlies 10.5 km^2 in the central part of the Turtle pluton (Figure 7 on page 15, Figure 17, Figure 18). The Core Facies is in contact with the Rim Sequence at the Schlieren Zone along most of its margin. The Core Facies has been observed to intrude the Rim Sequence at one location (Figure 13). Here a meter-wide dike of granodiorite with numerous mafic enclaves cross cuts a K-feldspar porphyritic granodiorite with fewer enclaves (-- Figure id 'figplt2' unknown -- no page.c). In the southeastern part of the map area, the Core Facies concordantly intrudes banded amphibolite and its central part Core Facies is stoped by the Target Granite (Figure 7).

The Core Facies is relatively homogenous unit (as compared to the Rim Sequence) in which no systematic, geographic variation of rock type was noted, however whole rock chemical data presented in Chapter 5 suggests that rocks proximal to the Target Granite are distinct from those distant from the younger intrusion (Figure 17).

Rocks of the Core Facies resemble the most mafic rocks of the Rim Sequence (Figure 14 and Chapter 5) and the granodiorite and quartz monzodiorite of the West Riverside Mountains 25 km southeast of the Turtle pluton (Figure 3 on page 6). Modal analyses are given in APPENDIX 1 and Figure 18. The range of rock type is granodiorite to quartz monzodiorite with color indices of 13 to 26.

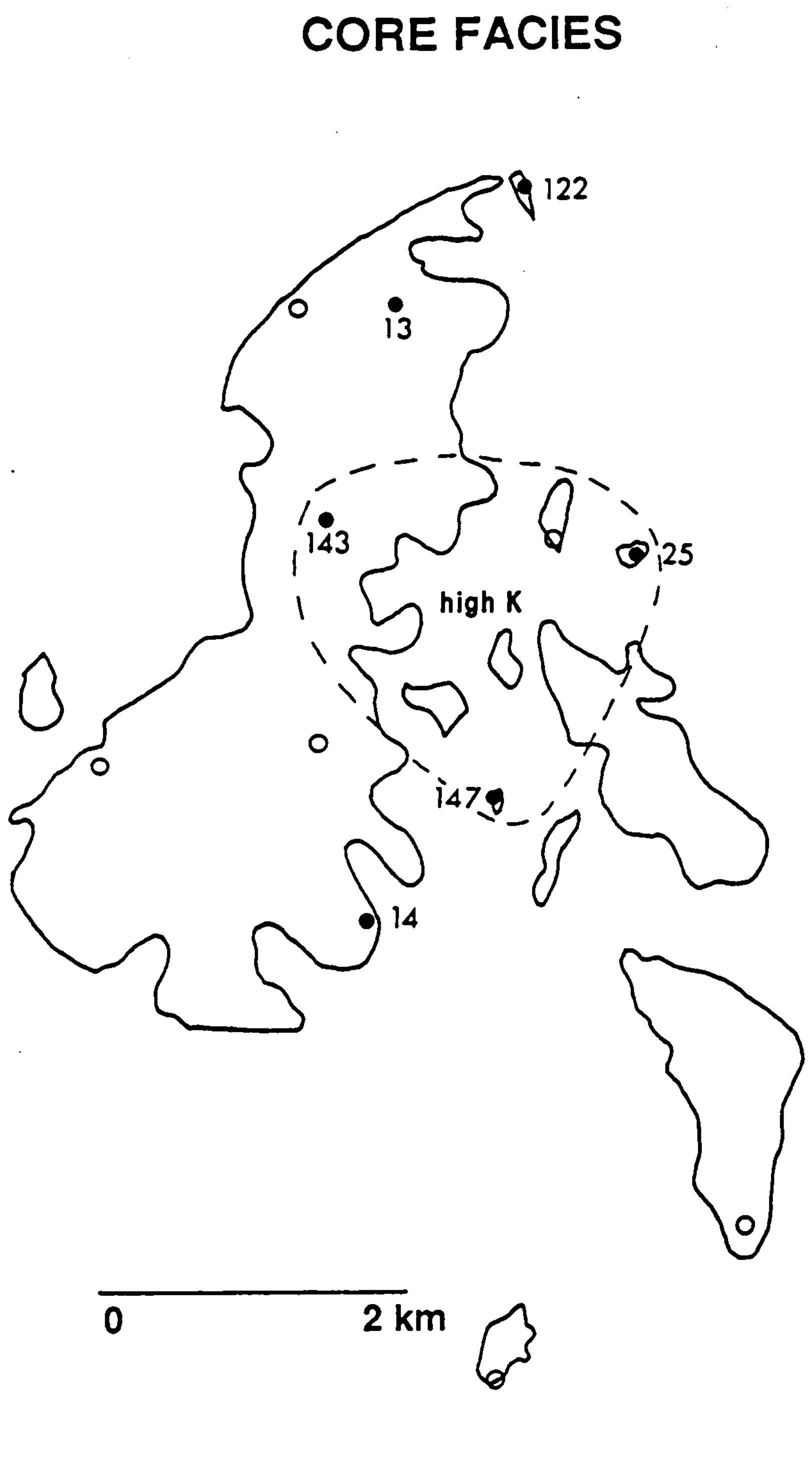

Figure 17. Outline map of the Core Facies: On this map of the Core Facies are given sample locations for modal (circles) and chemical (dots) analyses and the approximate limit of the high K facies found in the center of the unit near the Target Granite.

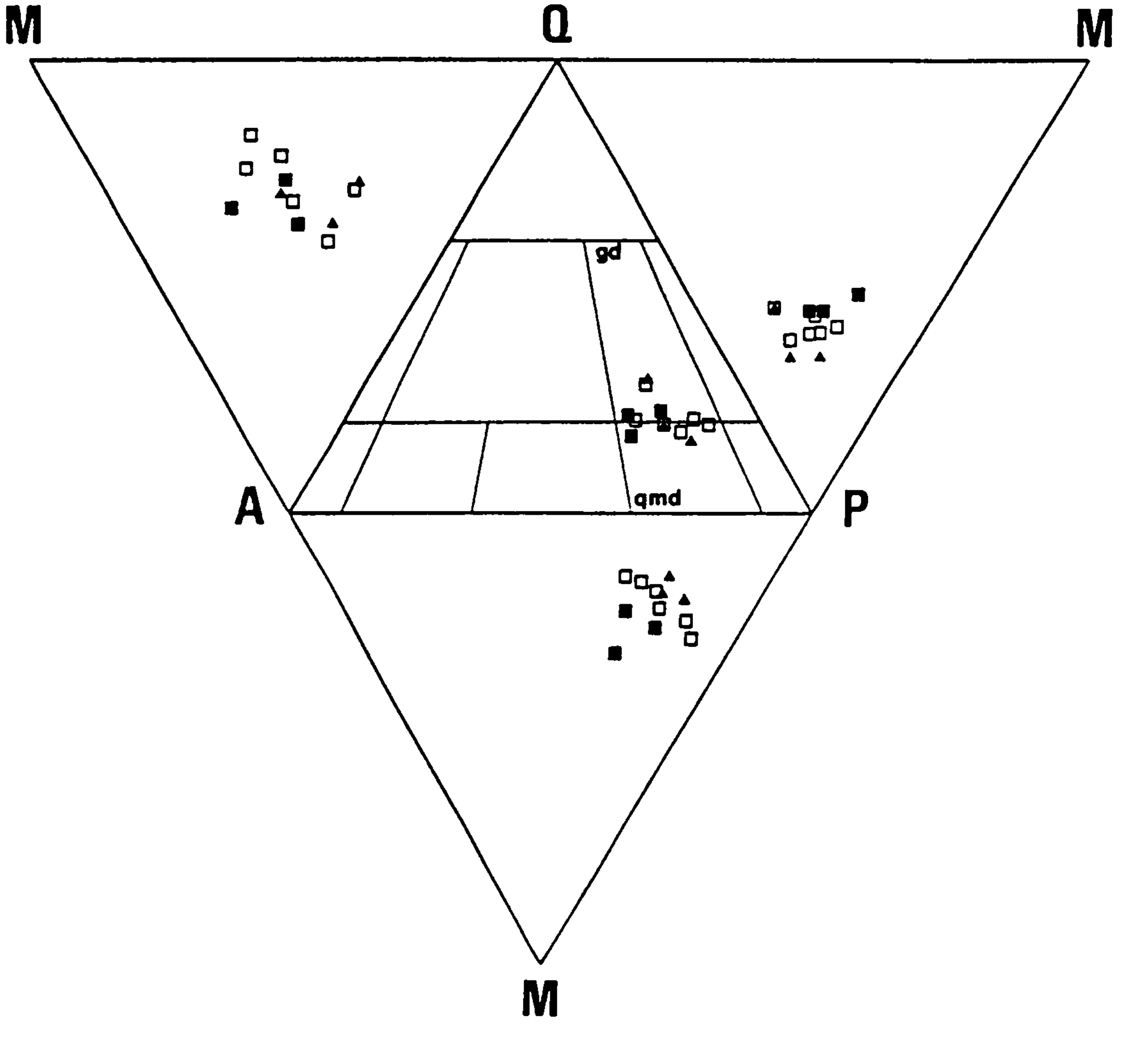

Figure 18. Modal composition of the Core Facies: The four modal components illustrated are potassium feldspar (A), plagioclase (P), quartz (Q), and the sum of all mafic minerals (M). Rock type varies from granodiorite to quartz monzodiorite. The high K rocks (filled square) contain more mafic minerals and alkali feldspar than other samples of the Core Facies (square). The composition of samples from the West Riverside Range (filled triangles) are comparable to the Core Facies. Rock classification after Streckeisen (1973).

Mineralogy

In hand specimen, both feldspars are generally white and indistinguishable, but in some samples taken from near the Target Granite, potassium feldspar is pink (CA84-143, CA84-147). In stained slabs, potassium feldspar is an interstitial, subhedral to anhedral mineral that is 1 to 3 mm in greatest dimension. Plagioclase is seriate and subhedral to euhedral in form. Most grains are 1 to 3 mm in length though in coarser grained samples (CA85-13, CA85-28, CA85-100) they reach 6 mm in length. Quartz grains are anhedral, gray and less than 3 mm in diameter. Biotite occurs mostly as subhedral and dispersed grains throughout a given specimen, but a small portion of the biotite occurs as hexagonal books to 2 mm in most samples. Hornblende grains are euhedral, black laths that range in size from 1 to 5 mm in most rocks but some contain sparse, larger crystals (to 10 mm). Cinnamon brown sphene to 2 mm in length is identifiable in hand specimen and other trace phases identified in thin section are apatite, zircon, and allanite.

Fabric and Enclaves of the Core Facies

Generally, the Core Facies lacks fabric except near the Schlieren Zone where a foliation defined by aligned minerals and mafic enclaves was observed. This lack of fabric is reflected in the equidimensional and/or randomly oriented microgranitoid enclaves that are common throughout the unit. Whereas microgranitoid enclaves occur in most outcrops, coarse-grained enclaves are much less common and are concentrated in the central portion of the facies. No mafic dikes or gneiss xenoliths were observed in this unit.

Four Deuce Hills

The eastern exposures of the Turtle pluton, called the Four Deuce Hills, comprise a significant area of the exposed pluton (5.3 km^2; Figure 19). The granite and granodiorite that underlie these hills have some textural, chemical, and isotopic similarities to the Rim Sequence and Core

Facies of the Turtle pluton, but the intrusive relationship of this unit to the other facies is unknown. The Four Deuce Hills are bounded on its western side by a low angle normal fault that has displaced this unit an unknown distance to the northeast relative to the Turtle pluton (Figure 4). The igneous rocks of the Four Deuce Hills were studied along a north to south traverse (D-D′). This facies is texturally similar to the Rim Sequence in the north but displays a distinct oikocrystic texture in the south. At the northern end of the traverse at the contact with Virginia May Gneiss (D), equigranular granite concordantly intrudes the gneiss like at the northern end of Traverse A-A′ in the Rim Sequence, and the progression of mineralogic and textural changes along traverse D-D′ is similar to those observed along A-A′ for about 2200 meters to sample location CA85-4. Equigranular granite becomes more coarse grained, and potassium feldspar becomes porphyritic. Further south along traverse D-D′, the rocks are texturally and chemically distinct from traverse A-A′ particularly with regard to biotite and potassium feldspar textures as described below and in ChapterS 4 and 5.

Traverse D-D′

This traverse follows the western edge of the Four Deuce Hills, along a well-exposed wash.

Potassium Feldspar

K-feldspars in granite at the northern end of the traverse are light pink, tabular (2/1) and have a maximum length of about 10 mm. In granodiorite about 50 to 2200 meters from the country rock contact (D), the potassium feldspar is distinctly porphyritic and is 10 to 40 mm in length (CA84-58). Approximately 2200 meters south of the contact and further south to D′ (Figure 19), this mineral is white to pale pink, oikocrystic, equidimensional, and less than 20 mm across (CA84-50). The distribution of rocks with oikocrystic texture are shown in Figure 19. The contact with porphyritic granodiorite is gradational over tens of meters.

FOUR DEUCE HILLS

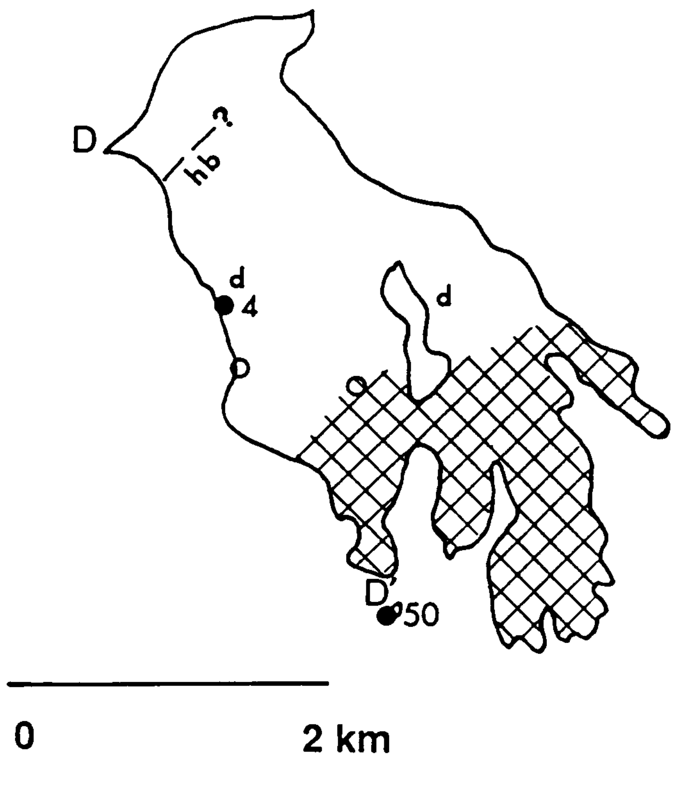

Figure 19. **Outline map of the Four Deuce Hills:** On this map of the Four Deuce Hills are given sample locations for modal and chemical analyses, the approximate area underlain by rocks containing oikocrystic, pale pink to white potassium feldspar phenocrysts (pattern), and the location of a detailed traverse (D-D'). Rocks containing hornblende occur south of a dashed line marked "hb". An area of dioritic enclaves (including hornblendites) is shown in the center of the rock unit. Mafic dikes with textures like microgranitoid enclaves occur at locations marked "d".

Plagioclase

At the northern end of the traverse, plagioclase crystals are white laths (2/1) that range in size from about 1 to 5 mm. Fifty meters from the contact (D), crystals reach a maximum length of 8 mm and is seriate with a size range of 1 to 8 mm which is maintained to the southern end of the traverse (D′;CA85-50).

Quartz

Quartz is a gray, equidimensional mineral that ranges in size from 1 to 6 mm throughout the traverse.

Biotite

The habit of biotite is distinctive in the rocks of the Four Deuce Hills as compared to the Rim Sequence. In hornblende-free granite at the northern 300 m of the traverse, biotite grains are subhedral, less than 3 mm across, and are dispersed throughout the rock. In granodiorite (hornblende bearing, see Figure 19), biotite occurs as conspicuous, euhedral, books 1 to 5 mm in diameter.

Hornblende

Hornblende-bearing rocks of the Four Deuce Hills are shown in Figure 19. Hornblende occurs as obvious, black laths that generally have a greater aspect ratio than rocks of the Rim Sequence (about 6 to 1 as compared to 2 or 3 to 1) and have maximum lengths of about 4 mm. Some hand samples contain rare hornblende phenocrysts to 8 mm (2/1 to 3/1).

Fe-Ti Oxides

Opaque oxides in the Four Deuce Hills have blocky morphologies that suggest they are magnetite. Maximum crystal size is about 0.2 mm.

Accessory Phases

All hornblende-bearing rocks contain green sphene (1 mm) that is euhedral to anhedral, and most of these rocks also contain euhedral orange-brown allanite. Apatite and zircon occur in all thin sections.

Fabrics and Enclaves

The rocks of the Four Deuce Hills are weakly foliated to nonfoliated as defined by alignment of minerals and enclaves. This is in contrast to the Rim Sequence which in some places has a well-defined fabric.

The granite and granodiorite of the Four Deuce Hills contain mafic enclaves and dikes with a range of mineralogies and textures. These rocks are described in detail in Chapter 2 and a brief overview is presented here.

Microgranitoid enclaves with textures and mineralogies like those observed in other facies of the Turtle pluton are common and comprise less than 1 % by volume of the Four Deuce Hills (visual estimate). Dikes with textures indistinguishable from these enclaves were observed cross-cutting granodiorite (Figure 10 and Figure 19). These dikes are 0.5 to 3 m thick and all have northeasterly strikes and moderate, southerly dips. Some dikes are offset on low angle normal faults along the west side of the Four Deuce Hills (Figure 10c\. Other dikes have convolute margins and are cut by granodiorite and aplitic dikes. A concentration of coarse-grained enclaves with dimensions of tens of meters occurs in the central part of these hills (Figure 4; Plate A). They consist of coarse- and very coarse-grained diorites and hornblendites and are intruded by more felsic dikes. The igneous relationships of these enclaves to the Turtle pluton are discussed in Chapter 2.

Aplite and Pegmatite Dikes

Pegmatitic and aplitic dikes are common in all facies of the Turtle pluton. Pegmatites are very coarse-grained and contain pink potassium feldspar, white plagioclase and gray quartz with muscovite, biotite and chlorite after biotite. Pegmatitic dikes range in thickness from 0.3 to 3 meters and occur in a variety of orientations. Aplitic dikes are medium- to fine-grained rocks, generally less than 1 meter-wide, and contain an assemblage like that of pegmatites, with or without garnet. Because garnet-bearing aplites are a readily identifiable subset of all aplites and pegmatites, and because they have potential use in geobarometry (see Chapter 3), garnet-bearing aplites were selected for detailed field and chemical investigation.

Garnet-bearing Aplites

Garnet-bearing aplitic dikes that are 10 to 65 cm thick were observed to intrude all facies of the Turtle pluton, Patton Granite, and Fortification Granodiorite, but no garnet-bearing aplites were observed in the Target Granite (Figure 20). Given these aplites were observed in the Core Facies adjacent to the Target Granite, some with strikes toward the younger granite, garnet aplites are assumed to pre-date the Target Granite and to post-date all facies of the Turtle pluton. Garnet-bearing aplites occur in a variety of orientations but a local preferred orientation is suggested by the field sampling given in Figure 20. Locations of aplites selected for chemical and isotopic study also appear in that figure.

Mineralogy

Garnet-bearing aplites are granitic in composition, and are composed of white plagioclase and potassium feldspar phenocrysts to 0.5 cm in length, clear to gray quartz phenocrysts to 0.3 cm across, groundmass feldspars and quartz about 1 mm in average grain size, biotite ($<$ 1 mm), phenocrysts of red garnet from 2 to 8 mm in diameter, and minor muscovite, magnetite, and ilmenite. Commonly, garnets are oikocrystic with quartz inclusions and well-developed crystal faces

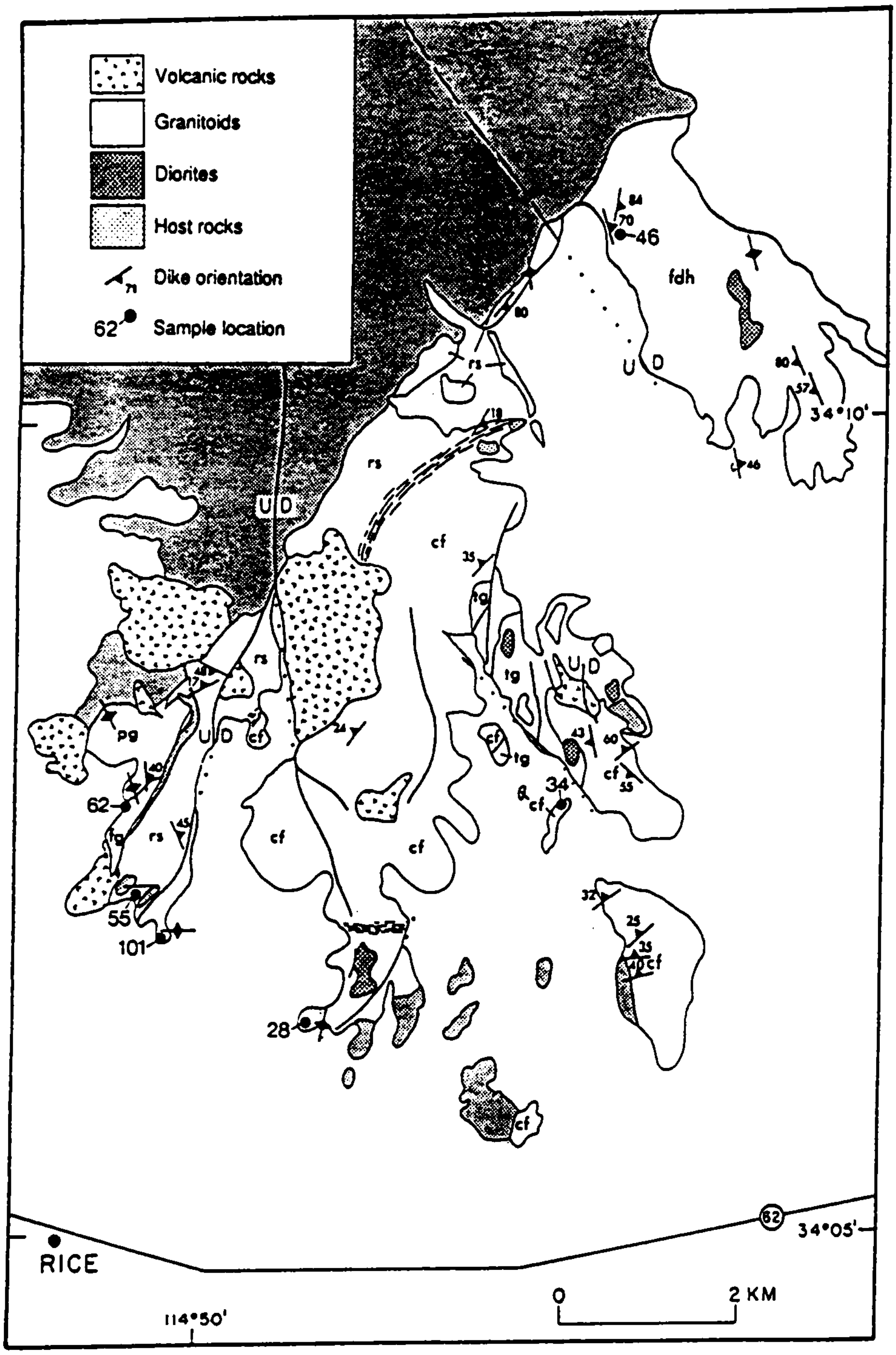

Figure 20. **Orientations of sampled garnet-bearing aplites:** These aplites occur in a variety of orientations with some local preferred orientation, and they occur in all plutonic units except the Target Granite (tg). Locations of rocks sampled for chemical study are given with sample numbers. Other granitoid units are rs = Rim Sequence, cf = Core Facies, fdh = Four Deuce Hills, pg = Patton Granite, and fg = Fortification Granodiorite.

(CA84-46), though some garnets contain only sparse inclusions (CA85-37). Surrounding all garnets are felsic zones 1 to 2 millimeters wide that are devoid of mafic minerals. Subhedral to anhedral muscovite (< 1 mm across) commonly occurs within plagioclase and its primary or secondary origin is ambiguous. Alteration is minor; plagioclase is sericitized and biotite is partially replaced by chlorite. Some aplites have a foliation subparallel to their walls that is defined by ribbon quartz, and brittlely deformed feldspars. This fabric was observed in aplite dikes of varying orientation within a single outcrop (CA84-12; N5S90E and N58E90E). A possible interpretation of such structures is that the much finer-grained, quartz-rich aplites that crisscross coarser-grained plutons take up post-crystallization strain (Brewer, 1987).

Other Intrusions in the Turtle Mountains and Environs

Early Cretaceous plutons occur in the Turtle Mountains and in adjacent ranges (Figure 3 on page 6 and Figure 5 on page 10). Ages of these intrusions are based on mineral K-Ar, whole rock Rb-Sr, and mineral U-Pb geochronology presented in Chapter 5. Intrusions known to be younger than the Turtle pluton, based on crosscutting relationships, are the Fortification Granodiorite and the Target Granite (Figure 7 on page 15). Intrusions modally similar to facies of the Turtle pluton that have similar K-Ar ages (Howard et al., 1982) include the Castle Rock pluton 10 km northeast of the Turtle pluton, porphyritic granodioritic bodies satellite to the Turtle pluton (3.5 km to the north), and the West Riverside Mountains, 25 km to the southeast (Figure 3). The field characteristics of these intrusions and relationship to the Turtle pluton are discussed below.

Fortification Granodiorite

At the western edge of the map area (Figure 7) the Rim Sequence is intruded by a fine- to medium-grained, biotite granodiorite that is light gray in outcrop (CA85-58, APPENDIX 1). This unit is refered to here as the Fortification Granodiorite. This intrusion contains no mafic enclaves but does contain xenolithic blocks of the Rim Sequence and of the Patton Granite. This unfoliated granodiorite is cut by garnet-bearing and garnet-free two mica aplite dikes and by few pegmatite dikes.

In hand specimen, the two feldspars and quartz share a similar size range from < 1 to 4 mm, and most grains are 1 to 2 mm in length. Potassium feldspar is white and interstitial or tabular. Plagioclase is white and tabular, whereas quartz is gray and equidimensional. Biotite occurs as euhedral to subhedral books less than 2 mm across. As determined from petrographic examination, trace phases include euhedral to subhedral zoned allanite with epidote rims, blocky opaque phases, and euhedral apatite and zircon.

Target Granite

A leucogranite, 0.6 km^2 in areal extent, stopes and dikes the Core Facies in the center of the field area (Figure 4, Figure 7, and Figure 21). This leucogranite is refered to here as the Target Granite. It contains many xenoliths of the Core Facies, Proterozoic rock types, and diorite, but few microgranitoid enclaves. Besides for being 30 Ma younger than the Turtle pluton, the Target Granite is isotopically distinct from the Turtle pluton. This unit is crosscut by pegmatite dikes, and less commonly by aplite dikes, and no garnet-bearing aplites were observed in this intrusion.

Mineralogy

The Target Granite is a fairly homogenous, medium- to fine-grained leucogranite with a color

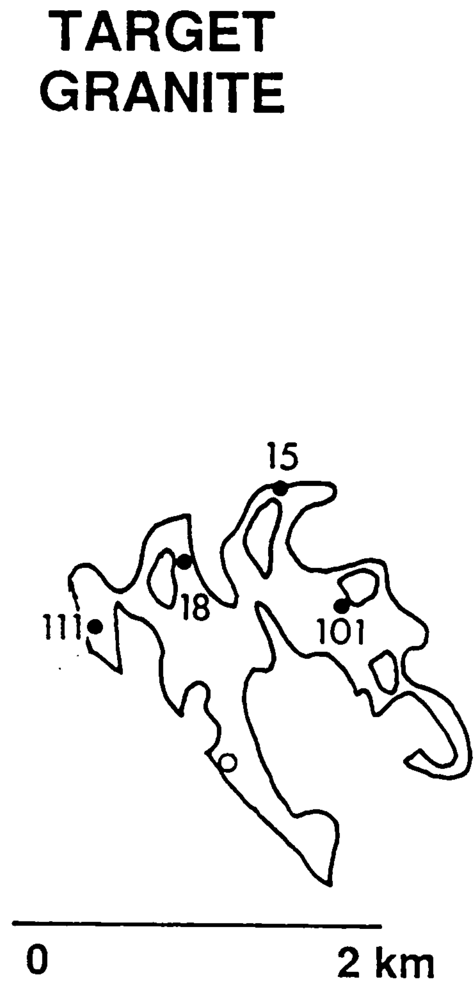

Figure 21. Outline map of the Target Granite: On this map of the Target Granite are given sample locations for modal and chemical analyses. This unit stopes the Core Facies.

index less than 5 (Figure 22). Potassium feldspar is pink, seriate, tabular and less than 1.5 cm in length. Plagioclase also is seriate but is white in color and has an average size smaller than K-feldspar (maximum length of about 0.4 cm). Quartz is clear to light gray and occurs in equidimensional or elongate aggregates (2/1) to about 1 cm in length. The mafic minerals are subhedral, dispersed biotite, and sparse hornblende. Accessory minerals are sphene, zircon and apatite.

Fabric and Enclaves

This unit has a weak or absent igneous foliation except in dikes where tabular feldspar and quartz define a foliation subparallel to dike walls. Mylonite zones less that 30 cm wide were observed to have north-south trends and moderate easterly dips. Brittle faults in the same area also have north-south trends but variable dips, and near these brittle faults, K-feldspar is darker pink in color, and biotite is chloritized.

The Target Granite contains xenoliths of quartz monzodiorite of the Core Facies, and of quartzofeldspathic gneiss and amphibolite similar to Proterozoic wall rock lithologies. Xenoliths vary in shape from blocks of quartz monzodiorite from 1 to tens of meters in greatest dimension, to sheets of Precambrian rocks that underlie dip slopes hundreds of meters across in the south-eastern portion of the exposed Target Granite (see Plate A). Several exposures of diorite occur in lowlands and crosscutting relationships with the leucogranite are unknown. Only a few microgranitoid enclaves were observed in the Target Granite and they are fine-grained discoids that are less than 30 centimeters long.

Satellite Stock North of the Turtle Pluton

About 3.5 kilometers north of the Turtle pluton occurs a granodiorite stock about 1 km^2 in area. This intrusion is closely associated with Jurassic or older diorites described by Howard et al.

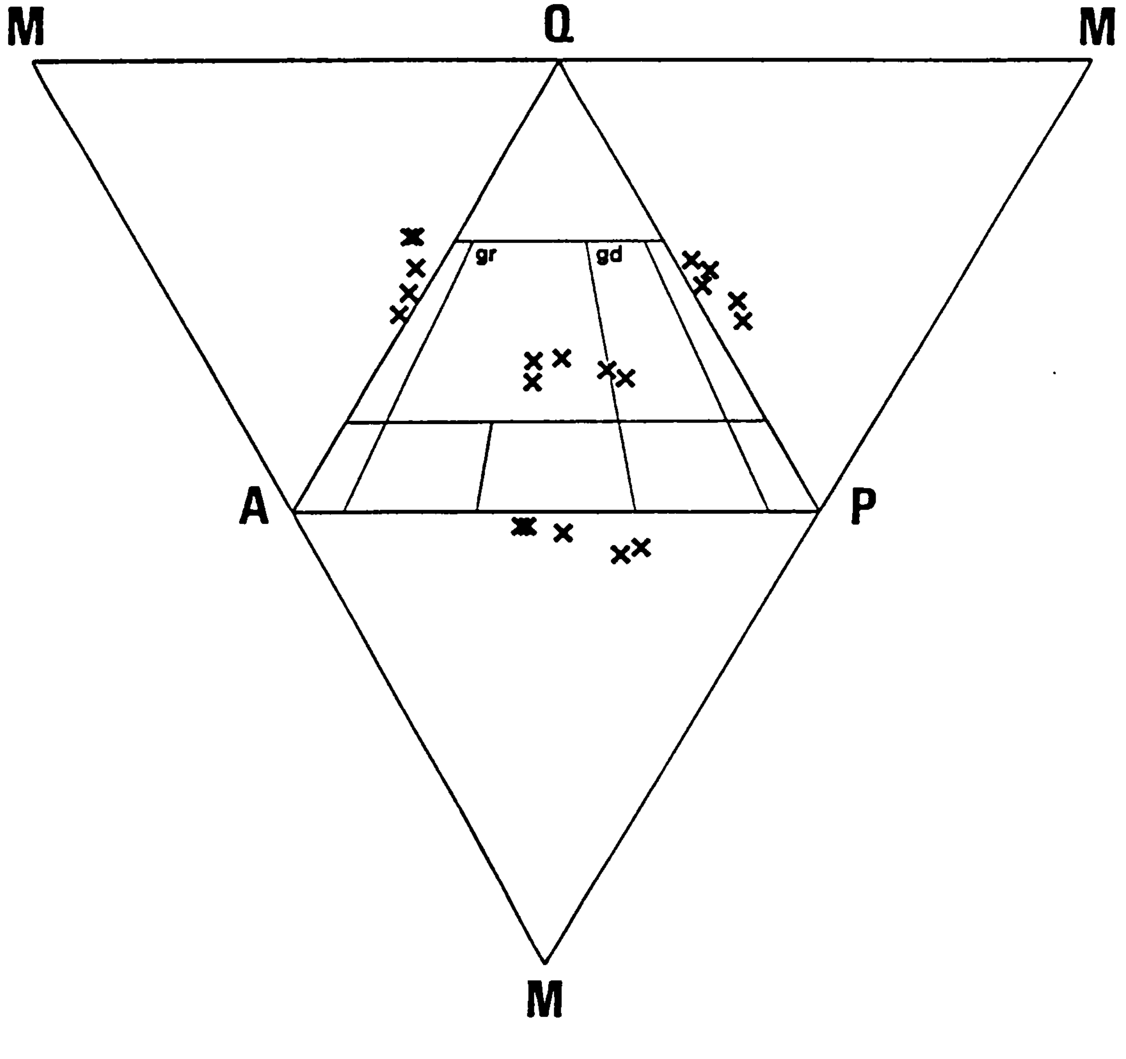

Figure 22. Modal composition of the Target Granite: The four modal components illustrated are potassium feldspar (A), plagioclase (P), quartz (Q), and the sum of all mafic minerals (M). This unit is composed of leucogranite and minor granodiorite. Rock classification after Streckeisen (1973).

(1982). The granodiorite contains potassium feldspar phenocrysts to several centimeters in length, gray quartz and white plagioclase 6 mm in greatest dimension, sparse euhedral hornblende and biotite books to 4 mm. The rock type resembles the coarsely porphyritic portion of the Rim Sequence of the Turtle pluton, however its isotopic character is distinct.

Castle Rock pluton

The Castle Rock pluton is located 10 km NNE of the Turtle pluton (Figure 3). It is composed of medium-grained hornblende-biotite granodiorite with rare, white potassium feldspar phenocrysts to 20 by 20 mm. K-feldspar is primarily interstitial (< 2 mm across) and is white in color. Plagioclase occurs as white euhedral laths, 1 to 4 mm in length, and quartz is gray, equidimensional, and 1 to 3 mm in diameter. Mafic minerals are euhedral and easily discernible in hand specimen. Biotite occurs as black, hexagonal books (1 to 2 mm across), and hornblende as black, tabular crystals (1/2 to 1/3) up to 3 mm in length. Accessory phases (determined petrographically) include cubic opaque minerals (to 0.2 mm), euhedral apatite and zircon, euhedral to subhedral, green sphene (to 1 mm in length), and euhedral to subhedral, zoned allanite (to 0.3 mm) enclosed in epidote.

The granodiorite of the Castle Rock pluton is generally unfoliated, and contains very sparse, mafic enclaves except along its borders. There, the granitoid is more strongly foliated and enclaves are more numerous. Throughout the body, aplites and pegmatites are rare.

The Castle Rock pluton resembles the rocks of the Four Deuce Hills. Similarities include granodioritic composition, euhedral biotite and hornblende, and white phenocrysts of potassium feldspar that are oikocrystic in some samples. There are chemical and isotopic similarities as well (ChapterS 4 and 5).

West Riverside Mountains

The West Riverside Mountains (Figure 5) are a homogenous block of foliated and unfoliated hornblende biotite quartz monzodiorite to granodiorite with sparse microgranitoid enclaves, and very rare coarse-grained ones. The granitoids are intruded by aplites, pegmatites, and basaltic to andesitic Tertiary (?) dikes commonly with NW strikes and moderate to steep dips. The entire range is cut by a series of northwest-trending subvertical faults.

The granitoids of the West Riverside Mountains have color indices of 10 to 20, comprised of subhedral, dispersed biotite as large as 2 mm, black hornblende laths (1/5) to 5 mm, and green, euhedral sphene up to 1.5 mm in length. Plagioclase occurs as seriate chalky white laths 1 to 5 mm long. Potassium feldspar is seriate and interstitial to tabular in form, and up to 5 mm in length. Rare, equant K-feldspar phenocrysts (to 20 mm across) with plagioclase rims were observed. Quartz is a gray, interstitial mineral. Trace phases are euhedral to subhedral sphene, euhedral zoned allanite with common epidote rims, opaque minerals, apatite and zircon.

Samples from the West Riverside Mountains are similar to the Core Facies of the Turtle pluton both modally and texturally except, in general, the rocks of the West Riverside Mountains are more altered and contain visible epidote and chlorite, particularly in rocks from the northwest part of the range. K-Ar geochronology on the West Riverside Mountains suggests an age very similar to K-Ar geochronology on the Turtle pluton (Howard et al., 1982), though the more intense post-emplacement alteration and faulting of the West Riverside Mountains suggest distinct post-emplacement histories.

Petrography of the Turtle Pluton and Target Granite

Introduction

Detailed petrographic study of the Turtle pluton and Target Granite was undertaken in order to determine the igneous mineral assemblage, secondary alteration effects, and orders of crystallization. A description of each mineral from the facies of the Turtle pluton and Target Granite is given below followed by a summary of orders of crystallization, by limits on crystallization conditions as determined from comparison to experimental systems, and by discussion of subsolidus reactions.

Rim Sequence of the Turtle pluton

Rock type, and mafic and trace mineralogy change systematically across the Rim Sequence from an ilmenite biotite granite with magnetite (ilmenite assemblage) to a biotite granodiorite with magnetite, to a biotite hornblende granodiorite with magnetite and sphene (magnetite assemblage) toward the interior (Figure 14 and Figure 15). All rock types from the Rim Sequence are granitoids and therefore contain essential plagioclase, potassium feldspar and quartz whose textural changes are discussed in detail in Field Relations (Figure 16).

Potassium Feldspar

Alkali feldspar changes greatly in abundance and size in this map unit as described in earlier sections. It is a seriate phase with a coarsely porphyritic texture in some granite and granodiorite samples (to 12 cm in length), and an interstitial one in granodiorite (1 to 3 mm) toward the core of the pluton. Modal abundance varies from 20 to 5 modal percent across the sequence (Figure 15). The feldspars are microperthite orthoclases that have Carlsbad and/or grid iron twinning in some grains. Potassium feldspar phenocrysts contain concentric zones of inclusions, particularly quartz, plagioclase, and biotite which divide optically continuous portions of a phenocryst. Alkali feldspar is a late crystallizing phase in all cases and includes all other mineral types (generally euhedral) from a given rock type. Myrmekite is developed in belts and fans at most orthoclase-plagioclase contacts.

Plagioclase

Plagioclase (oligoclase to andesine) is a seriate, tabular, zoned phase less than 0.8 cm in length. Inclusions found in cores are sparse biotite$\pm$opaque minerals while all other phases from a given rock may be found in the rims. Microprobe analyses show overall normal zonation trends (An_{31} to An_{14}) in ilmenite biotite granite. For all other rocks of the Rim Sequence, plagioclase has oscillatory zonation with a reversed chemical trend from albite-rich cores to anorthite-rich rims with a narrow more albitic overgrowth (see microprobe analyses, Chapter 3). The minimum and maximum anorthite contents of plagioclase from a given rock (range is about 20 mol %) both increase from the exterior to the interior of the Rim Sequence. Whereas many grains display Carlsbad, pericline and albite twin laws, some grains have no twins or patchy twins. Alteration is minor in the form of sericite, saussurite and/or calcite in fine cracks within plagioclase.

Quartz

Quartz shows strain and partial recrystallization in all specimens. It occurs as equidimensional to ellipsoidal aggregates to 1 cm in length. Strain and recrystallization are manifested as oscillatory extinction, deformation bands, development of subgrains, serrated quartz-quartz contacts, and as trails of fluid inclusions which probably lie along healed fractures. Sparse inclusions of all other phases if a given rock types are found in quartz.

Biotite

Biotite (1 to 5 mm) occurs in all rocks of the Rim Sequence and is the lone ferromagnesian silicate in granite except for trace muscovite. In hornblende-bearing granodiorite, it occurs adjacent to or separate from hornblende, or is enclosed in hornblende (Figure 23). The reverse relationship was very rarely observed. In all rock types, biotites have tan-brown-red brown pleochroism. Flakes are subhedral to anhedral, and commonly have digitate contacts with K-feldspar. Alteration products are green chlorite with violet to gray to brown anomalous extinction $\pm$ anhedral sphene, and a high relief, clear to golden aggregate of minerals that occur in lenticular patches. Apatite, zircon and opaque oxides were observed in this sheet silicate.

Hornblende

Euhedral to subhedral (1 to 8 mm) hornblende is found in all granodiorite samples except in a magnetite-biotite assemblage (BW84-18) that occurs between biotite granite and hornblende + biotite granodiorite. Hornblende commonly encloses biotite, and more rarely plagioclase, quartz, and iron oxides. The amphibole has light green-green-blue green pleochroism.

Figure 23. Photomicrographs from the Turtle pluton: a. Ragged biotite (bi, outlined by white dashes) in euhedral hornblende (hb) from sample granodiorite (BW84-23). Photo is 2.8 mm across. b. Two crystal shapes of apatite (equant = e and acicular = a) in Rim Sequence granite. Field of view 0.4 mm across. c. Typical hypidiomorphic-granular texture of Rim Sequence granodiorite (BW84-25). q = quartz, p = plagioclase, m = clot of hornblende, biotite, and alteration minerals. Photo is 2.8 mm across. d. Typical high K Core Facies quartz monzodiorite (CA84-147) with altered plagioclase (sericite = se and epidote = e), biotite (b), hornblende (h), euhedral sphene (s) and alteration in biotite (a). Unlabelled felsic phases are quartz, plagioclase and minor potassium feldspar. Sphene from this sample was used for U-Pb isotopic study. Photo is 2.8 mm across.

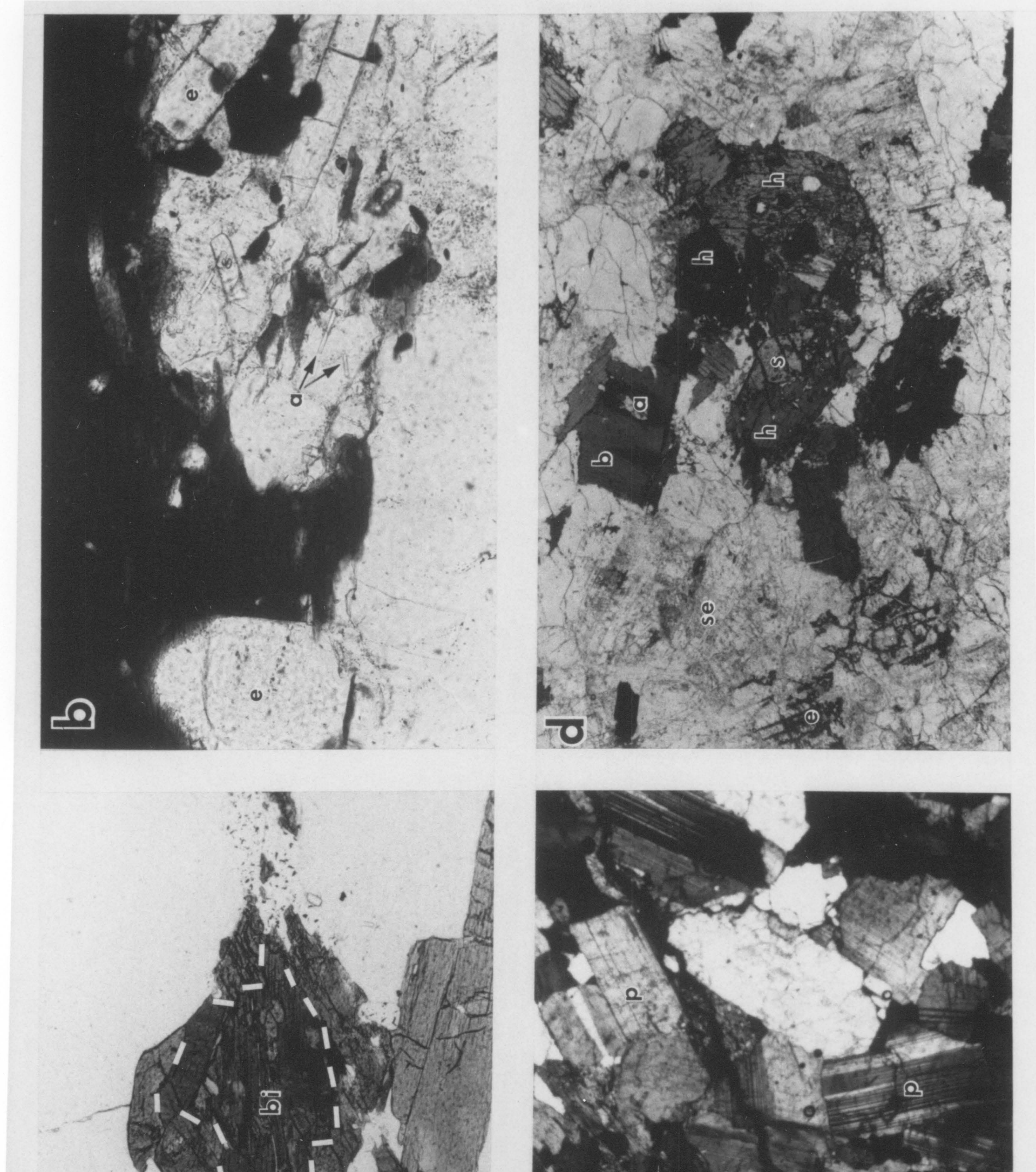
a
hb
bi
b
e
a
e
c
q
m
p
p
d
b
a
h
h
h
s
se
e

Muscovite

Muscovite occurs in biotite granite only (CA85-5, BW84-20) and it composes less than 1.0% of these rocks. It occurs as very fine to fine-grained crystals within plagioclase or along feldspar contacts with biotite. In 2 thin sections, muscovite displayed a primary crystallization habit: rectangular muscovite was included in biotite and in plagioclase.

Fe-Ti Oxides

Opaque minerals compose a small portion of these granitoids ($<$ 1 modal%). They are cubic and less than 0.3 mm across. The only phase observed within iron oxides is apatite. Microprobe analyses indicate that Mn-rich ilmenite with minor magnetite occurs in biotite granite (ilmenite assemblage) and that magnetite is the exclusive opaque phase in all other rocks (hornblende biotite granodiorite, or magnetite assemblage).

Accessory Phases

Accessory phases in the Rim Sequence are apatite, zircon, allanite, and sphene. Apatite is a conspicuous accessory in all thin sections and its morphology ranges from equant (up to 2 mm in diameter) to acicular ($<$ 0.05 mm in width) with extreme length to width ratios ($>$ 20/1). Apatite commonly occurs in mafic phases, particularly with magnetite. Zircons are euhedral, slightly elongate prisms with a length to width ratio of less than 4/1 and have a maximum length of 0.2 mm. Crystals are clear or light brown and some have optically distinct, darkened cores. Allanite is a euhedral, red-orange phase that is zoned and simply twinned. Usually, 1 to 6 grains were seen in thin section of hornblende + sphene + magnetite-bearing granodiorite while only 1 grain was observed in a biotite granite (BW84-18). In most instances, allanite grains are surrounded by pale green to clear epidote except where allanite is included in quartz. Sphene, 0.2 to 0.5 mm across, is a conspicuous green, subhedral to euhedral mineral in all hornblende-bearing hand specimens. In thin section, its morphology ranges from euhedral to subhedral prisms, to anhedral rims on magnetite. Opaque minerals are rarely included in euhedral sphene.

Secondary Phases

In decreasing order of abundance, the secondary phases that compose 1 to 3 modal % of rocks of the Rim Sequence are: chlorite, sericite, epidote and calcite. Green chlorite with violet or brown anomalous extinction commonly replaces biotite, especially biotite enclosed in hornblende. Sericite replaces core regions of some plagioclase grains and epidote and calcite are found in cracks in plagioclase.

Core Facies of the Turtle pluton

The Core Facies is composed of relatively homogenous, biotite hornblende granodiorite to quartz monzodiorites containing magnetite and sphene (Figure 18). These rocks are unfoliated to weakly foliated, medium-grained, hypidiomorphic granular rocks.

Potassium Feldspar

Potassium feldspar is a fine- to medium-grained, interstitial constituent of the Core Facies. It is cryptoperthitic to microperthitic orthoclase that is seen to enclose all other minerals of a given rock type. Grains frequently display grid iron twinning and patchy extinction. In the more felsic rocks, potassium feldspar phenocrysts (to 1 cm) include euhedra of hornblende, biotite, plagioclase and sphene and very rare quartz. Dustings of very fine unidentified inclusions lie within most feldspars but they are not so numerous as to make the feldspar "turbid" (Figure 23d). Myrmekite fans occur at many K-feldspar-plagioclase contacts. Commonly K-feldspar crystals are cracked.

Plagioclase

Plagioclases are subhedral, complexly zoned laths (less than 8 mm in length), infrequently with patchy cores and indistinct zonation bands. Common and complex twin laws occur. Plagioclases have oscillatory zonation but is generally reversely zoned from about An_{30} to An_{40} (core to rim). Plagioclase is most often inclusion free but sparse inclusions of of biotite, hornblende and apatite occur. Many plagioclase phenocrysts are cracked and veined by epidote (< 3 modal %) and there is some sericitization (Figure 23d).

Quartz

Quartz occurs as aggregates (to 3 mm in diameter) of strained and partially recrystallized grains and subgrains. This is a late crystallizing phase as evidenced by rare inclusions of all other phases in a given rock.

Biotite

Biotite occurs as subhedral and anhedral flakes to 4 mm across with tan-greenish brown-brown pleochroism. It occurs as isolated flakes or in contact with hornblende. Biotite contacts with K-feldspar are digitate and fine-grained dustings of opaques occur at these contacts. Green pleochroic chlorite fringes are common, and where included in hornblende, biotite is commonly replaced by pseudomorphs of green chlorite. Biotite includes all accessory phases, and plagioclase. Simplectic intergrowths of sphene and an unidentified phase occur as patches in biotite. Besides for chlorite, lenses of a moderately high relief, clear to brown colored, alteration product were observed.

Hornblende

Hornblende is subhedral to euhedral, for the most part, and displays light green-green-blue green pleochroism. Laths are commonly 1 to 8 mm in length and have aspect ratios of less than 3/1. Hornblende typically includes trace phases and biotite, but rarely the felsic minerals.

Fe-Ti Oxides

The opaque phase (< 1 modal %) is magnetite as deduced from microprobe analyses. This phase is cubic, about 1 mm across, and commonly occurs with biotite, hornblende and sphene.

Accessory Phases

Sphene is the most abundant trace phase. Large brown prismatic euhedra (to 2 mm) were observed in most thin sections (Figure 23d). Anhedral sphene rims opaque minerals (magnetite) where it is in contact with biotite or hornblende, and is observed in simplectic intergrowth with an unidentified mineral in biotite. Opaque phases are infrequently included in euhedral sphene. Apatite is prismatic and has a length to width ratio between 10/1 and 4/1. Largest crystals are up to 0.2 mm long. Zircon is equant to prismatic (to 0.2 mm long) and is included in all phases. Apatite and zircon together make up less than 1 modal % of this rock type and both are included in all major phases. Allanite, up to 2 mm in diameter, composes a small modal % of the Core Facies (< 1 %) but is conspicuous because of its red brown to red orange color in thin section. It is euhedral, zoned, has simple twins and commonly is surrounded by epidote (CA84-147).

Secondary Phases

Secondary phases comprise less than 5 modal % of all thin sections examined. Anhedral epidote is found as veins in plagioclase and as partial pseudomorphs of biotite and hornblende; it is also seen rimming allanite. Chlorite fringes biotite or pseudomorphs it entirely, particularly where biotite is enclosed in hornblende. It is green in plane light and has gray, brown or violet anomalous extinction in crossed polarized light. Sericite ± calcite is seen in plagioclases or between feldspars. Sphene rims opaques and is observed in simplectic intergrowth with an unidentified phase in biotite (-- Figure id 'figplt4' unknown --d.

Four Deuce Hills

The Four Deuce Hills are underlain by equigranular, biotite granite in the north and hornblende biotite granodiorite in the south. The changes of mineralogy and texture along a north-south traverse (D-D'; Figure 19) are presented below.

Potassium Feldspar

Potassium feldspar changes texture, abundance, size and color across the traverse. In the north, K-feldspar is seriate, tabular (to 8 mm in length) and pink with very sparse inclusions. In granodiorite, potassium feldspar is oikocrystic (to 20 mm across) and interstitial, and pink to white in color. It contains common, euhedral inclusions of plagioclase, biotite, hornblende, and opaque minerals, and sparse inclusions of quartz, apatite and zircon. In all rocks, K-feldspar is microperthitic orthoclase with Carlsbad and grid iron twinning. Myrmekite is commonly observed at plagioclase-potassium feldspar contacts.

Plagioclase

Plagioclase is a seriate, tabular mineral throughout the traverse and ranges in size from 1 to 5 mm in granite, and 1 to 8 mm in granodiorite. This mineral displays complex zonation patterns and common twin laws. Anorthite contents (determined optically) range from 22 to 29 % anorthite for granite, and 25 to 37 % anorthite for granodiorite. Inclusions of biotite in plagioclase were observed in granodiorite.

Quartz

In all rock types of the Four Deuce Hills, quartz occurs in gray, aggregates of grains and subgrains from 1 to 6 mm across. Evidence of partial recrystallization include oscillatory extinction, deformation bands, and development of subgrains. Rare inclusions of plagioclase, biotite, hornblende, and trace phases were observed.

Biotite

Biotite occurs as anhedral to subhedral flakes in all rock types of the Four Deuce Hills. In granite, grains are dispersed and less than 2 mm across. In granodiorite, they are seriate, from 1 to 3 mm across, and are found either in clusters with hornblende ± opaque minerals, or as individual, euhedral books. This euhedral habit of relatively large grains distinguishes this facies from the granodiorite of the Rim Sequence. Biotite displays tan-brown-red brown pleochroism, and includes accessory phases. Chlorite partially replaces some biotite.

Hornblende

Hornblende occurs in granodiorite of the Four Deuce Hills as euhedral, black, acicular crystals (l/w < 1/5) from 2 to 5 mm in length. Hornblende is light green-green-blue green pleochroic, and commonly includes brown biotite, chlorite, and accessory minerals.

Accessory Phases

Accessory phases include opaque minerals, apatite, zircon, sphene, and allanite. Sphene and allanite occur in granodioritic samples. Opaque minerals are cubic crystals (< 2 mm across). Apatite is equant to acicular with maximum length/width ratios of 20/1. Equant crystals are less than 1.5 mm in diameter while acicular ones are less than 0.3 mm across. Zircons are euhedral prisms commonly with l/w of less than 4/1 and a maximum length of 0.2 mm. Sphene is a euhedral prismatic to subhedral phase that commonly includes opaque phases. Maximum sphene length is 2 mm. Allanite is a euhedral to subhedral mineral (1 mm) that is zoned, commonly twinned, and commonly rimmed by epidote.

Turtle Pluton Crystallization Sequences and Magmatic Reactions

The Turtle pluton can be divided into three mineralogic facies: (1) biotite + ilmenite ± magnetite ± muscovite, (2) biotite + magnetite + sphene, and (3) hornblende + biotite + magnetite + sphene. Crystallization sequences based on petrographic observations are shown in Figure 24. The outstanding feature observed in these rocks is crystallization of biotite before hornblende. The textural evidence of crystallization of biotite before hornblende, and reaction to hornblende (ragged biotite within hornblende euhedra; see Figure 23b) is observed in all hornblende-bearing granitoids of the Turtle pluton (62 to 68 wt% SiO_2) as well as some mafic enclaves (50 to 53 wt% SiO_2) found within these rocks. This sequence has also been reported in rocks of the the Huntington Lake Quadrangle, Sierra Nevada (Bateman and Wones, 1972) and the Yerrington Batholith (Dilles, 1987). This is unlike the sequence, hornblende then biotite, described in Bowen's reaction series (Bowen, 1922) and in many other calcalkaline plutons (Bateman and Chappell, 1979; Speer, 1987, for example). The relative stability of these two mineral groups is controlled by numerous factors but it primarily depends on the activities of K_2O, CaO, and H_2O in the melt (Wones and Gilbert, 1982). As briefly summarized by Hewitt and Wones (1984), most intermediate calcalkaline magmas crystallize hornblende before biotite because these magmas contain a significant amount of water, and because CaO is relatively insoluble in these melts. Thus precipitation of Ca-bearing phases (clinopyroxene, hornblende and anorthite) is favored.

Crystallization conditions of the Turtle pluton (P, T, X) may be constrained by comparison of observed crystallization sequences to experiments on granitic and granodioritic compositions at 2 and 8 kb (Naney, 1983; Figure 25), particularly to the 2 kb experiments given the mesozonal characteristics of the Turtle pluton. The effects of bulk composition, H_2O contents, temperature and pressure on relative stabilities of hornblende and biotite in these experiments are summarized below: (1) hornblende is not a stable phase in granite in either the 2 or 8 kb experiment. (2) hornblende is stable in granodiorite with water contents greater than about 4 wt%. (3) an increase of pressure favors hornblende stability over biotite in granodiorite (Figure 25). Given these ex-

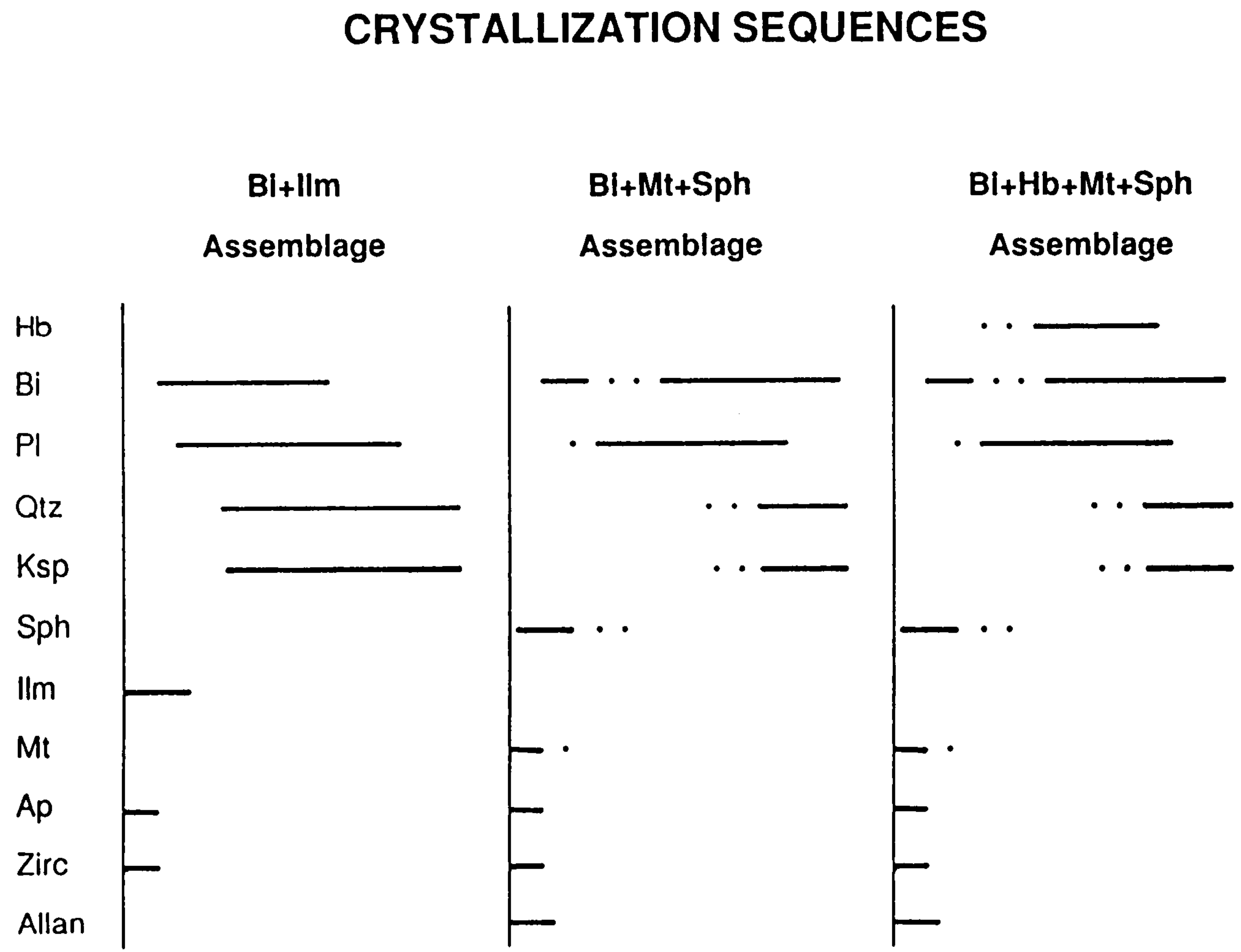

Figure 24. Rim Sequence crystallization sequences: Progressive crystallization is shown from left to right in each case. The Rim Sequence is composed of rocks with three mineral assemblages, that characterized by biotite + ilmenite in granites (left), by biotite + magnetite in granodiorite (center), and by hornblende + biotite + magnetite in granodiorite (right). Other essential differences among the three are the presence of sphene in all magnetite-bearing rocks, and the presence of allanite in most hornblende bearing rocks.

perimental results, the sequence biotite then hornblende could be the result of changes of several variables. These paths are: (1) change of bulk composition from granite to granodiorite. (2) increase of temperature in granodiorite. (3) increase of total pressure in granodiorite. (4) increase of H_2O pressure in granodiorite from less to more than 4 wt%.

Paths (1) and (2) (above) could be accomplished through addition of more mafic, hotter magma to a granitic one. Path (3) is considered geologically unlikely for a magma removed from its source region. Path (4) could result from addition of external H_2O, loss of other volatiles, or crystallization of minerals that contain less wt% H_2O than the melt (horizontal arrow, Figure 25).

In the case of the Turtle pluton, the accepted model must account for crystallization of biotite before hornblende not only in granodiorite but also in mafic enclaves (50 to 53 wt% SiO_2). This reaction observed in basaltic compositions makes a change in composition from an originally granitic one ($>$ 70 wt% SiO_2) an untenable explanation for the reaction. An increase of temperature, which requires addition of a hotter magma (magma mixing) is possible, and an increase of H_2O content from less to more than 4 wt% due to magma mixing, loss of other volatiles, or fractional crystallization can account for the textures observed in all rock types of the Turtle pluton.

The lack of pyroxenes as inclusions in any of the granitoids of the Turtle pluton and comparison to experiment suggests a maximum temperature for these magmas of less than about 750 and 800°C of granite and granodiorite, respectively.

Subsolidus Reactions in the Turtle Pluton

All other reactions observed in thin section are probably subsolidus. In the ilmenite biotite granite, low Ti-magnetite is exsolved from manganese-rich ilmenite (CA85-5, BW84-20). Production of extremely Mn-rich ilmenite is interpreted to result from oxidation (Czamanske and

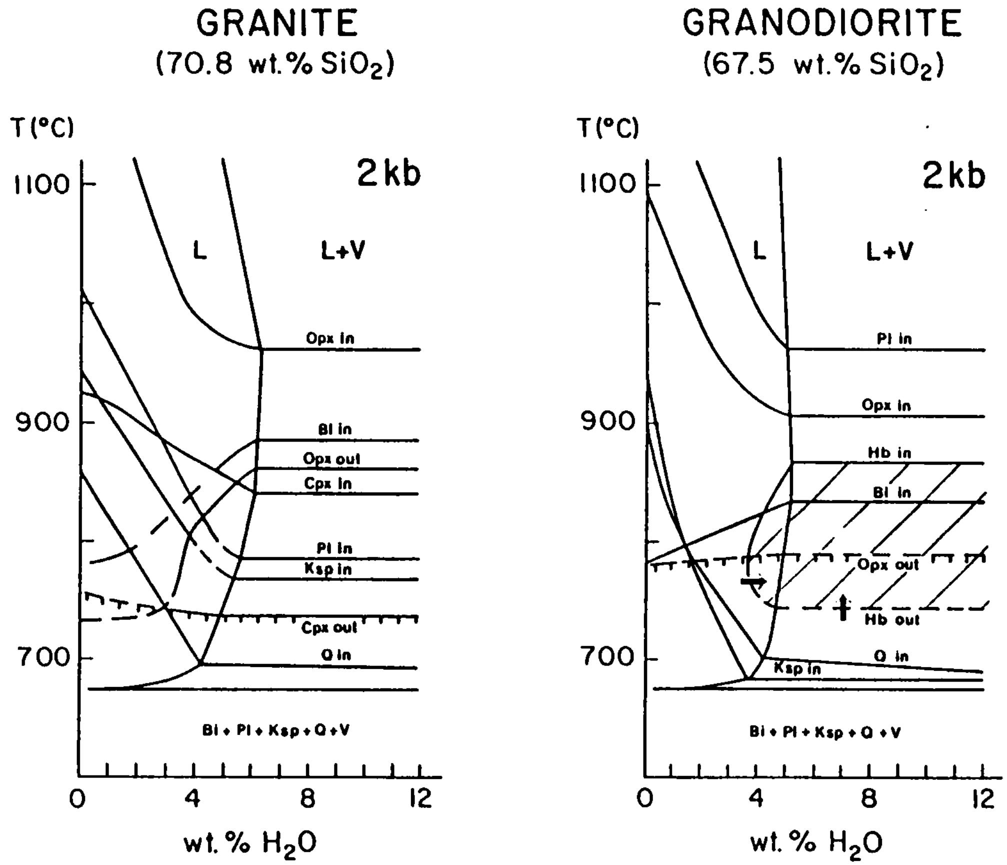

Simplified from Naney (1983)

Figure 25. Crystallization experiments on granite and granodiorite: These experiments were conducted at 2 kb total pressure with variable water contents. Lack of pyroxenes in the Turtle pluton suggests maximum magmatic temperatures in granite less than about 750°C (hatchured line). Hornblende is stable in the cross-hatched field in granodiorite. In order to explain the observed biotite to hornblende reaction, four paths are possible. (1) change of bulk composition from granite to granodiorite at about 735°C. (2) increase of total pressure in a granodioritic composition which expands hornblende stability relative to biotite (not shown). (3) increase of temperature from biotite to hornblende stability (vertical arrow). (4) increase of water pressure at a constant P and T to greater than about 4 wt% (horizontal arrow). Magma mixing could result in paths 3 and 4 whereas fractional crystallization could result in path 4.

Mihalik, 1972). In hornblende-bearing rocks, besides for sericitization of plagioclase and chloritization of biotite, other reactions suggested by petrographic evidence are:

(1) biotite = potassium feldspar + magnetite

(2) biotite = sphene + unidentified phases

(3) biotite + magnetite = sphene + unidentified phases.

Equation 1 results from oxidation of biotite and this suggests a late stage increase in f_{O_2} (Wones, 1981) which is also suggested by epidote rims on allanite (Affholter, 1988). Late stage oxidation is commonly observed in granitoid plutons (Czamanske and Mihalik, 1972; Czamanske and Wones, 1973; Czamanske et al., 1981).

Target Granite

The Target Granite is a biotite leucogranite that stopes and dikes the Core Facies. In the field, intrusive contacts are sharp but there is petrographic evidence of xenocrystic phases.

Potassium Feldspar

Potassium feldspars, roughly equant to 2 by 1 tabular microperthites that display grid iron and Carlsbad twinning, include all other phases. This seriate mineral has maximum dimensions of 10 to 1 mm. Some feldspars have optically distinct cores (xenocrystic ?) decorated by quartz that are chemically distinct as well (Chapter 3). K-feldspar includes all other phases.

Plagioclase

Subhedral laths of plagioclase (0.5 to 4 mm), though complexly zoned, have an overall normal chemical trend, have patchy cores, and are commonly bent and/or cracked. Some grains have conspicuous optical breaks dividing irregularly shaped, zoned cores from rims with more euhedral outlines (CA85-18). Sericitization is minor and tends to be concentrated in cores. Cracks are commonly filled by epidote.

Quartz

Quartz is moderately to strongly deformed in all specimens, and is recrystallized into sub-grains. Locally, quartz forms ribbons around more brittle phases such as feldspar.

Biotite

Biotite, the most abundant mafic phase, has tan-brown-red brown pleochroism and occurs as irregularly shaped grains that are partially chloritized in most case. In zones of high strain (CA85-15), biotite is recrystallized into retort-shaped crystals.

Hornblende

A few hornblende crystals (all < 1mm in length) were observed in this rock type (CA85-15, -101). Where unaltered, this phase is light green-green-blue green pleochroic. Grain types ranged from euhedral, unaltered examples, to grains partially replaced by a low birefringent, colorless phase interpreted as a serpentine mineral, to pseudomorphs composed of this serpentine mineral cut by 60°/120° crisscross of hematite reminiscent of hornblende cleavage.

Opaque Oxides

Opaques are cubic, less than 0.5 mm across, and are principally magnetite with lesser ilmenite (microprobe analyses).

Accessory Phases

Sphene (1 to 3 modal %) is euhedral, twinned and less than 1 mm in length. Apatite occurs as equant to acicular prisms whose maximum length is 0.1 mm. Zircons are slightly elongate, clear to pale brown prisms that commonly display growth zoning and rarely contain optically distinct cores (see Chapter 5).

Secondary Phases

Common secondary phases are green hornblende after biotite, a serpentine mineral after hornblende, sericite after plagioclase, and hematite after magnetite. Epidote was observed in cracks, particularly ones in plagioclase.

Crystallization Sequence and Reactions in the Target Granite

The crystallization sequence of the Target Granite for modally abundant minerals, biotite followed by plagioclase, quartz and K-feldspar, is a common one for granitic melts (Figure 26, Naney, 1983). It is unusual, however, that sparse hornblende occurs in rocks with up to 72 wt% SiO_2 (CA85-15 & 111) when in experiment at the range of crustal pressures, hornblende is not a stable phase in a 70.8 wt% SiO_2 melt (Naney, 1983). These experimental data, and the sparse hornblende population suggest hornblende may be xenocrystic. Optically discrete feldspar cores also lend credence to a xenocrystic component.

Other reactions observed in these rocks--chlorite after biotite, and sericite after plagioclase--are probably related to subsolidus alteration.

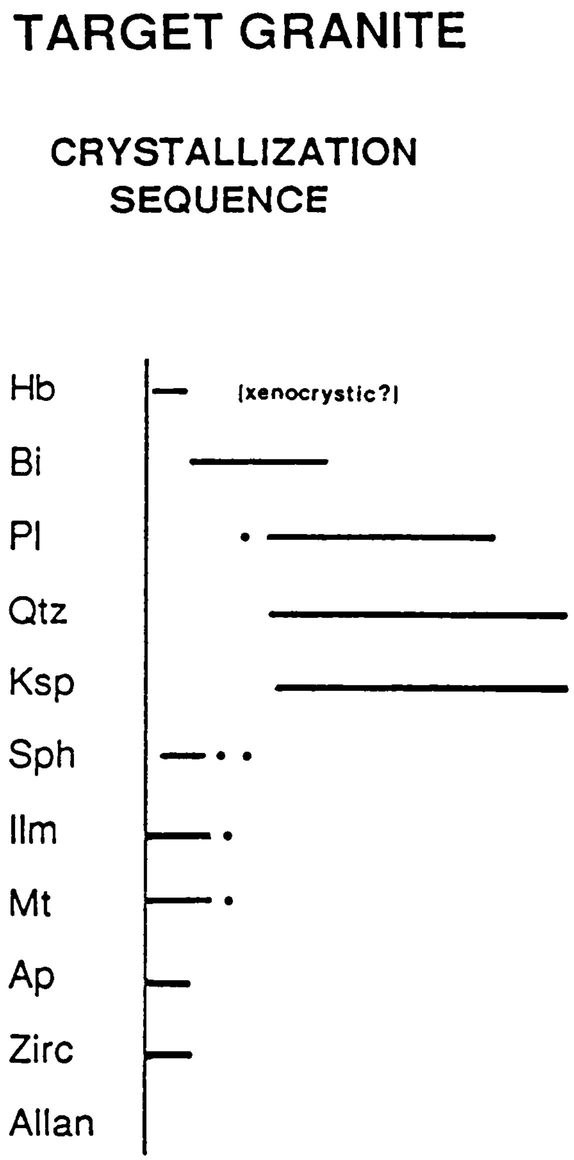

Figure 26. Target Granite crystallization sequence: Progressive crystallization is shown from left to right. The Target Granite has a common crystallization sequence for granites with the exception of sparse, early hornblende which may be xenocrystic.

Chapter 2

MAFIC ENCLAVES AND DIKES OF THE TURTLE PLUTON

Introduction

Fine- to very coarse-grained mafic rocks commonly occur in calcalkaline plutons as enclaves (inclusions) and dikes (Reid et al., 1983; Cantagrel et al., 1984; Didier, 1973 and 1987; Vernon, 1983; Kumar, 1988). Close spatial association suggests a genetic link of mafic rocks to the plutons and models of diorite to granite evolution through fractional crystallization or removal of restitic material have been proposed (Bateman et al., 1963; Bateman and Chappell, 1979; White and Chappell, 1977) though commonly observed igneous textures in enclaves makes unlikely a metamorphic or restitic origin (Vernon, 1983). Other models propose mixing of mantle derived mafic melts and granitic melts derived from the crust to generate the range of observed pluton and enclave compositions (for example, Barbarin, 1988; Stewart et al., 1988). Lastly, some mafic enclaves are thought to be xenoliths (Jurinski et al., 1989). Whether the mafic rocks of the Turtle pluton are comagmatic (early crystallizing liquids or "cognate xenoliths"), cogenetic (mixed magmas that have contributed to the evolution of the pluton), or unrelated (xenolithic) is unknown, and the ability to distinguish these possible sources through chemical and isotopic tests is contingent on lack of late stage, local chemical interaction between enclaves and host granitic magmas. Field relations, mineralogy, crystallization sequence, mineral chemistry, and geochemistry will be used to determine degree of local interaction and then probable sources of mafic rocks will be discussed.

The terminology for rocks in granitoids is discussed by Didier (1973) and by Vernon (1983). The word "enclave" is meant as a non-genetic term for one rock type enclosed in another. "Microgranitoid" denotes a granitic or hypidiomorphic-granular texture in a fine-grained rock. Grain size, crystal shape, and rock classification terminology is given in Chapter 1.

Three types of mafic rocks occur in the Turtle pluton: microgranitoid enclaves, medium- to coarse-grained dioritic enclaves referred to as "coarse-grained enclaves" to distinguish them from the microgranitoid variety that have different occurrences, textures, and compositions, and mafic dikes with textures like microgranitoid enclaves. Microgranitoid enclaves are fine- to medium-grained, equigranular to porphyritic bodies with maximum dimensions of less than 2 meters. They are common in outcrop in all facies of the Turtle pluton. Coarse-grained enclaves are medium- to very coarse-grained diorites and hornblendites with minimum dimension of three meters that occur in concentrations in the Four Deuce Hills, the Core Facies, and the southern part of the Rim Sequence. Mafic dikes occur in the Rim Sequence and Four Deuce Hills.

In order to examine local mafic rock-host granitoid interactions, mafic rocks and granitoid hosts were sampled close to one another. Three pairs of microgranitoid enclave-host pairs were sampled (Figure 27; BW84-23 & BW84-29, BW84-25 & BW84-25A, CA85-4 & CA84-45). One coarse-grained enclave was collected about 30 meters from BW84-25 and one mafic dike (CA85-4C) was sampled about 50 meters from CA85-4.

Field Observations

Field descriptions of enclaves and mafic dikes are based on observations throughout the pluton. In an effort to quantify the amount of microgranitoid enclave material in the pluton, its

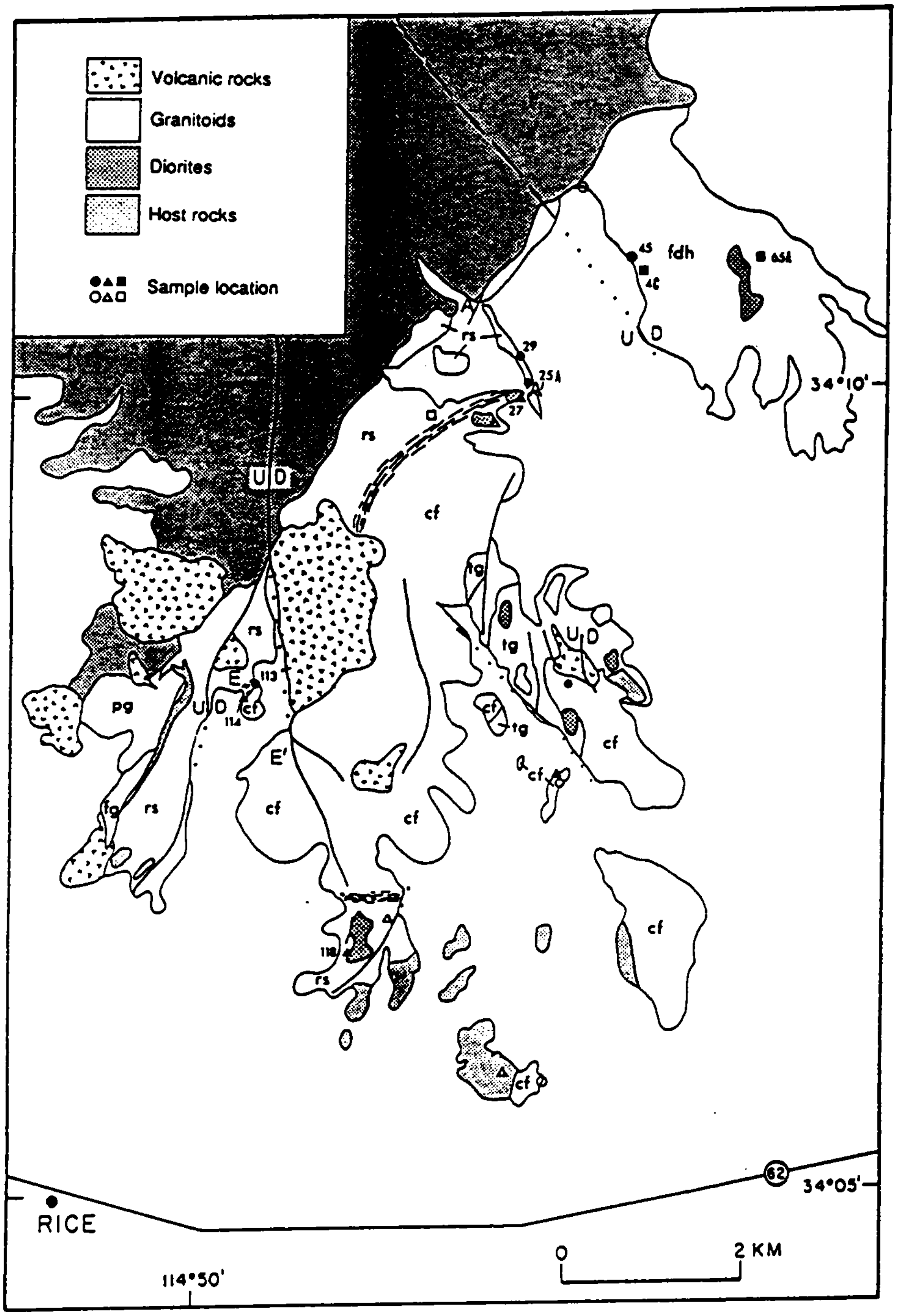

Figure 27. **Sample locations of mafic rocks:** This map of the Turtle pluton gives sample locations for modal (open symbols) and chemical (closed symbols) analyses of mafic rocks. Circle = microgranitoid enclave, square = mafic dike, triangle = dioritic enclave. Paired host rocks appear as stars. A-A' and E-E' are the two traverses along which enclave sizes and orientations were measured.

distribution, and its possible impact on the chemical evolution of the Turtle pluton, grid samplings of enclave size and orientation were taken along two traverses across the pluton (Figure 27).

Microgranitoid Enclaves

Fine- to medium-grained microgranitoid rocks form common enclaves throughout the Turtle pluton (Figure 8 on page 16) and were not seen in the Precambrian terrane. These enclaves have variable phenocryst contents. These enclaves have numerous features like those described in other plutons (Didier, 1973 and 1987; Vernon, 1983; Pabst, 1928; Link, 1969; Reid et al., 1983; Barbarin, 1988; Frost and Mahood, 1986; Kumar, 1988). Microgranitoid enclaves within the Turtle pluton occur singly, in matrix supported clusters (< 5 m in greatest dimension), and in large tabular swarms up to 5 by 100 m in size. Though most enclaves are ovoid, some are digitate, phacoid, and some truncated by schlieren. Most have sharp contacts against the enclosing granitoids but in the Core Facies, a several millimeter wide felsic halo primarily composed of plagioclase, quartz, and orthoclase, was observed surrounding some enclaves. No mafic or "chilled margins" were observed on enclaves within the Turtle pluton. In the porphyritic portion of the Rim Sequence, between enclaves in swarms, very coarse-grained granitic pegmatites are present.

Distribution, Size, and Orientation

In order to quantify enclave shape, orientation, and distribution, 18 horizontal and 19 vertical surfaces were sampled using a square meter grid along traverses (A-A′ and E-E′, Figure 27) across the Rim Sequence, and Schlieren Zone, and into the Core Facies. Grids were placed randomly on horizontal surfaces and on nearby vertical surfaces with strikes at high angle to the foliation. These grids are labelled A-S with a preceding H or V to indicate horizontal or vertical orientations.

Lengths, widths and orientations of enclaves are reported partly in Waugh (1985) (traverse A-A') and fully in APPENDIX 2. A summary of the results are given in Table 2 and in the figures below. The vertical axis is labelled X, horizontal one parallel to strike is labelled Y, and horizontal one perpendicular to strike, Z. As the selected surfaces expose random slices through enclaves and not necessarily the major axes of the enclaves, the total sampled enclave area is assumed to approximate enclave volume. This assumption is routinely made in modal analyses of rocks.

Enclaves are discoids with similar average dimensions on both horizontal and vertical surfaces (Table 2; X/Y/Z = 8.5/7.4/2.3), and are aligned parallel with the pluton-host rock contact and with igneous foliation of the Turtle pluton as shown in rose diagrams for the traverse segments (Figure 28). Such alignment of enclaves is commonly observed in plutons (Didier, 1973; Hutton, 1982; Vernon, 1983; Bateman, 1983;). Field observations here and elsewhere suggest a correlation of development of igneous foliation in granitoids and greater elongation ratios of enclaves (Hutton, 1982). The average length/width ratio (Y/Z) of enclaves in each horizontal grid along the traverses is given in geographic order from the country rock contact (left) into the Core Facies (right) in Figure 29. As the grid samplings were not taken at a regular interval, this figure is intended to show trends in the data. Enclaves are usually more elongate in the more foliated rocks toward the core, particularly in the Schlieren Zone (grids HL-HP, Figure 29). When present, foliation defined by alignment of platy and tabular minerals in an enclave is subparallel to the long dimension of the enclave, and lineation of tabular minerals is weak (subvertical) or absent. In foliated Rim Sequence rocks, where vertically aligned potassium feldspar phenocrysts suggest magmatic flow, enclaves have average measured dimensions of 10.0/3.7/8.3 (grids HG & VJ, Table 2).

The weak development of lineation and more common foliation within enclaves, and their oblate shape suggest that enclaves are weakly deformed by stretching during magmatic flow ($X \simeq Y$) and are more flattened parallel to wall rocks ($Y << X$). These observations are consistent with a model in which enclaves behaved as relatively rigid, mostly-crystalline spheres or ellipsoids in relatively plastic, partially crystalline granitic magma, were rotated into parallelism with flowing magmas (if nonspherical), and were flattened parallel to walls of the pluton during deformation of a nearly solid granite due to volume expansion from crystallization or intrusion of more magma into

Table 2. Summary of enclave field measurements (cm).

GRIDS++	n	AZIMUTH	Y	Z	AVERAGE Y/Z*	AVERAGE AREA	%AREA
AVG HORIZ	293	29.4	7.4	2.1	4.4	24.3	4.0
ST DEV		25.3	7.3	2.6	3.4	72.8	
AVG A-J	173	42.5	5.8	1.9	3.4	17.6	2.7
ST DEV		15.4	5.9	2.2	1.5	47.9	
AVG K-Q	88	22.6	10.8	2.3	6.7	37.8	7.4
ST DEV		13.4	9.2	3.3	4.9	110.9	
AVG R-T	32	-22.3	7.2	2.7	3.3	23.3	2.5
ST DEV		18.9	4.7	2.4	1.3	39.1	

	n	DIP	X	Z	AVERAGE X/Z*	AVERAGE AREA	%AREA
AVG VERT	297	53.0	8.5	2.5	4.5	30.9	4.8
ST. DEV.		18.8	7.4	3.1	2.9	82.0	
AVG A-J	153	58.5	7.7	1.9	4.7	21.0	3.2
ST. DEV.		12.3	7.4	2.1	2.9	57.0	
AVG K-Q	112	41.7	9.3	2.9	4.7	36.5	6.8
ST. DEV.		18.5	6.8	3.4	3.0	74.9	
AVG R-T	32	66.3	9.2	3.8	3.0	59.2	6.3
ST. DEV.		23.9	9.1	4.9	1.6	160.9	

++ A through J are from traverse of the Rim Sequence (A-A') and K through T are from traverse of the Schlieren Zone and into the Core Facies (E-E').

* This quantity= $\Sigma(1/w)/n$.

the center of a complex (Hutton, 1982). The most extreme flattening in normally zoned plutons is commonly close to wall rock contacts and this has been modelled as the result of strain concentration near the rigid walls (Bateman, 1983). In the Turtle pluton, strain is most extreme in the Schlieren Zone (Figure 29). This is probably due to intrusion of the Core Facies into the a more rigid Rim Sequence. Lack of excessive flattening at the Rim Sequence/wall rock contact is due to lack of strain build up, perhaps from magma flow out the top of a chamber, or due to deformation of country rock (Bateman, 1983).

Enclave areas were calculated from measurements assuming an elliptical shape (($\Pi/4$) × length × width). Calculated areas for enclaves from horizontal and vertical surfaces each yield a log normal distribution (Figure 30) and similar mean areas of 4.0 and 4.8%, respectively. The slightly larger calculated areas from vertical surfaces may be due to variation of surface orientation relative to strike. A similar pattern and small enclave area (< 1%) is reported from a detailed study of microgranitoid enclaves in the Tuolumne Intrusive Suite (Link, 1969). Two lines of evidence suggest total sampled area approximates total volume: similarity of calculated areas from both surfaces, and log normal size distributions (see Figure 30).

The area (volume) of microgranitoid enclave material within the Turtle pluton is small (4 to 5%) and enclaves are slightly more voluminous in the more mafic rocks of the core of the pluton as determined by grid sampling and field observations. The enclave areas in the Core Facies (2.5 and 6.3 %) and Schlieren Zone (7.4 and 6.8%) are greater than in the Rim Sequence (2.7 and 3.2%; see Table 2), though the discrepancy of calculated enclave areas from surfaces in the Core Facies suggests an inadequate sample size. A similar distribution of more microgranitoid enclaves in the core occurs in the reversely zoned Passadumkeag River pluton, Maine (Ayuso, 1984; Figure 1 on page 2). Conversely, in normally zoned plutons, enclaves are more numerous in mafic granitoids found at the rims of these intrusions (Pabst, 1928; Link, 1969; Bateman et al., 1963). Link (1969) and Pabst (1928) correlated color index of granitoids and volume of enclaves in normally zoned plutons, and suggested a genetic relationship of the two. These data from normally and reversely zoned plutons suggest that enclave abundance is small (< 5 volume %, Link, 1969 and this study),

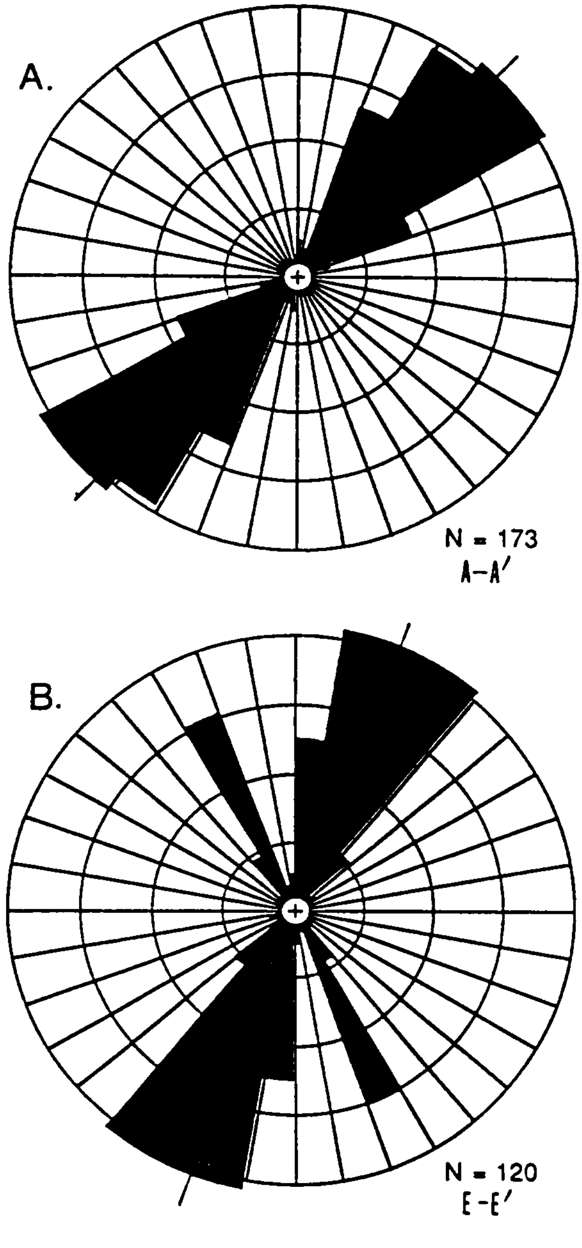

Figure 28. Orientations of microgranitoid enclaves: Orientations of enclaves and average orientations of nearby Turtle pluton-country rock contact (through-going lines) along traverses A-A′ (A) and E-E′ (B) are shown on rose diagrams. Generally, enclaves are aligned parallel to these contacts, a common occurrnce in calcalkaline plutons (Pabst, 1928; Hutton, 1982; Bateman, 1983). The secondary maximum in B is from enclaves sampled near E′, the ones furthest from the country rock which may parallel nearby unexposed Schlieren Zone, an internal igneous contact.

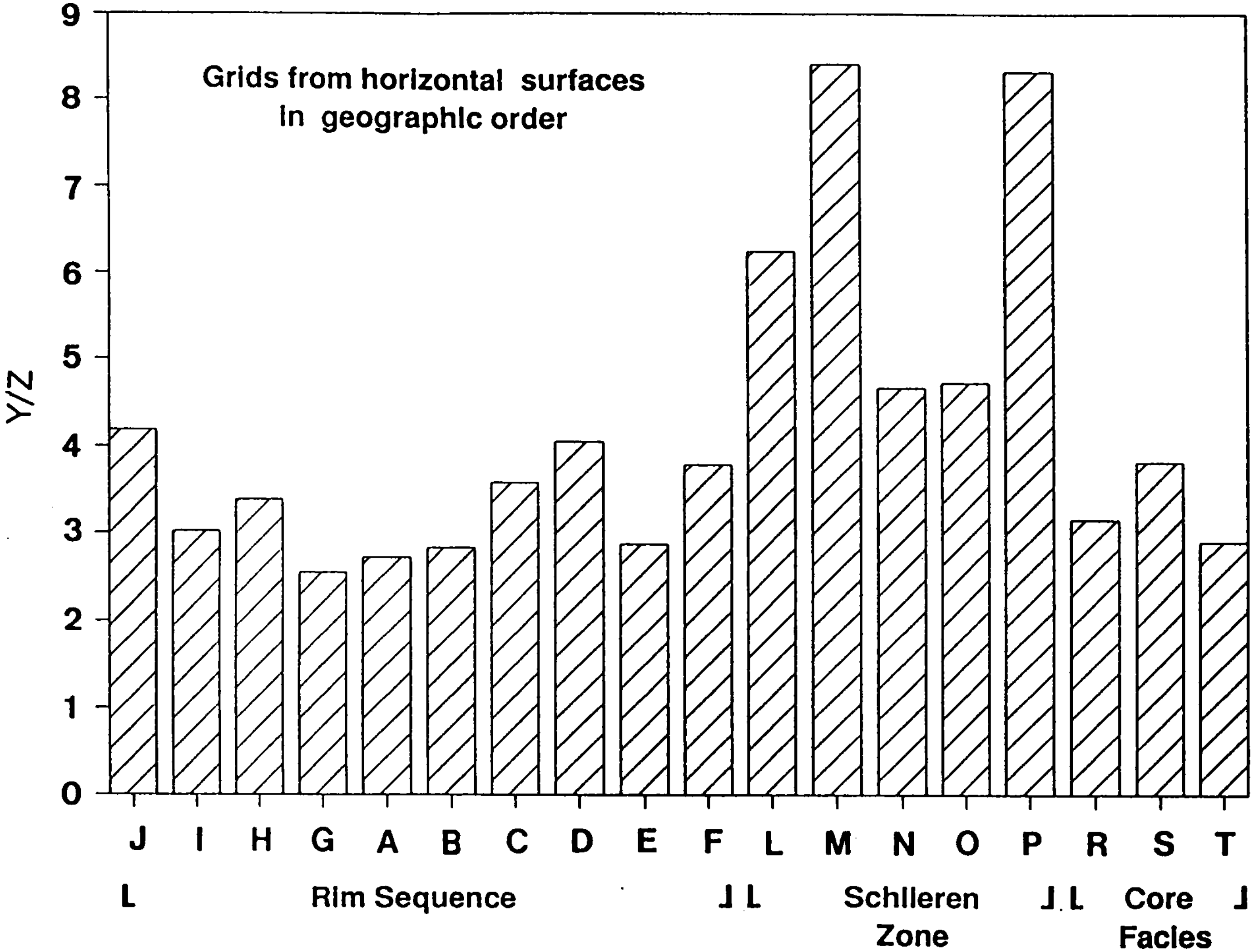

Figure 29. Length/width ratios of enclaves as measured on horizontal surfaces: This bar diagram shows average length/width ratios (Y/Z) for horizontal grids in geographic order from the country rock contact (left) to the Core Facies (right). Grids from traverse A-A′ are A-J. Those from traverse E-E′ are L through T. The ratios are greatest in the Schlieren Zone (grids L-P) where foliation in the host granitoids is best defined. There is no significant increase in flattening of enclaves at the country rock contact.

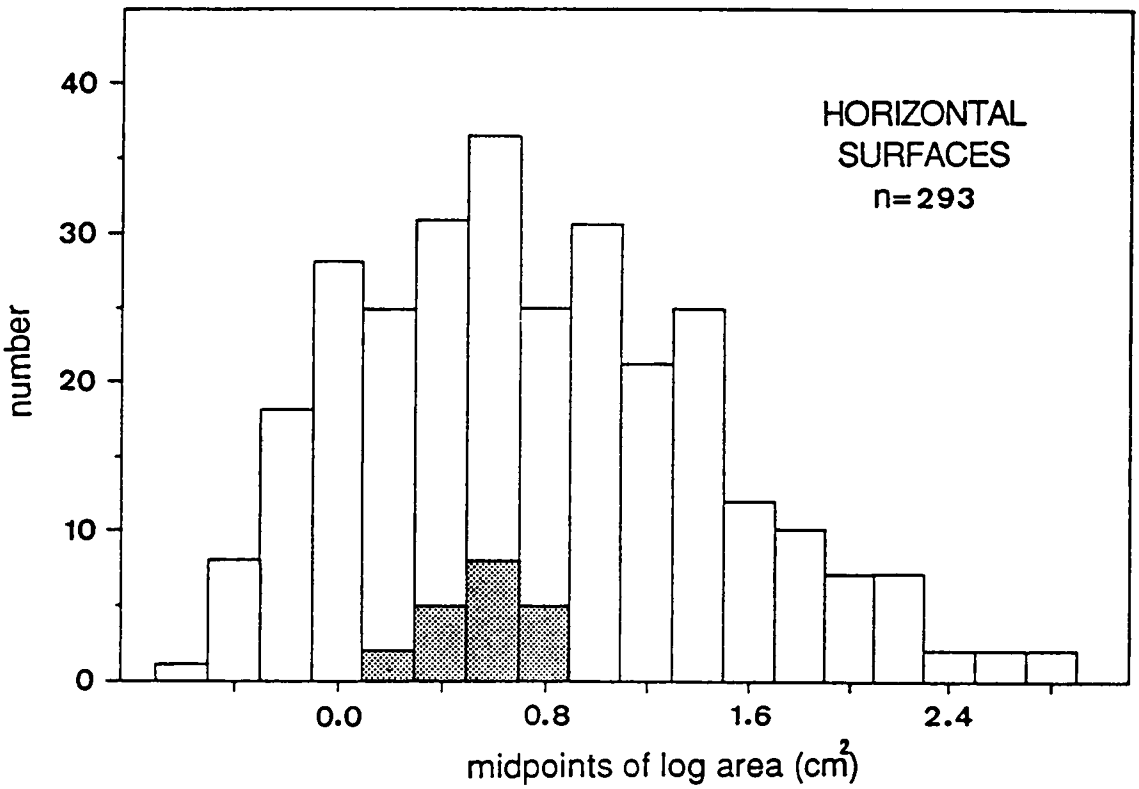

Figure 30. **Histogram of microgranitoid enclave areas:** This histogram shows the number of enclaves from horizontal grids in size classes on a log scale (cm^2). As an example, the enclaves from a single grid are shaded. Both the total population and most individual grids show a log normal distribution. The mean size is about 4 cm^2, a size at the small end of the total range of 1 to 500 cm^2. This distribution is in part due to sampling of a single surface through three dimensional enclaves.

and that abundance correlates with the presence of more mafic rocks and not with position (rim or core) in a plutonic system.

Mafic Dikes

Several mafic dikes with textures very similar to some enclaves (Figure 31 on page 90) occur in the peripheral units of the Turtle pluton, in the Rim Sequence (CA84-102, -103, -105, -170) and in the Four Deuce Hills (CA84-65A, -4C; see Figure 27 and Plate A). These dikes have widths from 5 cm to 3 m, have planar or curviplanar walls, commonly have more fine grained margins, have northeasterly strikes, may be offset on low angle normal faults, and are intruded by aplites (Figure 10 on page 21). One dike with curviplanar walls (CA86-65A) is itself diked and disrupted by its host granodiorite. Textural similarity of dikes and microgranitoid enclaves, and dike disruption suggest enclaves may be disaggregated dikes. If enclaves are the product of dike disruption, the occurrence of dikes only in the periphery of the Turtle pluton indicates an environment that allowed their preservation. Field evidence shows the Rim Sequence was emplaced before the Core Facies and thus the periphery of the pluton may have been crystalline enough to preserve dikes.

Synplutonic mafic dikes have been documented in a number of environments: the Coast Ranges of British Columbia (Roddick and Armstrong, 1959), the Klamath Mountains (Barnes et al., 1986), the Sierra Nevada (Pabst, 1928; Reid et al., 1983), Coastal Maine (Stewart et al., 1988), and the Malay Peninsula (Kumar, 1988). In these instances, disaggregation of dikes by granitic magmas is well documented, and suggests a genetic relationship of texturally similar dikes and enclaves.

Coarse-Grained Enclaves

Medium- to coarse-grained dioritic rocks occur locally in the Turtle pluton and in the Precambrian terrane (CA84-6C). Within the Turtle pluton, coarse-grained enclaves are concentrated in the southern portion of the Rim Sequence, in the Four Deuce Hills and in the Schlieren Zone, and are more sparse in the Core Facies. These diorites have a broad range of grain size from 3 mm in diorite to hornblendite with grain sizes of greater than 1 cm (CA84-65). Generally, the enclaves are ovoid and tens of meters long, and the shortest dimension of the smallest observed body is 3 meters (CA84-114). These bodies lack fabrics except where subhorizontal alignment of hornblende and plagioclase crystals suggests a cumulus origin (-- Figure id 'figplte' unknown --). Crosscutting relationships of these coarse-grained dioritic enclaves and host granitoids were not observed though contacts were examined carefully. These coarse-grained enclaves are distinct from microgranitoid enclaves in dimension, texture and grain size.

Petrography of Mafic Rocks

Introduction

The textural and mineralogic variation among enclaves and dikes, and comparison to host granitoid mineralogy is given below. There are two types of enclaves, microgranitoid and coarse-grained. Microgranitoid enclaves are divided into two textural subgroups: porphyritic and nonporphyritic, and these rocks are compared to texturally similar mafic dikes. For all cases examined in the Turtle pluton, microgranitoid enclaves contain a mineral assemblage that mimics the assemblage of their host rocks, and this is a common feature of microgranitoid enclaves in other

Figure 31. Thin section textures of mafic rocks: This photograph shows textures of 8 representative mafic rocks. a = non-porphyritic microgranitoid enclave. b = porphyritic microgranitoid enclave. c = porphyritic microgranitoid enclave. d = mafic dike. e = felsic coarse-grained enclave. f = coarse-grained enclave. g = coarse-grained enclave. h = coarse-grained enclave with cumulus texture.

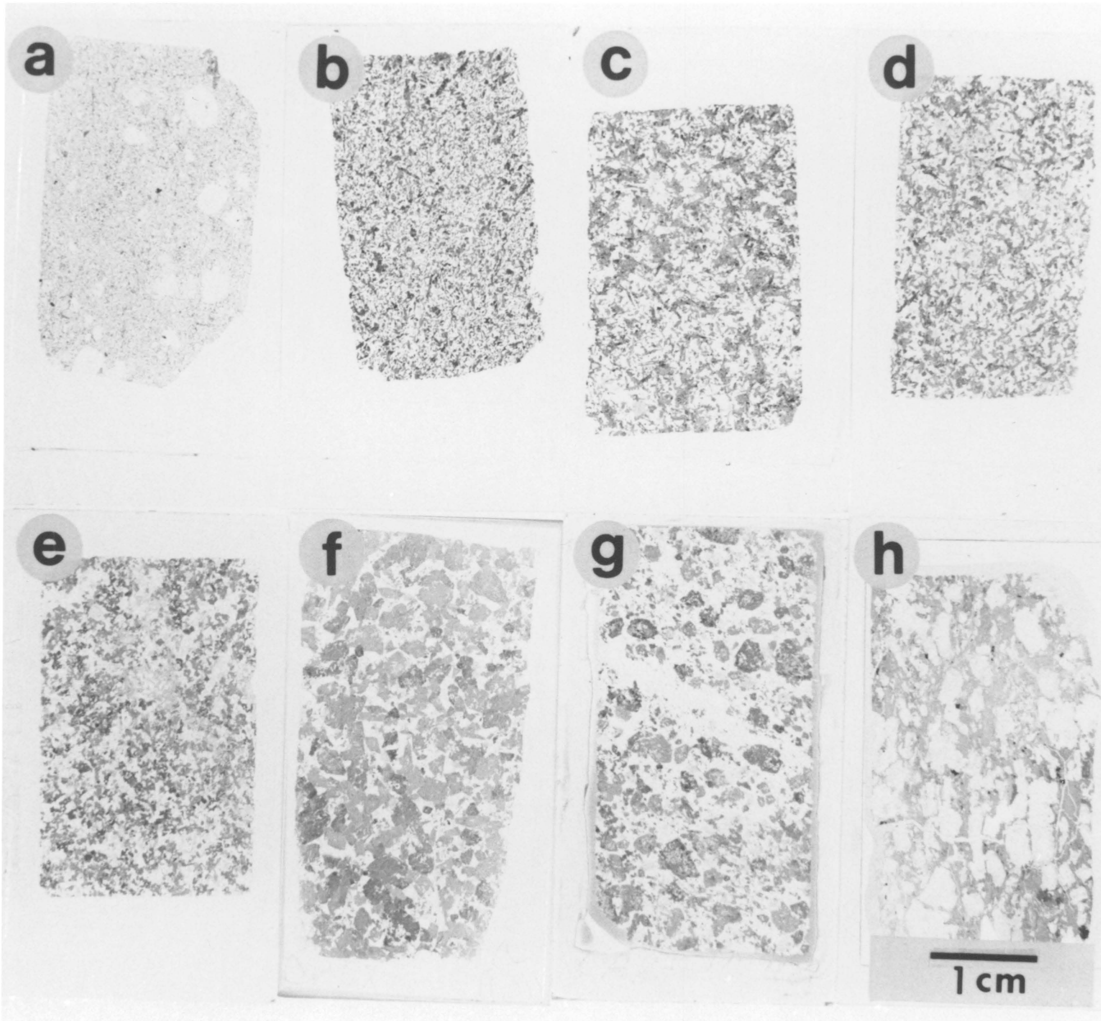
a
b
c
d
e
f
g
h
1 cm

plutons (Vernon, 1983; Didier, 1973). This suggests either enclaves are comagmatic with granitoids or that enclaves and their hosts have equilibrated at similar conditions. Coarse-grained enclaves in the Turtle pluton may have a different assemblage from their hosts and this suggests different histories for the two enclave types.

Microgranitoid Enclaves

Porphyritic and nonporphyritic microgranitoid enclaves occur in all facies of the Turtle pluton, and examples of texture are shown in Figure 31. Textures of these enclaves are variable even from enclave to enclave in a single swarm though the mineral assemblage of enclaves in a swarm is always consistent with that of the surrounding granitoid. Zoning within enclaves, such as changes of color index or concentrations of phenocrysts, were not observed. The porphyritic and nonporphyritic subgroups, contain similar characteristics. The groundmass of the porphyritic type resembles the equigranular, nonporphyritic type and the porphyritic type can be thought of as the result of addition of phenocrysts to the nonporphyritic type. A description of the nonporphyritic enclaves is followed by a description of phenocrysts found in the porphyritic type. Modal data are given in APPENDIX 1.

Nonporphyritic Microgranitoid Enclaves

These enclaves are medium- to fine-grained rocks (1 to 3 mm average grain size) and have an equigranular to seriate, hypidiomorphic texture. Enclaves that occur in biotite granite are composed of biotite + plagioclase + quartz ± K-feldspar ± opaque oxides + apatite + zircon. Enclaves found in hornblende-bearing rocks contain hornblende + biotite + plagioclase + quartz ± K-feldspar ± opaque oxides + apatite + zircon.

Potassium Feldspar

In stained thin sections and slabs, potassium feldspar composes less than one percent of the rock and is subhedral to anhedral.

Plagioclase

Plagioclase composes up to 56% of an enclave. It occurs as normally zoned, inclusion poor, euhedral laths with common twin laws, and as unzoned subhedral grains that share triple junction contacts with other plagioclase crystals and hornblende. Such granoblastic textures are taken as evidence of partial recrystallization of plagioclase under subsolidus conditions (Didier, 1973).

Quartz

Quartz is a minor constituent (< 5 modal%) in most samples but is more abundant in others (to 13 modal%). Where positively identified, it occurs as subequant grains with minor undulose extinction.

Biotite

Biotite occurs as subhedral to anhedral brown flakes (10 to 40 modal%) and it occurs adjacent to feldspar and hornblende (if present). Alteration to chlorite or a golden aggregate of unidentified minerals is more common. The textural relationships of biotite and hornblende are: 1) equilibrium. 2) optically continuous ragged patches of biotite in hornblende. 3) sub- to euhedral biotite grains crisscrossing hornblende.

Hornblende

Hornblende is found in all enclaves within hornblende-bearing granodiorites. This mineral is acicular to tabular (Figure 31), has light green-green-blue green pleochroism, and shows complex textural relations with biotite as discussed above. In some samples (CA84-47 and -103B) hornblende contains optically aligned, opaque oxides that occur near the enclosed biotite such that there is an inclusion free halo around biotite in hornblende. The cause of this texture is unknown but reactions involving hornblende and biotite are implicated.

Sphene

Sphene is a common accessory phase in enclaves ($\simeq$1 modal%). A few euhedral grains were observed (to 1mm in length), but generally, sphene is subhedral with inclusions of plagioclase and opaque oxides, or anhedral and associated with mafic silicates. The common subhedral texture of sphene with plagioclase inclusions suggests it ended crystallization after plagioclase began to crystallize. Its sparsity as inclusions in plagioclase phenocrysts also suggests it is a moderately late crystallizing phase.

Opaque Minerals

Blocky and acicular opaque oxides (< 1 mm across) compose less than 1 modal % of most enclaves and are commonly included in ferromagnesian silicates. EDAX analyses indicate that blocky grains are magnetite.

Apatite

Randomly oriented acicular apatites that commonly contain fluid inclusions are ubiquitous in mafic enclaves of the Turtle pluton. Crystals are euhedral with aspect ratios from 5 to 100, and have diameters less than 0.05 mm. There also are rare prismatic apatite grains with diameters of 0.4 to 0.15 mm and aspect ratios of less than 3. Among the acicular variety, few examples of Y-shaped or swallow tailed grains were seen but boudinaged trains and grains with stretched necks are common.

Zircon

Zircons observed in the groundmass are equant to prismatic grains to 0.2 mm in length commonly with broken terminations, or are acicular (l/w > 10; l = 0.3 mm; CA84-45, -113). Zircons occur as inclusions in phenocrysts as well.

Secondary Phases

Alteration of primary phases consists of sericitization of plagioclase, chloritization of biotite, and epidote and minor calcite in cracks. Only a few samples are pervasively altered and in these rocks remain little pristine plagioclase.

Porphyritic Microgranitoid Enclaves

Most enclaves are porphyritic and contain phenocrysts of quartz and plagioclase or aggregates of the two (2 to 8 mm in diameter). In enclaves from hornblende-bearing rocks, individual grains or clusters of amphibole are common (BW84-25A, -29, CA84-113), and phenocrysts of biotite in hornblende-bearing and hornblende-free rocks are very rare (CA84-113). Phenocrysts in microgranitoid enclaves have been interpreted as crystals from granitic magmas engulfed by mafic magma (Didier, 1987), however data presented below suggests other origins are possible.

Plagioclase Phenocrysts

Subhedral to euhedral plagioclase phenocrysts (andesine; 3 to 8 mm) display a range of morphologies, variable zonation profiles, and inclusion populations. Most phenocrysts occur in aggregates with or without quartz. These aggregates display synneusis type crystal outlines in which plagioclase-plagioclase contacts are curvilinear and contacts with other phases are planar crystal faces (Vance, 1969; CA84-62, -113). Individual crystals are euhedral to subhedral. Zonation style varies from well-defined (CA84-113) to patchy (CA84-62). Commonly, sericite in a zonation band divides a core of patchy or irregular zonation from a narrow rim of well-defined, concentric zonation bands. These cores may be inclusion-free, or may contain hornblende ± acicular apatite ± biotite ± opaque oxides ± zircon. On the other hand, rims may contain the phases listed above plus sphene, or may lack inclusions. Plagioclase with inclusions only in the rim and ones with inclusions only in the core may occur in a single specimen (CA84-113).

Quartz Phenocrysts

Quartz with few inclusions, occurs as aggregates or as single grains commonly with embayed margins. In either case, quartz displays pronounced undulose extinction with minor subgrain development (CA84-173, -43, BW84-28). Cracks filled with sericite or calcite crosscut these phenocrysts. Commonly, quartz occurs with plagioclase phenocrysts although in one sample (CA84-43), quartz occurs as single subhedral grains with crystal faces. No quartz crystal faces were observed in Turtle pluton granitoids and this suggests quartz phenocrysts are not exclusively xenocrysts from surrounding granitic rocks.

Quartz and plagioclase aggregates commonly occur as ocelli (rounded mineral grains or aggregates, rimmed by mafic mineral in some cases). This texture has been interpreted as the result of reaction (Didier, 1987).

Biotite Phenocrysts

Biotite phenocrysts (2 to 3 mm in diameter) are rare. Where they do occur, they contain acicular apatite and blocky opaques and are associated with chlorite ± high relief alteration phases.

Hornblende Phenocrysts

Hornblende phenocrysts occur as single crystals (about 3 mm long) or in clots (2 to 5 mm across). Single grains are euhedral and contain apatite, zircon and more rare opaque oxides and biotite (CA84-173). More ordinarily, amphibole phenocrysts occur in clusters of euhedral to subhedral grains that typically lack the biotite and aligned acicular opaque inclusions observed in groundmass hornblende (CA84-49). These clusters commonly contain blocky iron oxides and anhedral sphene.

Mafic Dikes

Mafic dikes have textures and modes very similar to porphyritic and nonporphyritic microgranitoid enclaves (Figure 31) except that dikes contain a greater modal abundance of secondary phases, particularly sericite after plagioclase, epidote after plagioclase or in veins, and chlorite after biotite (APPENDIX 1).

Coarse-Grained Enclaves

These enclaves in host biotite granite and hornblende biotite granodiorite are composed of hornblende + plagioclase ± biotite ± clinopyroxene ± sphene ± quartz ± K-feldspar ± apatite ± opaques ± zircon. Hornblende is modally dominant, comprising 50 to 90 % of a given specimen (APPENDIX 1 and field observation). These rocks are hornblendites to appinites (diorites that contain euhedral hornblende phenocrysts with smaller hornblende grains in the groundmass; Pitcher and Berger, 1973). Textures of some coarse-grained enclaves (excluding the very coarse-grained hornblendites) are shown in Figure 31. The major differences among these enclaves are the modal abundances of biotite, clinopyroxene, sphene, and opaque oxides (APPENDIX 1).

Potassium Feldspar

Interstitial potassium feldspar was positively identified in few samples and may comprise a small percentage of others (< 1%).

Plagioclase

Plagioclase (andesine) is interstitial to hornblende in most diorites but in rocks of lower color index, plagioclase laths are aligned with interstitial hornblende which suggests cumulus plagioclase. Plagioclase contains hornblende euhedra ± biotite ± subhedral to anhedral sphene ± opaque oxides. Many plagioclase grains have concentric zones of sericitization and zonation style ranges from well-defined to patchy.

Quartz

Quartz is a minor constituent of most coarse-grained enclaves (1 to 4 modal %). It is an interstitial phase with undulose extinction.

Biotite

Biotite content is variable in coarse-grained enclaves, from 1 to 16 modal % (including chlorite pseudomorphs). It occurs as large flakes or as euhedral to anhedral inclusion in hornblende, and rarely in plagioclase. Alteration products are chlorite, sphene, epidote and an unidentified high relief phase.

Hornblende

Hornblende is euhedral and frequently contains optically continuous shreds of brown biotite, cross flakes of biotite, rare anhedral plagioclase and sphene, and very rare opaque oxides. Hornblende is more abundant than biotite in all coarse-grained enclaves and occurs even in enclaves in hornblende-free granitoids. Euhedral hornblende crystals among euhedral to subhedral plagioclase and other phases suggests a cumulus texture. Pleochroism is light green-green-blue green and some grains display patchy color zonation.

Clinopyroxene

Pyroxene was observed in one specimen (BW84-27). It is colorless to light green, euhedral to subhedral and is associated with, and replaced by hornblende.

Opaque Oxides

Opaque minerals compose a small amount of these rocks. It occurs as blocky crystals and as a fine dusting in hornblende and biotite.

Sphene

This phase is commonly subhedral to anhedral and is found within hornblende and plagioclase. As in microgranitoid enclaves, its anhedral shape in contact with plagioclase, hornblende or biotite suggests co-crystallization with these phases. Some grains contain opaque oxides.

Apatite

Apatite crystal shape ranges from large equant and prismatic grains to 0.3 mm in diameter, to narrow acicular crystals ($<$ 0.1 mm in width). Acicular crystals are less abundant than found in microgranitoid enclaves though the same characteristics--fluid inclusions, boudinaged trains, and stretched necks--persist.

Zircon

Zircon occurs as extremely rare prismatic crystals in the major mineral phases.

Secondary Phases

Secondary phases in coarse grained enclaves are sericite, epidote, hematite, and minor calcite.

Implications of Textures and Crystallization Sequences

The textures of mafic enclaves and dikes are igneous with minor evidence of recrystallization in the form of subgrain development in quartz, and triple junction boundaries of plagioclase, and the development of biotite cross flakes in hornblende like those described by Frost and Mahood (1986). In general, textures of enclaves are hypidiomorphic granular, like those typical of granites with extended cooling histories. Textures that suggest undercooling are limited to the acicular morphology of apatite and zircon (Wyllie et al., 1963; Lofgren, 1974). Taken as a whole, mineral textures found in mafic rocks of the Turtle pluton suggest an early quenching event, then slower cooling, and development of a crystallization sequence (including biotite) generally like that of surrounding granitoids.

Mineral assemblages of microgranitoid enclaves reflect that of their hosts, whereas in some cases, coarse-grained enclaves and mafic dikes contain hornblende ± clinopyroxene where host granitoids do not. All mafic rocks have similar crystallization sequences as shown in Figure 32. Earliest crystallizing phases are apatite, zircon (when present), sphene, opaque oxides (when present), and clinopyroxene (when present), followed by hornblende (when present), then either biotite or plagioclase. Sphene and biotite did not complete crystallization until after nucleation of plagioclase. Late crystallizing interstitial phases are quartz and potassium feldspar. One coarse-grained enclave (BW84-27) is unique because it contains clinopyroxene that coexists with, and is replaced by hornblende. All coarse-grained enclaves, unlike microgranitoid ones, contain more hornblende than biotite.

The crystallization sequences and assemblages observed in mafic rocks are similar to those observed for granitoids of the Turtle pluton (Figure 24 on page 70). Five major differences exits. (1) Clinopyroxene was observed in a coarse-grained enclave whereas no pyroxene was observed in

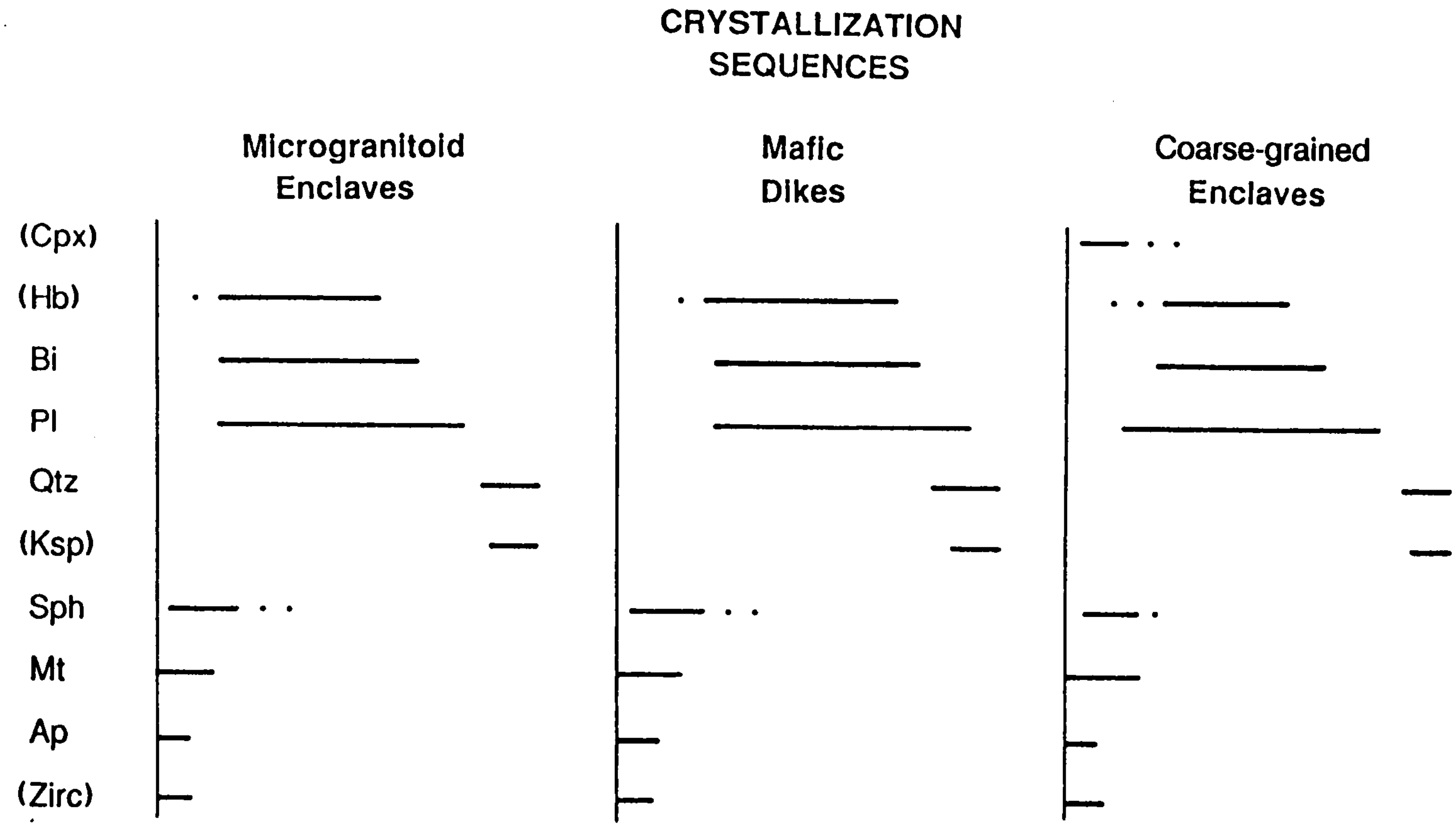

Figure 32. Crystallization sequences of mafic rocks: These are crystallization sequences (left to right in each case) of mafic rocks deduced from petrographic observations. As compared to crystallization experiments on basalts (Helz, 1973), these rocks could be produced by cooling of potassium rich basalts ($K_2O > 1$ wt%) with about 50 wt% silica. These crystallization sequences are similar to that of granitoids except for the presence of pyroxene in one sample, and the later crystallization of sphene in all cases.

granitoids. (2) Coarse-grained enclaves contain hornblende even when host granite does not. (3) Biotite is intergrown with hornblende, a range of textures which suggest co-crystallization in some and biotite before hornblende in others. (3) Sphene and biotite contain plagioclase inclusions and this suggests that these phases continued crystallizing after the onset of plagioclase production. Textures in granitoids indicate that sphene and biotite, for the most part, proceeded plagioclase. (4) Allanite was observed in only one mafic rock, an enclave in the Four Deuce Hills close to the country rock contact (CA84-43). These sequences may result from crystallization of a basalt containing SiO_2 of greater than 50 %, and K_2O of greater than 1 % and enough H_2O to stabilize hydrous phases (Helz, 1973). Such compositions of basalt can result from crustal contamination by assimilation or magma mixing with crustal sources.

It has been suggested that phenocrysts in enclaves are crystals from granitoid magmas engulfed in the mafic enclave (Cantagrel et al., 1984, for example). This is a possible source for some phenocrysts, however almost complete lack of some early crystallizing phases from granitoids in enclaves, allanite and phenocrystic biotite, and phenocrysts of quartz with crystal faces, a texture not observed in the Turtle pluton, suggest alternate sources for phenocrysts.

Mineral Chemistry

Mineral chemistries of phases from mafic rocks were investigated in order to constrain relationships among these rocks, and to determine the degree of interaction with host granitoids. The latter is also discussed in Chapter 5. Microprobe analyses of plagioclase, biotite, hornblende, and apatite are presented in this section, and are compared to host granitoid mineral compositions. All analyses appear in APPENDIX 4.

Plagioclase

Reconnaissance analyses of both phenocrystic and nonphenocrystic plagioclase in mafic rocks show normal zonation trends in all samples. For plagioclase traverses in five hornblende-bearing mafic rocks, anorthite contents range by about 20 %, and orthoclase contents generally from 1 to 1.5 %. Plagioclase in two microgranitoid enclaves have anorthite ranges from 28.1 to 37.2%, in a mafic dike from 41.1 to 47.6%, and in two coarse-grained enclaves from 33.0 to 40.2% (CA84-114) and 43.2 to 52.1% (BW84-27). Anorthite contents of these mafic rocks overlap those of granodiorites and quartz monzodiorites of the Turtle pluton (31.4 to 42.2%) and have greater anorthite contents in the cores. Plagioclase anorthite compositions in cores of grains from mafic rocks commonly exceed that of plagioclase grains in host granodiorites and quartz monzodiorites, but compositions of plagioclase rims overlap those of host granitoids (31.4 to 42.2 %). One microgranitoid enclave (6 cm^2 in area) from biotite granite (BW84-20A) contains normally zoned plagioclase with anorthite contents of 17.7 to 30.0%, and orthoclase contents of 0.6 to 1.9%. These compositions are very similar to analyses of its host granite (An = 17.4 to 30.3, Or = 0.6 to 2.7) in the same thin section.

Biotite

Biotite occurs in all analyzed mafic rocks and average analyses are given in Table 3 and Figure 33. Except for the enclave in biotite granite of the Rim Sequence (BW84-20A), biotite compositions are similar among mafic rocks. Two microgranitoid enclaves (BW84-29 and CA84-45) and a mafic dike (CA85-65A) have overlapping compositions. Fe/Fe + Mg contents range from 0.43 to 0.48, Al^{IV} from 2.10 to 2.55, Ti from 0.30 to 0.46, Mn from 0.04 to 0.10, and F from 0 to 0.2 (molecular abundances based on 24 oxygens). The mafic dike biotite has higher Fe/Fe + Mg

(0.47 to 0.48) and less F (0 to 0.1) than the two enclaves but their compositions overlap within error. Biotite from two coarse-grained enclaves have different compositions. Their chemical ranges are: Fe/Fe + Mg from 0.38 to 0.44, Al^{IV} from 2.43 to 2.50, Ti from 0.39 to 0.45, Mn from 0.02 to 0.03, and F is about 0.1. Compared to other enclaves, coarse-grained ones have lower Fe/Fe + Mg and Mn, higher Al^{IV} , and similar Ti and F.

The microgranitoid enclave from biotite granite is distinct from other mafic rocks with respect to all of these elements (see Figure 33) and has higher Fe/Fe + Mg (0.49 to 0.53), Mn (0.15 to 0.20), and F (0.3 to 0.5), similar to greater Al^{IV} (2.35 to 2.68), and lower Ti (0.22 to 0.38).

Biotite from microgranitoid enclaves are similar to their host rock compositions as shown by shaded fields for a granite (BW84-20) and a granodiorite (BW84-23) from the Rim Sequence (Figure 33) which are hosts for BW84-20A and BW84-29, respectively. These data suggest that either biotites in microgranitoid enclaves and granitoids crystallized under very similar conditions or that biotite has equilibrated with the surrounding host rock. No host rock data is available for the mafic dike. Biotites from coarse-grained enclaves have different mineral chemistries than microgranitoid ones, and biotite from one coarse-grained enclave-host granitoid pair (BW84-27 & BW84-25) are dissimilar. These data imply that coarse-grained enclaves maintain a distinct mineral chemistry.

Amphibole

Amphibole analyses from 2 microgranitoid enclaves, 2 coarse-grained enclaves and 1 dike are discussed below. All amphiboles are magnesiohornblendes except for some analyses of a mafic dike, which are edenites. Two microgranitoid enclaves contain hornblende with Fe/Fe + Mg of 0.40 to 0.45, Al^{IV} of 0.89 to 1.30, Ti of 0.09 to 0.16, Mn of 0.10 to 0.14 and F of 0 to 0.2 (molecular abundances based on 24 oxygens). Amphiboles from the mafic dike contain Fe/Fe + Mg of 0.43 to 0.47, Al^{IV} of 1.16 to 1.30, Ti of 0.13 to 0.17, Mn of 0.06 to 0.07, and F of 0 to 0.1. Comparatively, the mafic dike has greater Fe/Fe + Mg, Al^{IV} , Ti and lesser Mn and F than one enclave

Table 3. Average biotite analyses from mafic rocks.

	CA85-20a		CA84-45		BW84-29	
	m encl		m encl		m encl	
n	77		15		47	
	AVE	STD	AVE	STD	AVE	STD
SiO2	35.94	0.70	37.74	0.75	37.43	0.75
TiO2	2.69	0.39	3.11	0.23	3.32	0.30
Al2O3	16.27	0.56	15.23	1.02	15.75	0.90
FeO	18.29	0.53	17.31	0.47	17.71	0.43
MnO	1.26	0.10	0.63	0.05	0.60	0.06
MgO	9.84	0.37	12.08	0.42	12.34	0.41
CaO	0.02	0.01	0.10	0.07	0.03	0.04
Na2O	0.21	0.09	0.26	0.08	0.26	0.18
K2O	9.34	0.35	8.62	0.50	9.08	0.46
BaO	0.20	0.04	0.20	0.05	0.04	0.08
F	0.92	0.09	0.34	0.04	0.26	0.05
Cl	0.02	0.03	0.05	0.01	0.05	0.04
H2O	3.82	0.08	3.80	0.06	3.88	0.05
Total	98.82		99.45		100.76	
Si	5.51	0.07	5.69	0.09	5.58	0.08
Al4	2.49	0.07	2.31	0.09	2.42	0.08
Al6	0.45	0.09	0.39	0.09	0.35	0.09
Ti	0.31	0.04	0.35	0.03	0.37	0.03
Fe	2.35	0.06	2.18	0.06	2.21	0.07
Mn	0.16	0.01	0.08	0.01	0.08	0.01
Mg	2.25	0.08	2.71	0.08	2.74	0.07
Ca	0.00	0.00	0.02	0.01	0.00	0.01
Na	0.06	0.03	0.08	0.02	0.08	0.05
K	1.83	0.06	1.66	0.08	1.73	0.08
Ba	0.01	0.00	0.00	0.00	0.01	0.00
Cl	0.01	0.02	0.01	0.00	0.00	0.00
F	0.44	0.04	0.16	0.02	0.12	0.02
O	24.00		24.00		24.00	
Fe/Fe+Mg	0.511		0.446		0.446	

Table 3. Average biotite analyses from mafic rocks.

	CA84-65a		CA84-114		BW84-27	
	mdike		cg encl		cg encl	
n	6		3		2	
	AVE	STD	AVE	STD	AVE	STD
SiO2	37.37	0.67	36.87	0.65	37.35	0.03
TiO2	3.39	0.15	3.49	0.12	4.02	0.08
Al2O3	15.36	0.23	16.48	0.56	15.97	0.03
FeO	18.91	0.21	14.89	0.22	16.87	0.00
MnO	0.41	0.05	0.18	0.01	0.22	0.01
MgO	11.58	0.12	13.64	0.23	12.31	0.17
CaO	0.08	0.04	0.06	0.01	0.09	0.00
Na2O	0.14	0.04	0.34	0.04	0.30	0.01
K2O	9.15	0.32	8.75	0.13	8.62	0.05
BaO	0.24	0.17	0.20	0.07	0.22	0.02
F	0.14	0.05	0.16	0.07	0.15	0.11
Cl	0.04	0.04	0.00	0.00	0.00	0.00
H2O	3.92	0.04	3.93	0.05	3.95	0.04
Total	100.71		98.99		100.04	
Si	5.61	0.04	5.50	0.06	5.57	0.01
Al4	2.39	0.04	2.50	0.06	2.43	0.01
Al6	0.33	0.05	0.42	0.07	0.37	0.02
Ti	0.38	0.02	0.39	0.01	0.45	0.01
Fe	2.37	0.05	1.87	0.02	2.10	0.01
Mn	0.05	0.01	0.02	0.00	0.03	0.00
Mg	2.59	0.04	3.04	0.04	2.73	0.03
Ca	0.01	0.01	0.01	0.00	0.01	0.00
Na	0.04	0.01	0.11	0.00	0.09	0.00
K	1.75	0.05	1.66	0.01	1.64	0.00
Ba	0.02	0.00	0.01	0.00	0.01	0.00
Cl	0.01	0.00	0.01	0.02	0.00	0.00
F	0.07	0.03	0.07	0.04	0.07	0.05
O	24.00		24.00		24.00	
Fe/Fe+Mg	0.478		0.380		0.435	

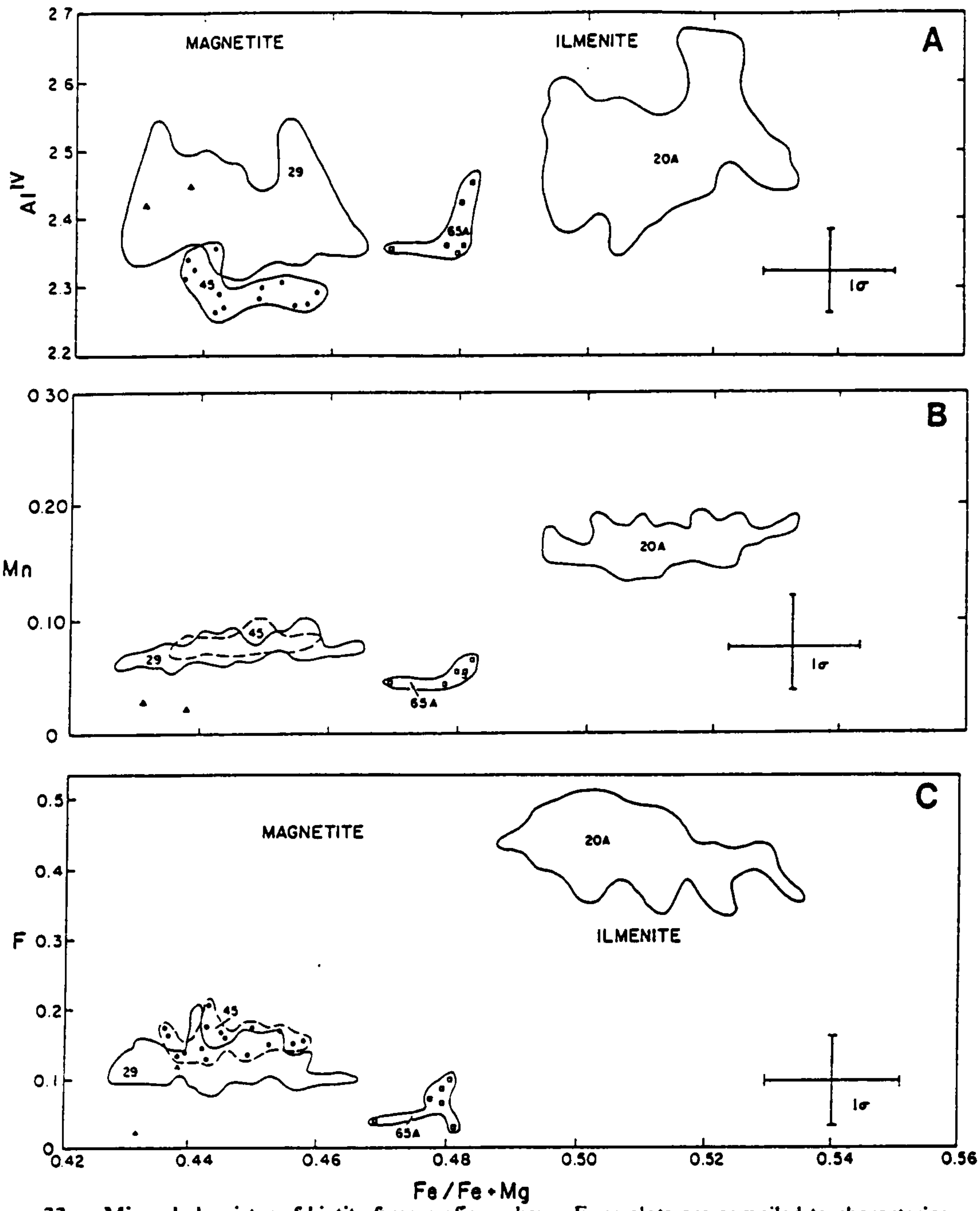

Figure 33. Mineral chemistry of biotite from mafic rocks: Four plots are compiled to characterize biotite chemistry. "MAGNETITE" and "ILMENITE" label the oxide assemblage of host granitoids. Samples 20A, 45, and 29 are microgranitoid enclaves (CA85-20A, CA84-45, BW84-29, respectively. 65A is a mafic dike (CA84-65A). Triangles are data from a dioritic enclave, BW84-27. Not shown at lower Fe/Fe+Mg are analyses of CA85-114, a dioritic enclave. This plot shows a microgranitoid enclave (20A) in ilmenite granite contains more Al^{IV}, Mn, and F and similar Ti than enclaves found in magnetite bearing-hornblende biotite granodiorites (45 and 29). Where host granitoid mineral compositions are known, biotites from enclaves have chemistries like their host granitoids (Figure 38 on page 133). Biotites from coarse-grained enclaves have similar or different chemistries than those from microgranitoid ones. Dikes are different from all analysed enclaves.

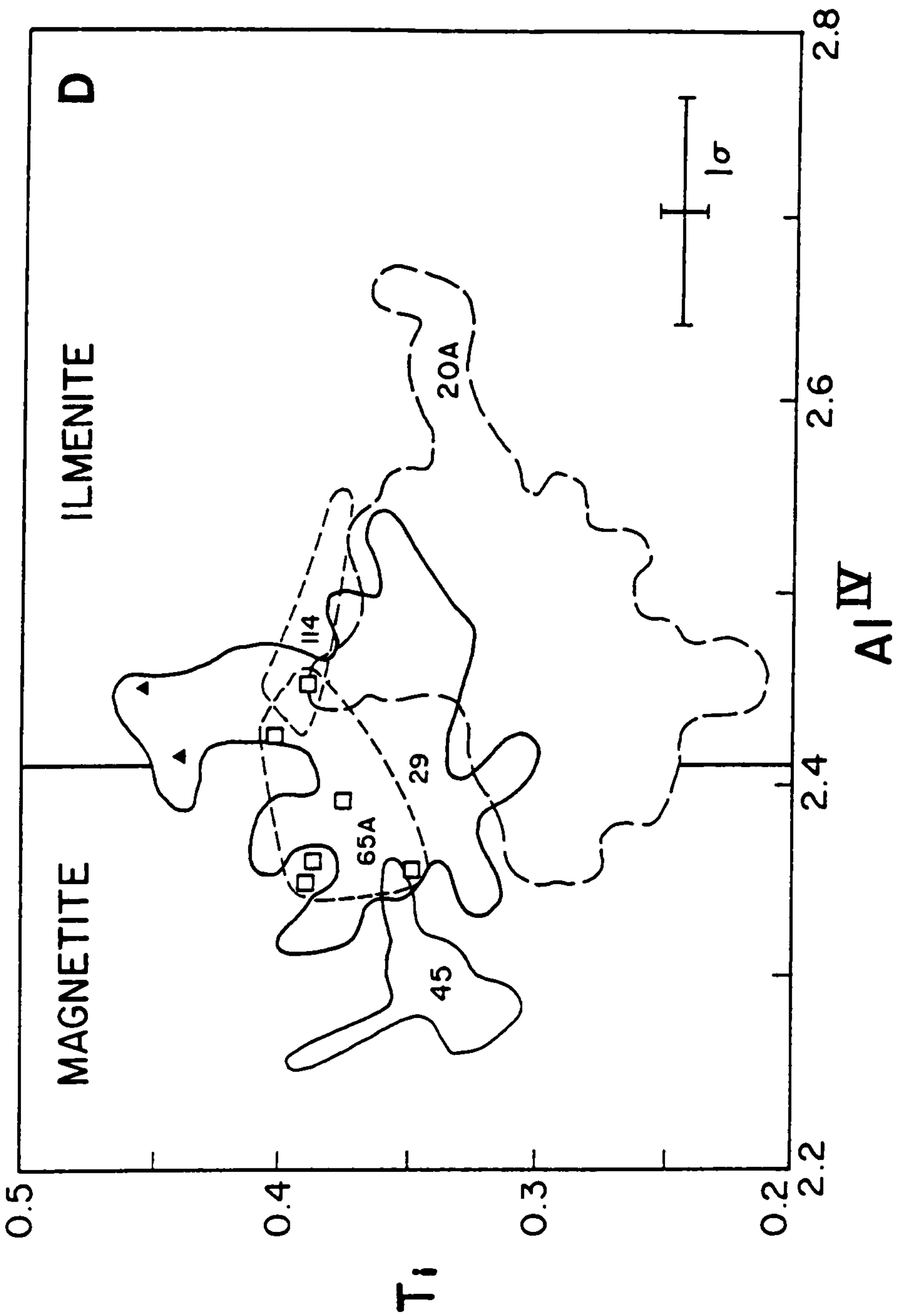
D
ILMENITE
MAGNETITE
20A
114
29
65A
45
1σ
0.5
0.4
0.3
0.2
2.2
2.4
2.6
2.8
Ti
Al IV

(CA84-45) but a similar composition to another (BW84-29). All three rocks occur in hornblende biotite granodiorite. Two coarse-grained enclaves contain hornblende with the following ranges Fe/Fe + Mg of 0.31 to 0.41, Al^{IV} of 0.89 to 1.30, Ti of 0.08 to 0.15, and F of 0 to 0.1. These values overlap those for microgranitoid enclaves except Fe/Fe + Mg and Al^{IV} extend to significantly lower values, and Mn concentrations are lower.

A comparison of amphibole analyses from the enclaves and granitoids is shown in Chapter 3 (Figure 39 on page 141). The amphiboles from one host rock-microgranitoid enclave pair (BW84-23 & -29) are only grossly similar. The enclave contains more Al^{IV} and Al^{VI}, Na and K, and less Fe than its host. For the one available coarse-grained enclave-host granitoid pair, (BW84-27 & BW84-25) the enclave has less Al^{IV}, more Al^{VI} , less Fe and K, and less Fe, more Mg, more Ca, less F, and has a lower Fe/Fe + Mg than its host. Unlike biotite, amphiboles both from microgranitoid and coarse-grained enclaves have mineral chemistries distinct from their hosts. These distinct chemistries can be marshalled to argue enclaves are not simple mineral segregations from granitoids.

Apatite

Preliminary apatite microprobe data indicate that one enclave contains apatite with composition similar to its host granite, and others have distinct compositions. Apatite is an early crystallizing, acicular phase in all microgranitoid enclaves and a mafic dike. It is early crystallizing in granitioids and it occurs in two crystal shapes--equant and acicular. Apatite compositions among the six rocks examined have overlapping mineral compositions except for F and MnO (Figure 34). There is a progressive increase in MnO and F contents in apatite from a microgranitoid enclave in granodiorite and a mafic dike, to apatite from a small microgranitoid enclave in granite, to apatite from granitoids. Acicular apatite from a mafic enclave (BW84-29; 13 analyses, 7 grains) and a mafic dike (CA84-65A; 5 analyses, 3 grains), both found in biotite hornblende granodiorite, have average formulas of $Ca_{4.7}$ $Fe_{0.01}$ $Mn_{0.01}$ $P_{3.0}$ O_{12} ($F_{0.5}OH_{0.5}$ and $Ca_{4.8}$ $Fe_{0.01}$ Mn_0 $P_{2.9}$ O_{12} ($F_{0.5}OH_{0.5}$), respectively, whereas apatite from a small enclave in biotite granite (BW84-20A) contains distinctly more Mn and F-- $Ca_{4.7}$ $Fe_{0.02}$ $Mn_{0.02}$ $P_{2.9}$ O_{12} ($F_{0.7}OH_{0.3}$) Acicular (15 analyses, 5 grains) and equant (25 analyses, 8 grains) apatite in granite (BW84-20A) have overlapping compositions though some analyses of acicular grains are relatively MnO poor. Equant apatite from granodiorite (BW84-23, 3 analyses, 2 grains) has a similar composition. Most importantly, a study of apatite in a single thin section of an enclave and host granite shows acicular apatite from the enclave (BW84-20A; 13 analyses, 5 grains) has a composition which overlaps that of the acicular apatite from its host (above), and overlaps the composition of equant apatite from its host (within errors). A survey of the literature suggests mafic rocks commonly contain less MnO and F than granitoids. Though errors are large given the range of MnO and F, these data indicate apatite from an enclave is not always chemically distinct from apatite in its host. The lack of distinction could be the result of its size, or longer residence time. One can disregard the possiblity these mafic rocks are mineral segregations from granitoids because: (1) mafic rocks lack equant apatite observed as an early crystallizing phase in granitoids, and (2) apatites can be chemically distinct. These mineral data suggest, in some cases, apatite from mafic rocks has equilibrated with its surroundings.

Conclusions from Mineral Chemistry

Though mafic rocks have bulk compositions different from granitic rocks ($SiO_2 = 65$ to 74 wt%), some mafic rocks have mineral chemistries that overlap those of the adjacent granitoids. The following minerals in microgranitoid enclaves and a mafic dike have overlapping compositions: biotite, plagioclase rims, and some apatite. Amphibole compositions are distinct. Coarse-grained enclaves, on the other hand, have mineral compositions different from the microgranitoid variety. These data indicate microgranitoid enclaves have crystallized under conditions like those of the

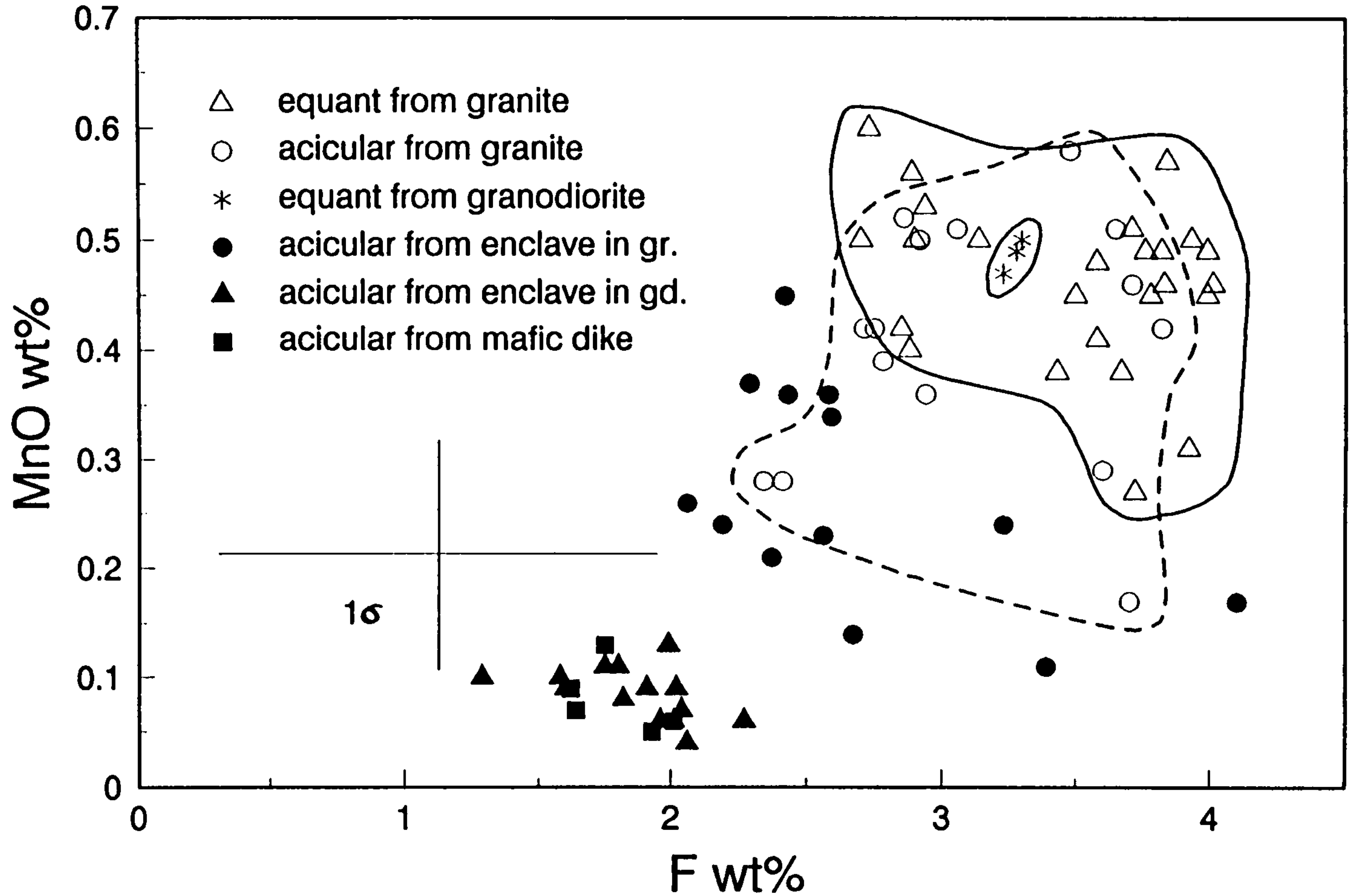

Figure 34. Apatite compositions from mafic rocks and granitoids: Mn and F contents of apatite are distinct in the rock types studied. Apatite from a mafic dike and a microgranitoid enclave in hornblende biotite granodiorite are poorer in both elements than apatite from an enclave in biotite granite. Equant and acicular apatite in granite and granodiorite contain more Mn and F than apatite in mafic rocks with the exception of apatite in a small enclave in granite (BW84-20A).

Turtle pluton, and/or they have equilibrated with the granitoids, that mafic dikes have some mineral compositions like that of granitoids, and that coarse-grained enclaves have maintained distinct mineral chemistries compared to their hosts.

Geochemistry

Introduction

Major and trace element geochemistry and Rb-Sr isotopic studies indicate these mafic rocks are high K basalts and andesites (terminology of Gill, 1981) with variable initial $^{87}Sr/^{86}Sr$ ratios. The microgranitoid enclaves are silica poor compared to the range of microgranitoid enclave compositions compiled from around the world by Didier (1973). The ranges of chemical composition and possible causes of that variation in all mafic rocks are discussed below.

Microgranitoid enclaves sampled for bulk chemistry averaged about 40×40×20 m in size. Samples exclude the region (2 to 3 cm) adjacent to host granitoids. Dikes and coarse-grained enclaves were sampled from core regions of the bodies.

Major Elements

Analyses of 5 microgranitoid enclaves, 3 coarse-grained enclaves, and 2 mafic dikes (Table 4) show calcalkaline trends using the FeO-MgO-alkalis criterion of Irvine and Baragar (1971), and they straddle the tholeitic/calcalkaline division (Fe/Mg versus SiO_2) of Miyashiro (1974). All mafic rocks are poorer in silica (50-55%) than the Turtle pluton granitoids (65 to 74 wt%). Major elements, with the exception of Ti, do not lie along the trend defined by their host granitoids (Figure 35 on page 115). For further discussion of the chemical relationship of mafic rocks to the Turtle pluton, see Chapters 4, 5 and 6.

Microgranitoid enclaves display a modest range of major element concentrations for the observed silica variation of 50.32 to 53.45 wt% (Figure 35). These rocks have similar contents of Al_2O_3, TiO_2, MnO, and P_2O_5, and variable FeO (7.57-10.33 wt%), MgO (4.51-6.71 wt%), CaO (7.33-9.50 wt%), Na_2O (2.02-3.33 wt%), and K_2O (1.21-2.00 wt%). Extending the high/low potassium subdivision of andesites (Gill, 1981) to basaltic rocks, the microgranitoid enclaves are high potassium basalts except for one medium K basalt (CA84-173, Figure 35). As compared to a compilation of enclave analyses by Didier (1973), these mafic rocks have lower SiO_2 and K_2O contents than most (50 to 54 in the range of 51 to 75 wt% and 1 to 2 in a range of 1 to 7 wt%, respectively).

Coarse-grained enclaves of the Turtle pluton contain more SiO_2 than most microgranitoid enclaves (52.59-54.79 wt%) and they contain less Al_2O_3 (12.20-15.35 wt%) and Na_2O (1.32-1.90 wt%), more CaO (9.17-10.67 wt%), and similar but variable FeO (7.93-9.01 wt%), MgO (6.61-9.96 wt%) and K_2O (0.87-2.01 wt%). One coarse-grained enclave (BW84-27) is a low K basalt and the other 2 samples are high K andesites. On Harker diagrams, coarse-grained enclaves plot as a distinct field from microgranitoid enclaves and dikes (Figure 35).

Relative to Turtle pluton granitoid analyses (65 to 74 wt% SiO_2) that define linear trends on Harker diagrams, coarse-grained enclaves contain more SiO_2 than microgranitoid enclaves and mafic dikes, but they do not lie intermediate to these mafic rocks and granitoids. This indicates no simple relationship ofthe three rock types. Distinct mineral chemistries of coarse-grained enclaves and whole rock chemistries suggest an origin different from microgranitoid enclaves and mafic dikes.

Table 4. Major and trace element chemistry of mafic rocks.

ID#	CA84-173	CA84-45	CA84-113	BW84-25a	BW84-29	CA84-65a	CA85-4c	BW84-27	CA84-114	CA85-118
TYPE	CFencl	FDHencl	CFencl	RSencl	RSencl	mdike	mdike	cg encl	cg encl	cg encl
SiO2	50.32	50.83	51.27	52.02	53.35	51.40	52.09	52.59	54.75	54.79
TiO2	1.16	0.98	0.98	1.10	1.21	1.27	1.52	1.17	0.58	1.26
Al2O3	18.19	16.20	18.70	18.60	18.31	17.26	15.47	15.35	12.20	15.03
FeO	10.21	10.33	9.20	8.52	7.51	9.93	9.17	8.69	9.01	7.93
MnO	0.28	0.48	0.20	0.25	0.32	0.26	0.15	0.19	0.30	0.16
MgO	4.51	6.85	4.84	6.71	5.00	5.52	7.05	7.62	9.96	6.61
CaO	9.44	7.33	8.41	8.90	7.52	9.14	9.50	10.64	9.17	10.01
Na2O	3.33	2.10	2.61	2.02	2.74	2.44	2.34	1.87	1.32	1.90
K2O	1.21	2.00	1.61	1.86	1.90	1.71	1.55	0.87	1.85	2.01
P2O5	0.41	0.29	0.44	0.45	0.30	0.40	0.36	0.20	0.26	0.26
LOI	0.48	1.54	0.85	1.13	0.76	1.30	0.96	1.14	1.38	1.17
SUM	99.54	98.93	99.11	101.56	98.92	100.63	100.16	100.33	100.78	101.13
A/CNK	0.77	0.86	0.89	0.88	0.91	0.78	0.69	0.67	0.59	0.65
AN	52.48	61.90	61.01	67.92	58.03	60.10	57.81	66.15	66.23	62.28
Q	0.00	0.00	0.00	0.00	2.49	0.00	0.00	2.68	3.61	4.28
Or	7.15	11.82	9.51	10.99	11.23	10.11	9.16	5.14	10.93	11.88
Ab	28.18	17.77	22.09	17.09	23.19	20.65	19.80	15.82	11.17	16.08
An	31.11	28.87	34.56	36.19	32.05	31.09	27.13	30.92	21.90	26.55
C	0.00	0.00	0.00	0.00	0.00	0.00	0.00	0.00	0.00	0.00
Di	10.95	4.64	3.58	4.13	2.73	9.69	14.51	16.85	17.87	17.57
Hy	5.24	28.28	24.88	28.68	23.49	21.39	24.48	25.08	32.23	20.61
Wo	0.00	0.00	0.00	0.00	0.00	0.00	0.00	0.00	0.00	0.00
Ol	13.27	3.48	0.77	0.21	0.00	3.07	0.40	0.00	0.00	0.00
Mt	0.00	0.00	0.00	0.00	0.00	0.00	0.00	0.00	0.00	0.00
Il	2.20	1.86	1.86	2.09	2.30	2.41	2.89	2.22	1.10	2.39
Ti	0.00	0.00	0.00	0.00	0.00	0.00	0.00	0.00	0.00	0.00
Ap	0.95	0.67	1.02	1.04	0.70	0.93	0.83	0.46	0.60	0.60
Ba		139	186	296	190	495		163		
Rb	29	111	67	60	93	55	54	22	64	45
Sr	520	286	524	502	345	630	473	376	234	410
F		870		260	770	1200				

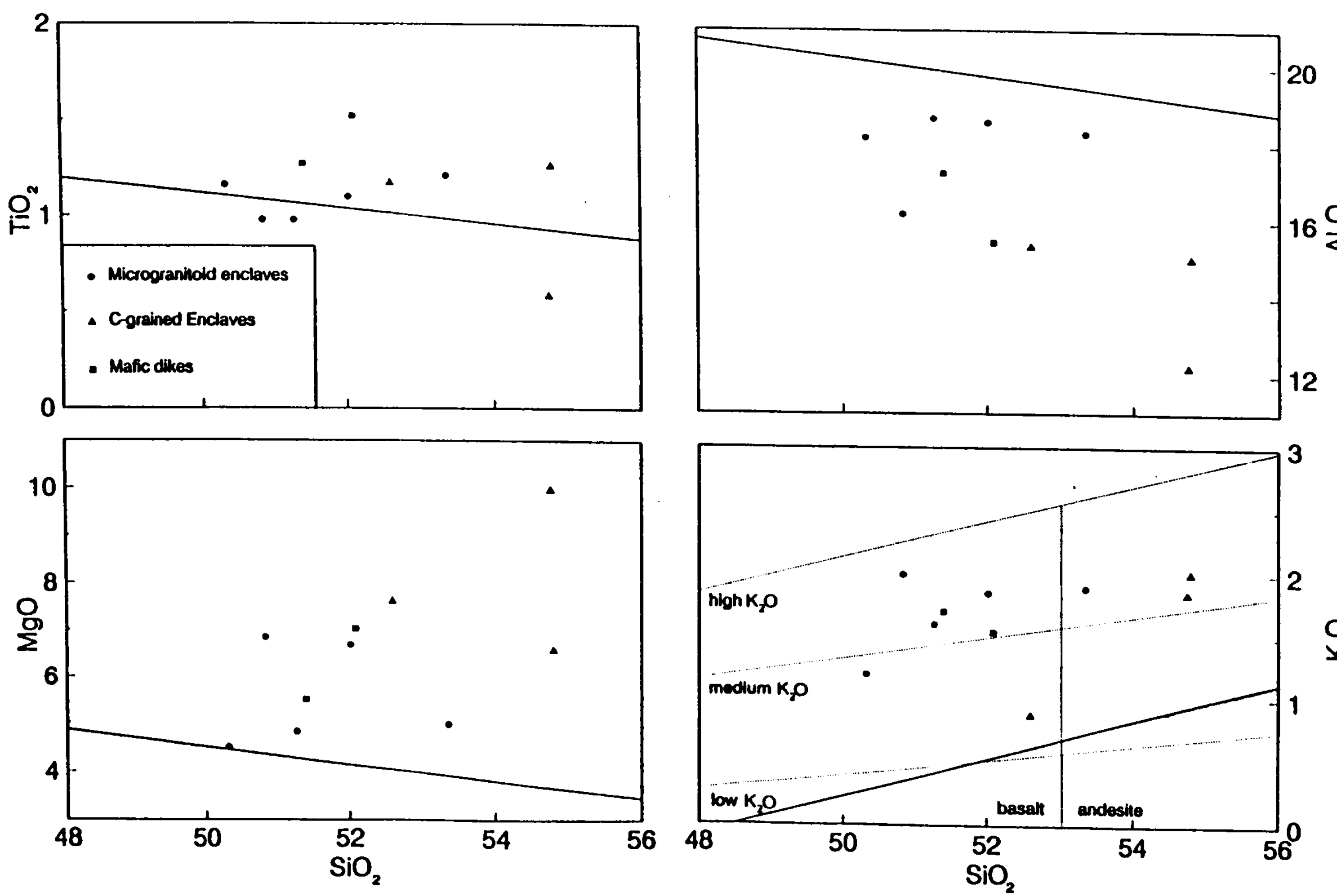

Figure 35. Major element chemistry of mafic rocks: Representative Harker diagrams show the MgO, TiO_2, Al_2O_3, and K_2O compositions of mafic rocks. A vector to Turtle pluton granitoid compositions is plotted as a solid line; it does not intersect mafic rock data. Microgranitoid and coarse-grained enclaves plot in separate fields, and mafic dikes have compositions similar to microgranitoid enclaves. All mafic rocks are medium to high K andesites and basalts (terminology of Gill, 1979, shown on K_2O diagram). Chemical variation among these three mafic rock types cannot be modelled as addition of granitic magma to one to form another.

Trace Elements

Selected trace elements (Ba, Rb, and Sr) from ten mafic rocks have a range of concentrations that overlap that of their host granitoids. Microgranitoid enclaves contain 139-296 ppm Ba, 29-111 ppm Rb, and 286-524 ppm Sr (Figure 36, and Chapter 4). Mafic dikes contain 495 ppm Ba (1 analysis), 54-55 ppm Rb, and 473-630 ppm Sr, and more Sr and less Rb than most microgranitoid enclaves. Compared to these mafic rocks, coarse-grained enclaves contain similar Ba (163 ppm), less Rb (22-64 ppm), and similar Sr (234-410 ppm) contents.

Microgranitoid enclaves have very similar Rb but lower Sr contents than their granitoid hosts (Figure 36 and Table 5). The similarity of Rb contents and biotite chemistries (Rb controlling phase in enclaves) from enclave and host suggest local equilibration of this phase.

Whole Rock Rb-Sr Isotope Geochemistry

Rb-Sr isotopic studies of mafic rocks were undertaken to test for isotopic equilibrium with host granitoids, and to evaluate sources of mafic rocks (also see Chapter 4).

The results of Rb-Sr isotopic studies are presented in Figure 36 and Table 5 on page 118. Enclaves and mafic dikes have variable $^{87}Sr/^{86}Sr$, $^{87}Rb/^{86}Sr$, and initial $^{87}Sr/^{86}Sr$ ($=Sr_i$, assuming a crystallization age of 130 Ma, that assumed for the Turtle pluton; see Chapter 4).

In Figure 36, compositions of nearby granitoids are compared to that of the mafic rocks. Microgranitoid enclaves have Sr_i similar to or greater than their hosts (solid tie lines). A mafic dike collected near an enclave-granitoid pair, has a much lower Sr_i than the other two rocks (dashed tie line). One coarse-grained enclave also has a distinctly lower Sr_i than a nearby microgranitoid enclave-host pair (dashed tie line). These data indicate the mafic rocks are not in isotopic equilib-

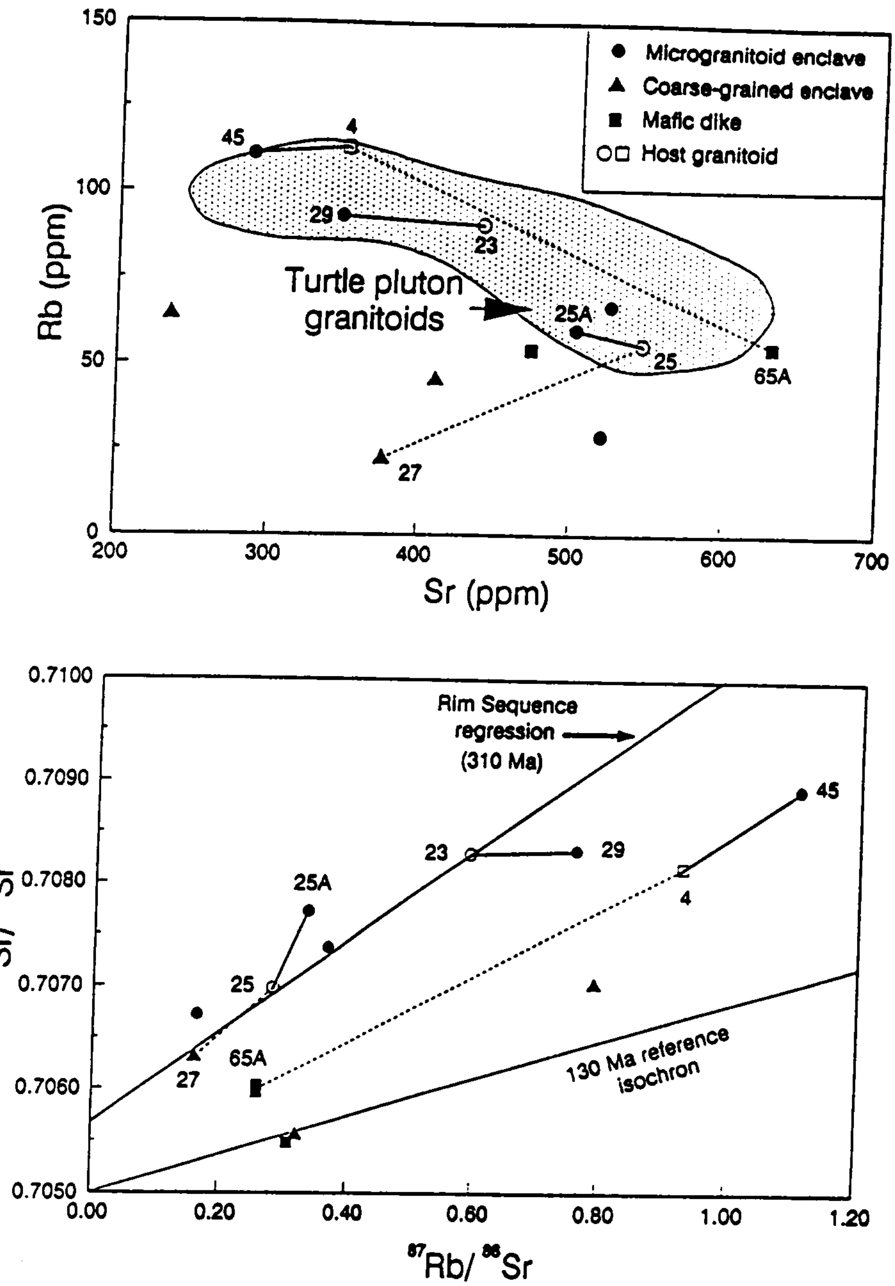

Figure 36. **Rb-Sr concentrations and isotopes of mafic rocks:** A. Microgranitoid enclaves have similar Rb and lesser Sr (solid tie lines) than their host (Rim Sequence = circle, Four Deuce Hills = square). Coarse-grained enclaves and mafic dikes contain less Rb and similar Sr concentrations than their hosts (dashed tie lines). Shaded field shows the range of compositions for granitoids. B. Enclaves from the Rim Sequence generally do not lie on the regression of Rim Sequence granitoid data, and microgranitoid enclaves have Sr_i > or < that of their hosts (solid tie lines). A microgranitoid enclave from the Four Deuce Hills (CA84-45) is more radiogenic than its host (CA85-4, square). Coarse-granied enclaves and mafic dikes are less radiogenic than their hosts (dashed lines). The scatter of the data from mafic rocks suggests no age significance can be assigned to the data.

Table 5. Geochemistry of mafic rock-host rock pairs.

	BW84-23 host gd	BW84-29 m encl
SiO2	66.90	53.35
K2O	2.82	1.90
FE#	0.66	0.60
Ba	688	190
Rb	90	91
Sr	440	346
Sr_i	0.7071	0.7069

	BW84-25 host gd	BW84-25a m encl	BW84-27 cg encl
SiO2	64.96	52.02	52.59
K2O	2.19	1.86	0.87
FE#	0.69	0.56	0.53
Ba	784	296	163
Rb	53	58	21
Sr	546	503	376
Sr_i	0.7065	0.7071	0.7060

	CA84-4 host gd	CA84-45 m encl	CA84-4c m dike
SiO2	68.18	50.83	52.09
K2O	3.72	2.00	1.55
FE#	0.68	0.60	0.57
Ba	985	186	495
Rb	112	108	55
Sr	357	284	613
Sr_i	0.7065	0.7069	0.7056

* FE# calculated from wt%, trace elements in ppm.

rium with adjacent Turtle pluton granitoids though some mafic rock compositions overlap the overall field (shaded) for granitoids.

Mafic rocks, except dikes, have Sr_i greater than 0.706. This value is generally accepted as a minimum crustal value (Kistler and Peterman, 1978). Dikes have lower Sr_i (0.7049-0.7055), ones intermediate between crustal values, and accepted mantle values as represented by MORB (Hart and Brooks, 1980).

Field evidence of disruption of mafic dikes by surrounding Turtle pluton granitoids, and the textural similarity of microgranitoid enclave and mafic dikes suggest these dikes are a potential source of this enclave type. The difference in Sr_i of enclaves and dikes may be the result of interaction of enclaves with granitoids due to their smaller size or longer residence time, however because some enclaves have Sr_i greater than their hosts (a result reported in another study, Holden et al, 1987) their isotopic compositions can not be modelled as mxing of dike compositions and adjacent host. A more radiogenic component is required.

Apatite Data

Isotopic studies were extended to minerals in order to test for isotopic equilibrium among minerals in enclaves. Apatite was selected for preliminary study because it is an early crystallizing phase, one likely to record a pre-crustal interaction signature. Apatite from one microgranitoid enclave (BW84-29; Sr_i of 0.7071 ± 1) has a similar Sr_i to the whole rock enclave (0.7075 ± 2). Low Rb content (5 ppm) indicate a pure apatite separate. Apatite could have grown from a liquid with a crustal value of Sr_i, or this mineral could have reached equilibrium with a contaminated liquid by diffusion in a geologically reasonable time span (Watson et al., 1985).

Causes of Chemical Variation Among Mafic Rocks

Introduction

There is no consensus on the origin of mafic enclaves, though many workers agree a mantle-derived mafic magma is likely (Vernom, 1983; Reid et al., 1983; Holden et al., 1987, as examples). Evidence of synplutonic dikes, and igneous textures of enclaves are the best evidence for a mafic magma source for microgranitoid enclaves. Crustal values of Sr_i indicate crustal interaction is a part of enclave evolution. Given these mafic rocks occur in granitoids of known composition, the effects of local interaction can be considered, and then previous history will be discussed.

Possible mechanisms that result in chemical variation among basaltic magmas are: (1) fractional crystallization, (2) variable degree of partial melting, (3) different sources, (4) variable contamination be it from magma mixing or assimilation (Yoder, 1976). With the limited number of chemical data, and their limited ranges, it is difficult to test these mechanisms. The range of Sr_i among mafic rocks indicates that (1) and (2) above (which do not commonly result in variable Sr_i) are not viable mechanisms alone.

Microgranitoid Enclaves and Mafic Dikes

In the field, the disaggregation of mafic dikes that have textures like microgranitoid enclaves suggests a genetic relationship of enclaves and dikes. Microgranitoid enclaves and dikes are similar with respect to major elements, though dikes generally contain less Rb, more Sr, and have lower Sr_i. The cause of this chemical difference could be either that dikes are different mafic magmas, or that enclaves have suffered more thorough contamination, perhaps from surrounding granitoids. The merits of these possibilities are discussed below with reference to granitoid composition.

Major element compositions of microgranitoid enclaves and dikes are shown with the regression of Rim Sequence data (65 to 74 wt% SiO_2; Figure 35). The ranges of composition of enclaves are not drawn out toward granitoid compositions, nor is there a consistent relationship of enclave and dike compositions with respect to that of granitoids. Therefore, simple contamination of dikes by granitoids to form enclaves is unlikely.

In order to test whether crustal contamination of microgranitoid enclaves is from a local source, parameters particularly sensitive to contamination of basalt by granite (K_2O and Rb) were compiled with Rb-Sr isotopic data for three microgranitoid enclave-host rock pairs, a coarse-grained enclave, and mafic dike (Table 5). For microgranitoid enclaves there is a strong positive correlation of K_2O, Rb and Sr_i and a weak one for Sr and Sr_i. The salient chemical features of these pairs are:

1. Rb concentrations in microgranitoid enclave and host are very similar.
2. K_2O contents are much lower in mafic rocks than granitoids but Rb and K_2O are positively correlated.
3. Enclaves contain less Sr than their hosts, and a mafic dike, more.
4. Initial $^{87}Sr/^{86}Sr$ of microgranitoid enclaves are similar to or greater than their hosts, and a mafic dike has a lower Sr_i than its host.

Variable Sr_i ratios of microgranitoid enclaves and their hosts indicate lack of isotopic equilibrium, a result also reported in another enclave-granitoid study (Holden et al., 1987). Sr concentrations and isotopic signature are controlled by plagioclase which suggests this mineral (cores?) is not in equilibrium with the whole rock. Lack of isotopic equilibrium rules out a comagmatic origin of mafic enclaves and granitoids (simple cumulates or "cognate xenoliths" or early crystallizing liquids). Lack of a colinear relationship of all enclaves and granitoids negates the possibility of a simple binary mixture of two magma end members (see Chapter 5), and suggests a more complicated origin of enclaves.Enclave history probably includes partial local equilibration given similarities of some mineral chemistries (biotite and plagioclase rims) and similar Rb contents (controlled by biotite). The greater initial Sr_i of enclaves relative to hosts observed in this study and in Holden et al. (1987) indicates crustal contamination prior to local interaction with host magmas.

In comparison, mafic dikes contain lower Rb and K_2O concentrations than all but one microgranitoid enclave (CA84-173) and dikes have lower Sr_i ratios (0.7049-0.7055) than any enclave. These data suggest that either dikes are from a different source than microgranitoid enclaves, have had a different contamination history, or dikes are somewhat less effected by their local environments.

Coarse-grained Enclaves

Coarse-grained enclaves do not have the consistent correlation of Rb, K_2O, and Sr_i displayed by microgranitoid enclaves. The coarse-grained enclave with greatest Sr_i contains the least K_2O and Rb. This enclave (BW84-27) was collected about 20 meters from a micorgranitoid enclave-host rock pair (BW84-25 and BW84-25A) and it is not in isotopic equilibrium with either of these rocks (see -- Table id " unknown --REFID=tabrbsr).

Coarse-grained enclaves have different mineral chemistries, whole rock geochemistries, and Sr_i than most microgranitoid enclaves. Conclusions from these data are these coarse-grained enclaves had a different history than microgranitoid ones, and they are not in chemical equilibrium with their hosts. These data suggest coarse-grained enclaves are comagmatic or xenolithic with respect to the Turtle pluton.

Comparison to Other Complexes

In order to compare compositions of enclaves from the Turtle pluton to those in other plutons, and to basalts, a plot of K_2O versus SiO_2 shows the mean enclave composition, and standard deviation from a given suite (Figure 37). This plot was selected because K_2O is among the most sensitive major elements to crustal contamination. Results show that enclaves from the

Turtle pluton (TP) have similar compositions and ranges to basalts from the same region ("bas" from northeastern Turtle Mountains, Hazlett, 1986), though Turtle pluton enclaves contain more SiO_2. The Turtle pluton enclaves are similar in composition and range to those from the Sierra Nevada (r = Reid et al., 1983; f = Frost and Mahood, 1987) and the Malay Peninsula (k = Kumar, 1988). Enclaves from two other reversely zoned plutons (a = Ayuso, 1982; w = Wernicke, 1987) display a much greater spread, have compositions close to that of hybrid granite/enclave from the Sierra Nevada (fh = Frost and Mahood, 1987), and may be hybrids also. A mean of enclave data from France (c = Cantagrel,et al., 1984). is more SiO_2 and K_2O rich than any of the other reported suites. The large variations in enclave composition observed in some complexes could be due to variable hybridization with host rocks.

This compilation indicates microgranitoid enclaves from the Turtle pluton are similar to other microgranitoid enclaves, and these basaltic and andesitic enclaves are distinct from "hybrid" andesitic enclaves that contain greater K_2O and Si_2O.

Conclusions

Microgranitoid enclaves have textures and compositions that suggest they are basaltic magmas. Lack of isotopic equilibrium of mafic enclaves and host granitoids indicates mafic rocks are not simple cumulates or mafic precursors of the Turtle pluton (i.e. they are not comagmatic), and they are not mixing end members (not cogenetic). Elevated K, and Rb (and Ba) contents and high Sr_i values (> 0.7060) are compatible with crustal contamination of basalt. The source of crustal component is unknown, however correlations of Rb and Sr concentrations, and similarities of mineral chemistries with hosts (biotite and plagioclase) suggest at least some local interaction. Lack of pervasive metamorphic textures in enclaves indicate this interaction is magma mixing. Because enclaves have higher Sr_i than their host rocks, crustal contamination before local interaction probably occurred.

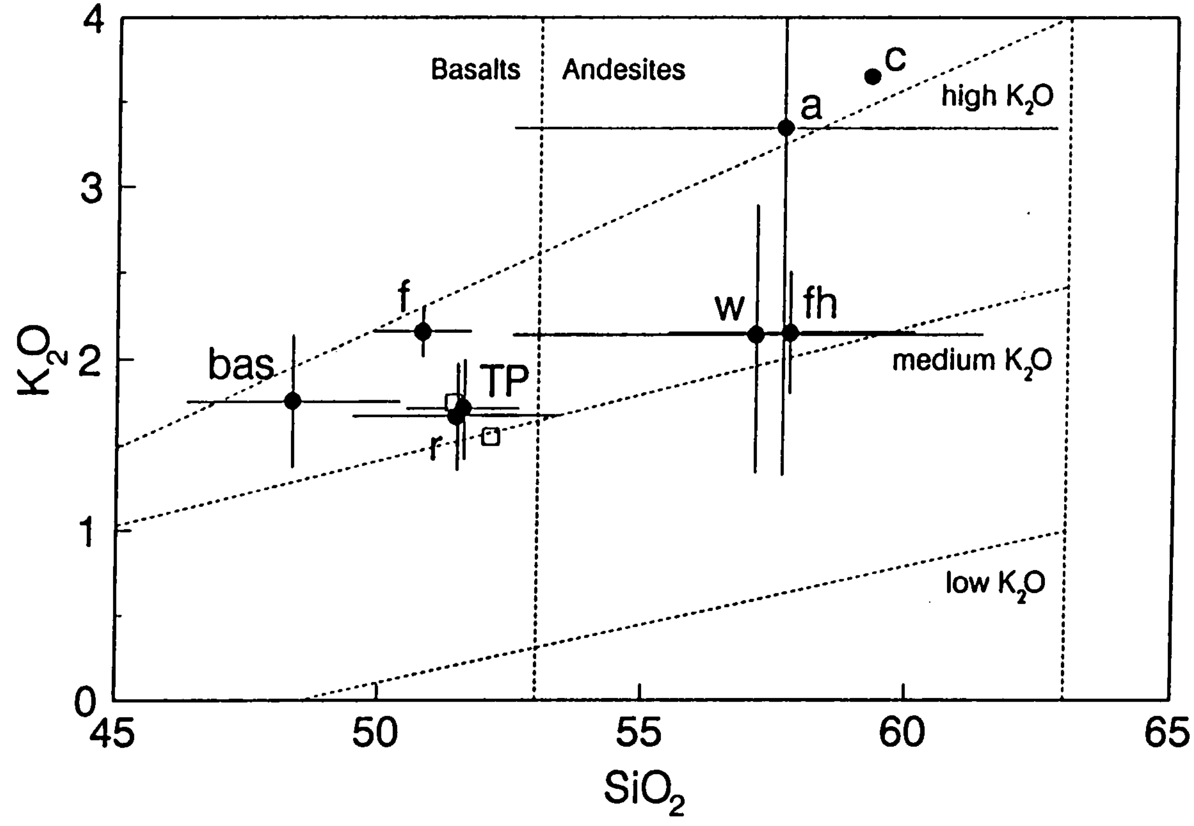

Figure 37. **Comparison of microgranitoid enclave compositions to other studies:** A plot of average K_2O versus SiO_2 (dot) was chosen to represent major element compositions of microgranitoid enclaves in this and other studies because potassium is the major element most sensitive to crustal contamination. All samples are medium to high K_2O basalts and andesites (terminology of Gill, 1979). Basaltic enclaves cluster and have smaller standard deviations (cross) than andesitic ones. Included in the andesitic group are rocks called "hybrids" (fh) of granitoids (f; Frost and Mahood, 1986) and basaltic magmas. The lowest K_2O rocks of the andesitic group have similar to higher K_2O but greater SiO_2 than the basaltic group. In order to compare compositional ranges of basalts to mafic rocks of the Turtle pluton, data from Tertiary basalts (bas) in the Turtle Mts. (and adjacent Mopah range) are given (Hazlett, 1986). Basalts have similar K_2O but lesser SiO_2 than enclaves and mafic dikes (squares, individual analyses) of the Turtle pluton (TP). Basalts and basaltic enclaves have similar ranges of composition. These data suggest all enclaves have been contaminated by crustal material and that andesitic ones are more thoroughly hybridized. a = Ayuso (1982). c = Cantagrel et al. (1983); r = Reid, et al.(1983); w = Wernicke (1986).

Initial $^{87}Sr/^{86}Sr$ of early crystallizing apatite from an enclave similar to that of the whole rock enclave and surrounding granodiorite suggest that even this early crystallizing mineral does not record a pre-crustal contamination ratio, and that Rb-Sr isotopes cannot be used to distinguish minerals from disaggregated enclaves dispersed in granitoids from those that grew from a granitic magma.

Mafic dikes have textures very similar to enclaves and field relations suggest microgranitoid enclaves may be disaggregated dikes. Dikes have lower Rb, K_2O, and Sr_i, and may be less affected by local environment than enclaves.

Coarse-grained enclaves have whole rock and mineral chemistries and isotopic signatures distinct from all other rock types from the Turtle pluton. These rocks of basaltic and andesitic compositions have cumulus textures, however, Sr-isotopic evidence suggest they are not simple cumulates from the Turtle pluton. No field or other evidence suggests a genetic relationship of coarse-grained and microgranitoid enclaves. It is difficult to evaluate the influence of surrounding granitic magma on these bodies except to state that the smallest body (CA84-114) of about 10 m^3 contains modal potassium feldspar and a greater Rb content than other coarse-grained enclaves. Initial $^{87}Sr/^{86}Sr$ range of 0.7050 to 0.7060 is intermediate between mantle and crustal values and suggests a hybrid origin.

Chapter 3

MINERAL CHEMISTRY AND INTENSIVE PARAMETERS

Mineral Chemistry

Mineral chemistries of plutonic rocks reflect crystallization conditions, coexisting phases (including fluids), and subsolidus reactions. Mineral compositions may be used to estimate pressure, temperature, and fugacities of volatiles from empirical and experimental geothermometers and geobarometers. In granitic systems, estimates of intensive variables are difficult because of the available mineral assemblage and the tendency for minerals to reequilibrate at subsolidus conditions (Wones, 1981). Nonetheless, in some instances, simply the presence of a mineral phase in a plutonic rock (magmatic epidote for example; Hammarstrom and Zen, 1987) or the order of crystallization define crystallization conditions. Mineral chemistries from granitoids and enclaves and, where possible, are used to limit the range of crystallization conditions.

All microprobe analyses are presented in APPENDIX 4 and methods in APPENDIX 3. Error analysis is based on 40 replicate analyses of a standard Kakanui hornblende and these are compared to accepted values from wet chemical analyses (APPENDIX 4). Error bars on all figures are equal to 2 standard deviations/mean for the Kakanui hornblende analyses times mid-range values for the mineral under discussion. This description of error may exaggerate the error for Mn as it occurs in small concentrations in the selected standard (0.01 cations per 24 oxygens).

Biotite

Average biotite analyses (24 oxygen basis) from major rock types appear in Table 6. Samples from the Turtle pluton are arranged geographically (rim to core) followed by mafic rocks, garnet aplites and the Target Granite. Biotite chemistries commonly reflect differences in whole rock composition, fluid composition, and may reflect source rock compositions (Wones, 1981).

Turtle pluton

Changes of biotite composition correlate with position, rock type and accessory assemblage as may be seen from average analyses in Table 6 and from Figure 38. Figure 38A shows the intermediate composition of these biotites relative to the siderophyllite-eastonite-annite-phlogopite quadralateral, and the distinctly Fe-enriched composition of biotite in ilmenite + muscovite ± magnetite-bearing granite or ilmenite assemblage ($Fe/Fe + Mg = Fe\# > 0.50$) as compared to magnetite-bearing granitoid or magnetite assemblage ($Fe\# < 0.50$). Ilmenite assemblage rocks contain biotite with more Al^{IV}, (2.37-2.62 per 24 oxygens), F (> 0.3), and Mn (> 0.13) than magnetite assemblage rocks (Figure 38A-C) but have similar Ti concentrations (0.25-0.45; Figure 38D). One granodiorite sample with an intermediate assemblage (biotite + magnetite + trace sphene and no hornblende; BW84-18) contains biotite with a composition intermediate to hornblende-bearing (magnetite facies) and hornblende-free (ilmenite facies) rocks. Biotite from this rock contains intermediate Mn and F concentrations but have Al^{IV} and Ti concentrations like biotite in rocks of the magnetite assemblage. Biotite from a rock with very little hornblende (2 modal %, BW84-19) contains more Mn and F than the other hornblende-bearing rocks but is otherwise similar. Thus there is a progression of Mn and F concentrations (cations per 24 oxygens) from the rim of the pluton into its core, from 0.16 Mn and 0.40 F in the ilmenite assemblage rocks to 0.07 Mn and 0.11 F in magnetite-bearing rocks.

Table 6. Average biotite analyses from granitoids.

	CA85-5		BW84-20		BW20A	
	RSgr		RSgr		RSgr	
n	14		4		40	
	AVG	STD	AVG	STD	AVG	STD
SiO2	35.54	0.44	36.39	0.30	36.22	0.82
TiO2	2.96	0.61	3.07	0.09	2.66	0.49
Al2O3	17.07	0.31	16.71	0.21	16.05	0.68
FeO	19.71	0.47	19.37	0.17	19.20	0.60
MnO	1.33	0.12	1.34	0.10	1.24	0.10
MgO	9.57	0.32	9.68	0.34	9.42	0.48
CaO	0.07	0.02	0.02	0.01	0.04	0.02
Na2O	0.08	0.02	0.10	0.01	0.06	0.08
K2O	9.84	0.19	9.30	0.10	9.63	0.36
BaO	0.21	0.08	0.09	0.07	0.22	0.08
F	0.79	0.09	0.89	0.14	0.89	0.08
Cl	0.03	0.01	0.00	0.00	0.00	0.00
H2O	3.55	0.04	3.52	0.05	3.50	0.10
Total	100.75		100.47		99.13	
Si	5.43	0.05	5.53	0.03	5.47	0.19
Al4	2.57	0.05	2.47	0.03	2.53	0.19
Al6	0.50	0.06	0.52	0.04	0.50	0.26
Ti	0.33	0.07	0.35	0.01	0.35	0.10
Fe	2.52	0.06	2.46	0.02	2.31	0.17
Mn	0.17	0.02	0.17	0.01	0.16	0.02
Mg	2.18	0.06	2.19	0.08	2.18	0.19
Ca	0.01	0.01	0.00	0.00	0.01	0.04
Na	0.02	0.01	0.03	0.00	0.06	0.05
K	1.91	0.03	1.80	0.02	1.79	0.12
Ba	0.01	0.00	0.01	0.00	0.01	0.00
Cl	0.01	0.00	0.01	0.00	0.01	0.01
F	0.38	0.04	0.43	0.07	0.42	0.10
O	24.00		24.00		24.00	
Fe/Fe+Mg	0.536		0.529		0.526	

Table 6. Average biotite analyses from granitoids.

	BW84-18		BW84-19		BW84-23	
	RSgd		RSgd		RSgd	
n	7		4		22	
	AVG	STD	AVG	STD	AVG	STD
SiO2	37.00	0.48	36.53	0.36	37.33	0.45
TiO2	3.00	0.34	2.58	0.20	3.22	0.46
Al2O3	15.60	0.57	15.98	0.24	15.53	0.50
FeO	17.85	0.55	17.96	0.75	17.39	0.79
MnO	1.24	0.12	0.86	0.03	0.63	0.06
MgO	11.44	0.26	12.15	0.46	11.94	0.43
CaO	0.04	0.02	0.09	0.01	0.02	0.05
Na2O	0.23	0.19	0.44	0.08	0.08	0.02
K2O	8.96	0.40	8.04	0.18	9.37	0.70
BaO	0.09	0.03	0.14	0.05	0.16	0.05
F	0.44	0.09	0.30	0.03	0.20	0.03
Cl	0.00	0.00	0.00	0.00	0.03	0.02
H2O	3.74	0.06	3.80	0.02	3.87	0.06
Total	99.62		98.88		99.78	
Si	5.61	0.03	5.55	0.02	5.63	0.04
Al4	2.39	0.03	2.45	0.02	2.37	0.04
Al6	0.39	0.09	0.41	0.04	0.39	0.08
Ti	0.34	0.04	0.30	0.02	0.36	0.05
Fe	2.26	0.06	2.28	0.11	2.19	0.08
Mn	0.16	0.02	0.11	0.00	0.08	0.01
Mg	2.59	0.07	2.75	0.09	2.68	0.13
Ca	0.01	0.00	0.01	0.00	0.00	0.01
Na	0.07	0.05	0.13	0.02	0.02	0.01
K	1.73	0.09	1.56	0.03	1.80	0.12
Ba	0.01	0.00	0.01	0.00	0.01	0.00
Cl	0.00	0.00	0.00	0.00	0.01	0.00
F	0.21	0.04	0.15	0.01	0.10	0.02
O	24.00		24.00		24.00	
Fe/Fe+Mg	0.467		0.453		0.450	

Table 6. Average biotite analyses from granitoids.

	BW84-25		CA84-147		CA84-102	
	RSgd		CFqmd		gap	
n	25		33		3	
	AVG	STD	AVG	STD	AVG	STD
SiO2	37.05	0.46	37.87	0.96	36.21	0.13
TiO2	2.91	0.47	2.08	0.61	3.02	0.13
Al2O3	15.31	0.31	15.95	0.65	16.32	0.24
FeO	18.77	0.42	18.03	0.73	21.56	0.22
MnO	0.53	0.05	0.49	0.04	1.20	0.07
MgO	11.61	0.43	12.48	0.55	8.40	0.31
CaO	0.06	0.06	0.01	0.07	0.03	0.01
Na2O	0.13	0.05	0.10	0.17	0.16	0.02
K2O	9.20	0.34	9.45	0.75	9.21	0.02
BaO	0.27	0.15	0.19	0.10	0.21	0.05
F	0.22	0.16	0.46	0.22	0.35	0.04
Cl	0.09	0.03	0.08	0.04	0.00	0.00
H2O	3.82	0.09	3.78	0.11	3.74	0.05
Total	99.97		100.97		100.41	
Si	5.62	0.05	5.62	0.06	5.55	0.02
Al4	2.38	0.05	2.38	0.06	2.45	0.02
Al6	0.35	0.06	0.40	0.10	0.50	0.01
Ti	0.33	0.05	0.32	0.07	0.35	0.02
Fe	2.38	0.06	2.34	0.08	2.76	0.04
Mn	0.07	0.01	0.06	0.01	0.16	0.01
Mg	2.62	0.10	2.63	0.10	1.92	0.06
Ca	0.01	0.01	0.01	0.01	0.00	0.00
Na	0.04	0.01	0.06	0.05	0.05	0.01
K	1.78	0.06	1.74	0.09	1.80	0.02
Ba	0.01	0.00	0.01	0.00	0.01	0.00
Cl	0.02	0.01	0.01	0.01	0.00	0.00
F	0.11	0.08	0.17	0.10	0.17	0.02
O	24.00		24.00		24.00	
Fe/Fe+Mg	0.476		0.470		0.590	

Table 6. Average biotite analyses from granitoids.

	CA84-46		CA84-111	
			TGgr	
n	10		15	
	AVG	STD	AVG	STD
SiO2	36.04	0.52	36.36	0.68
TiO2	3.11	0.29	3.23	0.72
Al2O3	16.44	0.26	16.19	0.52
FeO	17.94	0.53	17.70	0.41
MnO	1.49	0.09	0.88	0.07
MgO	10.32	0.40	11.34	0.35
CaO	0.06	0.04	0.09	0.04
Na2O	0.08	0.07	0.09	0.02
K2O	9.72	0.66	9.32	0.41
BaO	0.15	0.07	0.14	0.08
F	0.21	0.04	0.34	0.03
Cl	0.02	0.01	0.04	0.03
H2O	3.81	0.04	3.77	0.05
Total	99.39		99.49	
Si	5.51	0.02	5.52	0.68
Al4	2.49	0.02	2.48	0.72
Al6	0.47	0.05	0.42	0.52
Ti	0.36	0.03	0.37	0.41
Fe	2.30	0.09	2.25	0.07
Mn	0.19	0.01	0.11	0.35
Mg	2.35	0.08	2.57	0.04
Ca	0.01	0.01	0.01	0.02
Na	0.02	0.02	0.03	0.41
K	1.89	0.11	1.81	0.08
Ba	0.01	0.02	0.01	0.03
Cl	0.01	0.00	0.01	0.03
F	0.10	0.02	0.16	0.05
O	24.00		24.00	
Fe/Fe+Mg	0.494		0.467	

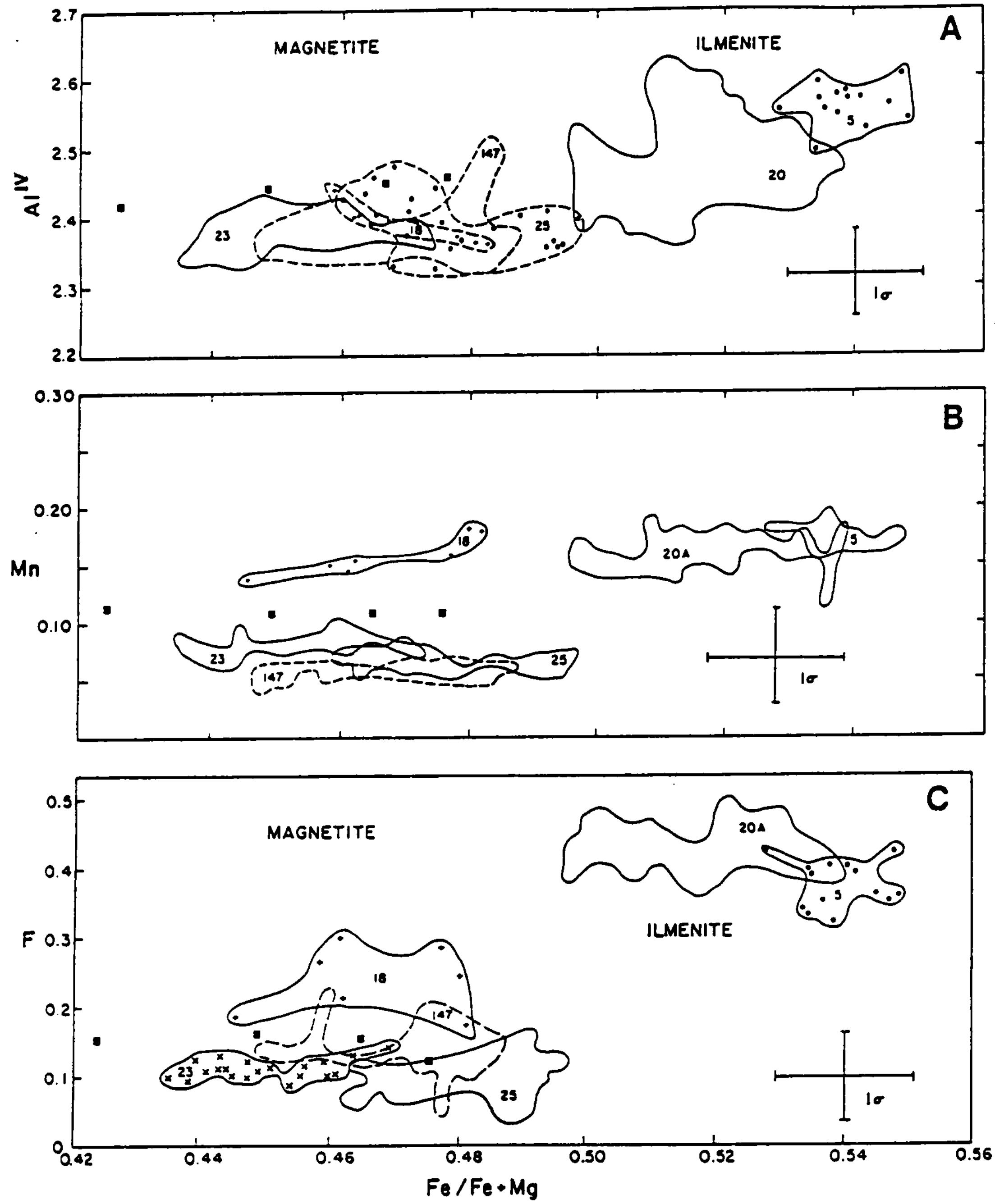

Figure 38. Biotite analyses from the Turtle pluton: A: Shows the intermediate composition of analyses on the biotite quadralateral, and the greater Fe/Fe + Mg (Fe#) and Al^{IV} of ilmenite assemblage granites (ILMENITE) as compared to the magnetite assemblage (MAGNETITE) of the Rim Sequence and Core Facies (CA84-147). B: Mn contents of biotites are greatest in hornblende-free rocks. (BW84-20 and BW84-18) and systematically decreases with increase of modal hornblende (distance into the pluton). C: Likewise, F contents of biotites in the ilmenite assemblage are greater than in magnetite assemblage rocks, and systematically decrease with distance into the pluton. D: Ti contents of ilmenite and magnetite assemblage rocks are similar.

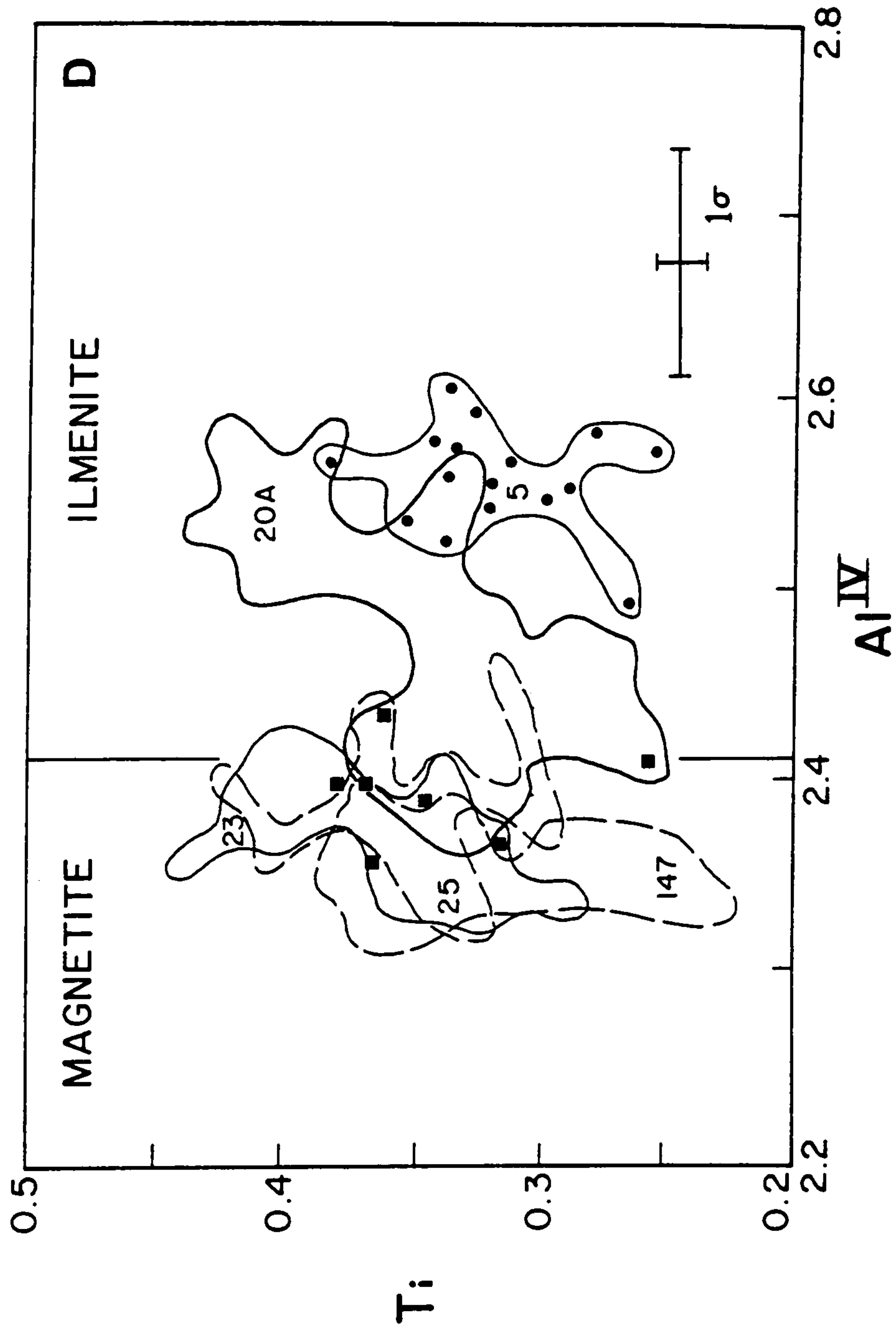
D
ILMENITE
MAGNETITE
20A
5
23
25
147
1σ
Ti
0.5
0.4
0.3
0.2
2.2
2.4
2.6
2.8
Al^{IV}

Some distinctions of biotite composition (Al, Fe#) correlate with opaque assemblage (± the appearance of muscovite) whereas other trace constituents (Mn, F) correlate with the modal absence of hornblende, and all variations correlate with geographic position in the Turtle pluton. Data compiled by Speer (1984) suggest the partition coefficient for Mn is greater for hornblende than biotite and the systematic decrease of Mn content of biotite from outer to inner Rim Sequence is probably influenced by the amount of coprecipitating hornblende. A similar decrease of F content in biotite may also reflect presence of a competing hydrous phase (amphibole) or changes of F/OH of coexisting fluids.

The chemistries of the two textural types of biotite discussed in Chapter 1, ragged biotite in hornblende and biotite in textural equilibrium with hornblende, overlap entirely in each of three samples of biotite + hornblende + sphene + magnetite granodiorite to quartz monzodiorite that were examined. There is also a lack of zonation in both the enclosed biotite and host hornblende euhedra. This suggests the two types of biotite crystallized in equilibrium, or that there were subtle shifts of physical parameters that allowed a shift of mineral stability from biotite to hornblende followed by biotite, or the 2 types of biotite reached equilibrium after crystallization.

Discussion

In order to understand chemical evolution of the Rim Sequence, mean biotite and whole rock analyses from a granite (BW84-20) and a granodiorite (BW84-18) are compared in Table 7. These samples were collected about 80 m apart in the field. The 2 rocks have the same crystallization sequence and assemblage except for opaque mineralogy (ilmenite ± magnetite versus magnetite) and the presence of trace muscovite in the granite and trace sphene in the granodiorite. The two whole rocks differ in silica content by 2.9 wt% and both rocks are weakly peraluminous ($Al/(Ca + Na + K) > 1$ & < 1.1). The major differences in biotite composition are F, Mg, Fe, Al and Si and lesser ones are Na and K. Biotite composition is antithetic with whole rock composition as described by de Albuquerque (1973) except for MgO and K_2O. Major element differences in biotite composition may be described by 3 exchanges:

Tschermak	$Al^{3+VI} + Al^{3+IV} = Si^{4+} + Mg^{2+}$
Fe-Tschermak	$Fe^{3+} + Al^{3+IV} = Si^{4+} + Mg^{2+}$
Fluorine-hydroxyl	$F^{1-} = OH^{1-}$.

These exchanges are affected by magma composition, fluid composition, temperature and pressure (Dymek, 1983). If these rocks represent liquid compositions or are related by fractional crystallization (see Chapter 5), the small observed difference in bulk rock composition should not greatly influence biotite chemistry. Given the proximity in the field, large differences in pressure or temperature are unlikely. Because biotite is the only modally significant hydrous phase in these rocks, F content of biotite should reflect that of the magma or coexisting fluid phase if other physical conditions are similar, and if subsolidus processes are insignificant (see Chapter 5). Therefore F enriched biotite from the very edge of the Rim Sequence (CA85-5 and BW84-20) co-existed with an F-richer fluid than magnetite assemblage rocks. This suggests a difference in fluid composition (and perhaps f_{O_2}) is the major cause of differences in biotite chemistry.

The question then becomes is the fluid composition in equilibrium with biotite an innate part of the pluton, or the result of interaction with country rock and/or fluids in equilibrium with country rock? As will be shown in Chapter 5, the samples being discussed have identical initial $^{87}Sr/^{86}Sr$ of 0.7082 and whole rock $\delta^{18}O$ of +6.5‰ (within error). Adjacent country rock has a much higher $^{87}Sr/^{86}Sr$ at 130 Ma of 0.8068 and $\delta^{18}O$ of +5.2‰ at the contact. From Sr isotopic data one can conclude no detectable assimilation of country rock (see Chapter 5), and based on homogenous whole rock $\delta^{18}O$ values throughout the pluton, probably a lack of interaction of fluids in equilibrium with country rock and the Turtle pluton. This is also supported by δD data (see Chapter 5). Ruling out external fluids in equilibrium with country rock and assimilation of country rock (Sr isotopic data), and noting the identical initial $^{87}Sr/^{86}Sr$ of the two rocks under discussion,

Table 7. Comparison of biotites, ilmenite and magnetite assemblages.

ILMENITE ASSEMBLAGE BW84-20a GRANITE bi+pl+ksp+qtz+ilm+musc				MAGNETITE ASSEMBLAGE BW84-18 GRANODIORITE bi+pl+ksp+qtz+mt+sph		
whole rock	average biotite	stand. dev.		average biotite	stand. dev.	whole rock
73.32	36.22	0.82	SiO2	37.00	0.48	70.45
14.55	16.05	0.68	Al2O3	15.60	0.57	15.23
1.49	19.20	0.60	FeO	17.85	0.55	2.20
0.46	9.42	0.48	MgO	11.44	0.26	0.88
	0.89	0.08	F	0.44	0.09	
1.07			A/CNK			1.07
0.7082			SR_i			0.7081
	5.47	0.19	Si	5.61	0.03	
	2.53	0.19	Al4	2.39	0.03	
	0.50	0.26	Al6	0.39	0.09	
	2.31	0.17	Fe	2.26	0.06	
	2.18	0.19	Mg	2.59	0.07	
	0.42	0.10	F	0.21	0.04	
	24.00		O	24.00		
0.645	0.526		Fe/(Fe+Mg)	0.467		0.584

A/CNK=molecular Al/(Ca+Na+K).
SR_i =initial $^{87}Sr/^{86}Sr$ at 130 Ma.

changes of F content of the magma and/or fluid as recorded in biotite composition is probably due to fractional crystallization.

Comparison to Biotite in Mafic Rocks

Compositions of biotite from microgranitoid enclaves and host granitoids are very similar (Figure 33 on page 107). General lack of metamorphic textures in enclaves and hosts suggests that biotite in these rock types reached equilibrium under magmatic conditions. Coarse-grained enclaves, on the other hand, have a different chemistry, including lower Fe and F contents, and probably did not equilibrate with the surrounding granitoids.

Amphibole

Average analyses of amphibole from granitoids, mafic dikes, and microgranitoid and coarse-grained enclaves appear in Table 8 and APPENDIX 4. Using the classification scheme of Hawthorne (1981) as modified from Leake (1978), assuming all Fe is 2+, and using the recalculation scheme of Robinson et al. (1982), site occupancies can be calculated. All Na + K occurs in the A-site and B-sites are full (1.98 to 2.10 = Ca + excess of C-site minus 5.00). All amphibole is calcic magnesio-hornblende except for amphibole from the Core Facies and some analyses of the mafic dike (CA84-65A). These are edenites (Na + K > 0.50; Figure 39).

Table 8. Average amphibole analyses from Turtle pluton and mafic rocks.

	BW84-19		BW84-23		BW84-25	
	RSgd		RSgd		RSgd	
n	9		29		41	
	AVG	STD	AVG	STD	AVG	STD
SiO2	46.28	1.10	46.36	0.79	45.42	0.94
TiO2	1.01	0.16	1.00	0.16	1.21	0.18
Al2O3	8.57	1.66	8.18	0.68	8.60	0.68
FeO	16.16	0.31	16.12	0.36	16.90	0.56
MnO	1.22	0.07	0.97	0.07	0.73	0.07
MgO	11.23	0.53	11.91	0.42	11.29	0.51
CaO	11.35	0.29	11.77	0.23	11.47	0.49
Na2O	0.97	0.08	0.86	0.09	0.86	0.12
K2O	0.74	0.09	0.77	0.06	0.99	0.28
BaO	0.08	0.05	0.11	0.04	0.10	0.05
F	0.20	0.05	0.09	0.08	0.11	0.06
Cl	0.00	0.00	0.07	0.06	0.11	0.07
H2O	1.92	0.02	1.95	0.03	1.91	0.04
Total	99.73		100.17		99.71	
Si	6.91	0.17	6.87	0.15	6.82	0.09
Al4	1.09	0.17	1.13	0.15	1.18	0.09
Al6	0.41	0.14	0.34	0.18	0.34	0.08
Ti	0.11	0.02	0.11	0.02	0.14	0.02
Fe	2.02	0.04	2.00	0.07	2.12	0.08
Mn	0.15	0.01	0.12	0.01	0.09	0.01
Mg	2.50	0.11	2.63	0.10	2.53	0.10
Ca	1.81	0.05	1.87	0.06	1.84	0.07
Na	0.28	0.02	0.25	0.03	0.25	0.03
K	0.14	0.02	0.14	0.01	0.19	0.06
Ba	0.01	0.00	0.01	0.00	0.01	0.00
F	0.09	0.02	0.06	0.03	0.06	0.03
O	24.00		24.00		24.00	
Fe/Fe+Mg	0.447	0.013	0.431	0.011	0.457	0.017

Table 8. Average amphibole analyses from Turtle pluton and mafic rocks.

	CA84-147		CA84-45		BW84-29	
	CFqmd		m encl		m encl	
n	25		19		27	
	AVG	STD	AVG	STD	AVG	STD
SiO2	44.80	0.56	47.66	0.77	46.28	0.75
TiO2	1.53	0.54	0.81	0.10	0.97	0.14
Al2O3	9.29	0.49	7.75	0.95	8.84	0.91
FeO	17.47	0.44	15.55	0.55	16.47	0.29
MnO	0.65	0.03	0.99	0.06	0.93	0.05
MgO	10.87	0.27	12.26	0.40	11.84	0.41
CaO	11.62	0.35	11.57	0.36	11.65	0.37
Na2O	1.14	0.16	0.98	0.10	1.02	0.10
K2O	1.09	0.11	0.69	0.08	0.85	0.06
BaO	0.11	0.04	0.13	0.02	0.03	0.03
F	0.18	0.07	0.04	0.02	0.07	0.07
Cl	0.15	0.10	0.24	0.08	0.12	0.10
H2O	1.88	0.04	1.91	0.05	1.95	0.05
Total	100.78		100.58		101.02	
Si	6.69	0.05	7.02	0.07	6.83	0.08
Al4	1.31	0.05	0.98	0.07	1.17	0.08
Al6	0.33	0.06	0.36	0.10	0.36	0.09
Ti	0.17	0.06	0.09	0.01	0.11	0.02
Fe	2.18	0.05	1.92	0.08	2.03	0.04
Mn	0.08	0.00	0.12	0.01	0.12	0.01
Mg	2.42	0.06	2.69	0.08	2.60	0.09
Ca	1.86	0.06	1.83	0.04	1.84	0.06
Na	0.33	0.05	0.28	0.03	0.30	0.03
K	0.21	0.02	0.13	0.02	0.16	0.01
Ba	0.01	0.00	0.01	0.00	0.00	0.00
F	0.09	0.03	0.11	0.04	0.07	0.05
O	24.00		24.00		24.00	
Fe/Fe+Mg	0.474	0.011	0.416	0.013	0.438	0.011

Table 8. Average amphibole analyses from Turtle pluton and mafic rocks.

	CA84-65a		BW84-27		CA84-114	
	mdike		cg encl		cg encl	
n	10		5		5	
	AVG	STD	AVG	STD	AVG	STD
SiO2	46.07	0.67	47.32	1.35	48.69	0.17
TiO2	1.39	0.11	1.02	0.25	0.97	0.05
Al2O3	9.18	0.40	8.44	1.43	6.40	0.13
FeO	16.78	0.36	14.42	0.34	11.91	0.26
MnO	0.54	0.03	0.33	0.04	0.27	0.03
MgO	11.61	0.37	12.81	0.75	14.44	0.53
CaO	11.90	0.12	12.11	0.24	12.22	0.07
Na2O	1.07	0.15	0.66	0.09	0.99	0.33
K2O	0.97	0.05	0.73	0.12	0.58	0.01
BaO	0.05	0.04	0.04	0.02	0.04	0.04
F	0.09	0.05	0.04	0.03	0.10	0.09
Cl	0.06	0.06	0.00	0.00	0.00	0.00
H2O	1.98	0.03	2.02	0.03	1.99	0.05
Total	101.68		99.95		98.60	
Si	6.76	0.06	6.95	0.15	7.17	0.04
Al4	1.24	0.06	1.05	0.15	0.83	0.04
Al6	0.35	0.02	0.41	0.11	0.28	0.03
Ti	0.15	0.01	0.11	0.03	0.11	0.01
Fe	2.06	0.05	1.77	0.05	1.47	0.04
Mn	0.07	0.00	0.04	0.01	0.03	0.00
Mg	2.54	0.07	2.80	0.14	3.17	0.10
Ca	1.87	0.02	1.91	0.03	1.93	0.01
Na	0.30	0.05	0.18	0.01	0.23	0.01
K	0.18	0.01	0.14	0.02	0.11	0.00
Ba	0.00	0.00	0.00	0.00	0.00	0.00
F	0.05	0.03	0.02	0.01	0.05	0.04
O	24.00		24.00		24.00	
Fe/Fe+Mg	0.448	0.013	0.388	0.016	0.316	0.011

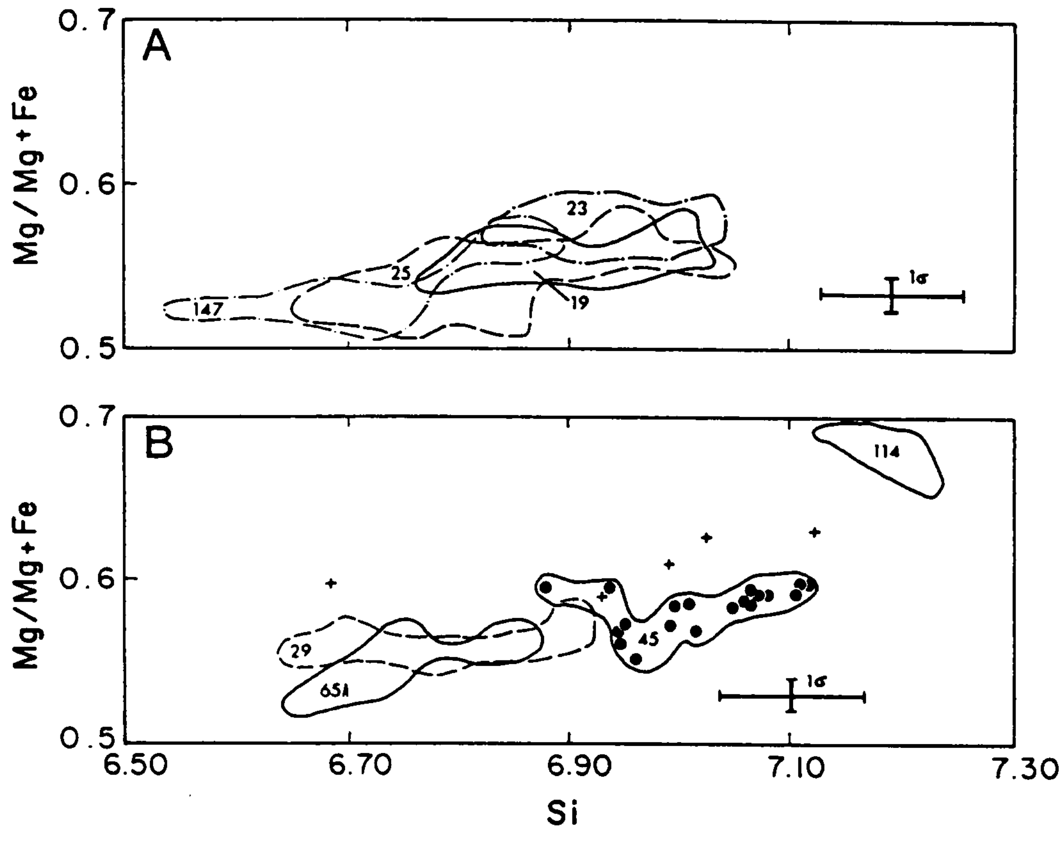

Figure 39. **Amphibole analyses from the Turtle pluton:** According to the classification scheme of Hawthorne (1981) as modified from Leake (1978), these amphiboles are calcic magnesiohornblendes with (Na+K < 0.50) except those from CA84-147 and CA84-65A, some of which are edenites (Na+K > 0.50). A. Analyses from the Rim Sequence rocks (BW84-19, BW84-23, BW84-25) contain more silica than most from the Core Facies (CA84-147), and have slightly greater Mg/(Mg+Fe). B. Amphibole from a microgranitoid enclave from the Four Deuce Hills (CA84-45) is more silica rich than one from the Rim Sequence (BW84-29A), and a mafic dike (CA84-65A). Hornblende from both coarse-grained enclaves (BW84-27, CA84-114) have greater Mg# than other mafic rocks. Amphibole compositions from a microgranitoid enclave (BW84-29)-granodiorite pair (BW84-23) show some overlap, whereas a coarse-grained enclave (BW84-27)-granodiorite pair (BW84-25) does not.

Turtle pluton

All hornblende from the Rim Sequence of the Turtle pluton is similar in composition (BW84-19, BW84-23, BW84-25). Analyses of the Core Facies (CA84-147) contain less silica and more Na + K than those in the Rim Sequence and amphibole composition may reflect the K-enriched nature of this sample (see Chapters 5 and 6).

Comparison to Amphibole in Mafic Rocks

Hornblende from mafic enclaves and dikes are grossly similar to those in granitoids. The one analyzed host rock/enclave pair (BW84-23 and BW84-29) have amphibole compositions that partially overlap; hornblende from the mafic rock commonly contains less Si. Amphibole from coarse-grained enclaves has greater Mg/(Mg + Fe) and silica contents than most granitoids and are distinct from those examined in microgranitoid enclaves.

Relations of Mafic Silicate and Whole Rock Compositions

Correlations of mineral and whole rock compositions have been reported by numerous investigators (Dodge et al., 1968; Allen, et al., 1975; Allen and Boettcher, 1978; Wones and Gilbert, 1981; de Albuquerque, 1973). Relations of silica contents of biotite and amphibole with whole rock silica are shown in Figure 40. For granitoids, there is a positive correlation of amphibole and whole rock silica (regression line), and a negative one for biotite and whole rock silica (regression line). Mafic rocks which contain less whole rock silica than granitic rocks have mineral compositions similar to their host granitoids. Data from mafic rocks define trends that have slopes like that of granitoids but different intercepts. Positive correlation of amphibole chemistry with whole rocks (melts) have been described by Dodge et al. (1968), Allen et al. (1975), Allen and Boettcher (1978), and Wones and Gilbert (1981) who suggest that amphibole chemistry reflects the silica activity of the melt. If this is the case, one would expect enclave amphibole to have lower silica contents than those of granitic rocks. This is not observed. De Albuquerque (1973) and Speer (1984) report a negative correlation of silica contents biotite and whole rock. Aluminum activity of the melt probably controls silica content of this sheet silicate, and biotite in enclaves is predicted to contain more Al and less Si. It does not. The overlapping silica contents of biotite in granitoids and mafic rocks, and likewise for amphibole suggest equilibration of the enclave and surrounding granitic magma.

Fe and Mg partitioning between biotite and amphibole, or $K_D = (X_{Fe}^{BI}/X_{Mg}^{BI})/(X_{Fe}^{HB}/X_{Mg}^{HB})$ are similar for the two biotite textural types, and suggests that no chemical distinction can be made. K_D for amphibole-biotite pairs is generally greater than or equal to 1 except for the high K Core Facies sample (CA84-147). It contains edenitic amphibole with a greater Fe# than coexisting biotite, and $K_D < 1$. Commonly, Fe# for biotite in igneous rocks are similar to that of coexisting amphibole (Speer, 1984), and K_D varies from 1.5 to 0.9 (de Albuquerque, 1973; Czamanske et al., 1981; Speer, 1984) but for a detailed study of one pluton (Liberty Hill, S.C.), tie line slopes vary from positive to negative (0.77 to 1.04, Speer, 1987). This suggests varying physical conditions are common within a single intrusion.

Plagioclase Feldspar

Average anorthite contents of plagioclase feldspar correlate with rock type. Granitoids of the Turtle pluton, Target Granite, garnet aplites, and mafic rocks were examined for range of anorthite content and zoning patterns. The results are shown in Figure 41.

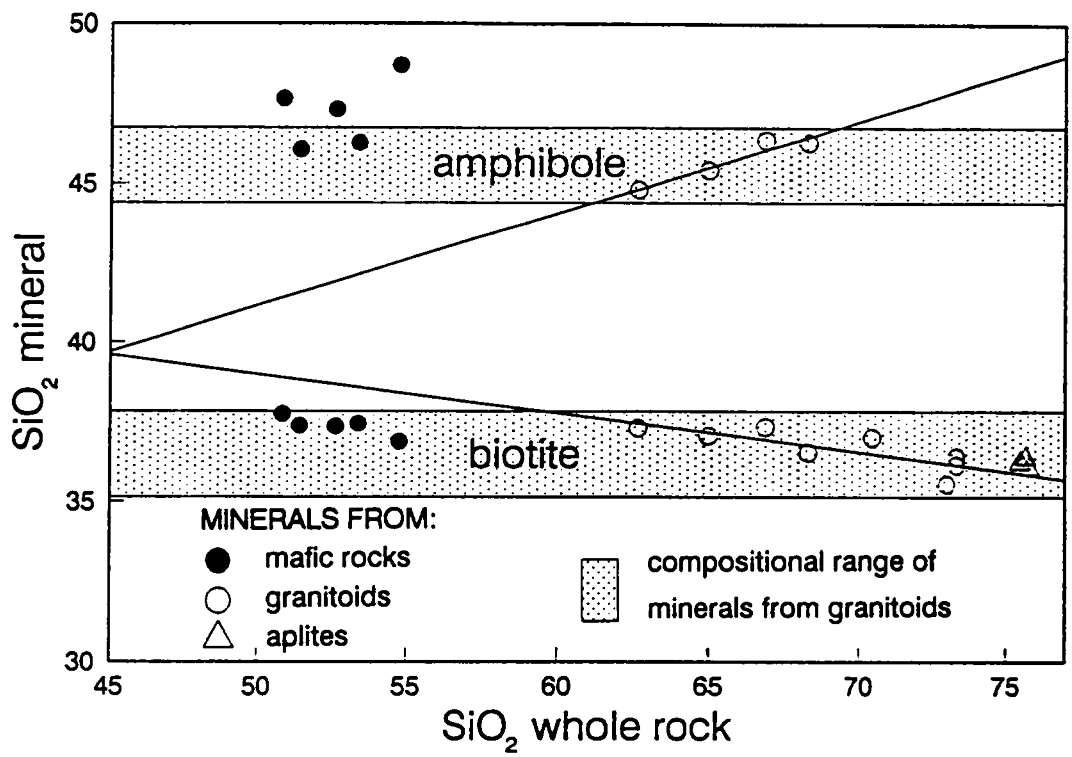

Figure 40. Silica contents of whole rocks and mafic silicates: As reported by other investigators (Dodge et al., 1968; de Albuquerque, 1973; Wones and Gilbert, 1981) there is a positive correlation of whole rock and amplibole silica contents, and a negative one for whole rock and biotite (solid lines). Mafic rocks, which contain less whole rock silica than granitoids, have biotite compositions very similar to those of granitoids and have amphiboles somewhat different average compositions. If amphiboles reflect the compositions of the magmas from which they grew as suggested by several authors (see text), amphiboles in mafic rocks should have lesser silica than those in granitoids. Similar compositions of minerals from enclaves and granitoid hosts suggest local equilibration.

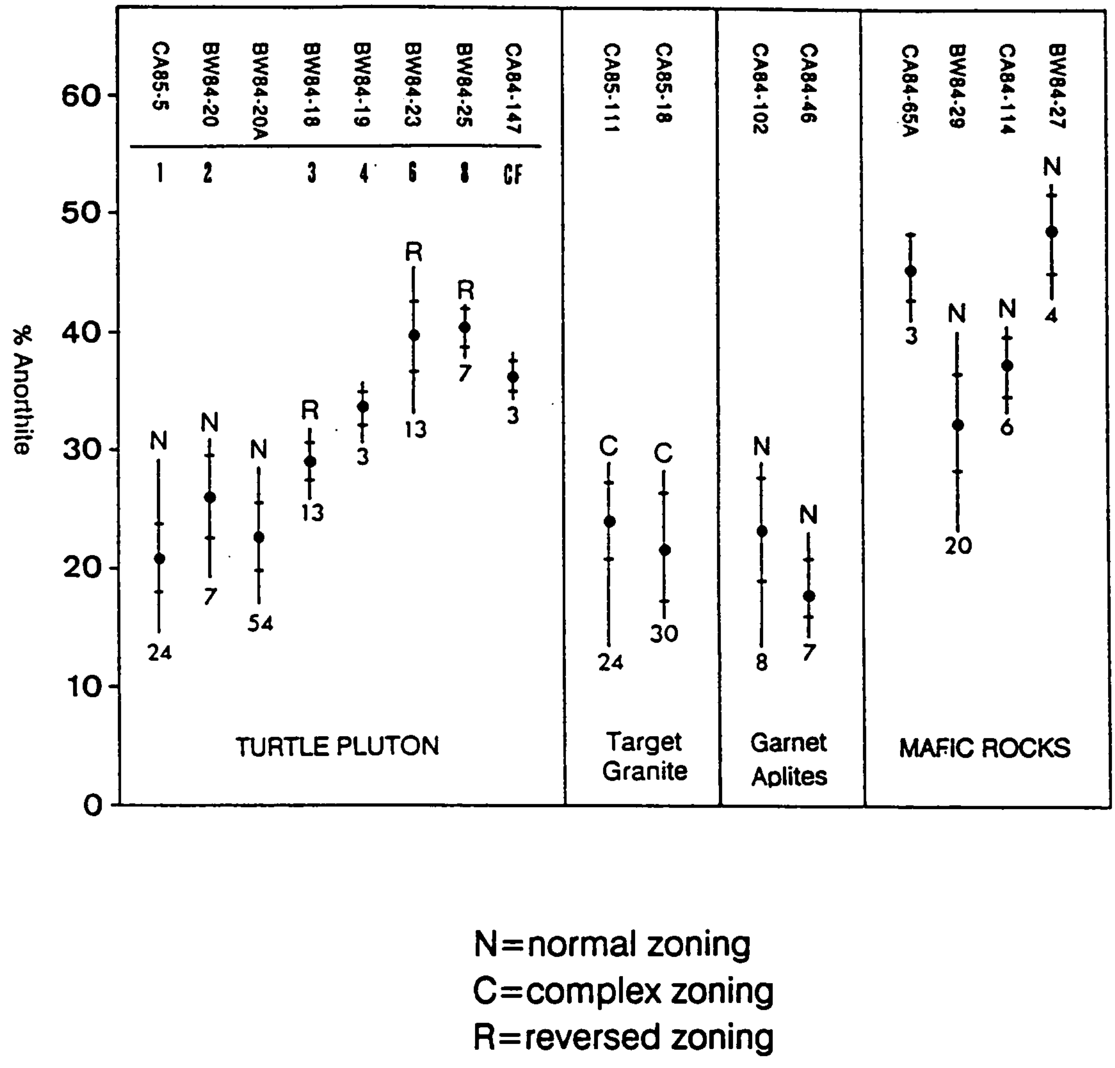

Figure 41. **Anorthite compositions and zoning patterns in plagioclase:** Average anorthite contents of plagioclase increase across the Rim Sequence (progression labelled 1 through 8 as in Figure 15 on page 34) from exterior to interior and into the Core Facies (left to right, labelled TURTLE PLUTON). Plagioclase from granites within 100 m of the country rock contact are normally zoned where as all other Rim Sequence rocks and the Core Facies are reversely zoned. Mafic rocks contain plagioclase with similar and greater anorthite contents and normal zonation patterns. Garnet-bearing aplites and the Target Granite have plagioclase with evolved compositions ($< An_{30}$).

Turtle Pluton

Anorthite content of plagioclase in the Rim Sequence correlates with position and increases steadily toward the Core Facies (Figure 41). The granite samples from the Rim Sequence display oscillatory but overall normal zoning patterns, have average anorthite contents of 21 to 25 %, standard deviations of about 2 %, and ranges of about 15 %. Analytical error is ± 1.5 mol.% anorthite (APPENDIX 4). Note that one sample has 54 analyses and that the standard deviation for this sample is similar to samples with many fewer analyses, thus a few analyses appear to be representative of the sample. In granodiorite, the plagioclase zoning patterns are oscillatory with a reversed trend and the rims show a return to normal zoning as exemplified by zoning patterns for two granodiorites (Figure 42).

Only 3 analyses are available from the Core Facies and this sample is anorthite poorer than the trend of the Rim Sequence. Petrographic observations indicate reversed zoning in most grains.

Other Rock Types

Plagioclase in the garnet aplites and the Target granite has evolved anorthite contents of less than 30 %. Garnet aplites have normal zoning, and the Target Granite, complex. Mafic rocks of the Turtle pluton have similar or greater anorthite contents than their host granitoids (An_{27} to An_{52}).

Discussion

The plagioclase textures in the Turtle pluton which must be explained are: (1) relatively small average grain size of equigranular granite at the margin, increase of grain size for 300 meters into

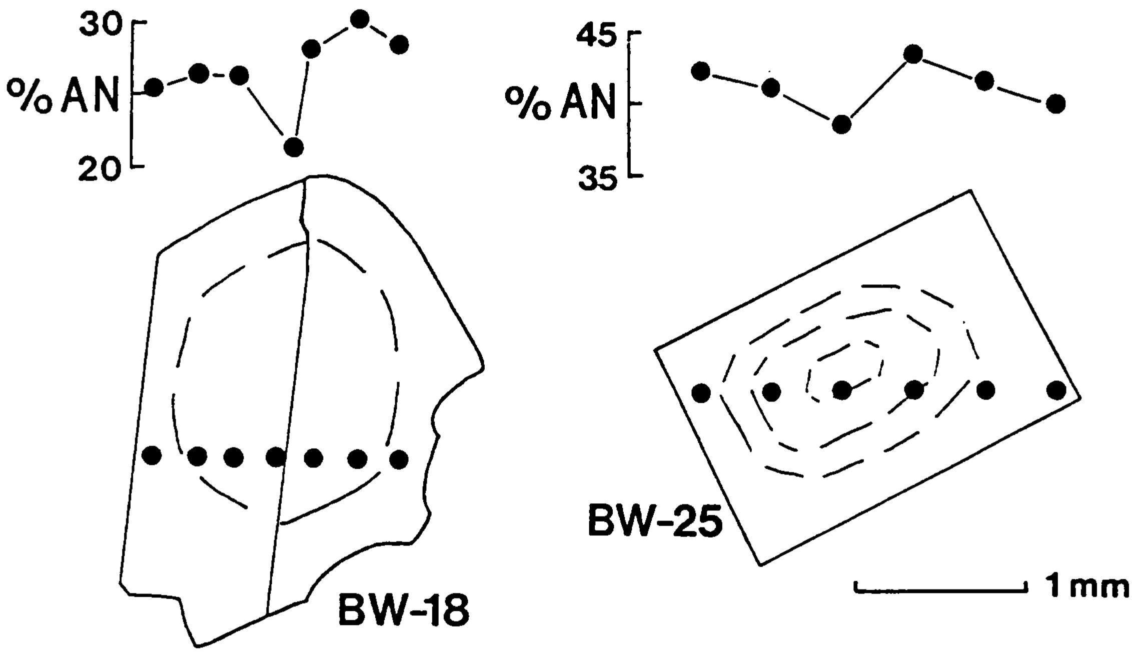

Figure 42. Plagioclase zonation patterns in two example granodiorites: Anorthite contents of plagioclase generally increases from core to rim, and has an overgrowth of more albitic composition.

the pluton, then a decreasing grain size into the Core Facies (Figure 16 on page 35). (2) the normal zoning of plagioclase in the Rim Sequence granite within about 100 meters of the country rock contact. (3) the reversed zoning of plagioclase in all other granitoids. (4) normal zoning in mafic enclaves.

As argued for biotite-hornblende reaction relationship (Reaction Section, Chapter 1), the parameters most likely to drive that reaction are increase in temperature, increase in water pressure, or change in composition to a more mafic one. The biotite to hornblende reaction could be produced either by fractional crystallization or by mixing with a more mafic magma. Likewise, plagioclase zoning patterns can be accounted for by either fractional crystallization (Loomis, 1982; Loomis and Welber, 1982) or magma mixing with a more mafic composition (Hibbard, 1981).

Plagioclase textures in the Turtle pluton listed above can be explained by undercooling and fractional crystallization of a predominantly crystal free magma due to intrusion. Progressive undercooling with no residual component build up in rim rocks (possibly from volatile loss) could yield normally zoned plagioclase, and a high degree of undercooling (chilled margin) would yield numerous small crystals (Loomis, 1982). In the core, slower cooling rates due to convection and previous local heating from conduction and build up of water or residual components in the melt from protracted fractional crystallization could allow formation of reversely zoned plagioclase (Loomis, 1982). At this lesser undercooling, crystal growth can keep pace with nucleation and fewer, larger crystals would form. The zoning patterns and crystal sizes observed in the Turtle pluton are predicted by Loomis and Welber (1982) for a crystallizing, dynamic, closed system, shallow pluton.

Normal zoning in enclaves could result from mechanisms like that described for the rim rocks (thermal undercooling).

Zoning patterns in feldspar could result from mixing with a more mafic and perhaps hotter magma (Hibbard, 1981). Granite with normally zoned feldspar could be uncontaminated magma, and granodiorite could be the result of mixing. The progressive increase of anorthite content of plagioclase cores from the Rim Sequence into the Core Facies suggests that no two rock samples had the same original liquid composition, and that a progressively more mafic (hotter?) liquid composition was in equilibrium with early plagioclase toward the interior of the Turtle pluton.

Like the reaction of biotite to hornblende, the dominant mechanism leading to observed plagioclase zoning patterns (fractional crystallization or magma mixing) cannot be resolved. In fact, whole rock geochemistry and isotopic studies presented in Chapters 4 and 5 suggest both must have been active.

Alkali Feldspar

Alkali feldspar in the Turtle pluton, Target Granite and garnet aplites is perthitic orthoclase with Or composition greater than 90%. Two feldspar geothermometry that yields temperatures less than 550°C (Green and Usdansky, 1986) indicates such high Or contents are the result of subsolidus reequilibration.

Sphene

Sphene occurs in all hornblende-bearing rocks in the study area and in a biotite granite sample that contains magnetite (BW84-18). Sphene analyses (APPENDIX 4) were preformed on euhedral to subhedral crystals from the Turtle pluton, and on microgranitoid and coarse-grained enclaves. The recalculation scheme assumes all iron is ferric. Compared to ideal sphene structure ($CaTiSiO_5$),the data indicate that the silica site is full to over full, Ca site is not full even with Mn, Mg, Ba, Na, and K, and the Ti site is full to overfull if Al and Fe (ferric) are incorporated. F contents (< 0.50 wt %) are in the detectable range. Oxide totals range from 93 to 98 wt % and qualitative microprobe REE analyses total 1.5 to 4.5 wt %.

As compared to sphene analyses from granites of the Mount Wheeler area, Nevada, the sphenes from this study contain less Al, and more Fe and REE (Lee, et al., 1969). In the Turtle pluton chemical diversity among sphenes may be described by:

$$Ti^{4+} + O^{2-} = Al^{3+} + OH^{1-}$$

$$F^{1-} = OH^{1-},$$

a substitution pair like that proposed for sphene by Franz and Spear (1985).

Opaque Minerals

Opaque oxides have been recalculated on the basis of 3 or 4 oxygens for ilmenite and magnetite, respectively, according to the method of Stormer (1983). Two assemblages occur in the Turtle pluton--titanomagnetite alone, and with manganoilmenite. Granite of the Rim Sequence, the ilmenite facies, contain both oxides. Ilmenite component in ilmenite ranges from 0.64 to 0.98 and Fe_{tot}/Mn (atomic) ranges from 9.04 to 0.45. Some ilmenites are extremely manganese rich (to 39 wt % MnO) and Mn-rich ilmenite has been interpreted to result from subsolidus reequilibration (Czamanske and Mihalik, 1972). All magnetite contains less than 0.015 ulvospinel component. This small ulvospinel composition restricts temperature and log fo_2 to between 590 °C and -17, and 500 °C and -24 (Spencer and Lindsley, 1981). Such low temperatures suggest subsolidus reequilibration. All other rocks from the Turtle pluton and Target Granite contain only magnetite with less than 0.01 ulvospinel. The exception is a single analysis of the Target Granite at 0.033.

One sample of a garnet aplite (CA84-46) contains both oxides but ilmenite is relatively Ti poor ($Ilm' = 0.06$ to 0.85) and $Fe_{tot}/Mn = 8.63$ to 0.29. Again magnetite contains less than 0.01 ulvospinel component and pairs yield subsolidus temperatures.

Apatite

Apatite occurs as equant and acicular grains in granitoids of the Turtle pluton. In a biotite granite (BW84-20A) both crystal shapes have very similar chemistries and an average formula of $Ca_{4.8}$ $Fe_{0.2}$ $Mn_{0.03}$ $P_{2.9}$ O_{12} ($OH_{0.1}$ $F_{0.9}$) with Cl contents below the detection limit (0.1 wt %). Three analyses from an equant grain in granodiorite (BW84-23) have an average composition of $Ca_{4.5}$ Fe_0 $Mn_{0.03}$ $P_{3.0}$ O_{12} ($OH_{0.2}$ $F_{0.8}$) which is relatively deficient in Ca and F as compared to those from granite.

Comparison to Mafic Rocks

Apatite from microgranitoid enclaves and a mafic dike primarily differs in Mn and F contents (see Chapter 3). An average apatite from an enclave in granodiorite is $Ca_{4.7}$ $Fe_{0.1}$ $Mn_{0.01}$ $P_{3.0}$ O_{12} ($OH_{0.5}$ $F_{0.5}$).

Muscovite

Muscovite from garnet aplites with apparent primary textures has a composition very similar to plutonic muscovite reviewed by Miller, et al. (1981). The average of 9 analyses from a garnet aplite (CA84-28) is $K_{1.70}$ $Na_{0.09}$ $Fe_{0.48}$ $Mg_{0.22}$ $Ti_{0.05}$ $Al_{5.35}$ $Si_{6.13}$ O_{20} ($OH_{3.92}$,$F_{0.07}$).

Garnet

Garnet from 3 aplites are spessertine-almandine-rich as can be seen from the average analyses below (Table 9). Such compositions are typical of plutonic garnets (Miller and Stoddard, 1980).

Intensive Variables

As in the studies of many other plutonic systems, estimates of physical conditions during emplacement and crystallization are difficult because of subsolidus reequilibration during slow cooling (Wones, 1981). In addition, small numbers of phases and complex solid solution series limit the potential number of geothermometers and geobarometers. In the case of the Turtle pluton, contact metamorphism of different bulk compositions cannot be used for estimates of pressure and temperature because of composition (mineral assemblage) and lack of contact effects. Thus estimates of physical conditions are from the plutonic rocks themselves.

Pressure

Field estimates of emplacement conditions may be obtained from contact geometries, degree of contact metamorphism, and presence of vesicles in saturated systems (Buddington, 1959). The Turtle pluton has sharp contacts, caused little contact metamorphism, and lacks vesicles, but these qualitative depth estimates from field criteria strongly depend on fluid content of the system. With these reservations in mind, intrusive style suggests a mesozonal emplacement level (2 to 4 kb).

Table 9. Average garnet compositions from aplites.

	CA84-28	CA84-46	CA84-102
TYPE	gap	gap	gap
number	9	2	7
SiO2	36.65	35.83	37.38
TiO2	0.18	0.56	0.36
Al2O3	20.99	19.81	18.82
FeO	20.67	12.94	16.35
MnO	22.48	29.77	24.75
MgO	1.34	1.23	1.38
CaO	0.49	0.87	0.72
Na2O	0.01	0.03	0.02
SUM	102.81	101.03	99.84
Si	2.939	3.068	2.936
Ti	0.011	0.022	0.034
Al4	0.051	0.000	0.030
Al6	1.932	1.820	1.883
Fe3+	0.068	0.180	0.118
Fe2+	1.318	0.942	0.769
Mn	1.527	1.720	2.066
Mg	0.160	0.169	0.150
Ca	0.042	0.063	0.077
Na	0.002	0.003	0.005
ALM	44.51	36.51	27.90
PYR	5.13	5.48	4.70
SPES	49.01	55.97	64.99
GROS	1.35	2.04	2.41

Pressure estimates can be obtained by hornblende geobarometry proposed by Hammarstrom and Zen (1986) and refined by Hollister et al. (1988). Caveats for use of this empirical barometer include: (1) appropriate mineral assemblage of Hb + Bi + Pl + Ksp + Q + Mt + Sph ± Ep and (2) silica activity fixed at 1 by presence of quartz during crystallization of hornblende. Results from averaged analyses of hornblende are given in Table 10. Calculated pressures from 2 granodiorites (BW84-23 and BW84-25) the three granitoids (BW84-23, -25 and CA84-147) are quite similar and yield pressures of about 3.5 kb (3.2 to 3.9 kb). (At these relatively low alumina contents, the two different calibrations yield small differences, less than the quoted error of 1 kb). Five microgranitoid and coarse-grained enclaves are quartz poor and K-feldspar poor but the similar calculated pressures (except CA85-114 and CA84-45) suggest they give geologically meaningful results.

Mineral assemblage itself restricts possible emplacement and/or source depths. Lack of primary epidote in the Turtle pluton granodiorite indicate emplacement pressures less than 8 kb (Naney, 1983; Zen and Hammarstrom, 1984; Hammarstrom and Zen, 1986). The range of stability of magmatic muscovite, much less its positive identification in thin section, is still in debate but the general consensus is that muscovite is not stable at pressures less than 3 to 4 kb (Zen, 1988). Presence of muscovite in the granite of the Turtle pluton and younger pegmatites and aplites suggest crystallization at pressures greater than 3 to 3.5 kb, similar to the 3.5 kb estimate from hornblende geobarometry.

Qualitative field data, mineral assemblage and hornblende geobarometry suggest crystallization at about 3.5 kb.

Temperature

Several geothermometers have been proposed for assemblages found in granitic rocks. For the Turtle pluton, potential geothermometers are two-feldspar (assuming a pressure), Fe-Ti oxide

Table 10. Hornblende geobarometry.

Sample	n		total Al	P(kb)[a]	P(kb)[b]
BW84-19	7	AVG	1.46	3.4	3.6
RSgd		STD	0.17	0.8	0.9
BW84-23	25	AVG	1.41	3.2	3.3
RSgd		STD	0.08	0.4	0.4
BW84-25	42	AVG	1.51	3.7	3.9
RSgd		STD	0.11	0.5	0.6
CA84-147	26	AVG	1.62	4.2	4.5
CFqmd		STD	0.07	0.3	0.4
BW84-29	25	AVG	1.51	3.7	3.9
m encl		STD	0.12	0.6	0.7
CA84-45	19	AVG	1.33	2.7	2.8
m encl		STD	0.10	0.5	0.6
CA84-65a	10	AVG	1.59	4.1	4.3
m dike		STD	0.07	0.4	0.4
CA84-114	5	AVG	1.11	1.7	1.6
cg encl		STD	0.02	0.1	0.1
BW84-27	3	AVG	1.46	3.4	3.6
cg encl		STD	0.26	0.1	0.1

[a] P= -3.92+5.03 Al , Hammarstrom & Zen, 1986.
[b] P= -4.76+5.64 Al , Hollister, et al., 1987.

which also yields oxygen fugacity information, biotite-apatite (OH-F exchange), and oxygen isotope exchange between minerals.

Microprobe analyses of adjacent plagioclase-potassium feldspar pairs (Green and Usdansky, 1986) and ilmenite-magnetite pairs (Stormer, 1983 and Spenser and Lindsley, 1981) both yield temperatures that suggest subsolidus reequilibration of these phases (< 550°C).

Apatite-biotite geothermometry based on OH-F exchange yielded variable results from magmatic (1000°C) to subsolidus (450°C) in a single sample of granite due to the variable F contents of both phases (up to 10 wt %, Ludington, 1978). A similar temperature range was obtained from this mineral pair in microgranitoid enclaves (1000 to 600°C). Such a broad range of temperatures (in part due to analytical uncertainty) is difficult to interpret.

Oxygen isotope thermometry is based on fractionation models from experiment (Bottinga and Javoy, 1975; Javoy et al., 1970). Using the fractionation constants of Bottinga and Javoy (1973 and 1975) oxygen isotope data yield temperatures between 630 and 715 °C from potassium feldspar-quartz pairs, 652 and 722 °C for hornblende-quartz pairs, and 526 to 549 °C for biotite-quartz from Rim Sequence granitoids (CA85-5, BW84-23, BW84-25) as given in Chapter 5. Biotite-quartz pairs from granitoids commonly give subsolidus results (Taylor and Sheppard, 1986), but other pairs suggest magmatic temperatures.

Temperature of the system may be estimated by comparison to crystallization experiments on similar compositions. Total lack of pyroxenes in the system suggests that temperatures near the emplacement level were less than 750 °C for granite and 780 °C for granodiorite (Naney, 1983; Figure 25 on page 72). All these data suggest crystallization temperatures of 780 to 630 °C with significant subsolidus reequilibration among some minerals.

Fugacity of Volatiles

Estimates of relative fugacities of volatile phases can be made from mineral assemblage and mineral chemistry. Redox reactions dependent on exchange of Fe-Ti and oxygen in opaque oxides have been calibrated to calculate T and fo_2 (Buddington and Linsley, 1964; Spencer and Lindsley, 1981). A change of opaque assemblage in the Rim Sequence of the Turtle pluton suggests a change in fo_2 from exterior to interior of the pluton, however this change from ilmenite to magnetite cannot be simply modelled as an exchange between two phases because of the ubiquitous presence of sphene, a Ti-bearing phase, in all magnetite assemblage rocks. A reaction involving these phases may be written:

$$3FeTiO_3 + 3CaO + 3SiO_2 + \frac{1}{2}O_2 = 3CaTiSiO_5 + Fe_3O_4$$

where CaO and O_2 are melt components (Zen, 1988). Quartz is present in both assemblages so that relative stability of opaque phases is controlled by activity of CaO and O_2 in the melt. Even this equation is an oversimplification as biotite contains significant Ti concentration (2.6 to 3.2 wt%) in both assemblages. The observed change in opaque assemblage cannot be used to define oxygen fugacity because the activities of Ti and Ca in the melts are unconstrained. Change in these activities could result in the change of mineralogy with no change of f_{O_2}, or a change of volatile composition could cause the same effect. As discussed in the section on biotite, F content of biotite in the ilmenite assemblage rocks suggests that ilmenite coexisted with magma or fluid enriched in F as compared to the magnetite-bearing assemblage. This F enrichment, suggested to result from fractional crystallization, could cause reduced f_{O_2}.

Finally, the reactions biotite to K-feldspar + magnetite (Wones and Eugster, 1965), and allanite to epidote (Affholter, 1987) indicate late stage or subsolidus oxidation, a common occurrence in plutonic environments (Czamanske and Wones, 1973; Wones, 1981).

Chapter 4

GEOCHEMISTRY

Introduction

The Turtle Pluton is a reversely zoned body composed of four facies, all of which are associated with microgranitoid and coarse-grained enclaves. Two younger intrusions, the Target Granite and Fortification Granodiorite, crosscut the Turtle pluton. Garnet aplites dike all facies of the Turtle pluton and Fortification Granodiorite, but were not observed in the Target Granite. Given these field relationships, whole rock chemical data are used to address the following questions:

1. What mechanism generated the zonation of the Rim Sequence (see Chapter 1)?
2. What is the chemical relationship of the Rim Sequence and Core Facies?
3. Are mafic rocks related to the Turtle Pluton?
4. Are garnet aplites differentiates of the Turtle Pluton?
5. What effect, if any, did the Target Granite have on the Turtle Pluton?
6. Are nearby intrusions, the West Riverside Range and Castle Rock pluton, chemically similar to the Turtle Pluton?

Major element, Rb and Sr analyses of 43 samples, and Ba analyses of 26 samples from the Turtle pluton, Target Granite, Precambrian host rocks and nearby granitoids were performed by X-ray Fluorescence spectrometry. Methods of sample preparation and analysis are given in APPENDIX 3. Additional analyses of country rock are supplied by K.A. Howard. Sample locations with identifying numbers are shown in Figure 5 on page 10, Figure 13 on page 32, Figure 17 on page 41, Figure 19 on page 45, Figure 20 on page 49, Figure 21 on page 52, and Figure 27 on page 80. Analyses and CIPW norms after Cox, Bell, and Pankhurst (1979) are given in Table 11.

Whole Rock Geochemical Data

Several processes have been proposed to explain chemical variations among plutonic rocks (see Chapter 1). The major mechanisms, fractional crystallization, magma mixing and assimilation (all either mixing or unmixing processes), can result in diagnostic major and trace element trends depending on how many end members (magmas, contaminants, or mineral phases) are involved. Involvement of just two, constant end members must result in linear trends (Bowen, 1928 White and Chappell, 1977; Langmuir et al., 1978). Mixing of two magmas can generate compositions between those two end members. Likewise, removal of a single phase or constant assemblage from a magma can generate a linear series of magmas. Involvement of more than two end members that are not mixed or unmixed in a constant proportion must yield curvilinear trends on element-element plots (Harker, 1909; Bowen, 1928). Fractional crystallization is considered an unmixing process in which a series of mineral phases is removed as a crystallizing assemblage changes with decreasing temperature. The trajectory of the evolving liquid changes with changing cumulate assemblage, and the resulting chemical trend is nonlinear (Bowen, 1928). In an intermediate composition magma system like the Turtle pluton, in which biotite, hornblende, plagioclase, and accessories are early crystallizing phases, the accumulation of a constant assemblage is unlikely, and fractional crystallization would be expected to result in curvilinear trends. Mixing of multiple magmas in changing proportion could also result in curvilinear trends.

Major elements can be relatively insensitive to such processes, especially over limited compositional ranges, because of their great abundances. Trace elements, on the other hand, because of their smaller concentrations and large distribution coefficients for some common minerals can

Table 11. Major and trace element analyses and CIPW norms.

ID#	BW84-20	CA85-5	BW84-18	BW84-19	BW84-22	BW84-23	BW84-24	BW84-25	CA85-120
TYPE	RSgr	RSgr	RSgd	RSgd	RSgd	RSgd	RSgd	RSgd	RSgd
SiO2	73.32	72.98	70.45	68.26	67.34	66.90	66.49	64.96	71.10
TiO2	0.20	0.21	0.28	0.40	0.43	0.45	0.47	0.53	0.31
Al2O3	14.55	14.50	15.23	15.65	16.25	16.31	16.14	16.56	15.63
FeO	1.49	1.89	2.20	3.21	3.21	3.43	3.61	4.41	2.92
MnO	0.08	0.10	0.11	0.11	0.10	0.10	0.11	0.10	0.06
MgO	0.46	0.53	0.88	1.29	1.26	1.77	1.56	1.95	0.77
CaO	1.87	1.82	2.61	3.52	3.93	4.12	4.18	5.22	2.78
Na2O	3.92	3.56	3.52	3.33	3.60	3.16	3.39	2.85	3.05
K2O	3.47	3.53	3.49	3.07	2.79	2.82	2.80	2.19	3.71
P2O5	0.09	0.07	0.12	0.16	0.18	0.19	0.20	0.23	0.14
LOI	0.30	0.28	0.44	0.37	0.76	0.84	0.67	0.51	0.28
SUM	99.75	99.47	99.33	99.37	99.85	100.09	99.62	99.51	100.75
A/CNK	1.07	1.12	1.07	1.04	1.02	1.04	1.00	1.01	1.12
AN	20.76	22.15	29.00	36.81	37.56	41.79	40.38	50.29	33.29
Q	31.63	32.76	28.33	25.65	23.48	24.18	22.58	23.18	30.19
Or	20.51	20.86	20.63	18.14	16.49	16.67	16.55	12.94	21.93
Ab	33.17	30.12	29.79	28.18	30.46	26.74	28.69	24.12	25.81
An	8.69	8.57	12.16	16.42	18.32	19.20	19.43	24.39	12.88
C	1.16	1.68	1.20	0.83	0.59	1.02	0.41	0.56	1.88
Di	0.00	0.00	0.00	0.00	0.00	0.00	0.00	0.00	0.00
Hy	3.70	4.63	5.97	8.65	8.51	10.15	9.94	12.27	6.88
Wo	0.00	0.00	0.00	0.00	0.00	0.00	0.00	0.00	0.00
Ol	0.00	0.00	0.00	0.00	0.00	0.00	0.00	0.00	0.00
Mt	0.00	0.00	0.00	0.00	0.00	0.00	0.00	0.00	0.00
Il	0.38	0.40	0.53	0.76	0.82	0.85	0.89	1.01	0.59
Ti	0.00	0.00	0.00	0.00	0.00	0.00	0.00	0.00	0.00
Ap	0.21	0.16	0.28	0.37	0.42	0.44	0.46	0.53	0.32
Ba	1100	1388	755	744	576	688	678	784	
Rb	102	93	103	92	87	90	85	53	100
Sr	276	293	309	382	428	439	434	558	336
F	500	630				290		550	

Table 11. Major and trace element analyses and CIPW norms.

ID#	CA85-4	CA84-50	CA84-143	CA84-147	CA85-122	CA86-14	CA85-13	CA84-158	CA85-85
TYPE	FDHgd	FDHgd	CFqmd	CFqmd	CFgd	CFgd	CFgd	CRgd	WRqmd
SiO2	68.18	67.41	63.03	62.59	61.68	58.68	64.81	68.42	66.12
TiO2	0.36	0.47	0.59	0.64	0.63	0.84	0.65	0.31	0.49
Al2O3	15.41	16.78	16.27	16.71	17.18	18.11	16.38	15.76	16.57
FeO	2.62	4.45	5.54	5.45	5.47	7.83	6.06	3.04	4.63
MnO	0.09	0.13	0.13	0.11	0.16	0.14	0.11	0.09	0.10
MgO	1.25	1.64	2.39	2.35	2.32	3.16	2.40	1.16	1.49
CaO	3.35	4.81	5.27	5.59	5.98	7.45	5.44	3.68	4.87
Na2O	3.73	3.00	2.33	2.48	2.73	2.62	2.56	3.22	2.94
K2O	3.72	2.88	3.35	3.03	1.91	1.73	2.87	3.29	3.00
P2O5	0.15	0.23	0.25	0.25	0.23	0.30	0.21	0.18	0.21
LOI	0.63	0.59	0.62	0.81	0.46	0.62	0.63	0.57	0.47
SUM	99.49	102.39	99.77	100.01	98.75	101.48	102.12	99.72	100.89
A/CNK	0.95	1.01	0.96	0.96	1.00	0.93	0.96	1.02	0.99
AN	31.00	46.83	54.94	54.87	54.94	59.48	53.31	38.53	47.81
Q	21.92	23.36	18.31	17.75	18.63	11.48	19.81	25.61	21.88
Or	21.98	17.02	19.80	17.91	11.29	10.22	16.96	19.44	17.73
Ab	31.56	25.39	19.72	20.99	23.10	22.17	21.66	27.25	24.88
An	14.32	22.36	24.04	25.52	28.16	32.55	24.73	17.08	22.79
C	0.00	0.53	0.00	0.00	0.30	0.00	0.00	0.64	0.14
Di	1.11	0.00	0.39	0.49	0.00	2.07	0.75	0.00	0.00
Hy	6.94	11.72	15.19	14.76	15.08	20.08	15.86	8.13	11.59
Wo	0.00	0.00	0.00	0.00	0.00	0.00	0.00	0.00	0.00
Ol	0.00	0.00	0.00	0.00	0.00	0.00	0.00	0.00	0.00
Mt	0.00	0.00	0.00	0.00	0.00	0.00	0.00	0.00	0.00
Il	0.68	0.89	1.12	1.22	1.20	1.60	1.23	0.59	0.93
Ti	0.00	0.00	0.00	0.00	0.00	0.00	0.00	0.00	0.00
Ap	0.35	0.53	0.58	0.58	0.53	0.70	0.49	0.42	0.49
Ba	985	1015	673	704	691			1063	
Rb	112	75	102	89	57	58	92	83	87
Sr	357	609	431	452	593	515	427	533	611
F				650					

Table 11. Major and trace element analyses and CIPW norms.

ID#	CA85-89	CA84-28	CA84-46	CA84-101	CA85-34	CA85-66	CA85-96	H79-123A	H84-92
TYPE	WRqmd	gap	gap	gap	gap	Xvm	Xvm	Xvm	Xvm
SiO2	66.05	76.57	75.80	75.49	74.70	75.72	73.56	75.10	72.20
TiO2	0.48	0.07	0.08	0.07	0.09	0.25	0.20	0.32	0.57
Al2O3	16.48	13.76	14.33	13.72	13.64	11.44	13.18	11.30	11.30
FeO	4.36	0.59	0.78	0.71	0.90	3.01	1.99	4.29	5.89
MnO	0.10	0.07	0.12	0.11	0.07	0.10	0.10	0.03	0.13
MgO	1.73	0.41	0.24	0.42	0.45	0.98	1.07	0.75	1.08
CaO	4.64	0.58	1.08	1.05	1.61	0.75	1.38	0.69	1.26
Na2O	2.98	3.67	3.00	3.40	2.82	2.36	2.50	2.48	1.55
K2O	2.69	4.85	5.89	5.17	4.29	4.40	4.40	4.07	4.71
P2O5	0.21	0.04	0.03	0.03	0.03	0.02	0.03	0.05	0.13
LOI	0.37	0.25	0.09	0.00	0.39	0.52	0.34	0.40	0.61
SUM	100.09	100.86	101.44	100.17	98.99	99.55	98.75	99.48	99.43
A/CNK	1.02	1.12	1.08	1.05	1.12	1.15	1.16	1.16	1.14
AN	46.19	7.77	16.90	14.84	24.61	15.24	23.92	12.87	29.16
Q	23.12	34.42	32.52	32.50	37.10	39.73	36.11	42.64	36.84
Or	15.90	28.66	34.81	30.55	25.35	26.00	26.00	24.05	27.84
Ab	25.22	31.05	25.39	28.77	23.86	19.97	21.15	20.99	13.12
An	21.65	2.62	5.16	5.01	7.79	3.59	6.65	3.10	5.40
C	0.73	1.51	1.13	0.69	1.50	1.48	1.87	1.68	1.67
Di	0.00	0.00	0.00	0.00	0.00	0.00	0.00	0.00	0.00
Hy	11.71	2.12	2.12	2.44	2.75	7.74	6.17	8.91	12.29
Wo	0.00	0.00	0.00	0.00	0.00	0.00	0.00	0.00	0.00
Ol	0.00	0.00	0.00	0.00	0.00	0.00	0.00	0.00	0.00
Mt	0.00	0.00	0.00	0.00	0.00	0.00	0.00	0.00	0.00
Il	0.91	0.13	0.15	0.13	0.17	0.47	0.38	0.61	1.08
Ti	0.00	0.00	0.00	0.00	0.00	0.00	0.00	0.00	0.00
Ap	0.49	0.09	0.07	0.07	0.07	0.05	0.07	0.12	0.30
Ba		415	830	1420					
Rb		144	119	105	125	140	134		128
Sr		73	187	196	282	62	320		100
F							700		

Table 11. Major and trace element analyses and CIPW norms.

ID#	H84-93	H79-118	H79-124	CA85-18	CA85-111	CA85-101	CA85-15	CA85-58
TYPE	Xvm	Xgg	Xag	TGgr	TGgr	TGgr	TGgr	FGDgd
SiO2	74.40	73.70	68.90	76.26	75.68	71.02	69.03	69.16
TiO2	0.02	0.24	0.75	0.14	0.17	0.29	0.30	0.37
Al2O3	13.70	13.50	13.40	13.37	14.08	15.46	15.62	16.76
FeO	0.63	2.20	5.15	1.15	1.43	2.40	2.39	3.33
MnO	0.02	0.03	0.08	0.07	0.07	0.08	0.09	0.07
MgO	0.12	2.32	1.09	0.23	0.48	1.32	0.83	0.92
CaO	1.18	1.30	2.33	1.26	1.57	2.69	2.98	3.51
Na2O	2.34	2.65	2.67	3.02	2.74	3.04	3.57	3.77
K2O	6.49	5.41	4.59	4.68	4.45	3.67	3.44	2.50
P2O5	0.05	0.06	0.29	0.03	0.06	0.10	0.10	0.16
LOI	0.53	0.51	0.47	0.29	1.49	0.57	0.85	0.54
SUM	99.48	101.92	99.72	100.50	102.22	100.64	99.20	101.09
A/CNK	1.06	1.08	0.99	1.09	1.16	1.12	1.05	1.10
AN	21.83	21.28	29.95	19.16	24.19	33.04	31.87	33.91
Q	32.88	29.90	26.40	36.91	37.67	29.98	25.91	26.65
Or	38.35	31.97	27.13	27.66	26.30	21.69	20.33	14.77
Ab	19.80	22.42	22.59	25.55	23.19	25.72	30.21	31.90
An	5.53	6.06	9.66	6.06	7.40	12.69	14.13	16.37
C	0.80	1.07	0.50	1.12	2.05	1.84	0.85	1.85
Di	0.00	0.00	0.00	0.00	0.00	0.00	0.00	0.00
Hy	1.40	9.29	10.62	2.58	3.67	7.36	6.13	7.93
Wo	0.00	0.00	0.00	0.00	0.00	0.00	0.00	0.00
Ol	0.00	0.00	0.00	0.00	0.00	0.00	0.00	0.00
Mt	0.00	0.00	0.00	0.00	0.00	0.00	0.00	0.00
Il	0.04	0.46	1.42	0.27	0.32	0.55	0.57	0.70
Ti	0.00	0.00	0.00	0.00	0.00	0.00	0.00	0.00
Ap	0.12	0.14	0.67	0.07	0.14	0.23	0.23	0.37
Ba				643			1248	
Rb	154	317	136	128	116	92	89	72
Sr	127	107	176	198	241	428	426	567
F								

be very sensitive to differentiation processes. The purpose of this chapter is to explore patterns of major and trace element data for the Turtle pluton, garnet aplites, and Target Granite, and to compare them to data from other rock types. Linear and curvilinear trends constrain potential mechanisms which lead to compositional variation.

All analyzed granitic rocks are calcalkaline according to the classification criteria of Irvine and Baragar (1971) and Miyashiro (1974). Major element data are presented in representative Harker diagrams (Figure 43) and trace element data (Ba, Rb, and Sr) on Harker diagrams and a plot of Rb versus Sr (Figure 44).

Rim Sequence

The Rim Sequence of the Turtle pluton is a gradational sequence that varies inward from the country rock contact from biotite granite with ilmenite, to biotite hornblende granodiorite with K-feldspar phenocrysts, to more equigranular biotite hornblende granodiorite with magnetite and sphene. This sequence is represented by 8 samples collected along a well-exposed wash (traverse A-A′, Figure 13 on page 32). The approximate distance of each sample from the country rock contact at A, their mineralogies, and sample numbers are given in Figure 15 on page 34. Two samples are biotite granites with ilmenite (CA85-5, & BW84-20, about 5 and 20 m from A, respectively), one biotite granodiorite with magnetite and trace sphene (BW84-18, about 100 m from A), and the rest are granodiorites with magnetite + sphene + allanite and variable biotite/hornblende ratios. An additional analysis of a hornblende biotite granodiorite with magnetite + sphene + allanite from the western portion of the Rim Sequence (CA85-120) is included to show the chemical similarity of a sample from elsewhere in the Rim Sequence to samples from traverse A-A′.

The eight analyses from the traverse contain variable silica contents (73.32 to 64.96 wt%) that decrease with distance into the pluton except for the two granite samples. Sample positions from point A at the country rock contact are labelled from 1 to 8 (Figure 43), and not only do major

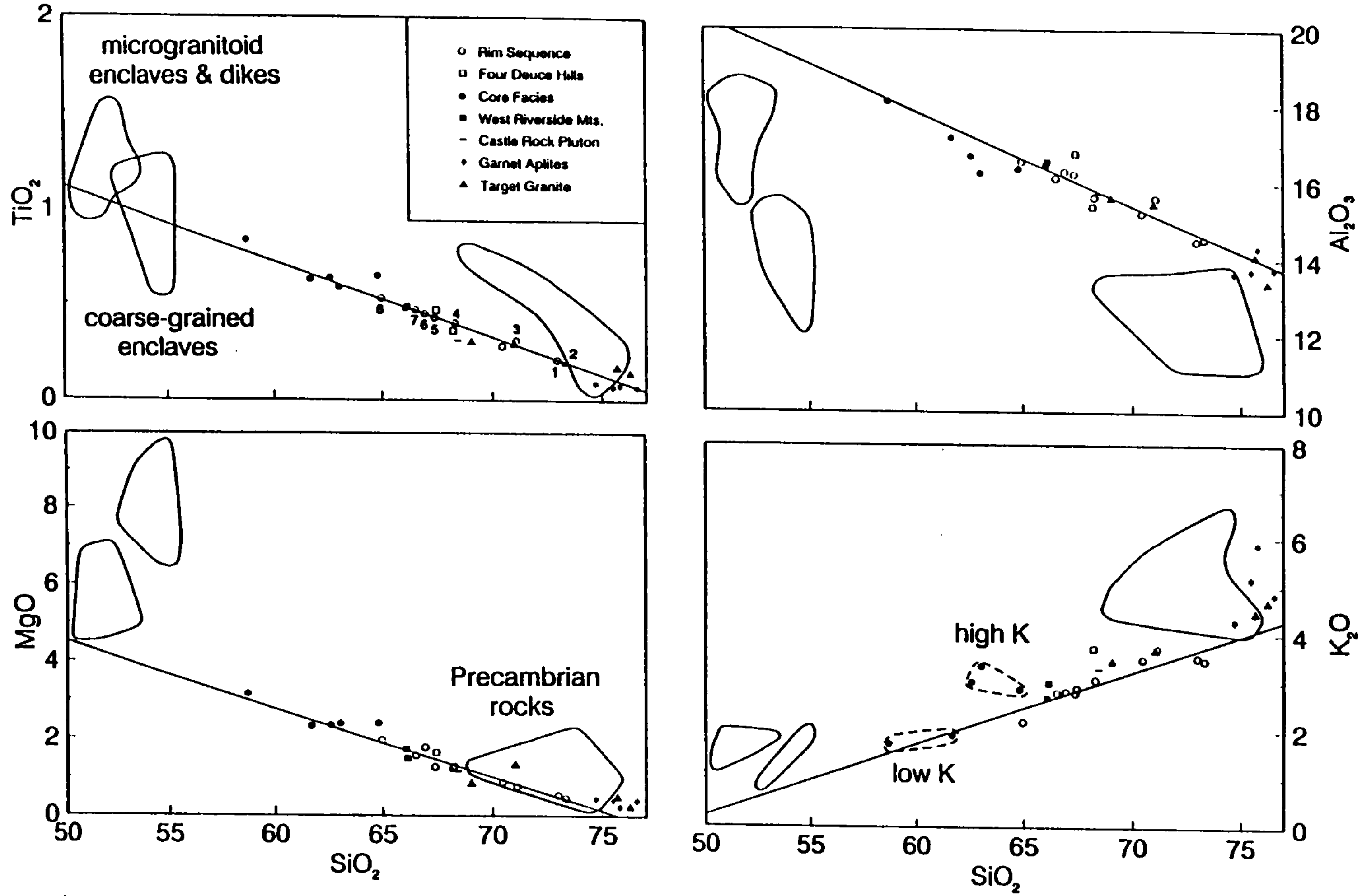

Figure 43. Major element Harker diagrams: These plots show variation of representative major elements with silica contents for all rock types studied. Circles = Rim Sequence traverse A-A' numbered in sequence from wall rock toward interior. Unnumbered circle = additional Rim Sequence sample (CA85-120). Outlined fields surround data from microgranitoid enclaves and mafic dikes, coarse-grained enclaves, and Proterozoic country rocks. Regression line is calculated from samples of the Rim Sequence traverse. Note linearity of the regressions for major elements other than K_2O and Al_2O_3. Also note that low K Core Facies rocks fall on this regression trend. With the exception of a few elements, neither mafic rocks nor country rocks lie on the regression and this suggests neither is involved in generation of chemical variation in the Turtle pluton.

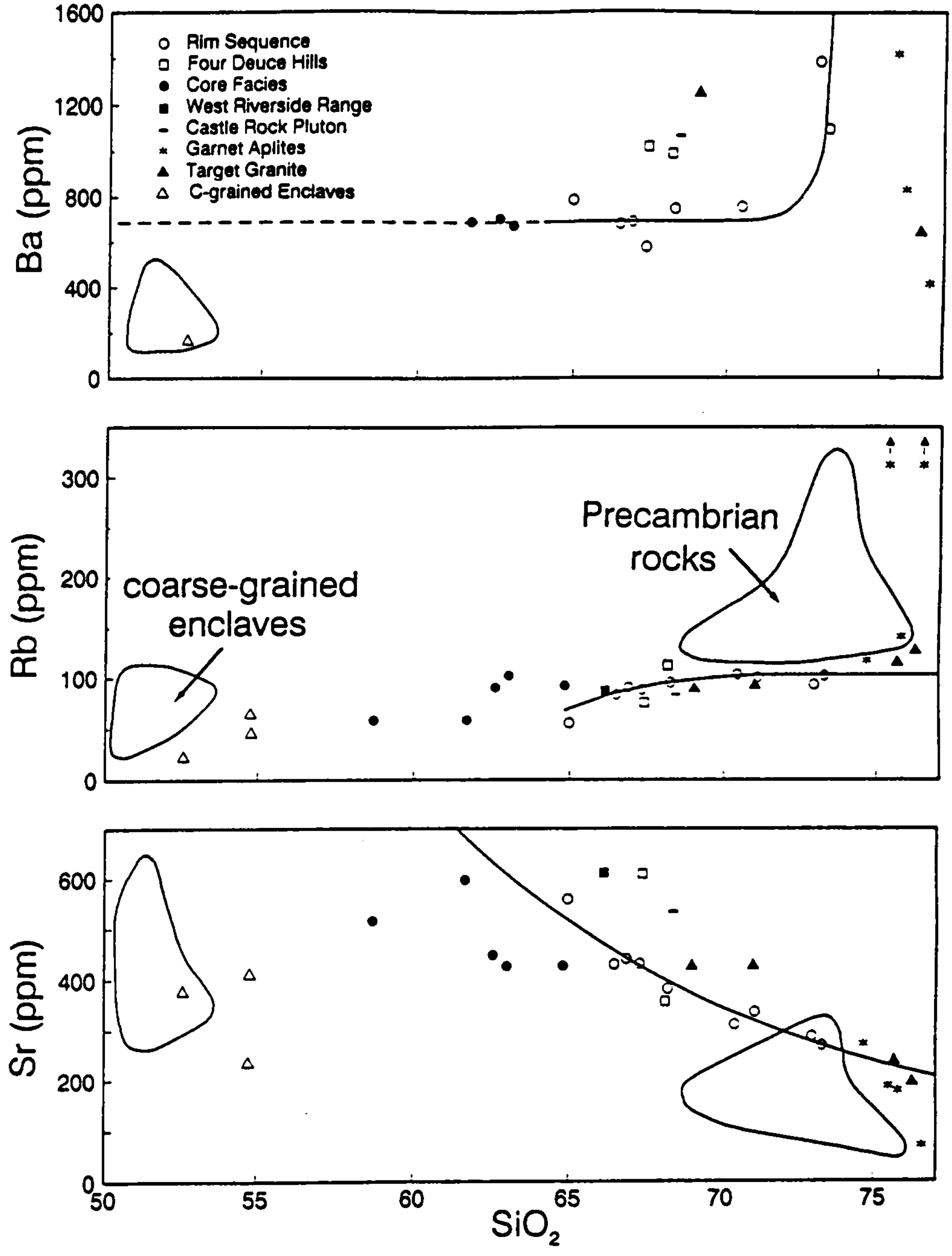

Figure 44. Trace element diagrams for granitoids and mafic rocks: These plots show variation of trace elements for all rock types studied. Whereas major element versus silica plots for the Rim Sequence data result in linear arrays, trace element trends are curvilinear (curves fit by eye). Mafic rocks (microgranitoid enclaves, dikes, and coase-granied enclaves) do not fall on Rim Sequence trends. The distinction of the high K and low K subgroups of the Core Facies are particularly evident on a plot of Rb versus Sr.

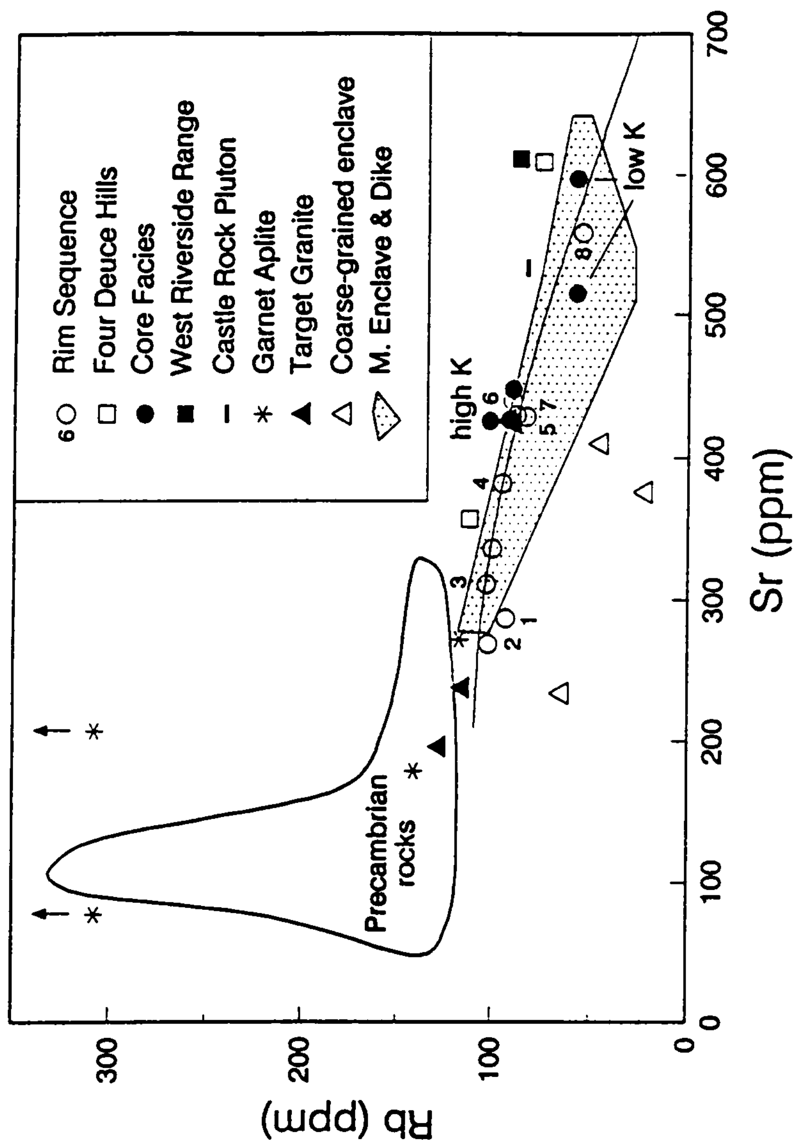
Rim Sequence
Four Deuce Hills
Core Facies
West Riverside Range
Castle Rock Pluton
Garnet Aplite
Target Granite
Coarse-grained enclave
M. Enclave & Dike
Precambrian rocks
high K
low K
Rb (ppm)
Sr (ppm)
0
100
200
300
400
500
600
700

element oxide concentrations correlate with position but the overall trends are linear for this 12 wt% silica range. Exceptions are MnO, Na_2O and K_2O. A measure of the linearity of these trends, the sum of the residuals squared (r^2) from linear regressions are greater than 0.95 (1.0 = perfect fit) except K_2O (0.86), Na_2O (0.65), and MnO (0.23). The range of MnO contents is 0.08 to 0.11, and is virtually constant at 0.10 to 0.11 for 7 of the 8 samples. From the country rock toward the interior of the pluton, Na_2O varies form 3.92 to 2.85 wt%, and K_2O from 3.53 to 2.19 wt%, and these alkalies have a concave downward trend on Harker diagrams. The elements with the largest percent change in concentration (CaO = 1.82 to 5.22 and FeO 1.49 to 4.41 wt%) both display linear trends. The ninth analysis from the Rim Sequence (unlabeled and not from the traverse) falls on the traverse trend for all major elements (Figure 43).

These data indicate the process that generated chemical diversity in the Rim Sequence was very orderly, and resulted in linear trends for all major elements but the alkalis. A two end member process readily accounts for most of these data.

Unlike most major elements that produce linear trends when plotted against silica, trace elements of the Rim Sequence yield curvilinear arrays. The ranges of composition of analyses from traverse A-A′ are great (576-1388 ppm for Ba, 55-103 ppm for Rb, and 269-558 ppm for Sr). There is a positive correlation of Ba and Rb with silica, and a negative one for Sr. The ninth Rim Sequence sample falls with traverse samples for Rb and Sr (no Ba available). Harker diagrams of the three trace elements yield strongly curvilinear trends and these results suggest a process involving more than two end members.

Four Deuce Hills

Two analyses of granodiorite from the Four Deuce Hills have silica contents of 76.41 and 68.18 wt%, and these analyses fall with those from the Rim Sequence for most oxides, exceptions being K_2O and Al_2O_3. These two rocks have Ba, Rb and Sr concentrations of 985-1015 ppm, 75-112 ppm, and 357-609 ppm, respectively. Though these samples are similar to the Rim Sequence with respect to major elements, these rocks have trace element concentrations that lie outside the band of Rim Sequence analyses.

Core Facies

Core Facies rocks, which appear to be moderately homogenous granodiorites in the field, are more restricted in composition than Rim Sequence rocks. Five samples from throughout the unit were selected for chemical analysis (Figure 17 on page 41). All are biotite hornblende granodiorites with magnetite + sphene + allanite except for one quartz monzodiorite (CA84-147). One granodiorite was analyzed because its low color index (17; CA85-13) suggested it may be a fractionate, and another (CA85-122) was collected on trend with traverse A-A′, about 200 m from BW84-25.

These rocks have a range of silica contents from 58.68 to 64.81 wt% with all but one analysis (CA86-14) between 61.68 and 64.81 wt %. The one outlier (CA86-14) is generally less evolved with higher Al_2O_3 and femic constituents, and lower K_2O. It is intermediate between other Core Facies rocks and microgranitoid enclaves of the Turtle pluton and may be a mixture of the two. The other four analyses have restricted major element compositions except for Al_2O_3 (16.27 to 17.18 wt%) and K_2O (1.91 to 3.35 wt%). Given the cluster of 4 samples and 1 outlier, for all major elements but Al_2O_3 and K_2O, it is not possible to distinguish linear versus curvilinear trends. For Al_2O_3, there is a curved array with a decrease in Al_2O_3 (about 1 wt%) with increasing silica. For K_2O, the data suggest two subgroups, a high K (> 2 wt%) and a low K (< 2 wt%) group, and the high K group occurs near the Target Granite (Figure 17 on page 41). This subdivision is supported by trace element and isotopic analyses.

Trace elements occur as complex patterns on Harker diagrams. High K rocks contain much more Rb and less Sr (90-102 ppm Rb and 426-448 ppm Sr) than low K rocks (58 ppm Rb and

515-597 ppm Sr). Ba contents of the two groups overlap and fall in the range 673 to 704 ppm (3 analyses). The prominent difference between the subgroups is apparent on a plot of Rb versus Sr (Figure 44). A process which strongly effects K_2O, Al_2O_3, Rb and Sr contents must be called upon to explain chemical differences among these five samples.

Garnet Aplites

Garnet aplites are fine-grained rocks of granitic composition which contain garnet + biotite ± muscovite. These four samples have a very limited range of oxide contents ($SiO_2 = 74.72$ to 75.92 wt%) except K_2O (4.33 to 5.81 wt%) and Na_2O (2.85 to 3.64 wt%). On Harker diagrams, these analyses cluster except for positive and negative linear slopes from K_2O and Na_2O with increasing silica.

Garnet aplites have a large range of trace element abundances given their limited major element ranges. Trace element contents are 415-1420 for Ba, 105-141 for Rb, and 70-272 ppm for Sr. On Harker, diagrams these trace element analyses define curvilinear fields that do not lie along the continuation of the Rim Sequence trend.

Target Granite

All four samples of Target Granite are granites that contain biotite, sphene, magnetite, ilmenite, and sparse hornblende. Given the granitic composition, chemical diversity is large (69.59 to 75.88 wt% SiO_2) and these four samples define linear trends with respect to all major elements except MnO, MgO and Na_2O for which there is scatter. Examples of chemical ranges are K_2O (3.47 to 4.68 wt%) for which there is a positive correlation with silica, and Al_2O_3 (13.37 to 15.62 wt%) and FeO (1.15 to 2.40) for which there is a negative correlation.

The Target Granite contains 643-1670 ppm Ba, 89-127 ppm Rb, and 196-425 ppm Rb. These rocks define curvilinear trends on plots of trace elements versus silica and these trends suggest a multiple end member differentiation process, probably fractional crystallization.

Precambrian Rocks

Country rocks immediately adjacent the Rim Sequence is Virginia May gneiss, a biotite bearing quartzofeldspathic gneiss associated with leucocratic dikes. The gneiss has a major element composition of 72.2 to 76.1 wt% SiO_2, 11.3 to 13.4 wt% Al_2O_3, 4.07 to 4.71 wt% K_2O, and 1.55 to 2.53 wt% Na_2O. A leucocratic dike is relatively enriched in K_2O (6.49 wt%) and Al_2O_3 (13.7 wt%) as compared to the enclosing gneiss. These gneisses have a limited range of Rb contents, and variable Sr contents (100-138 and 58-310 ppm, respectively) and contain more Rb than Rim Sequence granites. A single analysis of a mafic augen gneiss (H79-124) contains less SiO_2 (68.9 wt%) and has trace element concentrations similar to the Virginia May gneiss. The granitic gneiss found north of Rice (Xgg) contains 73.30 wt% Si_2O, and contains more Rb (317 ppm) than other Proterozoic rocks (128-154 ppm). For most of these elements, the country rocks are not colinear with Rim Sequence trends (see Figure 43 and Figure 44).

Nearby Early Cretaceous Intrusions

The rocks exposed in the West Riverside Mountains, 25 kilometers south of the Turtle Pluton, are similar to the mafic rocks of the Rim Sequence and the Core Facies in hand specimen and modal abundance (see Chapter 1). Two samples contain more silica than the Core Facies rocks and are very similar in major element composition to the most mafic portion of the Rim Sequence (BW84-25) except potassium and rubidium, in which they are enriched. These data suggest the rocks in the West Riverside Range could be an extension of the Turtle pluton, or a similar intrusion.

The Castle Rock pluton is a granodioritic intrusion 10 km north of the Turtle pluton that has oikocrystic potassium feldspar like the Four Deuce Hills. Its major and trace element chemistry is similar to granodiorites from the Four Deuce Hills and may be cogenetic with the Turtle pluton.

Discussion of Chemical Variation Among Rock Types

Rim Sequence

The Rim Sequence displays the largest chemical diversity of any of the rock types and major element chemical trends are linear, except for alkalis. Such linear trends can be modelled as dominantly mixing or unmixing of two end members which could be: (1) assimilation of country rock, (2) removal of a constant mineral assemblage from a parent magma, or (3) mixing of two magmas.

Along the Rim Sequence-country rock contact there is little evidence of contact effects--metamorphism or assimilation. Analyses of the Virginia May gneiss do not lie on an extension of most Rim Sequence major and trace element trends and could not be a bulk assimilant, and Rb-Sr isotopic data rule out even partial assimilation as a mechanism to generate chemical variation of the Rim Sequence (see Chapter 5).

If the range of Rim Sequence compositions and linear chemical trends are the result of fractional crystallization of early crystallizing phases preserved in these rocks, then the cumulate assemblage is of constant composition, lies on the Rim Sequence regression for major elements, is composed of primarily plagioclase and hornblende with lesser biotite (about 53 wt% SiO_2), and is roughly half an original magma volume with a composition like that of the most mafic rock of the sequence (63 wt% silica). The calculated cumulate assemblage assumes analyzed mineral compositions and minimum residual calculations from the program XLFRAC (Stormer and Nicholls, 1978). The constant assemblage, the composition of the assemblage with first crystallizing biotite much less abundant than hornblende, and such a large cumulate volume, are all unlikely.

Mixing of two magmas that bracket Rim Sequence data and lie on the regression line can explain most of the observed major element variation. A candidate for mafic end members is the low K group of the Core Facies. Microgranitoid enclaves do not lie on Rim Sequence trends and are not considered possible end members. Common $^{87}Sr/^{86}Sr$ data will be used to further limit the possible end member compositions (see Chapter 5 and 6). The felsic end member candidate is limited to the Rim Sequence granite itself. The Target Granite is a significantly younger intrusion. Oxygen and strontium isotopic data (including a younger age) rule out garnet aplites as an end member (Chapter 5).

Trace element and alkali trends, on the other hand, are curvilinear, and this indicates a process involving multiple end members must be invoked to explain their variation. Fractionation or accumulation of phases with large partition coefficients for these elements and alkalis (feldspars and biotite), that would not greatly effect concentrations of other major elements, can explain these curvilinear trends, but a fractionation model cannot account for linear trends of most major elements. These data suggest that more than one process needs to be considered in chemical modelling of the Rim Sequence, and that the model must incorporate magma mixing and a fractionation/accumulation mechanism involving minerals that contain K_2O, Na_2O, Rb and Sr.

Core Facies

The Core Facies has been subdivided into high K and low K groups. The low K group lies on trend with the Rim Sequence analyses, and major element, textural and mineralogic similarity of these to the most mafic granodiorites of the Rim Sequence suggest a genetic relationship of the two (see Chapter 1). High K Core Facies rocks, on the other hand, have a chemical signature distinct from the low K group. The occurrence of 2 of 3 Core Facies high K rocks near the Target Granite, and the splotchy distribution of K feldspar in these samples suggest metasomatism caused by the younger intrusion may be the source of chemical differences. A graphical comparison of a low K rock from the periphery of the Core Facies (CA85-122) and a high K rock proximal to the Target Granite (CA84-147) indicates the high K rocks are relatively enriched in K_2O, Rb and LOI constituents, and depleted in Al_2O_3, CaO, Na_2O, and Sr (Figure 45). These elements suggest a feldspar plus fluid exchange can account for most of the observed chemical differences with a loss of plagioclase (An_{44}) and gain of orthoclase (Or_{100}) + quartz + fluid components + additional potassium. An alteration model to account for the differences of these two groups will be further tested with isotopes (Chapter 5).

Garnet Aplites

The peraluminous and silica rich composition of aplites, and their cross cutting relationship with the Turtle pluton suggest they could be late differentiates of Turtle pluton magmas. Their major and trace element compositions generally lie on trend with Rim Sequence data, but oxygen and strontium isotopic data indicate these aplites are probably not related to the Turtle pluton.

Target Granite

The Target Granite stopes the Turtle pluton and therefore must have intruded after solidification of the Turtle pluton. This body has different major and trace element composition than the Turtle pluton, is about 30 Ma younger, and also has very different common Sr and oxygen isotopic signatures (Chapter 5).

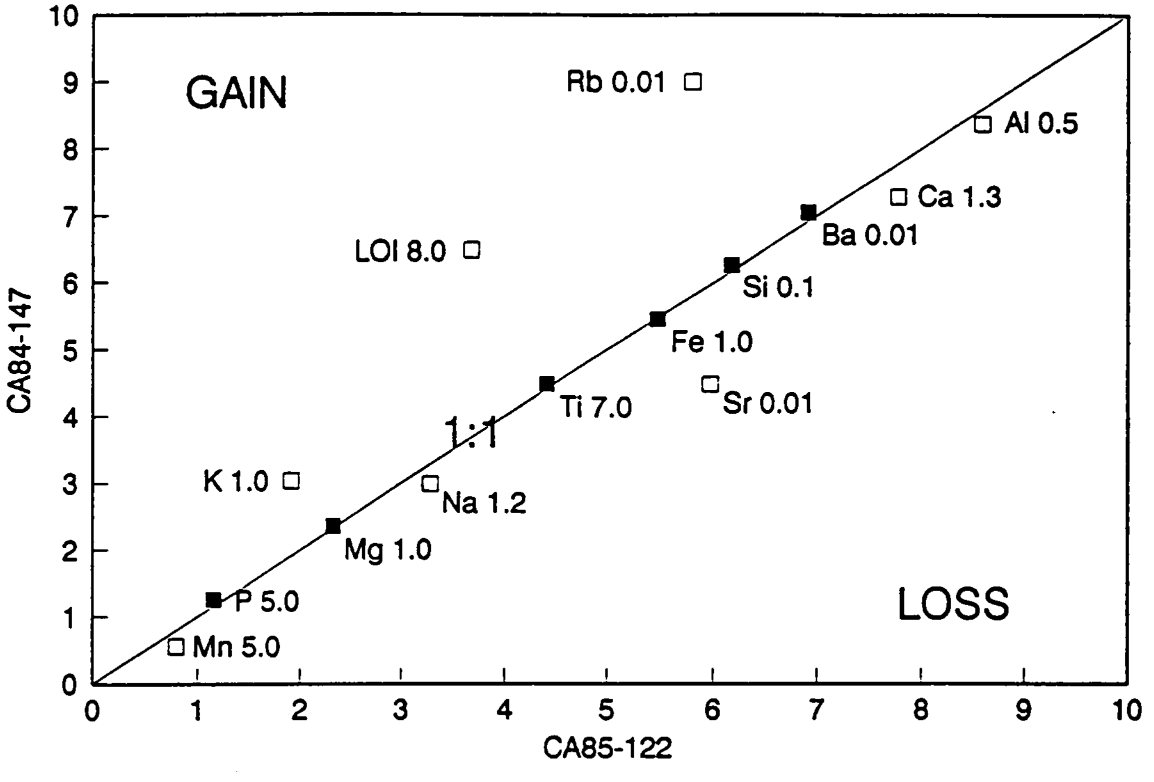

Figure 45. Chemical comparison of low and high K subgroups of the Core Facies: This isocon diagram is a graphical representation of changes of composition from a reference sample ("unaltered") to a second sample ("altered"; Grant, 1986). It is a plot of an element from the reference rock versus the same element in another sample, both multiplied by the same scaling factor (used to make the plot more legible). If the rocks are identical in composition, all elements would plot on a 1:1 slope. If elements in the reference are diluted by addition of another species, all elements would lie on a line but with a slope less than 1:1. Elements that are added to the reference rock will lie above a line passing through most elements (unchanged), and those lost would lie below. As compared to the low K subgroup (horizontal axis), the high K subgroup (vertical axis) contains more K_2O, H_2O, Rb and perhaps P_2O_5, and less Al_2O_3, CaO, Na_2O, and Sr. These changes can be modelled as a single reaction involving 2 feldspars and fluid (see text).

Chapter 5

ISOTOPE GEOCHEMISTRY

Introduction

Isotopes are valuable tools in discerning petrogenetic relationships. Radiogenic isotopes are used to determine the crystallization ages of the Turtle pluton and Target Granite. U-Pb ages of zircon and sphene are compared to mineral and whole rock Rb-Sr ages from these intrusions. Common isotopic ratios (Sr and Pb) are used to evaluate the genetic relationships of rock types from the study area and nearby Cretaceous intrusions, and to model their source characteristics. Stable isotopes (O and D) are employed to determine the role of post-crystallization fluid exchange on the Turtle pluton and Target Granite.

U-Pb Geochronology

If U and radiogenic Pb concentrations in a mineral are the result of radiogenic growth since crystallization, calculated ages, $^{207}Pb/^{235}U$, $^{206}Pb/^{238}U$, and $^{207}Pb/^{206}Pb$ should agree, and the sample is described as concordant (Wetherill, 1956), however, geologic factors such as the presence of a xenocrystic component and loss of radiogenic Pb through diffusion and episodic loss commonly result in the following age relationships in zircons: $^{206}Pb/^{238}U$ < $^{207}Pb/^{235}U$ < $^{207}Pb/^{206}Pb$, and the sample is described as discordant (Wetherill, 1956). Sphene, on the other hand, is usually concordant because inheritance is rare, and small concentrations of U as compared to zircon result in less radiation damage to the crystal, and thus relatively smaller losses of radiogenic Pb (Tilton and Grunenfelder, 1968; Tucker et al., 1986).

Errors of calculated ages depend on numerous factors (Mattinson, 1987; Ludwig, 1980). Minerals of Cretaceous age, because of relatively slow growth of ^{235}U and resulting small abundances of ^{207}Pb, are sensitive to common Pb and laboratory contamination (blank) corrections (Chen and Moore, 1982; Ludwig, 1980; Mattinson, 1987). Uncertainties associated with these corrections result in relatively large uncertainties in calculated ages (especially $^{207}Pb/^{206}Pb$) for young rocks. With these caveats in mind, ages interpreted from zircon and sphene data are assumed to represent crystallization ages of the Turtle pluton and Target Granite.

Turtle Pluton

Zircons were separated from 75 kg of Rim Sequence granite collected 10 m from the country rock contact (CA85-5). Three size fractions were separated: > 150, 85 to 75, and < 75 microns. The finest fraction was too small to analyze with confidence. Zircons from the other fractions comprise about 75% euhedral light brown crystals, 20 % clear ones, and about 5% violet ones, and many crystals display zoning (Figure 46). Brown crystals that contain darkened cores and the violet variety were removed prior to analysis.

The two fractions of zircon from the Rim Sequence are discordant (Figure 47) and yield U/Pb ages of 138 to 208 Ma and $^{207}Pb/^{206}Pb$ ages of 976 and 1058 Ma as given in Table 12. The lower and upper intercept ages from regression of these two points are 128 and 3100 Ma, but because of the small number of points and the small spread of composition, significant errors are associated with these ages.

Figure 46. Minerals used in U-Pb isotopic analyses: a. Zircons (75-85 microns) from the Rim Sequence granite (CA85-5) are generally clear and euhedral. Grains with darkened cores were removed before analysis. b. Zircons (85-100 microns) from the Target Granite (CA85-111) are euhedral and commonly display delicate growth zoning. c. Some zircons (85-100 microns) from the Target Granite (CA85-111) have optically distinct cores (left). Others contain mineral inclusions (center and right). d. A representative sphene (about 800 microns long) from the high K Core Facies rocks (CA84-147) is euhedral and contains inclusions (top left).

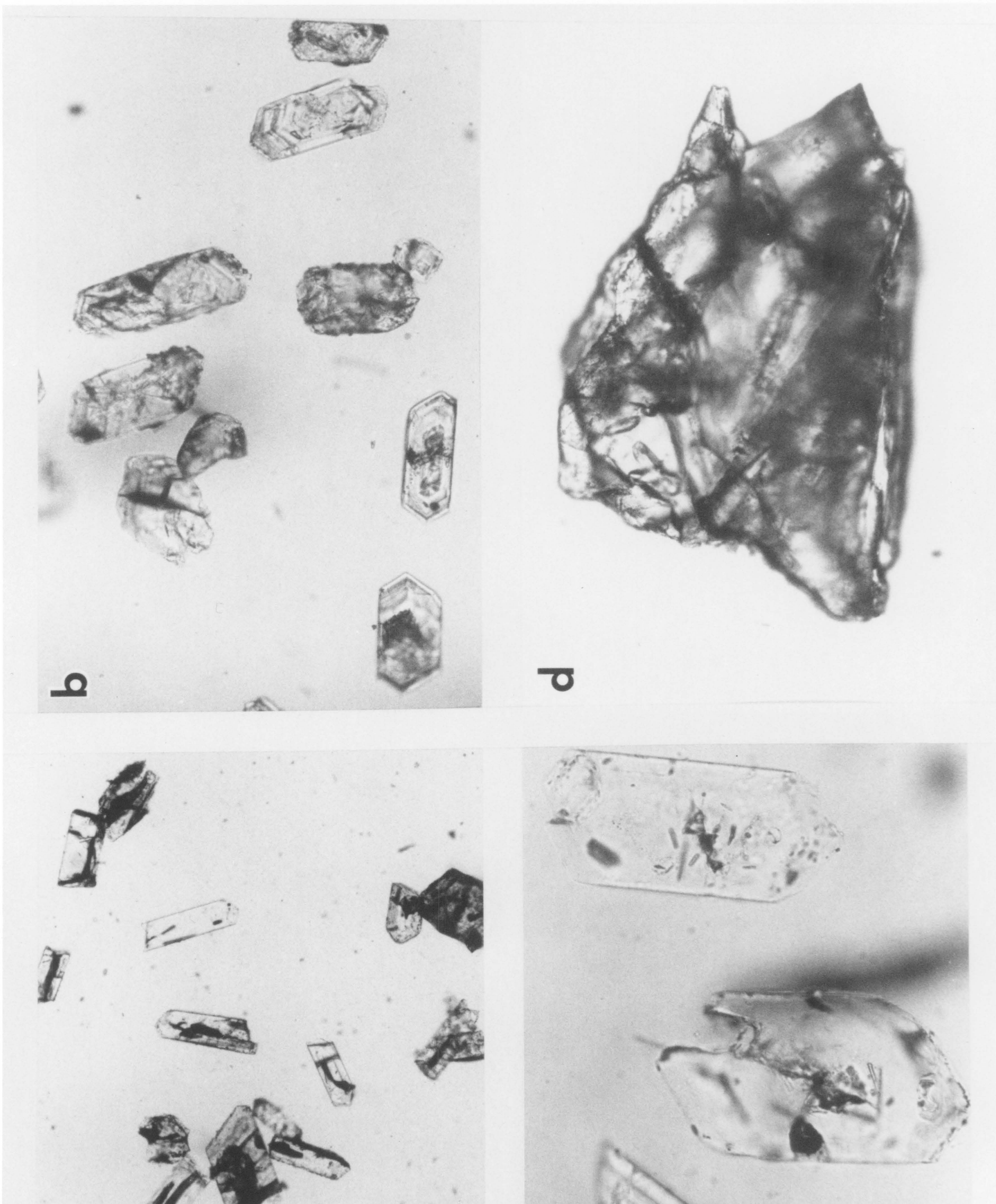
a
b
c
d

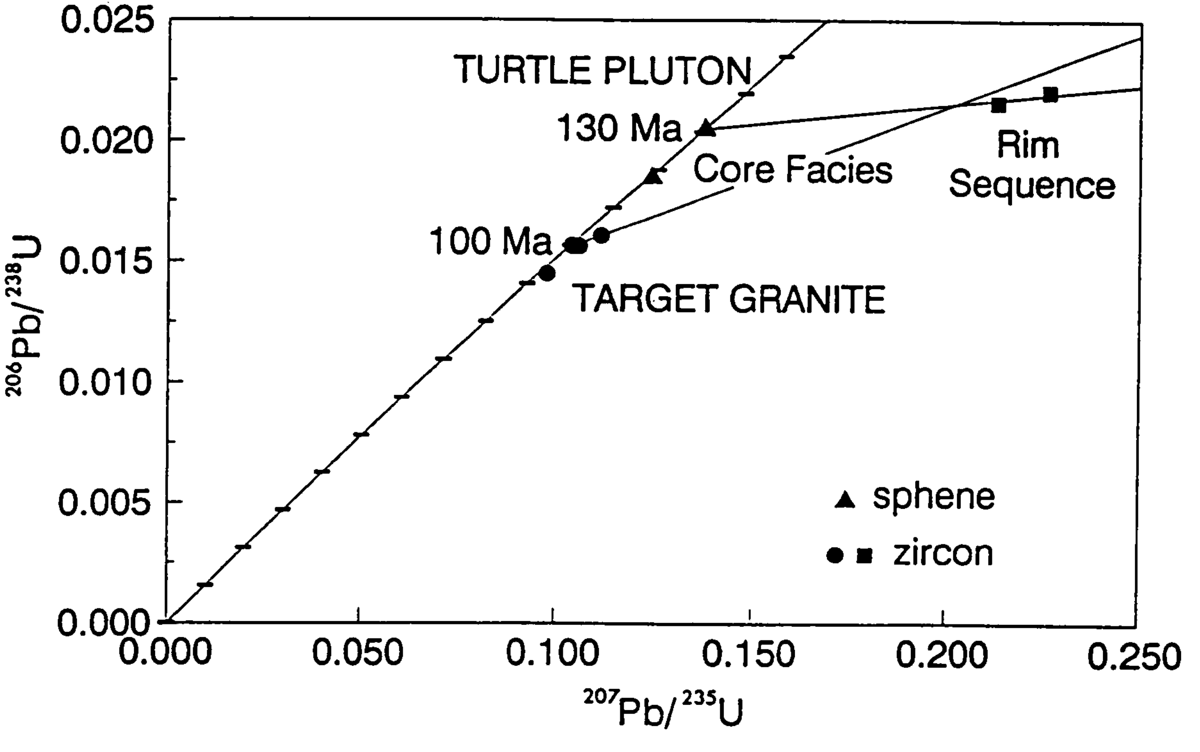

Figure 47. **Concordia diagram for Turtle Pluton and Target Granite:** This diagram shows that zircons from the Rim Sequence (square) are discordant, that one sphene fraction from the Core Facies (triangle) is concordant at 131 Ma and one has a similar $^{207}Pb/^{206}Pb$ age but lesser U/Pb ages, and that regression of the concordant sphene fraction and zircons yield a lower intercept age of 130 Ma and upper intercept age of 3.1 Ga for the Turtle pluton. Zircons from the Target Granite (dot) are concordant or mildly discordant. Regression of a concordant fraction (100 Ma) and the 2 fractions with greater $^{207}Pb/^{206}Pb$ ages yields a lower intercept age of 99 Ma, and an upper one of 1.7 Ga. This is similar to the age of Precambrian country rocks and suggests inheritance. A second possibility for discordance is contamination of the Target Granite by zircons from its host rock, the Turtle pluton. An fourth fraction from the Target Granite has a similar $^{207}Pb/^{206}Pb$ age to the concordant fraction but lesser U/Pb ages and suggests recent Pb loss or U gain.

Table 12. U-Pb isotope analyses of zircon and sphene.

Size	Concentration		Isotopic Ratios			Calculated Ratios		
	Pb	U	$^{206}Pb/^{204}Pb$	$^{207}Pb/^{204}Pb$	$^{208}Pb/^{204}Pb$	$^{207*}Pb/^{206*}Pb$	$^{206*}Pb/^{238}U$	$^{207*}Pb/^{235}U$
Target Granite zircon, CA84-111 % +								
100-150	34.1	2108	3676	192.1	537.8	0.04826 (112+29)	0.0156 (100±3)	0.1041 (101±3)
75-100	31.6	1891	3664	199.3	550.3	0.05038 (213±26)	0.0161 (103±3)	0.1115 (107±3)
45-75	30.7	2035	2578	141.0	382.5	0.04899 (148±31)	0.0145 (93±3)	0.0977 (95±3)
< 45	33.4	2049	2940	159.3	442.8	0.04920 (157±27)	0.0156 (100±2)	0.1059 (102±3)
Rim Sequence zircon, CA85-5 %% +								
> 150	15.0	651	3377	266.2	427.2	0.07462 (1058±22)	0.0220 (141±3)	0.2267 (208±5)
75-100	17.6	774	2654	204.5	376.3	0.07165 (976±24)	0.0216 (138±3)	0.2132 (196±4)
Core Facies sphene, CA84-147 %% ++								
1.8A nmag	7.3	140.4	111	20.2	140.1	0.04876 (137±17)	0.0205 (131±1)	0.1377 (131±1)
1.0A nmag	6.5	132.7	108	20.0	143.9	0.18504 (133±20)	0.0185 (118±1)	0.1239 (119±1)

+ Zircon data corrected for blank, and calibrated to NBS-983 standard.
% Assumed common Pb of 6/4=18.51, 7/4=15.62, 8/4=38.39.
++ Sphene data corrected for blank, and calibrated to CIT standard.
%% Assumed common Pb of 6/4=18.55, 7/4=15.62, 8/4=38.45.
Sizes in microns. Concentrations in ppm. Ages and errors given in parentheses.

Sphene was separated from 20 kg of Core Facies quartz monzodiorite. In thin section sphene occurs as euhedral crystals, or as anhedral grains associated with mafic phases (Figure 23 on page 60). Both types are medium brown. In order to avoid the anhedral type, grains larger than 150 microns were used in analysis. Sphene from this sample has a large range of magnetic susceptibilities (1.8 to 0.4 amps at 10° side tilt and 19° forward tilt on a Franz magnetic separator) which was utilized to split the population into fractions. Two fractions were analyzed, those separated between 0.8 and 1.0 amps, and those nonmagnetic at 1.8 amps.

The nonmagnetic fraction (1.8 amps) is concordant within error at 131 ± 1 Ma (see Table 12). The other fraction has a similar $^{207}Pb/^{206}Pb$ age of 133 ± 20 Ma, but lower Pb/U ages (118 ± 1) and this fraction may have suffered Pb loss (or U gain) as compared to the more nonmagnetic fraction. Perhaps the lower Pb/U ages are due to alteration of this rock by intrusion of the adjacent Target Granite.

The similarity in age of the concordant sphene fraction from the Core Facies (131 Ma), and the lower intercept of the two zircon fractions from the Rim Sequence (128 Ma), together yield a lower intercept age of 130 ± 1 Ma (Ludwig, 1984, Model 2). This age is interpreted to be the crystallization age of the Turtle pluton. This interpretation is tentative given the unusual range of magnetic susceptibilities of sphene and the differences in U/Pb ages of the two fractions, however ages determined from a series of radiogenic systems (see below) are supportive of this Early Cretaceous age. In terms of the petrologic interpretation which greatly depends on Rb-Sr isotopic data, an age difference of 10 Ma will change calculated initial $^{87}Sr/^{86}Sr$ by about 0.0001 for most samples, i.e. the level of experimental error. Thus a 10 Ma difference in model age will not effect petrologic interpretations.

Target Granite

Zircons were separated from 60 kg of the Target Granite collected away from contacts and xenoliths (CA85-111). Zircons were separated into four size fractions: > 85, 85-75, 75-45, and < 45 microns. All fractions contain euhedral, light brown to clear crystals that display delicate zoning, and some crystals contain optically distinct cores (Figure 46).

The results of zircon analyses appear in Table 12. One fraction, the coarsest, is concordant at 100 ± 3 Ma. Two fractions (85-75 and < 45 microns) have overlapping U/Pb ages, but greater $^{207}Pb/^{206}Pb$ ages (beyond errors) than the concordant one. One fraction (75-45 microns) has a $^{207}Pb/^{206}Pb$ age similar to that of the concordant fraction, but younger U/Pb ages (93 and 95 Ma). The fractions with $^{207}Pb/^{206}Pb$ ages greater than that of the concordant fraction suggest the presence of an inherited component and regression of these two fractions and the concordant one yields a lower intercept of 99 Ma (+ 4/-6 Ma, Ludwig, 1984, Model 1, and + 45/-30 Ma, Model 2), and an upper intercept of 1.7 ± 0.7 Ga (Ludwig, 1984, Models 1 and 2). The large error of the lower intercept is primarily the result of a small spread in the data and the parallelism of the regression and concordia. Upper intercept errors are large, but the agreement of this age with the age of exposed basement rocks in the area (this study, Wooden et al., 1988 and J.L. Wooden, unpublished data) suggests an interpretation of an inherited Precambrian component is valid. A second possibility is inheritance of zircon from the Turtle pluton which it intrudes (see regression, Figure 47). The fraction having lower U-Pb ages shares a $^{207}Pb/^{206}Pb$ age with the concordant one and is interpreted to have lost Pb (or gained U) relative to the concordant fraction.

The crystallization age of the Target Granite is concluded to be 100 ± 3 Ma based on data from a concordant zircon fraction.

Rb-Sr Isotopes

Introduction

Rb-Sr isotope data from rocks and minerals may be used for geochronology when isotopic equilibrium can be assumed. This criterion is fulfilled in the following cases: (1) suites of igneous rocks that result from fractional crystallization over geologically short time periods. (2) minerals in an igneous rock that crystallized from the same homogenous melt. (3) high grade metamorphic rocks where physical conditions allowed isotopic equilibration. Under other circumstances, when magmas are contaminated by country rock (assimilation) or by other magmas (magma mixing), or when metamorphic grades are low, isotopic equilibrium may not be achieved and pseudochrons or scatterchrons result (Brooks et al., 1972). In any case, when a crystallization age can be assigned from other methods, common or initial ratios of $^{87}Sr/^{86}Sr$ (Sr_i) may be used to test for petrogenetic relationships among rocks, and similar Sr_i values within ± 0.0002 indicate possible evolution from the same source.

Sr_i values can also yield information about source characteristics, whether the source is mature continental crust (> 0.7060), mantle derived melts (< 0.7035) or mixtures of the two (0.7035-0.7060; Kistler and Peterman, 1973; Hart and Brooks, 1981).

Isotopic data from Precambrian country rocks, the Turtle pluton, the Target Granite, and garnet aplites are used to define ages, magma relationships, and potential magma sources. All rocks analyzed for major elements were also analyzed for isotopic composition (Table 13) and locations are given in figure references below.

Table 13. Rb-Sr isotope analyses of whole rocks and minerals.

Sample	$^{87}Sr/^{86}Sr$	Rb	Sr	$^{87}Rb/^{86}Sr$	Sr_i
			Rim Sequence 130 Ma*		
85-5	0.71007	92.6	292.8	0.92	0.7084
bw-20	0.71021	102.4	275.6	1.08	0.7082
bw-18	0.70991	103.0	308.7	0.97	0.7081
bw-19	0.70908	91.9	382.3	0.70	0.7078
bw-22	0.70829	87.0	427.8	0.59	0.7072
bw-23	0.70823	90.4	439.2	0.60	0.7071
bw-24	0.70782	84.5	433.5	0.56	0.7068
bw-25	0.70698	52.8	545.8	0.28	0.7065
85-120w	0.70954	100.0	336.0	0.86	0.7079
			Four Deuce Hills 130 Ma*		
85-4	0.70816	111.5	357.1	0.90	0.7065
84-50	0.70699	75.2	609.4	0.36	0.7063
			High K Core Facies 130 Ma*		
84-143	0.70680	101.7	430.7	0.68	0.7055
84-147	0.70652	89.3	451.5	0.57	0.7055
84-147	0.70663	89.3	451.5	0.57	0.7056
85-25	0.70685	84.9	410.3	0.60	0.7057
85-13	0.70778	92.0	427.0	0.58	0.7067
			Low K Core Facies 130 Ma*		
85-122	0.70701	56.7	592.6	0.28	0.7065
86-14	0.70715	58.0	515.0	0.30	0.7066
			Microgranitoid Enclaves 130 Ma*		
bw-25as	0.70772	57.7	502.7	0.33	0.7071
bw-29s	0.70833	90.5	346.4	0.76	0.7069
84-45	0.70894	108.4	284.3	1.10	0.7069
84-113s	0.70737	65.9	523.7	0.36	0.7067
84-173	0.70672	28.4	507.3	0.16	0.7064
			Mafic Dikes 130 Ma*		
84-65a	0.70603	54.7	612.5	0.26	0.7056
84-65a	0.70596	54.7	612.5	0.26	0.7055
85-4c	0.70548	54.0	473.0	0.31	0.7049

Table 13. Rb-Sr isotope analyses of whole rocks and minerals.

Sample	$^{87}Sr/^{86}Sr$	Rb	Sr	$^{87}Rb/^{86}Sr$	Sr_i
		Coarse-grained Enclaves 130 Ma*			
bw-27	0.70630	20.7	376.3	0.16	0.7060
84-114	0.70702	63.9	234.2	0.79	0.7056
85-118	0.70555	45.6	412.0	0.32	0.7050
		Garnet Aplites 96 Ma**			
84-28	0.71557	144.2	73.1	5.71	0.7078
84-46	0.70982	118.6	187.3	1.83	0.7073
84-101	0.70978	104.9	196.4	1.55	0.7077
85-34	0.70834	125.0	282.2	1.28	0.7066
85-55	0.71646	158.7	66.9	6.87	0.7071
85-62	0.73288	337.5	52.1	18.79	0.7072
		Target Granite 100 Ma***			
85-18	0.70766	127.5	197.6	1.87	0.7050
85-111	0.70701	115.9	241.2	1.39	0.7050
85-101	0.70584	91.9	428.4	0.62	0.7050
85-15	0.70540	89.0	426.3	0.60	0.7045
		Castle Rock Pluton 130 Ma*			
84-158	0.70752	82.7	533.3	0.45	0.7067
		Virginia May Gneiss 130 Ma*			
85-5A	0.81330	100.0	75.0	3.90	0.8061
85-96	0.73300	134.3	320.4	1.22	0.7308
85-96	0.73332	134.3	320.4	1.22	0.7311
85-66	0.87001	140.1	62.4	6.60	0.8578
H84-92	0.79788	128.2	99.7	3.75	0.7909
H84-93	0.79229	154.4	126.5	3.56	0.7857
		Other Country Rocks 130*			
H79-118a+	0.92570	316.6	106.6	8.78	0.9095
H79-124+	0.76097	136.2	176.2	2.25	0.7568
86-8	0.74556	28.4	195.6	0.42	0.7448

* assumed age of the Turtle pluton, U-Pb.
** assumed age of aplites, Rb-Sr.
***assumed age of Target Granite, U-Pb.
\+ isotope dilution.

Table 13. Rb-Sr isotope analyses of whole rocks and minerals.

Mineral	$^{87}Sr/^{86}Sr$	Rb	Sr	$^{87}Rb/^{86}Sr$	Sr_i
	Rim Sequence Granite (CA85-5) 124 Ma $				
w.r.	0.70985	97.1	338.1	0.83	0.7084
ap ac	0.70881	17.5	271.7	0.19	0.7085
ap eq	0.70858	2.3	112.7	0.06	0.7085
ksp	0.71163	274.7	392.2	2.03	0.7081
ksp	0.71135	514.0	397.6	1.77	0.7082
biot	0.90650	509.7	13.4	112.07	0.7085
	High K Core Facies (CA84-147) 103 Ma $$				
w.r.#	0.70657	89.3	451.5	0.57	0.7057
sph0.4A	0.70623	0.6	38.3	0.05	0.7062
sph1.8A	0.70638	1.7	47.2	0.11	0.7062
ksp	0.70721	259.1	712.7	1.05	0.7057
biot	0.87855	559.9	13.9	118.21	0.7055
	Microgranitoid Enclave (BW84-29) 130 Ma*				
w.r.##	0.70833	90.5	346.4	0.76	0.7069
ap ac	0.70778	5.0	81.7	0.18	0.7074

++ conc. by isotope dilution unless otherwise noted.
$ age determined from 5 minerals & whole rock.
$$ age determined from 2 minerals & whole rock.
average of 2, concentrations from XRF.
concentrations from XRF.
** assumed age of the Turtle pluton.

Precambrian Rocks

Precambrian rocks (locations given in Figure 5 on page 10) were analyzed for Rb and Sr isotopic composition in order to test assimilation as a possible mechanism to produce the Turtle pluton, and to determine the age of the country rock.

As shown in Figure 48, analyses of the Virginia May gneiss, a quartzofeldspathic biotite gneiss that underlies a majority of the southern Turtle Mountains, result in an isochron with an age of 1.77 $\pm$0.04 Ga and an intercept of 0.7021$\pm$0.0014 ($\sqrt{MSRS}$ = 0.375, Model 2, York, 1969). This age incorporates two samples of gneiss collected within 2 km of the Turtle pluton and two samples collected near the Virginia May Mine, several kilometers north of the Turtle pluton (see Figure 5 on page 10). An analysis of one rock collected from within 10 m of the Turtle pluton (CA85-5A) falls above the isochron and may have been affected by the intrusion. This Proterozoic age is similar to $^{207}Pb/^{206}Pb$ age of whole rocks and feldspars from Precambrian rocks of the Turtle Mountains (Wooden et al., 1988 and J.L. Wooden, unpublished data) and to a high grade metamorphic event (1.7 Ga) documented in the eastern Mojave Desert (Silver, 1968; Wooden et al. 1988; Thomas et al., 1988; J.L. Anderson and J.E. Wright, unpublished data). The Sr_i of 0.702 is like that of the Bulk Earth Model at 1.77 Ga (DePaolo and Wasserburg, 1976), and this implies the gneiss did not experience significant radiogenic growth prior to isotopic homogenization at 1.77 Ga.

Analyses of two other rock types, the porphyritic granite gneiss (Xgg) and mafic augen gneiss (gneiss of Johnsons Well, Xag) also fall on the isochron and this suggests a minimum crystallization age of 1.77 Ga for these two metaigneous rock types. One rock type, an amphibolite (Xa) collected about 2 km north of the Turtle pluton, plots above the isochron and is not in isotopic equilibrium with the other Precambrian samples.

These data suggest a minimum crystallization age of 1.77 Ga for a majority of the terrane intruded by the Turtle pluton. In addition, these rocks are much more radiogenic (Sr_i = 0.730 to 0.909) than the Turtle pluton ($<$0.7084) as calculated at 130 Ma and are not colinear with Rim

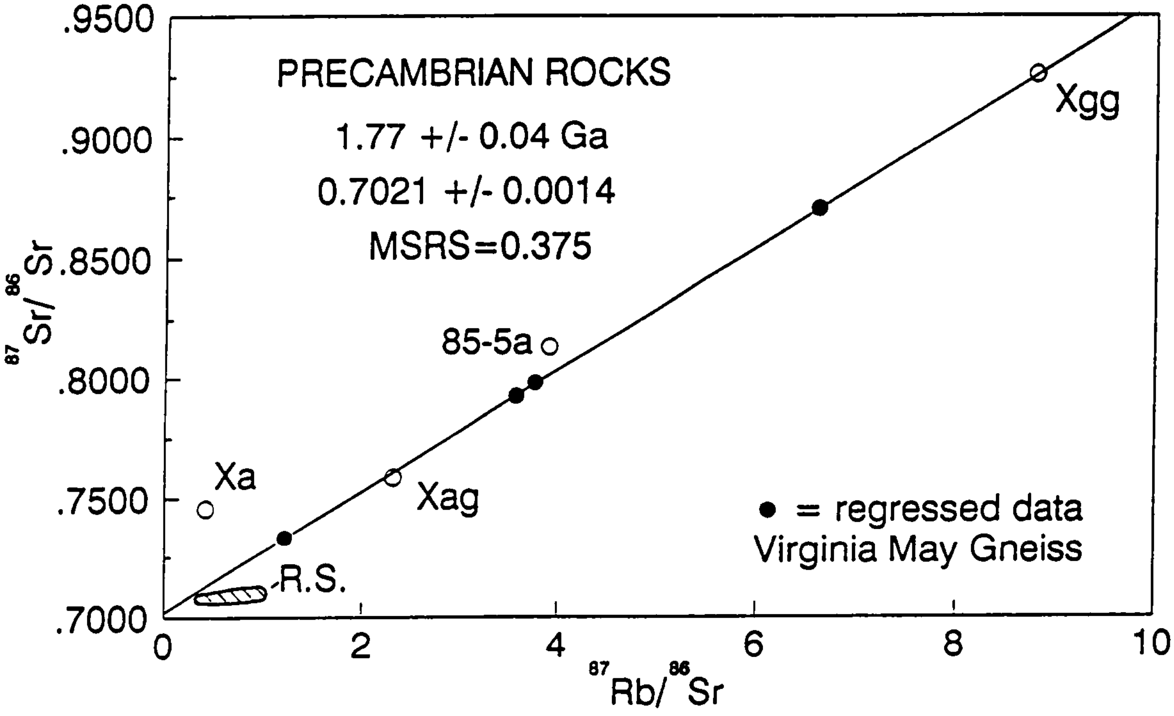

Figure 48. **Rb-Sr isochron diagram for Precambrian rocks:** The age of Precambrian rocks surrounding the Turtle pluton is 1.77 Ga as defined by four samples of the Virginia May Gneiss. The low Sr_i value approaches that of a bulk earth model (DePaolo and Wasserburg, 1976) and suggests little growth prior to homogenization at 1.77 Ga. One sample from the same unit and immediately adjacent the Turtle pluton does not fall on the isochron (circle) and was not included in the regression. Two other metaigneous rock units, the porphyritic granite gneiss of Rice (Xgg) and mafic augen gneiss (Gneiss of Johnsons Well; Xag) fall on the isochron and this suggests a minimum crystallization age of 1.77 Ga. One amphibolite (Xa) is more radiogenic than the other samples. A field marked "R.S.", the field of all Rim Sequence data, has a much lower slope and does not lie on the regression. These data indicate isotopic variation of these granitoids is not the result of contamination or partial melting of sampled Proterozoic rocks.

Sequence isotopic data (field labelled RS in Figure 49). This indicates that partial melting of sampled basement rocks cannot be the source of even the most radiogenic rocks of the Turtle pluton.

Turtle Pluton

The Turtle pluton is a reversely zoned intrusion composed of a Rim Sequence, a more mafic and homogenous Core Facies, and a lobe of granodiorite (Four Deuce Hills) of unknown relationship to the rest of the intrusion. Besides its unusual reversed zonation, petrography and mineral chemistry suggest processes other than fractional crystallization were operative in the Turtle pluton. The reaction texture of ragged biotite in euhedral hornblende and reversely zoned plagioclase in all rocks but Rim Sequence granites can be the result of magma mixing as well as fractional crystallization. Sr isotopes are used to test for these petrogenetic processes.

Rim Sequence

Sr isotope study of the Rim Sequence indicates that other processes besides fractional crystallization generated this rock sequence. Eight samples from traverse A-A′ of the Rim Sequence (Figure 13 on page 32) yield a linear array with the most radiogenic samples at the periphery of the pluton (samples 1 through 8, Figure 49). These data yield an apparent age of 310 ± 72 Ma and an intercept of 0.7057 ± 0.0008 ($\sqrt{MSRS} = 0.754$; Model 2, York, 1969) which is geologically unreasonable age given: (1) U-Pb geochronology indicates a 131 Ma crystallization age. (2) Rb-Sr mineral isochron yields a Cretaceous age. (3) There are no known Paleozoic igneous rocks in the eastern Mojave Desert. In order to point out the isotopic variability in this rock suite, 130 Ma reference isochrons that bracket the data are shown. Assuming this is the crystallization age, cal-

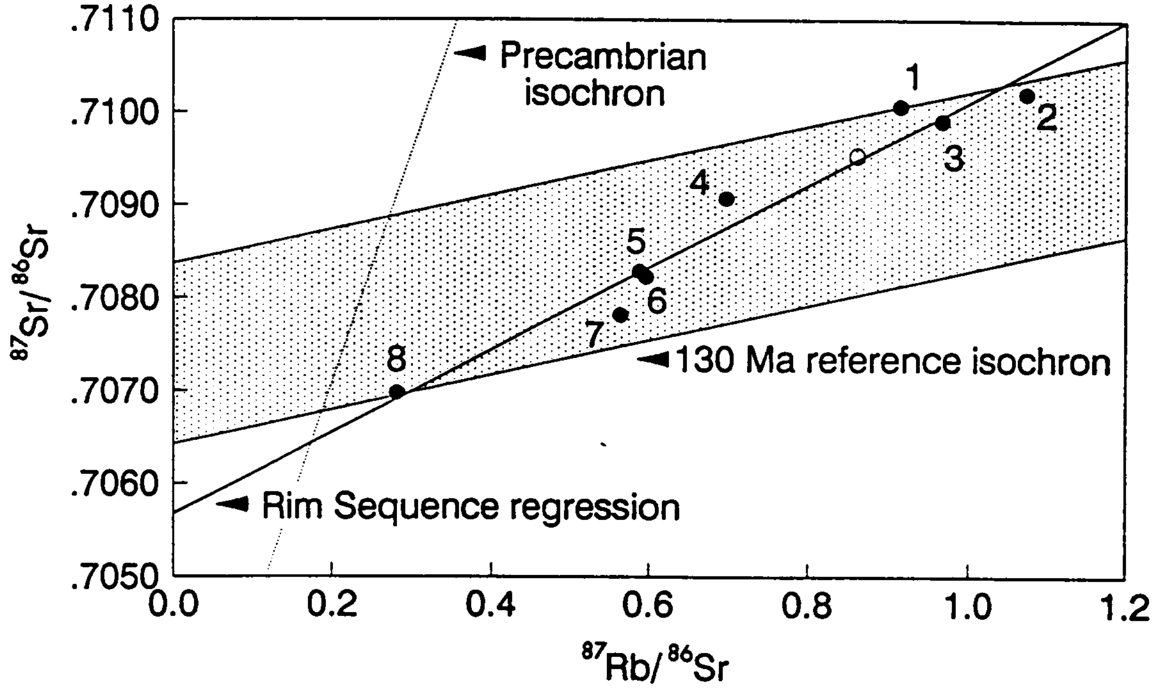

Figure 49. **Rb-Sr isochron diagram for the Rim Sequence:** Eight samples (dots) collected from the Rim Sequence traverse (A-A′) and numbered in sequence from country rock contact and into the pluton (1 to 8) define an apparent age of 310 Ma and intercept of 0.7057 and are more radiogenic at the rim (1) than toward the core (8). Hornblende-free samples (1-3) have similar Sr_i. An additional sample not from the traverse (circle) also falls on the regression. This 310 Ma age is interpreted as a false age generated by mixing of two magmas which have compositions that lie on the regression line and bracket the observed data. The least radiogenic possible end member is 0.7057, a value well above a pristine mantle signature. The range of resulting Sr_i is shown as a shaded field between two 130 Ma reference isochrons. Also shown is an isochron from Precambrian rocks which defines a much greater slope (1.77 Ga). None of the Precambrian samples are colinear with the Rim Sequence regression, thus these country rocks are neither sources nor contaminants of the Rim Sequence.

culated Sr_i vary from 0.7084 to 0.7065 systematically toward the Core Facies, except for the most radiogenic samples which share a calculated Sr_i of 0.7084 ± 0.0002. These samples labelled 1 through 3 are hornblende free granite and granodiorite (CA85-5, BW84-20, BW84-18). A ninth data point (circle) is from the Rim Sequence but not from the traverse (CA85-120). Like the major and trace element data, this sample fits the trend defined by the traverse samples. The pseudochron fit to the eight data points can be interpreted as the result of mixing two isotopically distinct end members that must lie on the regression line and bracket the data, and mechanisms that can account for isotopic variability are assimilation and magma mixing. Assimilation of exposed country rock can be discounted because of its radiogenic nature relative to the Rim Sequence (Figure 49). Magma mixing is the favored mechanism to account for systematic chemical and isotopic variation in the Rim Sequence and potential end members are discussed below.

An isochron based on 5 minerals and the whole rock from Rim Sequence granite (CA85-5; Figure 50), yields a Rb/Sr age of 124 ± 2 Ma and an intercept of 0.7085 ± 0.0003 ($\sqrt{MSRS} = 0.234$). This age approaches that from U-Pb geochronology from the same rock (130 Ma) and suggests Early Cretaceous crystallization. Also shown in Figure 50 are other analyses of hornblende-free rocks and these samples are isotopically homogenous with respect to Sr_i (0.7083 ± 0.0002). These granitic rocks at the margin of the intrusion that lack petrographic indicators of mixing (biotite to hornblende reaction and reversely zoned plagioclase) may be an end member of the mixing process that generated the Rim Sequence.

Core Facies

The Core Facies is composed of biotite hornblende granodiorite and quartz monzodiorite in the interior of the Turtle pluton. These rocks have been subdivided into high K and low K subgroups based on K_2O, Rb, and Sr contents. Six samples of the Core Facies have been analyzed for Rb and Sr isotopic composition (locations in Figure 17 on page 41). All high K samples were collected within a 1000 m of the Target Granite except one felsic sample (CA85-13) collected about

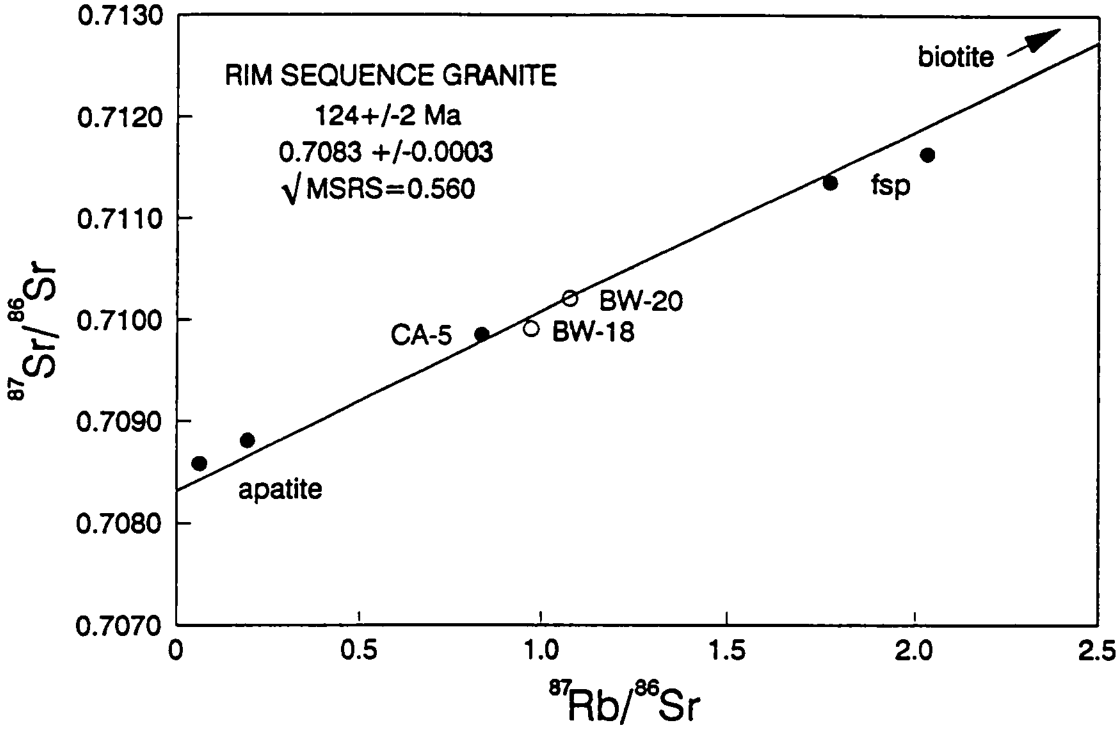

Figure 50. Rb-Sr isochron diagram for minerals from Rim Sequence granite: This mineral isochron is based on the following: equant apatite, acicular apatite, K-feldspar, feldspar, biotite, and whole rock (composition determined by isotope dilution). The resulting age of 124 Ma is somewhat less than the assumed crystallization age of 130 Ma based on U-Pb geochronology. Other whole rock analyses from hornblende free rocks of the Rim Sequence fall close to the isochron and this suggests these granites are in isotopic equilibrium and have not been affected by magma mixing.

1500 meters from the Target Granite. Low K rocks were collected from the periphery of the unit away from the younger intrusion. Rb-Sr isotopic data occur in two groups that generally correspond to the high and low K subgroups (Figure 51). The radiogenic group includes the low K samples (CA85-122 and CA86-14) and a high K sample (CA85-13). This group defines an array of Cretaceous age and Sr_i of about 0.7065. This is the common isotope composition of some granodiorites of the Rim Sequence. In fact, this group includes a sample (CA85-122) collected along the trend of the Rim Sequence traverse (A-A′). The relatively nonradiogenic group is a cluster of points that vary in common isotopic composition from 0.7055 to 0.7057. Of this relatively nonradiogenic group, the samples for which major element data are available were previously classified as high K.

The anomaly in the data set, the high K sample in the radiogenic group (CA85-13), could have attained a high K and Rb content through fractionation of "low K" magma. Two lines of evidence suggest its petrogenesis is different from other high K samples: (1) location away from the Target Granite, (2) Sr_i of 0.7067, a value more radiogenic than that calculated for the high K group (about 0.7056).

Differences in major and trace element data from the high and low K groups of the Core Facies were modelled as alteration by fluids associated with the younger Target Granite (see Chapter 4). Isotopic data support this model. The less radiogenic group (high K) has an isotopic composition between that of the more radiogenic (low K) group, and the Target Granite (Figure 52 on page 196).

Sr isotopic composition of minerals were determined from the same sample used for sphene U/Pb geochronology (CA84-147). This sample is a high K, quartz monzodiorite of the Core Facies that was collected about 800 m from the nearest exposure of the Target Granite. The preliminary isochron based on just 3 analyses (biotite, K-feldspar, and whole rock) suggests an age of 103 ± 2 Ma and an intercept of 0.7057 ± 0.0005 ($\sqrt{MSRS} = 0.392$). This age overlaps the U-Pb age for the Target Granite, the probable source of heat and fluids that caused alteration of this rock. Sphene separates used for U-Pb geochronology plot above the regression and are not in Rb/Sr isotopic equilibrium with other minerals. These sphenes could be xenocrystic except that their euhedral

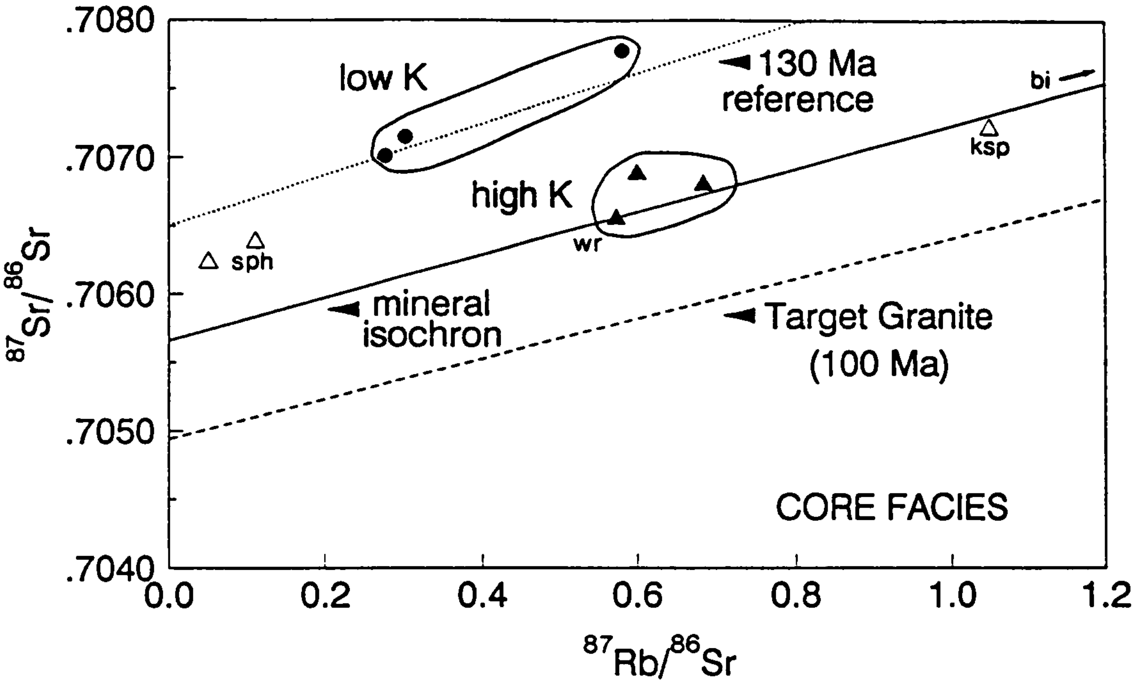

Figure 51. **Rb-Sr isochron diagram for the Core Facies:** Core Facies analyses fall into two subgroups that correspond generally to the low and high K subgroups. The more radiogenic group includes 2 low K samples (CA85-122, CA86-14) and one high K sample collected distant from the Target Granite (CA85-13). These three define a slope similar to 130 Ma (see reference isochron), and a Sr_i of 0.7065. The less radiogenic group (CA84-143, CA84-147, CA85-25) falls in a cluster and has Sr_i of about 0.7057 as calculated at 130 Ma. Geochemistry suggests the less radiogenic, high K group has been altered by the adjacent Target Granite, and this subgroup falls between the low K one and the regression for the Target Granite. A mineral isochron (103 Ma, biotite, feldspar, whole rock) from a sample of the high K group (CA84-147) defines an age similar to the Target Granite (100 Ma; U-Pb zircon). Sphene, used for U-Pb geochronology, falls above the mineral isochron.

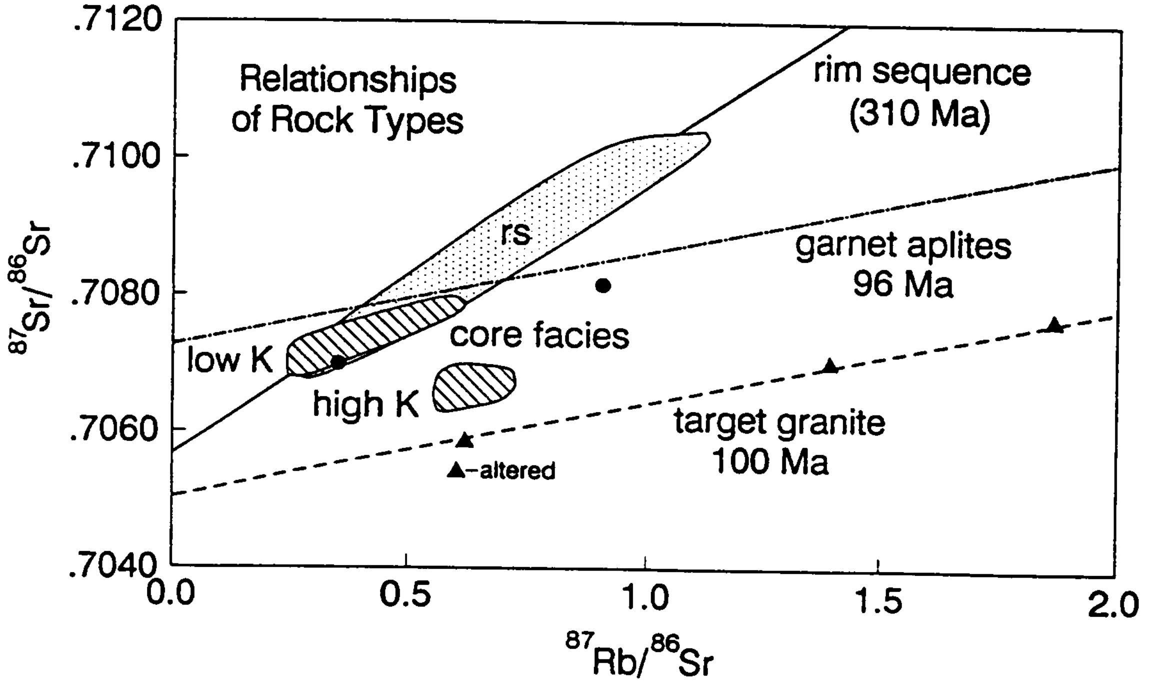

Figure 52. **Rb-Sr isochron diagram for all Cretaceous granitoids:** This diagram summarizes the relationships of granitoids. The Rim Sequence (rs) defines a 310 Ma pseudocron with Sr_i of 0.7057. Low K Core Facies rocks overlap the composition of the Rim Sequence and 2 analyses of the Four Deuce Hills (dots) have similar Sr_i. Mafic enclaves and dikes have a range of Sr_i and some overlap the Rim Sequence (see Chapter 2). High K Core Facies analyses are less radiogenic than any other rock of the Turtle pluton and these rocks cluster between low K Core Facies rocks and the Target Granite (triangles). The Target Granite has a U-Pb zircon age of 100 Ma and similar whole rock Rb-Sr age (103 Ma) defined by 3 samples. A fourth altered sample was excluded from the isochron. Garnet aplites have an age similar to the Target Granite (96 Ma), however they are much more radiogenic ($Sr_i = 0.7073$). These data suggest at least five separate magma sources.

shape and Cretaceous U-Pb age suggest this is not the case. More probably, these are relatively unaltered mineral phases in a rock affected by potassium and rubidium alteration. The sphene ($Sr_i = 0.7062$) may more closely approximate the original isotopic composition of the rock, one more similar to the low K subgroup ($Sr_i = 0.7065$-0.7067).

From geochemical data presented thus far, one can conclude:

1. The Core Facies samples have two distinct Sr isotopic signatures.
2. Most high K samples are less radiogenic ($Sr_i \simeq 0.7056$) than low K samples ($Sr_i \simeq 0.7065$).
3. The high K group yields an age like that of the Target Granite (100 Ma) that intrudes it, and may define an alteration halo surrounding the Target Granite.

Four Deuce Hills

Two analyses of granodiorite from the Four Deuce Hills suggest an age Early Cretaceous age, and fall close to the array defined by low K subgroup of the Core Facies (Figure 52). These data suggest the Four Deuce Hills ($Sr_i = 0.7063$-0.7065) are derived from a magma similar to the unaltered Core Facies ($\simeq 0.7065$).

Garnet-Bearing Aplites

Garnet-bearing aplites intrude all facies of the Turtle pluton but not the Target Granite. Six samples collected from throughout the study area (Figure 20 on page 49) yield an age of 96 ± 4 Ma and an intercept of 0.7073 ± 0.0004 ($\sqrt{MSRS} = 1.333$; Figure 53). These rocks are younger than the Turtle pluton and of similar age to the Target Granite, but are more radiogenic than the Target Granite. Therefore it is assumed these aplites are from a different magma than either pluton.

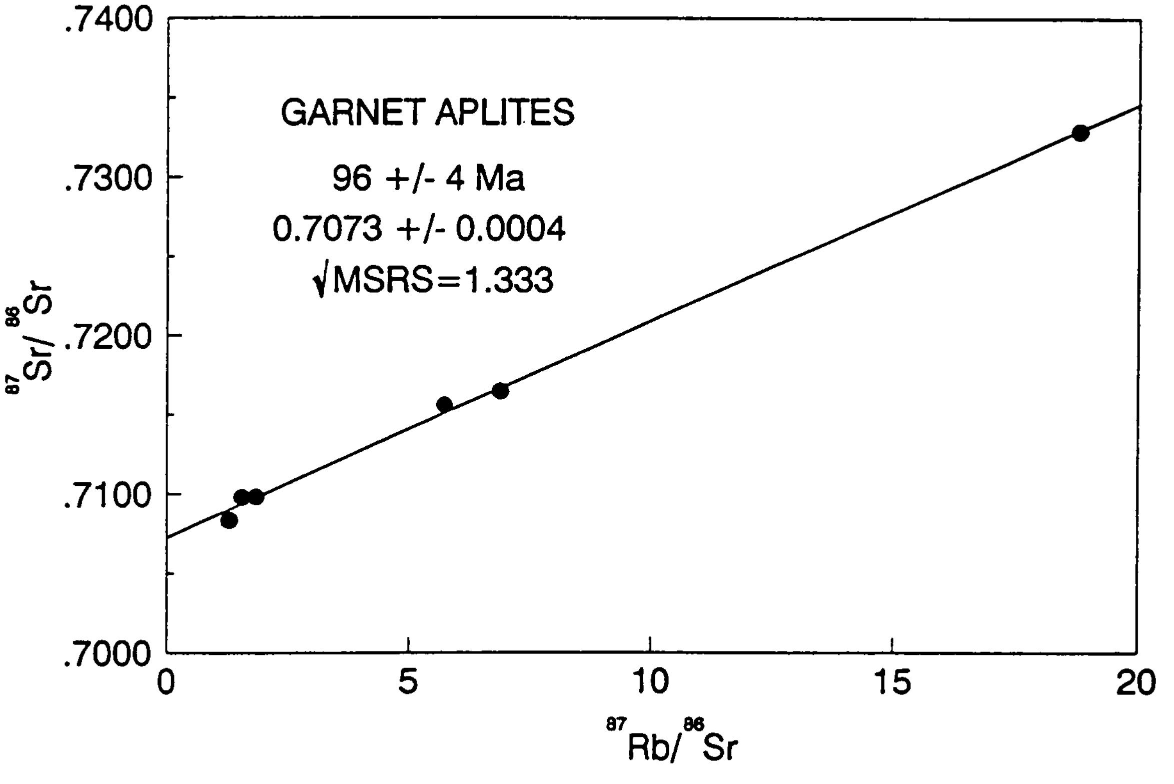

Figure 53. **Rb-Sr isochron diagram for garnet aplites:** Garnet aplites cross cut the Turtle pluton but not the Target Granite. The Rb-Sr age of garnet aplites is 96 Ma, an age that overlaps that of the Target granite (100 ± 3 Ma: U-Pb zircon), however the aplites are much more radiogenic (Sr_i = 0.7073) than the Target Granite (Sr_i = 0.705).

Target Granite

An isochron of 103 Ma and Sr_i of 0.705 is based on three samples of the Target Granite (Figure 52). A fourth sample of altered rock (CA85-15) was collected to test for alteration effects, and this sample lies below the isochron. This whole rock Rb-Sr age overlaps the U-Pb zircon age of 100 $\pm$3 Ma.

Summary and Discussion

Rb-Sr isotopic data from the Turtle pluton, associated mafic rocks, and Target Granite are summarized in Figure 52 and Figure 54.

The Rim Sequence data define an array (pseudochron of 310 Ma) and have a range of Sr_i from 0.7065 to 0.7084 (calculated at 130 Ma). Low K Core Facies rocks (CA85-122, CA86-14), one high K Core Facies sample (CA85-13), and samples from the Four Deuce Hills (CA84-50, CA85-4) have overlapping values of Sr_i (0.7063 to 0.7067). High K Core Facies data are distinctly less radiogenic (Sr_i = 0.7055 to 0.7057) and lie between fields of the low K Core Facies and Target Granite (Sr_i = 0.7045 to 0.7050 calculated at 100 Ma). Garnet aplites, with an age like that of the Target Granite, are much more radiogenic (0.7073 $\pm$ 0.0004) and probably are chemically unrelated to either intrusion. Mafic enclaves and dikes from the Rim Sequence, Core Facies, and Four Deuce Hills have Sr_i of 0.7049 to 0.7071. (at 130 Ma).

The range of isotopic compositions observed in the Rim Sequence must include mixing of two isotopic reservoirs. The radiogenic Precambrian rocks surrounding the Turtle pluton have been discounted as contaminants (Figure 49) and magma mixing is the favored mechanism to account for isotopic variability.

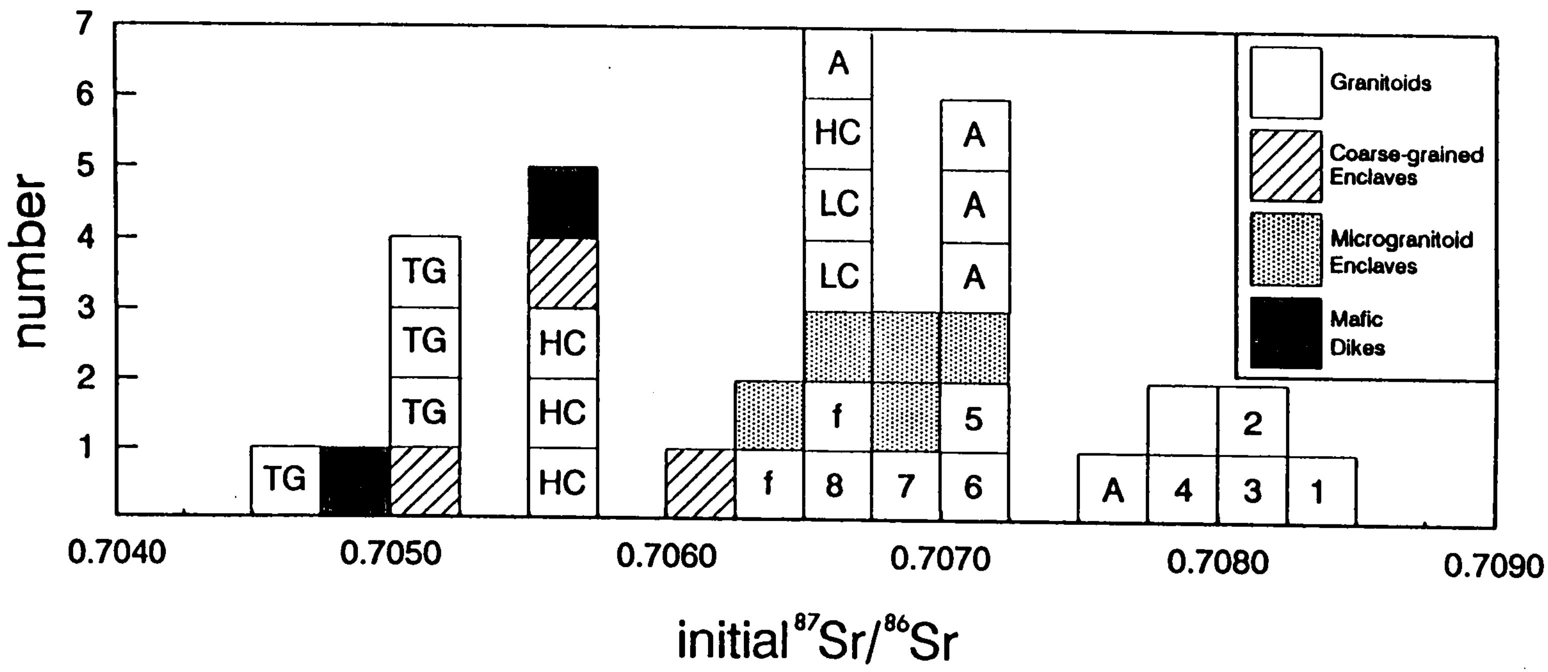

Figure 54. Histogram of inital Sr ratios: This figure shows the distribution of Sr_i for the Turtle pluton (Rim Sequence = 1 through 8, high K and low K Core Facies = HC and LC, respectively, Four Deuce Hills = f), mafic rocks (shaded), garnet aplites (A), and Target Granite (TG). Assuming a crystallization age of 130 Ma for all Turtle pluton samples, the Rim Sequence has a wide range of Sr_i values. The low K Core Facies, one high K sample (CA85-13, see text) and Four Deuce Hills samples overlap the primitive end of the Rim Sequence values and share Sr_i of about 0.7065. The high K Core Facies is less radiogenic (0.7055-0.7058), and has values closer to the younger Target Granite (0.7045-0.7050). Garnet aplites (96 Ma) have an age similar to the Target Granite (100 Ma, U-Pb on zircon) but are more radiogenic (≃0.7073) and therefore unrelated. Microgranitoid enclaves from the Turtle pluton have Sr_i that overlap that of their hosts, and coarse-grained enclaves and mafic dikes are less radiogenic.

To generate a linear array of compositions, only two end members can be involved in the mixing process and these end members must lie along the regression and bracket observed compositions. Possible mafic end members include rocks with Sr_i of 0.7065 or less but more than 0.7057 (the pseudochron intercept). The analyses that lie on the pseudochron and qualify as possible end members are the least radiogenic sample from the Rim Sequence (BW84-25), low K Core Facies samples (CA85-122, CA86-14), and a rock from the Four Deuce Hills (CA84-50). Most microgranitoid enclaves do not lie along the regression, and some have $Sr_i > 0.7065$ (Figure 36 on page 117). In addition examination of enclave-host pairs suggest enclaves are not in isotopic equilibrium with the surrounding rocks and therefore can not be an unmodified end member involved in generation of the Rim Sequence (Chapter 2). The granite of the Rim Sequence which composes a small volume of the exposed pluton is the most radiogenic unit in the pluton (0.7081 to 0.7084). These rocks lack mineralogic evidence of magma mixing and may approach the felsic end member composition. These isotopic extremes, Rim Sequence granite and low K Core Facies (and similar samples mentioned above) will be used in conjunction with major and trace element data to model the petrogenesis of the Turtle pluton (Chapter 6).

The similarity in Sr_i of low K Core Facies and Four Deuce Hills samples suggest derivation from a source with $Sr_i = 0.7065$, a possible end member of the Rim Sequence. Nearby Early Cretaceous intrusions, the Castle Rock pluton and West Riverside Mountains, have similar Sr_i (Figure 61 and Chapter 6).

These data indicate widespread occurrence of a 0.7065 source.

High K Core Facies rocks appear to be the result of alteration of low K Core Facies type by the Target Granite based on major and trace element chemistry, and Rb-Sr age determinations (103 Ma). The Target Granite is the least radiogenic rock unit studied. Its low Sr_i of 0.705 makes it unlikely these rocks were derived from a Precambrian terrane (much more radiogenic at 100 Ma; see Chapter 6), or from sources like that which produced the Turtle pluton (0.7065 to 0.7084). Instead, the Target Granite probably contains a significant mantle component (< 0.7035, Hart and Brooks, 1981).

The garnet aplites of similar age to the Target Granite are much more radiogenic (0.7073) and may be the result of low degrees of partial melting of crust by heating events contemporaneous with generation of the Target Granite.

These Sr isotopic data suggest at least five different melts with separate sources intruded the study area in the period 100 to 130 Ma and these are: two end members of the Rim Sequence, mafic magmas, the Target Granite, and garnet aplites. Common Pb and oxygen isotope data will be used to further constrain these sources.

Lead Isotopes

Introduction

Lead isotopes of potassium feldspars and whole rocks from the Turtle pluton and environs have been provided as part of a survey of the Precambrian and Mesozoic rocks of southern California and Arizona by Dr. Joe Wooden and Dr. Keith Howard of the USGS, Menlo Park. A discussion of techniques and errors appears in APPENDIX 3.

Lead isotope ratios from feldspars are considered the nonradiogenic or common lead signature of a rock because very little parent U or Th is incorporated in the crystal structure of potassium feldspar relative to their daughter, Pb. Thus feldspars in igneous rocks record the lead signatures of their source regions at the time of melting. The isotopic ratios of that lead, however, is the result of parent/daughter ratios (U/Pb and Th/Pb) of the source, the time allowed for the decay of those elements prior to the melting event, and the common Pb composition of the source. Consequently, Pb isotope studies of potassium feldspar from igneous rocks give insight into the ages and Pb, U and Th ratios of their source regions if a common Pb value for the source is assumed (Wooden et al., 1988, and references therein; see Chapter 6).

Lead isotopic data from potassium feldspars from the Turtle pluton, Target Granite, West Riverside Mountains, and the satellite stock north of the Turtle pluton (Figure 3 on page 6) are given in Table 14 and Figure 55. The data will be described by rock type, will be compared to data from Precambrian rocks of the Turtle Mountains, and will be used to evaluate petrogenetic relations among rock types in concert with common Sr data.

Analyses

Except for granite collected adjacent to Precambrian rocks (CA85-5), rocks of the Rim Sequence have a small range of $^{206}Pb/^{204}Pb$ (18.843-18.864) as compared to $^{207}Pb/^{204}Pb$ (15.629-15.674) and $^{208}Pb/^{204}Pb$ (38.585-38.883) and a regression of these data ($^{207}Pb/^{206}$ Pb) yields an age of 3.2 Ga. There are two interpretations of this slope: (1) this is the age of the source, one greater than that documented in the Turtle Mountains. (2) this is a false age generated by mixing of isotopically discrete magmas. The anomalous sample (CA85-5) is much more radiogenic than other samples ($^{206}Pb/^{204}Pb = 19.274$, $^{207}Pb/^{204}Pb = 15.704$, $^{208}Pb/^{204}Pb = 39.463$) and its composition is intermediate to the Rim Sequence data and adjacent whole rock analyses Virginia May gneiss (Table 14). It may have been affected by the surrounding Precambrian terrane.

Samples from the two Core Facies subgroups have very different Pb isotopic signatures and cannot be related by fractional crystallization alone. The low K group (Sr_i of 0.7065) has a Pb signature like the least radiogenic rocks of the Rim Sequence. The high K sample (Sr_i of 0.7057) is like the Target Granite and both have lower $^{206}Pb/^{204}Pb$ (16.532-16.554), $^{207}Pb/^{204}Pb$ (15.605-15.612) and $^{208}Pb/^{204}Pb$ (38.491-38.526) than the Rim Sequence. The lead data therefore support the model that high K core Facies rocks resulted from alteration by the Target Granite.

The samples from nearby Cretaceous intrusions, the West Riverside Mountains and the satellite body north of the Turtle pluton, have lower $^{206}Pb/^{204}Pb$ (18.219-18.470) and similar $^{207}Pb/^{204}Pb$ and $^{208}Pb/^{204}Pb$ to Cretaceous intrusions within the study area.

Table 14. Pb isotope analyses of K-feldspars and whole rocks.*

SAMPLE	TYPE	$^{206}Pb/^{204}Pb$	$^{207}Pb/^{204}Pb$	$^{208}Pb/^{204}Pb$
			Feldspar	
CA85-5	RSgr	19.279	15.705	39.471
CA85-5	RSgr	19.269	15.703	39.455
BW84-20	RSgr	18.843	15.657	38.883
BW84-18	RSgd	18.739	15.629	38.658
BW84-19	RSgd	18.849	15.650	38.721
BW84-23	RSgd	18.857	15.674	38.776
BW84-25	RSgd	18.864	15.652	38.585
CA85-122	CFgd	18.836	15.656	38.660
CA84-147	CFqmd	18.507	15.616	38.546
H79-486A	SATgr	18.470	15.630	38.550
H80-373	WRqmd	18.219	15.600	38.450
CA85-18	TG	18.532	15.605	38.491
CA85-111	TG	18.554	15.612	38.526
			Whole Rock	
CA85-5A	hostgn	22.147	16.025	42.036
CA85-96	hostgn	23.063	16.110	42.690

* Data provided by J.L. Wooden, USGS.

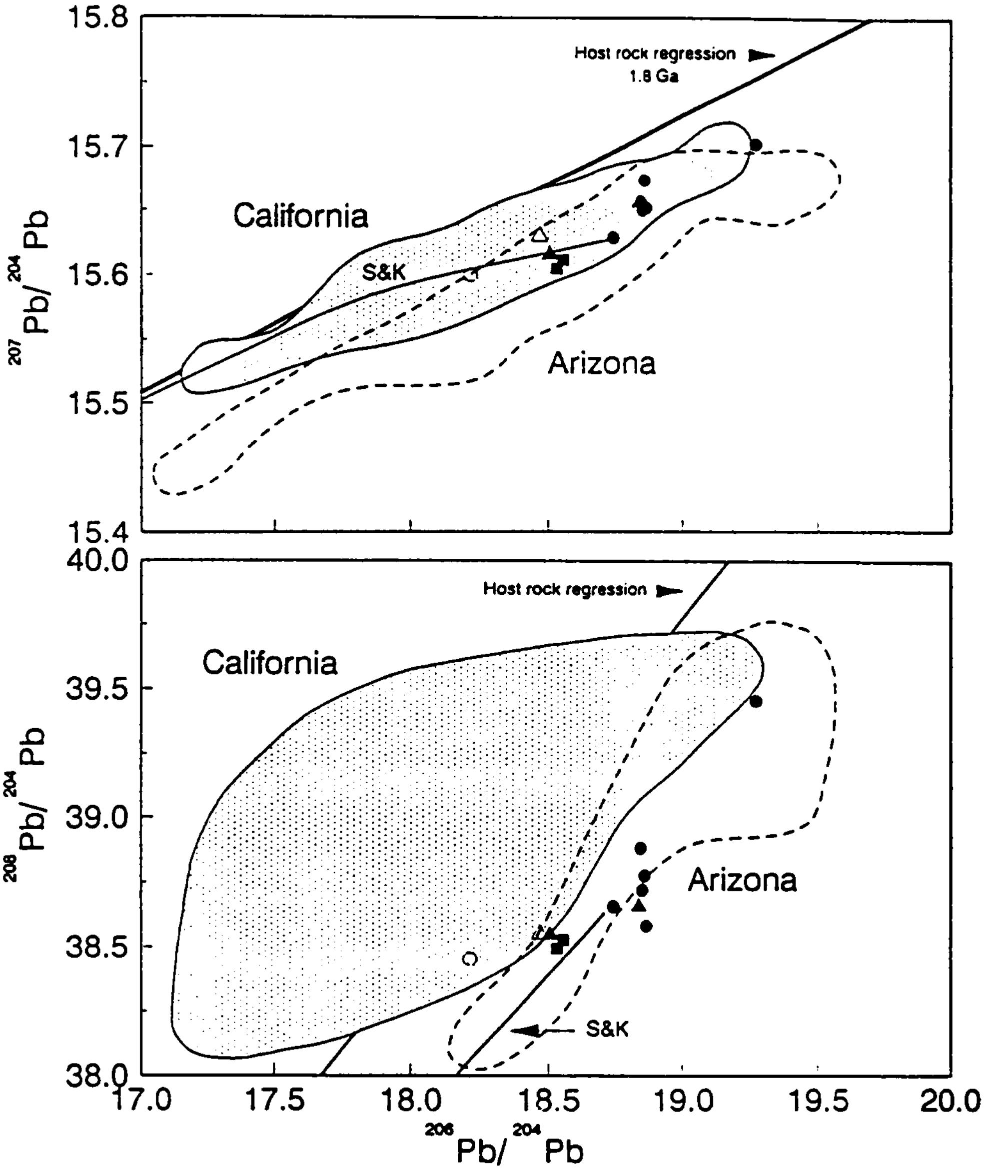

Figure 55. Pb isotope data from potassium feldspar and whole rocks: Pb feldspar data from the Rim Sequence (dots), except one sample adjacent to Precambrian gneisses, have relatively constant $^{206}Pb/^{204}Pb$, and define an age of 3.2 Ga (see text). High and low K Core Facies have different values (solid triangles), and the high K group is the less radiogenic of the two, and has a value similar to the Target Granite (solid squares). The West Riverside Mountains (open triangle) and the satellite body north of the Turtle pluton (circle) are less radiogenic than Rim Sequence samples, and have compositions grossly similar to the Target Granite. All analyses fall below a regression of whole rocks and feldspars from the Precambrian rocks of the Turtle Mountains that define an age of 1.8 Ga (solid line, data from Wooden et al., 1988 and J.L. Wooden, unpublished data). Samples from the Turtle pluton and Target Granite are more similar to those from western Arizona (field labelled Arizona) than to other Mesozoic intrusions of the Colorado River region in California (field labelled California), particularly with respect to $^{208}Pb/^{204}Pb$ (data from Wooden et al., 1988 and J.L. Wooden, unpublished data). The Pb evolution model of Stacey and Kramers (1975), marked "S&K" is included for reference.

A regression of Pb data from 12 whole rock and potassium feldspar samples from Precambrian rocks of the Turtle Mountains (including two samples of Virginia May gneiss from the study area) is given for comparison (J.L. Wooden, unpublished data). This regression results in a $^{207}Pb/^{206}Pb$ age of 1.8 Ga, one very similar to that obtained from Rb-Sr geochronology. Analyses from the Turtle pluton and Target Granite fall below the regression, particularly for thorium-derived ^{208}Pb, and like results from Rb-Sr data, suggest exposed Precambrian rocks are not the sources for these less radiogenic, Early Cretaceous plutons.

Discussion

General conclusions from these Pb isotope analyses are:

1. The Turtle pluton and Target Granite are less radiogenic in $^{208}Pb/^{204}Pb$ and $^{207}Pb/^{204}Pb$ than most analyzed Precambrian rocks in the Turtle Mountains and have similar compositions to Mesozoic rocks of the southwestern U.S., particularly to those from Arizona (see Chapter 6).
2. The Target Granite is less radiogenic in Pb composition ($^{208}Pb/^{204}Pb$, $^{207}Pb/^{204}Pb$, and $^{206}Pb/^{204}Pb$) than the Turtle pluton, except for the high K Core Facies sample that is probably altered by fluids associated with the Target Granite.
3. $^{207}Pb/^{206}Pb$ age of Precambrian rocks of the Turtle Mountains yield the same age as that obtained from Rb-Sr isotopic studies (1.8 Ga).

The conclusions about petrogenetic relationships and source characteristics are similar for both the Pb and Sr common isotopic studies. The behavior of the Pb isotopic data for the Rim Sequence is not as systematic as that for strontium, but generally there is a positive correlation of Sr_i and Pb isotopic data. This suggests the $^{207}Pb/^{206}Pb$ age of 3.2 Ga may be a pseudochron too, and not the true age.

Oxygen and Hydrogen Isotopes

Oxygen and hydrogen isotopic data provide information about the degree of subsolidus re-equilibration and, where there is little re-equilibration, information about source regions of igneous rocks. Whole rock oxygen isotope analyses from major rock types are compared, and mineral oxygen and deuterium analyses are used to evaluate isotopic equilibrium and fluid interactions.

Oxygen Isotopes

Oxygen isotopic ratios of 17 whole rocks and minerals from 6 samples (Table 15) were measured using techniques described in APPENDIX 3. Analytical error is ± 0.2 ‰. Eight samples from the Rim Sequence are those collected along traverse A-A′ (Figure 13 on page 32) and their compositional range is + 6.3 to + 6.5‰ for granites and + 6.7 to + 6.9‰ for granodiorites. Two analyses of high K Core Facies rocks have values similar to the Rim Sequence (+ 6.5 to + 6.7‰). The younger Target Granite and garnet aplite samples have heavier $\delta^{18}O$ ratios than the Turtle pluton (+ 7.4 to + 7.7‰, and + 8.0‰, respectively). As compared to their host Rim Sequence granodiorite (BW84-25), a microgranitoid enclave (BW84-25A) and coarse-grained enclave (BW84-27) have lighter $\delta^{18}O$ ratios (+ 5.7 and + 6.2‰) and this is probably a reflection of greater abundance of biotite which is greatly depleted in ^{18}O relative to ^{16}O as compared to other modal minerals ($\delta^{18}O$ of biotite = + 3.2, BW84-25). Analyses of the Virginia May gneiss collected 10 and 1000 m from the Turtle pluton have $\delta^{18}O$ that bracket values from the Turtle pluton (5.2 to 7.8‰, respectively).

Analyses of the Turtle pluton granitoids are unusual in two ways: (1) There is little variation of $\delta^{18}O$ (+ 6.3 to + 6.9‰) as compared to the large variation of Sr_i (0.7084 to 0.7057). (2) These samples have low $\delta^{18}O$ in comparison to most felsic and intermediate plutonic rocks (+ 7 to + 10‰; Taylor, 1974; O'Neill and Chappell, 1977). Oxygen isotope values from the Target Granite

Table 15. Oxygen and deuterium isotope analyses of whole rocks and minerals.

			$\delta^{18}O$ o/oo				T°C ++			δD o/oo
SAMPLE	TYPE	W.R.	Qtz	Ksp	Bi	Hb	Q-Ksp	Q-Bi	Q-Hb	Bi
CA85-5*	RSgr	+6.5	+7.8	+6.8	+2.6		715	526		-87*
BW84-20	RSgr	+6.3								
BW84-18	RSgr	+6.7								
BW84-19	RSgd	+6.8								
BW84-22	RSgd	+6.7								
BW84-23	RSgd	+6.8	+8.3	+7.1	+3.2	+4.9*	630	534	652	-79*
BW84-24	RSgd	+6.9								
BW84-25	RSgd	+6.6	+8.6	+7.5	+3.5	+5.7*	670	549	722	
CA84-143	CFgd	+6.7								
CA84-147	CFqmd	+6.5	+9.0	+7.1	+3.2	+5.2*	444	488	606	-67*
BW84-25a	m encl	+5.7								
BW84-27	cg encl	+6.2								
CA84-28	gap	+8.0								
CA85-18	TG	+7.7								
CA85-111	TG	+7.4	+8.3*	+7.2*	+2.7		670	507		-72*
CA85-96	hostgn	+7.8								
CA85-5a	hostgn	+5.2								

* Data provided by R. Brigham or L. Adami, USGS.
++ Temperatures from fractionation constants, Table 16.

(+7.4 to +7.7‰) are more like most granites but are still light as compared to the common range of +7 to +10‰ (Taylor, 1974).

Mineral analyses are used to ascertain degree of subsolidus fluid interaction. Based on laboratory measurements of oxygen fractionation among minerals at different temperatures, stable isotopes may be used to discern the degree of attainment and/or retention of equilibrium, and perhaps temperatures of formation (Javoy et al., 1970; Bottinga and Javoy, 1973 and 1975). Equilibrium criteria of O'Neil (1986) are:

1. Absence of isotopic reversals. Copious laboratory analyses indicate that the order of increasing $\delta^{18}O$ enrichment is Mt < Bi < Hb < Fsp < Q.
2. Lack of unusually large fractionation between minerals as compared to laboratory studies.
3. Temperature concordance of all minerals in a rock calculated from laboratory fractionation factors.

A plot of whole rock and mineral $\delta^{18}O$ versus distance from the Precambrian country rock into the Turtle pluton is given in Figure 56. It shows that all rocks of the Turtle pluton have similar values (average +6.7‰), that all samples show normal patterns of mineral $\delta^{18}O$ (first criterion), and there are no unusually large fractionations except for quartz-potassium feldspar from the Core Facies (second criterion). Temperature concordance (third criterion) is examined in isotherm plots that are based on fractionation constants given in Table 16 and on the equation relating fractionation constants (A and B, Table 16 on page 211) and temperature (T) (O'Neil, 1986):

$$10^3 \ln \alpha_{x-y} - B_{x-y} = A_{x-y}(10^6 T^{-2})$$

where x and y are minerals, Δ the difference of $\delta^{18}O$ for minerals x and y, and $10^3 \ln \alpha_{x-y} = \&$

On isotherm diagrams (Figure 57), minerals in equilibrium plot on a line. Relative to quartz, hornblende and potassium feldspar from the Turtle pluton yield similar slopes with magmatic temperatures of 652 to 722°C and 630 to 670°C, respectively, except for the Core Facies (606 and 444°C, respectively). Feldspar from the Target Granite also yields a magmatic temperature (670°C). Biotite-quartz pairs, on the other hand, yield distinctly greater slopes and lower temperatures than other minerals (488 to 549°C). Commonly, biotite-quartz pairs from plutonic rocks yield

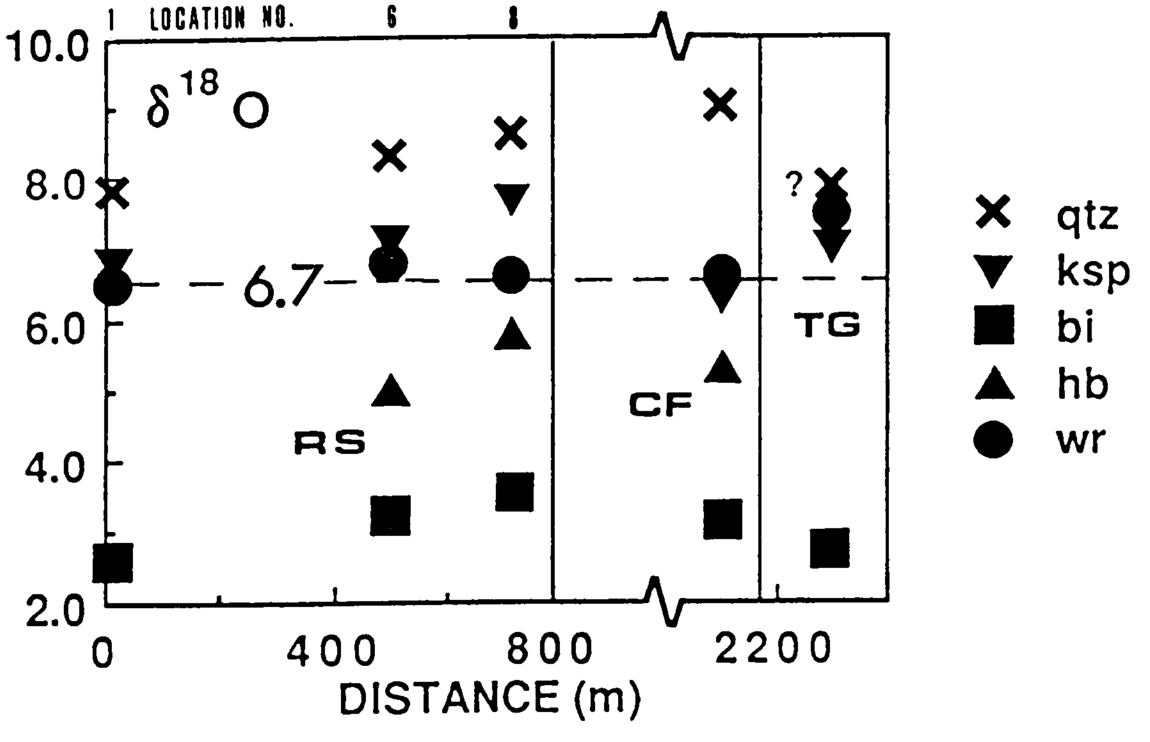

Figure 56. **Oxygen isotope values of rocks and minerals:** This figure shows the distribution of oxygen isotope values with distance into the Turtle pluton for the Rim Sequence (RS, sample numbers at top with position numbers as given in Figure 43 on page 165) and Core Facies (CF). The average value for the pluton is relatively constant for whole rocks (n = 10) and there is some systematic variation of mineral values with distance. There are no reversals in the sequence of mineral values commonly observed (qtz > fsp > hornblende > biotite). The Target Granite (TG) has a distinctly greater whole rock signature than the Turtle pluton.

Table 16. Oxygen isotope fractionation constants between quartz and other minerals.

	A	B	Reference
K-feldspar	0.97	0.0	a
Biotite	3.69	-0.6	b
Hornblende	3.15	-0.3	b

a=Bottinga and Javoy (1973)
b=Bottinga and Javoy (1975)

subsolidus temperatures (Taylor and Sheppard, 1986) which are thought to result from protracted cooling and fluid interaction with biotite (Giletti, 1987). If biotite is the only mineral affected by fluids then the whole rock, magmatic $\delta^{18}O$ is changed little by subsolidus fluid interactions because of the small modal percent biotite in the rocks and its small amount of oxygen per molar volume.

Hydrogen Isotopes

Hydrogen isotopes are sensitive indicators of subsolidus fluid exchange in plutonic rocks. The amount of hydrogen held in a rock is very small compared to a magma or fluid reservoir and minerals remain open to hydrogen exchange well below magmatic temperatures, consequently hydrous minerals act as passive recorders of fluid compositions under subsolidus conditions (Brigham and O'Neil, 1985).

δD of biotites were measured from three rocks of the Turtle pluton and one from the Target Granite in order to characterize amounts of fluid exchange in these plutons (Table 15). δD biotite for the Turtle pluton varies from -87 to -60 and decreases toward the core. Biotite from the Target Granite yields δD of -72. δD of most whole rocks for unaltered granitoids are in this range (-60 to -100 ‰; Taylor, 1986). These data indicate little or no contribution of meteoric waters.

Discussion

Oxygen and deuterium isotope studies of minerals from the Turtle pluton and Target Granite suggest whole rock $\delta^{18}O$ values have not been affected by subsolidus fluid interaction, except for high K Core Facies rocks which are interpreted as altered based on major and trace element data, and on common Sr and Pb isotopic data, and $\delta^{18}O$ of feldspar. These results suggest the relatively low and constant $\delta^{18}O$ for granitoids of the Turtle pluton (about +6.7‰) reflects the isotopic

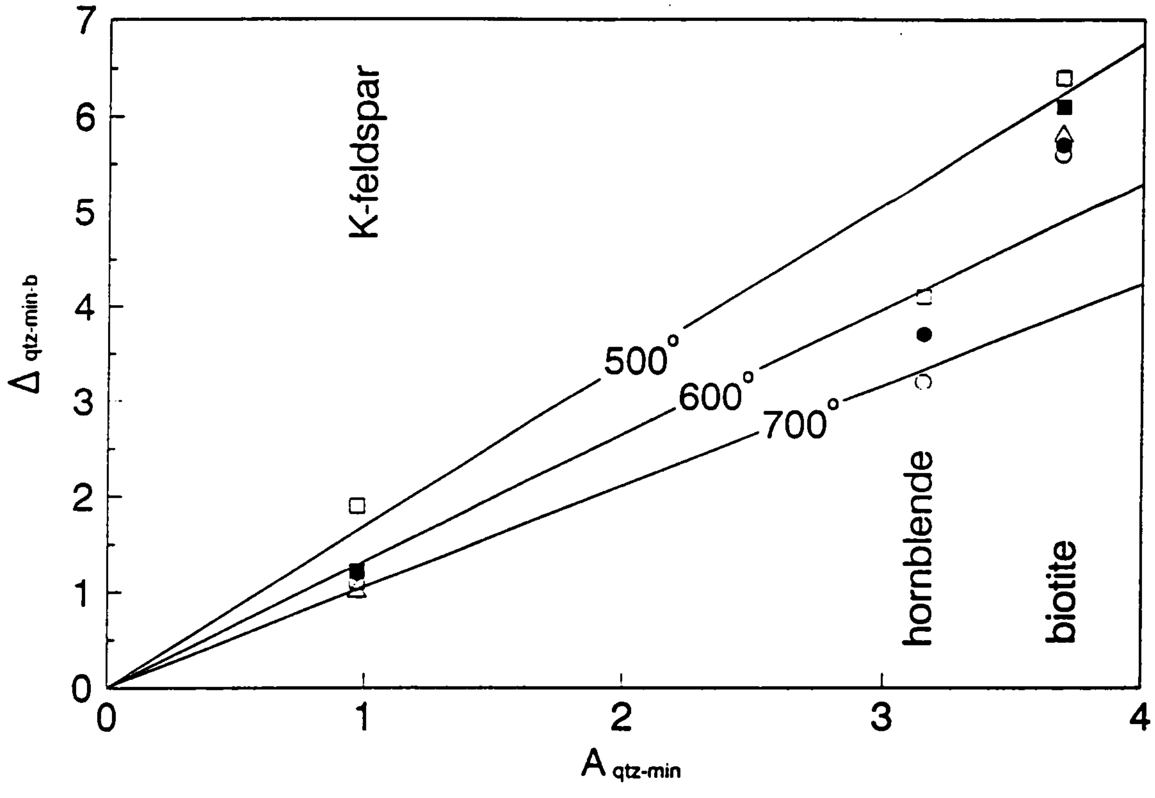

Figure 57. Isotherm diagram of mineral oxygen isotope data: Isotherm plots are based on the fractionation factors of Bottinga and Javoy (1973 and 1975) and the fractionation equation (see text). If all minerals in a rock are in equilibrium, they should fall along a single slope and define a single temperature. Sample symbols are: Rim Sequence granite (CA85-5) = triangle; 2 Rim Sequence granodiorites = dot (BW84-23) & circle (BW84-25); High K Core Facies = square(CA84-147); Target Granite = filled square (CA85-111). Relative to quartz, mineral pairs yield magmatic temperatures for hornblende and K-feldspar except for the Core Facies sample. In all cases, biotite records subsolidus temperatures which indicates this mineral is not in isotopic equilibrium with other minerals but has remained open to fluid interactions at a lower temperature. Given the small modal abundance and the small oxygen content per volume, this has a small effect on whole rock values.

signature of the source. Likewise, the distinctly higher value of the Target Granite (+7.4 and +7.7‰) is thought to reflect its source signature.

Chapter 6

PETROGENETIC MODEL AND SOURCE CONSTRAINTS

Introduction

A petrogenetic model for the reversely zoned Turtle pluton is based on field observations, major and trace element chemistry, and isotopic data. A chemical model is followed by a physical model of magma chamber evolution. Constraints on source characteristics for the Turtle pluton and Target Granite are derived from Sr and Pb isotopes, and these isotopic data are compared to those from other Cretaceous intrusions in the Colorado River region. Finally, the P-T-t history of the Turtle Mountains will be compared to those of flanking ranges.

Chemical Model of the Turtle pluton

The compelling features of the Turtle pluton that must be explained in any petrogenetic model are:

1. its reverse zoning

2. systematic changes in mineralogy and chemistry across the Rim Sequence
3. linear major element trends, except alkalis, observed for the Rim Sequence and low K Core Facies
4. curvilinear trace element (Ba, Rb, and Sr) and alkali trends of these rock types
5. changes of Sr_i from 0.7084 to 0.7065 across the Rim Sequence and into the Core Facies
6. chemical and isotopic differences of high and low K subgroups of the Core Facies
7. isotopic similarity of the Four Deuce Hills to the low K Core Facies.

Rim Sequence and Low K Core Facies

Chemical variations across the Rim Sequence and into the Core Facies cannot be explained by a single differentiation mechanism but must rely on at least two simultaneous processes.

On the basis of linear major element trends and variable Sr_i, it has been argued that a two end member process must be involved in generation of the Rim Sequence, and the favored mechanism is magma mixing (Chapter 3 and 5). The other principal two end member process, assimilation of country rock, has been eliminated because exposed host rocks are more radiogenic with respect to Sr isotopes and do not lie along an extension of Rim Sequence chemical trends. Based on Rb-Sr isotope study, suggested magma end members are Rim Sequence granite (rhyolitic composition) because of isotopic homogeneity of the granite and lack of petrographic evidence of mixing in those rocks, and low K Core Facies granodiorites and quartz monzodiorites (andesitic composition) because they are the most primitive rocks that lie on the Rim Sequence mixing line (Figure 52 on page 196).

Mafic enclaves and dikes are rejected as uncontaminated end members because they generally fail to lie on the Rim Sequence chemical trends for most major and trace elements, and Rb-Sr isotopes. Mafic rocks make up a small volume of the pluton ($<$ 5 area%), have had a complicated history including local interaction with granitoids, and appear to have had little influence on the chemical evolution of the Rim Sequence.

Two end member magma mixing explains some chemical features well, but cannot account for curvilinear trace and alkali element chemical trends. Such trends are the result of a multi-end member process which influences concentrations of these elements greatly, but does not effect that of other major elements (see Chapter 3). The favored mechanism is fractionation or accumulation of phases with large distribution coefficients for these elements (biotite, K-feldspar, and plagioclase).

Models of concomitant magma mixing and fractional crystallization have been cited in models of chemical evolution of plutons (Kistler et al., 1986; Barnes et al., 1987, as examples) and these models are based on the assimilation-fractional crystallization (AFC) model of DePaolo (1981). A model of magma mixing and fractionation for the Turtle pluton is adapted from this AFC model to account for the following:

1. Chemical changes across the Rim Sequence and into the Core Facies are orderly. In a pluton of this size and shape, one would expect disruption of the gradient by turbulent convection (Spera, 1984; Huppert et al., 1984) and therefore the observed chemical gradient must have been produced in situ and not at depth.
2. Mid-crustal plutons crystallize over a finite period, and cool primarily from their roofs and walls. Evidence which suggests exterior to interior, progressive crystallization includes: the fine grain size of Rim Sequence granite suggests a chilled margin, a dike of Core Facies intrudes the Rim Sequence, and mafic dikes found only in the Rim Sequence. The distribution of mafic dikes suggests this portion of the pluton was crystalline enough to preserve them while the core was dynamic enough to disaggregate them.
3. Rocks that approach end member compositions are exposed in the Turtle pluton. Granites of the Rim Sequence approach minimum melt compositions ($SiO_2 = 74$ wt%), and analyses of the low K Core Facies fall on chemical trends with the Rim Sequence.

DePaolo (1981) proposed a model of simultaneous mixing and fractional crystallization based on major and trace elements, and on the Rb-Sr isotopic system for mafic magma assimilating more felsic country rock. In the case of the Turtle pluton, the selected end members are first crystallizing Rim Sequence granite and low K Core Facies (contaminant). In the simple AFC model, fractionation in addition to mixing generates a curvilinear array of compositions that do not culminate in the contaminant composition (DePaolo, 1981; Figure 58) and this result is unsatisfactory given the Core Facies is assumed to be the contaminant. In order to circumvent this result, the felsic end member is allowed to evolve toward the contaminant composition. This approximates the orderly progression of chemical and field characteristics of the Turtle pluton and allows a model of in situ evolution of the magma chamber instead of maintenance of two isolated magma reservoirs that mix in constantly changing proportions in a third chamber.

The proposed AFC model is a stepwise approximation of Sr_i and trace element data. These variables were selected to constrain the model because Sr_i is sensitive to mixing and trace elements are sensitive to fractional crystallization. Sr_i vs SiO_2 is also given as an example of major element behavior. Assumptions made for the model are that mixing and fractional crystallization are about equally efficient though mixing dominates ($r = 1.05$), that an arbitrary ratio of 90% felsic and 10% mafic end members are mixed in a given step, and that 10% of the volume is removed by fractional crystallization of an assemblage with a constant K_D. The next step assumes this hybrid to be the new felsic end member and the process is repeated. Simultaneous fractional crystallization and mixing depend on the rates of assimilation (M_a) and crystallization (M_c), their ratio (r), the mass of the magma (M_m) as compared to the original mass (M_o), called F, the concentration of the elements and isotopes in the end members (X, Sr and SRI) the bulk distribution coefficient of the element (X_{solid}/X_{liquid}) or K_D, and on $Z = (r + K_D + 1)/(r-1)$ (DePaolo, 1981). Equations that describe the case where M_a and M_c are not equal are given in Table 17 along with the assumed end member compositions. For all three of these elements, Rim Sequence granite (BW84-20 and CA85-5) has concentrations which suggest it is a potassium feldspar cumulate relative to granodiorite (BW84-18, > Rb, > Ba, and < Sr). All three rocks share Sr_i of 0.7083 ± 0.0002, so that trace element concentrations between BW84-18 and the granites were used in the model in order to more closely approximate a liquid composition. Mafic end member concentrations mimic the low K Core Facies (CA85-122).

Where Sr_i (Y-axis) is plotted against elements other than Sr (X-axis), the Sr concentration of the end members still controls the curvature of a mixing line so that the behavior of Sr concentration as well as the element of interest must be known. The K_D that gives the best fit to the data for plots of Sr_i versus Sr constrain the Y-axis values for other elements. Visual best fit was then obtained by varying the K_D of Sr, then the K_D of the element of interest.

The results are shown in Figure 58 and in Table 17 and are compared to distribution coefficients for Rb, Sr and Ba-bearing minerals given by Arth (1976). The calculated model accurately

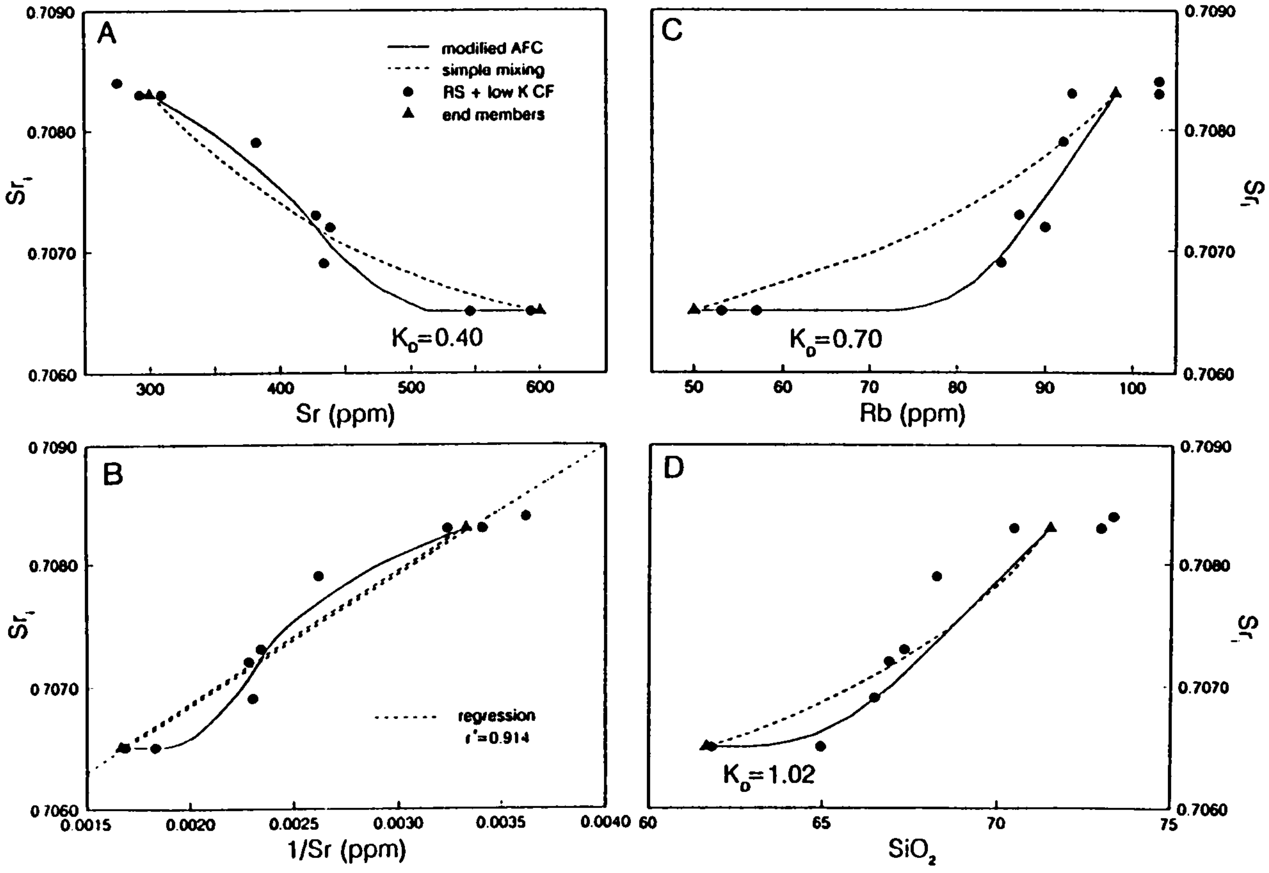

Figure 58. Results of modified AFC model: This adaptation of the AFC model of Depaolo (1981) allows progressive evolution of the felsic end member toward the mafic one. End members approach Rim Sequence granite and low K Core Facies (see Table 16). Best fit to the data is obtained by varying the K_D of the fractionated assemblage. Other constraints are given in the text. The model predicts Sr concentrations greater than simple mixing for mafic rocks, and ones less than simple mixing for felsic rocks (A & B) at K_D of 0.40. Note simple mixing would result in a straight line in B (Langmuir et al., 1978), instead the data define a sinusoidal curve with r^2 of 0.914 whereas a regression of the companion plot (A) yields r^2 of 0.947. In other words, if mixing were the only mechanism, data should be more linear in B than A and this is not observed. Thus another mechanism is assured. The model predicts Rb concentrations greater than mixing with K_D of 0.70. As an example of major element behavior, the model suggests little fractionation in the case of SiO_2 ($K_D \simeq 1$) but does not fit the data well. The calculated K_D for Sr, Rb and Ba (1.0, not shown) suggests biotite and feldspars are the dominant fractionated minerals (Table 16).

Table 17. Equations, end member compositions, and results of AFC modelling.

$$SRI = \frac{\frac{r}{r-1}\frac{Sr_m}{z}(1-F^{-z})\,SRI_m + Sr_f\,F^{-z}\,SRI_f}{\frac{r}{r-1}\frac{Sr_m}{z}(1-F^{-z}) + Sr_f\,F^{-z}}$$

$$Sr = \frac{-F^{-z}\,Sr_f}{(SRI-SRI_m)/(SRI_m-SRI_f)}$$

$$C = F^{-z} + (r/(r-1))(C_m/z\,C_f)(1-F^{-z})$$

where m=mafic, f=felsic, SRI= common isotopic ratio, Sr=concentration, and C=concentration of other elements.

Selected End Member Compositions

	MAFIC	FELSIC
SRI	0.7065	0.7083
SiO_2(wt%)	61.7	71.5
Sr (ppm)	300	600
Rb	50	98
Ba	690	760

Calculated K_D

	MODEL	Plag*	Ksp*	Biot*
Sr	0.40	4.4	4	v. low
Rb	0.70	0.04	0.4	2
Ba	1.05	0.3	6	10

*from Arth (1976)

predicts that Sr concentrations are greater than simple mixing for felsic rocks, and less than that of mixing for the more mafic ones at $K_D = 0.40$. This low calculated K_D value, relative to feldspars, suggests fractionation of a low K_D assemblage, one rich in quartz, biotite, ± hornblende, and poor in feldspar. The companion plot of Sr_i vs 1/Sr is provided to show the Rim Sequence does not plot as a straight line that would result from simple mixing but is sinusoidal, and, in fact is less linear ($r^2 = 0.914$) than Sr_i vs Sr ($r^2 = 0.947$). These results reconfirm processes more complicated than binary mixing have occurred. For Rb, the calculated K_D is 0.70 and the model predicts compositions richer in Rb than simple mixing would predict. If the rocks are assumed to approximate a liquid line of descent, the K_D cannot exceed 1 because the samples are enriched in this element relative to simple mixing. This value is greater than that of feldspars and suggests fractionation of feldspars plus biotite. Ba concentration is relatively unchanged (except for granites considered cumulates from the initial liquid and excluded from the model) and suggests removal of a neutral assemblage. Sr_i versus SiO_2 results in a sinusoidal trend which suggests fractionation of quartz among the most felsic rocks. The model does not provide a much better fit than simple mixing, except it does predict the relatively unradiogenic nature of the more mafic rocks. For all analyzed elements, if mixing is allowed to be more efficient than fractional crystallization ($r > 1.05$), or if the amount of crystallization is diminished ($F < 10\%$) as compared to the model, K_D values must increase. This model of chemical evolution in which the felsic end member is progressively contaminated and fractionated accounts for observed trace element variations, and is incorporated into a physical model of the magma chamber.

High K Core Facies

The high K rocks of the Core Facies differ from the low K group in major and trace element chemistry, and in common Pb and Sr ratios. The high K group has common isotope ratios more similar to the Target Granite which intrudes it than to the low K group of the Core Facies. Oxygen isotope mineral pairs indicate lower equilibration temperatures than those recorded in the Rim Sequence. Whole rock oxygen isotope values (+6.5 to +6.7‰), on the other hand, are like those of the Rim Sequence (+6.6 to 6.9‰) and not the Target Granite (+7.4 to +7.7‰). Oxygen isotope mineral pairs from high K Core Facies rocks suggest lower equilibration temperatures for quartz-feldspar than any pair from the Rim Sequence. δD of biotite is in the range of values considered "unaltered" (Taylor, 1974). These data suggest that high K rocks experienced potassic alteration by fluids with little meteoric component. The alteration particularly affected potassium feldspar, the principal host for Rb and Pb in these rocks. A Rb-Sr mineral age overlaps the U-Pb age of the Target Granite. The geographic location of high K rocks, and the geochronology indicate the younger intrusion is the source of fluids that caused alteration. All of these data indicate the high K group experienced potassic alteration by fluids associated with the younger Target Granite.

Four Deuce Hills

The limited data from the Four Deuce Hills suggest it is chemically similar to the granodioritic rocks of the Rim Sequence, the low K Core Facies and to the Castle Rock pluton. It may represent an apophysis from the Core Facies at depth, or may be a separate melt from a source like that of the Core Facies.

Physical Model of Evolution for the Turtle pluton

A physical model of the Turtle pluton based on field observation, whole rock geochemistry, and experimental and theoretical treatments of flow regimes in magma chambers is presented in Figure 59. The model must account for: orderly chemical gradients, reversed zonation of the pluton, preservation of mafic dikes in the Rim Sequence but not in the Core Facies, the Schlieren Zone, the presence of screens of Precambrian gneisses in the Schlieren Zone, and the similarity of the Four Deuce Hills to the Core Facies.

Geochemical data have been used to propose that both magma mixing and fractionation/ accumulation mechanisms led to chemical diversity in the Turtle pluton. In a cylindrical pluton with subvertical walls, a body of this size would most likely experience turbulent magma flow that would disrupt existent chemical gradients (Hubbert and Sparks, 1984; Spera, 1984). Orderly chemical gradients observed in the rocks probably represent in situ, progressive crystallization from the walls inward, and record a changing magma composition with time. A model of a steep-walled magma chamber that cools from the walls and roof, and undergoes sidewall crystallization and accumulation of buoyant, fractionated liquids at the roof (Baker and McBirney, 1985) is easily adapted to data from the Turtle pluton (Figure 59). Such a model allows formation of chemical gradients by removal of liquid from the site of side wall crystallization. Sr_i values are superimposed on the model of McBirney and Baker (1981) to indicate that the first magma to plate onto the walls is the most radiogenic (0.709), that a less radiogenic source at depth (< 0.706) is continuously added to the chamber which also adds heat and extends the life of the chamber, and that Sr_i of the chamber decreases with time and with distance into the pluton as mafic magma is incorporated. The initial granite has a small volume in comparison to the entire pluton, and could be the result of crustal melting above a pond of more mafic magma. Both magma types rose to a higher crustal level into unrelated Precambrian rocks, and the granite began to crystallize as mafic magma intruded it and mixed with it at a level now exposed in the Turtle pluton. Continued upward movement of the last part of the chamber to crystallize, the Core Facies, could result in the steep ductile deformation zone that divides the Rim Sequence from the Core Facies. Basaltic dikes with textures like microgranitoid enclaves observed throughout the pluton are only preserved in the outer portion of the pluton. This suggests small volumes of mafic magma were introduced into the chamber and disaggregated throughout its evolution, and that only late generations of dikes were preserved in the crystallized outer shell of the intrusion. These mafic dikes have lower Sr_i than any rock of the Turtle pluton and could represent the magmas that gave rise to the andesitic Core Facies through

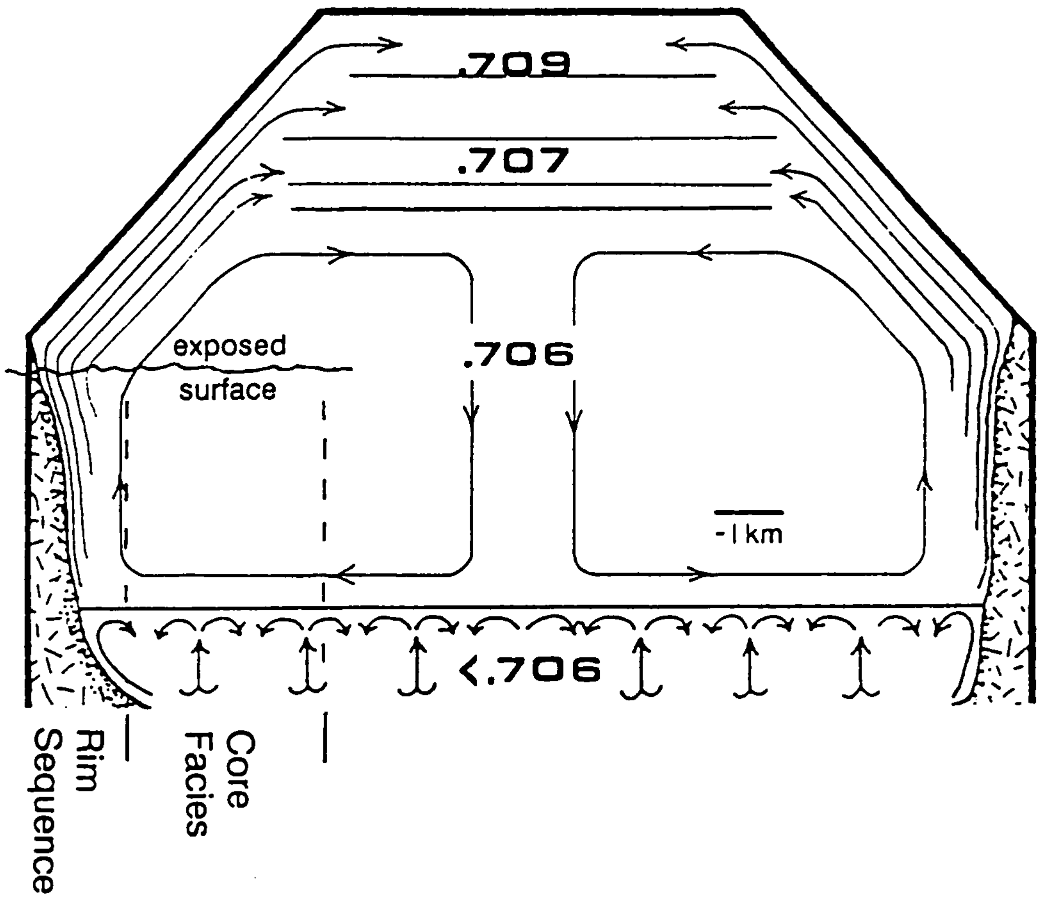

Figure 59. Physical model for evolution of the Turtle Pluton: This model of evolution for a steep-walled magma chamber in which crystallization from the walls and roof produces more buoyant fractionated liquids (McBirney and Baker, 1981), readily explains geochemical changes observed in the Turtle pluton. As adapted here, the first magma to crystallize is the most radiogenic (Sr_i = 0.709), a less radiogenic magma at depth (< 0.706) is added to the chamber, and the Sr_i of the chamber evolves with time.

mixing or crustal heating. It must be restated, however, that these basaltic magmas are not an end member of the process that generated the Rim Sequence.

Many of the mechanisms proposed to explain chemical zonation of reversely-zoned plutons (Chapter 1) cannot adequately explain the data from the Turtle pluton. Differentiation from interior to exterior due to addition of volatiles at the rim (Mutschler, 1980) can be discounted by the field evidence that the Core Facies intrudes the Rim Sequence. Rb-Sr isotopic evidence rules out contamination of the Rim Sequence by country rock (Ragland et al., 1980). Progressive partial melting of a single source (Hall, 1966) would result in homogenous Sr_i if isotopic equilibrium at anatexis is assumed. Similarly, restite unmixing would result in a single Sr_i (Ayuso and Wones, 1980). Flow differentiation could concentrate mafic enclaves and phenocrysts toward the interior of the intrusion but according to calculations by Barriere (1976) this mechanism is effective only when the conduit is less than 100 meters in diameter. Unrelated magmas compose the Turtle pluton, a mechanism suggested to form zoned plutons by Ragland et al., 1980, but geochronology indicates the magmas are the same age within errors. Hutchinson (1960) suggested intrusion of mafic magma into anatectic crustal melts and this may be the relationship of end members of the Rim Sequence. Rearrangement of a horizontally zoned chamber has been proposed to account for reversed zonation of an ash flow (Fridrich and Mahood, 1984) but the middle crustal depth of the Turtle pluton and wide spread steep foliations in country rocks suggest in situ, vertical zonation. Calculated flow regimes suggest previously developed gradients would be disrupted (Huppert and Sparks, 1984; Spera, 1984) and orderly gradients are observed. The mechanism proposed for the Turtle pluton is most like one proposed by Bourne and Danis (1987). They suggested emplacement of a large magma reservoir, onset of crystallization and movement of liquid toward the roof (Baker and McBirney, 1985), failure of the outer crust and escape of evolved liquid to form an "upper reservoir", then later tapping of lower zones to form diapirs that are emplaced in the core of the upper reservoir. Again, orderly zonation of the Turtle pluton suggests in situ evolution of the Rim Sequence, however emplacement of the chemically related Core Facies, development of the Schlieren Zone, and screens of Precambrian rocks in the Schlieren Zone could result from emplacement of the core into the previously formed daiapir that now forms the rim of the Turtle pluton.

Source Characteristics of End Member Magmas

Introduction

Source characteristics of magmas that gave rise to the Turtle pluton and Target Granite are constrained by ages of rocks exposed in the Turtle Mountains, by Rb/Sr, U/Pb, Th/Pb and Th/U ratios calculated from isotopic data, and by $\delta^{18}O$ of the exposed rocks. These values can be used to generally describe the source rock type (Table 18).

Turtle pluton

The Turtle pluton has been modelled as the result of mixing and concomitant fractionation of a rhyolitic magma like that of the outer Rim Sequence granite, and an andesitic one like the low K Core Facies rocks. The Rim Sequence granite has low color indices, approaches minimum melt compositions and lacks petrographic evidence of magma mixing. If it is assumed this magma is derived only from the crust of similar age to rocks exposed in the Turtle Mountains, then trace element ratios of the source can be calculated from Rb-Sr and U-Pb isotopes. Exposed Precambrian rocks of the Turtle Mountains range in age from 2.3 to 1.4 Ga (unpublished U-Pb zircon geochronology, J.L. Wooden; Wooden et al., 1988). Rocks immediately adjacent the pluton are 1.77 Ga and have $Sr_i = 0.702$, a value like that of the bulk earth model (DePaolo and Wasserburg,

Table 18. Characteristics of end member magmas.

	MAFIC	FELSIC
SiO_2	62 wt%	72 wt%
Sr_i	0.7065	0.7083
$\delta^{18}O$	+6.7‰	+6.4‰
$^{208}Pb/^{204}Pb$	38.60	38.88
Rb/Sr*		0.70-0.10
Th/U*		3.86-3.91
U/Pb*		0.14-0.15

* calculated, assuming source ages of 1.4 to 2.3 Ga.

1981) at that time (Figure 60), though all of these rocks are more radiogenic than the Turtle pluton at 130 Ma and cannot be its source. Assuming the source of Rim Sequence granite also had Sr_i like the bulk earth model, and an age between 2.3 to 1.4 Ga, an envelope of possible sources is defined on Sr isotope evolution diagram (Figure 60). These constraints limit the source to have Rb/Sr (ppm) between 0.07 and 0.10. Rocks that commonly have such ratios are amphibolites, granulites, mafic igneous rocks, and granulites.

If similar assumptions are made for common Pb, the source had initial Pb like that of the model of Stacey and Kramers (1974) and ages between 2.3 and 1.4 Ga, the source had U/Pb, Th/Pb and Th/U (ppm) of 0.14 to 0.15, 25.5 to 26.6, and 3.91 to 3.88, respectively. Rock types with such ratios are amphibolites and mafic igneous rocks. Granulites, because of previous melting, have Th/U much greater than the crustal average of 4 (Zartman and Doe, 1981) and therefore granulites are not possible source materials. These calculations suggest the source is mafic igneous rocks or amphibolites.

Whole rock and mineral oxygen isotope data suggest the $\delta^{18}O$ of Rim Sequence granites (+6.3 to +6.5‰) are inherited from the source. Such values are common in volcanic rocks, mafic intrusions, and metamorphic rocks exclusive of carbonates.

In summary, if a crustal source is assumed for the Rim Sequence granites, it is unlike the exposed basement rocks, and is probably a mafic plutonic rock (diorite, quartz diorite, or gabbro) or an amphibolite. Experimental studies suggest melting of undersaturated amphibolite can give rise to transitional metaluminous-peraluminous melts at temperatures between 910 and 940°C and at pressures greater than 4 kb (Ellis and Thompson, 1984).

The assumption of a single source is questionable for the mafic end member of the Turtle pluton (low K Core Facies) because its Sr_i (0.7065) is low for a mature, Precambrian crustal source (> 0.7060; Kistler and Peterman, 1973). If a purely crustal source is assumed, it is similar to that described for the felsic end member but with lower Rb/Sr and greater $\delta^{18}O$ (+6.7 to +6.9‰). Just as likely, it is a mixture of a mantle (< 0.7035) and crustal (> 0.7060) components.

Mafic rocks associated with the Turtle pluton have a range of Sr_i from 0.7050 to 0.7072 and these could be variably contaminated basaltic magmas from the mantle. Certainly the mafic dikes

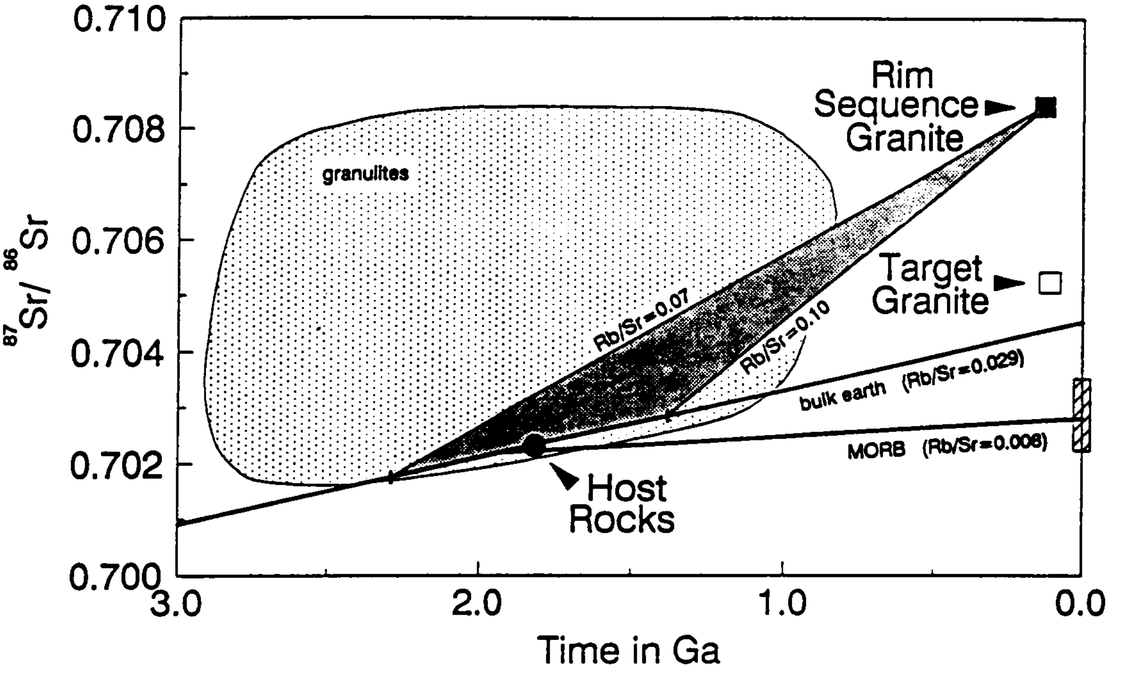

Figure 60. **Sr evolution diagram showing probable sources for Rim Sequence granite:** This evolution diagram shows Sr_i of Rim Sequence granite (filled square), Target Granite (square) and Precambrian rocks (dot) at their crystallization/homogenization ages. Assuming the source age is between 1.4 and 2.3 Ga, and has Sr_i like that of the bulk earth model of DePaolo and Wasserburg (1976), the source of the Rim Sequence has Rb/Sr ratio (ppm) between 0.07 and 0.10 which is similar to that for granulites (shaded field) compiled by Pettingill and Sinha (1984) and mafic igneous rocks. The much lower Sr_i of the Target Granite (0.705) suggests it contains a mantle component, here represented as MORB (ruled box and average growth line labelled "MORB", Hart and Brooks, 1981).

with Sr_i of 0.7049 to 0.7055 contain a mantle component. They plus a crustal source may have contributed to the Core Facies, and produced Sr_i that is intermediate between mature crust and mantle values.

Target Granite

The Target Granite is a leucogranite with a low Sr_i value of 0.705 as compared to mature continental crust (> 0.7060, Kistler and Peterman, 1973). This suggests a mantle contribution to this granitic intrusion. This low Sr_i is surprising given the granite contains only very sparse mafic inclusions that could be interpreted as a mantle component. This Target Granite is less radiogenic with respect to Pb and Sr isotopes, and has a greater $\delta^{18}O$ than the Turtle pluton, and must be derived from a different source or sources.

Regional Comparison of Cretaceous Plutons

The Turtle pluton and Target Granite have several unique features as compared to plutons in surrounding ranges. First of all, the ages of the Turtle pluton (130 Ma) and Target Granite (100 Ma) are greater than all Cretaceous plutons in surrounding ranges dated by U-Pb geochronology (J.L. Wooden, personal communication; Wright, et al., 1986). Secondly, K-Ar ages from biotite and hornblende from Cretaceous and pre-Cretaceous rocks of the Turtle Mountains yield ages of greater than 90 Ma whereas in flanking ranges (except the West Riverside Mountains, 95-101 Ma), they are less than 70 Ma (Howard et al., 1982; Hoisch et al., 1988; Martin et al., 1982; Davis et al., 1982). These data suggest the Late Cretaceous and Tertiary heating event that affected the surrounding ranges did not affect the Turtle Mountains or the West Riverside Mountains. Additionally, the plutons of the southern Turtle Mountains (Turtle pluton, Target Granite and Castle Rock Pluton) and West Riverside Mountains have common Sr and Pb ratios unlike many of the near by Cretaceous intrusions. These isotopic data are suggestive of a different source region.

A histogram of Sr_i values from Cretaceous plutons in surrounding ranges (this study for Goffs = Piute Mts.; Davis et al., 1982 for Whipple Mountains; John, 1987 for Chemehuevi Mts.; K.A. Howard, unpublished data) shows the Target Granite is less radiogenic than all others, that the low K Core Facies has Sr_i similar to some plutons of the Whipple Mountains, the West Riverside Mountains, and Castle Rock pluton, that the Rim Sequence has values similar to intrusions in the Whipple and Chemehuevi Mountains, and that most plutons in the Arica, Old Woman and Piute Mountains have $Sr_i > 0.7090$ (Figure 61). The sources for Cretaceous plutons to the west and south of the Turtle Mountains are metaluminous to peraluminous, are associated with nappes, and are distinctly more radiogenic (> 0.7090) than those plutons to the east and south east. The similar Sr_i of 0.7065 for the mafic portion of the Turtle pluton, the West Riverside Mountains and Castle Rock pluton and some rocks of the Whipple Mountains suggests these magmas are from a similar, widespread source.

A compilation of Pb isotopic data from potassium feldspars extracted form Mesozoic intrusions of the Colorado River Region and western Arizona appears on Pb isotope diagrams in Figure 55 on page 205 (Wooden et al., 1988; J.L. Wooden, unpublished data). The California field includes data from the Old Woman, Chemehuevi, and Iron Mountains, and ranges to the north and west (n = 50; Figure 3 on page 6). The Arizona field contains data from the southwestern part of the state (n = 41). Pb isotopic signatures of the Turtle pluton, Target Granite, and West Riverside Mountains are more similar to intrusions in Arizona than to those from ranges immediately surrounding the Turtle pluton. Pb data suggest the plutons of the study area were derived from sources with lower Th/U than Cretaceous plutons in flanking ranges (J.L. Wooden, personal communication, 1988).

Common Pb and Nd-Sm isotopic studies of Mesozoic intrusions and Precambrian rocks have been used to suggest fundamental differences of crustal age exist east and west of the Colorado River (1.7-1.8 and 2.0-2.3 Ga, respectively, Zartman, 1974; Bennett and DePaolo, 1987). Pb

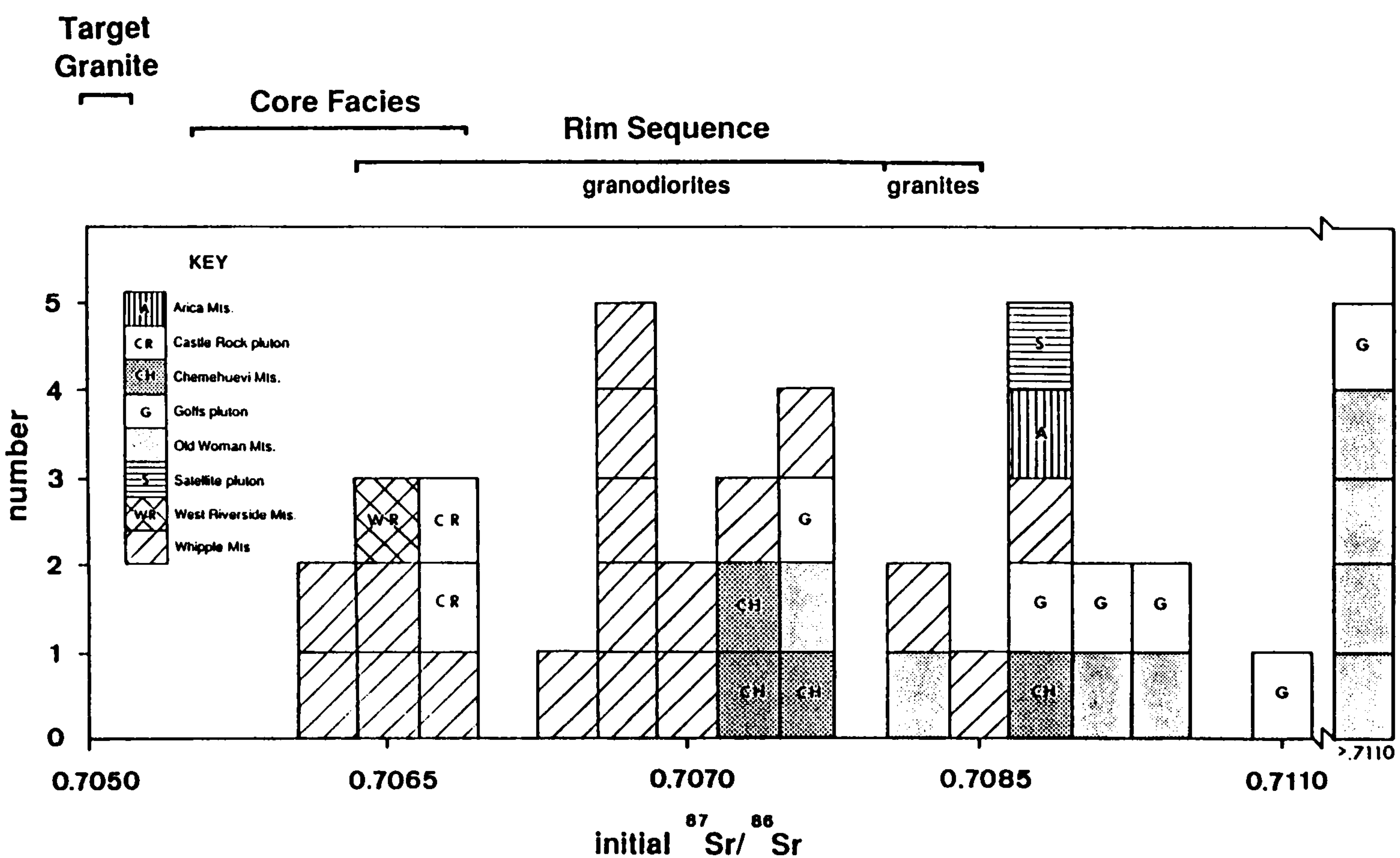

Figure 61. Histogram of initial Sr for ranges near the Turtle Mountains: This figure shows the distribution of Sr_i for the Turtle pluton and Target Granite relative to ratios from Cretaceous plutons in other ranges. Core Facies and some granodiorites from the Rim Sequence have values similar to the West Riverside Mts., the Castle Rock pluton, and some plutons of the Whipple Mts. Rim Sequence granites are similar to data from the Whipple and Chemehuevi Mts. Most analyses from ranges associated with nappes (Arica and Old Woman Mts., and Goffs pluton, Piute Mts.) are more radiogenic (>0.7085) than the most radiogenic rocks of the study area. These results indicate the Turtle pluton is petrogenetically more like plutons to the east than to the west.

isotopic studies of Tertiary and Quaternary volcanic rocks also suggest a fundamental change in mantle sources occurs in this area (Everson, 1979). With respect to common Sr and Pb isotopes, the Turtle pluton, Target Granite and West Riverside Mountains are more similar to Mesozoic rocks to the east and sources for these plutons probably belong to the eastern, younger province defined by Zartman, 1974. In addition, Rb-Sr and Pb isotopic studies of Precambrian rocks in the Turtle Mountains suggest a 1.8 Ga age, one like that of the eastern province. A reconnaissance study of Nd-isotopes suggests, however, that Precambrian rocks exposed in the Turtle Mountains belong to the older, western province (Bennett and DePaolo, 1987).

Differences in P-T-t Paths

Compilation of radiometric, geochemical and petrologic data from the Turtle pluton and flanking ranges allows comparison of the pressure-temperature-time (P-T-t) histories of these ranges. Data taken from studies of plutons and metamorphic rocks (this study; Anderson, 1988; Anderson et al., 1988; Hoisch, et al., 1988; Foster et al., 1988; Howard et al., 1982) are are shown in Figure 62.

Mineral chemistry, mineral assemblage, and U-Pb geochronology indicate the Turtle pluton was emplaced at 3.5 kb at 130 Ma, between 750 and 800°C. The pluton was solid at the time it was stoped by the Target Granite at 100 Ma, and the presence of muscovite in synchronous, two mica, garnet aplites suggests the terrane was still at midcrustal depths (3-4 kb) at the beginning of the Late Cretaceous. Biotite K-Ar ages from the Turtle pluton (98 Ma, Howard et al., 1982), K-feldspar $^{39}Ar/^{40}Ar$ from the Turtle Mountains (90 Ma, Foster et al., 1988), and a zircon fission track age from the western Turtle Mountains (88 Ma, Howard et al., 1982) all suggest the southern Turtle Mountains were not heated above 250°C after 90 Ma. The Cretaceous plutons of the study area were exposed by 20 Ma when Tertiary volcanic rocks covered the granitoids (Howard et al.,

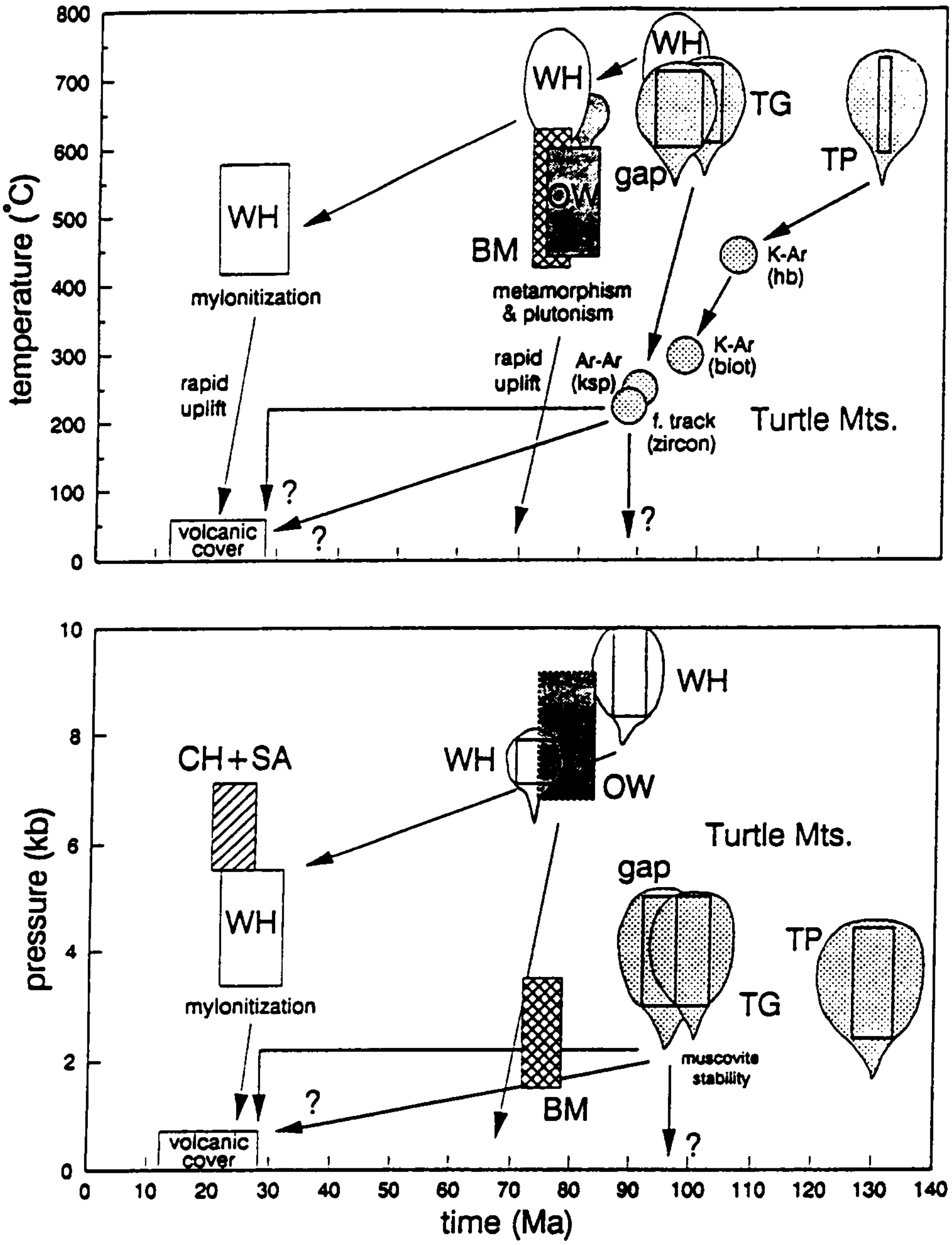

Figure 62. **P-T-t histories of the Turtle Mountains and surrounding ranges:** Data from metamorphic and plutonic rocks are compiled here in plots of pressure-time and temperature-time to show the differences in P-T-t paths for the southern Turtle Mountains and flanking ranges (references given in text). The Turtle Mountains cooled to below 250°C by about 90 Ma and were not reheated, while flanking ranges experienced metamorphism and plutonism in Late Cretaceous and Tertiary time. This suggests the Turtle Mountains acheived a high level in the crust during Early Cretaceous time while flanking ranges rose from middle to deep crustal levels in Late Cretaceous and Tertiary time.

1982). The range of possible P-T-t paths of the southern Turtle Mountains from pluton emplacement to exposure is given in Figure 62.

After the southern Turtle Mountains cooled through 250°C at 90 Ma, plutonism, metamorphism, and mylonitization occurred in the Old Woman Mountains to the west, the Big Maria Mountains to the south, and the Whipple Mountains to the east.

In the Whipple Mountains, deep-seated plutons were emplaced at 8-10 kb from 89 to 73 Ma (Anderson, 1988). These rocks were mylonitized at temperatures of about 500°C and pressures of 5 kb at 26 Ma (Anderson, 1988), and then experienced rapid uplift to the surface before about 30 Ma (Davis et al., 1982).

To the west and south, compressional tectonics produced nappes, high grade metamorphism (to sillimanite grade) and plutonism in the Old Woman Mountains and the Big and Little Maria Mountains (Figure 3 on page 6). Metamorphism in the Old Woman Mountains occurred prior to 74 Ma at pressures of about 8 kb, and emplacement of metaluminous and peraluminous plutons occurred shortly thereafter (Hoisch et al., 1988). Rapid uplift of the range occurred at about 70 Ma (Foster et al., 1988). Metamorphism of the Big Maria Mountains was contemporaneous with that in the Old Woman but at lower pressures (2-3 kb and 400-600°C; Hoisch et al., 1988).

These data indicate the southern Turtle Mountains cooled through 250°C by about 90 Ma and were not reheated during the Late Cretaceous event that affected ranges on three sides. The Turtle Mountains must have resided at crustal levels well above those now exposed in the Old Woman, Big Maria, and Whipple Mountains by Late Cretaceous time, and may represent a section similar to roof zones of these flanking ranges that were removed by tectonics and/or erosion. These P-T-t data and common isotope studies suggest that large contrasts in isotopic signatures of plutons over short distances are as much due to vertical movement as to strike-slip tectonics.

REFERENCES

Affholter, K.A. (1988) Synthesis and crystal chemistry of lanthanide allanites, 208 p. Ph.D. dissertation, Virginia Polytechnic Institute and State University, Blacksburg, Virginia.

Albee, A.L., and Ray, L. (1970) Correction factors for electron-probe microanalysis of silicates, oxides, carbonates, phosphates, and sulfates. Analytical Chemistry, 42, 1408-1414.

Allen, J.C., and Boettcher, A.L. (1978) Amphiboles in andesite and basalt: II. Stability as a function of P-T-f_{H_2O}-f_{O_2}. American Mineralogist, 63, 1074-1087.

Allen, J.C., Boettcher, A.L., and Marland, G. (1975) Amphiboles in andesite and basalt: I. Stability as a function of P-T-f_{O_2}. American Mineralogist, 60, 1069-1085.

Anderson, J.L. (1983) Proterozoic anorogenic granite plutonism of North America. Geological Society of America Memoir 161, 133-154.

Anderson, J.L. (1988) Core complexes of the Mojave-Sonoran Desert: Conditions of plutonism, mylonitization, and decompression. In W.G. Ernst, Ed., Metamorphism and Crustal Evolution of the Western United States, Rubey Volume VII, p. 502-525. Prentice-Hall, New Jersey.

Anderson, J.L., Barth, A.P., and Young, E.D. (1988) Mid-crustal roots of Cordilleran metamorphic core complexes. Geology, 16, 366-369.

Armstrong, R.L., and Suppe, J. (1973) Potassium-argon geochronometry of Mesozoic igneous rocks in Nevada, Utah, and southern California. Geological Society of America Bulletin, 80, 1375-1392.

Arth, J.G. (1976) Behavior of trace elements during magmatic processes-- a summary of theoretical models and their applications. Journal of Research, U.S. Geological Survey, 4, 41-47.

Ayuso, R.A. (1982) Geology of the Bottle Lake Complex, Maine. Ph.D. dissertation, 244 p. Virginia Polytechnic Institute and State University, Blacksburg, Virginia.

Ayuso, R.A. (1984) Field relations, crystallization, and petrography of reversely zoned granitic plutons in the Bottle Lake Complex, Maine, 58 p. U.S. Geological Survey Professional Paper 1320.

Ayuso, R.A., and Wones, D.R. (1980) Geology of the Bottle Lake Complex, Maine. In D.C. Roy and R.S. Naylor, Eds., The Geology of Northeastern Maine and Neighboring New Brunswick, p. 32-64. Boston College Press, Boston.

Baker, B.H., and McBirney, A.R. (1985) Liquid fractionation. Part III. Geochemistry of zoned magmas and the effects of crystal fractionation. Journal of Volcanology and Geothermal Research, 24, 55-81.

Baltz, R. (1982) Late Mesozoic folding and thrusting and Tertiary extensional faulting in the Arica Mountains, Riverside County, California. In E.G. Frost and D.L. Martin, Eds., Mesozoic-

Cenozoic Tectonic Evolution of the Colorado River Region, California, Arizona and Nevada (Anderson-Hamilton volume), p.582-597. Cordilleran Publishers, San Diego, California.

Barbarin, B. (1988) Field evidence for successive mixing and mingling between the Piolard Diorite and the Saint-Julien-la-Vetre Monzogranite (Nord-Forez, Massif Central, France). Canadian Journal of Earth Sciences, 25, 49-59.

Barnes, C.G., Allen, C.M., and Saleeby, J.B. (1986) Open- and closed-system characteristics of a tilted plutonic system, Klamath Mountains, California. Journal of Geophysical Research, 91, 6073-6090.

Barnes, C.G., Allen, C.M., and Brigham, R.H. (1987) Isotopic heterogeneity in a tilted plutonic system, Klamath Mountains, California. Geology, 15, 523-527.

Barriere, M. (1986) Flowage differentiation: limitation of the "Bagnold Effct" to the narrow intrusions. Contributions to Mineralogy and Petrology, 55, 139-145.

Bateman, P.C., Clark, L.D., Huber, N.K., and others (1963) The Sierra Nevada batholith--A synthesis of recent work across the central part. U.S. Geological Survey Professional Paper 414D, D1-D46.

Bateman, P.C., and Wones, D.R. (1972) Geologic map of the Huntington Lake quadrangle, central Sierra Nevada, California. U.S. Geological Survey, Geologic Quadrangle Map GQ 987, scale 1:62,500.

Bateman, P.C., and Chappell, B.W. (1979) Crystallization, fractionation, and solidification of the Tuolumne Intrusive Series, Yosemite National Park, California. Geological Society of America Bulletin, 90, 465-482.

Bateman, P.C. (1983) A summary of critical relations in the central part of the Sierra Nevada batholith, California, U.S.A. Geological Society of America Memoir 159, 241-254.

Bates, R.L., and Jackson, J.A. (1980) Glossary of Geology, 751 p. American Geophysical Institute, Falls Church, Virginia.

Bence, A.E., and Albee, A.L. (1968) Empirical correction factors for the electron microanalysis of silicates and oxides. Journal of Geology, 76, 382-403.

Bennett, V.C., and DePaolo, D.J. (1987) Proterozoic crustal history of the western United States as determined by neodymium isotopic mapping. Geological Society of America Bulletin, 99, 674-685.

Bishop, C.C. (1963) Geologic map of California, Needles sheet (1:250,000). California Division of Mines and Geology, San Francisco.

Bottinga, Y., and Javoy, M. (1973) Comments on oxygen isotope geothermometry. Earth and Planetary Science Letters, 20, 251-265.

Bottinga, Y., and Javoy, M. (1975) Oxygen isotope partitioning among minerals in igneous and metamorphic rocks. Reviews of Geophysics and Space Physics, 13, 401-418.

Bourne, J., and Danis, D. (1987) A proposed model for the formation of reversely zoned plutons based on a study of the Lacorne Complex, Superior Province, Quebec. Canadian Journal of Earth Sciences, 24, 2506-2520.

Bowen, N.L. (1922) The reaction principal in petrogenesis. Journal of Geology, 30, 177-198.

Bowen, N.L. (1928) The Evolution of the Igneous Rocks, 322 p. Princeton Univeristy Press, Princeton, N.J.

Brewer, W.M. (1987) Role of quartz-bearing dikes in incipient deformation of Whitestone leucogabbro from the Parry Sound Shear Zone, Ontario Canada. Seventh International Convention on Basement Tectonics, Queens University, 26.

Brigham, R.H., and O'Neil, J.R. (1985) Genesis and evolution of water in a two-mica pluton: A hydrogen isotope study. Chemical Geology, 49, 159-177.

Brooks, C. Hart, S.R., and Wendt, I. (1972) Realistic use of two error regression treatments as applied to rubidium strontium data. Reviews of Geophysics and Space Physics, 10, 551-577.

Buddington, A.F. (1959) Granite emplacement with special reference to North America. Geological Society of America Bulletin, 70, 671-747.

Cantagrel, J.-M., Didier, J., and Gourgaud, A. (1984) Magma mixing: origin of intermediate rocks and "enclaves" from volcanism to plutonism. Physics of the Earth and Planetary interiors, 35, 63-76.

Chen, J.H., and Moore, J.G. (1982) Uranium-lead isotopic ages from the Sierra Nevada Batholith, California. Journal of Geophysical Research, 87, 4761-4784.

Clayton, R.N., and Mayeda, T.K. (1963) The use of bromine pentafluoride in the extraction of oxygen from oxides and silicates for isotopic analysis. Geochemica et Cosmochemica Acta, 27, 43-52.

Coney, P.J., and Reynolds, S.J. (1977) Cordilleran Benioff zones. Nature, 275, 403-406.

Cox, K.G., Bell, J.D., and Pankhurst, R.J. (1979) The Interpretation of Igneous Rocks, 450 p. George Allen & Unwin, London.

Czamanske, G.K., and Wones, D.R. (1973) Oxidation during magmatic differentiation, Finnmarka Complex, Oslo area, Norway. Part II. Journal of Petrology, 14, 349-380.

Czamanske, G.K., Ishihara, S., and Atkin, S.A. (1981) Chemistry of rock-forming minerals of the Cretaceous-Paleocene batholith in southwestern Japan and implications for magma genesis. Journal of Geophysical Research, 86, 10431-10469.

Czamanske, G.K., and Mihalik, P. (1982) Oxidation during magmatic differentiation, Finnmarka Complex, Oslo area, Norway: Part I, the opaque oxides. Journal of Petrology, 13, 493-509.

Davis, G.A., Anderson, J.L., Frost, E.G., and Shackelford, T.J. (1980) Mylonitization and detachment faulting in the Whipple-Buckskin- Rawhide Mountains terrane, southeastern California and western Arizona. Geological Society of America Memoir 153, 79-129.

Davis, G.A., Anderson, J.L., Martin, D.L., Krummenacher, D., Frost, E.G., and Armstrong, R.L. (1982) Geologic and geochronologic relations in the lower plate of the Whipple Detachment Fault, Whipple Mountains, southeastern California, a progress report. In E.G. Frost and D.L. Martin, Eds., Mesozoic-Cenozoic Tectonic Evolution of the Colorado River Region, California, Arizona and Nevada (Anderson-Hamilton volume), p.1-28. Cordilleran Publishers, San Diego, California.

de Albuquerque, C.A.R. (1973) Geochemistry of biotites from granitic rocks, northern Portugal. Geochemica et Cosmochemica Acta, 37, 1779-1802.

DePaolo, D.J., and Wasserburg, G.J. (1976) Inferences about magma sources and mantle structure from variations of $^{143}Nd/^{144}Nd$. Geophysical Research Letter, 3, 743-746.

DePaolo, D.J. (1981) Trace element and isotopic effects of combined wallrock assimilation and fractional crystallization. Earth and Planetary Letters, 53, 189-202.

Dickinson, W.R. (1981) Plate tectonic evolution of the southern Cordillera. In W.R. Dickinson and W.D. Payne, Eds., Relations of tectonics to ore deposits in the southern Cordillera, vol. XIV, p. 113-135. Arizona Geological Society Digest.

Didier, J. (1973) Granites and their enclaves, 393 p. Elsevier, Amsterdam.

Didier, J. (1987) Contribution of enclave studies to the understanding of origin and evolution of granitic magmas. Geologische Rundschau, 76, 41-50.

Dilles, J.H. (1987) Petrology of the Yerington Batholith, Nevada: evidence for evolution of porphyry copper ore deposits. Economic Geology, 82, 1750-1789.

Dodge, F.C.W., Moore, J.G., Papike, J.J., and May, R.E. (1968) Hornblendes from granitic rocks of the Central Sierra Nevada batholith, California. Journal of Petrology, 9, 378-410.

Dodge, F.C.W., Smith, V.C., and Mays, R.E. (1969) Biotites from granitic rocks of the central Sierra Nevada batholith, California. Journal of Petrology, 10, 250-271.

Dostal, J. (1975) Geochemistry and petrology of the Loon Lake pluton, Ontario. Canadian Journal of Earth Sciences, 12, 1331-1345.

Dymek, R.F (1983) Titanium, aluminum and interlayer cation substitution in biotite from high-grade gneisses, West Greenland. American Mineralogist, 68, 880-899.

Ellis, D.J., and Thompson, A.B. (1986) Subsolidus and partial melting reactions in the quartz-excess $CaO + MgO + Al_2O_3 + SiO_2 + H_2O$ system under water-excess and water deficient conditions to 10 kb: some implications for the origin of peraluminous melts from mafic rocks. Journal of Petrology, 27, 91-121.

Everson, L.E. (1979) Regional variations in the lead isotopic characteristics of Late Cenozoic basalts from the southwestern United States, Ph.D. dissertation, 454 p. California Institute of Technology, Pasdena.

Farmer, G.L., and DePaolo, D.J. (1984) Origin of Mesozoic and Tertiary granite in the western United States and implications for pre-Mesozoic crustal structure 2. Nd and Sr Isotopic studies of unmineralized and Cu- and Mo-mineralized granite in the Precambrian craton. Journal of Geophysical Research, 89, 10414-10161.

Faure, G. (1977) Principles of Isotope Geochemistry, 464 p. John Wiley & Sons, New York.

Foster,D.A., Harrison, T.M., Miller, C.F., Howard, K.A., and John, B.E. (1988) Mesozoic and Cenozoic thermal history of the eastern Mojave Desert, California: insights from $^{40}Ar/^{39}Ar$ geochronology. Geological Society of America Abstracts with Programs, 20, A17.

Franz, G., and Spear, F.S. (1985) Aluminous titanite (sphene) from the eclogite zone, south central Tauern Window, Austria. Chemical Geology, 50, 33-46.

Fridrich, C.J., and Mahood, G.A. (1984) Reverse zoning in the resurgent intrusions of the Grizzly Peak cauldron, Sawatch Range, Colorado. Geological Society of America Bulletin, 95, 779-787.

Frost, T.P., and Mahood, G.A. (1987) Field, chemical, and physical constraints on mafic-felsic magma interaction in the Lamark Granodiorite, Sierra Nevada, California. Geological Society of America Bulletin, 99, 272-291.

Frost, E.G., and Okaya, D.A. (1986) Application of seismic reflection profiles to tectonic analysis in mineral exploration. Arizona Geological Society Digest, 16, 137-151.

Giletti, B.J. (1986) Diffusion effects on oxygen isotope temperatures of slowly cooled igneous and metamorphic rocks. Earth and Planetary Science Letters, 77, 218-228.

Gill, J.G. (1981) Orogenic Andesites and Plate Tectonics, 390 p. Springer-Verlag, Berlin.

Grant, J.A. (1986) The isocon diagram--A simple solution to Gresens' equation for metasomatic alteration. Economic Geology, 81, 1976-1982.

Green, N.L., and Usdansky, S.I. (1986) Ternary-feldspar mixing relations and thermobarometery. American Mineralogist, 71, 1100-1108.

Hall, A. (1966) A petrogenetic study of the Rosses granite Complex, Donegal. Journal of Petrology, 7, 202-220.

Hamilton, W. (1982) Structural evolution of the Big Maria Mountains, northeastern Riverside County, southeastern California. In E.G. Frost and D.L. Martin, Eds., Mesozoic-Cenozoic Tectonic Evolution of the Colorado River Region, California, Arizona and Nevada (Anderson-Hamilton volume), p. 1-28. San Diego, California, Cordilleran Publishers.

Hammarstrom, J.M., and Zen, E-an. (1986) Aluminum in hornblende: an empirical igneous geobarometer. American Mineralogist, 71, 1297-1313.

Harker, A. (1909) The Natural History of Igneous Rocks, 309 p. New York.

Hart, S.R., and Brooks, C. (1977) The geochemistry and evolution of the early Precambrian mantle. Contributions to Mineralogy and Petrolgy, 61, 109-128.

Hart, S.R., and Brooks, C. (1980) Sources of terrestrial basalts: an isotopic view point. In Basaltic Volcanism on the Terrestrial Planets, Chapter 7.4.2 of Basaltic Volcanism Study Project, Lunar and Planetary Institute, Pergammon Press, Inc., New York.

Hawthorne, F.C. (1982) Crystal chemistry of the amphiboles. In D.R. Veblen, Ed., Amphiboles and other hydrous pyroboles--mineralogy. Reviews in Mineralogy, Volume 9A, p. 1-102. Mineralogical Society of America.

Hayes, J.M. (1983) Practice and principles of isotopic measurements in organic geochemistry. In Organic geochemistry of contemporaneous and ancient sediments, p. 5-1-5-31. Great Lakes Section, SEPM, Bloomington.

Hazlett, R.W. (1986) Geology of a Tertiary volcanic center, Mopah Range, San Bernardino County, California, 303 p. Ph.D. dissertation, University of Southern California, Los Angeles.

Helz, R.T. (1976) Phase relations of basalts in their melting ranges at $P_{H_2O} = 5$ kb. Part II. Melt Compositions. Journal of Petrology, 17, 139-193.

Hewitt, D.A., and Wones, D.R. (1984) Experimental phase relations of the micas. In S.W. Bailey, Ed., Micas, Reviews in Mineralogy, Volume 13, p. 201-256. Mineralogical Society of America.

Hibbard, M.J. (1981) The magma mixing origin of mantled feldspars. Contributions to Mineralogy and Petrology, 76, 158-170.

Hill, R.I., Chappell, B.W., and Silver, L.T. (1988) San Jacinto Intrusive Complex 2. Geochemistry, Journal of Geophysical Research, 93, 10349-10372.

Hill, R.I., and Silver, L.T. (1988) San Jacinto Intrusive Complex 3. Constraints on crustal magma chamber processes from strontium isotope heterogeneity. Journal of Geophysical Research, 93, 10373-10388.

Hoisch, T.D. (1987) Heat transport by fluids during Late Cretaceous regional metamorphism in the Big Maria Mountains, southeastern California. Geological Society of America Bulletin, 98, 549-553.

Hoisch, T.D., Miller, C.F., Heizler, M.T., Harrison, T.M., and Stoddard, E.F. (1988) Late Cretaceous Regional Metamorphism in Southeastern California. In W.G. Ernst, Ed., Metamorphism and Crustal Evolution of the Western United States, Rubey Volume VII, p. 538-571. Prentice-Hall, New Jersey.

Holden, P., Halliday, A.N., and Stephens, W.E. (1987) Neodymium and strontium isotope content of microdiorite enclaves points to mantle input to granitoid production. Nature, 330, 53-56.

Hollister, L.S., Grissom, G.C., Peters, E.K., Stowell, H.H., and Sisson. V.G. (1987) Confirmation of the empirical correlation of Al in hornblende with pressure of solidification of calc-alkaline plutons. American Mineralogist, 72, 231-239.

Howard, K.A., and Shaw, S.E. (1982) Mesozoic plutonism in the eastern Mojave Desert, California. Geological Society of America Abstracts with Programs, 14, 174.

Howard, K.A., Stone, P., Pernokas, M.A., and Marvin, R.F. (1982) Geologic and geochronologic reconnaissance of the Turtle Mountains area, California: West border of the Whipple detachment terrane. In E.G. Frost and D.L. Martin, Eds., Mesozoic-Cenozoic Tectonic Evolution of the Colorado River Region, California, Arizona and Nevada (Anderson-Hamilton volume), p. 314-354. Cordilleran Publishers, San Diego, California.

Howard, K.A., Nielson, J.E., Simpson, R.W., Hazlett, R.W., Alminas, H.V., Nakata, J.K., and McDonnell, J.R., Jr. (1988) Mineral Resources of the Turtle Mountains Wilderness Study Area, San Bernardino County, California, 28 p. U.S. Geological Survey Bulletin 1713-B.

Howard, K.A., and John, B.E. (1988) Crustal extension along a rooted system of imbricate low-angle faults: Colorado River extensional corridor, California and Arizona. In Coward, M.P., Dewey, J.F., and Hancock, P.L., Eds., Continental Extensional Tectonics, Geological Society Special Paper, 28, 299-311.

Huppert, H.E., and Sparks, R.S.J. (1984) Double-diffusive convection due to crystallization in magma. Annual Reviews of Earth and Planetary Sciences, 12, 11-37.

Hutchinson, R.M. (1960) Petrotectonics and petrochemistry of late Precambrian batholiths of central Texas and the north end of Pikes Peak batholith, Colorado: 21st International Geological Congress, Copenhagen, 95-107.

Hutton, D.H.W. (1982) A method for the determination of the initial shape of deformed xenoliths in granitoids. Tectonophysics, 85, 45-50.

Irvine, T.N., and Baragar, W.R.A. (1971) A guide to the chemical classification of igneous rocks. Canadian Journal of Earth Sciences, 8, 523-548.

Jacobson, R.R.E., MacLoed, W.N., and Black, R. (1958) Ring complexes in the Younger Granite Province of northern Nigeria, 72 p. Geological Society of London Memoir.

Javoy, M., Fourcade, S., and Allegre, C.J. (1970) Graphical method for examination of 18O/16O fractionations in silicate rocks. Earth and Planetary Science Letters, 10, 12-16.

John, B.E. (1986) Structural and intrusive history of the Chemehuevi Mountains area, southeastern California and Western Arizona, Ph.D. dissertation, 295 p. University of California, Santa Barbara.

Jurinski, J.B., and Sinha, A.K. (1989) Igneous complexes within the Coastal Maine Magmatic Province: evidence for a Silurian tensional environment. Geological Society of America Abstracts with Programs, 21, 25.

Kistler, R.W. (1974) Phanerozoic batholiths in western North America: A summary of some recent work on variations in time, space, chemistry, and isotopic compositions. Annual Review Earth and Planetary Science, 2, 403-418.

Kistler, R.W., and Peterman, Z.E. (1978) Reconstruction of crustal blocks of California on the basis of inital strontium isotopic compositions of Mesozoic Granitic rocks. U.S. Geological Survey Professional Paper, 1071, 1-17.

Kistler, R.W., Chappell, B.W., Peck, D.L., and Bateman, P.C. (1986) Isotopic variation in the Tuolumne Intrusive Suite, central Sierra Nevada, California. Contributions to Mineralogy and Petrology, 94, 205-220.

Krogh, T.E. (1973) A low-contamination method for hydrothermal decomposition of zircon and extraction of U and Pb for isotopic age determinations. Geochemica Cosmochemica Acta, 37, 485-494.

Kumar, S.C. (1988) Microgranular enclaves in granitoids: agents of magma mixing. Journal of Southeast Asian Earth Sciences, 2, 109-121.

Langmuir, C.H., Volke, R.D., Jr., Hanson, G.N., and Hart, S.R. (1978) A general mixing equation with application to Icelandic basalts. Earth and Planetary Science Letters, 37, 380-392.

Leake, B.E. (1978) Nomenclature of amphiboles. Canadian Journal of Earth Sciences, 16, 501-520.

Lee, D.E., Mays, R.E., von Loenen, R.E., and Rose, H.J. (1969) Accessory sphene from hybrid rocks of the Mount Wheeler Mine area, Nevada. U.S. Geological Survey Professional Paper, 650B, B41-B46.

Link, A.J. (1970) Inclusions in the Half Dome Quartz Monzonite, Yosemite National Park-California. Ph.D. dissertation, 113 p. Northwestern University, Evanston, Illinois.

Lofgren, G. (1974) An experimental study of plagioclase crystal morphology: isothermal crystallization. American Journal of Science, 274, 243-274.

Loomis, T.P. (1982) Numerical simulations of crystallization processes of plagioclase in complex melts: the origin of irregular and oscillatory zoning in plagioclase. Contributions to Mineralogy and Petrology, 81, 219-229.

Loomis, T.P, and Welber, P.W. (1982) Crystallization processes in the Rocky Hill Granodiorite pluton, California: an interpretation based on compositional zoning of plagioclase. Contributions to Mineralogy and Petrology, 81, 230-239.

Ludington, S. (1978) The biotite-apatite geothermometer revisited. American Mineralogist, 63, 551-553.

Ludwig, K.R. (1980) Calculations of uncertainties of U-Pb isotope data. Earth and Planetary Science Letters, 46, 212-220.

Ludwig, K.R. (1984) PBDAT; a program for reduction of Pb-U-Th isotope data, for use with HP-86/87 microcomputers, 54 p. U.S. Geological Survey Open File Report 84-113.

Ludwig, K.R. (1987) ISOPLOT version 2: a plotting and regression program for isotope geochemistry, for use with HP series 200/300 computers, 62 p. U.S. Geological Survey Open File Report 87-0601.

Ludwig, K.R., and Silver, L.T. (1977) Lead-isotope inhomogeneity in Precambrian igneous K-feldspars. Geochemica Cosmochemica Acta, 41, 1457-1471.

Maaloe, S., and Wyllie, P.J. (1975) Water content of a granitic magma deduced from the sequence of crystallization determined experimentally with water-undersaturated conditions. Contributions to Mineralogy and Petrology, 52, 175-191.

Martin, D.L., Krummenacher, D., and Frost, E.G. (1982) K-Ar Geochronologic record of Mesozoic and Tertiary tectonics of the Big Maria-Little Maria-Riverside Mountains terrane. In E.G. Frost and D.L. Martin, Eds., Mesozoic-Cenozoic Tectonic Evolution of the Colorado River Region, California, Arizona and Nevada (Anderson-Hamilton volume), p.408-432. Cordilleran Publishers, San Diego, California.

Mattinson, J.M. (1987) U-Pb ages of zircons: a basic examination of error propagation. Chemical Geology, 66, 151-162.

McBirney, A.R., Baker, B.H., and Nilson, R.H. (1985) Liquid fractionation. Part I: basic principles and experimental simulations. Journal of Volcanology and Geothermal Research, 24, 1-24.

Miller, C.F., and Stoddard, E.F. (1981) The role of manganese in the paragenesis of magmatic garnet: An example from the Old Woman-Piute Range, California. Journal of Geology, 89, 233-246.

Miller, C.F., Stoddard, E.F., Bradfish, L.J., and Dollase, W.A. (1981) Composition of plutonic muscovite: genetic implications. Canadian Mineralogist, 19, 25-34.

Miller, C.F., Howard, K.A., and Hoisch, T.D. (1982) Mesozoic thrusting, metamorphism, and plutonism, Old Woman-piute Range, southeastern California. In E.G. Frost and D.L. Martin, Eds., Mesozoic-Cenozoic Tectonic Evolution of the Colorado River Region, California, Arizona and Nevada (Anderson-Hamilton volume), p.561-581. Cordilleran Publishers, San Diego, California.

Miyashiro, A. (1974) Volcanic rock series in island arcs and active continental margins. American Journal of Science, 274, 321-355.

Mutschler, F.E. (1980) Crystallization of a soda granite: Treasure Mountain Dome, Colorado, and the genesis of stockwork molybdenum deposits. New Mexico Geological Society Special Publication 6, 199-205.

Nabelek, P.I., Papike, J.J., and Laul, J.C. (1986) The Notch Peak Granite Stock, Utah: Origin of reverse zoning and petrogenesis. Journal of Petrology, 27, 1035-1039.

Naney, M.T. (1983) Phase equilibria of rock-forming ferromagnesian silicates in granitic systems. American Journal of Science, 283, 993-1033.

Norrish, K., and Chappell, B.W. (1977) X-ray fluorescence spectroscopy. In Zussman, J., Ed., Physical Methods in Determinative Mineralogy, p. 201-272. John Wiley & Sons, New York.

O'Neil, J.R. (1986) Theoretical and experimental aspects of isotopic fractionation. In Valley, J.W., Taylor, H.P, Jr., and O'Neil, J.R., Eds. Stable Isotopes in high temperature geological processes, Reviews in Mineralogy, Volume 16, p. 1-37. Mineralogical Society of America.

O'Neill, J.R., and Chappell, B.W. (1977) Oxygen and hydrogen isotope relations in the Berridale batholith. Journal of the Geological Society of London, 133, 559-571.

Pabst, A. (1928) Observations on inclusions in the granitic rocks of the Sierra Nevada. University of California Publication of Geological Sciences, 17, 325-386.

Pettingill, H.S., Sinha, A.K., and Tatsumoto, M. (1984) Age and origin of anorthosites, charnokites, and granulites in the central Virginia Blue Ridge: Nd and Sr isotopic evidence. Contributions to Mineralogy and Petrology, 85, 279-291.

Pitcher, W.S., and Berger, A.R. (1972) The Geology of Donegal: a Study of Granite Emplacement and Unroofing, 435 p. Wiley Interscience, New York.

Ragland, P.C., and Butler, J.R. (1972) Crystallization of the West Farrington pluton, North Carolina, U.S.A. Journal of Petrology, 13, 381-404.

Ragland, P.C., Billings, G.K., and Adams, J.A.S. (1968) Magmatic differentiation and autometasomatism in a zoned granitic batholith from Central Texas, U.S.A. In L.H. Ahrens, ed, Origin and distribution of the elements, p.795-823. Pergamon Press, Oxford and New York.

Reid, J.B., Evans, O.C., and Fates, D.G. (1983) Magma mixing in granitic rocks of the central Sierra Nevada, California. Earth and Planetary Sciences, 66, 243-261.

Robinson, P., Spear, F.S., Schumacher, J.C., Laird, J., Evens, B.W., and Doolan, B.L. (1982) Phase relations of metamorphic amphiboles: natural occurrence and theory. In Veblen, D.R., and Ribbe, P.H., Eds. Amphiboles: petrology and experimental phase relations, Reviews in Mineralogy, Volume 9B. p. 1-211. Mineralogical Society of America.

Roddick, J.A., and Armstrong, J.E. (1959) Relict dikes in the Coast Mountains near Vancouver, B.C. Journal of Geology, 67, 603-613.

Rucklidge, J.C. (1971) Specifications of Fortran program SUPPERRECAL. Department of Geology, University of Toronto.

Silver, L.T. (1968) Precambrian batholiths of Arizona. Geological Society of America Special Paper, 121, 558-559.

Solberg, T.N., and Speer, J.A. (1982) QALL, a 16-element analytical scheme for efficient petrologic work on an automated ARL-SEMQ; application to mica reference samples. Microbeam Analysis 1982, 422-426.

Spencer, K.J., and Lindsley, D.H. (1981) A solution model for coexisting iron-titanium oxides. American Mineralogist, 66, 1189-1201.

Speer, J.A. (1984) Micas in Igneous Rocks. In S.W. Bailey, Ed., Micas, Reviews in Mineralogy, Volume 13, p. 201-256, Mineralogical Society of America.

Speer, J.A. (1987) Evolution of magmatic AFM mineral assemblages in granitoid rocks: the hornblende + melt = biotite reaction in the Liberty Hill pluton, South Carolina. American Mineralogist, 72, 863-878.

Spera, F.J. (1984) Some numerical experiments on the withdrawal of magma from crustal reservoirs. Journal of Geophysical Research, 89B, 8222-8236.

Stacey, J.S., and Kramers, J.D. (1975) Approximation of terrestrial lead isotope evolution by a two-stage model. Earth and Planetary Science Letters, 26, 207-211.

Steiger, R.H., and Jaeger, E. (1977) Subcommission on geochronology: convention on the use of decay constants in geo- and cosmochemistry. Earth and Planetary Science Letters, 36, 359-362.

Stewart, D.B., Arth, J.G., and Flohr, M.J.K. (1988) Petrogenesis of the South Penobscot Intrusive Suite, Maine. American Journal of Science, 288-A, 75-114.

Stephens, W.E., and Halliday, A.N. (1980) Discontinuities in the composition surface of a zoned pluton, Criffell, Scotland. Bulletin of the Geological Society of America, 91, 165-170.

Stormer, J.C., Jr. (1983) The effects of recalculation on estimates of temperature and oxygen fugacity from analyses of multicomponent iron-titanium oxides. American Mineralogist, 68, 586-594.

Stormer, J.C., and Nicholls, J. (1978) XLFRAC: A program for the interactive testing of magmatic differentiation models. Computers and Geosciences, 4, 143-159.

Streckeisen, A.L. (1973) Plutonic rocks. Geotimes, 18, 26-30.

Swanson, S.E. (1977) Relation of nucleation and crystal-growth rate to the development of granitic textures. American Mineralogist, 62, 966-978.

Taylor, H.P., Jr. (1974) The application of oxygen and hydrogen isotope studies to problems of hydrothermal alteration and ore deposits. Economic Geology, 69, 843-883.

Taylor, H.P. (1986) Igneous rocks: II. Isotopic case studies of circumpacific magmatism. In Valley, J.W., Taylor, H.P, Jr., and O'Neil, J.R., Eds. Stable Isotopes in high temperature geological processes. Reviews in Mineralogy, 16, 273-318.

Taylor, H.P., and Sheppard, S.M.F. (1986) Igneous rocks: I. Processes of isotopic fractionation and isotope systematics. In Valley, J.W., Taylor, H.P, Jr., and O'Neil, J.R., Eds. Stable Isotopes in high temperature geological processes. Reviews in Mineralogy, 16, 227-269.

Thomas, W.M., Clark, H.S., Young, E.D., Orrell, S.E., and Anderson, J.L. (1988) Proterozoic high-grade metamorphism in the Colorado River Region, Nevada, Arizona, and California. In W.G. Ernst, Ed., Metamorphism and Crustal Evolution of the Western United States, Rubey Volume VII, p. 526-537. Prentice-Hall, New Jersey.

Tilton, G.R., and Grunenfelder, M.H. (1968) Sphene: uranium-lead ages. Science, 159, 1458-1460.

Tindle, A.G., and Pierce, J.A. (1981) Petrogenetic modelling of in situ fractional crystallization in the zoned Loch Doon pluton, Scotland. Contributions to Mineralogy and Petrology, 78, 196-207.

Tucker, R.D., Raheim, A., Krogh, T.E., and Corfu, F. (1987) Uranium-lead zircon and titanite ages from the northern portion of the Western Gneiss Region, south-central Norway. Earth and Planetary Science Letters, 81, 203-211.

Vance, J.A. (1969) On synneusis. Contributions to Mineralogy and Petrology, 24, 7-29.

Vernon, R.H. (1983) Restite, xenoliths and microgranitoid enclaves in granites. J., and Proceedings of the Royal Society of New South Wales, 116, 77-103.

Watson, E.B., Harrison, T.M., and Ryerson, F.J. (1985) Diffusion of Sm, Sr, and Pb in fluorapatite. Geochem Cosmochem Acta, 49, 1813-1823.

Waugh, B.J. (1985) The origin of mafic enclaves within a granodioritic pluton of the Turtle Mountains, CA. B.A. thesis, 50 p. Carleton College, Northfield, Minnesota.

Wernicke, R.S. (1987) Geology, petrography and geochemistry of the El Topo Pluton, Baja, California Norte, Mexico. M.S. thesis, 226 p. San Diego State Univeristy, San Diego, California.

Wetherill, G.W. (1956) Discordant uranium-lead ages, 1. Transactions of the American Geophysical Union, 37, 320-326.

White, A.J.R., and Chappell, B.W. (1977) Ultrametamorphism and granitoid genesis. Tectonophysics, 43, 7-22.

Wones, D.R., and Eugster, H.P. (1965) Stability of biotite: experiment, theory, and applications. American Mineralogist, 50, 1228-1272.

Wones, D.R. (1981) Mafic silicates as indicators of intensive variables in granitic magmas. Mining Geology, 31, 191-212.

Wones, D.R., and Gilbert, M.C. (1982) Amphiboles in the igneous environment. In D.R. Veblen and P.H. Ribbe, Eds., Amphiboles: Petrology and Experimental Phase Relations, Reviews in Mineralogy, Volume 9B, p. 355-390, Mineralogical Society of America.

Wooden, J., Stacey, J., Howard, K., and Miller, D. (1988) Pb isotope evidence for the formation of Proterozoic crust in the southwestern United States. In W.G. Ernst, Ed., Metamorphism and Crustal Evolution of the Western United States, Rubey Volume VII, p. 69-86. Prentice-Hall, New Jersey.

Woodward-McNeil and Associates (1974) in Southern California Edison Company, Information concerning site characteristics, Vidal Nuclear Generating Station, Appendices 2.5E and 2.5-1.

Wright, J.E., Anderson, J.L., and Davis, G.A. (1986) Timing of plutonism, mylonitization, and decompression in a metamorphic core complex, Whipple Mountains, CA. Geological Society of America Abstracts with Programs, 18, 201.

Wyllie, P.J., Cox, K.G., and Biggar, G.M. (1962) The habit of apatite in synthetic systems and igneous rocks. Journal of Petrology, 3, 238-243.

Yoder, H.S. (1976) Generation of Basaltic Magma, 265 p. National Academy of Sciences, Washington, D.C.

York, D (1969) Least-squares fitting of a straight line with correlated errors. Earth and Planetary Science Letters, 5, 320-324.

Zartman, R.E. (1974) Lead isotopic provinces in the cordillera of the western United States and their geologic significance. Economic Geology, 69, 792-805.

Zartman, R.E., and Doe, B.R. (1981) Plumbotectonics--the model. Tectonophysics, 75, 135-162.

Zen, E., and Hammarstrom, J.M. (1984) Magmatic epidote and its petrologic significance. Geology, 12, 515-518.

Zen, E. (1988) Phase relations of peraluminous granitic rocks and their petrogenetic implications. Annual Review Earth and Planetary Science, 16, 21-51.

Ziebold, T.O., and Ogilvie, R.E. (1964) An empirical method for electron microanalysis. Analytical Chemistry, 36, 322-327.

APPENDIX 1. Percent modal minerals from stained slabs

SAMPLE	TYPE	PLAG	KSP	QTZ	MAFIC
CA85-5	RSgr	42.7	26.7	24.0	6.6
BW84-20	RSgr	43.5	23.1	29.1	4.3
BW84-18	RSgd	48.4	18.7	29.7	3.1
BW84-19	RSgd	40.1	19.5	28.8	11.6
BW84-22	RSgd	41.2	17.5	27.3	13.9
BW84-23	RSgd	54.5	9.9	21.1	14.5
BW84-24	RSgd	51.6	14.8	24.3	9.3
BW84-25	RSgd	57.6	7.1	17.7	17.6
CA85-36	RSgd	44.6	21.2	32.5	1.7
CA85-120	RSgd	52.8	17.2	25.6	4.4
CA84-50	FDHgd	45.9	17.4	30.3	6.4
CA84-58	FDHgd	43.5	19.6	31.5	5.4
CA84-61A	FDHgd	44.6	22.4	27.1	5.9
CA85-4	FDHgd	46.4	18.2	24.3	11.1
CA84-1	CFqmd	50.4	12.0	14.6	23.0
CA84-143	CFqmd	44.2	20.2	18.2	17.4
CA84-147	CFqmd	41.7	19.2	12.7	26.4
CA84-131	CFgd	49.1	20.3	18.7	12.0
CA85-10	CFgd	46.8	15.5	24.9	12.8
CA85-13	CFgd	51.0	15.4	16.7	17.0
CA85-28	CFgd	54.3	7.6	15.2	22.8
CA85-100	CFgd	48.1	13.8	17.5	20.6
CA85-41	CFgd	53.9	9.7	17.0	19.4
CA85-85	WRgd	55.0	16.4	17.6	11.1
CA85-86	WRgd	47.1	14.5	25.7	12.7
CA85-89	WRgd	57.7	12.5	13.8	15.9
CA84-141	TGgr	30.0	39.3	29.1	1.7
CA85-101	TGgr	40.9	23.2	30.2	5.7
CA85-111	TGgr	33.1	30.9	33.1	3.0
CA85-15	TGgr	44.9	21.7	28.3	5.1
CA85-18	TGgr	28.0	37.3	32.9	1.9
CA85-71	PATgd	41.5	25.4	26.5	6.7
CA85-58	FORTgd	54.6	10.4	29.3	5.7
CA84-158	CRgd	45.2	14.4	29.2	11.1
CA85-40	Xgg	22.6	37.7	36.4	3.2
CA84-11	Xa	26.8	***	4.5	68.7
CA84-5	Xa	43.0	***	0.0	57.0
CA84-6B	Xa	34.0	***	14.2	51.8
CA85-5A	Xvm	25.8	***	58.4	15.8
CA85-96	Xvm	37.2	***	52.4	10.3

***little dectectable potassium feldspar.

APPENDIX 1. Percent modal minerals counted from thin sections.

SAMPLE	TYPE	PLAG	KSPAR	QTZ	C.I.*	BIOT	HB	CPX	SPH	OPQ	APAT	ALLAN	MUSC	SERIC	EPID	CHLOR	CALCITE
BW84-20	RSgr				4.3	3.4	0.0	0.0	0.0	0.4	0.0	0.0	0.2	0.3	0.0	0.0	0.0
BW84-18	RSgd				3.1	2.7	0.0	0.0	0.0	0.3	0.0	0.0	0.1	0.0	0.0	0.0	0.0
BW84-19	RSgd	for femic constituents			11.6	8.7	1.6	0.0	0.6	0.5	0.0	0.0	0.0	0.1	0.0	0.0	0.0
BW84-22	RSgd	see above			13.9	9.2	3.4	0.0	0.3	0.7	0.0	0.1	0.0	0.1	0.1	0.0	0.0
BW84-23	RSgd				14.5	9.8	3.7	0.0	0.3	0.3	0.0	0.2	0.0	0.1	0.1	0.0	0.0
BW84-24	RSgd				9.3	4.9	3.4	0.0	0.3	0.4	0.0	0.1	0.0	0.1	0.1	0.0	0.0
BW84-25	RSgd				17.6	8.9	6.9	0.0	0.5	1.0	0.0	0.1	0.0	0.1	0.1	0.0	0.0
BW84-29	encl	39.8	0.6	10.7	38.8	11.1	26.1	0.0	1.2	0.3	0.0	0.0		10.0	0.0	0.1	0.0
BW84-25A	encl	46.2	0.5	1.1	47.2	11.3	34.8	0.0	1.1	0.0	0.0	0.0		3.1	0.3	1.6	0.0
84-5	non p enc	43.0	0.0	0.0	55.1	11.5	42.2	0.0	1.2	0.2	1.1	0.0		0.4	0.2	0.2	0.0
84-45	encl	39.8	0.4	3.8	52.4	11.0	41.1	0.0	0.1	0.2	0.0	0.0		2.8	0.4	0.4	0.0
84-43	encl	46.8	0.0	13.0	37.6	36.4	0.0	0.0	0.0	1.2	1.4	0.4		0.4	0.2	0.2	0.0
84-103B	encl	40.8	0.0	0.0	52.4	17.0	32.6	0.0	2.6	0.2	0.7	0.0		4.0	2.0	0.1	0.0
84-113	encl	55.8	0.3	0.4	41.9	19.0	20.9	0.0	0.9	1.1	0.0	0.0		0.9	0.6	0.0	0.1
84-173	encl	44.6	0.7	3.8	41.5	11.0	29.0	0.0	0.9	0.6	0.2	0.0		6.5	2.8	0.0	0.0
85-4c	dike	21.4	0.0	2.2	50.8	4.2	44.6	0.0	1.8	0.2	0.8	0.0		18.4	0.2	5.6	0.6
84-65A	dike	30.1	0.0	4.8	38.8	0.3	37.5	0.0	0.7	0.3	0.1	0.0		18.9	3.3	4.1	0.0
84-170c	dike	24.0	0.0	0.2	47.6	0.0	46.2	0.0	0.8	0.6	0.4	0.0		20.8	0.4	6.6	0.0
85-6a	diorite	30.3	0.0	0.0	45.8	0.0	44.6	0.0	1.2	0.0	0.0	0.0		20.5	1.6	1.8	0.0
84-27	diorite	29.6	0.6	6.2	56.2	0.2	51.2	3.0	1.6	0.2	0.0	0.0		7.0	0.0	0.4	0.0
84-24	diorite	20.4	0.0	3.4	64.2	16.2	48.0	0.0	0.0	0.0	0.0	0.0		11.6	0.2	0.2	0.0
84-134b	diorite	32.6	0.0	1.6	63.6	6.2	56.4	0.0	0.8	0.2	0.0	0.0		1.8	0.0	0.4	0.0
84-118	diorite	31.8	0.0	10.4	43.8	1.2	41.4	0.0	1.2	0.0	0.0	0.0		12.6	0.4	1.0	0.0
84-114	diorite	26.1	0.9	8.9	58.3	8.8	49.5	0.0	0.0	0.0	0.2	0.0		5.1	0.5	0.0	0.0

* C.I. = color index

APPENDIX 2. Enclave field measurements from horizontal surfaces (cm).

		AZM	Y	Z	Y/Z	LOGY/Z	AREA	LOGAREA
HJ	1	22	16.00	4.00	4.00	0.60	50.26	1.70
	2	6	10.00	7.00	1.43	0.15	54.98	1.74
	3	20	11.00	4.00	2.75	0.44	34.56	1.54
	4	7	3.00	1.30	2.31	0.36	3.06	0.49
	5	20	16.00	4.00	4.00	0.60	50.26	1.70
	6	28	15.00	2.00	7.50	0.88	23.56	1.37
	7	27	7.70	2.00	3.85	0.59	12.09	1.08
	8	70	1.00	0.50	2.00	0.30	0.39	-0.41
	9	25	1.80	0.30	6.00	0.78	0.42	-0.37
	10	25	2.00	0.50	4.00	0.60	0.79	-0.10
	11	40	4.50	1.00	4.50	0.65	3.53	0.55
	12	44	7.00	2.50	2.80	0.45	13.74	1.14
	13	40	11.00	2.00	5.50	0.74	17.28	1.24
	14	36	8.00	1.00	8.00	0.90	6.28	0.80
	15	20	7.60	1.00	7.60	0.88	5.97	0.78
	16	20	3.00	0.70	4.29	0.63	1.65	0.22
	17	32	9.50	1.90	5.00	0.70	14.18	1.15
	18	15	3.00	1.40	2.14	0.33	3.30	0.52
	19	25	2.00	0.70	2.86	0.46	1.10	0.04
	20	30	20.00	6.00	3.33	0.52	94.25	1.97
SUM							391.66	
AVERAGE		28	7.96	2.19	4.19	0.58	19.58	0.86
ST DEV		14	5.45	1.83	1.87	0.20	24.48	0.71
HI	1	35	7.30	4.00	1.83	0.26	22.93	1.36
	2	27	5.00	1.00	5.00	0.70	3.93	0.59
	3	45	2.40	1.30	1.85	0.27	2.45	0.39
	4	4	1.30	0.80	1.63	0.21	0.82	-0.09
	5	2	1.70	0.60	2.83	0.45	0.80	-0.10
	6	43	2.70	0.70	3.86	0.59	1.48	0.17
	7	35	6.30	1.50	4.20	0.62	7.42	0.87
SUM							39.83	
AVERAGE		27	3.81	1.41	3.03	0.44	5.69	0.46
ST DEV		16	2.20	1.10	1.24	0.18	7.36	0.49
HH	1	41	1.80	0.60	3.00	0.48	0.85	-0.07
	2	10	2.60	0.70	3.71	0.57	1.43	0.16
	3	56	1.80	0.30	6.00	0.78	0.42	-0.37
	4	12	18.00	9.00	2.00	0.30	127.23	2.10
	5	20	2.00	1.50	1.33	0.12	2.36	0.37
	6	35	7.00	1.60	4.38	0.64	8.80	0.94
	7	23	9.00	2.70	3.33	0.52	19.08	1.28
	8	28	4.20	1.00	4.20	0.62	3.30	0.52
	9	35	3.00	1.00	3.00	0.48	2.36	0.37
	10	24	2.50	1.10	2.27	0.36	2.16	0.33
	11	42	3.80	1.40	2.71	0.43	4.18	0.62

APPENDIX 2. Enclave field measurements from horizontal surfaces (cm).

		AZM	Y	Z	Y/Z	LOGY/Z	AREA	LOGAREA
	12	7	2.40	0.60	4.00	0.60	1.13	0.05
	13	14	3.70	0.90	4.11	0.61	2.62	0.42
SUM							175.91	
AVERAGE		27	4.75	1.72	3.39	0.50	13.53	0.52
ST DEV		14	4.33	2.18	1.16	0.16	33.17	0.61
HG	1	67	2.00	1.00	2.00	0.30	1.57	0.20
	2	60	26.00	7.00	3.71	0.57	142.94	2.16
	3	65	3.20	2.00	1.60	0.20	5.03	0.70
	4	30	4.80	1.90	2.53	0.40	7.16	0.86
	5	50	2.60	1.00	2.60	0.41	2.04	0.31
	6	52	1.70	0.60	2.83	0.45	0.80	-0.10
	7	49	0.90	0.80	1.13	0.05	0.57	-0.25
	8	40	1.50	0.70	2.14	0.33	0.82	-0.08
	9	50	1.00	1.00	1.00	0.00	0.79	-0.10
	10	60	6.70	2.20	3.05	0.48	11.58	1.06
	11	44	4.00	1.50	2.67	0.43	4.71	0.67
	12	60	39.00	16.00	2.44	0.39	490.07	2.69
	13	28	19.00	7.00	2.71	0.43	104.45	2.02
	14	28	2.50	1.00	2.50	0.40	1.96	0.29
	15	50	9.00	2.00	4.50	0.65	14.14	1.15
	16	37	1.40	0.80	1.75	0.24	0.88	-0.06
	17	34	17.00	7.00	2.43	0.39	93.46	1.97
	18	70	21.00	9.00	2.33	0.37	148.44	2.17
	19	21	2.50	0.50	5.00	0.70	0.98	-0.01
	20	50	1.00	0.50	2.00	0.30	0.39	-0.41
SUM							1032.78	
AVERAGE		47	8.34	3.18	2.55	0.38	51.64	0.76
ST DEV		14	10.26	3.29	2.57	0.38	103.20	0.79
HA	1	72	10.00	5.00	2.00	0.30	39.27	1.59
	2	67	2.00	0.80	2.50	0.40	1.26	0.10
	3	65	0.90	0.40	2.25	0.35	0.28	-0.55
	4	50	2.00	0.50	4.00	0.60	0.79	-0.10
	5	80	4.00	1.00	4.00	0.60	3.14	0.50
	6	51	2.00	1.00	2.00	0.30	1.57	0.20
	7	68	21.00	4.00	5.25	0.72	65.97	1.82
	8	45	2.50	1.50	1.67	0.22	2.95	0.47
	9	68	2.20	1.20	1.83	0.26	2.07	0.32
	10	75	2.00	0.80	2.50	0.40	1.26	0.10
	11	66	2.00	0.50	4.00	0.60	0.79	-0.10
	12	57	9.00	7.60	1.18	0.07	53.72	1.73
	13	61	4.00	1.40	2.86	0.46	4.40	0.64
	14	54	4.70	2.30	2.04	0.31	8.49	0.93
	15	44	5.00	1.80	2.78	0.44	7.07	0.85
SUM							193.01	

APPENDIX 2. Enclave field measurements from horizontal surfaces (cm).

		AZM	Y	Z	Y/Z	LOGY/Z	AREA	LOGAREA
AVERAGE		62	4.89	1.99	2.72	0.40	12.87	0.57
ST DEV		11	5.00	1.96	1.08	0.17	20.76	0.68
HB	1	25	4.00	2.00	2.00	0.30	6.28	0.80
	2	51	2.00	0.60	3.33	0.52	0.94	-0.03
	3	32	2.00	0.70	2.86	0.46	1.10	0.04
	4	52	7.20	2.40	3.00	0.48	13.57	1.13
	5	51	6.20	2.00	3.10	0.49	9.74	0.99
	6	45	2.20	0.30	7.33	0.87	0.52	-0.29
	7	54	4.00	1.60	2.50	0.40	5.03	0.70
	8	45	1.50	0.50	3.00	0.48	0.59	-0.23
	9	43	2.00	0.90	2.22	0.35	1.41	0.15
	10	29	2.60	1.00	2.60	0.41	2.04	0.31
	11	43	1.80	1.10	1.64	0.21	1.56	0.19
	12	43	2.00	0.50	4.00	0.60	0.79	-0.10
	13	30	6.00	4.00	1.50	0.18	18.85	1.28
	14	37	7.00	2.80	2.50	0.40	15.39	1.19
	15	44	4.20	2.10	2.00	0.30	6.93	0.84
	16	37	2.50	1.60	1.56	0.19	3.14	0.50
	17	32	6.00	2.00	3.00	0.48	9.42	0.97
	18	46	2.80	1.00	2.80	0.45	2.20	0.34
SUM							99.50	
AVERAGE		41	3.67	1.51	2.83	0.42	5.53	0.49
ST DEV		8	1.92	1.48	2.88	0.43	10.71	0.47
HC	1	81	2.00	0.96	1.29	0.16	22.23	0.51
	2	55	2.50	0.50	5.00	0.70	0.98	-0.01
	3	40	8.20	2.80	2.93	0.47	18.03	1.26
	4	50	3.80	1.10	3.45	0.54	3.28	0.52
	5	32	3.00	0.50	6.00	0.78	1.18	0.07
	6	54	1.50	0.60	2.50	0.40	0.71	-0.15
	7	47	2.80	1.90	1.47	0.17	4.18	0.62
	8	39	2.90	1.10	2.64	0.42	2.51	0.40
	9	54	16.00	3.90	4.10	0.61	49.01	1.69
	10	54	5.90	1.50	3.93	0.59	6.95	0.84
	11	49	3.00	0.50	6.00	0.78	1.18	0.07
	12	52	2.00	0.60	3.33	0.52	0.94	-0.03
	13	50	4.20	1.50	2.80	0.45	4.95	0.69
	14	50	12.20	2.70	4.52	0.65	25.87	1.41
	15	48	4.20	0.80	5.25	0.72	2.64	0.42
	16	52	6.60	1.50	4.40	0.64	7.78	0.89
	17	39	6.50	1.80	3.61	0.56	9.19	0.96
	18	62	3.20	1.40	2.29	0.36	3.52	0.55
	19	35	1.50	0.60	2.50	0.40	0.71	-0.15
SUM							165.82	
AVERAGE		50	4.84	1.38	3.58	0.52	8.73	0.56

APPENDIX 2. Enclave field measurements from horizontal surfaces (cm).

		AZM	Y	Z	Y/Z	LOGY/Z	AREA	LOGAREA
ST DEV		10	3.70	0.90	1.34	0.18	11.97	0.52
HD	1	57	1.70	0.70	2.43	0.39	0.93	-0.03
	2	50	3.00	0.50	6.00	0.78	1.18	0.07
	3	70	6.00	1.90	3.16	0.50	8.95	0.95
	4	52	9.00	1.40	6.43	0.81	9.90	1.00
	5	52	1.20	0.50	2.40	0.38	0.47	-0.33
	6	52	3.60	0.60	6.00	0.78	1.70	0.23
	7	63	5.00	1.40	3.57	0.55	5.50	0.74
	8	61	14.50	2.50	5.80	0.76	28.47	1.45
	9	62	3.40	1.10	3.09	0.49	2.94	0.47
	10	52	6.10	0.90	6.78	0.83	4.31	0.63
	11	33	6.50	2.50	2.60	0.41	12.76	1.11
	12	54	5.00	1.00	5.00	0.70	3.93	0.59
	13	45	2.50	0.70	3.57	0.55	1.37	0.14
	14	56	29.00	10.20	2.84	0.45	232.31	2.37
	15	57	22.00	5.10	4.31	0.63	88.12	1.95
	16	61	5.50	1.60	3.44	0.54	6.91	0.84
	17	50	8.90	5.50	1.62	0.21	38.44	1.58
SUM							187.45	
AVERAGE		55	7.82	2.24	4.06	0.57	26.36	0.81
ST DEV		8	7.26	2.45	1.57	0.17	55.66	0.70
HE	1	46	8.00	6.20	1.29	0.11	38.95	1.59
	2	56	11.00	3.00	3.67	0.56	25.92	1.41
	3	48	3.50	0.80	4.38	0.64	2.20	0.34
	4	38	2.50	0.70	3.57	0.55	1.37	0.14
	5	40	2.00	0.70	2.86	0.46	1.10	0.04
	6	38	2.00	1.20	1.67	0.22	1.88	0.28
	7	38	1.50	0.50	3.00	0.48	0.59	-0.23
	8	44	4.40	1.50	2.93	0.47	5.18	0.71
	9	28	1.00	0.50	2.00	0.30	0.39	-0.41
	10	54	5.50	2.00	2.75	0.44	8.64	0.94
	11	46	3.00	1.00	3.00	0.48	2.36	0.37
	12	48	2.00	1.00	2.00	0.30	1.57	0.20
	13	52	3.00	0.50	6.00	0.78	1.18	0.07
	14	45	2.80	1.00	2.80	0.45	2.20	0.34
	15	35	4.50	1.60	2.81	0.45	5.65	0.75
	16	45	6.00	2.70	2.22	0.35	12.72	1.10
	17	36	20.00	7.50	2.67	0.43	117.81	2.07
	18	51	3.50	1.00	3.50	0.54	2.75	0.44
	19	25	7.60	4.80	1.58	0.20	28.65	1.46
SUM							261.12	
AVERAGE		43	4.94	2.01	2.88	0.43	13.74	0.61
ST DEV		8	4.34	1.97	1.06	0.16	26.78	0.65

APPENDIX 2. Enclave field measurements from horizontal surfaces (cm).

		AZM	Y	Z	Y/Z	LOGY/Z	AREA	LOGAREA
HF	1	36	1.50	0.80	1.88	0.27	0.94	-0.03
	2	21	2.50	0.80	3.13	0.49	1.57	0.20
	3	34	1.70	0.60	2.83	0.45	0.80	-0.10
	4	25	2.40	1.00	2.40	0.38	1.88	0.28
	5	42	2.20	0.70	3.14	0.50	1.21	0.08
	6	48	2.20	0.90	2.44	0.39	1.56	0.19
	7	31	4.00	1.00	4.00	0.60	3.14	0.50
	8	35	6.00	1.80	3.33	0.52	8.48	0.93
	9	48	3.10	0.50	6.20	0.79	1.22	0.09
	10	30	3.60	1.00	3.60	0.56	2.83	0.45
	11	45	21.00	2.00	10.50	1.02	32.99	1.52
	12	37	5.00	1.40	3.57	0.55	5.50	0.74
	13	67	5.80	3.30	1.76	0.24	15.03	1.18
	14	42	2.00	0.70	2.86	0.46	1.10	0.04
	15	38	1.50	0.30	5.00	0.70	0.35	-0.45
	16	42	1.50	0.30	5.00	0.70	0.35	-0.45
	17	35	20.50	6.80	3.01	0.48	109.48	2.04
	18	40	2.00	0.70	2.86	0.46	1.10	0.04
	19	30	3.50	1.00	3.50	0.54	2.75	0.44
	20	36	3.50	1.00	3.50	0.54	2.75	0.44
	21	36	9.20	3.00	3.07	0.49	21.68	1.34
	22	35	2.60	0.30	8.67	0.94	0.61	-0.21
	23	58	4.50	1.10	4.09	0.61	3.89	0.59
	24	25	11.00	5.00	2.20	0.34	43.20	1.64
	25	55	2.10	1.00	2.10	0.32	1.65	0.22
SUM							266.05	
AVERAGE		39	5.00	1.48	3.79	0.53	10.64	0.47
ST DEV		10	5.18	1.51	2.00	0.18	22.78	0.64
HL	1	35	13.00	2.00	6.50	0.81	20.42	1.31
	2	46	3.00	0.50	6.00	0.78	1.18	0.07
	3	44	6.00	2.50	2.40	0.38	11.78	1.07
	4	41	11.00	3.00	3.67	0.56	25.92	1.41
	5	39	13.50	2.00	6.75	0.83	21.21	1.33
	6	30	2.00	1.00	2.00	0.30	1.57	0.20
	7	34	5.00	1.00	5.00	0.70	3.93	0.59
	8	25	12.00	1.50	8.00	0.90	14.14	1.15
	9	26	6.00	1.00	6.00	0.78	4.71	0.67
	10	16	6.00	0.50	12.00	1.08	2.36	0.37
	11	12	13.00	3.00	4.33	0.64	30.63	1.49
	12	20	13.50	2.00	6.75	0.83	21.21	1.33
	13	23	17.00	2.00	8.50	0.93	26.70	1.43
	14	33	4.50	0.50	9.00	0.95	1.77	0.25
	15	36	1.50	0.50	3.00	0.48	0.59	-0.23
	16	29	32.00	5.00	6.40	0.81	125.66	2.10
	17	28	4.00	1.00	4.00	0.60	3.14	0.50

APPENDIX 2. Enclave field measurements from horizontal surfaces (cm).

		AZM	Y	Z	Y/Z	LOGY/Z	AREA	LOGAREA
	18	36	60.00	12.00	5.00	0.70	565.47	2.75
	19	24	6.00	1.00	6.00	0.78	4.71	0.67
	20	32	8.00	2.25	3.56	0.55	14.14	1.15
	21	12	4.00	1.00	4.00	0.60	3.14	0.50
	22	18	4.50	1.50	3.00	0.48	5.30	0.72
	23	12	11.00	1.50	7.33	0.87	12.96	1.11
	24	12	3.00	1.00	3.00	0.48	2.36	0.37
	25	34	32.00	9.00	3.56	0.55	226.19	2.35
	26	30	9.00	3.50	2.57	0.41	24.74	1.39
	27	36	3.00	0.50	6.00	0.78	1.18	0.07
	28	28	5.00	0.50	10.00	1.00	1.96	0.29
	29	25	11.00	7.00	1.57	0.20	60.47	1.78
	30	34	10.00	1.00	10.00	1.00	7.85	0.90
	31	20	14.00	0.50	28.00	1.45	5.50	0.74
SUM							1252.87	
AVERAGE		28	11.08	2.30	6.25	0.72	40.42	0.96
ST DEV		9	11.47	2.60	4.72	0.25	105.48	0.69
HN	1	22	16.00	2.50	6.40	0.81	31.42	1.50
	2	20	15.00	2.00	7.50	0.88	23.56	1.37
	3	29	4.00	1.00	4.00	0.60	3.14	0.50
	4	25	9.00	1.50	6.00	0.78	10.60	1.03
	5	32	9.00	1.50	6.00	0.78	10.60	1.03
	6	38	7.50	1.50	5.00	0.70	8.84	0.95
	7	40	5.50	1.00	5.50	0.74	4.32	0.64
	8	17	7.50	0.50	15.00	1.18	2.95	0.47
	9	15	20.00	5.00	4.00	0.60	78.54	1.90
	10	10	11.00	1.00	11.00	1.04	8.64	0.94
	11	0	15.00	2.00	7.50	0.88	23.56	1.37
	12	4	10.00	1.00	10.00	1.00	7.85	0.90
	13	0	4.00	1.00	4.00	0.60	3.14	0.50
	14	18	20.00	2.50	8.00	0.90	39.27	1.59
	15	15	6.00	1.00	6.00	0.78	4.71	0.67
	16	23	19.00	2.00	9.50	0.98	29.84	1.47
	17	0	15.00	1.50	10.00	1.00	17.67	1.25
	18	23	9.00	0.50	18.00	1.26	3.53	0.55
	19	13	13.50	2.00	6.75	0.83	21.21	1.33
	20	6	9.00	0.50	18.00	1.26	3.53	0.55
SUM							336.93	
AVERAGE		18	11.25	1.58	8.41	0.88	16.85	1.02
ST DEV		12	4.99	0.99	4.15	0.19	17.77	0.42
HO	1	20	42.00	24.00	1.75	0.24	791.66	2.90
	2	20	12.00	0.50	24.00	1.38	4.71	0.67
	3	65	4.00	3.00	1.33	0.12	9.42	0.97
	4	45	2.00	1.00	2.00	0.30	1.57	0.20

APPENDIX 2. Enclave field measurements from horizontal surfaces (cm).

		AZM	Y	Z	Y/Z	LOGY/Z	AREA	LOGAREA
HR	1	-53	22.00	10.50	2.10	0.32	181.42	2.26
	2	-25	4.00	1.00	4.00	0.60	3.14	0.50
	3	-35	3.00	1.00	3.00	0.48	2.36	0.37
	4	-28	3.50	1.00	3.50	0.54	2.75	0.44
	5	-28	5.00	3.00	1.67	0.22	11.78	1.07
	6	-30	10.50	3.00	3.50	0.54	24.74	1.39
	7	-40	8.50	2.00	4.25	0.63	13.35	1.13
	8	-36	6.00	1.50	4.00	0.60	7.07	0.85
	9	-26	3.00	1.00	3.00	0.48	2.36	0.37
	10	-40	14.00	5.50	2.55	0.41	60.47	1.78
SUM							309.44	
AVERAGE		-34	7.95	2.95	3.16	0.48	30.94	1.02
ST DEV		8	5.81	2.86	0.81	0.13	52.92	0.61
HS	1	-68	18.00	10.00	1.80	0.26	141.37	2.15
	2	-27	9.00	2.00	4.50	0.65	14.14	1.15
	3	-27	5.00	1.00	5.00	0.70	3.93	0.59
	4	-12	4.00	1.50	2.67	0.43	4.71	0.67
	5	-23	13.00	5.00	2.60	0.41	51.05	1.71
	6	-25	11.00	2.50	4.40	0.64	21.60	1.33
	7	-22	6.00	3.00	2.00	0.30	14.14	1.15
	8	0	3.00	0.50	6.00	0.78	1.18	0.07
	9	-25	4.00	2.00	2.00	0.30	6.28	0.80
	10	-25	2.50	0.50	5.00	0.70	0.98	-0.01
	11	-22	3.00	0.50	6.00	0.78	1.18	0.07
SUM							260.55	
AVERAGE		-25	7.14	2.59	3.82	0.54	23.69	0.88
ST DEV		16	4.79	2.67	1.56	0.19	39.73	0.67
HT	1	5	9.00	3.00	3.00	0.48	21.21	1.33
	2	-5	7.00	1.50	4.67	0.67	8.25	0.92
	3	-25	14.00	4.50	3.11	0.49	49.48	1.69
	4	-5	4.00	3.50	1.14	0.06	11.00	1.04
	5	25	4.00	1.50	2.67	0.43	4.71	0.67
	6	30	10.00	5.00	2.00	0.30	39.27	1.59
	7	-25	5.00	2.00	2.50	0.40	7.85	0.90
	8	-15	5.00	2.00	2.50	0.40	7.85	0.90
	9	-22	5.00	2.50	2.00	0.30	9.82	0.99
	10	-25	7.00	3.00	2.33	0.37	16.49	1.22
	11	-35	3.00	0.50	6.00	0.78	1.18	0.07
SUM							177.10	
AVERAGE		-9	6.64	2.64	2.90	0.42	16.10	1.03
ST DEV		20	3.11	1.28	1.29	0.18	14.44	0.42

APPENDIX 2. Enclave field measurements from horizontal surfaces (cm).

		AZM	Y	Z	Y/Z	LOGY/Z	AREA	LOGAREA
	5	20	24.00	9.00	2.67	0.43	169.64	2.23
	6	25	7.00	1.00	7.00	0.85	5.50	0.74
	7	60	4.00	2.50	1.60	0.20	7.85	0.90
	8	12	6.00	2.50	2.40	0.38	11.78	1.07
	9	0	5.00	3.00	1.67	0.22	11.78	1.07
	10	-10	4.00	1.00	4.00	0.60	3.14	0.50
	11	10	3.00	1.00	3.00	0.48	2.36	0.37
SUM							1019.42	
AVERAGE		24.27	10.27	4.41	4.67	0.47	92.67	1.06
ST DEV		22.44	11.65	6.59	6.30	0.35	225.94	0.77
HP	1	12	16.00	2.00	8.00	0.90	25.13	1.40
	2	12	31.00	15.00	2.07	0.32	365.20	2.56
	3	12	4.00	1.50	2.67	0.43	4.71	0.67
	4	8	5.00	1.50	3.33	0.52	5.89	0.77
	5	5	3.50	1.00	3.50	0.54	2.75	0.44
	6	5	3.50	0.50	7.00	0.85	1.37	0.14
	7	8	9.00	1.50	6.00	0.78	10.60	1.03
	8	9	5.00	0.50	10.00	1.00	1.96	0.29
	9	5	8.50	3.00	2.83	0.45	20.03	1.30
	10	10	5.00	1.50	3.33	0.52	5.89	0.77
	11	10	13.00	4.00	3.25	0.51	40.84	1.61
SUM							484.38	
AVERAGE		9	9.41	2.91	4.73	0.62	44.03	1.00
ST DEV		3	7.87	3.95	2.48	0.21	102.23	0.66
HQ								
	1	15	22.00	3.00	7.33	0.87	51.83	1.71
	2	42	14.00	2.00	7.00	0.85	21.99	1.34
	3	30	7.00	0.50	14.00	1.15	2.75	0.44
	4	30	6.00	0.50	12.00	1.08	2.36	0.37
	5	25	4.00	1.00	4.00	0.60	3.14	0.50
	6	30	16.00	4.00	4.00	0.60	50.26	1.70
	7	30	18.00	2.00	9.00	0.95	28.27	1.45
	8	15	11.00	2.00	5.50	0.74	17.28	1.24
	9	15	9.00	1.50	6.00	0.78	10.60	1.03
	10	17	2.00	0.50	4.00	0.60	0.79	-0.10
	11	32	10.00	1.00	10.00	1.00	7.85	0.90
	12	25	3.00	1.50	2.00	0.30	3.53	0.55
	13	32	7.00	1.00	7.00	0.85	5.50	0.74
	14	32	9.00	1.00	9.00	0.95	7.07	0.85
	15	32	24.00	1.00	24.00	1.38	18.85	1.28
SUM							162.00	
AVERAGE		27	10.80	1.50	8.32	0.85	15.47	0.93
ST DEV		11	6.49	0.95	5.22	0.25	16.02	0.51

APPENDIX 2. Enclave field measurements from vertical surfaces (cm).

		AZM	DIP	X	Z	X/Z	LOGX/Z	AREA	LOGAREA
VA	1	350	33.00	15.00	4.00	3.75	0.57	47.12	1.67
	2	350	61.00	9.00	2.50	3.60	0.56	17.67	1.25
	3	350	42.00	20.00	1.20	16.67	1.22	18.85	1.28
	4	350	57.00	5.60	1.40	4.00	0.60	6.16	0.79
	5	350	48.00	12.70	3.30	3.85	0.59	32.92	1.52
	6	350	69.00	5.00	0.80	6.25	0.80	3.14	0.50
	7	350	56.00	29.70	1.50	19.80	1.30	34.99	1.54
	8	350	83.00	6.30	2.20	2.86	0.46	10.89	1.04
	9	350	47.00	11.40	3.60	3.17	0.50	32.23	1.51
	10	350	62.00	17.50	1.70	10.29	1.01	23.36	1.37
SUM								227.33	
AVERAGE			55.80	13.22	2.22	7.42	0.76	22.73	1.25
ST DEV			13.53	7.31	1.04	5.83	0.29	13.34	0.35
VB	1	350	39.00	12.60	1.70	7.41	0.87	16.82	1.23
	2	350	58.00	8.00	2.00	4.00	0.60	12.57	1.10
	3	350	52.00	5.00	1.00	5.00	0.70	3.93	0.59
	4	350	52.00	2.50	0.50	5.00	0.70	0.98	-0.01
SUM								34.30	
AVERAGE			50.25	7.03	1.30	5.35	0.72	8.57	0.73
ST DEV			6.94	3.76	0.59	1.26	0.10	6.39	0.49
VC	1	327	99.00	2.30	0.70	3.29	0.52	1.26	0.10
	2	327	54.00	2.00	0.70	2.86	0.46	1.10	0.04
	3	327	69.00	1.70	0.60	2.83	0.45	0.80	-0.10
	4	327	64.00	4.00	0.90	4.44	0.65	2.83	0.45
	5	327	52.00	9.00	1.00	9.00	0.95	7.07	0.85
	6	327	67.00	3.00	1.10	2.73	0.44	2.59	0.41
	7	327	73.00	7.00	3.50	2.00	0.30	19.24	1.28
	8	327	49.00	2.10	0.30	7.00	0.85	0.49	-0.31
	9	327	57.00	1.00	0.50	2.00	0.30	0.39	-0.41
	10	327	60.00	8.20	2.50	3.28	0.52	16.10	1.21
	11	327	66.00	1.50	0.30	5.00	0.70	0.35	-0.45
	12	327	57.00	9.60	1.50	6.40	0.81	11.31	1.05
	13	327	55.00	4.60	0.80	5.75	0.76	2.89	0.46
	14	327	61.00	1.70	0.60	2.83	0.45	0.80	-0.10
SUM								67.24	
AVERAGE			63.07	4.12	1.07	4.24	0.58	4.80	0.32
ST DEV			11.97	2.93	0.86	2.03	0.20	6.05	0.57
VD	1	345	73.00	12.00	5.50	2.18	0.34	51.83	1.71
	2	345	72.00	5.80	2.00	2.90	0.46	9.11	0.96
	3	345	59.00	1.80	1.60	1.13	0.05	2.26	0.35
	4	345	55.00	13.00	1.70	7.65	0.88	17.36	1.24
	5	345	66.00	4.60	1.40	3.29	0.52	5.06	0.70
	6	345	68.00	1.50	0.60	2.50	0.40	0.71	-0.15

APPENDIX 2. Enclave field measurements from vertical surfaces (cm).

		AZM	DIP	X	Z	X/Z	LOGX/Z	AREA	LOGAREA
	7	345	49.00	31.00	6.00	5.17	0.71	146.08	2.16
	8	345	68.00	6.00	0.60	10.00	1.00	2.83	0.45
	9	345	55.00	4.00	1.30	3.08	0.49	4.08	0.61
	10	345	51.00	2.00	0.80	2.50	0.40	1.26	0.10
	11	345	70.00	6.00	2.50	2.40	0.38	11.78	1.07
	12	345	60.00	1.20	0.40	3.00	0.48	0.38	-0.42
	13	345	55.00	2.70	0.50	5.40	0.73	1.06	0.03
	14	345	37.00	3.80	0.90	4.22	0.63	2.69	0.43
	15	345	37.00	2.00	1.70	1.18	0.07	2.67	0.43
	16	345	50.00	2.50	0.60	4.17	0.62	1.18	0.07
	17	345	47.00	5.30	1.40	3.79	0.58	5.83	0.77
	18	345	55.00	15.30	3.60	4.25	0.63	43.26	1.64
SUM								309.41	
AVERAGE			57.06	6.69	1.84	3.82	0.52	17.19	0.67
ST DEV			10.67	7.13	1.59	2.14	0.23	34.33	0.67
VE	1	354	52.00	4.00	1.60	2.50	0.40	5.03	0.70
	2	354	56.00	1.00	0.20	5.00	0.70	0.16	-0.80
	3	354	59.00	11.30	4.00	2.83	0.45	35.50	1.55
	4	354	68.00	1.50	0.40	3.75	0.57	0.47	-0.33
	5	354	64.00	8.50	2.00	4.25	0.63	13.35	1.13
	6	354	62.00	22.50	7.00	3.21	0.51	123.70	2.09
	7	354	77.00	5.00	1.20	4.17	0.62	4.71	0.67
	8	354	47.00	14.00	3.50	4.00	0.60	38.48	1.59
SUM								221.40	
AVERAGE			60.63	8.48	2.49	3.71	0.56	27.67	0.82
ST DEV			8.80	6.82	2.12	0.77	0.09	38.96	0.92
VF	1	4	62.00	3.00	0.80	3.75	0.57	1.88	0.28
	2	4	48.00	1.50	0.40	3.75	0.57	0.47	-0.33
	3	4	48.00	4.00	0.50	8.00	0.90	1.57	0.20
	4	4	60.00	3.90	1.00	3.90	0.59	3.06	0.49
	5	4	48.00	1.50	0.60	2.50	0.40	0.71	-0.15
	6	4	58.00	11.50	3.00	3.83	0.58	27.10	1.43
	7	4	61.00	1.40	0.30	4.67	0.67	0.33	-0.48
	8	4	74.00	1.00	0.60	1.67	0.22	0.47	-0.33
	9	4	67.00	9.70	2.40	4.04	0.61	18.28	1.26
	10	4	62.00	5.60	1.20	4.67	0.67	5.28	0.72
	11	4	65.00	3.00	0.50	6.00	0.78	1.18	0.07
	12	4	47.00	1.30	0.30	4.33	0.64	0.31	-0.51
	13	4	58.00	3.00	0.30	10.00	1.00	0.71	-0.15
	14	4	56.00	5.00	0.70	7.14	0.85	2.75	0.44
	15	4	65.00	3.60	1.60	2.25	0.35	4.52	0.66
	16	4	44.00	3.30	0.60	5.50	0.74	1.56	0.19
SUM								70.17	
AVERAGE			57.69	3.89	0.93	4.75	0.63	4.39	0.24

APPENDIX 2. Enclave field measurements from vertical surfaces (cm).

		AZM	DIP	X	Z	X/Z	LOGX/Z	AREA	LOGAREA
ST DEV			8.29	2.86	0.76	2.11	0.19	7.23	0.56
VG	1	340	61.00	2.00	1.00	2.00	0.30	1.57	0.20
	2	340	68.00	2.00	0.50	4.00	0.60	0.79	-0.10
	3	340	60.00	1.30	0.40	3.25	0.51	0.41	-0.39
	4	340	72.00	3.00	0.50	6.00	0.78	1.18	0.07
	5	340	63.00	1.70	0.20	8.50	0.93	0.27	-0.57
	6	340	72.00	1.70	0.30	5.67	0.75	0.40	-0.40
	7	340	63.00	5.00	0.60	8.33	0.92	2.36	0.37
	8	340	70.00	18.00	2.80	6.43	0.81	39.58	1.60
	9	340	68.00	1.80	0.70	2.57	0.41	0.99	-0.00
	10	340	72.00	5.00	0.60	8.33	0.92	2.36	0.37
	11	340	67.00	10.00	3.60	2.78	0.44	28.27	1.45
	12	340	69.00	16.00	1.50	10.67	1.03	18.85	1.28
	13	340	66.00	27.00	4.00	6.75	0.83	84.82	1.93
	14	340	67.00	10.00	2.00	5.00	0.70	15.71	1.20
	15	340	74.00	1.10	0.30	3.67	0.56	0.26	-0.59
	16	340	64.00	29.00	4.00	7.25	0.86	91.10	1.96
	17	340	57.00	4.00	0.70	5.71	0.76	2.20	0.34
SUM								291.11	
AVERAGE			66.65	8.15	1.39	5.70	0.71	17.12	0.51
ST DEV			4.63	8.79	1.32	2.38	0.20	28.18	0.85
VH	1	18	67.00	2.00	0.60	3.33	0.52	0.94	-0.03
	2	18	77.00	16.20	3.80	4.26	0.63	48.35	1.68
	3	18	72.00	10.00	2.50	4.00	0.60	19.63	1.29
	4	18	67.00	1.50	0.60	2.50	0.40	0.71	-0.15
	5	18	84.00	8.00	2.00	4.00	0.60	12.57	1.10
	6	18	61.00	2.00	0.50	4.00	0.60	0.79	-0.10
	7	18	52.00	4.50	2.50	1.80	0.26	8.84	0.95
	8	18	76.00	4.00	2.20	1.82	0.26	6.91	0.84
	9	18	74.00	7.50	3.50	2.14	0.33	20.62	1.31
	10	18	45.00	2.00	0.50	4.00	0.60	0.79	-0.10
	11	18	51.00	1.70	0.60	2.83	0.45	0.80	-0.10
	12	18	62.00	1.50	0.60	2.50	0.40	0.71	-0.15
	13	18	65.00	4.70	1.00	4.70	0.67	3.69	0.57
SUM								125.33	
AVERAGE			65.62	5.05	1.61	3.22	0.49	9.64	0.55
ST DEV			10.92	4.20	1.16	0.96	0.14	13.13	0.65
VI	1	328	66.00	5.00	0.70	7.14	0.85	2.75	0.44
	2	328	61.00	12.00	1.50	8.00	0.90	14.14	1.15
	3	328	74.00	6.50	0.80	8.13	0.91	4.08	0.61
	4	328	57.00	5.00	0.50	10.00	1.00	1.96	0.29
	5	328	49.00	3.00	0.50	6.00	0.78	1.18	0.07
	6	328	56.00	7.00	1.00	7.00	0.85	5.50	0.74

APPENDIX 2. Enclave field measurements from vertical surfaces (cm).

		AZM	DIP	X	Z	X/Z	LOGX/Z	AREA	LOGAREA
	7	328	70.00	3.00	0.50	6.00	0.78	1.18	0.07
	8	328	87.00	10.00	0.80	12.50	1.10	6.28	0.80
	9	328	77.00	19.50	3.50	5.57	0.75	53.60	1.73
	10	328	39.00	3.00	1.00	3.00	0.48	2.36	0.37
	11	328	2.00	1.80	0.60	3.00	0.48	0.85	-0.07
	12	328	53.00	1.80	0.60	3.00	0.48	0.85	-0.07
SUM								94.72	
AVERAGE			57.58	6.47	1.00	6.61	0.78	7.89	0.51
ST DEV			20.98	4.98	0.80	2.77	0.20	14.24	0.51
VJ	1	351	60.00	24.00	12.00	2.00	0.30	226.19	2.35
	2	351	56.00	1.80	0.80	2.25	0.35	1.13	0.05
	3	351	74.00	9.00	3.40	2.65	0.42	24.03	1.38
	4	351	55.00	9.00	2.00	4.50	0.65	14.14	1.15
	5	351	71.00	3.50	1.00	3.50	0.54	2.75	0.44
	6	351	54.00	13.00	3.00	4.33	0.64	30.63	1.49
	7	351	54.00	4.00	1.30	3.08	0.49	4.08	0.61
	8	351	52.00	8.00	2.00	4.00	0.60	12.57	1.10
	9	351	51.00	16.50	3.00	5.50	0.74	38.88	1.59
	10	351	19.00	8.20	0.60	13.67	1.14	3.86	0.59
	11	351	51.00	9.20	2.50	3.68	0.57	18.06	1.26
	12	351	51.00	4.50	0.80	5.63	0.75	2.83	0.45
	13	351	70.00	2.60	1.70	1.53	0.18	3.47	0.54
	14	351	59.00	9.00	1.80	5.00	0.70	12.72	1.10
	15	351	59.00	31.50	5.80	5.43	0.73	143.49	2.16
	16	351	51.00	3.80	0.90	4.22	0.63	2.69	0.43
	17	351	59.00	2.50	1.00	2.50	0.40	1.96	0.29
	18	351	66.00	16.00	5.00	3.20	0.51	62.83	1.80
	19	351	52.00	4.00	1.50	2.67	0.43	4.71	0.67
	20	351	67.00	1.50	1.00	1.50	0.18	1.18	0.07
	21	351	67.00	43.00	18.00	2.39	0.38	607.88	2.78
	22	351	61.00	5.00	1.00	5.00	0.70	3.93	0.59
	23	351	61.00	3.00	1.50	2.00	0.30	3.53	0.55
	24	351	51.00	10.00	2.80	3.57	0.55	21.99	1.34
	25	351	51.00	21.00	4.00	5.25	0.72	65.97	1.82
	26	351	41.00	12.50	2.50	5.00	0.70	24.54	1.39
	27	351	31.00	2.80	0.60	4.67	0.67	1.32	0.12
	28	351	54.00	7.00	2.50	2.80	0.45	13.74	1.14
	29	351	45.00	2.50	1.50	1.67	0.22	2.95	0.47
	30	351	40.00	6.00	1.00	6.00	0.78	4.71	0.67
	31	351	49.00	14.00	2.00	7.00	0.85	21.99	1.34
	32	351	46.00	8.50	0.50	17.00	1.23	3.34	0.52
	33	351	37.00	9.00	3.50	2.57	0.41	24.74	1.39
	34	351	62.00	18.70	6.00	3.12	0.49	88.12	1.95
	35	351	51.00	26.00	5.80	4.48	0.65	118.43	2.07
	36	351	36.00	18.00	4.00	4.50	0.65	56.55	1.75

APPENDIX 2. Enclave field measurements from vertical surfaces (cm).

		AZM	DIP	X	Z	X/Z	LOGX/Z	AREA	LOGAREA
	37	351	55.00	20.00	3.50	5.71	0.76	54.98	1.74
	38	351	61.00	12.00	3.50	3.43	0.54	32.99	1.52
	39	351	53.00	3.00	1.00	3.00	0.48	2.36	0.37
	40	351	53.00	4.00	1.50	2.67	0.43	4.71	0.67
	41	351	55.00	1.00	0.40	2.50	0.40	0.31	-0.50
SUM								1771.28	
AVERAGE			53.44	10.45	2.88	4.27	0.57	43.20	1.05
ST DEV			10.73	8.96	3.19	2.87	0.22	99.83	0.71
VK	1	30	34.00	7.00	4.00	1.75	0.24	21.99	1.34
	2	30	25.00	5.00	4.00	1.25	0.10	15.71	1.20
	3	30	45.00	18.00	5.00	3.60	0.56	70.68	1.85
	4	30	50.00	23.00	9.00	2.56	0.41	162.57	2.21
	5	30	51.00	14.00	7.00	2.00	0.30	76.97	1.89
	6	30	65.00	2.00	1.00	2.00	0.30	1.57	0.20
	7	30	21.00	9.00	4.50	2.00	0.30	31.81	1.50
	8	30	90.00	2.00	1.00	2.00	0.30	1.57	0.20
	9	30	65.00	9.00	4.00	2.25	0.35	28.27	1.45
	10	30	90.00	11.00	3.00	3.67	0.56	25.92	1.41
SUM								437.06	
AVERAGE			53.60	10.00	4.25	2.31	0.34	43.71	1.32
ST DEV			22.95	6.43	2.32	0.73	0.13	46.33	0.63
VL	1	25	46.00	23.00	8.00	2.88	0.46	144.51	2.16
	2	25	18.00	13.00	2.00	6.50	0.81	20.42	1.31
	3	25	15.00	9.00	1.50	6.00	0.78	10.60	1.03
	4	25	30.00	32.00	10.50	3.05	0.48	263.89	2.42
	5	25	36.00	5.50	1.00	5.50	0.74	4.32	0.64
	6	25	14.00	33.00	11.00	3.00	0.48	285.09	2.45
	7	25	28.00	4.00	1.50	2.67	0.43	4.71	0.67
	8	25	12.00	22.50	5.50	4.09	0.61	97.19	1.99
	9	25	6.00	7.00	1.50	4.67	0.67	8.25	0.92
	10	25	8.00	4.00	1.00	4.00	0.60	3.14	0.50
	11	25	35.00	4.00	0.50	8.00	0.90	1.57	0.20
	12	25	30.00	7.00	1.30	5.38	0.73	7.15	0.85
	13	25	39.00	5.00	1.00	5.00	0.70	3.93	0.59
	14	25	36.00	7.00	1.00	7.00	0.85	5.50	0.74
	15	25	36.00	11.00	3.50	3.14	0.50	30.24	1.48
	16	25	32.00	16.00	3.50	4.57	0.66	43.98	1.64
	17	25	35.00	9.50	3.00	3.17	0.50	22.38	1.35
	18	25	19.00	10.00	2.00	5.00	0.70	15.71	1.20
	19	25	18.00	6.00	1.30	4.62	0.66	6.13	0.79
	20	25	27.00	13.00	5.00	2.60	0.41	51.05	1.71
	21	25	33.00	7.50	2.50	3.00	0.48	14.73	1.17
	22	25	10.00	9.00	3.00	3.00	0.48	21.21	1.33
	23	25	43.00	5.00	0.80	6.25	0.80	3.14	0.50

APPENDIX 2. Enclave field measurements from vertical surfaces (cm).

		AZM	DIP	X	Z	X/Z	LOGX/Z	AREA	LOGAREA
	24	25	0.00	7.00	1.50	4.67	0.67	8.25	0.92
	25	25	28.00	2.00	0.50	4.00	0.60	0.79	-0.10
	26	25	33.00	5.00	1.50	3.33	0.52	5.89	0.77
	27	25	12.00	9.00	2.00	4.50	0.65	14.14	1.15
	28	25	20.00	17.00	5.00	3.40	0.53	66.76	1.82
	29	25	10.00	11.00	3.00	3.67	0.56	25.92	1.41
SUM								1190.55	
AVERAGE			24.45	10.83	2.94	4.37	0.62	41.05	1.16
ST DEV			12.04	7.77	2.71	1.39	0.13	70.82	0.62
VM	1	0	46.00	7.00	1.00	7.00	0.85	5.50	0.74
	2	0	55.00	25.00	20.00	1.25	0.10	392.69	2.59
	3	0	0.00	3.00	1.00	3.00	0.48	2.36	0.37
	4	0	35.00	5.00	1.50	3.33	0.52	5.89	0.77
	5	0	80.00	3.00	1.00	3.00	0.48	2.36	0.37
	6	0	90.00	5.00	3.00	1.67	0.22	11.78	1.07
	7	0	42.00	18.00	4.00	4.50	0.65	56.55	1.75
	8	0	16.00	8.00	5.00	1.60	0.20	31.42	1.50
	9	0	0.00	5.00	4.00	1.25	0.10	15.71	1.20
	10	0	44.00	3.00	1.00	3.00	0.48	2.36	0.37
	11	0	55.00	17.00	5.50	3.09	0.49	73.43	1.87
	12	0	38.00	6.00	2.50	2.40	0.38	11.78	1.07
	13	0	90.00	5.00	3.00	1.67	0.22	11.78	1.07
	14	0	46.00	27.00	14.00	1.93	0.29	296.87	2.47
SUM								920.46	
AVERAGE			45.50	9.79	4.75	2.76	0.39	65.75	1.23
ST DEV			27.42	8.03	5.33	1.48	0.21	117.15	0.70
VN	1	335	54	5.00	0.50	10.00	1.00	1.96	0.29
	2	335	32	6.00	1.50	4.00	0.60	7.07	0.85
	3	335	45	15.00	4.00	3.75	0.57	47.12	1.67
	4	335	56	6.50	1.00	6.50	0.81	5.10	0.71
	5	335	47	4.50	2.00	2.25	0.35	7.07	0.85
	6	335	52	2.50	1.00	2.50	0.40	1.96	0.29
	7	335	36	14.00	5.50	2.55	0.41	60.47	1.78
	8	335	45	8.50	2.00	4.25	0.63	13.35	1.13
	9	335	36	14.00	4.00	3.50	0.54	43.98	1.64
	10	335	36	20.00	5.00	4.00	0.60	78.54	1.90
	11	335	37	6.50	1.50	4.33	0.64	7.66	0.88
	12	335	36	4.00	0.50	8.00	0.90	1.57	0.20
	13	335	34	4.00	0.50	8.00	0.90	1.57	0.20
	14	335	42	3.00	1.00	3.00	0.48	2.36	0.37
	15	335	43	7.00	1.00	7.00	0.85	5.50	0.74
	16	335	43	10.00	1.00	10.00	1.00	7.85	0.90
	17	335	56	5.00	1.00	5.00	0.70	3.93	0.59
	18	335	48	8.50	2.25	3.78	0.58	15.02	1.18

APPENDIX 2. Enclave field measurements from vertical surfaces (cm).

		AZM	DIP	X	Z	X/Z	LOGX/Z	AREA	LOGAREA
	19	335	48	10.00	3.00	3.33	0.52	23.56	1.37
	20	335	44	18.00	4.00	4.50	0.65	56.55	1.75
	21	335	50	8.50	2.50	3.40	0.53	16.69	1.22
	22	335	38	3.50	0.50	7.00	0.85	1.37	0.14
	23	335	36	4.00	0.25	16.00	1.20	0.79	-0.10
	24	335	44	4.00	0.50	8.00	0.90	1.57	0.20
	25	335	49	6.00	1.00	6.00	0.78	4.71	0.67
	26	335	49	4.00	1.00	4.00	0.60	3.14	0.50
	27	335	47	3.00	0.50	6.00	0.78	1.18	0.07
	28	335	31	7.00	1.00	7.00	0.85	5.50	0.74
	29	335	54	30.00	18.00	1.67	0.22	424.10	2.63
SUM								851.25	
AVERAGE			43.72	8.34	2.33	5.49	0.68	29.35	0.87
ST DEV			7.22	6.10	3.29	2.98	0.22	77.39	0.65
VO	1	30	45.00	2.00	1.00	2.00	0.30	1.57	0.20
	2	30	25.00	5.00	2.00	2.50	0.40	7.85	0.90
	3	30	36.00	6.00	3.50	1.71	0.23	16.49	1.22
	4	30	18.00	23.00	15.00	1.53	0.19	270.95	2.43
	5	30	45.00	11.00	3.00	3.67	0.56	25.92	1.41
	6	30	32.00	11.00	7.00	1.57	0.20	60.47	1.78
	7	30	55.00	16.00	5.00	3.20	0.51	62.83	1.80
	8	30	55.00	3.00	2.00	1.50	0.18	4.71	0.67
	9	30	90.00	1.50	1.00	1.50	0.18	1.18	0.07
SUM								454.72	
AVERAGE			44.56	8.72	4.39	2.13	1.22	25.26	25.69
ST DEV			20.01	6.82	4.18	0.77	1.07	62.61	62.44
VP	1	277	52.00	7.50	1.00	7.50	0.88	5.89	0.77
	2	277	53.00	13.50	2.00	6.75	0.83	21.21	1.33
	3	277	53.00	8.00	1.00	8.00	0.90	6.28	0.80
	4	277	48.00	4.50	0.50	9.00	0.95	1.77	0.25
	5	277	58.00	4.50	0.50	9.00	0.95	1.77	0.25
	6	277	55.00	3.50	1.50	2.33	0.37	4.12	0.62
	7	277	53.00	7.50	1.00	7.50	0.88	5.89	0.77
	8	277	51.00	3.50	1.00	3.50	0.54	2.75	0.44
	9	277	58.00	11.50	1.50	7.67	0.88	13.55	1.13
	10	277	54.00	20.00	5.00	4.00	0.60	78.54	1.90
	11	277	53.00	20.50	2.50	8.20	0.91	40.25	1.60
	12	277	57.00	4.50	0.50	9.00	0.95	1.77	0.25
	13	277	46.00	3.00	1.00	3.00	0.48	2.36	0.37
	14	277	56.00	13.00	1.30	10.00	1.00	13.27	1.12
	15	277	48.00	8.50	1.00	8.50	0.93	6.68	0.82
	16	277	54.00	5.50	0.30	18.33	1.26	1.30	0.11
	17	277	54.00	11.00	1.50	7.33	0.87	12.96	1.11
	18	277	58.00	7.00	0.50	14.00	1.15	2.75	0.44

APPENDIX 2. Enclave field measurements from vertical surfaces (cm).

		AZM	DIP	X	Z	X/Z	LOGX/Z	AREA	LOGAREA
	19	277	55.00	7.50	1.00	7.50	0.88	5.89	0.77
	20	277	50.00	4.00	0.50	8.00	0.90	1.57	0.20
	21	277	50.00	2.50	1.00	2.50	0.40	1.96	0.29
SUM								232.51	
AVERAGE			53.14	8.14	1.24	7.70	0.83	11.07	0.73
ST DEV			3.33	5.04	0.99	3.62	0.22	17.50	0.48
VR	1	48	63.00	6.00	1.00	6.00	0.78	4.71	0.67
	2	48	85.00	15.00	4.00	3.75	0.57	47.12	1.67
	3	48	90.00	6.00	2.50	2.40	0.38	11.78	1.07
	4	48	90.00	3.00	1.00	3.00	0.48	2.36	0.37
	5	48	90.00	3.50	1.50	2.33	0.37	4.12	0.62
	6	48	87.00	4.00	1.00	4.00	0.60	3.14	0.50
	7	48	84.00	16.00	3.00	5.33	0.73	37.70	1.58
	8	48	90.00	9.50	3.50	2.71	0.43	26.11	1.42
	9	48	90.00	5.00	1.50	3.33	0.52	5.89	0.77
	10	48	85.00	9.50	1.00	9.50	0.98	7.46	0.87
	11	48	84.00	12.00	4.00	3.00	0.48	37.70	1.58
	12	48	90.00	3.00	1.00	3.00	0.48	2.36	0.37
SUM								190.45	
AVERAGE			85.67	7.71	2.08	4.03	0.57	15.87	0.96
ST DEV			7.27	4.43	1.19	1.97	0.17	15.84	0.47
VS	1	335	50.00	10.00	5.00	2.00	0.30	39.27	1.59
	2	335	70.00	3.00	1.00	3.00	0.48	2.36	0.37
	3	335	55.00	3.00	1.00	3.00	0.48	2.36	0.37
	4	335	40.00	3.00	2.00	1.50	0.18	4.71	0.67
	5	335	50.00	2.50	2.00	1.25	0.10	3.93	0.59
	6	335	70.00	5.00	2.00	2.50	0.40	7.85	0.90
	7	335	80.00	2.00	1.00	2.00	0.30	1.57	0.20
	8	335	42.00	43.00	26.00	1.65	0.22	878.05	2.94
	9	335	60.00	4.00	1.00	4.00	0.60	3.14	0.50
SUM								943.24	
AVERAGE			57.44	8.39	4.56	2.32	0.34	104.80	0.90
ST DEV			12.87	12.44	7.68	0.83	0.15	273.61	0.82
VT	1	325	70.00	30.00	15.00	2.00	0.30	353.42	2.55
	2	325	0.00	1.00	1.00	1.00	0.00	0.79	-0.10
	3	325	44.00	7.50	2.50	3.00	0.48	14.73	1.17
	4	325	46.00	5.00	2.50	2.00	0.30	9.82	0.99
	5	325	65.00	13.00	6.00	2.17	0.34	61.26	1.79
	6	325	55.00	20.00	4.50	4.44	0.65	70.68	1.85
	7	325	67.00	24.00	8.00	3.00	0.48	150.79	2.18
	8	325	55.00	14.00	6.00	2.33	0.37	65.97	1.82
	9	325	0.00	5.00	4.00	1.25	0.10	15.71	1.20
	10	325	85.00	3.00	1.00	3.00	0.48	2.36	0.37

APPENDIX 2. Enclave field measurements from vertical surfaces (cm).

	AZM	DIP	X	Z	X/Z	LOGX/Z	AREA	LOGAREA
11	325	90.00	5.00	3.50	1.43	0.15	13.74	1.14
SUM							759.26	
AVERAGE		52.45	11.59	4.91	2.33	0.33	69.02	1.36
ST DEV		28.24	9.07	3.80	0.94	0.18	99.59	0.74

APPENDIX 3

Introduction

All sample preparations and analyses were performed by the author at Virginia Tech unless noted otherwise.

Electron Microprobe

Major and trace element compositions of minerals were determined with an automated ARL SEMQ microprobe following the procedure of Solberg and Speer (1982). Accelerating voltage was 15 kV, and beam current 20 nA. Data from the probe was immediately reduced using the correction scheme of Ziebold and Ogilvie (1964), Bence and Albee (1986), and Albee and Ray (1970) on a PDP-11 attached to the microprobe. Errors on individual analyses are assumed to be 2 standard deviations/mean for elements in Kakanui hornblende, a mineral not used in calibration. Analyses of Kakanui hornblende, means, standard deviations, and comparisons to wet chemical analyses are given in Appendix 4. Elemental abundances on an oxygen basis suitable for a mineral type, and H_2O contents were calculated using the Fortran program SUPERRECAL (Rucklidge, 1971) on the mainframe IBM system.

Whole Rock Preparation

Whole rock samples weighing 1 to 25 kg (weight dependent on grain size) were processed through a jaw crusher and final powders were prepared in a tungsten carbide shatter box. In both steps, cleaning and precontamination techniques were used.

Major Element Analyses

Major element compositions were analyzed from glass disks placed in a Philips Sequential X-ray Analysis System Model 1450 using wave length dispersive techniques of Norrish and Chappell (1977). Glass disks were made from whole rock powders, an oxidizer ($LiNO_3$) and La based flux (Spectroflux) fired in Pt crucibles over a bunsen burner and cast in an aluminum mold. Major element calibrations were based on analyses of USGS standard rock powders PCC-1, GSP-1, BCR-1, AVG-1, and G-2. Errors in the calibrations suggest the following precisions: 1% for SiO_2, Al_2O_3, TiO_2, FeO, CaO, and K_2O; 3% for MgO, MnO and Na_2O, and less than 0.01% for P_2O_5. All calibrations were performed by H.N.T. Pendrak.

Whole Rock Ba, Rb, and Sr Concentrations by XRF

Ba, Rb and Sr concentrations were determined with a Philips Sequential X-Ray Analysis System Model 1450 by H.N.T. Pendrak using pressed powder pellets and following the method of Norrish and Chappell (1977). Calibrations were based on analyses of the following standards--G-2, AGV-1, BCR-1, GSP-1, NBS-607, and PCC-1. Yttrium corrected Mo corrections were applied to the data. Replicate analyses (n = 3 or 4) of randomly selected pellets indicate a precision of better than 1.5% (2 sigma/mean) for Rb contents greater than 100 ppm and Sr greater than 50 ppm. These replicates suggest a precision in Rb/Sr of 1.1% (2 sigma). Ba precision is probably better than 3%.

Mineral Preparation

Whole rock samples weighing 10 to 100 kg were processed through a jaw crusher and then repeatedly run through a roller mill until 95% of the material passed through a 425 micron screen. The particles were separated by Wilfley Table, heavy liquid, and magnetic separation techniques. Mineral separates were hand picked under a microscope to insure purity, and then were washed in acid solutions before dissolution.

Isotope Analyses

All reagent grade HCl, HNO_3, HBr, and HF, and dionized H_2O used in extraction of elements of interest were produced by subboiling distillation in teflon. In the case of HF used in zircon analyses, it was doubly distilled. Both HCl and H_2O were distilled in a quartz still prior to teflon distillation. Savillex bombs used in all sample dissolution but zircon, teflon bombs used for zircon, and PMP beakers used for collection were washed in warm, dilute reagent HNO_3, and refluxed with warm teflon distilled 6N HCl.

Isotopic ratios were determined using a modified and automated AVCO 35 cm radius, 90° sector, solid source mass spectrometer interfaced with a PDP-11 computer. Magnetic field was switched and controlled by a Varian FR-41 gaussmeter/controller. All ratios were integrated by HP integrating voltmeter, and were processed by the computer following the procedure of Hart and Brooks (1977).

Rb & Sr Isotope Analyses

For whole rocks, 0.1 g of powdered sample were dissolved in a mixture of HF + HNO_3 in 5 or 10 ml Savillex bombs at about 170°C on a hot plate for 2-3 days, then evaporated and redissolved in HCL. Mineral samples varied in size from 0.01 to 0.04 g and were washed with dilute HNO_3, water, and acetone prior to weighing. Known amounts of sample were spiked with known amounts of mixed ^{87}Rb and ^{84}Sr solution, then treated as above. Some whole rock samples were also spiked (see below). Samples were equilibrated with 1-2 ml of 2.5 N HCl, and centrifuged in microcentrifuge tubes. About half this solution was loaded onto a cation exchange column, which consisted of 0.5 cm diameter pyrex glass tube with a fitted blown silica frit, filled with 3 ml of AG 50w×8, 200-400 mesh resin with a bed length of about 20 cm, previously washed with HCl and water, and conditioned with 2.5N HCl. After loading on the column, samples were eluted with 2.5N HCl.

Rb and Sr were run in the mass spectrometer as phosphates on a previously degassed Re filament onto which a slurry of Ta_2O_5 had been dried to produce a coating of the oxide. After loading and drying, the filament was heated to a dull red glow. The filament and holder were then loaded into the spectrometer.

$^{87}Sr/^{86}Sr$ ratios were corrected to a $^{86}Sr/^{88}Sr$ ratio of 0.1194 during the run by computer. Between 60 and 140 cycles of data were collected until a standard error on $^{87}Sr/^{86}Sr$ of 0.0001 or better was obtained. For spiked samples, this ratio (previously normalized to a $^{86}Sr/^{88}Sr$ of 0.1194) was calculated in a LOTUS 1-2-3 spread sheet knowing the concentrations in the spike. All reported $^{87}Sr/^{86}Sr$ values are normalized by a multiplicative factor of 0.99982 based on the known value of Eimer and Armand $SrCO_3$ standard of 0.70800, and the measured ratio of 0.708127 (n = 23; standard error of the mean = 0.000013). $^{87}Rb/^{86}Sr$ ratios, corrected $^{87}Sr/^{86}Sr$, and model initial ratios were calculated in a LOTUS 1-2-3 spread sheet.

Sr blanks (n = 7) averaged 220 pg (± 90 pg, 1 sigma) and Rb blanks (n = 5) averaged 194 pg (± 130 pg, 1 sigma) during the period of analysis of unknowns and are negligible for the concentrations examined.

Regressions were calculated according to York (1969) as presented by Faure (1977) as a Fortran program. All ages and square roots of the mean of the sum of residuals squared ($\sqrt{MSRS}$) are from York (1969) model II. The decay constant of ^{87}Rb used as 1.42×10^{-11}/yr (Steiger and Jaeger, 1977).

Concentrations of Rb and Sr in some whole rock samples and all mineral separates were analyzed by isotope dilution using a mixed ^{87}Rb-^{84}Sr spike solution. Replicate analyses of spiked NBS standard feldspar (NBS-607) were used to calibrate the spike, and to cross calibrate with the XRF analyses (see below). Average of four runs indicate a concentration of 0.0231 ± 0.0003 micromoles/gram Sr and 0.04036 ± 0.0007 micromoles/gram Rb. These analyses suggest a precision of better than 1.8% for Rb and Sr, and of 0.94% for Rb/Sr.

Comparison of Techniques

Ten whole rock samples were analyzed by both isotope dilution and XRF. In 9 of 10 cases, Rb concentrations by isotope dilution were greater than by XRF (mean ID/XRF = 107.6%, 1 sigma = 9.4%). In all 10 cases, Sr concentrations were greater by isotope dilution than XRF (mean ID/XRF = 108.7%, 1 sigma = 4.1%). Because of this discrepancy in the techniques, isochrons were constructed from analyses by one method or the other, except for a preliminary isochron for the Core Facies (CA84-147) for which whole rock concentrations were determined by XRF, and minerals by isotope dilution.

Zircon U-Pb

Zircon separates were divided into size fractions by sieving, and were hand picked under a microscope to remove impurities. Samples were washed with warm HNO_3, then rinsed with water and teflon distilled acetone. A size fraction was divided into two populations and one was spiked with a mixed $^{235}U/^{208}$ Pb solution. Spike concentrations for U in this solution was determined by adding known shelf solutions and was found to be 0.03286 ± 0.00013 (1 sigma) micromoles/gm for U based on 3 runs. A concentration of 0.2101 micromoles/gram is assumed from a previous calibration (Sinha, personnal communication). The samples and spike were placed in teflon bombs with a mixture of 90% teflon distilled 48% HF and 14N HNO_3, put in MONEL screw top sleeves, and place in an oven at 220°C for 7 days (after Krogh, 1973).

Samples were checked for total dissolution, were evaporated and converted to chloride by addition of HCl. Separation of U and Pb was accomplished by a 3.1N HCl and H_2O based elution on 0.5 cm diameter teflon columns with fitted blown silica frits, filled with a bed length of 2 cm of AG 1-×8 200-400 mesh resin (after Krogh, 1973). Total Pb blanks ranged from 0.64 to 1.29 ng, and averaged 1.03 ng (n = 4) and a U blank was 2.93 ng. These blank corrections cause minor changes in calculated U-Pb ages.

Sphene U-Pb

About 10 g of sphene was separated from 35 kg of a sample of the Core Facies (CA84-147) by method described above. The sphenes displayed a wide range of magnetic susceptibilities, from 0.4 to 1.8 A at 10° forward tilt and 5° side tilt on a Franz magnetic separator (7 fractions). Two fractions (nonmag at 1.8A and 1.0-1.2 A) were analysed. Grains greater than 425 microns from these separates were used in analysis. After hand picking, sphenes were washed in hot HNO_3 for 30 minutes, rinsed with water, and distilled acetone. 100 to 120 milligrams of sample were split, weighed and spiked with a mixed U-Pb solution (as described for zircons) and placed in a 5 ml Savillex screw top bomb. Dissolution was accomplished by adding HF and HNO_3 and heating on a hot plate at about 180°C for 9 days. Closed bombs were occassionally placed in an ultrasonic cleaner in order to break up the dissolving material. The sample was evaporated and the process repeated for another 9 days. Pb and U were extracted by elution with HBr, HCl, and dilute HF in 15 ml pyrex columns with a 0.5 cm diameter. Columns were filled with a bed length of 15 cm of AG 1-x8 200-400 mesh resin. These separates were then treated like the zircon samples described above. As a clean up procedure, Pb and U solutions were eluted in teflon columns with HCl and H_2O (like elution described for zircons). Pb was loaded in phosphoric acid on silica gel previously dried on a Re filament. U as loaded in phosphoric acid on Ta_2O_5 previously dried on a Re filament. In both cases, the sample was heated to a dull red glow before being placed into the mass spectrometer. 90% peak heights were obtained for both elements at 1.5A and 300 to 1000 mV.

Total Pb blank run with these samples was 5.6 ng, but while the procedure was designed, ranged up to 7.6 ng. This level of contamination is due to the large amounts of acid (particularly HF) used in dissolution and elution, and is significant given the amount of Pb (^{207}Pb) in these samples. Assumed blank composition is 204:206:207:208 = 1:19.4:15.9:39.3 (Sinha, personal communication). A single U blank for this lab during the period of analysis is 4.9 ng was used in blank correction. Measurements of CIT Pb standard during this period resulted in isotopic ratios of $^{206}Pb/^{208}Pb = 2.177$, $^{207}Pb/^{206}Pb = 0.9296$, and $^{206}Pb/^{204}Pb = 16.579$ (J.P. Hogan, personal communication, 1988). Calibration factors applied to the data are 0.9971, 1.0012, and 1.0028, respectively.

U-Pb Calculations and Errors

Isotopic ratios corrected for blanks and calibration, Pb and U concentrations, and ages were calculated in a LOTUS 1-2-3 spread sheet. Errors on the ages were determined in a Fortran program called PBDAT (Ludwig, 1984) using standard errors from the raw mass spectrometer data, and errors in concentration and composition of spikes and blanks calculated from multiple runs. Errors on regressions were calculated from errors determined in PBDAT in a Fortran program called ISOPLOT (Ludwig, 1987). Decay constants employed are $^{238}U = 1.5525 \times 10^{-10}$/yr and $^{235}U = 9.8485 \times 10^{-10}$/yr (Steiger and Jaeger, 1977).

Feldspar Pb

Feldspar Pb analyses were performed by Dr. J.L. Wooden at USGS in Menlo Park. Feldspar separates provided by the author were leached with 6N HCl, 7N HNO_3, and 3% HF to remove surface contamination and labile Pb (Ludwig and Silver, 1977). 150 to 250 mg samples were dissolved in HF and HNO_3, dried and converted to chlorides, dried and equilibrated with 0.6N HBr. Pb was separated using 0.6N HBr and 6N HCl on an anion exchange column. The elution procedure was done twice. Samples were loaded on Re filaments with silica gel and H_3PO_4 and run on a single collector Finnigan/Mat 261 mass spectrometer. Lead isotopic ratios are corrected for fractionation by empirical factors derived from runs of standards NBS-981 and NBS-982, and average 0.1% per mass unit. Total uncertainties on individual ratios are $\pm 0.1\%$ (2 sigma). Blanks are generally less than 2 nanograms.

Oxygen Isotopes

Analyses of whole rocks and minerals were done by the author in the laboratory of J.R. O'Neil at the USGS in Menlo Park, CA. Some replicate mineral analyses were performed by L. Adami or R. Brigham there. Analyses of whole rocks and minerals were performed on 0.10 to 0.15 mg of sample that was dried over night in an oven, then weighed and placed in a vessel where a positive pressure of dry N_2 expanded over the trap. After loading, all 10 vessels in the system were capped and brought to 1+ atmospheres N_2 pressure. Furnaces were adjusted to 150°C and samples were heated and evacuated at high vacuum for at least 1 hour. After cool down in liquid N_2, the reagent ClF_3 was added in proportion to sample size and condensed with liquid nitrogen in each vessel. Furnaces were used to bring each vessel to 550-600°C overnight. ClF_3 was condensed at liquid nitrogen temperature, and removed, and O_2 was converted to CO_2 in a chamber with a hot graphite rod. Gas yields were recorded before and after conversion. The general method is after Clayton and Mayeda (1963). A standard (African Glass Sand) was run twice with each batch of eight samples in order to judge the quality of the runs. All samples were run in duplicate or triplicate until duplication of values better than 0.2 ‰ was achieved.

Oxygen isotopic composition was determined on a Nier-type double collecting isotope ratio mass spectrometer. Data is reported in δ terminology relative to the standard SMOW (Hayes, 1983).

Deuterium Analyses

Deuterium analyses of four biotite separates were performed by personnel in J.R. O'Neil's laboratory in Menlo Park. H_2O is isolated by freezing and/or condensing other volatiles. H_2O is reacted with uranium, and H_2 gas is frozen onto a charcoal base. Sample was run on a Neir-type double collecting mass spectrometer. Data are reported in δ terminology relative to the standard SMOW.

APPENDIX 4: Introduction

Analyses of oxides in minerals in weight percent are followed by calculated numbers of cations on an n oxygen basis, where n is selected according to ideal mineral formula.

Microprobe analyses of minerals are listed in the following order:

- Kakanui hornblende standard
- feldspars
- biotite
- hornblende
- garnet
- muscovite
- opaque minerals
- apatite

Under each mineral, sample orders are:

- Rim Sequence
- Core Facies
- Other granitoids
- Garnet aplites
- Mafic rocks

APPENDIX 4: KAKANUI HORNBLENDE STANDARD (24 Oxygen)

SMPL#	SiO2	Al2O3	TiO2	FeO	MnO	MgO	CaO	Na2O	K2O	F	TOTAL
1014	40.42	14.36	4.87	10.66	0.10	12.96	10.17	2.55	2.02	0.13	98.24
1016	40.80	14.04	4.97	10.32	0.08	12.93	10.32	2.46	2.02	0.19	98.13
1017	40.91	14.37	4.62	10.64	0.10	13.05	10.00	2.58	2.01	0.16	98.43
1068	40.24	14.78	4.54	10.66	0.07	13.20	9.91	2.53	1.96	0.23	98.12
1087	40.45	13.34	4.84	10.68	0.08	12.93	10.04	2.73	2.00	0.12	97.21
1088	41.02	13.58	4.83	10.53	0.09	12.90	10.09	2.45	2.04	0.12	97.65
1089	40.29	13.65	4.79	10.72	0.10	13.05	10.09	2.49	2.00	0.18	97.36
1092	40.91	14.37	4.99	10.57	0.08	12.34	10.17	2.57	1.99	0.21	98.20
1099	41.38	14.55	4.87	10.63	0.08	12.64	10.21	2.67	2.04	0.20	99.27
1133	41.46	14.22	4.84	10.65	0.10	12.66	10.03	2.41	2.00	0.22	98.59
1204	41.74	14.39	4.81	10.74	0.06	13.00	10.08	2.18	2.04	0.10	99.14
1251	40.98	14.69	4.81	10.69	0.09	12.80	10.03	2.40	1.98	0.20	98.67
1281	40.59	14.26	4.93	10.63	0.09	12.41	10.63	2.23	2.00	0.17	97.94
1331	40.81	14.27	4.87	10.67	0.09	12.81	9.99	1.78	1.97	0.08	97.34
1429	40.81	14.33	4.89	10.52	0.08	12.76	10.08	2.59	2.01	0.18	98.24
2167	40.77	14.63	4.55	10.53	0.10	13.04	10.09	2.73	2.03	0.23	98.70
3004	41.80	14.21	4.63	10.48	0.20	12.99	10.25	2.44	2.10	0.27	99.37
3006	41.28	14.05	4.78	10.62	0.14	13.04	10.02	2.51	2.09	0.15	98.68
3007	41.03	14.18	5.00	10.40	0.12	12.90	10.01	2.53	2.09	0.16	98.42
3008	41.87	14.48	4.81	10.39	0.12	13.07	10.53	2.53	2.08	0.11	99.99
3009	41.45	14.29	4.90	10.54	0.11	13.25	10.26	2.45	2.11	0.13	99.49
3010	41.45	14.62	4.48	10.62	0.13	13.39	10.16	2.31	2.07	0.15	99.38
3045	39.94	14.32	4.94	10.49	0.06	13.23	9.95	2.37	2.11	0.25	97.66
3048	41.30	14.27	4.74	10.42	0.08	13.18	9.97	2.68	2.11	0.22	98.97
3124	42.30	14.02	4.67	10.51	0.07	13.30	10.26	2.57	2.09	0.24	100.03
3406	39.24	14.46	4.97	10.47	0.13	13.07	9.78	2.42	2.19	0.19	96.92
3477	39.17	14.21	4.82	10.35	0.13	13.12	9.83	2.50	2.14	0.16	96.43
4004	40.83	14.40	4.83	10.33	0.08	13.33	10.17	2.60	2.09	0.17	98.83
4064	39.96	13.74	5.25	10.26	0.08	13.11	9.67	2.81	2.11	0.18	97.17
4065	39.96	13.98	4.92	10.23	0.13	13.32	9.84	2.78	2.08	0.20	97.44
4066	41.18	13.81	4.98	10.48	0.13	13.24	10.19	2.67	2.09	0.26	99.03
4116	40.98	14.00	4.92	10.20	0.12	13.11	10.07	2.10	2.09	0.31	97.90

APPENDIX 4: KAKANUI HORNBLENDE STANDARD (24 Oxygen)

SMPL#	SiO2	Al2O3	TiO2	FeO	MnO	MgO	CaO	Na2O	K2O	F	TOTAL
4162	40.97	14.05	4.88	10.29	0.07	13.27	10.29	2.74	2.10	0.22	98.88
4169	40.16	14.32	4.73	10.52	0.11	13.30	10.10	2.55	2.10	0.21	98.10
4170	40.34	14.25	4.76	10.54	0.10	13.24	10.10	2.46	2.13	0.16	98.07
4173	40.44	14.09	5.05	10.41	0.11	13.32	10.30	2.50	2.10	0.19	98.51
4205	40.39	14.02	4.79	10.64	0.09	13.23	10.18	2.41	2.09	0.18	98.02
6089	41.36	14.28	4.80	10.56	0.10	13.25	10.24	2.79	2.10	0.24	99.72
AVG	40.84	14.20	4.83	10.51	0.10	13.05	10.11	2.50	2.06	0.19	98.40
STD	0.66	0.30	0.15	0.14	0.03	0.24	0.18	0.20	0.05	0.05	0.85
%2STD/AVG	3.25	4.22	6.03	2.74	53.52	3.72	3.60	15.91	5.10	50.93	1.72

SMPL#	Si	Al4	Al6	Ti	Fe	Mn	Mg	Ca	Na	K	F	Fe#
1014	5.931	2.069	0.415	0.537	1.308	0.012	2.835	1.599	0.726	0.378	0.060	0.316
1016	5.981	2.019	0.406	0.548	1.265	0.010	2.825	1.621	0.699	0.378	0.088	0.309
1017	5.979	2.021	0.454	0.508	1.301	0.012	2.843	1.566	0.731	0.375	0.074	0.314
1068	5.903	2.097	0.459	0.501	1.308	0.009	2.886	1.558	0.720	0.367	0.107	0.312
1087	6.006	1.994	0.340	0.540	1.326	0.010	2.861	1.597	0.786	0.379	0.056	0.317
1088	6.044	1.956	0.402	0.535	1.297	0.011	2.833	1.593	0.700	0.383	0.056	0.314
1089	5.971	2.029	0.354	0.534	1.329	0.013	2.882	1.602	0.715	0.378	0.084	0.316
1092	5.992	2.008	0.473	0.550	1.295	0.010	2.694	1.596	0.730	0.372	0.097	0.325
1099	5.995	2.005	0.479	0.531	1.288	0.010	2.730	1.585	0.750	0.377	0.092	0.321
1133	6.039	1.961	0.479	0.530	1.297	0.012	2.748	1.565	0.681	0.372	0.101	0.321
1204	6.040	1.960	0.494	0.523	1.300	0.007	2.804	1.563	0.612	0.377	0.046	0.317
1251	5.969	2.031	0.490	0.527	1.302	0.011	2.779	1.565	0.678	0.368	0.092	0.319
1281	5.970	2.030	0.442	0.545	1.308	0.011	2.721	1.675	0.636	0.375	0.079	0.325
1331	6.014	1.986	0.492	0.540	1.315	0.011	2.814	1.577	0.509	0.370	0.037	0.318
1429	5.976	2.024	0.448	0.538	1.288	0.010	2.785	1.581	0.735	0.375	0.083	0.316
2167	5.946	2.054	0.461	0.499	1.284	0.012	2.835	1.577	0.772	0.378	0.106	0.312
3004	6.043	1.957	0.463	0.503	1.267	0.024	2.799	1.588	0.684	0.387	0.123	0.312

APPENDIX 4: KAKANUI HORNBLENDE STANDARD (24 Oxygen)

SMPL#	Si	Al4	Al6	Ti	Fe	Mn	Mg	Ca	Na	K	F	Fe#
3004	6.043	1.957	0.463	0.503	1.267	0.024	2.799	1.588	0.684	0.387	0.123	0.312
3006	6.018	1.982	0.432	0.524	1.295	0.017	2.833	1.565	0.709	0.389	0.069	0.314
3007	5.994	2.006	0.435	0.549	1.271	0.015	2.809	1.567	0.717	0.389	0.074	0.312
3008	6.016	1.984	0.467	0.520	1.248	0.015	2.799	1.621	0.705	0.381	0.050	0.308
3009	5.992	2.008	0.426	0.533	1.274	0.013	2.855	1.589	0.687	0.389	0.059	0.309
3010	5.991	2.009	0.482	0.487	1.284	0.016	2.885	1.573	0.647	0.382	0.069	0.308
3045	5.893	2.107	0.383	0.548	1.294	0.007	2.910	1.573	0.678	0.397	0.117	0.308
3048	5.998	2.002	0.440	0.518	1.266	0.010	2.853	1.551	0.755	0.391	0.101	0.307
3124	6.070	1.930	0.441	0.504	1.261	0.009	2.845	1.577	0.715	0.383	0.109	0.307
3406	5.846	2.154	0.384	0.557	1.304	0.016	2.902	1.561	0.699	0.416	0.090	0.310
3477	5.865	2.135	0.372	0.543	1.296	0.016	2.928	1.577	0.726	0.409	0.076	0.307
4004	5.944	2.056	0.415	0.529	1.258	0.010	2.893	1.586	0.734	0.388	0.078	0.303
4064	5.929	2.071	0.331	0.586	1.273	0.010	2.899	1.537	0.808	0.399	0.084	0.305
4065	5.913	2.087	0.350	0.547	1.266	0.016	2.938	1.560	0.798	0.393	0.094	0.301
4066	5.951	2.049	0.303	0.541	1.267	0.016	2.852	1.578	0.748	0.385	0.119	0.308
4116	6.006	1.994	0.424	0.542	1.250	0.015	2.864	1.581	0.597	0.391	0.144	0.304
4117	6.029	1.971	0.417	0.541	1.260	0.017	2.857	1.588	0.644	0.396	0.069	0.306
4129	5.990	2.010	0.417	0.510	1.285	0.012	2.854	1.597	0.742	0.387	0.091	0.310
4162	5.966	2.034	0.377	0.534	1.253	0.009	2.880	1.606	0.774	0.390	0.101	0.303
4169	5.905	2.095	0.386	0.523	1.294	0.014	2.915	1.591	0.727	0.394	0.098	0.307
4170	5.929	2.071	0.397	0.526	1.296	0.012	2.900	1.590	0.701	0.399	0.074	0.309
4173	5.919	2.081	0.349	0.556	1.274	0.014	2.906	1.615	0.709	0.392	0.088	0.305
4205	5.942	2.058	0.373	0.530	1.309	0.011	2.901	1.605	0.687	0.392	0.084	0.311
6089	5.989	2.011	0.426	0.523	1.279	0.012	2.875	1.527	0.780	0.384	0.092	0.308
AVG	5.972	2.028	0.419	0.532	1.286	0.012	2.846	1.583	0.709	0.385	0.085	0.311
STD	0.050	0.050	0.048	0.019	0.020	0.003	0.057	0.025	0.056	0.011	0.022	0.006
%2STD/AVG	1.68	4.96	23.08	6.96	3.17	52.17	3.99	3.16	15.88	5.49	51.56	3.70
WET CHEM	5.900	2.570		0.520	1.340	0.010	2.780	1.610	0.800	0.380		
DELTA	0.072	-0.542		0.011	-0.054	0.002	0.066	-0.027	-0.091	0.005		

APPENDIX 4: PLAGIOCASE ANALYSES (8 Oxygen) CA85-5 RSgr

SMPL#	SiO2	Al2O3	FeO	CaO	BaO	Na2O	K2O	TOTAL
3327	62.15	22.65	0.05	3.72	0.02	8.26	0.31	97.16
3328	60.87	23.81	0.05	4.73	0.05	8.29	0.40	98.20
3329	60.01	24.10	0.05	5.38	0.08	7.27	0.30	97.19
3330	61.12	23.95	0.05	4.82	0.05	7.80	0.28	98.07
3331	61.12	23.94	0.04	4.94	0.06	7.91	0.42	98.43
3332	62.10	22.81	0.05	3.98	0.00	8.92	0.52	98.38
3333	62.07	22.94	0.06	3.85	0.05	8.81	0.51	98.29
3334	62.20	23.01	0.06	3.90	0.00	9.02	0.49	98.68
3335	62.14	23.15	0.06	3.96	0.00	9.24	0.43	98.98
3336	62.60	23.07	0.05	3.86	0.01	9.32	0.47	99.38
3337	63.12	23.43	0.02	3.63	0.00	9.60	0.11	99.91
3338	61.70	23.76	0.04	4.67	0.04	8.80	0.22	99.23
3339	62.10	23.40	0.05	4.30	0.07	8.55	0.21	98.68
3341	62.28	22.96	0.05	3.95	0.04	8.75	0.41	98.44
3343	62.55	22.98	0.04	3.86	0.01	8.30	0.45	98.19
3345	61.06	23.64	0.04	4.74	0.03	8.05	0.37	97.93
3347	61.72	23.88	0.05	4.56	0.03	8.36	0.34	98.94
3348	62.50	22.96	0.05	3.88	0.03	8.11	0.21	97.74
3361	62.04	23.70	0.02	4.44	0.06	8.45	0.20	98.91
3367	62.39	23.42	0.03	4.22	0.07	8.91	0.14	99.18
3368	63.90	22.86	0.01	2.97	0.00	9.58	0.07	99.39
3372	66.94	21.02	0.05	1.03	0.03	10.44	0.17	99.68
3374	66.73	20.42	0.02	0.54	0.03	10.39	0.21	98.34
3376	61.05	24.25	0.03	4.38	0.00	8.36	0.19	98.26
3377	63.11	23.08	0.04	3.90	0.03	8.66	0.12	98.94
AVG	62.38	23.17	0.04	3.93	0.03	8.73	0.30	98.58
STD	1.54	0.85	0.01	1.05	0.02	0.73	0.14	0.68

APPENDIX 4: PLAGIOCASE ANALYSES (8 Oxygen) CA85-5 RSgr (continued)

SMPL#	Si	Al	Fe	Ca	Ba	Na	K	AN	AB	OR
3327	2.814	1.208	0.002	0.180	0.000	0.725	0.018	19.5	78.5	2.0
3328	2.744	1.265	0.002	0.228	0.001	0.724	0.023	23.4	74.3	2.4
3329	2.728	1.291	0.002	0.262	0.001	0.641	0.017	28.5	69.7	1.8
3330	2.751	1.270	0.002	0.232	0.001	0.681	0.016	25.0	73.3	1.7
3331	2.745	1.267	0.002	0.238	0.001	0.689	0.024	25.0	72.5	2.5
3332	2.792	1.208	0.002	0.192	0.000	0.777	0.030	19.2	77.8	3.0
3333	2.791	1.216	0.002	0.185	0.001	0.768	0.029	18.8	78.2	3.0
3334	2.787	1.215	0.002	0.187	0.000	0.784	0.028	18.7	78.5	2.8
3335	2.777	1.219	0.002	0.190	0.000	0.800	0.025	18.7	78.8	2.5
3336	2.786	1.210	0.002	0.184	0.000	0.804	0.027	18.1	79.2	2.7
3337	2.789	1.220	0.001	0.172	0.000	0.822	0.006	17.2	82.2	0.6
3338	2.752	1.249	0.001	0.223	0.001	0.761	0.013	22.4	76.3	1.3
3339	2.777	1.233	0.002	0.206	0.001	0.741	0.012	21.5	77.3	1.3
3341	2.796	1.215	0.002	0.190	0.001	0.762	0.023	19.5	78.2	2.4
3343	2.806	1.215	0.002	0.185	0.000	0.722	0.026	19.8	77.4	2.8
3345	2.753	1.256	0.002	0.229	0.001	0.704	0.021	24.0	73.8	2.2
3347	2.757	1.257	0.002	0.218	0.001	0.724	0.019	22.7	75.3	2.0
3348	2.810	1.217	0.002	0.187	0.001	0.707	0.012	20.6	78.0	1.3
3361	2.769	1.246	0.001	0.212	0.001	0.731	0.011	22.2	76.6	1.2
3367	2.777	1.228	0.001	0.201	0.001	0.769	0.008	20.6	78.6	0.8
3368	2.827	1.192	0.000	0.141	0.000	0.822	0.004	14.6	85.0	0.4
3372	2.935	1.086	0.002	0.048	0.001	0.888	0.010	5.1	93.9	1.1
3374	2.957	1.066	0.001	0.026	0.001	0.893	0.012	2.8	95.9	1.3
3376	2.743	1.284	0.001	0.211	0.000	0.728	0.011	22.2	76.6	1.2
3377	2.804	1.208	0.001	0.186	0.001	0.746	0.007	19.8	79.4	0.7
AVG	2.791	1.222	0.002	0.189	0.001	0.757	0.017	19.6	78.6	1.8
STD	0.052	0.050	0.001	0.051	0.000	0.058	0.008	5.4	5.7	0.8

APPENDIX 4: POTASSIUM FELDSPAR ANALYSES (8 Oxygen) CA85-5 RSgr

SMPL#	SiO2	Al2O3	FeO	CaO	BaO	Na2O	K2O	TOTAL
3362	62.95	19.10	0.03	0.03	0.59	0.40	15.69	98.79
3363	63.03	18.95	0.06	0.07	0.94	0.95	15.43	99.43
3364	62.61	18.99	0.07	0.02	1.40	0.38	16.10	99.57
3365	63.32	19.00	0.05	0.08	1.28	1.36	14.88	99.97
3366	63.41	18.94	0.08	0.04	1.07	0.77	15.29	99.60
3369	62.72	19.09	0.05	0.05	1.40	0.89	15.39	99.59
3371	63.29	18.99	0.07	0.03	0.34	0.53	16.25	99.50
3373	64.20	18.90	0.05	0.04	0.37	1.56	14.84	99.96
3375	64.45	19.23	0.04	0.04	0.32	2.05	13.45	99.58
3378	63.28	18.71	0.05	0.08	0.62	0.65	15.94	99.33
AVG	63.33	18.99	0.06	0.05	0.83	0.95	15.33	99.53
STD	0.56	0.13	0.01	0.02	0.42	0.52	0.77	0.31

SMPL#	Si	Al	Fe	Ca	Ba	Na	K	AN	AB	OR
3362	2.953	1.056	0.001	0.002	0.011	0.036	0.939	0.2	3.7	96.1
3363	2.947	1.044	0.002	0.004	0.017	0.086	0.920	0.4	8.5	91.1
3364	2.943	1.052	0.003	0.001	0.026	0.035	0.965	0.1	3.5	96.4
3365	2.948	1.042	0.002	0.004	0.023	0.123	0.883	0.4	12.2	87.4
3366	2.959	1.041	0.003	0.002	0.020	0.070	0.910	0.2	7.1	92.7
3369	2.940	1.055	0.002	0.003	0.026	0.081	0.920	0.3	8.1	91.6
3371	2.954	1.044	0.003	0.002	0.006	0.048	0.967	0.2	4.7	95.1
3373	2.963	1.028	0.002	0.002	0.007	0.140	0.874	0.2	13.8	86.0
3375	2.967	1.043	0.002	0.002	0.006	0.183	0.790	0.2	18.8	81.0
3378	2.962	1.032	0.002	0.004	0.011	0.059	0.952	0.4	5.8	93.8
AVG	2.954	1.044	0.002	0.003	0.015	0.086	0.912	0.3	8.6	91.1
STD	0.009	0.009	0.001	0.001	0.008	0.046	0.050	0.1	4.7	4.7

APPENDIX 4: PLAGIOCLASE ANALYSES (8 Oxygen) BW84-20 RSgr

SMPL#	SiO2	Al2O3	FeO	CaO	BaO	Na2O	K2O	TOTAL
1193	63.65	23.04	0.00	3.83	0.00	7.59	0.16	98.27
1194	62.98	23.34	0.00	4.57	0.08	6.78	0.20	97.95
1195	62.94	23.51	0.00	4.64	0.04	6.96	0.18	98.27
1196	62.52	23.76	0.00	4.63	0.00	6.29	0.17	97.37
1197	62.15	24.24	0.00	5.56	0.07	6.88	0.20	99.10
1198	62.27	23.39	0.00	4.76	0.01	6.58	0.17	97.18
1200	63.91	23.18	0.00	3.56	0.01	7.70	0.12	98.48
AVG	62.92	23.49	0.00	4.51	0.03	6.97	0.17	98.09
STD	0.62	0.37	0.00	0.61	0.03	0.47	0.03	0.61

SMPL#	Si	Al	Fe	Ca	Ba	Na	K	AN	AB	OR
1193	2.835	1.209	0.000	0.183	0.000	0.655	0.009	21.6	77.3	1.1
1194	2.817	1.230	0.000	0.219	0.001	0.588	0.011	26.8	71.9	1.3
1195	2.808	1.236	0.000	0.222	0.001	0.602	0.010	26.6	72.2	1.2
1196	2.806	1.257	0.000	0.223	0.000	0.547	0.010	28.6	70.1	1.3
1197	2.763	1.270	0.000	0.265	0.001	0.593	0.011	30.5	68.2	1.3
1198	2.807	1.242	0.000	0.230	0.000	0.575	0.010	28.2	70.6	1.2
1200	2.838	1.213	0.000	0.169	0.000	0.663	0.007	20.1	79.0	0.8
AVG	2.811	1.237	0.000	0.216	0.000	0.603	0.010	26.1	72.8	1.2
STD	0.023	0.020	0.000	0.029	0.000	0.039	0.001	3.5	3.7	0.2

APPENDIX 4: POTASSIUM FELDSPAR ANALYSES (8 Oxygen) BW84-20 RSgr

SMPL#	SiO2	Al2O3	FeO	CaO	BaO	Na2O	K2O	TOTAL
1201	64.26	19.20	0.00	0.00	0.86	0.80	14.40	99.52
1202	63.79	18.42	0.00	0.00	0.75	0.48	14.55	97.99

SMPL#	Si	Al	Fe	Ca	Ba	Na	K	AN	AB	OR
1201	2.974	1.047	0.000	0.000	0.016	0.072	0.850	0.0	7.8	92.2
1202	2.998	1.020	0.000	0.000	0.014	0.044	0.872	0.0	4.8	95.2

APPENDIX 4: PLAGIOCLASE ANALYSES (8 Oxygen) BW84-18 RSgd

SMPL#	SiO2	Al2O3	FeO	CaO	BaO	Na2O	K2O	TOTAL
1073	60.76	24.76	0.05	5.60	0.00	7.61	0.25	99.03
1074	61.50	24.53	0.05	5.68	0.00	7.82	0.25	99.83
1075	61.41	24.59	0.04	5.41	0.01	7.31	0.25	99.02
1079	60.57	24.65	0.04	5.97	0.00	7.16	0.20	98.59
1080	60.59	24.77	0.13	5.84	0.02	6.98	0.43	98.76
1081	60.59	24.89	0.12	5.99	0.00	7.31	0.42	99.32
1082	60.96	24.82	0.10	5.72	0.04	7.52	0.42	99.58
1083	60.62	24.79	0.09	5.98	0.00	6.95	0.39	98.82
1152	62.07	25.00	0.05	5.59	0.13	7.58	0.24	100.66
1153	62.20	24.60	0.05	5.29	0.01	8.04	0.21	100.40
1154	62.74	24.09	0.05	5.28	0.02	8.09	0.17	100.44
1155	61.47	24.80	0.04	5.89	0.00	7.39	0.18	99.77
1156	62.32	24.36	0.04	5.64	0.00	7.75	0.30	100.41
AVG	61.37	24.67	0.07	5.68	0.02	7.50	0.29	99.59
STD	0.73	0.23	0.03	0.24	0.03	0.35	0.09	0.69

SMPL#	Si	Al	Fe	Ca	Ba	Na	K	AN	AB	OR
1073	2.717	1.305	0.002	0.268	0.000	0.660	0.014	28.5	70.1	1.5
1074	2.729	1.283	0.002	0.270	0.000	0.673	0.014	28.2	70.3	1.5
1075	2.739	1.292	0.001	0.259	0.000	0.632	0.014	28.6	69.8	1.5
1079	2.719	1.304	0.002	0.287	0.000	0.623	0.011	31.2	67.6	1.2
1080	2.717	1.309	0.005	0.281	0.000	0.607	0.025	30.8	66.5	2.7
1081	2.707	1.310	0.004	0.287	0.000	0.633	0.024	30.4	67.1	2.5
1082	2.715	1.303	0.004	0.273	0.001	0.649	0.024	28.9	68.6	2.5
1083	2.716	1.309	0.003	0.287	0.000	0.604	0.022	31.4	66.2	2.4
1152	2.729	1.295	0.002	0.263	0.002	0.646	0.013	28.5	70.1	1.4
1153	2.740	1.277	0.002	0.250	0.000	0.687	0.012	26.3	72.4	1.3
1154	2.762	1.250	0.002	0.249	0.000	0.690	0.010	26.2	72.7	1.1
1155	2.725	1.295	0.001	0.280	0.000	0.635	0.010	30.3	68.6	1.1
1156	2.747	1.265	0.001	0.266	0.000	0.662	0.017	28.1	70.1	1.8
AVG	2.728	1.292	0.002	0.271	0.000	0.646	0.016	29.0	69.2	1.7
STD	0.015	0.018	0.001	0.013	0.001	0.026	0.005	1.6	2.0	0.6

APPENDIX 4: POTASSIUM FELDSPAR ANALYSES (8 Oxygen) BW84-18 RSgd

SMPL#	SiO2	Al2O3	FeO	CaO	BaO	Na2O	K2O	TOTAL
1070	63.26	18.87	0.00	0.02	0.20	0.53	14.91	97.79
1071	65.32	19.24	0.01	0.03	0.22	4.68	9.49	98.99
1076	64.07	18.94	0.03	0.00	0.07	0.49	15.28	98.88
AVG	64.22	19.02	0.01	0.02	0.16	1.90	13.23	98.55
STD	0.85	0.16	0.01	0.01	0.07	1.97	2.65	0.54

SMPL#	Si	Al	Fe	Ca	Ba	Na	K	AN	AB	OR
1070	2.976	1.046	0.000	0.001	0.004	0.048	0.895	0.1	5.1	94.8
1071	2.979	1.034	0.000	0.001	0.004	0.414	0.552	0.1	42.8	57.1
1076	2.981	1.038	0.001	0.000	0.001	0.044	0.907	0.0	4.6	95.4
AVG	2.979	1.039	0.000	0.001	0.003	0.169	0.785	0.1	17.5	82.4
STD	0.002	0.005	0.000	0.000	0.001	0.173	0.165	0.0	17.9	17.9

APPENDIX 4: PLAGIOCLASE ANALYSES (8 Oxygen) BW84-19 RSgd

SMPL#	SiO2	Al2O3	FeO	CaO	BaO	Na2O	K2O	TOTAL
1266	60.61	25.99	0.08	6.56	0.03	6.65	0.22	100.14
1267	60.40	25.20	0.04	5.86	0.00	6.99	0.13	98.62
1269	59.93	25.63	0.13	6.33	0.00	6.39	0.42	98.83
AVG	60.31	25.61	0.08	6.25	0.01	6.68	0.26	99.20
STD	0.28	0.32	0.04	0.29	0.01	0.25	0.12	0.67

SMPL#	Si	Al	Fe	Ca	Ba	Na	K	AN	AB	OR
1266	2.680	1.354	0.003	0.311	0.001	0.570	0.012	34.8	63.8	1.3
1267	2.706	1.330	0.001	0.281	0.000	0.607	0.007	31.4	67.8	0.8
1269	2.685	1.353	0.005	0.304	0.000	0.555	0.024	34.4	62.9	2.7
AVG	2.690	1.346	0.003	0.299	0.000	0.577	0.014	33.6	64.8	1.6
STD	0.011	0.011	0.002	0.013	0.000	0.022	0.007	1.5	2.1	0.8

APPENDIX 4: POTASSIUM FELDSPAR ANALYSES (8 Oxygen) BW84-19 RSgd

SMPL#	SiO2	Al2O3	FeO	CaO	BaO	Na2O	K2O	TOTAL
1272	64.79	18.81	0.05	0.00	0.32	0.45	15.19	99.61
1273	65.26	18.81	0.01	0.00	0.54	0.68	14.75	100.05

SMPL#	Si	Al	Fe	Ca	Ba	Na	K	AN	AB	OR
1272	2.993	1.024	0.002	0.000	0.006	0.040	0.895	0.0	4.3	95.7
1273	2.997	1.018	0.000	0.000	0.010	0.061	0.864	0.0	6.6	93.4

APPENDIX 4: PLAGIOCLASE ANALYSES (8 Oxygen) BW84-23 RSgd

SMPL#	SiO2	Al2O3	FeO	CaO	BaO	Na2O	K2O	TOTAL
1347	59.78	24.95	0.11	5.56	0.00	6.00	0.22	96.62
1348	60.20	25.87	0.08	6.94	0.00	6.00	0.20	99.29
1350	60.20	25.18	0.03	7.03	0.00	5.89	0.28	98.61
1351	59.14	26.04	0.08	6.36	0.06	5.47	0.22	97.37
1352	58.97	26.59	0.07	7.51	0.08	4.90	0.20	98.32
1355	59.74	25.90	0.03	6.18	0.03	5.37	0.19	97.44
1365	58.36	25.84	0.10	7.92	0.07	5.49	0.29	98.07
1366	60.06	25.41	0.01	6.28	0.08	5.91	0.08	97.83
1367	56.28	28.29	0.06	6.84	0.00	5.04	0.20	96.71
1368	59.72	26.17	0.05	6.54	0.00	5.57	0.12	98.17
1369	60.34	25.56	0.07	7.36	0.05	5.79	0.20	99.37
1370	60.12	25.75	0.09	7.03	0.05	5.31	0.30	98.65
1373	60.63	25.09	0.08	6.59	0.00	5.74	0.37	98.50
AVG	59.50	25.90	0.07	6.78	0.03	5.58	0.22	98.07
STD	1.11	0.82	0.03	0.60	0.03	0.34	0.07	0.83

APPENDIX 4: PLAGIOCLASE ANALYSES (8 Oxygen) BW84-23 RSgd (continued)

SMPL#	Si	Al	Fe	Ca	Ba	Na	K	AN	AB	OR
1347	2.716	1.336	0.004	0.271	0.000	0.528	0.013	33.4	65.0	1.6
1348	2.681	1.358	0.003	0.331	0.000	0.518	0.011	38.5	60.2	1.3
1350	2.699	1.330	0.001	0.338	0.000	0.512	0.016	39.0	59.1	1.8
1351	2.678	1.389	0.003	0.309	0.001	0.480	0.013	38.5	59.9	1.6
1352	2.651	1.408	0.003	0.362	0.001	0.427	0.011	45.3	53.4	1.4
1355	2.696	1.377	0.001	0.299	0.001	0.470	0.011	38.3	60.3	1.4
1365	2.645	1.380	0.004	0.385	0.001	0.482	0.017	43.6	54.5	1.9
1366	2.703	1.348	0.000	0.303	0.001	0.516	0.005	36.8	62.6	0.6
1367	2.573	1.524	0.002	0.335	0.000	0.447	0.012	42.2	56.3	1.5
1368	2.680	1.384	0.002	0.314	0.000	0.485	0.007	39.0	60.2	0.9
1369	2.687	1.341	0.003	0.351	0.001	0.500	0.011	40.7	58.0	1.3
1370	2.691	1.358	0.003	0.337	0.001	0.461	0.017	41.3	56.6	2.1
1373	2.717	1.325	0.003	0.316	0.000	0.499	0.021	37.8	59.7	2.5
AVG	2.678	1.374	0.002	0.327	0.001	0.487	0.013	39.6	58.9	1.5
STD	0.037	0.050	0.001	0.029	0.000	0.029	0.004	3.0	3.0	0.5

APPENDIX 4: POTASSIUM FELDSPAR ANALYSES (8 Oxygen) BW84-23 RSgd

SMPL#	SiO2	Al2O3	FeO	CaO	BaO	Na2O	K2O	TOTAL
1343	64.29	19.76	0.00	0.03	0.63	1.09	13.55	99.35
1344	63.64	19.54	0.02	0.00	0.53	0.57	14.74	99.04
1345	63.74	19.55	0.00	0.00	0.49	0.66	14.55	98.99
AVG	63.89	19.62	0.01	0.01	0.55	0.77	14.28	99.13
STD	0.29	0.10	0.01	0.01	0.06	0.23	0.52	0.16

SMPL#	Si	Al	Fe	Ca	Ba	Na	K	AN	AB	OR
1343	2.964	1.073	0.000	0.001	0.011	0.097	0.797	0.1	10.8	89.1
1344	2.959	1.070	0.001	0.000	0.010	0.051	0.874	0.0	5.5	94.5
1345	2.961	1.070	0.000	0.000	0.009	0.059	0.862	0.0	6.4	93.6
AVG	2.961	1.071	0.000	0.000	0.010	0.069	0.844	0.0	7.6	92.4
STD	0.002	0.001	0.000	0.000	0.001	0.020	0.034	0.1	2.3	2.4

APPENDIX 4: PLAGIOCLASE ANALYSES (8 Oxygen) BW84-25 RSgd

SMPL#	SiO2	Al2O3	FeO	CaO	BaO	Na2O	K2O	TOTAL
1289	59.27	26.00	0.14	7.61	0.07	6.17	0.18	99.44
1290	59.11	26.45	0.10	7.52	0.00	5.55	0.33	99.06
1291	59.26	25.62	0.10	7.14	0.03	6.17	0.19	98.51
1292	60.20	26.17	0.09	7.36	0.08	5.60	0.32	99.82
1293	59.68	26.48	0.09	7.71	0.00	5.64	0.28	99.88
1294	59.63	25.91	0.09	7.24	0.00	6.20	0.23	99.30
1308	59.50	25.80	0.10	7.44	0.11	5.98	0.21	99.14
AVG	59.52	26.06	0.10	7.43	0.04	5.90	0.25	99.31
STD	0.34	0.30	0.02	0.19	0.04	0.27	0.06	0.44

SMPL#	Si	Al	Fe	Ca	Ba	Na	K	AN	AB	OR
1289	2.649	1.370	0.005	0.364	0.001	0.535	0.010	40.0	58.9	1.1
1290	2.645	1.395	0.004	0.361	0.000	0.482	0.019	41.9	55.9	2.2
1291	2.668	1.359	0.004	0.344	0.001	0.539	0.011	38.5	60.3	1.2
1292	2.671	1.368	0.003	0.350	0.001	0.482	0.018	41.2	56.7	2.1
1293	2.650	1.385	0.003	0.367	0.000	0.486	0.016	42.2	55.9	1.8
1294	2.664	1.364	0.003	0.347	0.000	0.537	0.013	38.7	59.9	1.4
1308	2.664	1.361	0.004	0.357	0.002	0.519	0.012	40.2	58.4	1.4
AVG	2.659	1.372	0.004	0.356	0.001	0.511	0.014	40.4	58.0	1.6
STD	0.010	0.012	0.001	0.008	0.001	0.025	0.003	1.4	1.7	0.4

APPENDIX 4: PLAGIOCLASE ANALYSES (8 Oxygen) CA84-147 CFqmd

SMPL#	SiO2	Al2O3	FeO	CaO	BaO	Na2O	K2O	TOTAL
2199	58.37	26.38	0.03	7.28	0.00	7.23	0.11	99.39
2200	57.49	27.23	0.07	7.84	0.00	6.92	0.19	99.75
2201	58.37	25.68	0.05	7.16	0.00	7.18	0.16	98.60
AVG	58.08	26.43	0.05	7.43	0.00	7.11	0.15	99.25
STD	0.41	0.63	0.02	0.30	0.00	0.14	0.03	0.48

APPENDIX 4: PLAGIOCLASE ANALYSES (8 Oxygen) CA84-147 CFqmd (continued)

SMPL#	Si	Al	Fe	Ca	Ba	Na	K	AN	AB	OR
2199	2.619	1.395	0.001	0.349	0.000	0.628	0.006	35.5	63.9	0.6
2200	2.578	1.439	0.003	0.377	0.000	0.602	0.011	38.1	60.8	1.1
2201	2.639	1.368	0.002	0.347	0.000	0.629	0.009	35.2	63.9	0.9
AVG	2.612	1.401	0.002	0.358	0.000	0.620	0.009	36.3	62.9	0.9
STD	0.025	0.029	0.001	0.014	0.000	0.012	0.002	1.3	1.4	0.2

APPENDIX 4: POTASSIUM FELDSPAR ANALYSES (8 Oxygen) CA84-147 CFqmd

SMPL#	SiO2	Al2O3	FeO	CaO	BaO	Na2O	K2O	TOTAL
2181	63.50	18.65	0.01	0.05	0.53	1.04	14.23	98.02
2182	64.59	19.51	0.06	0.05	0.83	1.15	14.04	100.23
2202	64.28	18.42	0.00	0.00	0.39	1.07	14.31	98.47
2205	63.17	18.97	0.00	0.00	0.73	0.32	15.25	98.44
AVG	63.89	18.86	0.03	0.03	0.58	1.09	14.19	98.79
STD	0.57	0.47	0.03	0.02	0.18	0.04	0.12	0.85

SMPL#	Si	Al	Fe	Ca	Ba	Na	K	AN	AB	OR
2181	2.981	1.032	0.000	0.003	0.010	0.095	0.852	0.3	10.0	89.7
2182	2.965	1.055	0.002	0.002	0.015	0.102	0.822	0.2	11.0	88.8
2202	2.999	1.012	0.000	0.000	0.007	0.097	0.852	0.0	10.2	89.8
2205	2.968	1.050	0.000	0.000	0.013	0.029	0.914	0.0	3.1	96.9
AVG	2.978	1.037	0.001	0.001	0.011	0.081	0.860		8.6	91.3
STD	0.013	0.017	0.001	0.001	0.003	0.030	0.033	0.1	3.2	3.3

APPENDIX 4: POTASSIUM FELDSPAR ANALYSES (8 Oxygen) CA84-28 gap

SMPL#	SiO2	Al2O3	FeO	CaO	BaO	Na2O	K2O	TOTAL
3411	62.76	18.74	0.05	0.07	0.71	0.66	15.78	98.77
3413	62.88	19.07	0.06	0.07	1.03	1.42	14.43	98.96
3414	62.80	18.92	0.05	0.07	1.10	1.41	14.50	98.85
3415	62.07	18.90	0.05	0.07	1.05	1.45	14.15	97.74
3417	62.56	19.03	0.04	0.05	0.98	1.58	14.54	98.78
3418	62.47	19.00	0.04	0.06	1.01	1.44	14.64	98.66
3419	62.86	19.06	0.04	0.06	0.74	1.21	15.02	98.99
3421	62.30	18.87	0.04	0.05	1.23	1.38	14.86	98.73
3422	62.00	18.70	0.55	0.04	1.14	0.41	16.04	98.88
3423	62.78	18.78	0.07	0.03	0.50	0.24	16.57	98.97
3444	62.52	18.91	0.06	0.07	0.97	1.08	15.25	98.86
3448	62.64	18.88	0.06	0.06	1.09	0.96	15.31	99.00
3449	62.10	18.80	0.05	0.05	0.80	0.50	16.01	98.31
3453	63.15	18.83	0.08	0.01	0.22	0.19	16.77	99.25
3455	62.44	18.97	0.05	0.12	0.57	1.13	14.95	98.23
3456	61.76	18.66	0.04	0.07	1.03	1.08	14.83	97.47
3457	61.80	18.53	0.03	0.05	1.11	1.01	14.89	97.42
3458	60.97	18.32	0.03	0.03	0.98	0.86	15.09	96.28
3464	62.89	19.03	0.04	0.06	0.75	0.90	15.59	99.26
3465	62.47	18.93	0.04	0.07	1.04	1.30	15.00	98.85
3466	62.07	19.12	0.03	0.07	1.08	1.23	14.78	98.38
3467	62.92	19.11	0.04	0.06	0.99	1.14	15.13	99.39
3468	61.03	18.12	0.04	0.08	0.79	1.14	15.23	96.43
3470	62.87	18.80	0.05	0.08	1.02	1.28	14.96	99.06
3471	62.42	18.93	0.05	0.06	1.04	1.10	15.19	98.79
3472	62.40	18.80	0.03	0.06	0.99	1.09	15.09	
AVG	62.38	18.84	0.07	0.06	0.92	1.05	15.18	98.49
STD	0.53	0.23	0.10	0.02	0.22	0.37	0.62	0.80

APPENDIX 4: POTASSIUM FELDSPAR ANALYSES (8 Oxygen) CA84-28 gap (continued)

SMPL#	Si	Al	Fe	Ca	Ba	Na	K	AN	AB	OR
3411	2.955	1.040	0.002	0.004	0.013	0.060	0.948	0.4	5.9	93.7
3413	2.945	1.053	0.002	0.004	0.019	0.129	0.862	0.4	13.0	86.6
3414	2.947	1.046	0.002	0.004	0.020	0.128	0.868	0.4	12.8	86.8
3415	2.943	1.056	0.002	0.004	0.020	0.133	0.856	0.4	13.4	86.2
3417	2.942	1.054	0.002	0.003	0.018	0.144	0.872	0.3	14.1	85.6
3418	2.941	1.054	0.002	0.003	0.019	0.131	0.879	0.3	12.9	86.8
3419	2.947	1.053	0.002	0.003	0.014	0.110	0.898	0.3	10.9	88.8
3421	2.941	1.050	0.002	0.003	0.023	0.126	0.895	0.3	12.3	87.4
3422	2.936	1.044	0.022	0.002	0.021	0.038	0.969	0.2	3.8	96.0
3423	2.953	1.041	0.003	0.002	0.009	0.022	0.994	0.2	2.2	97.6
3444	2.944	1.049	0.002	0.004	0.018	0.099	0.916	0.4	9.7	89.9
3448	2.948	1.047	0.002	0.003	0.020	0.088	0.919	0.3	8.7	91.0
3449	2.946	1.051	0.002	0.003	0.015	0.046	0.969	0.3	4.5	95.2
3453	2.958	1.039	0.003	0.001	0.004	0.017	1.002	0.1	1.7	98.2
3455	2.945	1.054	0.002	0.006	0.011	0.103	0.899	0.6	10.2	89.2
3456	2.947	1.049	0.002	0.004	0.019	0.100	0.902	0.4	9.9	89.7
3457	2.953	1.043	0.001	0.003	0.021	0.094	0.907	0.3	9.4	90.3
3458	2.948	1.044	0.001	0.002	0.019	0.081	0.931	0.2	8.0	91.8
3464	2.947	1.051	0.002	0.003	0.014	0.082	0.932	0.3	8.1	91.6
3465	2.941	1.050	0.002	0.004	0.019	0.119	0.901	0.4	11.6	88.0
3466	2.935	1.065	0.001	0.004	0.02	0.113	0.891	0.4	11.0	86.8
3467	2.944	1.054	0.002	0.003	0.018	0.103	0.903	0.3	10.2	89.5
3468	2.950	1.032	0.002	0.004	0.015	0.107	0.939	0.4	10.2	89.4
3470	2.951	1.040	0.002	0.004	0.019	0.116	0.896	0.4	11.4	88.2
3471	2.943	1.052	0.002	0.003	0.019	0.101	0.913	0.3	9.9	89.8
3472	2.948	1.047	0.001	0.003	0.018	0.100	0.909	0.3	9.9	89.8
AVG	2.946	1.048	0.003	0.003	0.017	0.096	0.914	0.3	9.4	90.2
STD	0.005	0.007	0.004	0.001	0.004	0.033	0.037	0.1	3.3	3.4

APPENDIX 4: PLAGIOCLASE ANALYSES (8 Oxygen) CA84-46 gap

SMPL#	SiO2	Al2O3	FeO	CaO	BaO	Na2O	K2O	TOTAL
3500	63.16	22.35	0.30	3.06	0.03	8.75	1.64	99.29
3501	63.40	22.31	0.09	3.24	0.00	8.86	0.41	98.31
3502	63.35	22.70	0.07	3.57	0.00	8.65	0.18	98.52
3503	62.58	21.91	0.07	3.31	0.00	8.16	0.44	96.47
3504	61.07	22.98	0.08	4.40	0.05	7.83	0.36	96.77
3505	62.57	21.93	0.12	3.20	0.04	8.75	0.15	96.76
3516	62.58	22.78	0.03	3.61	0.02	8.29	0.16	97.47
AVG	62.67	22.42	0.11	3.48	0.02	8.47	0.48	97.66
STD	0.74	0.39	0.08	0.42	0.02	0.35	0.49	0.99

SMPL#	Si	Al	Fe	Ca	Ba	Na	K	AN	AB	OR
3500	2.822	1.177	0.011	0.147	0.001	0.758	0.093	14.7	76.0	9.3
3501	2.838	1.177	0.003	0.155	0.000	0.769	0.023	16.4	81.2	2.4
3502	2.825	1.193	0.003	0.171	0.000	0.748	0.010	18.4	80.5	1.1
3503	2.847	1.175	0.003	0.161	0.000	0.720	0.026	17.8	79.4	2.9
3504	2.782	1.234	0.003	0.215	0.001	0.692	0.021	23.2	74.6	2.3
3505	2.841	1.173	0.005	0.156	0.001	0.770	0.009	16.7	82.4	1.0
3516	2.818	1.209	0.001	0.174	0.000	0.724	0.009	19.2	79.8	1.0
AVG	2.825	1.191	0.004	0.168	0.000	0.740	0.027	18.0	79.1	2.8
STD	0.020	0.021	0.003	0.021	0.000	0.027	0.028	2.5	2.6	2.7

APPENDIX 4: PLAGIOCLASE ANALYSES (8 Oxygen) CA84-102 gap

SMPL#	SiO2	Al2O3	FeO	CaO	BaO	Na2O	K2O	TOTAL
1320	63.65	23.69	0.00	4.41	0.00	6.47	0.21	98.43
1321	64.78	21.72	0.00	2.81	0.00	6.29	0.20	95.80
1322	62.83	23.16	0.00	4.11	0.00	6.81	0.25	97.16
1323	63.28	23.10	0.01	3.99	0.04	6.99	0.28	97.69
1324	63.59	23.06	0.00	4.12	0.03	6.66	0.28	97.74
1325	63.31	23.13	0.00	4.33	0.00	7.01	0.21	97.99
1326	65.27	21.50	0.00	2.48	0.00	8.32	0.20	97.77
1405	60.36	25.54	0.06	6.15	0.01	8.24	0.18	100.54
AVG	63.38	23.11	0.01	4.05	0.01	7.10	0.23	97.89
STD	1.37	1.16	0.02	1.04	0.02	0.72	0.04	1.24

SMPL#	Si	Al	Fe	Ca	Ba	Na	K	AN	AB	OR
1320	2.823	1.238	0.000	0.210	0.000	0.556	0.012	27.0	71.5	1.5
1321	2.924	1.155	0.000	0.136	0.000	0.551	0.012	19.5	78.8	1.7
1322	2.827	1.228	0.000	0.198	0.000	0.594	0.014	24.6	73.7	1.7
1323	2.834	1.219	0.000	0.191	0.001	0.607	0.016	23.5	74.6	2.0
1324	2.842	1.214	0.000	0.197	0.001	0.577	0.016	24.9	73.0	2.0
1325	2.828	1.217	0.000	0.207	0.000	0.607	0.012	25.1	73.5	1.5
1326	2.910	1.130	0.000	0.118	0.000	0.719	0.011	13.9	84.8	1.3
1405	2.673	1.333	0.002	0.292	0.000	0.707	0.010	28.9	70.1	1.0
AVG	2.833	1.217	0.000	0.194	0.000	0.615	0.013	23.4	75.0	1.6
STD	0.071	0.056	0.001	0.049	0.000	0.060	0.002	4.4	4.4	0.3

APPENDIX 4: POTASSIUM FELDSPAR ANALYSES (8 Oxygen) CA84-102 gap

SMPL#	SiO2	Al2O3	FeO	CaO	BaO	Na2O	K2O	TOTAL
1023	64.98	18.40	0.00	0.03	1.38	1.38	13.76	99.93
1024	65.16	18.49	0.00	0.03	1.18	1.41	13.68	99.95
1312	64.36	18.89	0.00	0.03	1.12	0.89	13.40	98.69
1313	64.11	18.34	0.02	0.03	1.28	0.92	13.76	98.46
1434	62.83	18.97	0.00	0.00	0.69	0.32	15.46	98.27
AVG	64.29	18.62	0.00	0.02	1.13	0.98	14.01	99.06
STD	0.82	0.26	0.01	0.01	0.24	0.40	0.74	0.73

SMPL#	Si	Al	Fe	Ca	Ba	Na	K	AN	AB	OR
1023	3.001	1.001	0.000	0.001	0.025	0.124	0.811	0.1	13.2	86.6
1024	3.002	1.004	0.000	0.001	0.021	0.126	0.804	0.1	13.5	86.4
1312	2.993	1.035	0.000	0.001	0.020	0.080	0.795	0.1	9.1	90.8
1313	3.000	1.011	0.001	0.002	0.023	0.083	0.821	0.2	9.2	90.6
1434	2.962	1.054	0.000	0.000	0.013	0.029	0.930	0.0	3.0	97.0
AVG	2.992	1.021	0.000	0.001	0.020	0.088	0.832	0.1	9.6	90.3
STD	0.015	0.020	0.000	0.001	0.004	0.036	0.050	0.1	3.8	3.8

APPENDIX 4: PLAGIOCLASE ANALYSES (8 Oxygen) BW84-29 m encl

SMPL#	SiO2	Al2O3	FeO	CaO	BaO	Na2O	K2O	TOTAL
1485	58.74	27.13	0.07	7.87	0.01	7.24	0.19	101.25
1486	59.62	25.78	0.08	6.59	0.01	7.85	0.31	100.24
1487	61.82	24.40	0.12	5.83	0.00	8.34	0.26	100.77
1488	60.92	25.24	0.04	6.40	0.00	7.96	0.12	100.68
1489	58.50	27.05	0.09	8.16	0.06	6.75	0.12	100.73
1490	60.10	25.58	0.06	6.43	0.07	7.79	0.17	100.20
1491	60.79	24.81	0.04	6.10	0.00	7.99	0.13	99.86
1492	60.51	25.28	0.01	6.55	0.00	7.92	0.11	100.38
1493	59.07	26.26	0.08	7.69	0.00	7.31	0.16	100.57
1494	59.41	25.79	0.09	6.71	0.00	7.84	0.15	99.99
1496	59.20	26.30	0.03	5.83	0.03	7.37	0.52	99.29
1497	59.46	26.73	0.01	7.32	0.06	7.00	0.17	100.75
1498	58.94	25.85	0.05	7.26	0.03	7.42	0.14	99.69
1499	58.50	27.03	0.07	7.62	0.04	7.04	0.13	100.43
1501	61.47	25.03	0.05	5.86	0.06	8.42	0.20	101.09
1504	60.41	25.72	0.01	6.92	0.02	7.89	0.12	101.09
1505	60.06	26.29	0.11	7.10	0.00	7.85	0.20	101.61
1510	58.84	26.17	0.03	7.27	0.00	7.23	0.78	100.32
1511	60.63	25.91	0.07	6.07	0.00	8.45	0.23	101.36
AVG	59.84	25.91	0.06	6.82	0.02	7.67	0.22	100.54
STD	0.98	0.74	0.03	0.71	0.02	0.48	0.16	0.58

SMPL#	Si	Al	Fe	Ca	Ba	Na	K	AN	AB	OR
1485	2.595	1.412	0.003	0.372	0.000	0.620	0.011	37.1	61.8	1.1
1486	2.653	1.352	0.003	0.314	0.000	0.677	0.018	31.1	67.1	1.8
1487	2.726	1.268	0.004	0.275	0.000	0.713	0.015	27.4	71.1	1.5
1488	2.690	1.313	0.001	0.303	0.000	0.682	0.007	30.5	68.8	0.7
1489	2.595	1.414	0.003	0.388	0.001	0.580	0.007	39.8	59.5	0.7
1490	2.669	1.339	0.002	0.306	0.001	0.671	0.010	31.0	68.0	1.0
1491	2.704	1.300	0.001	0.291	0.000	0.689	0.007	29.5	69.8	0.7
1492	2.682	1.320	0.000	0.311	0.000	0.680	0.006	31.2	68.2	0.6

APPENDIX 4: PLAGIOCLASE ANALYSES (8 Oxygen) BW84-29 m encl ontinued)

SMPL#	Si	Al	Fe	Ca	Ba	Na	K	AN	AB	OR
1493	2.624	1.374	0.003	0.366	0.000	0.630	0.009	36.4	62.7	0.9
1494	2.649	1.355	0.003	0.321	0.000	0.678	0.009	31.8	67.3	0.9
1496	2.647	1.386	0.001	0.279	0.001	0.639	0.030	29.4	67.4	3.2
1497	2.626	1.391	0.000	0.346	0.001	0.599	0.010	36.2	62.7	1.0
1498	2.639	1.364	0.002	0.348	0.001	0.644	0.008	34.8	64.4	0.8
1499	2.600	1.416	0.003	0.363	0.001	0.607	0.007	37.2	62.1	0.7
1501	2.704	1.297	0.002	0.276	0.001	0.718	0.011	27.5	71.4	1.1
1504	2.663	1.336	0.000	0.327	0.000	0.674	0.007	32.4	66.9	0.7
1505	2.639	1.361	0.004	0.334	0.000	0.669	0.011	32.9	66.0	1.1
1510	2.625	1.376	0.001	0.348	0.000	0.625	0.044	34.2	61.5	4.3
1511	2.665	1.342	0.003	0.286	0.000	0.720	0.013	28.1	70.7	1.3
AVG	2.652	1.353	0.002	0.324	0.000	0.659	0.013	32.6	66.2	1.3
STD	0.037	0.041	0.001	0.034	0.000	0.040	0.009	3.5	3.5	0.9

APPENDIX 4: PLAGIOCLASE ANALYSES (8 Oxygen) CA84-65A mdike

SMPL#	SiO2	Al2O3	FeO	CaO	BaO	Na2O	K2O	TOTAL
1399	60.35	26.33	0.10	7.74	0.00	5.99	0.17	100.68
1400	57.46	27.95	0.06	9.02	0.01	5.41	0.12	100.03
1401	58.78	27.84	0.03	8.59	0.00	5.32	0.10	100.66
AVG	58.86	27.37	0.06	8.45	0.00	5.57	0.13	100.46
STD	1.18	0.74	0.03	0.53	0.00	0.30	0.03	0.30

SMPL#	Si	Al	Fe	Ca	Ba	Na	K	AN	AB	OR
1399	2.659	1.367	0.004	0.365	0.000	0.512	0.010	41.1	57.7	1.1
1400	2.562	1.469	0.002	0.431	0.000	0.468	0.007	47.6	51.7	0.8
1401	2.594	1.448	0.001	0.406	0.000	0.455	0.006	46.8	52.5	0.7
AVG	2.605	1.428	0.002	0.401	0.000	0.478	0.008	45.2	54.0	0.9
STD	0.040	0.044	0.001	0.027	0.000	0.024	0.002	2.9	2.7	0.2

APPENDIX 4: PLAGIOCLASE ANALYSES (8 Oxygen) CA84-114 cg encl

SMPL#	SiO2	Al2O3	FeO	CaO	BaO	Na2O	K2O	TOTAL
1467	57.41	26.89	0.12	8.30	0.12	6.76	0.25	99.85
1468	60.07	25.90	0.12	7.00	0.00	7.67	0.25	101.01
1469	59.61	25.95	0.05	7.25	0.00	7.35	0.20	100.41
1470	58.21	26.50	0.04	8.02	0.00	6.86	0.26	99.89
1471	59.35	26.78	0.02	7.86	0.04	7.24	0.05	101.34
1472	57.64	27.59	0.07	8.42	0.03	6.79	0.17	100.71
AVG	58.72	26.60	0.07	7.81	0.03	7.11	0.20	100.54
STD	1.01	0.58	0.04	0.52	0.04	0.34	0.07	0.55

SMPL#	Si	Al	Fe	Ca	Ba	Na	K	AN	AB	OR
1467	2.578	1.423	0.005	0.399	0.002	0.589	0.014	39.8	58.8	1.4
1468	2.653	1.348	0.004	0.331	0.000	0.657	0.014	33.0	65.6	1.4
1469	2.647	1.358	0.002	0.345	0.000	0.633	0.011	34.9	64.0	1.1
1470	2.605	1.397	0.001	0.385	0.000	0.595	0.015	38.7	59.8	1.5
1471	2.615	1.390	0.001	0.371	0.001	0.618	0.003	37.4	62.3	0.3
1472	2.564	1.446	0.003	0.401	0.001	0.586	0.010	40.2	58.8	1.0
AVG	2.610	1.394	0.003	0.372	0.001	0.613	0.011	37.3	61.5	1.1
STD	0.033	0.034	0.001	0.026	0.001	0.026	0.004	2.6	2.6	0.4

APPENDIX 4: PLAGIOCLASE ANALYSES (8 Oxygen) BW84-27 cg encl

SMPL#	SiO2	Al2O3	FeO	CaO	BaO	Na2O	K2O	TOTAL
1380	59.37	26.03	0.09	7.71	0.00	5.45	0.23	98.88
1381	57.66	27.88	0.10	9.50	0.00	4.91	0.23	100.28
1382	57.22	27.73	0.08	9.28	0.00	4.57	0.22	99.10
1389	58.79	27.15	0.03	8.46	0.01	4.95	0.10	99.49
AVG	58.26	27.20	0.08	8.74	0.00	4.97	0.20	99.44
STD	0.86	0.73	0.03	0.71	0.00	0.31	0.06	0.53

SMPL#	Si	Al	Fe	Ca	Ba	Na	K	AN	AB	OR
1380	2.660	1.374	0.003	0.370	0.000	0.473	0.013	43.2	55.3	1.5
1381	2.565	1.462	0.004	0.453	0.000	0.424	0.013	50.9	47.6	1.5
1382	2.570	1.468	0.003	0.447	0.000	0.398	0.013	52.1	46.4	1.5
1389	2.619	1.425	0.001	0.404	0.000	0.428	0.006	48.2	51.1	0.7
AVG	2.604	1.432	0.003	0.419	0.000	0.431	0.011	48.6	50.1	1.3
STD	0.039	0.037	0.001	0.034	0.000	0.027	0.003	3.4	3.4	0.3

APPENDIX 4: PLAGIOCLASE ANALYSES (8 Oxygen) CA85-18 TGgr

SMPL#	SiO2	Al2O3	FeO	CaO	BaO	Na2O	K2O	TOTAL
3259	61.31	22.84	0.08	4.12	0.00	7.31	0.21	95.87
3260	60.03	23.66	0.07	4.07	0.00	8.02	0.11	95.96
3262	57.75	23.71	0.08	4.12	0.00	7.43	0.15	93.24
3263	60.62	23.70	0.17	4.17	0.01	7.65	0.41	96.73
3264	60.75	23.61	0.13	4.50	0.07	8.06	0.51	97.63
3265	60.68	23.33	0.14	3.97	0.00	7.86	0.56	96.54
3266	61.70	23.04	0.11	3.93	0.00	8.01	0.53	97.32
3267	61.85	23.21	0.10	4.28	0.01	8.49	0.16	98.10
3270	60.62	24.43	0.11	4.25	0.00	8.44	0.30	98.15
3273	61.57	23.47	0.11	4.37	0.01	7.80	0.49	97.82
3275	62.08	22.95	0.14	3.79	0.05	7.99	0.33	97.33
3277	60.92	23.75	0.11	4.74	0.00	8.53	0.33	98.38
3283	61.61	22.69	0.09	3.93	0.03	7.37	0.27	95.99
3284	61.44	23.33	0.09	4.41	0.03	7.31	0.26	96.87
3285	59.76	23.81	0.10	4.25	0.00	6.97	0.26	95.15
3289	61.55	23.20	0.07	4.18	0.00	7.81	0.23	97.04
3294	61.25	23.57	0.11	4.02	0.02	7.72	0.25	96.94
3295	62.06	22.55	0.10	3.65	0.03	7.94	0.25	96.58
3307	62.14	23.39	0.03	3.60	0.06	7.41	0.09	96.72
3308	61.00	23.59	0.13	4.89	0.07	6.97	0.21	96.86
3309	61.48	23.55	0.15	3.94	0.03	8.33	0.21	97.69
3310	61.64	23.33	0.14	4.28	0.12	7.12	0.15	96.78
3311	61.12	23.19	0.15	4.51	0.04	6.26	0.22	95.49
3312	61.42	23.18	0.14	4.09	0.02	6.99	0.32	96.16
3313	61.82	23.00	0.10	3.97	0.03	7.27	0.29	96.48
3314	63.35	22.59	0.03	3.02	0.01	8.54	0.07	97.61
3315	61.27	23.18	0.17	4.14	0.00	7.40	0.28	96.44
3316	62.22	22.69	0.06	3.50	0.04	7.73	0.07	96.31
AVG	61.25	23.31	0.11	4.10	0.02	7.67	0.27	96.72
STD	0.97	0.42	0.04	0.37	0.03	0.54	0.13	1.04

APPENDIX 4: PLAGIOCLASE ANALYSES (8 Oxygen) CA85-18 TGgr (continued)

SMPL#	Si	Al	Fe	Ca	Ba	Na	K	AN	AB	OR
3259	2.805	1.231	0.003	0.202	0.000	0.648	0.012	23.4	75.2	1.4
3260	2.753	1.279	0.003	0.200	0.000	0.713	0.006	21.8	77.6	0.7
3262	2.722	1.317	0.003	0.208	0.000	0.679	0.009	23.2	75.8	1.0
3263	2.757	1.270	0.006	0.203	0.000	0.675	0.024	22.5	74.8	2.7
3264	2.754	1.261	0.005	0.219	0.001	0.708	0.029	22.9	74.1	3.0
3265	2.772	1.256	0.005	0.194	0.000	0.696	0.033	21.0	75.4	3.6
3266	2.793	1.229	0.004	0.191	0.000	0.703	0.031	20.6	76.0	3.4
3267	2.780	1.229	0.004	0.206	0.000	0.740	0.009	21.6	77.5	0.9
3270	2.732	1.297	0.004	0.205	0.000	0.737	0.017	21.4	76.9	1.8
3273	2.776	1.247	0.004	0.211	0.000	0.682	0.028	22.9	74.0	3.0
3275	2.805	1.222	0.005	0.184	0.001	0.700	0.019	20.4	77.5	2.1
3277	2.743	1.260	0.004	0.229	0.000	0.745	0.019	23.1	75.0	1.9
3283	2.814	1.221	0.003	0.192	0.001	0.653	0.016	22.3	75.8	1.9
3284	2.787	1.247	0.003	0.214	0.001	0.643	0.015	24.5	73.7	1.7
3285	2.755	1.293	0.004	0.210	0.000	0.623	0.015	24.8	73.5	1.8
3289	2.789	1.239	0.003	0.203	0.000	0.686	0.013	22.5	76.1	1.4
3294	2.780	1.260	0.004	0.195	0.000	0.679	0.014	22.0	76.5	1.6
3295	2.822	1.208	0.004	0.178	0.001	0.700	0.014	20.0	78.5	1.6
3307	2.808	1.246	0.001	0.174	0.001	0.649	0.005	21.0	78.4	0.6
3308	2.768	1.261	0.005	0.238	0.001	0.613	0.012	27.6	71.0	1.4
3309	2.774	1.252	0.006	0.190	0.001	0.729	0.012	20.4	78.3	1.3
3310	2.795	1.247	0.005	0.208	0.002	0.626	0.009	24.7	74.3	1.1
3311	2.799	1.251	0.006	0.221	0.001	0.556	0.013	28.0	70.4	1.6
3312	2.800	1.245	0.005	0.200	0.000	0.618	0.019	23.9	73.8	2.3
3313	2.808	1.231	0.004	0.193	0.001	0.640	0.017	22.7	75.3	2.0
3314	2.841	1.194	0.001	0.145	0.000	0.743	0.004	16.3	83.3	0.4
3315	2.790	1.244	0.006	0.202	0.000	0.653	0.016	23.2	75.0	1.8
3316	2.824	1.214	0.002	0.170	0.001	0.680	0.004	19.9	79.6	0.5
AVG	2.782	1.249	0.004	0.200	0.000	0.678	0.016	22.5	75.8	1.7
STD	0.029	0.026	0.001	0.019	0.001	0.046	0.008	2.2	2.5	0.8

APPENDIX 4: POTASSIUM FELDSPAR ANALYSES (8 Oxygen) CA85-18 TGgr

SMPL#	SiO2	Al2O3	FeO	CaO	BaO	Na2O	K2O	TOTAL
3291	63.00	18.77	0.06	0.03	0.14	0.67	16.08	98.75
3293	63.06	18.61	0.08	0.02	0.16	0.42	16.44	98.79
3299	63.34	18.59	0.07	0.03	0.10	0.59	16.14	98.86
3301	62.25	18.51	0.04	0.02	0.71	0.42	15.81	97.76
3302	62.09	18.60	0.11	0.02	0.25	0.27	16.17	97.51
3303	62.86	18.79	0.08	0.04	0.42	0.83	15.46	98.48
3304	62.12	18.38	0.04	0.03	0.48	0.83	15.04	96.92
3305	61.86	18.51	0.08	0.02	0.94	0.33	16.08	97.82
3306	62.27	19.11	0.06	0.11	1.67	2.05	13.32	98.59
AVG	62.54	18.65	0.07	0.04	0.54	0.71	15.62	98.16
STD	0.50	0.20	0.02	0.03	0.48	0.51	0.90	0.65

SMPL#	Si	Al	Fe	Ca	Ba	Na	K	AN	AB	OR
3291	2.960	1.039	0.002	0.002	0.003	0.061	0.964	0.2	5.9	93.9
3293	2.966	1.031	0.003	0.001	0.003	0.038	0.986	0.1	3.7	96.2
3299	2.970	1.027	0.003	0.002	0.002	0.054	0.965	0.2	5.3	94.5
3301	2.960	1.037	0.002	0.001	0.013	0.039	0.959	0.1	3.9	96.0
3302	2.947	1.040	0.004	0.001	0.005	0.025	0.979	0.1	2.5	97.4
3303	2.958	1.042	0.003	0.002	0.008	0.076	0.928	0.2	7.6	92.2
3304	2.967	1.034	0.002	0.002	0.009	0.077	0.916	0.2	7.7	92.1
3305	2.950	1.040	0.003	0.001	0.018	0.031	0.978	0.1	3.1	96.8
3306	2.933	1.061	0.002	0.006	0.031	0.187	0.800	0.6	18.8	80.6
AVG	2.957	1.039	0.003	0.002	0.010	0.065	0.942	0.2	6.5	93.3
STD	0.011	0.009	0.001	0.001	0.009	0.046	0.055	0.2	4.7	4.8

APPENDIX 4: PLAGIOCLASE ANALYSES (8 Oxygen) CA85-111 TGgr

SMPL#	SiO2	Al2O3	FeO	CaO	BaO	Na2O	K2O	TOTAL
3203	60.94	23.94	0.10	4.62	0.00	8.63	0.17	98.40
3207	59.91	24.37	0.14	4.91	0.00	8.03	0.19	97.55
3211	59.94	24.33	0.09	5.23	0.00	8.25	0.11	97.95
3212	60.49	23.85	0.07	4.94	0.05	8.74	0.09	98.23
3213	57.31	26.64	0.12	4.71	0.00	8.02	0.08	96.88
3215	57.62	25.95	0.15	5.46	0.02	7.40	0.21	96.81
3216	61.62	23.19	0.11	4.24	0.00	9.04	0.19	98.39
3217	60.48	23.94	0.08	3.98	0.02	9.00	0.12	97.62
3220	59.83	23.25	0.10	4.83	0.07	7.96	0.18	96.22
3221	59.53	23.13	0.08	4.46	0.00	8.47	0.23	95.90
3223	60.58	23.22	0.11	4.36	0.11	8.98	0.21	97.57
3228	58.37	25.02	0.21	4.78	0.03	7.26	0.32	95.99
3229	58.62	25.42	0.19	4.74	0.04	7.18	0.30	96.49
3230	59.16	25.65	0.22	4.78	0.02	7.15	0.31	97.29
3231	58.89	25.46	0.22	4.82	0.03	6.73	0.29	96.44
3232	59.62	25.56	0.21	4.80	0.06	6.54	0.29	97.08
3233	59.82	24.88	0.09	4.24	0.00	8.70	0.17	97.90
3234	60.53	24.02	0.13	5.05	0.01	8.47	0.19	98.40
3235	60.65	23.87	0.08	5.04	0.00	8.60	0.13	98.37
3236	62.70	22.06	0.04	2.90	0.13	8.28	2.58	98.69
3237	59.96	24.09	0.11	4.20	0.01	7.50	0.19	96.06
3238	58.90	24.93	0.10	5.48	0.04	7.72	0.21	97.38
3240	60.77	23.08	0.10	4.28	0.00	7.36	0.19	95.78
3241	60.30	24.03	0.06	4.53	0.02	7.97	0.14	97.05
AVG	59.86	24.33	0.12	4.64	0.03	8.00	0.30	97.27
STD	1.18	1.07	0.05	0.52	0.03	0.71	0.48	0.89

APPENDIX 4: PLAGIOCLASE ANALYSES (8 Oxygen) CA85-111 TGgr (continued)

SMPL#	Si	Al	Fe	Ca	Ba	Na	K	AN	AB	OR
3203	2.740	1.269	0.004	0.223	0.000	0.752	0.010	22.6	76.3	1.0
3207	2.717	1.303	0.005	0.239	0.000	0.706	0.011	25.0	73.8	1.2
3211	2.711	1.297	0.003	0.253	0.000	0.723	0.006	25.8	73.6	0.6
3212	2.730	1.268	0.003	0.239	0.001	0.765	0.005	23.7	75.8	0.5
3213	2.622	1.436	0.005	0.231	0.000	0.711	0.005	24.4	75.1	0.5
3215	2.635	1.398	0.006	0.267	0.000	0.656	0.012	28.6	70.2	1.3
3216	2.770	1.229	0.004	0.204	0.000	0.788	0.011	20.3	78.6	1.1
3217	2.738	1.277	0.003	0.193	0.000	0.790	0.007	19.5	79.8	0.7
3220	2.750	1.259	0.004	0.238	0.001	0.709	0.011	24.8	74.0	1.1
3221	2.747	1.258	0.003	0.221	0.000	0.758	0.014	22.3	76.3	1.4
3223	2.754	1.244	0.004	0.212	0.002	0.792	0.012	20.9	78.0	1.2
3228	2.682	1.355	0.008	0.235	0.001	0.647	0.019	26.1	71.8	2.1
3229	2.677	1.368	0.007	0.232	0.001	0.636	0.017	26.2	71.9	1.9
3230	2.678	1.368	0.008	0.232	0.000	0.627	0.018	26.5	71.5	2.1
3231	2.684	1.367	0.008	0.235	0.001	0.595	0.017	27.7	70.2	2.0
3232	2.694	1.361	0.008	0.232	0.001	0.573	0.017	28.2	69.7	2.1
3233	2.704	1.325	0.003	0.205	0.000	0.762	0.010	21.0	78.0	1.0
3234	2.727	1.275	0.005	0.244	0.000	0.740	0.011	24.5	74.4	1.1
3235	2.732	1.267	0.003	0.243	0.000	0.751	0.007	24.3	75.0	0.7
3236	2.828	1.173	0.002	0.140	0.002	0.724	0.148	13.8	71.5	14.6
3237	2.737	1.296	0.004	0.205	0.000	0.664	0.011	23.3	75.5	1.3
3238	2.682	1.338	0.004	0.267	0.001	0.682	0.012	27.8	71.0	1.2
3240	2.787	1.247	0.004	0.210	0.000	0.654	0.011	24.0	74.7	1.3
3241	2.740	1.287	0.002	0.221	0.000	0.702	0.008	23.7	75.4	0.9
AVG	2.719	1.303	0.005	0.226	0.000	0.704	0.017	24.0	74.3	1.8
STD	0.045	0.060	0.002	0.026	0.001	0.061	0.028	3.2	2.8	2.7

APPENDIX 4: POTASSIUM FELDSPAR ANALYSES (8 Oxygen) CA85-111 TGgr

SMPL#	SiO2	Al2O3	FeO	CaO	BaO	Na2O	K2O	TOTAL
3196	63.05	18.74	0.08	0.09	0.55	1.04	15.19	98.74
3198	62.74	18.62	0.08	0.07	0.53	0.99	15.29	98.32
3199	63.10	18.66	0.17	0.05	0.45	1.43	14.68	98.54
3200	63.18	18.50	0.05	0.03	0.36	0.94	15.57	98.63
3201	62.54	18.43	0.03	0.01	0.26	0.67	15.95	97.89
3209	63.23	18.81	0.04	0.02	0.22	0.76	16.01	99.09
3210	63.59	19.02	0.04	0.19	0.39	2.52	12.74	98.49
3218	62.69	18.66	0.07	0.03	0.19	0.63	15.92	98.19
3225	62.25	18.29	0.04	0.03	0.15	0.92	15.38	97.06
3226	62.10	18.17	0.05	0.05	0.13	0.67	15.79	96.96
AVG	62.85	18.59	0.07	0.06	0.32	1.06	15.25	98.19
STD	0.44	0.24	0.04	0.05	0.15	0.54	0.93	0.66

SMPL#	Si	Al	Fe	Ca	Ba	Na	K	AN	AB	OR
3196	2.958	1.036	0.003	0.005	0.010	0.095	0.909	0.5	9.4	90.1
3198	2.958	1.035	0.003	0.004	0.010	0.091	0.920	0.4	9.0	90.6
3199	2.961	1.032	0.007	0.003	0.008	0.130	0.879	0.3	12.8	86.9
3200	2.969	1.025	0.002	0.002	0.007	0.086	0.933	0.2	8.4	91.4
3201	2.966	1.030	0.001	0.001	0.005	0.062	0.965	0.1	6.0	93.9
3209	2.961	1.038	0.002	0.001	0.004	0.069	0.956	0.1	6.7	93.2
3210	2.962	1.044	0.002	0.009	0.007	0.228	0.757	0.9	22.9	76.2
3218	2.959	1.038	0.003	0.002	0.004	0.058	0.958	0.2	5.7	94.1
3225	2.969	1.028	0.002	0.002	0.003	0.085	0.935	0.2	8.3	91.5
3226	2.969	1.024	0.002	0.003	0.002	0.062	0.963	0.3	6.0	93.7
AVG	2.963	1.033	0.003	0.003	0.006	0.097	0.918	0.3	9.5	90.1
STD	0.004	0.006	0.002	0.002	0.003	0.048	0.059	0.2	4.9	5.1

APPENDIX 4: PLAGIOCLASE ANALYSES (8 Oxygen) BW84 20A THREE ENCLAVE TRAVERSES

SMPL#	SiO2	Al2O3	FeO	CaO	Na2O	K2O	TOTAL
4179	63.52	22.31	0.08	3.97	8.11	0.21	98.20
4180	64.22	22.17	0.06	3.67	8.91	0.21	99.24
4181	61.88	23.38	0.36	3.72	8.26	0.18	97.78
4182	63.03	22.56	0.05	4.19	8.46	0.15	98.44
4184	62.96	22.70	0.22	4.06	8.18	0.22	98.34
4185	62.28	22.76	0.10	4.43	7.35	0.27	97.19
4187	62.71	22.09	0.07	3.83	8.01	0.19	96.90
4188	63.37	22.24	0.09	3.74	7.41	0.27	97.12
4190	62.79	22.66	0.05	4.38	7.23	0.20	97.31
4191	61.86	22.96	0.07	4.28	7.56	0.21	96.94
4192	61.66	23.38	0.03	5.12	7.40	0.19	97.78
4193	63.09	22.68	0.03	4.05	8.31	0.20	98.36
4195	62.73	22.69	0.07	4.40	8.06	0.19	98.14
4196	62.12	23.55	0.02	4.88	7.88	0.21	98.66
4198	62.96	22.29	0.05	3.82	8.86	0.13	98.11
4200	61.02	23.33	0.09	4.56	7.82	0.16	96.98
4201	61.12	23.74	0.01	5.23	8.39	0.13	98.62
4202	61.75	23.37	0.00	5.04	8.59	0.13	98.88
4204	62.90	22.57	0.18	3.99	9.34	0.13	99.11
4205	63.42	22.29	0.08	3.76	9.51	0.18	99.24
4206	62.99	22.78	0.04	4.05	9.41	0.15	99.42
4207	61.93	23.55	0.05	5.08	9.18	0.10	99.89
4209	63.41	22.85	0.03	4.12	8.93	0.19	99.53
4210	61.08	24.10	0.04	5.71	7.83	0.17	98.93
4211	62.03	23.12	0.09	4.39	8.62	0.16	98.41
4212	63.04	22.43	0.05	4.10	8.61	0.16	98.39
4213	61.82	23.28	0.05	4.80	8.34	0.19	98.48
4215	61.79	23.61	0.04	5.07	7.73	0.15	98.39
4217	61.60	23.38	0.13	4.99	7.17	0.16	97.43
4218	60.47	24.18	0.08	4.83	6.66	0.13	96.35
4219	62.40	22.57	0.04	4.28	8.06	0.17	97.52
4221	60.60	24.11	0.09	5.71	7.28	0.12	97.91
4223	62.41	23.29	0.09	4.18	7.96	0.19	98.12

APPENDIX 4: PLAGIOCLASE ANALYSES (8 Oxygen) BW84-20A THREE ENCLAVE TRAVERSES

SMPL#	SiO2	Al2O3	FeO	CaO	Na2O	K2O	TOTAL
4225	61.77	23.44	0.04	4.31	8.14	0.26	97.96
4226	61.70	23.76	0.10	4.96	8.35	0.15	99.02
4265	61.82	21.98	0.03	4.03	7.95	0.22	96.03
4266	61.54	23.49	0.03	5.26	7.20	0.21	97.73
4268	62.81	22.70	0.04	4.37	8.46	0.19	98.57
4269	63.15	22.26	0.05	3.91	8.36	0.22	97.95
4270	62.63	22.83	0.06	4.50	8.27	0.27	98.56
4271	63.94	22.33	0.10	3.98	9.20	0.20	99.75
4272	61.52	23.96	0.02	5.01	8.15	0.18	98.84
4273	62.98	22.93	0.07	4.32	8.58	0.18	99.06
5012	64.28	22.47	0.06	3.95	8.68	0.20	99.64
5013	63.99	22.73	0.06	4.01	8.48	0.17	99.44
5014	63.32	22.87	0.10	4.22	8.45	0.24	99.20
5015	63.78	23.28	0.11	4.27	9.07	0.15	100.66
5019	63.40	23.13	0.12	3.78	8.09	0.10	98.62
5021	62.62	23.60	0.02	4.98	7.81	0.13	99.16
5022	60.94	22.99	0.06	4.99	7.39	0.20	96.57
5023	62.16	22.74	0.10	3.93	8.20	0.15	97.28
5024	63.96	23.06	0.07	4.23	7.99	0.15	99.46
5025	63.15	22.81	0.11	4.35	7.58	0.17	98.17
5027	62.79	24.17	0.08	5.32	7.39	0.14	99.89
5028	63.65	23.96	0.04	5.42	7.86	0.12	101.05
5030	63.59	24.03	0.07	5.14	7.99	0.10	100.92
5031	64.60	23.07	0.12	4.53	8.79	0.18	101.29
5032	64.26	23.15	0.18	3.91	8.86	0.09	100.45
5033	64.11	23.08	0.02	4.42	8.47	0.15	100.25
5034	64.14	23.33	0.01	4.60	7.97	0.08	100.13
5035	62.15	24.90	0.05	4.90	8.08	0.12	100.20
5036	63.54	23.59	0.02	5.17	8.17	0.17	100.66
5039	60.92	22.72	0.20	3.45	7.80	0.19	95.28
5040	64.59	23.12	0.03	4.04	8.05	0.60	100.43

APPENDIX 4: PLAGIOCLASE ANALYSES (8 Oxygen) BW84-20A THREE ENCLAVE TRAVERSES

SMPL#	SiO2	Al2O3	FeO	CaO	Na2O	K2O	TOTAL
5042	64.81	23.05	0.09	4.01	8.89	0.13	100.98
5043	64.03	23.92	0.04	5.14	8.30	0.16	101.59
5044	62.29	25.10	0.04	5.33	8.27	0.15	101.18
5045	64.06	23.46	0.05	4.56	8.43	0.13	100.69
AVG	62.73	23.13	0.07	4.47	8.19	0.18	98.78
STD	1.06	0.64	0.06	0.54	0.58	0.07	1.36

SMPL#	Si	Al	Fe	Ca	Na	K	AN	AB	OR
4179	2.841	1.176	0.003	0.190	0.703	0.012	21.0	77.7	1.3
4180	2.848	1.158	0.002	0.174	0.766	0.012	18.3	80.5	1.3
4181	2.784	1.240	0.014	0.179	0.721	0.010	19.7	79.2	1.1
4182	2.820	1.189	0.002	0.201	0.734	0.009	21.3	77.8	1.0
4184	2.818	1.197	0.008	0.195	0.710	0.013	21.2	77.3	1.4
4185	2.818	1.214	0.004	0.215	0.645	0.016	24.5	73.6	1.8
4187	2.842	1.180	0.003	0.186	0.704	0.011	20.6	78.1	1.2
4188	2.855	1.181	0.003	0.181	0.647	0.016	21.4	76.7	1.9
4190	2.830	1.203	0.002	0.211	0.632	0.011	24.7	74.0	1.3
4191	2.803	1.226	0.003	0.208	0.664	0.012	23.5	75.1	1.4
4192	2.779	1.242	0.001	0.247	0.647	0.011	27.3	71.5	1.2
4193	2.822	1.195	0.001	0.194	0.721	0.011	21.0	77.9	1.2
4195	2.814	1.200	0.003	0.211	0.701	0.011	22.9	75.9	1.2
4196	2.778	1.241	0.001	0.234	0.683	0.012	25.2	73.5	1.3
4198	2.826	1.179	0.002	0.184	0.771	0.007	19.1	80.1	0.7
4200	2.771	1.248	0.003	0.222	0.688	0.009	24.2	74.9	1.0
4201	2.746	1.257	0.000	0.252	0.731	0.007	25.5	73.8	0.7
4202	2.764	1.233	0.000	0.242	0.746	0.007	24.3	75.0	0.7
4204	2.805	1.186	0.007	0.191	0.808	0.007	19.0	80.3	0.7
4205	2.824	1.169	0.003	0.179	0.821	0.010	17.7	81.3	1.0
4206	2.802	1.194	0.001	0.193	0.812	0.009	19.0	80.1	0.9
4207	2.752	1.233	0.002	0.242	0.791	0.006	23.3	76.1	0.6
4209	2.813	1.194	0.001	0.196	0.768	0.011	20.1	78.8	1.1

APPENDIX 4: PLAGIOCLASE ANALYSES (8 Oxygen) BW84-20A THREE ENCLAVE TRAVERSES

SMPL#	Si	Al	Fe	Ca	Na	K	AN	AB	OR
4210	2.736	1.272	0.001	0.274	0.680	0.010	28.4	70.5	1.0
4211	2.785	1.223	0.003	0.211	0.750	0.009	21.8	77.3	0.9
4212	2.824	1.184	0.002	0.197	0.748	0.009	20.6	78.4	0.9
4213	2.776	1.232	0.002	0.231	0.726	0.011	23.9	75.0	1.1
4215	2.772	1.248	0.002	0.244	0.672	0.009	26.4	72.6	1.0
4217	2.782	1.244	0.005	0.241	0.628	0.009	27.4	71.5	1.0
4218	2.756	1.299	0.003	0.236	0.589	0.008	28.3	70.7	1.0
4219	2.816	1.200	0.002	0.207	0.705	0.010	22.5	76.5	1.1
4221	2.736	1.283	0.003	0.276	0.637	0.007	30.0	69.2	0.8
4223	2.798	1.231	0.003	0.201	0.692	0.011	22.2	76.5	1.2
4225	2.780	1.243	0.002	0.208	0.710	0.015	22.3	76.1	1.6
4226	2.757	1.251	0.004	0.237	0.724	0.009	24.4	74.6	0.9
4265	2.831	1.186	0.001	0.198	0.706	0.013	21.6	77.0	1.4
4266	2.774	1.248	0.001	0.254	0.629	0.012	28.4	70.3	1.3
4268	2.810	1.197	0.001	0.209	0.734	0.011	21.9	76.9	1.2
4269	2.834	1.177	0.002	0.188	0.727	0.013	20.3	78.3	1.4
4270	2.804	1.204	0.002	0.216	0.718	0.015	22.8	75.7	1.6
4271	2.830	1.165	0.004	0.189	0.789	0.011	19.1	79.8	1.1
4272	2.752	1.263	0.001	0.240	0.707	0.010	25.1	73.9	1.0
4273	2.805	1.204	0.003	0.206	0.741	0.010	21.5	77.4	1.0
5012	2.839	1.170	0.002	0.187	0.743	0.011	19.9	79.0	1.2
5013	2.831	1.185	0.002	0.190	0.727	0.010	20.5	78.4	1.1
5014	2.812	1.197	0.004	0.201	0.727	0.014	21.3	77.2	1.5
5015	2.799	1.204	0.004	0.201	0.772	0.008	20.5	78.7	0.8
5019	2.822	1.213	0.004	0.180	0.698	0.006	20.4	79.0	0.7
5021	2.783	1.236	0.001	0.237	0.673	0.007	25.8	73.4	0.8
5022	2.782	1.237	0.002	0.244	0.654	0.012	26.8	71.9	1.3
5023	2.811	1.212	0.004	0.190	0.719	0.009	20.7	78.3	1.0
5024	2.825	1.200	0.003	0.200	0.684	0.008	22.4	76.7	0.9
5025	2.823	1.202	0.004	0.208	0.657	0.010	23.8	75.1	1.1
5027	2.769	1.256	0.003	0.251	0.632	0.008	28.2	70.9	0.9

APPENDIX 4: PLAGIOCLASE ANALYSES (8 Oxygen) BW84-20ATHREE ENCLAVE TRAVERSES

SMPL#	Si	Al	Fe	Ca	Na	K	AN	AB	OR
5028	2.778	1.232	0.001	0.253	0.665	0.007	27.4	71.9	0.8
5030	2.779	1.238	0.003	0.241	0.677	0.006	26.1	73.3	0.6
5031	2.815	1.185	0.004	0.211	0.743	0.010	21.9	77.1	1.0
5032	2.817	1.196	0.007	0.184	0.753	0.005	19.5	79.9	0.5
5033	2.817	1.195	0.001	0.208	0.721	0.008	22.2	76.9	0.9
5034	2.814	1.206	0.000	0.216	0.678	0.004	24.1	75.5	0.4
5035	2.738	1.293	0.002	0.231	0.690	0.007	24.9	74.4	0.8
5036	2.787	1.219	0.001	0.243	0.695	0.010	25.6	73.3	1.1
5039	2.804	1.232	0.008	0.170	0.696	0.011	19.4	79.4	1.3
5040	2.829	1.193	0.001	0.190	0.684	0.034	20.9	75.3	3.7
5042	2.827	1.185	0.003	0.187	0.752	0.007	19.8	79.5	0.7
5043	2.784	1.225	0.001	0.239	0.700	0.009	25.2	73.8	0.9
5044	2.726	1.294	0.001	0.250	0.702	0.008	26.0	73.1	0.8
5045	2.803	1.210	0.002	0.214	0.715	0.007	22.9	76.4	0.7
AVG	2.799	1.216	0.003	0.213	0.709	0.010	22.9	76.0	1.1
STD	0.030	0.033	0.002	0.026	0.047	0.004	2.9	2.9	0.4

APPENDIX 4: PLAGIOCLASE ANALYSES (8 Oxygen) BW84-20A THREE GRANITE TRAVERSES

SMPL#	SiO2	Al2O3	FeO	CaO	Na2O	K2O	TOTAL
4227	62.78	22.62	0.11	4.07	8.63	0.23	98.44
4228	62.64	23.05	0.05	3.97	8.18	0.35	98.24
4230	62.31	23.13	0.04	4.56	8.36	0.34	98.74
4231	62.31	23.17	0.01	4.61	8.40	0.29	98.79
4232	61.39	23.78	0.05	4.50	8.81	0.24	98.77
4233	61.94	23.61	0.04	4.40	8.60	0.33	98.92
4234	62.25	23.13	0.02	4.57	9.24	0.29	99.50
4237	62.35	23.19	0.05	4.78	8.64	0.25	99.26
4240	60.72	24.32	0.03	4.57	7.49	0.41	97.54
4241	63.00	23.20	0.05	3.96	8.82	0.12	99.15
4242	62.16	23.27	0.04	4.83	8.14	0.30	98.74
4243	62.34	23.23	0.02	4.56	7.53	0.34	98.02
4244	59.92	24.97	0.03	4.57	7.49	0.28	97.27
4245	63.29	22.83	0.02	4.18	8.12	0.21	98.65
4248	63.31	22.99	0.01	4.14	9.01	0.18	99.64
4250	61.98	23.32	0.04	3.88	8.05	0.34	97.61
4251	61.62	23.85	0.03	3.72	8.77	0.27	98.26
4252	63.33	22.80	0.06	3.65	9.03	0.17	99.04
4256	62.62	23.33	0.03	4.27	9.17	0.16	99.58
4260	60.63	25.23	0.03	4.85	7.87	0.20	98.81
4261	61.37	23.41	0.03	4.76	8.13	0.24	97.94
4263	62.57	22.85	0.08	3.47	8.70	0.12	97.79
4274	62.16	22.14	1.98	3.87	9.10	0.26	99.51
4275	63.57	22.73	0.03	4.01	9.34	0.22	99.90
4276	61.54	23.76	0.06	4.77	8.25	0.29	98.67
4277	64.34	22.70	0.04	3.93	9.10	0.17	100.28
4281	60.95	23.59	1.15	4.62	8.01	0.30	98.62
4282	61.66	23.41	0.05	5.15	7.82	0.27	98.36
4283	62.15	23.49	0.10	5.14	7.14	0.17	98.19
4285	62.99	22.57	0.08	4.02	7.72	0.24	97.62
4286	62.31	23.23	0.02	4.88	7.26	0.27	97.97
4288	63.69	22.23	0.02	3.51	9.14	0.18	98.77

APPENDIX 4: PLAGIOCLASE ANALYSES (8 Oxygen) BW84-20A THREE GRANITE TRAVERSES

SMPL#	SiO2	Al2O3	FeO	CaO	Na2O	K2O	TOTAL
4289	62.52	23.05	0.03	4.43	8.08	0.29	98.40
4290	62.85	23.22	0.00	4.78	7.68	0.32	98.85
4291	63.14	22.92	0.08	4.14	8.77	0.19	99.24
4292	63.58	22.62	0.05	3.81	9.01	0.19	99.26
4293	63.65	22.29	0.02	3.91	8.48	0.18	98.53
4294	61.46	23.32	0.14	5.11	7.77	0.19	97.99
4295	62.84	22.94	0.02	4.48	8.39	0.15	98.82
4296	63.67	22.45	0.04	3.89	9.12	0.20	99.37
4297	63.08	23.13	0.00	4.44	8.46	0.15	99.26
4298	62.93	23.43	0.03	4.70	8.23	0.34	99.66
5052	64.47	24.02	0.22	4.33	8.82	0.14	102.00
5056	61.86	24.47	0.01	6.31	7.89	0.18	100.72
5057	62.64	23.96	0.02	5.35	8.11	0.26	100.34
5058	63.64	23.55	0.03	4.99	8.26	0.26	100.73
5060	64.86	23.25	0.03	4.51	8.89	0.30	101.84
5065	64.86	22.73	0.00	4.16	8.97	0.20	100.92
5067	64.71	22.70	0.00	4.19	8.39	0.20	100.19
5069	64.12	23.84	0.01	5.22	7.72	0.23	101.14
5070	64.65	23.32	0.02	4.55	8.39	0.17	101.10
5075	64.94	23.00	0.01	4.44	8.56	0.11	101.06
5076	63.03	22.54	0.21	3.69	8.19	0.18	97.84
5079	64.13	24.11	0.04	4.89	8.00	0.26	101.43
AVG	62.77	23.26	0.10	4.43	8.37	0.24	99.17
STD	1.14	0.62	0.30	0.52	0.54	0.07	1.15

APPENDIX 4: PLAGIOCLASE ANALYSES (8 Oxygen) BW84·20A THREE GRANITE TRAVERSES

SMPL#	Si	Al	Fe	Ca	Na	K	AN	AB	OR
4227	2.813	1.194	0.004	0.195	0.750	0.013	20.4	78.3	1.4
4228	2.806	1.217	0.002	0.191	0.710	0.020	20.7	77.1	2.2
4230	2.789	1.220	0.001	0.219	0.725	0.019	22.7	75.3	2.0
4231	2.786	1.221	0.000	0.221	0.728	0.017	22.9	75.4	1.8
4232	2.753	1.256	0.002	0.216	0.766	0.014	21.7	76.9	1.4
4233	2.769	1.244	0.001	0.211	0.746	0.019	21.6	76.4	1.9
4234	2.773	1.214	0.001	0.218	0.798	0.016	21.1	77.3	1.6
4237	2.779	1.218	0.002	0.228	0.747	0.014	23.1	75.5	1.4
4240	2.745	1.295	0.001	0.221	0.656	0.024	24.5	72.8	2.7
4241	2.801	1.215	0.002	0.189	0.760	0.007	19.8	79.5	0.7
4242	2.780	1.226	0.001	0.231	0.706	0.017	24.2	74.0	1.8
4243	2.800	1.230	0.001	0.219	0.656	0.019	24.5	73.4	2.1
4244	2.718	1.335	0.001	0.222	0.659	0.016	24.7	73.5	1.8
4245	2.821	1.199	0.001	0.200	0.702	0.012	21.9	76.8	1.3
4248	2.804	1.200	0.000	0.196	0.774	0.010	20.0	79.0	1.0
4250	2.794	1.239	0.002	0.187	0.703	0.020	20.5	77.3	2.2
4251	2.768	1.262	0.001	0.179	0.764	0.015	18.7	79.7	1.6
4252	2.816	1.195	0.002	0.174	0.778	0.010	18.1	80.9	1.0
4256	2.780	1.220	0.001	0.203	0.789	0.009	20.3	78.8	0.9
4260	2.711	1.330	0.001	0.232	0.682	0.011	25.1	73.7	1.2
4261	2.768	1.244	0.001	0.230	0.711	0.014	24.1	74.5	1.5
4263	2.813	1.210	0.003	0.167	0.758	0.007	17.9	81.3	0.8
4274	2.789	1.171	0.074	0.186	0.792	0.015	18.7	79.8	1.5
4275	2.812	1.185	0.001	0.190	0.801	0.012	18.9	79.9	1.2
4276	2.759	1.255	0.002	0.229	0.717	0.017	23.8	74.5	1.8
4277	2.827	1.175	0.001	0.185	0.775	0.010	19.1	79.9	1.0
4281	2.745	1.252	0.043	0.223	0.699	0.017	23.7	74.4	1.8
4282	2.770	1.239	0.002	0.248	0.681	0.015	26.3	72.1	1.6
4283	2.785	1.240	0.004	0.247	0.620	0.010	28.2	70.7	1.1
4285	2.831	1.195	0.003	0.194	0.673	0.014	22.0	76.4	1.6
4286	2.798	1.229	0.001	0.235	0.632	0.015	26.6	71.7	1.7
4288	2.839	1.168	0.001	0.168	0.790	0.010	17.4	81.6	1.0

APPENDIX 4: PLAGIOCLASE ANALYSES (8 Oxygen) BW84-20A THREE GRANITE TRAVERSES

SMPL#	Si	Al	Fe	Ca	Na	K	AN	AB	OR
4289	2.801	1.217	0.001	0.213	0.702	0.017	22.9	75.3	1.8
4290	2.801	1.219	0.000	0.228	0.664	0.018	25.1	73.0	2.0
4291	2.807	1.201	0.003	0.197	0.756	0.011	20.4	78.4	1.1
4292	2.822	1.183	0.002	0.181	0.775	0.011	18.7	80.1	1.1
4293	2.840	1.172	0.001	0.187	0.734	0.010	20.1	78.8	1.1
4294	2.772	1.239	0.005	0.247	0.679	0.011	26.4	72.5	1.2
4295	2.802	1.205	0.001	0.214	0.725	0.009	22.6	76.5	0.9
4296	2.825	1.174	0.001	0.185	0.785	0.011	18.9	80.0	1.1
4297	2.802	1.211	0.000	0.211	0.729	0.008	22.3	76.9	0.8
4298	2.788	1.223	0.001	0.223	0.707	0.019	23.5	74.5	2.0
5052	2.790	1.225	0.008	0.201	0.740	0.008	21.2	78.0	0.8
5056	2.726	1.270	0.000	0.298	0.674	0.010	30.3	68.6	1.0
5057	2.762	1.245	0.001	0.253	0.693	0.015	26.3	72.1	1.6
5058	2.789	1.216	0.001	0.234	0.702	0.015	24.6	73.8	1.6
5060	2.813	1.188	0.001	0.210	0.747	0.017	21.6	76.7	1.7
5065	2.832	1.169	0.000	0.195	0.759	0.011	20.2	78.7	1.1
5067	2.840	1.174	0.000	0.197	0.714	0.011	21.4	77.4	1.2
5069	2.794	1.224	0.000	0.244	0.652	0.013	26.8	71.7	1.4
5070	2.816	1.197	0.001	0.212	0.708	0.009	22.8	76.2	1.0
5075	2.827	1.180	0.000	0.207	0.723	0.006	22.1	77.2	0.6
5076	2.829	1.192	0.008	0.177	0.713	0.010	19.7	79.2	1.1
5079	2.787	1.235	0.001	0.228	0.674	0.014	24.9	73.6	1.5
AVG	2.793	1.219	0.004	0.211	0.722	0.013	22.3	76.3	1.4
STD	0.030	0.036	0.011	0.025	0.045	0.004	2.8	3.0	0.4

APPENDIX 4: BIOTITE ANALYSES (24 Oxygen) CA85-5 RSgr

SMPL#	SIO2	AL2O3	TIO2	FEO	MNO	MGO	CAO	NA2O	K2O	BAO	F	CL	H2O	TOTAL
3350	34.15	17.26	4.93	19.41	0.96	9.00	0.14	0.07	9.37	0.39	0.74	0.03	3.54	99.99
3352	35.80	17.31	2.46	19.03	1.45	10.57	0.04	0.06	10.04	0.19	1.01	0.02	3.48	101.46
3353	35.66	16.91	2.93	20.11	1.29	9.44	0.05	0.09	10.11	0.13	0.75	0.05	3.56	101.08
3355	35.69	17.10	2.99	19.89	1.41	9.60	0.05	0.08	10.04	0.16	0.67	0.03	3.62	101.33
3356	35.76	16.26	3.08	20.66	1.36	9.59	0.08	0.08	9.73	0.13	0.88	0.03	3.50	101.14
3357	35.99	17.01	3.33	20.05	1.30	9.58	0.05	0.05	10.05	0.24	0.84	0.04	3.57	102.10
3358	35.48	17.46	2.79	19.13	1.23	9.35	0.10	0.12	9.64	0.13	0.81	0.03	3.52	99.79
3359	35.43	17.22	2.94	20.31	1.36	9.46	0.06	0.09	9.91	0.19	0.73	0.03	3.59	101.32
3360	35.96	16.61	2.95	20.18	1.36	9.61	0.07	0.08	9.82	0.15	0.82	0.03	3.54	101.18
3384	35.93	16.98	2.31	19.50	1.33	9.58	0.06	0.10	9.92	0.13	0.70	0.03	3.57	100.14
3388	35.50	17.04	2.60	19.56	1.50	9.48	0.07	0.10	9.75	0.24	0.73	0.03	3.55	100.15
3389	35.30	17.40	2.83	19.36	1.39	9.50	0.06	0.08	9.79	0.31	0.69	0.04	3.58	100.33
3390	35.34	17.17	2.71	19.41	1.29	9.51	0.07	0.08	9.80	0.34	0.82	0.03	3.51	100.08
3391	35.62	17.28	2.53	19.35	1.41	9.72	0.08	0.05	9.72	0.20	0.88	0.04	3.50	100.38
AVG	35.54	17.07	2.96	19.71	1.33	9.57	0.07	0.08	9.84	0.21	0.79	0.03	3.55	
STD	0.44	0.31	0.61	0.47	0.12	0.32	0.02	0.02	0.19	0.08	0.09	0.01	0.04	

APPENDIX 4: BIOTITE ANALYSES (24 Oxygen) CA85-5 RSgr

SMPL#	SI	AL4	AL6	TI	FE	MN	MG	CA	NA	K	BA	F	FE#	NA+K
3349	5.426	2.574	0.566	0.256	2.575	0.166	2.214	0.025	0.027	1.845	0.010	0.406	0.538	1.872
3350	5.252	2.748	0.380	0.570	2.497	0.125	2.063	0.023	0.021	1.838	0.024	0.360	0.548	1.859
3352	5.417	2.583	0.504	0.280	2.408	0.186	2.384	0.006	0.018	1.938	0.008	0.483	0.503	1.956
3353	5.439	2.561	0.478	0.336	2.565	0.167	2.146	0.008	0.027	1.967	0.011	0.362	0.544	1.994
3355	5.421	2.579	0.482	0.342	2.527	0.181	2.173	0.008	0.024	1.945	0.008	0.322	0.538	1.969
3356	5.462	2.538	0.388	0.354	2.639	0.176	2.183	0.013	0.024	1.895	0.010	0.425	0.547	1.919
3357	5.429	2.571	0.453	0.378	2.530	0.166	2.154	0.008	0.015	1.934	0.008	0.401	0.540	1.949
3358	5.442	2.558	0.597	0.322	2.454	0.160	2.138	0.016	0.036	1.886	0.014	0.393	0.534	1.922
3359	5.393	2.607	0.482	0.337	2.585	0.175	2.146	0.010	0.027	1.924	0.008	0.351	0.546	1.951
3360	5.473	2.527	0.452	0.338	2.569	0.175	2.180	0.011	0.024	1.906	0.011	0.395	0.541	1.930
3384	5.505	2.495	0.570	0.266	2.498	0.173	2.188	0.010	0.030	1.938	0.009	0.339	0.533	1.968
3388	5.451	2.549	0.534	0.300	2.512	0.195	2.170	0.012	0.030	1.909	0.014	0.354	0.537	1.939
3389	5.406	2.594	0.545	0.326	2.479	0.180	2.168	0.010	0.024	1.912	0.019	0.334	0.533	1.936
3390	5.431	2.569	0.540	0.313	2.494	0.168	2.178	0.012	0.024	1.921	0.020	0.399	0.534	1.945
3391	5.446	2.554	0.559	0.291	2.474	0.183	2.215	0.013	0.015	1.895	0.012	0.426	0.528	1.910
AVG	5.426	2.574	0.502	0.334	2.520	0.172	2.180	0.012	0.024	1.910	0.012	0.383	0.536	1.935
STD	0.054	0.054	0.063	0.071	0.057	0.015	0.065	0.005	0.005	0.034	0.005	0.042	0.011	0.034

APPENDIX 4: BIOTITE ANALYSES (24 Oxygen) BW84-20 RSgr

SMPL#	SIO2	AL2O3	TIO2	FEO	MNO	MGO	CAO	NA2O	K2O	BAO	F	CL	H2O	TOTAL
1189	36.59	16.83	3.08	19.62	1.38	9.56	0.02	0.11	9.26	0.16	0.96	0.00	3.51	101.08
1190	36.75	16.69	3.20	19.26	1.34	9.18	0.01	0.10	9.42	0.01	0.79	0.00	3.57	100.32
1191	36.22	16.94	2.98	19.18	1.46	9.93	0.02	0.08	9.37	0.03	1.09	0.00	3.44	100.74
1199	36.00	16.39	3.00	19.40	1.19	10.06	0.03	0.09	9.15	0.14	0.73	0.00	3.57	99.75
AVG	36.39	16.71	3.07	19.37	1.34	9.68	0.02	0.10	9.30	0.09	0.89	0.00	3.52	
STD	0.30	0.21	0.09	0.17	0.10	0.34	0.01	0.01	0.10	0.07	0.14	0.00	0.05	

SMPL#	SI	AL4	AL6	TI	FE	MN	MG	CA	NA	K	BA	F	FE#	NA+K
1189	5.533	2.467	0.531	0.350	2.481	0.177	2.155	0.003	0.032	1.786	0.009	0.459	0.535	1.818
1190	5.581	2.419	0.568	0.365	2.446	0.172	2.078	0.002	0.029	1.825	0.001	0.379	0.541	1.854
1191	5.493	2.507	0.521	0.340	2.433	0.188	2.245	0.003	0.024	1.813	0.002	0.523	0.520	1.837
1199	5.510	2.490	0.467	0.345	2.483	0.154	2.295	0.005	0.027	1.786	0.008	0.353	0.520	1.813
AVG	5.529	2.471	0.522	0.350	2.461	0.173	2.193	0.003	0.028	1.803	0.005	0.429	0.529	1.831
STD	0.033	0.033	0.036	0.009	0.022	0.012	0.083	0.001	0.003	0.017	0.004	0.067	0.009	0.016

APPENDIX 4: BIOTITE ANALYSES (24 Oxygen) BW84-18 RSgd

SMPL#	SIO2	AL2O3		TIO2	FEO	MNO	MGO	CAO	NA2O	K2O	BAO	F	CL	H2O	TOTAL
1077	36.45	15.09		3.26	17.53	1.19	11.44	0.01	0.08	9.28	0.11	0.39	nd	3.72	98.55
1078	36.14	15.32		3.11	17.51	1.16	11.60	0.01	0.05	9.31	0.07	0.49	nd	3.66	98.43
1135	37.44	15.20		3.22	18.51	1.41	11.16	0.02	0.09	9.34	0.08	0.31	nd	3.83	100.61
1136	37.41	15.03		3.12	18.69	1.43	11.35	0.03	0.12	9.29	0.08	0.46	nd	3.76	100.77
1143	37.40	16.17		2.80	18.10	1.26	11.12	0.07	0.24	8.51	0.08	0.54	nd	3.73	100.02
1150	36.96	15.69		3.23	17.49	1.14	11.46	0.06	0.43	8.56	0.08	0.56	nd	3.69	99.35
1151	37.17	16.67		2.25	17.11	1.09	11.94	0.06	0.57	8.45	0.15	0.35	nd	3.82	99.63
AVG	37.00	15.60		3.00	17.85	1.24	11.44	0.04	0.23	8.96	0.09	0.44		3.74	
STD	0.48	0.57		0.34	0.55	0.12	0.26	0.02	0.19	0.40	0.03	0.09		0.06	

SMPL#	SI	AL4	AL6	TI	FE	MN	MG	CA	NA	K	BA	F	FE#	NA+K
1077	5.598	2.402	0.328	0.376	2.251	0.155	2.619	0.002	0.024	1.818	0.007	0.189	0.462	1.842
1078	5.561	2.439	0.339	0.360	2.253	0.151	2.660	0.002	0.015	1.827	0.004	0.238	0.459	1.842
1135	5.642	2.358	0.341	0.365	2.333	0.180	2.507	0.003	0.026	1.795	0.005	0.148	0.482	1.821
1136	5.639	2.361	0.308	0.354	2.356	0.183	2.550	0.005	0.035	1.786	0.005	0.219	0.480	1.821
1143	5.630	2.370	0.498	0.317	2.278	0.161	2.495	0.011	0.070	1.634	0.005	0.257	0.477	1.704
1150	5.601	2.399	0.403	0.368	2.217	0.146	2.589	0.010	0.126	1.655	0.005	0.268	0.461	1.781
1151	5.590	2.410	0.544	0.254	2.152	0.139	2.676	0.010	0.166	1.621	0.009	0.166	0.446	1.787
AVG	5.609	2.391	0.394	0.342	2.263	0.159	2.585	0.006	0.066	1.734	0.006	0.212	0.467	1.800
STD	0.027	0.027	0.085	0.040	0.064	0.015	0.066	0.004	0.054	0.085	0.002	0.042	0.012	0.045

APPENDIX 4: BIOTITE ANALYSES (24 Oxygen) BW84-19 RSgd

SMPL#	SIO2	AL2O3	TIO2	FEO	MNO	MGO	CAO	NA2O	K2O	BAO	F	CL	H2O	TOTAL
1260	36.98	16.36	2.29	16.82	0.91	12.80	0.08	0.42	7.99	0.08	0.31	0.00	3.83	98.87
1278	36.48	16.03	2.76	18.19	0.84	11.75	0.10	0.46	8.27	0.11	0.32	0.00	3.79	99.10
1279	36.68	15.77	2.78	17.93	0.83	12.36	0.08	0.34	8.13	0.17	0.33	0.00	3.80	99.20
1280	35.99	15.76	2.50	18.90	0.85	11.69	0.09	0.55	7.78	0.20	0.25	0.00	3.78	98.34
AVG	36.53	15.98	2.58	17.96	0.86	12.15	0.09	0.44	8.04	0.14	0.30	0.00	3.80	
STD	0.36	0.24	0.20	0.75	0.03	0.46	0.01	0.08	0.18	0.05	0.03	0.00	0.02	

SMPL#	SI	AL4	AL6	TI	FE	MN	MG	CA	NA	K	BA	F	FE#	NA+K
1260	5.577	2.423	0.485	0.260	2.121	0.116	2.877	0.013	0.123	1.537	0.005	0.148	0.424	1.660
1278	5.544	2.456	0.415	0.315	2.312	0.108	2.662	0.016	0.136	1.603	0.007	0.154	0.465	1.739
1279	5.557	2.443	0.373	0.317	2.272	0.107	2.791	0.013	0.100	1.571	0.010	0.158	0.449	1.671
1280	5.529	2.471	0.382	0.289	2.428	0.111	2.677	0.015	0.164	1.524	0.012	0.121	0.476	1.688
AVG	5.552	2.448	0.414	0.295	2.283	0.111	2.752	0.014	0.131	1.559	0.009	0.145	0.453	1.690
STD	0.018	0.018	0.044	0.023	0.110	0.003	0.088	0.001	0.023	0.031	0.003	0.014	0.019	0.030

APPENDIX 4: BIOTITE ANALYSES (24 Oxygen) BW84-23 RSgd

SMPL#	SIO2	AL2O3	TIO2	FEO	MNO	MGO	CAO	NA2O	K2O	BAO	F	CL	H2O	TOTAL
1358	37.66	16.60	3.41	17.20	0.60	11.27	0.01	0.07	9.38	0.08	0.19	nd	3.93	100.40
1359	37.60	15.95	3.48	17.85	0.63	11.32	0.01	0.09	9.34	0.17	0.27	nd	3.88	100.59
1360	37.83	15.95	3.59	17.71	0.71	11.47	0.01	0.09	9.44	0.00	0.25	nd	3.91	100.96
1363	37.56	15.44	3.56	18.55	0.62	11.68	0.02	0.08	9.28	0.14	0.17	nd	3.93	101.03
1364	37.63	14.68	3.89	18.75	0.58	11.73	0.00	0.12	9.24	0.08	0.21	nd	3.90	100.81
4206	37.06	15.35	3.44	17.63	0.63	12.20	0.00	0.10	9.58	0.20	0.18	0.03	3.89	100.29
4207	37.63	15.96	3.72	17.27	0.67	11.55	0.00	0.05	9.82	0.22	0.19	0.04	3.92	101.04
4208	37.28	15.13	3.13	17.66	0.57	12.44	0.00	0.10	9.60	0.16	0.21	0.05	3.87	100.20
4209	37.45	15.57	3.15	17.48	0.52	12.30	0.00	0.10	9.59	0.18	0.25	0.05	3.87	100.51
4210	37.32	15.29	2.78	17.85	0.63	12.34	0.00	0.08	9.57	0.19	0.23	0.04	3.86	100.18
4211	36.72	15.22	2.94	17.79	0.60	12.12	0.00	0.11	9.61	0.17	0.21	0.03	3.83	99.35
4212	37.70	15.23	3.17	18.06	0.65	12.05	0.00	0.12	9.68	0.14	0.22	0.04	3.89	100.95
4213	37.13	15.38	3.51	17.75	0.63	11.68	0.00	0.09	9.43	0.20	0.19	0.05	3.87	99.91
4224	37.01	16.18	3.40	16.12	0.60	11.52	0.00	0.09	9.66	0.21	0.23	0.07	3.83	98.92
4225	37.88	15.58	3.55	17.42	0.64	12.18	0.00	0.05	9.70	0.19	0.19	0.03	3.94	101.35
4226	37.66	15.65	3.17	16.87	0.56	11.98	0.00	0.09	9.46	0.21	0.20	0.03	3.88	99.76
4227	37.40	15.96	3.32	17.48	0.67	11.79	0.00	0.07	9.60	0.20	0.16	0.04	3.92	100.61
4228	37.98	16.25	3.07	16.73	0.57	12.01	0.00	0.09	9.86	0.20	0.18	0.04	3.94	100.92
4236	36.09	14.50	1.73	15.01	0.54	13.24	0.20	0.10	6.31	0.14	0.12	0.07	3.67	91.72
4238	37.21	15.39	2.83	16.79	0.72	11.76	0.00	0.04	9.68	0.18	0.20	0.02	3.83	98.65
4239	36.99	15.56	2.48	16.74	0.66	12.17	0.07	0.04	8.81	0.15	0.18	0.04	3.82	97.71
4257	36.55	14.84	3.53	17.88	0.77	11.80	0.13	0.06	9.40	0.17	0.23	0.04	3.81	99.21
AVG	37.33	15.53	3.22	17.39	0.63	11.94	0.02	0.08	9.37	0.16	0.20	0.03	3.87	
STD	0.45	0.50	0.46	0.79	0.06	0.43	0.05	0.02	0.70	0.05	0.03	0.02	0.06	

APPENDIX 4: BIOTITE ANALYSES (24 Oxygen) BW84-23 RSgd

SMPL#	SI	AL4	AL6	TI	FE	MN	MG	CA	NA	K	BA	F	FE#	NA+K
1358	5.614	2.386	0.530	0.382	2.144	0.076	2.504	0.002	0.020	1.784	0.005	0.090	0.461	1.804
1359	5.624	2.376	0.435	0.391	2.233	0.080	2.524	0.002	0.026	1.782	0.010	0.128	0.469	1.808
1360	5.628	2.372	0.424	0.402	2.203	0.089	2.543	0.002	0.026	1.791	0.000	0.118	0.464	1.817
1363	5.610	2.390	0.328	0.400	2.317	0.078	2.600	0.003	0.023	1.768	0.008	0.080	0.471	1.791
1364	5.641	2.359	0.234	0.439	2.350	0.074	2.621	0.000	0.035	1.767	0.005	0.100	0.473	1.802
4206	5.577	2.423	0.300	0.389	2.219	0.080	2.737	0.000	0.029	1.839	0.012	0.086	0.448	1.868
4207	5.606	2.394	0.407	0.417	2.151	0.085	2.565	0.000	0.014	1.866	0.013	0.090	0.456	1.880
4208	5.614	2.386	0.298	0.354	2.224	0.073	2.792	0.000	0.029	1.844	0.009	0.100	0.443	1.873
4209	5.611	2.389	0.360	0.355	2.190	0.066	2.747	0.000	0.029	1.833	0.011	0.118	0.444	1.862
4210	5.625	2.375	0.340	0.315	2.250	0.080	2.772	0.000	0.023	1.840	0.011	0.110	0.448	1.863
4211	5.590	2.410	0.320	0.337	2.265	0.077	2.750	0.000	0.032	1.866	0.010	0.101	0.452	1.898
4212	5.640	2.360	0.325	0.357	2.260	0.082	2.687	0.000	0.035	1.847	0.008	0.104	0.457	1.882
4213	5.606	2.394	0.343	0.399	2.241	0.081	2.629	0.000	0.026	1.816	0.012	0.091	0.460	1.842
4224	5.606	2.394	0.495	0.387	2.042	0.077	2.601	0.000	0.026	1.866	0.012	0.110	0.440	1.892
4225	5.623	2.377	0.348	0.396	2.162	0.080	2.695	0.000	0.014	1.836	0.011	0.089	0.445	1.850
4226	5.660	2.340	0.432	0.358	2.120	0.071	2.684	0.000	0.026	1.813	0.012	0.095	0.441	1.839
4227	5.596	2.404	0.410	0.374	2.187	0.085	2.629	0.000	0.020	1.832	0.012	0.076	0.454	1.852
4228	5.641	2.359	0.484	0.343	2.078	0.072	2.659	0.000	0.026	1.868	0.012	0.085	0.439	1.894
4236	5.773	2.227	0.506	0.208	2.008	0.073	3.157	0.034	0.031	1.287	0.009	0.061	0.389	1.318
4238	5.671	2.329	0.436	0.324	2.140	0.093	2.672	0.000	0.012	1.882	0.011	0.096	0.445	1.894
4239	5.663	2.337	0.470	0.286	2.143	0.086	2.777	0.011	0.012	1.720	0.009	0.087	0.436	1.732
4257	5.580	2.420	0.249	0.405	2.283	0.100	2.685	0.021	0.018	1.830	0.010	0.111	0.460	1.848
AVG	5.627	2.373	0.385	0.364	2.191	0.080	2.683	0.003	0.024	1.799	0.010	0.097	0.450	1.823
STD	0.040	0.040	0.082	0.049	0.083	0.008	0.131	0.008	0.007	0.118	0.003	0.015	0.017	0.117

APPENDIX 4: BIOTITE ANALYSES (24 Oxygen) BW84-25 RSgd

SMPL#	SIO2	AL2O3	TIO2	FEO	MNO	MGO	CAO	NA2O	K2O	BAO	F	CL	H2O	TOTAL
1298	37.71	15.97	3.78	18.82	0.50	11.11	0.02	0.20	9.19	0.04	0.08	nd	4.00	101.42
1299	37.90	15.74	3.63	18.96	0.44	11.00	0.03	0.23	9.11	0.07	0.12	nd	3.97	101.20
4268	36.73	14.98	3.22	18.75	0.44	12.20	0.03	0.11	9.32	0.24	0.13	0.10	3.87	100.12
4269	36.26	15.04	2.74	19.19	0.51	12.43	0.15	0.11	8.44	0.18	0.22	0.11	3.79	99.17
4270	37.15	15.43	2.92	18.48	0.52	11.93	0.00	0.12	9.57	0.31	0.15	0.10	3.88	100.56
4271	36.41	15.38	3.39	18.51	0.57	11.83	0.02	0.09	9.36	0.27	0.16	0.09	3.85	99.93
4272	36.68	15.47	3.16	18.67	0.60	11.62	0.02	0.06	9.56	0.31	0.14	0.08	3.87	100.24
4273	36.83	15.91	2.32	18.28	0.57	12.05	0.02	0.11	9.60	0.26	0.85	0.07	3.54	100.41
4291	36.87	15.27	2.63	18.57	0.60	12.03	0.11	0.08	9.00	0.20	0.12	0.08	3.86	99.42
4292	37.12	15.20	2.92	18.94	0.52	12.00	0.00	0.12	9.63	0.19	0.20	0.10	3.86	100.80
4293	36.25	15.44	2.64	18.70	0.47	11.82	0.13	0.13	8.43	0.25	0.13	0.10	3.81	98.30
5143	37.07	15.62	2.59	18.34	0.65	11.62	0.10	0.13	8.96	0.27	0.20	0.11	3.82	99.48
5144	36.72	14.90	3.06	19.04	0.55	10.99	0.17	0.06	9.22	0.25	0.19	0.10	3.79	99.04
5145	37.12	15.04	3.31	19.00	0.52	11.41	0.00	0.10	9.51	0.31	0.16	0.09	3.86	100.43
5147	37.32	15.19	3.02	18.86	0.51	11.57	0.00	0.13	9.48	0.19	0.59	0.08	3.67	100.61
5150	37.77	15.39	1.26	17.41	0.51	12.43	0.08	0.05	8.98	0.24	0.19	0.12	3.80	98.23
5171	36.70	14.93	2.73	18.82	0.49	11.68	0.15	0.23	9.06	0.90	0.19	0.12	3.80	99.80
5172	37.57	14.97	3.00	19.14	0.55	11.43	0.01	0.14	9.26	0.35	0.25	0.11	3.83	100.61
5173	36.87	15.20	3.18	19.36	0.55	11.23	0.04	0.15	9.38	0.28	0.29	0.10	3.79	100.42
5174	37.26	15.25	3.00	19.27	0.54	11.07	0.04	0.21	9.21	0.32	0.23	0.12	3.82	100.34
5175	37.44	15.27	2.93	19.44	0.44	11.19	0.05	0.14	9.42	0.34	0.19	0.10	3.86	100.81
5176	36.55	15.24	2.91	19.17	0.56	10.91	0.20	0.19	9.16	0.26	0.22	0.13	3.77	99.27
5180	37.74	15.76	2.44	18.29	0.58	11.68	0.00	0.09	9.47	0.23	0.20	0.08	3.87	100.43
5182	36.93	14.80	2.81	18.53	0.51	11.55	0.11	0.13	8.44	0.27	0.19	0.09	3.79	98.15
5183	37.35	15.24	3.04	18.75	0.44	11.56	0.01	0.10	9.20	0.27	0.22	0.10	3.84	100.12
AVG	37.05	15.31	2.91	18.77	0.53	11.61	0.06	0.13	9.20	0.27	0.22	0.09	3.82	
STD	0.46	0.31	0.47	0.42	0.05	0.43	0.06	0.05	0.34	0.15	0.16	0.03	0.09	

APPENDIX 4: BIOTITE ANALYSES (24 Oxygen) BW84-25 RSgd

SMPL#	SI	AL4	AL6	TI	FE	MN	MG	CA	NA	K	BA	F	FE#	NA+K
1298	5.600	2.400	0.394	0.422	2.337	0.063	2.459	0.003	0.058	1.741	0.002	0.038	0.487	1.799
1299	5.641	2.359	0.402	0.406	2.360	0.055	2.440	0.005	0.066	1.730	0.004	0.056	0.492	1.796
4268	5.565	2.435	0.239	0.367	2.376	0.056	2.755	0.005	0.032	1.801	0.014	0.062	0.463	1.833
4269	5.541	2.459	0.250	0.315	2.453	0.066	2.831	0.025	0.033	1.645	0.011	0.106	0.464	1.678
4270	5.598	2.402	0.338	0.331	2.329	0.066	2.680	0.000	0.035	1.839	0.018	0.071	0.465	1.874
4271	5.528	2.472	0.280	0.387	2.350	0.073	2.677	0.003	0.026	1.813	0.016	0.077	0.467	1.839
4272	5.557	2.443	0.319	0.360	2.366	0.077	2.624	0.003	0.018	1.847	0.018	0.067	0.474	1.865
4273	5.574	2.426	0.411	0.264	2.314	0.073	2.718	0.003	0.032	1.853	0.015	0.407	0.460	1.885
4291	5.607	2.393	0.344	0.301	2.362	0.077	2.727	0.018	0.024	1.746	0.012	0.058	0.464	1.770
4292	5.593	2.407	0.292	0.331	2.387	0.066	2.695	0.000	0.035	1.851	0.011	0.095	0.470	1.886
4293	5.571	2.429	0.367	0.305	2.403	0.061	2.708	0.021	0.039	1.652	0.015	0.063	0.470	1.691
5143	5.628	2.372	0.423	0.296	2.329	0.084	2.630	0.016	0.038	1.735	0.016	0.096	0.470	1.773
5144	5.635	2.365	0.329	0.353	2.443	0.071	2.514	0.028	0.018	1.805	0.015	0.092	0.493	1.823
5145	5.616	2.384	0.297	0.377	2.404	0.067	2.573	0.000	0.029	1.835	0.018	0.077	0.483	1.864
5147	5.634	2.366	0.336	0.343	2.381	0.065	2.603	0.000	0.038	1.825	0.011	0.282	0.478	1.863
5150	5.766	2.234	0.535	0.145	2.223	0.066	2.829	0.013	0.015	1.749	0.014	0.092	0.440	1.764
5171	5.608	2.392	0.296	0.314	2.405	0.063	2.660	0.025	0.068	1.766	0.054	0.092	0.475	1.834
5172	5.668	2.332	0.329	0.340	2.415	0.070	2.570	0.002	0.041	1.782	0.021	0.119	0.484	1.823
5173	5.591	2.409	0.307	0.363	2.455	0.071	2.538	0.006	0.044	1.814	0.017	0.139	0.492	1.858
5174	5.641	2.359	0.362	0.342	2.440	0.069	2.498	0.006	0.062	1.778	0.019	0.110	0.494	1.840
5175	5.645	2.355	0.357	0.332	2.451	0.056	2.515	0.008	0.041	1.811	0.020	0.091	0.494	1.852
5176	5.603	2.397	0.355	0.335	2.457	0.073	2.493	0.033	0.056	1.791	0.016	0.107	0.496	1.847
5180	5.671	2.329	0.461	0.276	2.298	0.074	2.616	0.000	0.026	1.815	0.014	0.095	0.468	1.841
5182	5.676	2.324	0.356	0.325	2.382	0.066	2.646	0.018	0.039	1.655	0.016	0.092	0.474	1.694
5183	5.644	2.356	0.358	0.345	2.369	0.056	2.604	0.002	0.029	1.773	0.016	0.105	0.476	1.802
AVG	5.616	2.384	0.349	0.331	2.380	0.067	2.624	0.010	0.038	1.778	0.016	0.108	0.476	1.816
STD	0.049	0.049	0.064	0.052	0.056	0.007	0.105	0.010	0.014	0.059	0.009	0.075	0.013	0.058

APPENDIX 4: BIOTITE ANALYSES (24 Oxygen) CA84-147 CFqmd

SMPL#	SIO2	AL2O3	TIO2	FEO	MNO	MGO	CAO	NA2O	K2O	BAO	F	CL	H2O	TOTAL
2172	35.80	15.32	2.12	17.52	0.45	11.52	0.09	0.60	7.96	0.09	0.44	nd	3.60	95.51
2173	35.17	18.08	2.07	16.84	0.48	11.54	0.11	0.64	7.46	0.18	0.29	nd	3.75	96.61
2177	36.21	16.30	4.09	17.93	0.39	10.77	0.20	0.34	8.69	0.14	0.23	nd	3.84	99.13
2178	36.11	16.08	3.96	18.05	0.48	10.78	0.04	0.30	8.74	0.30	0.24	nd	3.81	98.89
2180	36.62	16.14	3.82	17.97	0.49	10.83	0.03	0.33	8.81	0.33	0.21	nd	3.86	99.44
2183	35.17	16.44	3.15	17.73	0.48	11.08	0.10	0.49	8.01	0.13	0.31	nd	3.71	96.80
2185	35.76	15.58	3.29	18.14	0.46	11.03	0.08	0.45	8.35	0.06	0.37	nd	3.69	97.26
2192	36.74	15.46	2.41	18.95	0.42	11.62	0.07	0.47	7.97	0.08	0.24	nd	3.80	98.23
2193	37.24	15.43	2.91	19.14	0.48	11.31	0.05	0.30	8.88	0.04	0.32	nd	3.81	99.91
2194	36.74	15.76	2.88	18.44	0.40	11.17	0.05	0.38	8.63	0.09	0.24	nd	3.81	98.59
2195	36.80	15.33	2.89	18.66	0.47	11.44	0.05	0.30	8.75	0.24	0.11	nd	3.87	98.91
5099	37.68	15.02	2.80	19.13	0.51	12.05	0.00	0.11	9.29	0.54	0.29	0.11	3.83	101.36
5100	37.50	14.68	2.90	19.28	0.42	11.89	0.00	0.09	9.36	0.40	0.33	0.10	3.79	100.74
5101	37.36	14.91	2.87	19.28	0.45	11.97	0.00	0.11	9.43	0.28	0.24	0.09	3.84	100.83
5109	37.69	15.32	2.27	18.76	0.46	12.29	0.00	0.05	9.35	0.24	0.76	0.10	3.60	100.89
5114	36.99	15.76	1.87	19.04	0.51	12.60	0.00	0.12	8.70	0.24	0.28	0.10	3.81	100.02
5115	37.68	15.66	1.62	18.83	0.51	12.77	0.06	0.07	8.62	0.15	0.27	0.08	3.84	100.16
5117	38.20	15.31	2.40	19.05	0.44	12.65	0.00	0.10	9.49	0.20	0.28	0.09	3.89	102.10
5118	37.72	15.33	3.27	19.26	0.41	12.02	0.00	0.05	9.48	0.19	0.35	0.10	3.84	102.02
5119	37.91	14.97	3.35	19.36	0.45	11.95	0.00	0.29	9.62	0.22	0.26	0.08	3.89	102.35
5120	37.67	15.00	3.11	19.37	0.49	11.98	0.00	0.08	9.58	0.19	0.43	0.09	3.79	101.78
5121	37.87	15.18	2.84	18.79	0.45	12.02	0.00	0.14	9.62	0.20	0.26	0.08	3.87	101.32
5122	38.49	16.20	2.78	18.81	0.41	11.61	0.00	0.06	9.76	0.25	0.26	0.10	3.92	102.65
5127	37.69	16.33	2.94	17.22	0.40	11.74	0.00	0.03	9.63	0.14	1.39.	0.07	3.34	100.92
5128	37.84	15.91	2.82	18.00	0.48	11.67	0.00	0.05	9.47	0.18	0.26	0.10	3.86	100.64
5129	38.15	15.11	3.02	19.43	0.50	11.70	0.00	0.08	9.66	0.26	0.37	0.09	3.83	102.20
5130	38.34	15.30	3.28	18.99	0.49	11.58	0.00	0.06	9.54	0.24	0.31	0.08	3.88	102.09
5131	38.15	15.29	3.39	18.96	0.51	11.71	0.00	0.06	9.66	0.35	0.24	0.09	3.91	102.32
5132	38.23	15.50	3.36	19.06	0.49	11.71	0.00	0.10	9.68	0.29	0.66	0.08	3.73	102.89
5133	38.53	15.39	3.31	19.22	0.53	11.75	0.00	0.08	9.74	0.34	0.32	0.09	3.90	103.20
5135	38.48	16.38	2.05	18.45	0.46	12.22	0.00	0.07	9.78	0.17	0.34	0.08	3.89	102.37
5141	37.84	16.77	2.62	17.24	0.37	11.94	0.07	0.11	9.15	0.17	0.47	0.06	3.79	100.60

APPENDIX 4: BIOTITE ANALYSES (24 Oxygen) CA84-147 CFqmd (continued)

SMPL#	SIO2	AL2O3	TIO2	FEO	MNO	MGO	CAO	NA2O	K2O	BAO	F	CL	H2O	TOTAL
5142	37.87	15.95	2.08	18.03	0.49	12.48	0.01	0.10	9.45	0.19	0.46	0.08	3.78	100.97
AVG	37.29	15.67	2.83	18.62	0.46	11.78	0.04	0.20	9.02	0.21	0.36	0.06	3.80	
STD	0.96	0.65	0.61	0.73	0.04	0.55	0.07	0.17	0.75	0.10	0.22	0.04	0.11	

SMPL#	SI	AL4	AL6	TI	FE	MN	MG	CA	NA	K	BA	F	FE#	NA+K
2172	5.631	2.369	0.471	0.251	2.305	0.060	2.701	0.015	0.183	1.597	0.006	0.219	0.460	1.780
2173	5.423	2.577	0.708	0.240	2.172	0.063	2.652	0.018	0.191	1.467	0.011	0.141	0.450	1.658
2177	5.497	2.503	0.413	0.467	2.276	0.050	2.437	0.033	0.100	1.683	0.008	0.110	0.483	1.783
2178	5.510	2.490	0.401	0.454	2.303	0.062	2.452	0.007	0.089	1.701	0.018	0.116	0.484	1.790
2180	5.548	2.452	0.429	0.435	2.277	0.063	2.446	0.005	0.097	1.702	0.020	0.101	0.482	1.799
2183	5.463	2.537	0.472	0.368	2.303	0.063	2.565	0.017	0.148	1.587	0.008	0.152	0.473	1.735
2185	5.545	2.455	0.391	0.384	2.352	0.060	2.549	0.013	0.135	1.651	0.004	0.181	0.480	1.786
2192	5.628	2.372	0.419	0.278	2.428	0.054	2.653	0.011	0.140	1.557	0.005	0.116	0.478	1.697
2193	5.634	2.366	0.384	0.331	2.421	0.062	2.550	0.008	0.088	1.713	0.002	0.153	0.487	1.801
2194	5.611	2.389	0.448	0.331	2.355	0.052	2.543	0.008	0.113	1.681	0.005	0.116	0.481	1.794
2195	5.618	2.382	0.376	0.332	2.382	0.061	2.603	0.008	0.089	1.704	0.014	0.053	0.478	1.793
5099	5.649	2.351	0.302	0.316	2.398	0.065	2.693	0.000	0.032	1.776	0.032	0.137	0.471	1.808
5100	5.661	2.339	0.272	0.329	2.434	0.054	2.675	0.000	0.026	1.802	0.024	0.158	0.476	1.828
5101	5.631	2.369	0.279	0.325	2.430	0.057	2.689	0.000	0.032	1.813	0.017	0.114	0.475	1.845
5109	5.665	2.335	0.378	0.257	2.358	0.059	2.753	0.000	0.015	1.792	0.010	0.361	0.461	1.807
5114	5.591	2.409	0.398	0.213	2.407	0.065	2.839	0.000	0.035	1.677	0.014	0.134	0.459	1.712
5115	5.663	2.337	0.436	0.183	2.367	0.065	2.861	0.010	0.020	1.652	0.009	0.128	0.453	1.672
5117	5.661	2.339	0.334	0.267	2.361	0.055	2.794	0.000	0.029	1.794	0.012	0.131	0.458	1.823
5118	5.607	2.393	0.292	0.366	2.394	0.052	2.663	0.000	0.014	1.797	0.011	0.165	0.473	1.811
5119	5.628	2.372	0.246	0.374	2.403	0.057	2.644	0.000	0.083	1.821	0.013	0.122	0.476	1.904
5120	5.627	2.373	0.267	0.349	2.420	0.062	2.667	0.000	0.023	1.825	0.011	0.203	0.476	1.848
5121	5.659	2.341	0.332	0.319	2.348	0.057	2.677	0.000	0.041	1.834	0.012	0.123	0.467	1.875
5122	5.662	2.338	0.471	0.308	2.314	0.051	2.546	0.000	0.017	1.831	0.014	0.121	0.476	1.848
5127	5.634	2.366	0.511	0.331	2.153	0.051	2.616	0.000	0.009	1.836	0.008	0.657	0.451	1.845
5128	5.660	2.340	0.465	0.317	2.252	0.061	2.602	0.000	0.015	1.807	0.011	0.123	0.464	1.822

APPENDIX 4: BIOTITE ANALYSES (24 Oxygen) CA84-147 CFqmd (continued)

SMPL#	SI	AL4	AL6	TI	FE	MN	MG	CA	NA	K	BA	F	FE#	NA+K
5129	5.671	2.329	0.318	0.338	2.415	0.063	2.592	0.000	0.023	1.832	0.015	0.174	0.482	1.855
5130	5.681	2.319	0.353	0.366	2.353	0.062	2.558	0.000	0.017	1.803	0.014	0.145	0.479	1.820
5131	5.651	2.349	0.319	0.378	2.349	0.064	2.585	0.000	0.017	1.825	0.020	0.112	0.476	1.842
5132	5.640	2.360	0.335	0.373	2.352	0.061	2.575	0.000	0.029	1.822	0.017	0.308	0.477	1.851
5133	5.663	2.337	0.328	0.366	2.362	0.066	2.574	0.000	0.023	1.826	0.020	0.149	0.479	1.849
5135	5.666	2.334	0.508	0.227	2.272	0.057	2.682	0.000	0.020	1.837	0.010	0.158	0.459	1.857
5141	5.629	2.371	0.569	0.293	2.145	0.047	2.648	0.011	0.032	1.736	0.010	0.221	0.448	1.768
5142	5.653	2.347	0.458	0.233	2.251	0.062	2.777	0.002	0.029	1.799	0.011	0.217	0.448	1.828
AVG	5.617	2.383	0.396	0.324	2.337	0.059	2.632	0.005	0.059	1.745	0.013	0.170	0.470	1.804
STD	0.062	0.062	0.096	0.066	0.077	0.005	0.101	0.008	0.052	0.094	0.006	0.104	0.012	0.056

APPENDIX 4: BIOTITE ANALYSES (24 Oxygen) CA84-45 m encl

SMPL#	SIO2	AL2O3	TIO2	FEO	MNO	MGO	CAO	NA2O	K2O	BAO	F	CL	H2O	TOTAL
5196	37.59	15.31	3.11	17.19	0.64	11.66	0.03	0.26	8.93	0.23	0.32	0.05	3.79	99.11
5204	35.59	18.49	2.98	16.46	0.60	11.52	0.08	0.28	8.44	0.19	0.36	0.06	3.78	98.83
5210	36.93	14.26	2.82	17.63	0.62	11.78	0.12	0.20	8.25	0.31	0.31	0.05	3.70	96.98
5211	37.44	14.54	3.06	17.90	0.64	11.88	0.12	0.27	8.42	0.32	0.32	0.06	3.76	98.73
5220	38.49	15.01	3.13	17.96	0.79	12.33	0.01	0.13	9.48	0.18	0.37	0.05	3.86	101.79
5221	38.70	15.05	2.94	17.65	0.65	12.45	0.04	0.19	9.28	0.21	0.28	0.04	3.90	101.38
5222	38.30	15.64	3.80	16.70	0.59	11.24	0.13	0.22	8.68	0.17	0.36	0.04	3.83	99.70
5223	37.09	14.63	3.37	16.34	0.61	11.57	0.16	0.27	7.96	0.21	0.30	0.06	3.71	96.28
5225	37.81	13.65	3.20	17.17	0.57	12.45	0.25	0.16	7.63	0.18	0.36	0.05	3.72	97.20
5237	38.14	15.70	2.79	17.26	0.63	12.18	0.13	0.28	8.04	0.15	0.44	0.06	3.78	99.58
5238	38.04	15.48	3.11	17.26	0.62	12.39	0.14	0.29	8.43	0.16	0.30	0.06	3.86	100.14
5239	37.76	15.11	3.17	17.38	0.64	12.51	0.05	0.36	8.85	0.16	0.29	0.04	3.85	100.17
5240	38.23	15.14	2.98	17.41	0.62	12.60	0.01	0.46	9.14	0.19	0.35	0.04	3.85	101.02
5241	38.31	15.25	2.98	17.68	0.57	12.16	0.02	0.23	8.94	0.20	0.29	0.04	3.87	100.54
5243	37.66	15.14	3.16	17.63	0.62	12.47	0.15	0.29	8.80	0.18	0.38	0.04	3.81	100.33
AVG	37.74	15.23	3.11	17.31	0.63	12.08	0.10	0.26	8.62	0.20	0.34	0.05	3.80	
STD	0.75	1.02	0.23	0.47	0.05	0.42	0.07	0.08	0.50	0.05	0.04	0.01	0.06	

APPENDIX 4: BIOTITE ANALYSES (24 Oxygen) CA84-45 m encl

SMPL#	SI	AL4	AL6	TI	FE	MN	MG	CA	NA	K	BA	F	FE#	NA+K
5196	5.692	2.308	0.424	0.354	2.177	0.082	2.632	0.005	0.076	1.725	0.014	0.153	0.453	1.801
5204	5.377	2.623	0.669	0.339	2.080	0.077	2.594	0.013	0.082	1.627	0.011	0.172	0.445	1.709
5210	5.728	2.272	0.335	0.329	2.287	0.081	2.724	0.020	0.060	1.632	0.019	0.152	0.456	1.692
5211	5.709	2.291	0.321	0.351	2.283	0.083	2.700	0.020	0.080	1.638	0.019	0.154	0.458	1.718
5220	5.700	2.300	0.320	0.349	2.224	0.099	2.722	0.002	0.037	1.791	0.010	0.173	0.450	1.828
5221	5.733	2.267	0.360	0.328	2.187	0.082	2.749	0.006	0.055	1.753	0.012	0.131	0.443	1.808
5222	5.726	2.274	0.482	0.427	2.088	0.075	2.505	0.021	0.064	1.655	0.010	0.170	0.455	1.719
5223	5.742	2.258	0.410	0.392	2.115	0.080	2.670	0.027	0.081	1.572	0.013	0.147	0.442	1.653
5225	5.804	2.196	0.273	0.369	2.204	0.074	2.849	0.041	0.048	1.494	0.011	0.175	0.436	1.542
5237	5.710	2.290	0.479	0.314	2.161	0.080	2.718	0.021	0.081	1.535	0.009	0.208	0.443	1.616
5238	5.677	2.323	0.399	0.349	2.154	0.078	2.756	0.022	0.084	1.605	0.009	0.142	0.439	1.689
5239	5.658	2.342	0.326	0.357	2.178	0.081	2.794	0.008	0.105	1.691	0.009	0.137	0.438	1.796
5240	5.686	2.314	0.339	0.333	2.165	0.078	2.793	0.002	0.133	1.734	0.011	0.165	0.437	1.867
5241	5.715	2.285	0.395	0.334	2.206	0.072	2.704	0.003	0.067	1.701	0.012	0.137	0.449	1.768
5243	5.643	2.357	0.316	0.356	2.209	0.079	2.785	0.024	0.084	1.682	0.011	0.180	0.442	1.766
AVG	5.687	2.313	0.390	0.352	2.181	0.080	2.713	0.016	0.076	1.656	0.012	0.160	0.446	1.731
STD	0.091	0.091	0.095	0.027	0.058	0.006	0.084	0.011	0.022	0.079	0.003	0.020	0.007	0.084

APPENDIX 4: BIOTITE ANALYSES (24 Oxygen) BW84-29 m encl

SMPL#	SIO2	AL2O3	TIO2	FEO	MNO	MGO	CAO	NA2O	K2O	BAO	F	CL	H2O	TOTAL
1438	37.09	15.36	2.97	17.94	0.58	12.00	0.03	0.15	9.22	0.21	0.25	0.00	3.84	99.64
1439	35.90	16.35	2.64	18.16	0.64	12.28	0.05	0.76	8.00	0.17	0.34	0.00	3.78	99.07
1445	36.95	15.67	3.28	18.29	0.56	12.10	0.03	0.15	9.01	0.18	0.21	0.00	3.89	100.32
1446	37.03	14.83	3.32	17.54	0.53	11.78	0.01	0.17	9.13	0.13	0.27	0.00	3.79	98.53
1447	37.46	15.32	2.87	18.10	0.72	12.02	0.06	0.15	9.18	0.16	0.28	0.00	3.85	100.17
1448	36.88	14.78	3.52	18.30	0.70	11.18	0.06	0.14	9.24	0.30	0.23	0.00	3.81	99.14
1450	37.08	14.94	3.54	17.92	0.58	11.58	0.03	0.10	9.13	0.25	0.21	0.00	3.84	99.20
1451	37.06	15.49	3.30	17.91	0.58	12.31	0.01	0.16	9.27	0.11	0.34	0.00	3.83	100.37
1452	36.72	15.31	3.35	17.96	0.59	11.94	0.03	0.10	9.26	0.12	0.27	0.00	3.82	99.47
1454	35.00	15.54	2.91	17.32	0.71	11.59	0.06	0.56	7.97	0.18	0.19	0.00	3.72	95.75
1484	36.01	16.23	3.87	18.41	0.61	11.45	0.07	0.45	8.78	0.08	0.24	0.00	3.85	100.05
4015	38.03	15.10	3.36	17.71	0.55	12.34	0.00	0.05	9.70	0.00	0.22	0.05	3.91	101.02
4016	37.07	15.75	3.64	17.67	0.61	12.37	0.00	0.18	9.55	0.00	0.24	0.05	3.89	101.02
4017	37.54	14.78	3.40	18.02	0.59	12.69	0.00	0.13	9.64	0.00	0.22	0.04	3.89	100.94
4018	37.71	15.08	3.59	17.93	0.58	12.48	0.00	0.10	9.60	0.00	0.27	0.03	3.89	101.26
4022	38.04	15.01	3.28	18.13	0.70	12.67	0.00	0.05	9.74	0.00	0.24	0.04	3.92	101.82
4023	38.07	15.18	3.13	18.64	0.69	12.51	0.00	0.11	9.43	0.00	0.22	0.04	3.93	101.95
4024	38.46	15.10	3.31	18.34	0.66	12.80	0.00	0.08	9.78	0.00	0.31	0.05	3.92	102.81
4025	38.31	14.99	3.24	18.12	0.62	12.85	0.00	0.08	9.68	0.00	0.29	0.05	3.91	102.14
4030	38.57	15.08	3.38	17.88	0.67	12.61	0.00	0.12	9.63	0.00	0.22	0.04	3.96	102.16
4031	38.26	15.30	3.19	17.67	0.51	13.00	0.00	0.12	9.26	0.00	0.22	0.05	3.94	101.52
4032	38.00	15.37	3.28	17.74	0.57	12.99	0.00	0.16	9.41	0.00	0.27	0.04	3.92	101.75
4033	37.80	15.05	3.34	17.82	0.56	12.79	0.00	0.10	9.58	0.00	0.27	0.03	3.89	101.23
4034	37.82	14.85	3.28	17.90	0.62	12.67	0.00	0.07	9.60	0.00	0.25	0.04	3.89	100.99
4041	38.06	15.54	3.29	17.36	0.50	13.03	0.07	0.11	8.58	0.00	0.22	0.04	3.93	100.73
4042	38.90	15.22	3.62	18.04	0.62	12.53	0.13	0.06	9.47	0.00	0.27	0.04	3.97	102.87
4053	37.60	15.36	3.15	18.18	0.52	12.57	0.00	0.51	8.97	0.00	0.35	0.05	3.84	101.10
4056	37.09	16.21	3.12	17.51	0.68	12.47	0.07	0.25	9.31	0.00	0.31	0.07	3.86	100.95
4059	36.96	16.26	2.94	17.38	0.61	12.65	0.00	0.20	9.50	0.00	0.29	0.07	3.86	100.72
4068	37.92	15.54	2.85	17.17	0.54	12.82	0.01	0.28	8.82	0.00	0.28	0.08	3.86	100.17
4069	36.95	16.87	3.35	17.04	0.56	12.16	0.01	0.38	8.95	0.00	0.33	0.09	3.84	100.53
4077	37.11	15.96	3.02	17.46	0.60	12.43	0.04	0.51	8.39	0.00	0.21	0.09	3.87	99.69

APPENDIX 4: BIOTITE ANALYSES (24 Oxygen) BW84-29 m encl (continued)

SMPL#	SIO2	AL2O3		TIO2	FEO	MNO	MGO	CAO	NA2O	K2O	BAO	F	CL	H2O	TOTAL
4078	37.27	16.15		2.72	17.51	0.66	12.42	0.03	0.63	8.41	0.00	0.28	0.10	3.84	100.02
4081	37.27	16.00		2.79	17.80	0.67	12.10	0.03	0.52	8.40	0.00	0.31	0.10	3.82	99.81
4083	37.64	15.50		3.08	17.59	0.60	12.51	0.00	0.27	9.20	0.00	0.42	0.06	3.80	100.67
4084	37.16	15.33		3.81	17.96	0.62	12.14	0.13	0.27	8.84	0.00	0.24	0.06	3.87	100.43
4085	36.19	19.13		3.44	16.77	0.56	11.73	0.09	0.40	8.34	0.00	0.25	0.13	3.91	100.94
4086	38.27	15.59		3.62	17.54	0.56	12.50	0.19	0.18	9.23	0.00	0.21	0.07	3.96	101.92
4087	38.05	15.97		3.48	17.26	0.47	12.54	0.02	0.36	8.87	0.00	0.22	0.07	3.94	101.25
4088	37.43	16.48		3.44	17.41	0.56	12.29	0.02	0.39	8.90	0.00	0.28	0.06	3.90	101.16
4089	38.13	15.63		3.50	17.75	0.63	12.62	0.01	0.30	9.21	0.00	0.26	0.08	3.93	102.05
4090	37.81	15.76		3.68	17.70	0.61	12.70	0.00	0.30	9.23	0.00	0.25	0.07	3.93	102.04
4091	36.84	17.34		3.24	16.90	0.55	12.46	0.04	0.53	8.50	0.00	0.32	0.10	3.86	100.68
4093	36.32	18.84		3.60	16.59	0.53	12.01	0.04	0.47	8.27	0.00	0.24	0.14	3.92	100.97
4094	37.61	16.73		3.56	17.40	0.51	12.26	0.00	0.35	8.87	0.00	0.25	0.08	3.93	101.55
4095	37.63	16.33		3.86	17.38	0.59	12.25	0.01	0.38	8.96	0.00	0.18	0.08	3.96	101.61
4097	38.01	16.05		3.96	17.43	0.57	11.97	0.02	0.37	8.86	0.00	0.22	0.07	3.94	101.47
AVG	37.43	15.75		3.32	17.71	0.60	12.34	0.03	0.26	9.08	0.04	0.26	0.05	3.88	
STD	0.75	0.90		0.30	0.43	0.06	0.41	0.04	0.18	0.46	0.08	0.05	0.04	0.05	

SMPL#	SI	AL4	AL6	TI	FE	MN	MG	CA	NA	K	BA	F	FE#	NA+K
1438	5.615	2.385	0.355	0.338	2.271	0.074	2.708	0.005	0.044	1.780	0.012	0.120	0.456	1.824
1439	5.459	2.541	0.389	0.302	2.310	0.082	2.783	0.008	0.224	1.552	0.010	0.164	0.454	1.776
1445	5.555	2.445	0.331	0.371	2.299	0.071	2.711	0.005	0.044	1.728	0.011	0.100	0.459	1.772
1446	5.658	2.342	0.328	0.381	2.241	0.069	2.683	0.002	0.050	1.779	0.008	0.130	0.455	1.829
1447	5.640	2.360	0.358	0.325	2.279	0.092	2.697	0.010	0.044	1.763	0.009	0.133	0.458	1.807
1448	5.637	2.363	0.298	0.405	2.339	0.091	2.547	0.010	0.041	1.801	0.018	0.111	0.479	1.842
1450	5.638	2.362	0.315	0.405	2.279	0.075	2.625	0.005	0.029	1.771	0.015	0.101	0.465	1.800
1451	5.569	2.431	0.311	0.373	2.251	0.074	2.757	0.002	0.047	1.777	0.006	0.162	0.449	1.824
1452	5.574	2.426	0.312	0.382	2.280	0.076	2.701	0.005	0.029	1.793	0.007	0.130	0.458	1.822

APPENDIX 4: BIOTITE ANALYSES (24 Oxygen) BW84-29 m encl (continued)

SMPL#	SI	AL4	AL6	TI	FE	MN	MG	CA	NA	K	BA	F	FE#	NA+K
1454	5.501	2.499	0.380	0.344	2.277	0.095	2.715	0.010	0.171	1.598	0.011	0.094	0.456	1.769
4015	5.664	2.336	0.314	0.376	2.206	0.069	2.739	0.000	0.014	1.843	nd	0.104	0.446	1.857
4016	5.531	2.469	0.300	0.408	2.205	0.077	2.751	0.000	0.052	1.817	nd	0.113	0.445	1.869
4017	5.615	2.385	0.221	0.382	2.254	0.075	2.829	0.000	0.038	1.839	nd	0.104	0.443	1.877
4018	5.614	2.386	0.259	0.402	2.232	0.073	2.769	0.000	0.029	1.823	nd	0.127	0.446	1.852
4022	5.637	2.363	0.259	0.366	2.247	0.088	2.799	0.000	0.014	1.841	nd	0.112	0.445	1.855
4023	5.636	2.364	0.284	0.348	2.308	0.087	2.760	0.000	0.032	1.781	nd	0.103	0.455	1.813
4024	5.646	2.354	0.257	0.365	2.251	0.082	2.801	0.000	0.023	1.831	nd	0.144	0.446	1.854
4025	5.654	2.346	0.260	0.360	2.236	0.077	2.827	0.000	0.023	1.822	nd	0.135	0.442	1.845
4030	5.677	2.323	0.293	0.374	2.201	0.084	2.766	0.000	0.034	1.808	nd	0.102	0.443	1.842
4031	5.650	2.350	0.313	0.354	2.182	0.064	2.862	0.000	0.034	1.744	nd	0.103	0.433	1.778
4032	5.613	2.387	0.288	0.364	2.191	0.071	2.860	0.000	0.046	1.773	nd	0.126	0.434	1.819
4033	5.624	2.376	0.262	0.374	2.217	0.071	2.836	0.000	0.029	1.818	nd	0.127	0.439	1.847
4034	5.645	2.355	0.256	0.368	2.234	0.078	2.818	0.000	0.020	1.827	nd	0.118	0.442	1.847
4041	5.637	2.363	0.349	0.366	2.150	0.063	2.876	0.011	0.032	1.621	nd	0.103	0.428	1.653
4042	5.679	2.321	0.298	0.397	2.203	0.077	2.727	0.020	0.017	1.763	nd	0.125	0.447	1.780
4053	5.602	2.398	0.298	0.353	2.265	0.066	2.791	0.000	0.147	1.704	nd	0.165	0.448	1.851
4056	5.528	2.472	0.375	0.350	2.183	0.086	2.770	0.011	0.072	1.770	nd	0.146	0.441	1.842
4059	5.522	2.478	0.384	0.330	2.171	0.077	2.817	0.000	0.058	1.810	nd	0.137	0.435	1.868
4068	5.659	2.341	0.392	0.320	2.143	0.068	2.852	0.002	0.081	1.679	nd	0.132	0.429	1.760
4069	5.504	2.496	0.465	0.375	2.123	0.071	2.700	0.002	0.110	1.701	nd	0.155	0.440	1.811
4077	5.573	2.427	0.397	0.341	2.193	0.076	2.782	0.006	0.148	1.607	nd	0.100	0.441	1.755
4078	5.582	2.418	0.432	0.306	2.193	0.084	2.773	0.005	0.183	1.607	nd	0.133	0.442	1.790
4081	5.600	2.400	0.433	0.315	2.237	0.085	2.710	0.005	0.151	1.610	nd	0.147	0.452	1.761
4083	5.621	2.379	0.349	0.346	2.197	0.076	2.785	0.000	0.078	1.752	nd	0.198	0.441	1.830
4084	5.568	2.432	0.275	0.429	2.250	0.079	2.711	0.021	0.078	1.689	nd	0.114	0.454	1.767
4085	5.338	2.662	0.663	0.382	2.069	0.070	2.579	0.014	0.114	1.569	nd	0.117	0.445	1.683
4086	5.628	2.372	0.330	0.400	2.157	0.070	2.740	0.030	0.051	1.731	nd	0.098	0.440	1.782
4087	5.614	2.386	0.390	0.386	2.130	0.059	2.758	0.003	0.103	1.669	nd	0.103	0.436	1.772
4088	5.542	2.458	0.417	0.383	2.156	0.070	2.712	0.003	0.112	1.681	nd	0.131	0.443	1.793
4089	5.610	2.390	0.320	0.387	2.184	0.079	2.768	0.002	0.086	1.728	nd	0.121	0.441	1.814

APPENDIX 4: BIOTITE ANALYSES (24 Oxygen) BW84-29 m encl (continued)

SMPL#	SI	AL4	AL6	TI	FE	MN	MG	CA	NA	K	BA	F	FE#	NA+K
4090	5.567	2.433	0.301	0.407	2.179	0.076	2.787	0.000	0.086	1.733	nd	0.116	0.439	1.819
4091	5.464	2.536	0.494	0.361	2.096	0.069	2.754	0.006	0.152	1.608	nd	0.150	0.432	1.760
4093	5.350	2.650	0.620	0.399	2.044	0.066	2.637	0.006	0.134	1.554	nd	0.112	0.437	1.688
4094	5.538	2.462	0.441	0.394	2.143	0.064	2.691	0.000	0.100	1.666	nd	0.116	0.443	1.766
4095	5.544	2.456	0.380	0.428	2.142	0.074	2.690	0.002	0.109	1.684	nd	0.084	0.443	1.793
4097	5.602	2.398	0.390	0.439	2.148	0.071	2.630	0.003	0.106	1.666	nd	0.103	0.450	1.772
1484	5.439	2.561	0.328	0.440	2.326	0.078	2.578	0.011	0.132	1.692	0.005	0.115	0.474	1.824
AVG	5.582	2.418	0.350	0.372	2.210	0.076	2.744	0.005	0.076	1.728	0.011	0.123	0.446	1.803
STD	0.077	0.077	0.086	0.032	0.066	0.008	0.075	0.006	0.051	0.084	0.003	0.022	0.010	0.048

APPENDIX 4: BIOTITE ANALYSES (24 Oxygen) CA84-65 mdike

SMPL#	SIO2	AL2O3	TIO2	FEO	MNO	MGO	CAO	NA2O	K2O	BAO	F	CL	H2O	TOTAL
1402	37.05	15.16	3.30	19.12	0.40	11.58	0.14	0.09	8.71	0.28	0.21	0.00	3.86	99.90
1403	36.35	15.20	3.40	19.03	0.50	11.49	0.07	0.11	8.92	0.45	0.06	0.00	3.90	99.48
1404	36.88	15.07	3.54	19.15	0.43	11.65	0.09	0.12	9.00	0.45	0.19	0.00	3.88	100.45
4105	37.78	15.54	3.10	18.59	0.36	11.80	0.10	0.21	9.11	0.00	0.09	0.07	3.95	100.70
4106	38.31	15.64	3.52	18.85	0.42	11.47	0.04	0.16	9.63	0.10	0.14	0.08	3.98	102.34
4107	37.87	15.57	3.46	18.70	0.35	11.46	0.02	0.13	9.50	0.18	0.16	0.07	3.93	101.40
AVG	37.37	15.36	3.39	18.91	0.41	11.58	0.08	0.14	9.15	0.24	0.14	0.04	3.92	
STD	0.67	0.23	0.15	0.21	0.05	0.12	0.04	0.04	0.32	0.17	0.05	0.04	0.04	

SMPL#	SI	AL4	AL6	TI	FE	MN	MG	CA	NA	K	BA	F	FE#	NA+K
1403	5.546	2.454	0.279	0.390	2.428	0.065	2.613	0.011	0.033	1.736	0.027	0.029	0.482	1.769
1404	5.572	2.428	0.255	0.402	2.420	0.055	2.624	0.015	0.035	1.734	0.027	0.091	0.480	1.769
1402	5.608	2.392	0.311	0.376	2.420	0.051	2.612	0.023	0.026	1.681	0.017	0.101	0.481	1.707
4105	5.644	2.356	0.380	0.348	2.323	0.046	2.628	0.016	0.061	1.736	0.000	0.043	0.469	1.797
4106	5.650	2.350	0.368	0.390	2.325	0.052	2.521	0.006	0.046	1.812	0.006	0.065	0.480	1.858
4107	5.639	2.361	0.370	0.387	2.328	0.044	2.543	0.003	0.038	1.804	0.011	0.075	0.478	1.842
AVG	5.610	2.390	0.327	0.382	2.374	0.052	2.590	0.012	0.040	1.751	0.015	0.067	0.478	1.790
STD	0.039	0.039	0.048	0.017	0.049	0.007	0.042	0.007	0.011	0.045	0.010	0.025	0.004	0.050

APPENDIX 4: BIOTITE ANALYSES (24 Oxygen) CA84-114 cg encl

SMPL#	SIO2	AL2O3	TIO2	FEO	MNO	MGO	CAO	NA2O	K2O	BAO	F	CL	H2O	TOTAL
1464	37.48	16.52	3.64	14.89	0.20	13.80	0.05	0.28	8.91	0.12	0.19	0.00	3.96	100.04
1465	35.97	17.14	3.35	14.62	0.18	13.32	0.08	0.38	8.60	0.20	0.23	0.00	3.85	97.92
1466	37.17	15.77	3.49	15.16	0.17	13.80	0.05	0.35	8.75	0.28	0.06	0.00	3.97	99.02
AVG	36.87	16.48	3.49	14.89	0.18	13.64	0.06	0.34	8.75	0.20	0.16	0.00	3.93	
STD	0.65	0.56	0.12	0.22	0.01	0.23	0.01	0.04	0.13	0.07	0.07	0.00	0.05	

SMPL#	SI	AL4	AL6	TI	FE	MN	MG	CA	NA	K	BA	F	FE#	NA+K
1464	5.539	2.461	0.416	0.405	1.840	0.025	3.040	0.008	0.080	1.679	0.007	0.089	0.377	1.759
1466	5.566	2.434	0.348	0.393	1.898	0.022	3.080	0.008	0.102	1.671	0.016	0.028	0.381	1.773
1465	5.438	2.562	0.492	0.381	1.849	0.023	3.002	0.013	0.111	1.658	0.012	0.110	0.381	1.769
AVG	5.502	2.498	0.420	0.387	1.874	0.023	3.041	0.011	0.107	1.665	0.014	0.069	0.381	1.767
STD	0.064	0.064	0.072	0.006	0.024	0.001	0.039	0.002	0.004	0.006	0.002	0.041	0.000	0.006

APPENDIX 4: BIOTITE ANALYSES (24 Oxygen) BW84-27 cg encl

SMPL#	SIO2	AL2O3	TIO2	FEO	MNO	MGO	CAO	NA2O	K2O	BAO	F	CL	H2O	TOTAL
1377	37.38	16.00	4.09	16.87	0.20	12.48	0.09	0.28	8.67	0.19	0.25	0.00	3.91	100.41
1378	37.32	15.94	3.94	16.87	0.23	12.13	0.09	0.31	8.56	0.24	0.04	0.00	3.99	99.66
AVG	37.35	15.97	4.02	16.87	0.22	12.31	0.09	0.30	8.62	0.22	0.15	0.00	3.95	
STD	0.03	0.03	0.08	0.00	0.01	0.17	0.00	0.01	0.05	0.02	0.11	0.00	0.04	

SMPL#	SI	AL4	AL6	TI	FE	MN	MG	CA	NA	K	BA	F	FE#	NA+K
1378	5.582	2.418	0.391	0.443	2.110	0.029	2.704	0.014	0.090	1.633	0.014	0.019	0.438	1.723
1377	5.555	2.445	0.357	0.457	2.097	0.025	2.764	0.014	0.081	1.643	0.011	0.118	0.431	1.724
AVG	5.569	2.432	0.374	0.450	2.104	0.027	2.734	0.014	0.086	1.638	0.013	0.068	0.435	1.735
STD	0.013	0.013	0.017	0.007	0.007	0.002	0.030	0.000	0.004	0.005	0.001	0.050	0.003	0.362

APPENDIX 4: BIOTITE ANALYSES (24 Oxygen) CA85-102 gap

SMPL#	SIO2	AL2O3		TIO2	FEO	MNO	MGO	CAO	NA2O	K2O	BAO	F	CL	H2O	TOTAL
1020	36.05	16.08		3.18	21.87	1.12	7.97	0.01	0.13	9.24	0.15	0.40	0.00	3.69	99.89
1021	36.38	16.64		3.00	21.47	1.29	8.62	0.04	0.18	9.18	0.21	0.30	0.00	3.80	101.11
1022	36.20	16.23		2.87	21.35	1.20	8.62	0.03	0.17	9.20	0.27	0.36	0.00	3.73	100.23
AVG	36.21	16.32		3.02	21.56	1.20	8.40	0.03	0.16	9.21	0.21	0.35	0.00	3.74	
STD	0.13	0.24		0.13	0.22	0.07	0.31	0.01	0.02	0.02	0.05	0.04	0.00	0.05	

SMPL#	SI	AL4	AL6	TI	FE	MN	MG	CA	NA	K	BA	F	FE#	NA+K
1020	5.565	2.435	0.490	0.369	2.823	0.146	1.834	0.002	0.039	1.819	0.009	0.195	0.606	1.858
1021	5.530	2.470	0.510	0.343	2.729	0.166	1.953	0.007	0.053	1.780	0.013	0.144	0.583	1.833
1022	5.558	2.442	0.494	0.331	2.741	0.156	1.973	0.005	0.051	1.802	0.016	0.175	0.581	1.853
AVG	5.551	2.449	0.498	0.348	2.764	0.156	1.920	0.005	0.048	1.800	0.013	0.171	0.590	1.848
STD	0.015	0.015	0.009	0.016	0.042	0.008	0.061	0.002	0.006	0.016	0.003	0.021	0.011	0.011

APPENDIX 4: BIOTITE ANALYSES (24 Oxygen) CA84-46 gap

SMPL#	SIO2	AL2O3	TIO2	FEO	MNO	MGO	CAO	NA2O	K2O	BAO	F	CL	H2O	TOTAL
3506	34.65	16.08	2.72	19.26	1.36	10.28	0.07	0.26	7.78	0.10	0.15	0.06	3.72	96.49
3507	36.12	16.49	3.53	17.63	1.61	9.71	0.04	0.06	9.85	0.17	0.20	0.01	3.82	99.24
3508	35.78	16.33	3.09	18.31	1.64	9.91	0.04	0.04	9.76	0.30	0.17	0.01	3.81	99.19
3509	36.11	16.65	3.36	17.88	1.50	10.01	0.03	0.07	9.81	0.19	0.19	0.02	3.81	99.63
3510	36.02	16.74	2.67	17.39	1.55	10.18	0.04	0.04	10.02	0.13	0.21	0.02	3.80	98.81
3511	36.07	16.62	3.01	17.93	1.47	10.16	0.06	0.12	9.68	0.24	0.21	0.02	3.81	99.40
3512	36.19	16.15	3.21	17.75	1.43	11.03	0.04	0.04	10.03	0.11	0.27	0.01	3.81	100.07
3513	36.34	16.44	3.32	17.81	1.46	10.59	0.03	0.03	10.07	0.05	0.22	0.01	3.85	100.22
3514	36.66	16.79	2.82	17.31	1.38	10.86	0.04	0.03	10.15	0.07	0.27	0.01	3.84	100.23
3515	36.45	16.07	3.42	18.15	1.54	10.47	0.18	0.06	10.03	0.12	0.21	0.02	3.85	100.57
AVG	36.04	16.44	3.11	17.94	1.49	10.32	0.06	0.08	9.72	0.15	0.21	0.02	3.81	
STD	0.52	0.26	0.29	0.53	0.09	0.40	0.04	0.07	0.66	0.07	0.04	0.01	0.04	

SMPL#	SI	AL4	AL6	TI	FE	MN	MG	CA	NA	K	BA	F	FE#	NA+K
3506	5.456	2.544	0.439	0.322	2.536	0.181	2.413	0.012	0.079	1.562	0.006	0.075	0.512	1.641
3507	5.528	2.472	0.502	0.406	2.257	0.209	2.215	0.007	0.018	1.923	0.010	0.097	0.505	1.941
3508	5.506	2.494	0.467	0.358	2.356	0.214	2.273	0.007	0.012	1.916	0.018	0.083	0.509	1.928
3509	5.509	2.491	0.502	0.385	2.281	0.194	2.276	0.005	0.021	1.909	0.001	0.092	0.501	1.930
3510	5.533	2.467	0.563	0.308	2.234	0.202	2.331	0.007	0.012	1.963	0.008	0.102	0.489	1.975
3511	5.516	2.484	0.511	0.346	2.293	0.190	2.316	0.010	0.036	1.888	0.014	0.102	0.498	1.924
3512	5.500	2.500	0.392	0.367	2.256	0.184	2.498	0.007	0.012	1.944	0.007	0.130	0.475	1.956
3513	5.507	2.493	0.443	0.378	2.257	0.187	2.392	0.005	0.009	1.947	0.003	0.105	0.485	1.956
3514	5.537	2.463	0.525	0.320	2.186	0.177	2.445	0.006	0.009	1.955	0.004	0.129	0.472	1.964
3515	5.521	2.479	0.390	0.390	2.299	0.198	2.364	0.029	0.018	1.938	0.007	0.101	0.493	1.956
AVG	5.511	2.489	0.473	0.358	2.296	0.194	2.352	0.010	0.023	1.895	0.008	0.102	0.494	1.917
STD	0.022	0.022	0.054	0.031	0.091	0.012	0.082	0.007	0.020	0.113	0.005	0.017	0.013	0.093

APPENDIX 4: BIOTITE ANALYSES (24 Oxygen) CA85-111 TGgr

SMPL#	SIO2	AL2O3	TIO2	FEO	MNO	MGO	CAO	NA2O	K2O	BAO	F	CL	H2O	TOTAL
3129	36.48	16.55	3.52	17.22	0.87	10.61	0.17	0.08	8.47	0.10	0.35	0.03	3.75	98.20
3130	36.01	16.53	3.38	17.79	0.96	11.10	0.07	0.13	9.04	0.05	0.36	0.05	3.75	99.22
3132	36.96	16.03	3.55	18.01	0.94	11.23	0.09	0.09	9.53	0.13	0.33	0.03	3.83	100.75
3133	36.84	16.07	3.75	17.81	0.89	11.11	0.06	0.12	9.65	0.17	0.29	0.03	3.84	100.63
3135	36.76	16.04	3.57	18.02	0.90	11.01	0.12	0.10	9.52	0.18	0.31	0.03	3.82	100.38
3137	36.44	16.96	1.82	17.63	0.84	11.95	0.07	0.11	9.48	0.06	0.33	0.02	3.79	99.50
3138	35.74	16.58	1.93	16.96	0.80	11.20	0.08	0.11	9.24	0.09	0.35	0.03	3.68	96.79
3139	36.56	16.93	1.65	17.16	0.81	11.71	0.08	0.08	9.67	0.07	0.41	0.06	3.72	98.91
3140	35.34	15.10	3.50	18.54	0.79	10.94	0.06	0.05	8.68	0.38	0.26	0.02	3.71	97.37
3141	36.98	15.49	3.48	17.89	0.89	11.70	0.03	0.06	9.76	0.22	0.35	0.03	3.81	100.69
3142	37.44	15.78	3.61	18.24	0.87	11.55	0.05	0.08	9.89	0.22	0.36	0.03	3.85	101.97
3143	37.22	16.09	3.66	17.50	0.76	11.68	0.06	0.04	9.70	0.09	0.38	0.02	3.83	101.03
3145	35.20	16.76	3.74	17.44	0.94	11.26	0.17	0.09	8.75	0.12	0.35	0.10	3.72	98.64
3146	35.91	15.66	3.68	17.77	1.03	11.50	0.09	0.09	9.25	0.13	0.33	0.09	3.74	99.27
3147	35.56	16.35	3.61	17.50	0.96	11.50	0.09	0.08	9.15	0.07	0.32	0.08	3.75	99.02
AVG	36.36	16.19	3.23	17.70	0.88	11.34	0.09	0.09	9.32	0.14	0.34	0.04	3.77	
STD	0.68	0.52	0.72	0.41	0.07	0.35	0.04	0.02	0.41	0.08	0.03	0.03	0.05	

APPENDIX 4: BIOTITE ANALYSES (24 Oxygen) CA85-111 TGgr

SMPL#	SI	AL4	AL6	TI	FE	MN	MG	CA	NA	K	BA	F	FE#	NA+K
3129	5.567	2.433	0.544	0.404	2.198	0.112	2.413	0.028	0.024	1.649	0.006	0.169	0.477	1.673
3130	5.481	2.519	0.446	0.387	2.265	0.124	2.518	0.011	0.038	1.755	0.003	0.173	0.474	1.793
3132	5.550	2.450	0.386	0.401	2.262	0.120	2.513	0.014	0.026	1.825	0.008	0.157	0.474	1.851
3133	5.538	2.462	0.385	0.424	2.239	0.113	2.490	0.010	0.035	1.850	0.010	0.138	0.473	1.885
3135	5.544	2.456	0.395	0.405	2.273	0.115	2.475	0.019	0.029	1.831	0.011	0.148	0.479	1.860
3137	5.524	2.476	0.554	0.207	2.235	0.108	2.700	0.011	0.032	1.833	0.004	0.158	0.453	1.865
3138	5.562	2.438	0.602	0.226	2.207	0.105	2.598	0.013	0.033	1.834	0.005	0.172	0.459	1.867
3139	5.571	2.429	0.611	0.189	2.187	0.105	2.660	0.013	0.024	1.880	0.004	0.198	0.451	1.904
3140	5.517	2.483	0.295	0.411	2.421	0.104	2.546	0.010	0.015	1.728	0.023	0.128	0.487	1.743
3141	5.567	2.433	0.315	0.394	2.252	0.113	2.625	0.005	0.018	1.874	0.013	0.167	0.462	1.892
3142	5.568	2.432	0.333	0.404	2.268	0.110	2.560	0.008	0.023	1.876	0.013	0.169	0.470	1.899
3143	5.555	2.445	0.385	0.411	2.184	0.096	2.598	0.010	0.012	1.847	0.005	0.179	0.457	1.859
3145	5.389	2.611	0.412	0.431	2.233	0.122	2.569	0.028	0.027	1.709	0.007	0.169	0.465	1.736
3146	5.485	2.515	0.304	0.423	2.270	0.133	2.618	0.015	0.027	1.802	0.008	0.159	0.464	1.829
3147	5.430	2.570	0.372	0.415	2.235	0.124	2.617	0.015	0.024	1.782	0.004	0.155	0.461	1.806
AVG	5.523	2.477	0.423	0.369	2.249	0.114	2.567	0.014	0.026	1.805	0.008	0.163	0.467	1.831
STD	0.053	0.053	0.103	0.082	0.055	0.009	0.073	0.006	0.007	0.066	0.005	0.016	0.010	0.066

APPENDIX 4: BIOTITE ANALYSES (24 Oxygen) BW84-20A THREE ENCLAVE TRAVERSES

SMPL#	SIO2	AL2O3	TIO2	FEO	MNO	MGO	CAO	NA2O	K2O	BAO	SrO	F	TOTAL
6005	35.54	15.99	1.83	17.34	1.09	10.58	0.02	0.25	9.08	0.21	0.12	0.92	92.97
6008	35.88	15.71	2.37	18.02	1.21	10.14	0.01	0.12	9.39	0.17	0.08	0.97	94.07
6009	35.80	15.80	2.31	17.79	1.21	10.24	0.00	0.14	9.35	0.13	0.08	0.99	93.84
6010	36.54	15.97	2.66	17.78	1.15	9.11	0.01	0.19	9.46	0.23	0.10	0.79	93.99
6011	34.72	17.13	2.83	17.18	1.15	8.84	0.04	0.33	8.79	0.20	0.13	0.80	92.14
6012	34.69	16.01	3.76	18.00	1.31	9.20	0.01	0.33	9.20	0.28	0.13	0.83	93.75
6014	34.50	17.96	2.33	17.90	1.29	9.43	0.00	0.31	9.29	0.22	0.09	0.95	94.27
6015	35.67	16.27	2.75	17.97	1.25	9.57	0.01	0.12	9.23	0.15	0.09	0.94	94.02
6016	36.42	16.97	2.64	17.61	1.18	9.53	0.01	0.20	9.02	0.24	0.07	0.94	94.83
6017	35.69	15.93	2.95	18.40	1.18	9.91	0.01	0.19	9.41	0.23	0.08	0.93	94.91
6018	36.06	15.90	2.50	17.98	1.24	10.03	0.01	0.18	9.25	0.12	0.08	0.94	94.29
6019	35.92	16.15	2.66	18.41	1.42	10.18	0.02	0.24	9.64	0.13	0.07	1.02	95.86
6020	36.10	16.60	2.74	17.92	1.27	10.14	0.02	0.23	9.31	0.19	0.06	1.05	95.63
6021	35.51	16.27	3.18	18.38	1.33	9.59	0.02	0.28	9.26	0.27	0.08	0.83	95.00
6022	35.26	15.94	3.03	18.90	1.40	9.83	0.01	0.29	9.33	0.20	0.07	0.78	95.04
6023	35.60	15.66	2.41	18.77	1.36	10.22	0.02	0.18	9.55	0.21	0.06	1.05	95.09
6024	35.30	15.81	3.09	18.50	1.32	9.70	0.01	0.19	9.51	0.19	0.09	0.85	94.56
6025	35.51	16.16	2.73	18.38	1.28	9.66	0.00	0.26	9.19	0.21	0.09	0.87	94.34
6026	35.05	15.98	2.41	18.09	1.20	9.69	0.08	0.34	9.28	0.21	0.13	0.86	93.32
6028	36.04	15.67	2.17	17.61	1.17	10.06	0.02	0.17	9.16	0.18	0.09	0.92	93.26
6029	35.26	15.80	2.76	18.63	1.31	9.58	0.02	0.16	9.64	0.22	0.09	0.87	94.34
6030	35.25	16.70	2.96	17.83	1.13	9.25	0.00	0.25	9.14	0.25	0.09	0.84	93.69
6033	34.63	16.49	1.91	17.34	1.31	9.97	0.00	0.39	9.37	0.21	0.12	0.82	92.56
6034	35.65	15.98	2.68	18.69	1.44	10.12	0.04	0.14	9.85	0.14	0.05	0.85	95.63
6035	36.83	17.51	2.48	17.07	1.17	9.21	0.01	0.25	8.66	0.25	0.10	0.85	94.39
6036	36.81	16.60	2.42	17.30	1.10	9.53	0.01	0.16	8.99	0.19	0.06	0.84	94.01
6038	35.70	15.96	2.81	18.66	1.34	9.97	0.02	0.21	9.67	0.21	0.07	1.00	95.62
6039	35.43	16.14	2.85	18.51	1.35	9.82	0.03	0.25	9.71	0.20	0.08	0.98	95.35
6040	34.87	16.34	2.81	17.30	1.04	9.30	0.02	0.32	8.89	0.19	0.10	0.87	92.05
6041	35.52	15.89	3.05	19.01	1.40	9.75	0.03	0.23	9.62	0.26	0.06	1.05	95.87
6042	35.78	15.57	2.19	18.56	1.44	10.35	0.00	0.18	9.37	0.17	0.07	1.06	94.74

SMPL#	SIO2	AL2O3	TIO2	FEO	MNO	MGO	CAO	NA2O	K2O	BAO	SrO	F	TOTAL
6043	35.77	15.58	3.01	19.35	1.37	9.62	0.02	0.12	9.75	0.19	0.07	0.83	95.68
6044	35.80	16.49	2.78	18.17	1.26	10.11	0.02	0.24	9.46	0.18	0.06	0.88	95.45
6045	35.92	16.49	2.74	18.29	1.22	10.26	0.01	0.23	9.49	0.23	0.06	1.01	95.95
6047	35.15	15.97	2.63	18.40	1.30	9.84	0.00	0.22	9.15	0.18	0.07	0.92	93.83
6048	35.60	16.47	2.50	18.46	1.30	10.16	0.02	0.37	9.38	0.24	0.06	0.96	95.52
6049	34.99	17.06	2.98	18.19	1.47	9.53	0.02	0.49	9.05	0.28	0.09	0.86	95.01
6050	34.45	17.95	2.84	17.80	1.42	9.08	0.01	0.44	8.57	0.28	0.10	0.70	93.64
6052	34.02	17.15	3.04	17.82	1.35	9.23	0.02	0.27	9.14	0.20	0.08	0.78	93.10
6067	36.93	16.41	3.40	18.61	1.26	9.31	0.04	0.19	9.70	0.17	0.07	0.86	96.95
6068	36.86	16.10	2.62	18.72	1.26	10.26	0.02	0.19	9.66	0.24	0.07	1.19	97.19
6072	36.49	16.31	2.63	18.48	1.25	9.96	0.00	0.21	9.41	0.25	0.07	0.89	95.95
6073	36.78	15.78	2.42	18.70	1.27	10.22	0.02	0.11	9.70	0.18	0.07	0.83	96.08
6074	36.47	15.74	2.81	18.87	1.26	10.07	0.02	0.13	9.59	0.15	0.05	0.90	96.06
6078	36.02	16.06	3.16	18.54	1.27	9.69	0.02	0.16	9.64	0.23	0.06	0.90	95.75
6079	36.33	15.87	2.73	19.31	1.36	9.79	0.04	0.12	9.76	0.19	0.06	0.88	96.44
6080	36.42	16.03	2.71	18.46	1.27	9.84	0.00	0.19	9.36	0.20	0.06	0.88	95.42
6081	35.34	15.75	2.78	18.16	1.26	9.65	0.00	0.14	9.38	0.20	0.11	0.89	93.66
6082	36.10	16.04	2.64	18.55	1.33	9.73	0.02	0.29	9.05	0.13	0.08	0.92	94.88
6083	35.55	15.91	3.13	19.15	1.33	9.65	0.00	0.35	9.02	0.17	0.08	0.87	95.21
6086	36.97	15.97	2.49	18.43	1.28	10.26	0.03	0.09	9.69	0.23	0.06	0.94	96.44
6087	36.04	15.98	3.06	18.79	1.30	9.91	0.02	0.09	9.63	0.20	0.07	0.90	95.99
6088	36.35	16.25	2.56	18.64	1.19	9.75	0.02	0.22	9.12	0.21	0.08	0.84	95.23
6089	36.28	15.97	3.10	18.85	1.44	9.31	0.03	0.24	9.15	0.15	0.09	0.79	95.40
6090	35.51	16.44	2.28	18.07	1.30	10.06	0.02	0.16	9.49	0.19	0.07	0.96	94.55
6092	36.68	16.05	2.19	18.33	1.31	10.38	0.02	0.19	9.14	0.21	0.07	0.98	95.55
6093	36.73	15.86	2.27	18.87	1.38	10.37	0.02	0.10	9.55	0.21	0.06	1.02	96.44
6095	36.69	16.00	3.11	18.45	1.29	9.87	0.03	0.04	9.84	0.22	0.05	0.96	96.55
6096	36.30	17.06	2.28	17.15	1.06	10.09	0.02	0.21	9.17	0.18	0.08	0.91	94.51
6097	36.70	16.34	3.25	18.34	1.28	9.74	0.02	0.12	9.67	0.19	0.08	0.86	96.59
6098	36.21	16.15	3.13	18.54	1.22	10.02	0.02	0.15	9.50	0.16	0.07	0.85	96.02

APPENDIX 4: BIOTITE ANALYSES (24 Oxygen) BW84-20A THREE ENCLAVE TRAVERSES

SMPL#	SIO2	AL2O3	TIO2	FEO	MNO	MGO	CAO	NA2O	K2O	BAO	SrO	F	TOTAL
6099	35.32	17.14	3.69	17.51	1.38	9.17	0.01	0.29	8.75	0.15	0.13	0.87	94.41
6100	35.50	17.27	2.89	17.84	1.29	10.18	0.01	0.23	8.72	0.22	0.11	0.88	95.14
6101	36.23	16.71	2.63	17.62	1.17	9.93	0.01	0.24	8.86	0.25	0.09	0.96	94.70
6102	35.90	17.16	2.71	18.62	1.29	9.52	0.03	0.30	8.75	0.22	0.08	0.87	95.45
6103	36.25	16.16	1.93	19.13	1.19	10.19	0.02	0.18	9.43	0.25	0.06	0.93	95.72
6104	35.73	17.36	1.59	18.24	1.15	10.15	0.03	0.24	8.55	0.13	0.11	0.84	94.12
6118	36.60	15.75	2.73	19.12	1.26	9.56	0.00	0.17	9.41	0.25	0.06	0.90	95.81
6121	36.99	15.76	2.32	19.00	1.30	10.36	0.04	0.12	9.86	0.16	0.04	1.15	97.10
6122	37.23	16.15	2.84	18.64	1.18	9.91	0.04	0.02	9.98	0.21	0.05	0.99	97.24
6123	36.89	16.14	2.81	18.55	1.17	10.15	0.05	0.05	10.04	0.25	0.05	0.96	97.11
6124	36.81	15.54	2.57	18.32	1.22	10.08	0.01	0.10	9.59	0.19	0.06	1.01	95.50
6126	35.90	17.19	2.77	18.09	1.14	9.91	0.02	0.27	9.51	0.21	0.06	1.02	96.09
6127	36.33	15.33	1.96	17.83	1.02	9.74	0.01	0.25	8.59	0.17	0.11	0.89	92.23
6128	36.73	16.02	2.85	18.67	1.20	10.38	0.04	0.05	9.95	0.12	0.05	0.93	96.99
6129	36.91	16.93	2.42	18.26	1.16	9.94	0.00	0.32	9.04	0.17	0.09	1.17	96.41
6130	36.92	15.85	2.59	18.79	1.18	10.25	0.01	0.12	9.64	0.21	0.07	0.92	96.55
AVG	35.94	16.27	2.69	18.29	1.26	9.84	0.02	0.21	9.34	0.20	0.08	0.92	95.05
STD	0.70	0.56	0.39	0.53	0.10	0.37	0.01	0.09	0.35	0.04	0.02	0.09	1.24

SMPL#	Si	Al4	Al6	Ti	Fe	Mn	Mg	Ca	Na	K	Ba	Sr	F	Fe#
6005	5.55	2.46	0.49	0.22	2.26	0.14	2.46	0.00	0.08	1.81	0.01	0.45	0.45	0.479
6008	5.56	2.45	0.42	0.28	2.33	0.16	2.34	0.00	0.04	1.85	0.01	0.48	0.48	0.499
6009	5.55	2.45	0.43	0.27	2.31	0.16	2.37	0.00	0.04	1.85	0.01	0.49	0.49	0.494
6010	5.65	2.36	0.55	0.31	2.30	0.15	2.10	0.00	0.06	1.86	0.01	0.39	0.39	0.523
6011	5.46	2.54	0.63	0.34	2.26	0.15	2.07	0.01	0.10	1.76	0.01	0.40	0.40	0.522
6012	5.41	2.59	0.36	0.44	2.35	0.17	2.14	0.00	0.10	1.83	0.02	0.41	0.41	0.523
6014	5.34	2.67	0.61	0.27	2.32	0.17	2.17	0.00	0.09	1.83	0.01	0.47	0.46	0.516
6015	5.52	2.48	0.48	0.32	2.32	0.16	2.21	0.00	0.04	1.82	0.01	0.46	0.46	0.513

APPENDIX 4: BIOTITE ANALYSES (24 Oxygen) BW84-20A THREE ENCLAVE TRAVERSES

SMPL#	Si	Al4	Al6	Ti	Fe	Mn	Mg	Ca	Na	K	Ba	Sr	F	Fe#
6016	5.55	2.45	0.60	0.30	2.25	0.15	2.17	0.00	0.06	1.75	0.01	0.45	0.45	0.509
6017	5.49	2.51	0.38	0.34	2.37	0.15	2.27	0.00	0.06	1.85	0.01	0.45	0.45	0.510
6018	5.56	2.44	0.45	0.29	2.32	0.16	2.30	0.00	0.05	1.82	0.01	0.46	0.46	0.502
6019	5.48	2.52	0.38	0.31	2.35	0.18	2.31	0.00	0.07	1.88	0.01	0.49	0.49	0.504
6020	5.48	2.52	0.46	0.31	2.28	0.16	2.30	0.00	0.07	1.80	0.01	0.50	0.50	0.498
6021	5.46	2.54	0.41	0.37	2.36	0.17	2.20	0.00	0.08	1.82	0.02	0.40	0.40	0.518
6022	5.44	2.56	0.34	0.35	2.44	0.18	2.26	0.00	0.09	1.84	0.01	0.38	0.38	0.519
6023	5.49	2.51	0.34	0.28	2.42	0.18	2.35	0.00	0.05	1.88	0.01	0.51	0.51	0.507
6024	5.47	2.53	0.36	0.36	2.40	0.17	2.24	0.00	0.06	1.88	0.01	0.42	0.42	0.517
6025	5.49	2.51	0.44	0.32	2.38	0.17	2.23	0.00	0.08	1.81	0.01	0.43	0.43	0.516
6026	5.49	2.51	0.44	0.28	2.37	0.16	2.26	0.01	0.10	1.85	0.01	0.43	0.43	0.512
6028	5.61	2.39	0.48	0.25	2.29	0.15	2.33	0.00	0.05	1.82	0.01	0.45	0.43	0.495
6029	5.48	2.52	0.38	0.32	2.42	0.17	2.22	0.00	0.05	1.91	0.01	0.43	0.43	0.522
6030	5.47	2.53	0.53	0.35	2.32	0.15	2.14	0.00	0.08	1.81	0.02	0.41	0.41	0.520
6033	5.46	2.54	0.52	0.23	2.29	0.18	2.34	0.00	0.12	1.88	0.01	0.41	0.41	0.494
6034	5.47	2.53	0.36	0.31	2.40	0.19	2.31	0.01	0.04	1.93	0.01	0.41	0.41	0.509
6035	5.60	2.40	0.74	0.28	2.17	0.15	2.09	0.00	0.07	1.68	0.02	0.41	0.41	0.510
6036	5.64	2.36	0.64	0.28	2.22	0.14	2.18	0.00	0.05	1.76	0.01	0.41	0.41	0.505
6038	5.47	2.53	0.35	0.32	2.39	0.17	2.28	0.00	0.06	1.89	0.01	0.49	0.49	0.512
6039	5.45	2.55	0.37	0.33	2.38	0.18	2.25	0.01	0.08	1.90	0.01	0.48	0.48	0.514
6040	5.50	2.51	0.53	0.33	2.28	0.14	2.18	0.00	0.10	1.79	0.01	0.43	0.43	0.511
6041	5.44	2.56	0.31	0.35	2.44	0.18	2.23	0.01	0.07	1.88	0.02	0.51	0.41	0.523
6042	5.52	2.48	0.36	0.25	2.40	0.19	2.38	0.00	0.05	1.85	0.01	0.52	0.52	0.501
6043	5.50	2.50	0.32	0.35	2.49	0.18	2.20	0.00	0.04	1.91	0.01	0.40	0.40	0.530
6044	5.47	2.53	0.43	0.32	2.32	0.16	2.30	0.00	0.07	1.84	0.01	0.43	0.43	0.502
6045	5.46	2.54	0.41	0.31	2.32	0.16	2.32	0.00	0.07	1.84	0.01	0.49	0.49	0.500
6047	5.47	2.53	0.40	0.31	2.40	0.17	2.28	0.00	0.07	1.82	0.01	0.45	0.45	0.512
6048	5.45	2.55	0.42	0.29	2.36	0.17	2.32	0.00	0.11	1.83	0.01	0.47	0.47	0.505
6049	5.38	2.62	0.47	0.35	2.34	0.19	2.18	0.00	0.15	1.78	0.02	0.42	0.42	0.517
6050	5.35	2.65	0.63	0.33	2.31	0.19	2.10	0.00	0.13	1.70	0.02	0.34	0.34	0.524
6052	5.34	2.66	0.51	0.36	2.34	0.18	2.16	0.00	0.08	1.83	0.01	0.39	0.39	0.520

APPENDIX 4: BIOTITE ANALYSES (24 Oxygen) BW84-20A THREE ENCLAVE TRAVERSES

SMPL#	Si	Al4	Al6	Ti	Fe	Mn	Mg	Ca	Na	K	Ba	Sr	F	Fe#
6067	5.55	2.45	0.46	0.38	2.34	0.16	2.09	0.01	0.06	1.86	0.01	0.41	0.41	0.529
6068	5.53	2.47	0.38	0.30	2.35	0.16	2.30	0.00	0.06	1.85	0.01	0.57	0.57	0.506
6072	5.54	2.46	0.46	0.30	2.35	0.16	2.25	0.00	0.06	1.82	0.02	0.43	0.43	0.510
6073	5.59	2.41	0.41	0.28	2.38	0.16	2.31	0.00	0.03	1.88	0.01	0.40	0.40	0.507
6074	5.55	2.45	0.37	0.32	2.40	0.16	2.28	0.00	0.04	1.86	0.01	0.43	0.43	0.512
6078	5.50	2.50	0.39	0.36	2.37	0.16	2.21	0.00	0.05	1.88	0.01	0.44	0.44	0.518
6079	5.53	2.47	0.37	0.31	2.46	0.18	2.22	0.01	0.04	1.89	0.01	0.42	0.42	0.525
6080	5.56	2.44	0.44	0.31	2.36	0.16	2.24	0.00	0.06	1.82	0.01	0.43	0.43	0.513
6081	5.51	2.49	0.41	0.33	2.37	0.17	2.24	0.00	0.04	1.87	0.01	0.44	0.44	0.514
6082	5.54	2.46	0.44	0.31	2.38	0.17	2.23	0.00	0.09	1.77	0.01	0.45	0.45	0.517
6083	5.47	2.53	0.35	0.36	2.46	0.17	2.21	0.00	0.10	1.77	0.01	0.42	0.42	0.527
6086	5.58	2.42	0.43	0.28	2.33	0.16	2.31	0.01	0.03	1.87	0.01	0.45	0.45	0.502
6087	5.49	2.51	0.36	0.35	2.40	0.17	2.25	0.00	0.03	1.87	0.01	0.43	0.43	0.515
6088	5.56	2.44	0.48	0.29	2.38	0.15	2.22	0.00	0.07	1.78	0.01	0.41	0.41	0.517
6089	5.55	2.45	0.43	0.36	2.41	0.19	2.12	0.01	0.07	1.79	0.01	0.38	0.38	0.532
6090	5.48	2.52	0.47	0.27	2.33	0.17	2.31	0.00	0.05	1.87	0.01	0.47	0.47	0.502
6092	5.58	2.42	0.45	0.25	2.33	0.17	2.35	0.00	0.06	1.77	0.01	0.47	0.47	0.498
6093	5.56	2.44	0.39	0.26	2.39	0.18	2.34	0.00	0.03	1.85	0.01	0.49	0.49	0.505
6095	5.55	2.46	0.39	0.35	2.33	0.17	2.22	0.01	0.01	1.90	0.01	0.46	0.46	0.512
6096	5.54	2.46	0.61	0.26	2.19	0.14	2.30	0.00	0.06	1.79	0.01	0.44	0.44	0.488
6097	5.53	2.47	0.44	0.37	2.31	0.16	2.19	0.00	0.04	1.86	0.01	0.41	0.41	0.514
6098	5.50	2.50	0.39	0.36	2.36	0.16	2.27	0.00	0.04	1.84	0.01	0.41	0.41	0.509
6099	5.42	2.58	0.52	0.43	2.25	0.18	2.10	0.00	0.09	1.71	0.01	0.42	0.42	0.517
6100	5.41	2.59	0.51	0.33	2.27	0.17	2.31	0.00	0.07	1.69	0.01	0.42	0.42	0.496
6101	5.53	2.47	0.54	0.30	2.25	0.15	2.26	0.00	0.07	1.73	0.02	0.46	0.46	0.499
6102	5.47	2.54	0.54	0.31	2.37	0.17	2.16	0.01	0.09	1.70	0.01	0.42	0.42	0.523
6103	5.54	2.46	0.45	0.22	2.44	0.15	2.32	0.00	0.05	1.84	0.02	0.45	0.45	0.513
6104	5.49	2.51	0.64	0.18	2.35	0.15	2.33	0.01	0.07	1.68	0.01	0.41	0.41	0.502
6118	5.58	2.42	0.42	0.31	2.44	0.16	2.17	0.00	0.05	1.83	0.02	0.43	0.43	0.529
6121	5.57	2.43	0.37	0.26	2.39	0.17	2.33	0.01	0.04	1.89	0.01	0.55	0.55	0.507

APPENDIX 4: BIOTITE ANALYSES (24 Oxygen) BW84-20A THREE ENCLAVE TRAVERSES

SMPL#	Si	Al4	Al6	Ti	Fe	Mn	Mg	Ca	Na	K	Ba	Sr	F	Fe#
6122	5.58	2.42	0.43	0.32	2.34	0.15	2.21	0.01	0.01	1.91	0.01	0.47	0.47	0.514
6123	5.55	2.45	0.41	0.32	2.33	0.15	2.27	0.01	0.02	1.93	0.02	0.46	0.46	0.506
6124	5.61	2.39	0.40	0.30	2.34	0.16	2.29	0.00	0.03	1.87	0.01	0.49	0.49	0.505
6126	5.44	2.57	0.50	0.32	2.29	0.15	2.24	0.00	0.08	1.84	0.01	0.49	0.49	0.506
6127	5.70	2.30	0.53	0.23	2.34	0.14	2.28	0.00	0.08	1.72	0.01	0.44	0.44	0.507
6128	5.53	2.47	0.37	0.32	2.35	0.15	2.33	0.01	0.02	1.91	0.01	0.44	0.44	0.502
6129	5.54	2.46	0.54	0.27	2.29	0.15	2.22	0.00	0.09	1.73	0.01	0.56	0.56	0.508
6130	5.58	2.42	0.40	0.29	2.37	0.15	2.31	0.00	0.04	1.86	0.01	0.44	0.44	0.507
AVG	5.51	2.49	0.45	0.31	2.35	0.16	2.25	0.00	0.06	1.83	0.01	0.44	0.44	0.511
STD	0.07	0.07	0.09	0.04	0.06	0.01	0.08	0.00	0.03	0.06	0.00	0.04	0.04	0.010

APPENDIX 4: BIOTITE ANALYSES (24 Oxygen) BW84-20A THREE GRANITE TRAVERSES

SMPL#	SIO2	AL2O3	TIO2	FEO	MNO	MGO	CAO	NA2O	K2O	BAO	SrO	F	TOTAL
6053	35.31	15.94	3.69	17.79	1.35	9.44	0.03	0.12	9.65	0.19	0.07	0.79	94.37
6054	34.85	16.09	3.25	17.85	1.41	9.69	0.04	0.17	9.61	0.24	0.06	0.94	94.20
6055	35.26	16.32	3.35	17.88	1.35	9.54	0.04	0.08	9.61	0.27	0.06	0.88	94.64
6056	34.78	16.88	3.60	17.46	1.25	9.13	0.01	0.20	8.95	0.31	0.06	0.76	93.39
6057	34.98	16.02	3.62	17.72	1.33	9.59	0.03	0.10	9.67	0.20	0.05	0.93	94.24
6058	34.76	17.42	3.52	18.11	1.24	9.57	0.03	0.21	9.34	0.36	0.08	0.86	95.50
6059	34.32	17.77	3.09	18.16	1.18	9.61	0.02	0.26	9.28	0.27	0.09	0.82	94.87
6060	34.46	17.18	3.18	18.28	1.33	9.42	0.02	0.22	9.38	0.41	0.08	0.89	94.85
6062	35.74	16.46	2.89	18.45	1.07	9.94	0.03	0.27	9.40	0.18	0.07	0.88	95.38
6105	35.28	18.29	2.35	17.83	1.19	9.61	0.02	0.10	9.29	0.21	0.11	0.86	95.14
6106	36.11	16.42	3.59	18.51	1.13	9.57	0.00	0.21	9.20	0.17	0.09	0.99	95.99
6107	36.58	15.95	3.61	18.98	1.30	9.67	0.04	0.07	9.80	0.23	0.06	1.00	97.29
6108	37.22	16.63	2.92	17.72	1.07	9.46	0.01	0.11	8.83	0.23	0.08	0.88	95.16
6109	36.58	16.12	2.98	18.54	1.18	10.00	0.01	0.12	9.38	0.24	0.07	0.97	96.19
6110	36.33	15.88	3.13	19.24	1.33	10.10	0.03	0.04	9.76	0.29	0.07	0.88	97.08
6111	36.76	16.50	2.91	18.23	1.22	9.40	0.07	0.21	8.95	0.18	0.08	0.95	95.46
6112	35.72	16.32	3.01	18.96	1.22	9.44	0.00	0.18	9.26	0.15	0.08	0.99	95.33
6113	35.61	16.37	2.94	18.97	1.26	9.78	0.02	0.19	9.42	0.31	0.08	0.92	95.87
6114	36.34	16.29	2.77	18.94	1.36	9.75	0.02	0.20	9.60	0.23	0.04	0.92	96.46
6131	36.59	16.20	3.17	19.34	1.32	9.94	0.04	0.08	9.85	0.46	0.07	1.05	98.11
6133	36.49	16.57	4.39	17.79	1.13	8.62	0.01	0.14	9.63	0.21	0.06	0.88	95.92
6134	37.24	15.67	3.24	18.15	1.12	9.99	0.04	0.13	9.89	0.22	0.05	1.05	96.79
6138	36.96	15.78	2.69	18.80	1.30	9.99	0.00	0.15	9.71	0.18	0.08	0.95	96.59
6139	36.69	15.65	3.25	19.01	1.37	9.37	0.05	0.26	9.60	0.17	0.07	0.82	96.31
6142	36.79	16.51	2.65	18.31	1.24	10.27	0.00	0.19	9.13	0.22	0.06	0.87	96.24
6143	36.55	15.87	2.27	18.38	1.05	11.15	0.01	0.22	8.19	0.22	0.05	0.82	94.78
6144	37.42	16.19	1.96	17.52	1.30	10.94	0.02	0.18	9.72	0.21	0.06	1.06	96.58
6147	36.58	18.76	2.34	16.86	1.12	8.94	0.00	0.50	8.29	0.12	0.10	0.81	94.42
6149	35.87	15.66	2.80	18.91	1.33	9.58	0.00	0.10	9.32	0.23	0.05	0.84	94.69

APPENDIX 4: BIOTITE ANALYSES (24 Oxygen) BW84-20A THREE GRANITE TRAVERSES

SMPL#	SIO2	AL2O3	TIO2	FEO	MNO	MGO	CAO	NA2O	K2O	BAO	SrO	F	TOTAL
6150	36.22	16.05	2.66	19.20	1.24	9.42	0.04	0.06	9.63	0.22	0.06	0.89	95.69
6151	35.97	15.84	2.47	18.88	1.33	9.58	0.02	0.13	9.36	0.35	0.05	0.97	94.95
6152	35.94	15.65	2.91	19.25	1.35	9.50	0.05	0.12	9.57	0.45	0.06	1.12	95.97
6153	35.85	15.91	2.47	18.85	1.37	9.76	0.04	0.12	9.58	0.24	0.05	0.92	95.16
6154	35.08	16.29	2.97	18.76	1.35	9.03	0.02	0.18	9.41	0.24	0.06	0.80	94.19
6155	37.04	15.98	2.77	18.19	1.19	9.94	0.01	0.21	9.24	0.12	0.10	0.81	95.60
6156	36.68	16.51	3.14	18.64	1.30	9.90	0.02	0.22	9.68	0.18	0.05	0.87	97.19
6157	36.98	15.91	2.38	18.66	1.12	10.44	0.00	0.11	9.47	0.20	0.07	1.00	96.34
6158	37.12	16.29	2.25	18.24	1.32	10.33	0.00	0.20	9.43	0.24	0.08	0.91	96.41
6159	36.39	16.13	2.45	18.43	1.27	10.25	0.02	0.18	9.48	0.19	0.07	0.97	95.83
6160	36.43	15.77	2.59	19.77	1.26	9.79	0.00	0.15	9.56	0.24	0.06	0.96	96.58
AVG	36.10	16.35	2.96	18.44	1.25	9.74	0.02	0.17	9.40	0.24	0.07	0.91	95.64
STD	0.82	0.68	0.49	0.60	0.10	0.48	0.02	0.08	0.36	0.08	0.02	0.08	1.00

SMPL#	Si	Al4	Al6	Ti	Fe	Mn	Mg	Ca	Na	K	Ba	Sr	F	Fe#
6053	5.54	2.46	0.36	0.30	2.51	0.16	2.22	0.00	0.04	1.85	0.01	0.46	0.36	0.531
6054	5.47	2.54	0.37	0.43	2.30	0.18	2.18	0.01	0.04	1.91	0.01	0.39	0.46	0.514
6055	5.42	2.58	0.36	0.38	2.32	0.19	2.24	0.01	0.05	1.91	0.02	0.46	0.43	0.508
6056	5.44	2.56	0.41	0.39	2.31	0.18	2.20	0.01	0.02	1.89	0.02	0.43	0.37	0.513
6057	5.41	2.59	0.51	0.42	2.27	0.17	2.12	0.00	0.06	1.78	0.02	0.37	0.46	0.518
6058	5.43	2.58	0.35	0.42	2.30	0.18	2.22	0.01	0.03	1.91	0.01	0.46	0.42	0.509
6059	5.32	2.68	0.46	0.41	2.32	0.16	2.18	0.01	0.06	1.82	0.02	0.42	0.40	0.515
6060	5.28	2.72	0.51	0.36	2.34	0.15	2.21	0.00	0.08	1.82	0.02	0.40	0.44	0.515
6062	5.35	2.65	0.73	0.86	1.64	0.27	1.40	0.29	0.09	1.39	0.01	0.28	0.43	0.539
6105	5.46	2.54	0.43	0.33	2.36	0.14	2.27	0.01	0.08	1.83	0.01	0.43	0.42	0.510
6106	5.38	2.62	0.67	0.27	2.27	0.15	2.18	0.00	0.03	1.81	0.01	0.42	0.48	0.510
6107	5.47	2.53	0.41	0.41	2.35	0.15	2.16	0.00	0.06	1.78	0.01	0.48	0.48	0.520
6108	5.50	2.50	0.33	0.41	2.39	0.17	2.17	0.01	0.02	1.88	0.01	0.48	0.42	0.524
6109	5.63	2.37	0.60	0.33	2.24	0.14	2.13	0.00	0.03	1.71	0.01	0.42	0.46	0.512

APPENDIX 4: BIOTITE ANALYSES (24 Oxygen) BW84-20A THREE GRANITE TRAVERSES

SMPL#	Si	Al4	Al6	Ti	Fe	Mn	Mg	Ca	Na	K	Ba	Sr	F	Fe#
6110	5.54	2.46	0.41	0.34	2.35	0.15	2.26	0.00	0.04	1.81	0.01	0.46	0.42	0.510
6111	5.49	2.51	0.32	0.36	2.43	0.17	2.28	0.01	0.01	1.88	0.02	0.42	0.46	0.517
6112	5.58	2.42	0.53	0.33	2.31	0.16	2.13	0.01	0.06	1.73	0.01	0.46	0.48	0.521
6113	5.47	2.53	0.42	0.35	2.43	0.16	2.16	0.00	0.05	1.81	0.01	0.48	0.44	0.530
6114	5.44	2.56	0.39	0.34	2.42	0.16	2.23	0.00	0.06	1.84	0.02	0.45	0.44	0.521
6131	5.51	2.49	0.42	0.32	2.40	0.18	2.20	0.00	0.06	1.86	0.01	0.44	0.50	0.521
6133	5.68	2.32	0.53	0.29	2.08	0.13	2.35	0.00	0.08	1.79	0.01	0.54	0.42	0.470
6134	5.52	2.48	0.48	0.50	2.25	0.15	1.94	0.00	0.04	1.86	0.01	0.42	0.50	0.537
6138	5.44	2.56	0.64	0.33	2.27	0.16	2.11	0.01	0.16	1.70	0.01	0.33	0.45	0.518
6139	5.59	2.41	0.40	0.31	2.38	0.17	2.25	0.00	0.04	1.87	0.01	0.45	0.39	0.514
6142	5.48	2.52	0.49	0.41	2.16	0.15	2.19	0.00	0.16	1.77	0.01	0.39	0.42	0.496
6143	5.55	2.45	0.48	0.30	2.31	0.16	2.31	0.00	0.06	1.76	0.01	0.42	0.40	0.500
6144	5.57	2.43	0.42	0.26	2.34	0.14	2.53	0.00	0.07	1.59	0.01	0.40	0.50	0.481
6147	4.39	3.61	2.02	0.20	1.74	0.12	1.51	0.02	0.27	1.36	0.01	0.26	0.39	0.536
6149	5.56	2.44	0.79	0.19	2.15	0.13	2.33	0.01	0.14	1.55	0.01	0.34	0.41	0.479
6150	5.54	2.46	0.40	0.33	2.44	0.17	2.21	0.00	0.03	1.84	0.01	0.41	0.43	0.525
6151	5.54	2.46	0.44	0.31	2.46	0.16	2.15	0.01	0.02	1.88	0.01	0.43	0.47	0.533
6152	5.55	2.45	0.42	0.29	2.43	0.17	2.20	0.00	0.04	1.84	0.02	0.47	0.54	0.525
6153	5.51	2.49	0.33	0.34	2.47	0.18	2.17	0.01	0.04	1.87	0.03	0.54	0.45	0.532
6154	5.52	2.48	0.41	0.29	2.43	0.18	2.24	0.01	0.04	1.88	0.01	0.45	0.39	0.520
6155	5.46	2.54	0.45	0.35	2.44	0.18	2.10	0.00	0.05	1.87	0.02	0.39	0.39	0.538
6156	5.62	2.38	0.47	0.32	2.31	0.15	2.25	0.00	0.06	1.79	0.01	0.39	0.41	0.507
6157	5.50	2.50	0.42	0.35	2.34	0.17	2.21	0.00	0.06	1.85	0.01	0.41	0.48	0.514
6158	5.59	2.41	0.42	0.27	2.36	0.14	2.35	0.00	0.03	1.82	0.01	0.48	0.43	0.501
6159	5.59	2.41	0.49	0.26	2.30	0.17	2.32	0.00	0.06	1.81	0.01	0.43	0.47	0.498
6160	5.53	2.47	0.43	0.28	2.34	0.16	2.32	0.00	0.05	1.84	0.01	0.47	0.46	0.502
AVG	5.47	2.53	0.50	0.35	2.31	0.16	2.18	0.01	0.06	1.79	0.01	0.43	0.42	0.515
STD	0.19	0.19	0.26	0.10	0.17	0.02	0.19	0.04	0.05	0.12	0.00	0.06	0.10	0.015

APPENDIX 4: HORNBLENDE ANALYSES (24 Oxygen) BW84-19 RSgd

SMPL#	SIO2	AL2O3	TIO2	FEO	MNO	MGO	CAO	NA2O	K2O	BAO	F	CL	H2O	TOTAL
1262	45.39	10.01	1.16	16.38	1.17	10.73	11.01	1.08	0.82	0.10	0.14	nd	1.94	99.93
1263	43.87	12.38	1.09	15.79	1.18	10.50	10.85	1.05	0.75	0.02	0.20	nd	1.91	99.59
1264	45.98	9.45	1.08	16.19	1.23	10.74	11.00	1.02	0.87	0.13	0.14	nd	1.94	99.77
1265	46.32	7.88	1.19	16.71	1.14	11.05	11.62	0.93	0.81	0.06	0.18	nd	1.92	99.81
1274	46.70	7.64	0.89	16.11	1.21	11.14	11.53	0.87	0.70	0.08	0.22	nd	1.89	98.98
1275	47.98	6.70	0.77	15.72	1.14	11.51	11.43	1.02	0.60	0.19	0.20	nd	1.94	99.20
1276	47.23	7.29	0.76	15.94	1.35	12.30	11.49	0.92	0.60	0.09	0.16	nd	1.95	100.08
1284	46.68	7.94	1.02	16.50	1.33	11.65	11.67	0.83	0.76	0.02	0.30	nd	1.88	100.58
1285	46.39	7.87	1.15	16.08	1.23	11.46	11.54	1.00	0.73	0.07	0.22	nd	1.90	99.64
AVG	46.28	8.57	1.01	16.16	1.22	11.23	11.35	0.97	0.74	0.08	0.20		1.92	
STD	1.10	1.66	0.16	0.31	0.07	0.53	0.29	0.08	0.09	0.05	0.05		0.02	

SMPL#	SI	AL4	AL6	TI	FE	MN	MG	CA	NA	K	BA	F	FE#	NA+K
1262	6.766	1.234	0.524	0.130	2.042	0.148	2.384	1.758	0.312	0.156	0.006	0.066	0.461	0.468
1263	6.543	1.457	0.719	0.122	1.970	0.149	2.334	1.734	0.295	0.143	0.001	0.094	0.458	0.438
1264	6.855	1.145	0.515	0.121	2.019	0.155	2.387	1.757	0.303	0.165	0.008	0.066	0.458	0.468
1265	6.929	1.071	0.318	0.134	2.090	0.144	2.464	1.862	0.296	0.155	0.004	0.085	0.459	0.451
1274	7.017	0.983	0.369	0.101	2.024	0.154	2.495	1.856	0.271	0.134	0.005	0.105	0.448	0.405
1275	7.172	0.828	0.352	0.087	1.965	0.144	2.564	1.830	0.252	0.114	0.011	0.095	0.434	0.366
1276	7.007	0.993	0.281	0.085	1.978	0.170	2.720	1.826	0.293	0.114	0.005	0.075	0.421	0.407
1284	6.922	1.078	0.309	0.114	2.046	0.167	2.575	1.854	0.264	0.144	0.001	0.141	0.443	0.408
1285	6.944	1.056	0.332	0.129	2.013	0.156	2.557	1.851	0.241	0.139	0.004	0.104	0.440	0.380
AVG	6.906	1.094	0.413	0.114	2.016	0.154	2.498	1.814	0.281	0.140	0.005	0.092	0.447	0.421
STD	0.166	0.166	0.136	0.017	0.038	0.009	0.114	0.047	0.023	0.017	0.003	0.022	0.013	0.035

APPENDIX 4: HORNBLENDE ANALYSES (24 Oxygen) BW84-23 RSgd

SMPL#	SIO2	AL2O3	TIO2	FEO	MNO	MGO	CAO	NA2O	K2O	BAO	F	CL	H2O	TOTAL
1311	46.32	7.93	1.32	16.35	0.75	11.77	11.70	0.77	0.82	0.12	0.20	nd	1.92	99.97
1332	46.60	9.36	1.01	15.27	0.96	12.01	11.31	0.89	0.66	0.00	0.18	nd	1.95	100.20
1334	47.41	7.62	1.08	15.80	0.99	12.35	11.65	0.83	0.67	0.11	0.18	nd	1.95	100.64
1335	47.88	7.52	1.03	15.66	0.96	12.47	11.51	0.92	0.68	0.10	0.24	nd	1.93	100.90
1338	45.49	8.76	1.25	16.88	0.94	11.22	11.63	0.86	0.90	0.01	0.20	nd	1.91	100.05
1339	47.84	7.48	1.06	15.64	1.06	12.08	11.86	0.96	0.72	0.06	0.32	nd	1.89	100.97
1340	46.16	7.99	1.30	16.22	1.03	11.16	11.83	0.92	0.79	0.09	0.06	nd	1.97	99.52
1341	46.76	7.72	1.05	16.15	1.09	12.27	11.68	0.85	0.77	0.07	0.12	nd	1.97	100.50
1342	47.40	7.30	1.11	15.93	0.99	11.73	11.78	0.93	0.70	0.15	0.24	nd	1.91	100.17
1361	47.17	7.96	1.19	16.24	1.02	11.78	11.79	0.93	0.76	0.20	0.06	nd	2.01	101.11
1362	46.91	8.19	1.16	16.30	0.96	11.59	11.42	0.67	0.76	0.05	0.10	nd	1.98	100.09
4215	46.00	8.57	0.98	16.29	0.89	11.94	11.98	0.99	0.77	0.11	0.03	0.12	1.96	100.63
4217	46.16	8.10	1.16	16.50	1.00	12.22	12.07	1.08	0.84	0.11	0.03	0.13	1.96	101.36
4218	46.83	7.76	1.03	15.92	0.95	12.47	11.86	1.02	0.75	0.13	0.03	0.10	1.98	100.83
4220	45.53	8.97	0.71	16.05	0.89	11.78	11.65	0.88	0.78	0.13	0.05	0.07	1.95	99.44
4221	47.12	7.41	1.06	15.79	1.00	12.74	12.03	0.90	0.70	0.18	0.03	0.10	1.98	101.04
4222	46.80	7.55	1.21	15.75	1.04	12.65	11.99	0.92	0.71	0.13	0.03	0.08	1.99	100.85
4231	47.21	8.10	0.80	15.96	0.87	11.45	12.03	0.73	0.79	0.11	0.03	0.16	1.94	100.18
4232	45.56	8.45	0.73	15.86	1.00	11.56	11.85	0.79	0.76	0.10	0.04	0.10	1.93	98.73
4240	46.27	8.07	0.94	16.40	0.97	11.82	11.87	0.83	0.79	0.11	0.03	0.12	1.95	100.17
4242	46.03	8.52	0.91	15.99	0.92	12.08	12.02	0.74	0.72	0.14	0.04	0.09	1.96	100.16
4243	46.01	8.01	0.96	16.40	1.07	12.21	12.01	0.75	0.81	0.13	0.03	0.14	1.94	100.47
4244	45.99	7.97	0.88	16.39	0.95	12.05	11.92	0.82	0.83	0.15	0.03	0.10	1.95	100.03
4245	45.87	8.12	0.96	16.47	1.03	12.00	11.91	0.83	0.80	0.13	0.03	0.13	1.94	100.22
4246	45.91	8.07	0.84	16.45	0.98	11.94	11.90	0.82	0.80	0.12	0.03	0.18	1.91	99.95
4249	45.22	8.10	0.76	16.52	1.04	11.71	11.65	0.89	0.76	0.15	0.03	0.15	1.90	98.88
4250	45.52	8.74	0.80	16.35	0.96	11.74	11.53	0.80	0.78	0.11	0.04	0.12	1.93	99.42
4255	44.60	10.79	0.85	15.46	0.90	10.89	11.06	0.81	0.83	0.10	0.07	0.11	1.92	98.39
4261	45.89	8.22	1.00	16.47	1.00	11.82	11.88	0.88	0.85	0.11	0.04	0.08	1.96	100.20
AVG	46.36	8.18	1.00	16.12	0.97	11.91	11.77	0.86	0.77	0.11	0.09	0.12	1.95	
STD	0.79	0.68	0.16	0.36	0.07	0.42	0.23	0.09	0.06	0.04	0.08	0.03	0.03	

APPENDIX 4: HORNBLENDE ANALYSES (24 Oxygen) BW84-23 RSgd

SMPL#	SI	AL4	AL6	TI	FE	MN	MG	CA	NA	K	BA	F	FE#	NA+K
1311	6.904	1.096	0.297	0.148	2.038	0.095	2.615	1.869	0.205	0.156	0.007	0.094	0.438	0.361
1332	6.869	1.131	0.494	0.112	1.882	0.120	2.639	1.786	0.220	0.124	0.000	0.084	0.416	0.344
1334	6.981	1.019	0.304	0.120	1.946	0.123	2.711	1.838	0.254	0.126	0.006	0.084	0.418	0.380
1335	7.027	0.973	0.328	0.114	1.922	0.119	2.728	1.810	0.236	0.127	0.006	0.111	0.413	0.363
1338	6.798	1.202	0.340	0.140	2.110	0.119	2.499	1.862	0.267	0.172	0.001	0.095	0.458	0.439
1339	7.030	0.970	0.326	0.117	1.922	0.132	2.646	1.867	0.245	0.135	0.003	0.149	0.421	0.380
1340	6.912	1.088	0.322	0.146	2.031	0.131	2.491	1.898	0.279	0.151	0.005	0.028	0.449	0.430
1341	6.921	1.079	0.267	0.117	1.999	0.137	2.707	1.852	0.264	0.145	0.004	0.056	0.425	0.409
1342	7.034	0.966	0.311	0.124	1.977	0.124	2.595	1.873	0.245	0.132	0.009	0.113	0.432	0.377
1361	6.941	1.059	0.321	0.132	1.998	0.127	2.584	1.859	0.265	0.143	0.012	0.028	0.436	0.408
1362	6.942	1.058	0.371	0.129	2.017	0.120	2.557	1.811	0.267	0.143	0.003	0.047	0.441	0.410
4215	6.820	1.180	0.317	0.109	2.020	0.112	2.638	1.903	0.285	0.146	0.006	0.056	0.434	0.431
4217	6.814	1.186	0.224	0.129	2.037	0.125	2.689	1.909	0.309	0.158	0.006	0.061	0.431	0.467
4218	6.910	1.090	0.259	0.114	1.965	0.119	2.743	1.875	0.292	0.141	0.008	0.047	0.417	0.433
4220	6.818	1.182	0.401	0.080	2.010	0.113	2.629	1.869	0.256	0.149	0.008	0.033	0.433	0.405
4221	6.936	1.064	0.221	0.117	1.944	0.125	2.795	1.897	0.257	0.131	0.010	0.047	0.410	0.388
4222	6.903	1.097	0.215	0.134	1.943	0.130	2.781	1.895	0.263	0.134	0.008	0.037	0.411	0.397
4231	6.995	1.005	0.409	0.089	1.977	0.109	2.529	1.910	0.210	0.149	0.006	0.075	0.439	0.359
4232	6.872	1.128	0.374	0.083	2.001	0.128	2.599	1.915	0.231	0.146	0.006	0.048	0.435	0.377
4240	6.890	1.110	0.306	0.105	2.042	0.122	2.624	1.894	0.240	0.150	0.006	0.057	0.438	0.390
4242	6.841	1.159	0.334	0.102	1.988	0.116	2.676	1.914	0.213	0.136	0.008	0.042	0.426	0.349
4243	6.845	1.155	0.249	0.107	2.040	0.135	2.707	1.914	0.216	0.154	0.008	0.066	0.430	0.370
4244	6.868	1.132	0.271	0.099	2.047	0.120	2.682	1.907	0.237	0.158	0.009	0.047	0.433	0.395
4245	6.842	1.158	0.269	0.108	2.054	0.130	2.668	1.903	0.240	0.152	0.008	0.061	0.435	0.392
4246	6.864	1.136	0.286	0.094	2.057	0.124	2.661	1.906	0.238	0.153	0.007	0.085	0.436	0.391
4249	6.845	1.155	0.290	0.087	2.091	0.133	2.642	1.890	0.261	0.147	0.009	0.072	0.442	0.408
4250	6.827	1.173	0.372	0.090	2.051	0.122	2.625	1.853	0.233	0.149	0.006	0.057	0.439	0.382
4256	6.156	1.844	1.229	0.094	1.725	0.105	2.262	1.614	0.222	0.131	0.006	0.063	0.433	0.353
4261	6.844	1.156	0.289	0.112	2.054	0.126	2.628	1.898	0.254	0.162	0.006	0.038	0.439	0.416
AVG	6.871	1.129	0.345	0.112	1.996	0.122	2.633	1.869	0.248	0.145	0.006	0.065	0.431	0.393
STD	0.153	0.153	0.180	0.018	0.074	0.009	0.102	0.059	0.025	0.011	0.003	0.028	0.011	0.029

APPENDIX 4: HORNBLENDE ANALYSES (24 Oxygen) BW84-25 RSgd

SMPL#	SIO2	AL203	TIO2	FEO	MNO	MGO	CAO	NA2O	K2O	BAO	F	CL	H2O	TOTAL
1296	45.58	9.16	1.21	17.50	0.71	10.94	11.70	0.79	0.95	0.02	0.24	nd	1.90	100.70
1297	45.80	9.31	1.17	16.57	0.67	10.76	11.26	0.81	0.95	0.00	0.22	nd	1.90	99.42
1303	47.21	7.88	1.19	16.27	0.77	11.58	11.61	0.80	0.81	0.00	0.12	nd	1.97	100.21
1304	45.18	8.88	1.36	17.36	0.86	10.64	11.73	0.74	0.98	0.00	0.04	nd	1.98	99.75
1305	44.39	9.03	1.60	17.20	0.81	10.63	11.86	0.71	1.03	0.05	0.20	nd	1.89	99.40
1309	44.78	9.11	1.13	17.15	0.78	11.02	11.49	0.81	0.91	0.00	0.08	nd	1.95	99.21
1310	46.39	8.04	1.34	16.43	0.64	11.70	11.58	0.71	0.83	0.14	0.25	nd	1.89	99.94
4274	45.68	7.99	1.05	16.88	0.72	11.62	11.91	0.66	0.81	0.13	0.06	0.06	1.95	99.52
4275	45.78	8.79	0.92	16.37	0.74	11.42	11.30	0.70	0.92	0.12	0.07	0.04	1.96	99.13
4279	44.85	8.92	1.27	17.50	0.73	11.33	12.00	1.05	1.04	0.11	0.12	0.10	1.93	100.95
4280	44.48	9.50	1.38	16.66	0.63	11.09	11.00	0.83	1.05	0.16	0.19	0.13	1.87	98.97
4281	45.05	9.18	1.20	17.29	0.66	11.38	11.39	0.83	1.00	0.13	0.09	0.10	1.93	100.23
4282	44.80	8.62	1.46	17.39	0.71	11.31	11.87	0.98	1.04	0.06	0.11	0.12	1.91	100.38
4283	45.02	8.40	1.15	17.21	0.71	11.56	11.83	0.86	0.91	0.13	0.08	0.24	1.86	99.96
4284	45.67	8.25	1.44	16.73	0.88	11.83	12.11	0.98	0.94	0.10	0.09	0.08	1.96	101.06
4286	47.19	7.19	1.36	15.88	0.82	12.67	12.08	0.87	0.71	0.10	0.05	0.09	1.98	100.99
4287	46.24	7.74	1.22	16.50	0.86	12.17	12.16	0.86	0.83	0.11	0.10	0.12	1.94	100.85
4288	45.74	8.29	1.28	17.13	0.78	11.68	12.13	0.88	0.88	0.12	0.07	0.13	1.94	101.05
4289	44.75	8.88	1.21	17.30	0.78	11.25	12.03	0.97	0.97	0.13	0.08	0.13	1.92	100.04
4290	44.70	9.10	0.95	17.40	0.73	11.16	11.91	0.90	0.97	0.08	0.10	0.11	1.92	100.03
4294	44.68	9.08	1.01	17.59	0.81	11.11	12.02	0.77	0.99	0.12	0.08	0.08	1.94	100.28
4295	43.55	9.90	1.09	17.45	0.73	10.78	10.23	0.68	1.94	0.11	0.08	0.12	1.88	98.54
4296	44.61	9.81	1.26	17.64	0.71	10.99	10.21	0.68	2.26	0.14	0.08	0.09	1.93	100.41
4298	45.88	8.12	1.26	16.85	0.80	11.85	11.94	0.80	0.86	0.14	0.06	0.09	1.96	100.61
5148	44.97	9.03	1.11	15.84	0.64	11.16	10.88	0.81	0.93	0.10	0.21	0.15	1.84	97.57
5151	46.62	7.69	1.08	15.89	0.72	12.10	11.33	0.92	0.74	0.16	0.10	0.13	1.92	99.40
5153	45.73	7.61	1.32	15.49	0.72	11.91	11.18	0.85	0.81	0.09	0.08	0.12	1.90	97.81
5155	45.26	8.04	0.86	16.53	0.71	11.24	11.32	0.92	0.76	0.11	0.08	0.14	1.88	97.85
5160	43.44	9.13	0.91	17.70	0.64	10.75	10.52	0.94	1.44	0.12	0.07	0.14	1.86	97.66
5162	44.60	8.84	1.21	17.23	0.65	10.55	11.07	0.92	1.01	0.14	0.09	0.10	1.89	98.30
5165	45.15	8.66	1.04	17.64	0.72	10.45	11.16	0.83	0.97	0.09	0.09	0.19	1.86	98.85
5166	47.10	7.45	1.31	16.48	0.65	11.84	11.48	1.00	0.79	0.13	0.07	0.12	1.95	100.37

APPENDIX 4: HORNBLENDE ANALYSES (24 Oxygen) BW84-25 RSgd (continued)

SMPL#	SIO2	AL2O3	TIO2	FEO	MNO	MGO	CAO	NA2O	K2O	BAO	F	CL	H2O	TOTAL
5168	45.51	8.68	1.39	17.10	0.67	11.24	11.44	1.18	1.01	0.13	0.13	0.23	1.87	100.58
5169	45.75	8.23	1.36	16.77	0.72	11.57	11.45	0.97	0.88	0.10	0.08	0.17	1.90	99.95
5177	45.69	8.60	1.42	17.00	0.85	11.36	11.62	0.92	1.02	0.06	0.12	0.11	1.93	100.70
5178	47.44	8.08	0.91	16.54	0.70	11.31	11.10	0.78	0.93	0.18	0.10	0.16	1.92	100.15
5179	47.10	7.62	1.21	16.52	0.83	11.99	11.78	0.72	0.75	0.15	0.08	0.14	1.94	100.83
5184	44.43	8.31	1.51	16.55	0.69	10.67	11.16	1.07	1.02	0.12	0.28	0.17	1.80	97.78
5188	44.96	10.14	0.98	16.37	0.68	10.68	10.60	0.69	0.88	0.13	0.18	0.08	1.90	98.27
5189	44.76	9.00	1.39	17.79	0.68	10.55	11.37	1.03	1.06	0.12	0.09	0.16	1.89	99.89
5190	45.85	8.42	1.29	17.11	0.69	11.22	11.45	0.99	0.94	0.14	0.08	0.26	1.86	100.30
AVG	45.42	8.60	1.21	16.90	0.73	11.29	11.47	0.86	0.99	0.10	0.11	0.13	1.91	
STD	0.94	0.68	0.18	0.56	0.07	0.51	0.49	0.12	0.28	0.05	0.06	0.03	0.04	

SMPL#	SI	AL4	AL6	TI	FE	MN	MG	CA	NA	K	BA	F	FE#	NA+K
1296	6.771	1.229	0.375	0.135	2.174	0.089	2.422	1.862	0.288	0.180	0.001	0.113	0.473	0.468
1297	6.853	1.147	0.494	0.132	2.073	0.085	2.400	1.805	0.229	0.181	0.000	0.104	0.463	0.410
1303	6.987	1.013	0.361	0.132	2.014	0.097	2.554	1.841	0.232	0.153	0.000	0.056	0.441	0.385
1304	6.783	1.217	0.355	0.154	2.180	0.109	2.381	1.887	0.233	0.188	0.000	0.019	0.478	0.421
1305	6.709	1.291	0.318	0.182	2.174	0.104	2.395	1.921	0.217	0.199	0.003	0.096	0.476	0.416
1309	6.759	1.241	0.379	0.128	2.165	0.100	2.479	1.858	0.208	0.175	0.000	0.038	0.466	0.383
1310	6.906	1.094	0.317	0.150	2.046	0.081	2.596	1.847	0.234	0.158	0.008	0.118	0.441	0.392
4274	6.864	1.136	0.278	0.119	2.121	0.092	2.602	1.917	0.192	0.155	0.008	0.029	0.449	0.347
4275	6.871	1.129	0.426	0.104	2.055	0.094	2.555	1.817	0.204	0.176	0.007	0.019	0.446	0.380
4279	6.694	1.306	0.263	0.143	2.184	0.092	2.520	1.919	0.304	0.198	0.006	0.047	0.464	0.502
4280	6.724	1.276	0.417	0.157	2.106	0.081	2.499	1.782	0.243	0.202	0.009	0.062	0.457	0.445
4281	6.737	1.263	0.355	0.135	2.162	0.084	2.537	1.825	0.241	0.191	0.008	0.047	0.460	0.432
4282	6.718	1.282	0.241	0.165	2.181	0.090	2.528	1.907	0.285	0.199	0.004	0.057	0.463	0.484
4283	6.768	1.232	0.256	0.130	2.164	0.090	2.590	1.906	0.251	0.174	0.008	0.114	0.455	0.425
4284	6.776	1.224	0.218	0.161	2.076	0.111	2.616	1.925	0.282	0.178	0.006	0.038	0.442	0.460
4286	6.945	1.055	0.192	0.151	1.955	0.102	2.779	1.905	0.248	0.133	0.006	0.042	0.413	0.381

APPENDIX 4: HORNBLENDE ANALYSES (24 Oxygen) BW84-25 RSgd (continued)

SMPL#	SI	AL4	AL6	TI	FE	MN	MG	CA	NA	K	BA	F	FE#	NA+K
4287	6.857	1.143	0.209	0.136	2.046	0.108	2.690	1.932	0.247	0.157	0.006	0.056	0.432	0.404
4288	6.791	1.209	0.241	0.143	2.127	0.098	2.585	1.930	0.253	0.167	0.007	0.061	0.451	0.420
4289	6.709	1.291	0.277	0.136	2.169	0.099	2.514	1.932	0.282	0.185	0.008	0.062	0.463	0.467
4290	6.719	1.281	0.331	0.107	2.187	0.093	2.500	1.918	0.262	0.186	0.005	0.052	0.467	0.448
4294	6.708	1.292	0.314	0.114	2.209	0.103	2.486	1.933	0.224	0.190	0.007	0.038	0.471	0.414
4295	6.659	1.341	0.443	0.125	2.231	0.095	2.457	1.676	0.202	0.378	0.007	0.058	0.476	0.580
4296	6.694	1.306	0.429	0.142	2.214	0.090	2.458	1.642	0.198	0.433	0.008	0.043	0.474	0.631
4298	6.825	1.175	0.248	0.141	2.096	0.101	2.627	1.903	0.231	0.163	0.008	0.042	0.444	0.394
5148	6.850	1.150	0.471	0.127	2.018	0.083	2.534	1.776	0.239	0.161	0.006	0.072	0.443	0.400
5151	6.964	1.036	0.318	0.121	1.985	0.091	2.694	1.813	0.266	0.141	0.009	0.061	0.424	0.407
5153	6.939	1.061	0.300	0.151	1.966	0.093	2.694	1.818	0.250	0.157	0.005	0.058	0.422	0.407
5155	6.905	1.095	0.350	0.099	2.109	0.092	2.556	1.850	0.272	0.148	0.007	0.068	0.452	0.420
5160	6.709	1.291	0.371	0.106	2.286	0.084	2.475	1.741	0.281	0.284	0.007	0.068	0.480	0.565
5162	6.804	1.196	0.393	0.139	2.198	0.084	2.399	1.809	0.272	0.197	0.008	0.048	0.478	0.469
5165	6.853	1.147	0.402	0.119	2.239	0.093	2.364	1.815	0.244	0.188	0.005	0.091	0.486	0.432
5166	6.982	1.018	0.283	0.146	2.043	0.082	2.616	1.823	0.287	0.149	0.008	0.056	0.439	0.436
5168	6.789	1.211	0.315	0.156	2.133	0.085	2.499	1.828	0.341	0.192	0.008	0.109	0.460	0.533
5169	6.843	1.157	0.293	0.153	2.098	0.091	2.579	1.835	0.281	0.168	0.006	0.080	0.449	0.449
5177	6.797	1.203	0.305	0.159	2.115	0.107	2.519	1.852	0.265	0.194	0.003	0.052	0.456	0.459
5178	7.034	0.966	0.445	0.101	2.051	0.088	2.499	1.763	0.224	0.176	0.010	0.075	0.451	0.400
5179	6.956	1.044	0.283	0.134	2.040	0.104	2.639	1.864	0.206	0.141	0.009	0.065	0.436	0.347
5184	6.820	1.180	0.323	0.174	2.124	0.090	2.441	1.835	0.318	0.200	0.007	0.083	0.465	0.518
5188	6.797	1.203	0.603	0.111	2.070	0.087	2.406	1.717	0.202	0.170	0.008	0.038	0.462	0.372
5189	6.746	1.254	0.344	0.158	2.242	0.087	2.370	1.836	0.301	0.204	0.007	0.076	0.486	0.505
5190	6.847	1.153	0.329	0.145	2.137	0.087	2.497	1.832	0.287	0.179	0.008	0.123	0.461	0.466
AVG	6.816	1.184	0.338	0.137	2.121	0.093	2.526	1.844	0.252	0.189	0.006	0.064	0.457	0.441
STD	0.093	0.093	0.083	0.020	0.079	0.008	0.097	0.069	0.035	0.055	0.003	0.026	0.017	0.061

APPENDIX 4: HORNBLENDE ANALYSES (24 Oxygen) CA84-147 CFqmd

SMPL#	SIO2	AL2O3	TIO2	FEO	MNO	MGO	CAO	NA2O	K2O	BAO	F	CL	H2O	TOTAL
2168	44.25	9.66	1.31	17.11	0.65	10.70	11.97	1.24	1.01	0.00	0.16	nd	1.92	99.98
2169	44.44	9.31	1.29	17.60	0.62	10.76	11.86	1.19	1.10	0.15	0.14	nd	1.93	100.39
2170	44.09	9.45	1.13	17.06	0.63	10.95	11.80	1.13	0.97	0.09	0.25	nd	1.86	99.41
2174	43.88	9.12	1.55	17.44	0.63	10.79	11.88	0.93	1.12	0.07	0.10	nd	1.93	99.44
2175	45.20	8.24	1.20	15.75	0.62	11.84	11.68	1.12	0.79	0.06	0.21	nd	1.88	98.59
2176	44.25	9.69	1.51	17.13	0.58	10.68	11.76	1.08	1.10	0.01	0.10	nd	1.95	99.84
5097	45.31	9.17	1.36	17.98	0.64	10.76	11.89	1.28	1.22	0.09	0.23	0.15	1.89	101.97
5103	44.78	9.18	0.99	17.85	0.65	10.74	11.73	1.09	1.05	0.13	0.14	0.24	1.85	100.42
5104	44.50	9.64	1.03	17.64	0.65	10.52	11.44	1.66	1.08	0.13	0.10	0.14	1.90	100.43
5105	44.91	8.98	1.31	18.21	0.66	10.59	11.64	1.18	1.13	0.12	0.20	0.21	1.85	100.99
5106	44.74	9.04	1.68	17.59	0.65	11.01	11.59	1.04	1.19	0.17	0.21	0.26	1.83	101.00
5107	45.15	9.10	1.05	17.63	0.68	11.00	11.62	0.97	1.01	0.11	0.14	0.20	1.87	100.53
5108	44.23	9.38	1.28	17.57	0.71	10.56	11.06	0.99	1.04	0.15	0.15	0.15	1.86	99.13
5110	44.82	8.99	1.58	17.49	0.62	11.00	11.64	1.23	1.19	0.14	0.24	0.17	1.86	100.97
5111	45.73	9.05	1.53	17.54	0.68	11.08	11.74	1.45	1.13	0.10	0.23	0.23	1.87	102.36
5112	45.22	9.12	1.53	17.42	0.64	11.15	11.67	1.20	1.12	0.13	0.23	0.12	1.90	101.45
5116	44.98	9.52	1.53	17.25	0.61	10.83	11.47	1.24	1.20	0.13	0.38	0.26	1.79	101.19
5123	45.43	9.15	1.76	17.75	0.63	10.91	11.91	1.14	1.21	0.09	0.19	0.17	1.90	102.24
5124	43.39	10.86	1.50	17.20	0.63	10.63	10.99	1.03	1.04	0.13	0.15	0.32	1.80	99.67
5125	44.63	10.12	1.60	17.47	0.64	10.64	11.59	1.09	1.17	0.10	0.17	0.36	1.80	101.38
5126	45.22	9.51	1.65	17.72	0.71	10.80	11.70	1.20	1.18	0.17	0.17	0.20	1.89	102.12
5137	44.77	8.61	3.93	17.47	0.61	10.79	10.33	0.81	0.81	0.14	0.07	0.14	1.93	100.41
5138	45.21	9.26	1.52	17.44	0.66	11.20	11.98	1.18	1.03	0.13	0.08	0.19	1.92	101.80
5139	45.75	8.92	1.74	17.70	0.70	11.05	11.77	1.10	1.13	0.17	0.18	0.16	1.91	102.28
5140	45.01	9.09	1.65	17.83	0.65	10.83	11.78	1.05	1.21	0.13	0.24	0.19	1.86	101.52
AVG	44.80	9.29	1.53	17.47	0.65	10.87	11.62	1.14	1.09	0.11	0.18	0.20	1.88	
STD	0.56	0.49	0.54	0.44	0.03	0.27	0.35	0.16	0.11	0.04	0.07	0.06	0.04	

APPENDIX 4: HORNBLENDE ANALYSES (24 Oxygen) CA84-147 CFqmd

SMPL#	SI	AL4	AL6	TI	FE	MN	MG	CA	NA	K	BA	F	FE#	NA+K
2168	6.658	1.342	0.371	0.148	2.153	0.083	2.400	1.930	0.306	0.194	0.000	0.076	0.473	0.500
2169	6.671	1.329	0.317	0.146	2.209	0.079	2.407	1.907	0.361	0.211	0.009	0.066	0.479	0.572
2170	6.665	1.335	0.349	0.128	2.157	0.081	2.467	1.911	0.349	0.187	0.005	0.120	0.466	0.536
2174	6.641	1.359	0.267	0.176	2.207	0.081	2.434	1.926	0.332	0.216	0.004	0.048	0.476	0.548
2175	6.837	1.163	0.306	0.137	1.992	0.079	2.669	1.893	0.273	0.152	0.004	0.100	0.427	0.425
2176	6.650	1.350	0.366	0.171	2.153	0.074	2.392	1.894	0.326	0.211	0.001	0.048	0.474	0.537
5097	6.712	1.288	0.312	0.151	2.227	0.080	2.376	1.887	0.368	0.230	0.005	0.070	0.484	0.598
5103	6.726	1.274	0.351	0.112	2.242	0.083	2.405	1.888	0.317	0.201	0.008	0.114	0.482	0.518
5104	6.682	1.318	0.388	0.116	2.215	0.083	2.355	1.841	0.483	0.207	0.008	0.066	0.485	0.690
5105	6.724	1.276	0.308	0.147	2.280	0.084	2.363	1.867	0.343	0.216	0.007	0.099	0.491	0.559
5106	6.686	1.314	0.277	0.189	2.198	0.082	2.452	1.856	0.301	0.227	0.010	0.123	0.473	0.528
5107	6.754	1.246	0.358	0.118	2.206	0.086	2.453	1.862	0.281	0.193	0.006	0.095	0.473	0.474
5108	6.714	1.286	0.392	0.146	2.230	0.091	2.389	1.799	0.291	0.201	0.009	0.072	0.483	0.492
5110	6.697	1.303	0.280	0.178	2.186	0.078	2.450	1.864	0.356	0.227	0.008	0.080	0.472	0.583
5111	6.731	1.269	0.300	0.169	2.159	0.085	2.431	1.851	0.414	0.212	0.006	0.107	0.470	0.626
5112	6.710	1.290	0.304	0.171	2.162	0.080	2.466	1.855	0.345	0.212	0.008	0.056	0.467	0.557
5116	6.697	1.303	0.367	0.171	2.148	0.077	2.403	1.830	0.358	0.228	0.008	0.122	0.472	0.586
5123	6.699	1.301	0.289	0.195	2.189	0.079	2.398	1.882	0.326	0.228	0.005	0.079	0.477	0.554
5124	6.544	1.456	0.474	0.170	2.169	0.080	2.390	1.776	0.301	0.200	0.008	0.153	0.476	0.501
5125	6.630	1.370	0.402	0.179	2.170	0.081	2.356	1.845	0.314	0.222	0.006	0.169	0.479	0.536
5126	6.677	1.323	0.332	0.183	2.188	0.089	2.377	1.851	0.344	0.222	0.010	0.093	0.479	0.566
5137	6.673	1.327	0.185	0.440	2.178	0.077	2.397	1.650	0.234	0.154	0.008	0.066	0.476	0.388
5138	6.682	1.318	0.295	0.169	2.156	0.083	2.467	1.897	0.338	0.194	0.008	0.089	0.466	0.532
5139	6.736	1.264	0.284	0.193	2.180	0.087	2.425	1.857	0.314	0.212	0.010	0.075	0.473	0.526
5140	6.695	1.305	0.288	0.185	2.218	0.082	2.401	1.877	0.303	0.230	0.008	0.089	0.480	0.533
AVG	6.692	1.308	0.326	0.172	2.183	0.082	2.421	1.860	0.331	0.207	0.007	0.091	0.474	0.539
STD	0.051	0.051	0.056	0.060	0.050	0.004	0.061	0.055	0.047	0.020	0.003	0.030	0.011	0.059

APPENDIX 4: HORNBLENDE ANALYSES (24 Oxygen) CA84-45 m encl

SMPL#	SIO2	AL2O3	TIO2	FEO	MNO	MGO	CAO	NA2O	K2O	BAO	F	CL	H2O	TOTAL
5230	47.55	8.21	0.81	16.15	0.93	12.19	11.73	0.97	0.88	0.13	0.03	0.28	1.91	101.77
5214	47.26	10.82	0.75	14.12	0.88	11.69	11.02	1.05	0.60	0.11	0.07	0.19	1.95	100.51
5201	48.51	6.57	0.80	15.47	1.09	12.98	11.65	0.94	0.60	0.19	0.04	0.22	1.93	100.99
5208	47.79	6.98	0.79	15.45	1.06	12.58	11.40	0.96	0.63	0.13	0.03	0.49	1.78	100.07
5199	46.33	8.14	0.68	16.53	0.97	11.50	11.15	0.80	0.77	0.14	0.05	0.18	1.90	99.14
5203	46.91	8.31	0.90	16.04	0.96	11.93	11.24	0.86	0.86	0.14	0.03	0.27	1.89	100.34
5197	46.94	7.71	0.81	15.86	0.92	11.84	11.37	0.84	0.73	0.08	0.07	0.26	1.86	99.29
5209	47.67	7.27	0.74	15.54	1.05	12.38	11.23	1.02	0.64	0.15	0.03	0.20	1.92	99.84
5193	48.36	6.84	0.96	15.26	1.06	12.61	11.54	0.98	0.62	0.16	0.03	0.20	1.94	100.56
5217	47.82	7.92	0.68	16.10	0.93	12.11	11.96	1.13	0.73	0.12	0.03	0.21	1.94	101.68
5192	47.27	6.71	0.86	14.81	0.99	12.35	11.39	0.89	0.64	0.12	0.07	0.16	1.90	98.16
5232	47.33	9.10	0.95	14.74	0.96	12.18	11.26	1.00	0.63	0.13	0.04	0.17	1.95	100.44
5244	48.90	7.32	0.85	15.43	0.97	12.79	12.18	0.87	0.65	0.12	0.01	0.25	1.95	102.29
5202	47.25	7.09	0.84	15.39	0.99	12.32	11.34	0.98	0.64	0.10	0.06	0.31	1.84	99.15
5236	48.18	7.72	0.80	15.60	1.05	12.41	12.12	1.07	0.70	0.12	0.05	0.24	1.93	101.99
5215	48.58	7.59	0.69	15.76	1.03	12.50	11.99	0.90	0.67	0.09	0.02	0.20	1.96	101.98
5229	48.31	7.82	0.97	15.63	1.06	12.33	12.11	1.11	0.73	0.13	0.03	0.23	1.95	102.41
5207	46.02	7.87	0.89	16.05	0.92	11.60	11.26	1.05	0.76	0.16	0.06	0.38	1.79	98.81
5233	48.57	7.17	0.64	15.59	1.04	12.70	11.90	1.13	0.64	0.12	0.02	0.15	1.98	101.65
AVG	47.66	7.75	0.81	15.55	0.99	12.26	11.57	0.98	0.69	0.13	0.04	0.24	1.91	
STD	0.77	0.95	0.10	0.55	0.06	0.40	0.36	0.10	0.08	0.02	0.02	0.08	0.05	

APPENDIX 4: HORNBLENDE ANALYSES (24 Oxygen) CA84-45 m encl

SMPL#	SI	AL4	AL6	TI	FE	MN	MG	CA	NA	K	BA	F	FE#	NA+K
5192	7.113	0.887	0.302	0.097	1.864	0.126	2.770	1.836	0.260	0.123	0.007	0.076	0.402	0.383
5193	7.108	0.892	0.292	0.106	1.876	0.132	2.762	1.817	0.279	0.116	0.009	0.093	0.404	0.395
5197	7.015	0.985	0.373	0.091	1.982	0.116	2.637	1.821	0.243	0.139	0.005	0.123	0.429	0.382
5199	6.958	1.042	0.399	0.077	2.076	0.123	2.574	1.794	0.233	0.148	0.008	0.086	0.446	0.381
5201	7.111	0.889	0.246	0.088	1.897	0.135	2.836	1.830	0.267	0.112	0.011	0.102	0.401	0.379
5202	7.061	0.939	0.310	0.094	1.923	0.125	2.744	1.816	0.284	0.122	0.006	0.147	0.412	0.406
5203	6.945	1.055	0.395	0.100	1.986	0.120	2.633	1.783	0.247	0.162	0.008	0.126	0.430	0.409
5207	6.945	1.055	0.344	0.101	2.026	0.118	2.609	1.821	0.307	0.146	0.009	0.181	0.437	0.453
5208	7.079	0.921	0.298	0.088	1.914	0.133	2.778	1.809	0.276	0.119	0.008	0.230	0.408	0.395
5209	7.068	0.932	0.338	0.083	1.927	0.132	2.736	1.784	0.293	0.121	0.009	0.094	0.413	0.414
5214	6.880	1.120	0.736	0.082	1.719	0.109	2.536	1.719	0.296	0.111	0.006	0.087	0.404	0.407
5215	7.051	0.949	0.349	0.075	1.913	0.127	2.704	1.865	0.253	0.124	0.005	0.092	0.414	0.377
5217	6.989	1.011	0.353	0.075	1.968	0.115	2.638	1.873	0.320	0.136	0.007	0.097	0.427	0.456
5229	6.997	1.003	0.331	0.106	1.893	0.130	2.662	1.879	0.312	0.135	0.007	0.105	0.416	0.447
5230	6.948	1.052	0.361	0.089	1.973	0.115	2.655	1.836	0.275	0.164	0.007	0.129	0.426	0.439
5232	6.936	1.064	0.508	0.105	1.807	0.119	2.661	1.768	0.284	0.118	0.007	0.079	0.404	0.402
5233	7.074	0.926	0.304	0.070	1.899	0.128	2.757	1.857	0.319	0.119	0.007	0.069	0.408	0.438
5236	7.007	0.993	0.330	0.087	1.897	0.129	2.690	1.889	0.302	0.130	0.007	0.110	0.414	0.432
5244	7.067	0.933	0.313	0.092	1.865	0.119	2.755	1.886	0.244	0.120	0.007	0.114	0.404	0.364
AVG	7.019	0.981	0.362	0.090	1.916	0.124	2.691	1.825	0.279	0.130	0.007	0.113	0.416	0.408
STD	0.068	0.068	0.103	0.011	0.077	0.007	0.076	0.043	0.026	0.015	0.001	0.038	0.013	0.028

APPENDIX 4: HORNBLENDE ANALYSES (24 Oxygen) BW84-29 m encl

SMPL#	SIO2	AL2O3	TIO2	FEO	MNO	MGO	CAO	NA2O	K2O	BAO	F	CL	H2O	TOTAL
1435	46.77	7.86	0.98	15.94	0.94	12.42	11.87	1.16	0.71	0.00	0.10	nd	1.98	100.73
1436	45.50	8.64	0.99	16.37	0.97	11.52	11.87	1.18	0.83	0.00	0.14	nd	1.94	99.95
1437	46.06	8.36	0.95	16.45	1.00	11.63	11.97	1.13	0.80	0.07	0.16	nd	1.94	100.52
1440	45.14	8.77	1.04	16.42	0.97	11.54	11.94	1.10	0.82	0.10	0.14	nd	1.93	99.91
1441	45.16	8.66	1.01	16.68	0.96	11.39	11.94	0.80	0.84	0.04	0.37	nd	1.82	99.67
4012	47.26	8.14	1.01	16.55	0.94	12.19	11.76	1.10	0.85	0.00	0.05	0.13	1.97	101.95
4013	46.80	8.45	1.16	16.66	1.06	12.04	11.81	0.95	0.85	0.00	0.03	0.12	1.98	101.91
4014	46.01	11.50	0.87	16.44	0.88	11.45	11.48	1.00	0.84	0.01	0.04	0.10	2.01	102.63
4020	46.27	8.46	0.85	16.07	0.92	12.58	10.43	0.90	1.02	0.07	0.04	0.09	1.96	99.66
4021	45.01	10.40	1.44	17.03	0.89	10.43	10.80	0.96	1.04	0.00	0.06	0.15	1.92	100.13
4027	46.57	8.53	0.87	16.91	0.92	11.85	11.95	1.08	0.83	0.03	0.03	0.09	1.99	101.65
4028	46.88	8.55	0.84	16.51	0.88	12.11	11.99	0.92	0.82	0.03	0.04	0.10	1.99	101.66
4029	47.53	8.05	0.88	16.28	0.96	12.19	11.87	0.93	0.78	0.03	0.03	0.10	1.99	101.62
4035	46.49	8.28	0.86	16.31	0.93	11.96	11.58	1.03	0.82	0.09	0.04	0.09	1.97	100.45
4036	46.60	8.19	0.88	16.37	0.92	11.94	11.63	0.86	0.80	0.05	0.03	0.11	1.96	100.34
4037	46.24	8.60	0.94	16.58	0.88	11.87	11.54	1.06	0.85	0.07	0.03	0.14	1.95	100.75
4038	46.22	8.66	1.02	16.77	0.90	11.84	11.62	1.12	0.88	0.02	0.03	0.09	1.98	101.15
4039	46.48	8.43	1.06	16.69	0.96	12.05	11.73	0.93	0.85	0.04	0.03	0.07	1.99	101.31
4040	47.13	8.30	1.11	16.50	0.97	12.17	11.87	0.85	0.82	0.05	0.03	0.13	1.98	101.91
4044	47.36	8.56	1.05	16.71	0.97	11.92	12.04	1.05	0.89	0.06	0.03	0.12	2.00	102.76
4049	46.99	8.18	0.93	16.25	0.92	12.29	11.90	1.14	0.81	0.04	0.04	0.54	1.78	101.81
4052	45.64	10.20	0.96	16.32	0.82	11.58	11.47	1.13	0.89	0.00	0.05	0.24	1.91	101.21
4055	46.30	8.92	0.68	16.90	0.96	11.82	11.87	0.95	0.87	0.06	0.04	0.13	1.96	101.46
4064	44.73	10.23	1.12	16.50	0.99	11.47	11.33	1.08	0.91	0.00	0.07	0.14	1.93	100.50
4067	46.63	8.31	1.01	16.47	0.92	11.98	11.62	1.07	0.85	0.03	0.04	0.16	1.94	101.03
4071	46.47	8.56	0.94	16.32	0.95	11.99	11.69	1.12	0.85	0.01	0.03	0.12	1.96	101.01
4076	45.24	10.90	0.86	15.61	0.86	11.53	11.07	1.07	0.78	0.04	0.07	0.15	1.93	100.11
AVG	46.28	8.84	0.97	16.47	0.93	11.84	11.65	1.02	0.85	0.03	0.07	0.14	1.95	
STD	0.75	0.91	0.14	0.29	0.05	0.41	0.37	0.10	0.06	0.03	0.07	0.09	0.05	

APPENDIX 4: HORNBLENDE ANALYSES (24 Oxygen) BW84-29 m encl

SMPL#	SI	AL4	AL6	TI	FE	MN	MG	CA	NA	K	BA	F	FE#	NA+K
1435	6.908	1.092	0.275	0.109	1.969	0.118	2.734	1.878	0.301	0.134	0.000	0.047	0.419	0.435
1436	6.803	1.197	0.326	0.111	2.047	0.123	2.567	1.902	0.336	0.158	0.000	0.066	0.444	0.494
1437	6.845	1.155	0.309	0.106	2.044	0.126	2.576	1.906	0.340	0.152	0.004	0.075	0.442	0.492
1440	6.762	1.238	0.310	0.117	2.057	0.123	2.577	1.916	0.328	0.157	0.006	0.066	0.444	0.485
1441	6.776	1.224	0.307	0.114	2.093	0.122	2.547	1.919	0.320	0.161	0.002	0.176	0.451	0.481
4012	6.905	1.095	0.306	0.111	2.022	0.116	2.655	1.841	0.312	0.158	0.000	0.060	0.432	0.470
4013	6.849	1.151	0.306	0.128	2.039	0.131	2.626	1.852	0.270	0.159	0.000	0.056	0.437	0.429
4014	6.655	1.345	0.615	0.095	1.989	0.108	2.468	1.779	0.280	0.155	0.001	0.046	0.446	0.435
4020	6.889	1.111	0.374	0.095	2.001	0.116	2.792	1.664	0.260	0.194	0.004	0.042	0.417	0.454
4021	6.711	1.289	0.538	0.161	2.123	0.112	2.318	1.725	0.278	0.198	0.000	0.071	0.478	0.476
4027	6.844	1.156	0.321	0.096	2.078	0.115	2.596	1.882	0.308	0.156	0.002	0.042	0.445	0.464
4028	6.867	1.133	0.343	0.093	2.022	0.109	2.644	1.882	0.261	0.153	0.002	0.046	0.433	0.414
4029	6.949	1.051	0.335	0.097	1.990	0.119	2.656	1.859	0.264	0.145	0.002	0.046	0.428	0.409
4035	6.893	1.107	0.339	0.096	2.022	0.117	2.643	1.839	0.296	0.155	0.005	0.042	0.433	0.451
4036	6.911	1.089	0.342	0.098	2.030	0.116	2.639	1.848	0.247	0.151	0.003	0.052	0.435	0.398
4037	6.845	1.155	0.346	0.105	2.053	0.110	2.619	1.830	0.304	0.161	0.004	0.066	0.439	0.465
4038	6.822	1.178	0.329	0.113	2.070	0.113	2.605	1.838	0.321	0.166	0.001	0.042	0.443	0.487
4039	6.844	1.156	0.307	0.117	2.055	0.120	2.645	1.851	0.266	0.160	0.002	0.033	0.437	0.426
4040	6.885	1.115	0.314	0.122	2.016	0.120	2.650	1.858	0.241	0.153	0.003	0.060	0.432	0.394
4044	6.872	1.128	0.336	0.115	2.028	0.119	2.578	1.872	0.295	0.165	0.003	0.055	0.440	0.460
4049	6.887	1.113	0.300	0.103	1.992	0.114	2.685	1.869	0.324	0.151	0.002	0.250	0.426	0.475
4052	6.716	1.284	0.484	0.106	2.008	0.102	2.540	1.808	0.322	0.167	0.000	0.112	0.442	0.489
4055	6.819	1.181	0.367	0.075	2.082	0.120	2.595	1.873	0.271	0.163	0.003	0.061	0.445	0.434
4064	6.649	1.351	0.441	0.125	2.051	0.125	2.541	1.805	0.311	0.173	0.000	0.066	0.447	0.484
4067	6.879	1.121	0.324	0.112	2.032	0.115	2.634	1.837	0.306	0.160	0.002	0.075	0.435	0.466
4071	6.854	1.146	0.342	0.104	2.013	0.119	2.636	1.847	0.320	0.160	0.001	0.056	0.433	0.480
4076	6.696	1.304	0.597	0.096	1.932	0.108	2.544	1.755	0.307	0.147	0.002	0.070	0.432	0.454
AVG	6.827	1.173	0.364	0.108	2.032	0.117	2.604	1.842	0.296	0.160	0.002	0.070	0.438	0.456
STD	0.079	0.079	0.089	0.015	0.039	0.006	0.085	0.057	0.028	0.013	0.002	0.045	0.011	0.029

APPENDIX 4: HORNBLENDE ANALYSES (24 Oxygen) CA84-65A mdike

SMPL#	SIO2	AL2O3	TIO2	FEO	MNO	MGO	CAO	NA2O	K2O	BAO	F	CL	H2O	TOTAL
1392	45.49	9.48	1.39	17.25	0.52	11.15	12.00	0.82	0.93	0.11	0.20	nd	1.93	101.27
1393	45.37	9.06	1.46	16.85	0.58	11.45	11.80	0.89	0.98	0.00	0.14	nd	1.95	100.53
1397	46.38	8.85	1.43	16.63	0.51	11.62	11.87	0.94	0.95	0.02	0.00	nd	2.04	101.24
1398	45.12	9.94	1.57	17.57	0.56	11.03	11.79	1.05	1.05	0.06	0.06	nd	2.00	101.80
4100	46.26	9.27	1.32	16.41	0.54	12.18	11.72	1.31	0.96	0.00	0.07	0.21	1.94	102.19
4101	47.07	8.70	1.15	16.49	0.51	12.11	12.15	1.10	0.91	0.09	0.07	0.08	2.00	102.43
4109	45.59	9.62	1.50	16.80	0.50	11.34	11.92	1.14	1.08	0.07	0.08	0.09	1.97	101.70
4110	46.71	9.04	1.29	16.66	0.59	11.67	11.82	1.20	0.92	0.03	0.09	0.08	1.99	102.09
4111	45.73	9.22	1.45	16.80	0.55	11.53	11.96	1.22	0.99	0.07	0.09	0.05	1.99	101.65
4112	47.00	8.59	1.32	16.38	0.49	11.98	11.93	1.05	0.94	0.06	0.07	0.07	2.00	101.88
AVG	46.07	9.18	1.39	16.78	0.54	11.61	11.90	1.07	0.97	0.05	0.09	0.10	1.98	
STD	0.67	0.40	0.11	0.36	0.03	0.37	0.12	0.15	0.05	0.04	0.05	0.05	0.03	

SMPL#	SI	AL4	AL6	TI	FE	MN	MG	CA	NA	K	BA	F	FE#	NA+K
1392	6.724	1.276	0.376	0.155	2.132	0.065	2.457	1.901	0.235	0.175	0.006	0.094	0.465	0.410
1393	6.747	1.253	0.334	0.163	2.095	0.073	2.538	1.880	0.236	0.186	0.000	0.066	0.452	0.422
1397	6.820	1.180	0.353	0.158	2.045	0.064	2.547	1.870	0.254	0.178	0.001	0.000	0.445	0.432
1398	6.652	1.348	0.379	0.174	2.166	0.070	2.424	1.862	0.269	0.197	0.003	0.028	0.472	0.466
4100	6.748	1.252	0.341	0.145	2.002	0.067	2.648	1.832	0.370	0.179	0.000	0.097	0.431	0.549
4101	6.843	1.157	0.334	0.126	2.005	0.063	2.624	1.893	0.310	0.169	0.005	0.037	0.433	0.479
4109	6.705	1.295	0.372	0.166	2.066	0.062	2.486	1.878	0.325	0.203	0.004	0.042	0.454	0.528
4110	6.817	1.183	0.372	0.142	2.033	0.073	2.539	1.848	0.340	0.171	0.002	0.037	0.445	0.511
4111	6.729	1.271	0.328	0.160	2.067	0.069	2.529	1.886	0.348	0.186	0.004	0.023	0.450	0.534
4112	6.861	1.139	0.339	0.145	2.000	0.061	2.607	1.866	0.297	0.175	0.003	0.032	0.434	0.472
AVG	6.765	1.235	0.353	0.153	2.061	0.067	2.540	1.872	0.298	0.182	0.003	0.046	0.448	0.480
STD	0.064	0.064	0.019	0.013	0.054	0.004	0.068	0.020	0.046	0.011	0.002	0.029	0.013	0.047

APPENDIX 4: HORNBLENDE ANALYSES (24 Oxygen) CA84-114 cg encl

SMPL#	SIO2	AL2O3	TIO2	FEO	MNO	MGO	CAO	NA2O	K2O	BAO	F	CL	H2O	TOTAL
1459	49.03	6.49	0.95	11.80	0.33	14.99	12.31	0.82	0.57	0.11	0.00	nd	2.06	99.46
1460	48.59	6.61	0.94	11.69	0.26	14.80	12.29	0.76	0.58	0.03	0.16	nd	1.97	98.68
1461	48.63	6.33	1.02	11.61	0.23	14.25	12.12	0.88	0.58	0.02	0.22	nd	1.92	97.81
1462	48.63	6.34	1.03	12.20	0.27	13.50	12.19	0.83	0.60	0.00	0.00	nd	2.02	97.61
1463	48.56	6.24	0.91	12.23	0.27	14.68	12.20	1.64	0.58	0.04	0.14	nd	1.97	99.46
AVG	48.69	6.40	0.97	11.91	0.27	14.44	12.22	0.99	0.58	0.04	0.10		1.99	
STD	0.17	0.13	0.05	0.26	0.03	0.53	0.07	0.33	0.01	0.04	0.09		0.05	

SMPL#	SI	AL4	AL6	TI	FE	MN	MG	CA	NA	K	BA	F	FE#	NA+K
1459	7.145	0.855	0.259	0.104	1.438	0.041	3.256	1.922	0.226	0.106	0.006	0.000	0.306	0.332
1460	7.132	0.868	0.276	0.104	1.435	0.032	3.238	1.933	0.233	0.109	0.002	0.074	0.307	0.342
1461	7.205	0.795	0.310	0.114	1.439	0.029	3.147	1.924	0.218	0.110	0.001	0.103	0.314	0.328
1462	7.222	0.778	0.331	0.115	1.515	0.034	2.988	1.940	0.253	0.114	0.000	0.000	0.336	0.367
1463	7.154	0.846	0.237	0.101	1.507	0.034	3.223	1.926	0.237	0.109	0.002	0.065	0.319	0.346
AVG	7.172	0.828	0.283	0.108	1.467	0.034	3.170	1.929	0.233	0.110	0.002	0.048	0.316	0.343
STD	0.035	0.035	0.034	0.006	0.036	0.004	0.098	0.007	0.012	0.003	0.002	0.041	0.011	0.014

APPENDIX 4: HORNBLENDE ANALYSES (24 Oxygen) BW84-27 cg encl

SMPL#	SIO2	AL2O3	TIO2	FEO	MNO	MGO	CAO	NA2O	K2O	BAO	F	CL	H2O	TOTAL
1375	44.94	11.10	1.23	14.05	0.35	11.79	11.65	0.60	0.84	0.05	0.06	nd	1.99	98.65
1376	46.82	8.19	1.32	15.00	0.35	12.18	12.28	0.66	0.87	0.06	0.06	nd	2.00	99.79
1379	47.79	8.12	1.07	14.57	0.25	12.81	12.28	0.54	0.76	0.01	0.06	nd	2.02	100.28
1385	48.53	6.75	0.68	14.15	0.36	13.76	12.26	0.67	0.57	0.03	0.00	nd	2.04	99.80
1386	48.54	8.06	0.80	14.33	0.34	13.51	12.09	0.82	0.63	0.04	0.00	nd	2.07	101.23
AVG	47.32	8.44	1.02	14.42	0.33	12.81	12.11	0.66	0.73	0.04	0.04		2.02	
STD	1.35	1.43	0.25	0.34	0.04	0.75	0.24	0.09	0.12	0.02	0.03		0.03	

SMPL#	SI	AL4	AL6	TI	FE	MN	MG	CA	NA	K	BA	F	FE#	NA+K
1386	7.023	0.977	0.398	0.087	1.734	0.042	2.914	1.874	0.188	0.116	0.002	0.000	0.373	0.304
1379	6.987	1.013	0.386	0.118	1.781	0.031	2.792	1.924	0.187	0.142	0.001	0.028	0.389	0.329
1376	6.928	1.072	0.357	0.147	1.856	0.044	2.686	1.947	0.172	0.164	0.003	0.028	0.409	0.336
1375	6.683	1.317	0.628	0.138	1.747	0.044	2.613	1.856	0.193	0.159	0.003	0.028	0.401	0.352
1385	7.123	0.877	0.291	0.075	1.737	0.045	3.010	1.928	0.154	0.107	0.002	0.000	0.366	0.261
AVG	6.949	1.051	0.412	0.113	1.771	0.041	2.803	1.906	0.179	0.138	0.002	0.017	0.388	0.316
STD	0.147	0.147	0.114	0.028	0.046	0.005	0.145	0.035	0.014	0.023	0.001	0.014	0.016	0.032

APPENDIX 4: GARNET ANALYSES (12 Oxygens) CA84-102 gap

SMPL#	SiO2	TiO2	Al2O3	FeO	MnO	MgO	CaO	Na2O	TOTAL
3018	38.05	0.24	18.41	16.57	24.64	1.46	0.84	0.03	100.24
3019	37.19	0.30	18.48	16.56	24.85	1.44	0.65	0.04	99.51
3315	37.32	0.56	18.76	16.37	24.43	1.44	0.69	0.00	99.57
3316	37.39	0.10	18.89	16.08	24.94	1.30	0.81	0.00	99.51
3317	37.28	0.51	19.24	16.42	24.86	1.30	0.69	0.02	100.32
3318	37.24	0.32	18.74	16.11	24.81	1.30	0.65	0.03	99.20
3319	37.18	0.50	19.21	16.35	24.71	1.41	0.68	0.00	100.04
AVG	37.38	0.36	18.82	16.35	24.75	1.38	0.72	0.02	99.84
STD	0.28	0.16	0.30	0.18	0.16	0.07	0.07	0.02	0.38

	Si	Ti	Al4	Al6	Fe3+	Fe2+	Mn	Mg	Ca	Na	ALM	PYR	SPES	GROS
3315	3.065	0.035	0.000	1.816	0.184	0.940	1.700	0.176	0.061	0.000	36.72	5.75	55.54	1.99
3316	3.076	0.006	0.000	1.831	0.169	0.937	1.738	0.159	0.071	0.000	35.98	5.17	56.54	2.31
3317	3.045	0.031	0.000	1.852	0.148	0.973	1.720	0.158	0.060	0.003	36.65	5.17	56.23	1.96
3318	3.071	0.020	0.000	1.821	0.179	0.932	1.733	0.160	0.057	0.005	36.30	5.23	56.62	1.86
3319	3.045	0.031	0.000	1.854	0.146	0.974	1.714	0.172	0.060	0.000	36.53	5.61	55.90	1.96
3018	3.104	0.015	0.000	1.770	0.230	0.900	1.702	0.178	0.073	0.005	36.65	5.77	55.21	2.37
3019	3.068	0.019	0.000	1.796	0.204	0.939	1.736	0.177	0.057	0.006	36.72	5.69	55.77	1.83
AVG	3.068	0.022	0.000	1.820	0.180	0.942	1.720	0.169	0.063	0.003	36.51	5.48	55.97	2.04
STD	0.019	0.010	0.000	0.028	0.028	0.024	0.015	0.008	0.006	0.002	0.25	0.26	0.48	0.20

APPENDIX 4: GARNET ANALYSES (12 Oxygens) CA84-28 gap

SMPL#	SiO2	TiO2	Al2O3	FeO	MnO	MgO	CaO	Na2O	TOTAL
3430	36.87	0.13	20.81	21.59	20.86	1.35	0.51	0.00	102.12
3431	36.36	0.28	20.66	20.59	22.50	1.27	0.52	0.04	102.22
3432	36.88	0.28	20.37	20.52	23.74	1.28	0.52	0.01	103.60
3437	37.03	0.09	21.94	20.61	21.92	1.37	0.46	0.01	103.43
3438	36.44	0.17	20.86	20.23	23.35	1.30	0.49	0.02	102.86

APPENDIX 4: GARNET ANALYSES (12 Oxygens) CA84-28 gap (continued)

SMPL#	SiO2	TiO2	Al2O3	FeO	MnO	MgO	CaO	Na2O	TOTAL
3439	36.60	0.08	21.15	20.28	22.83	1.35	0.43	0.02	102.74
3440	36.66	0.18	21.02	21.10	22.21	1.38	0.52	0.00	103.07
3441	36.66	0.20	21.03	20.54	22.40	1.38	0.46	0.02	102.69
3443	36.37	0.18	21.03	20.61	22.51	1.34	0.49	0.00	102.53
AVG	36.65	0.18	20.99	20.67	22.48	1.34	0.49	0.01	102.81
STD	0.22	0.07	0.40	0.40	0.78	0.04	0.03	0.01	0.47

SMPL#	Si	Ti	Al4	Al6	Fe3+	Fe2+	Mn	Mg	Ca	Na	ALM	PYR	SPES	GROS
3430	2.966	0.008	0.026	1.947	0.053	1.399	1.421	0.162	0.044	0.000	47.16	5.26	46.15	1.43
3431	2.935	0.017	0.048	1.918	0.082	1.308	1.539	0.153	0.045	0.006	44.45	4.89	49.22	1.44
3432	2.949	0.017	0.034	1.885	0.115	1.257	1.608	0.153	0.045	0.002	43.17	4.81	50.60	1.42
3437	2.934	0.005	0.061	1.987	0.013	1.353	1.471	0.162	0.039	0.002	44.96	5.33	48.42	1.28
3438	2.929	0.010	0.061	1.915	0.085	1.274	1.590	0.156	0.042	0.003	43.18	4.96	50.52	1.33
3439	2.935	0.005	0.060	1.939	0.061	1.299	1.551	0.161	0.037	0.003	43.74	5.18	49.89	1.19
3440	2.933	0.011	0.056	1.926	0.074	1.338	1.505	0.165	0.045	0.000	45.16	5.28	48.13	1.44
3441	2.940	0.012	0.048	1.940	0.060	1.317	1.522	0.165	0.040	0.003	44.36	5.32	49.03	1.29
3443	2.926	0.011	0.063	1.930	0.070	1.317	1.534	0.161	0.042	0.000	44.40	5.15	49.10	1.34
AVG	2.939	0.011	0.051	1.932	0.068	1.318	1.527	0.160	0.042	0.002	44.51	5.13	49.01	1.35
STD	0.011	0.004	0.012	0.026	0.026	0.040	0.054	0.004	0.003	0.002	1.15	0.18	1.29	0.08

APPENDIX 4: GARNET ANALYSES (12 Oxygens) CA84-46 gap

SMPL#	SiO2	TiO2	Al2O3	FeO	MnO	MgO	CaO	Na2O	TOTAL
4479	35.97	0.46	19.82	12.89	30.03	1.20	0.87	0.01	101.25
4480	35.69	0.65	19.80	12.99	29.50	1.25	0.87	0.05	100.80

SMPL#	Si	Ti	Al4	Al6	Fe3+	Fe2+	Mn	Mg	Ca	Na	ALM	PYR	SPES	GROS
4479	2.941	0.028	0.031	1.878	0.122	0.759	2.079	0.146	0.076	0.002	27.69	4.59	65.34	2.39
4480	2.931	0.040	0.029	1.887	0.113	0.779	2.052	0.153	0.077	0.008	28.10	4.82	64.65	2.43

APPENDIX 4: MUSCOVITE ANALYSES (24 Oxygens) CA84-28 gap

SMPL#	SiO2	TiO2	Al2O3		FeO	MnO	MgO	CaO	Na2O	K2O	F	H2O	TOTAL
	45.03	0.38	32.73		4.35	0.04	1.17	0.05	0.43	9.89	0.20	4.28	98.55
3425	46.55	0.11	31.24		4.18	0.10	1.07	0.02	0.13	10.12	0.18	4.28	97.98
3434	45.69	0.71	31.45		4.63	0.11	1.41	0.03	0.31	9.07	0.18	4.27	97.86
3435	45.45	0.81	31.67		4.69	0.12	1.39	0.04	0.41	9.65	0.19	4.29	98.71
3451	43.10	0.05	35.28		3.91	0.08	1.07	0.06	0.42	9.70	0.14	4.29	98.10
3459	44.77	0.57	33.66		3.81	0.06	0.85	0.03	0.27	9.30	0.13	4.31	97.76
3460	43.82	0.67	32.88		4.08	0.07	1.04	0.06	0.40	9.83	0.10	4.27	97.22
3461	43.03	0.42	33.61		3.89	0.06	0.89	0.05	0.32	9.92	0.14	4.20	96.53
3462	42.98	0.41	34.62		3.98	0.06	0.95	0.07	0.48	9.56	0.12	4.27	97.50
AVG	44.49	0.46	33.02		4.17	0.08	1.09	0.05	0.35	9.67	0.15	4.27	97.80
STD	1.24	0.25	1.33		0.30	0.03	0.19	0.02	0.10	0.31	0.03	0.03	0.63

SMPL#	Si	Ti	Al4	Al6	Fe	Mn	Mg	Ca	Na	K	F	H	Fe#
3424	6.164	0.039	1.836	3.444	0.498	0.005	0.239	0.007	0.114	1.727	0.087	3.909	0.676
3425	6.389	0.011	1.611	3.442	0.480	0.012	0.219	0.003	0.035	1.772	0.078	3.919	0.687
3434	6.273	0.073	1.727	3.361	0.532	0.013	0.289	0.004	0.083	1.588	0.078	3.911	0.648
3435	6.216	0.083	1.784	3.321	0.536	0.014	0.283	0.006	0.109	1.683	0.082	3.914	0.654
3451	5.916	0.005	2.084	3.623	0.449	0.009	0.219	0.009	0.112	1.698	0.061	3.928	0.672
3459	6.129	0.059	1.871	3.560	0.436	0.007	0.173	0.004	0.072	1.624	0.056	3.936	0.716
3460	6.080	0.070	1.920	3.455	0.473	0.008	0.215	0.009	0.108	1.739	0.044	3.952	0.688
3461	6.012	0.044	1.988	3.545	0.455	0.005	0.185	0.007	0.087	1.768	0.062	3.914	0.711
3462	5.937	0.043	2.063	3.572	0.460	0.007	0.196	0.010	0.129	1.684	0.052	3.935	0.701
AVG	6.124	0.047	1.876	3.480	0.480	0.009	0.224	0.007	0.094	1.698	0.067	3.924	0.684
STD	0.147	0.025	0.147	0.096	0.034	0.003	0.038	0.002	0.027	0.059	0.014	0.014	0.022

APPENDIX 4: FE-TI OXIDES (3 or 4 Oxygens) CA85-5 RSgr

SMPL#	TiO2	Al2O3	FeO	MnO	MgO	CaO	Cr3O4	TOTAL
3318	54.19	0.15	16.70	33.32	0.12	0.140	0.10	104.72
3319	54.60	1.19	22.96	27.96	0.16	0.130	0.11	107.11
3320	52.57	0.06	15.84	34.88	0.10	0.120	0.11	103.68
3321	0.22	0.12	91.35	0.40	0.11	0.120	0.14	92.46
3322	51.68	0.18	33.14	15.25	0.17	0.130	0.12	100.67
3323	52.21	0.06	31.78	17.63	0.15	0.100	0.06	101.99
3324	50.99	0.03	33.40	17.75	0.13	0.090	0.06	102.45
3325	48.02	0.07	27.32	16.94	0.14	0.130	0.07	92.69
3326	52.40	0.11	31.26	19.35	0.14	0.120	0.13	103.51
3393	0.29	0.23	87.21	0.22	0.11	0.130	0.08	88.27
3394	0.20	0.12	88.58	0.25	0.08	0.140	0.12	89.49
3395	0.52	0.84	86.06	0.21	0.22	0.210	0.13	88.19
3398	53.82	0.06	25.29	22.76	0.11	0.130	0.05	102.22
3399	50.82	1.57	28.29	12.89	0.28	0.220	0.11	94.18

SMPL#	Ti	Al	Fe	Mn	Mg	Ca	Cr	O	Xilm'	Xusp'
3318	0.970	0.004	0.332	0.671	0.004	0.004	0.003	3.000	0.254	0.927
3319	0.944	0.032	0.441	0.544	0.005	0.003	0.003	3.000	0.312	0.893
3320	0.950	0.002	0.318	0.710	0.004	0.003	0.003	3.000	0.201	0.882
3321	0.006	0.005	2.943	0.013	0.006	0.005	0.003	4.000	0.930	0.006
3322	0.962	0.005	0.686	0.320	0.006	0.003	0.003	3.000	0.590	0.940
3323	0.962	0.002	0.651	0.366	0.005	0.003	0.003	3.000	0.563	0.944
3324	0.935	0.001	0.681	0.366	0.005	0.002	0.002	3.000	0.540	0.910
3325	0.971	0.002	0.614	0.386	0.006	0.004	0.003	3.000	0.534	0.947
3326	0.950	0.003	0.630	0.395	0.005	0.003	0.003	3.000	0.518	0.926
3393	0.009	0.011	2.933	0.007	0.007	0.006	0.003	4.000	0.913	0.008
3394	0.006	0.006	2.952	0.008	0.005	0.006	0.002	4.000	0.942	0.006
3395	0.016	0.039	2.861	0.007	0.013	0.009	0.003	4.000	0.828	0.015
3398	0.990	0.002	0.517	0.471	0.004	0.003	0.003	3.000	0.482	0.976
3399	0.978	0.047	0.605	0.279	0.011	0.006	0.003	3.000	0.469	0.909

APPENDIX 4: FE-TI OXIDES (3 or 4 Oxygens) BW84-20a RSgr

SMPL#	TiO2	Al2O3	FeO	MnO	MgO	CaO	Cr3O4	TOTAL
1064	0.25	1.42	86.96	0.33	0.05	0.160		89.17
1065	0.22	0.10	91.92	0.34	0.00	0.130		92.71
1176	0.20	0.45	88.87	0.34	0.00	0.160		90.02
1178	0.23	0.30	88.65	0.35	0.03	0.180		89.74
1179	34.76	0.22	54.53	5.94	0.04	0.110		95.60
1180	75.71	0.58	17.61	0.28	0.01	0.100		94.29
1181	47.38	0.12	33.27	16.47	0.05	0.100		97.39
1186	0.27	0.26	89.60	0.34	0.03	0.140		90.64
1187	0.20	0.12	88.51	0.31	0.00	0.120		89.26
1188	0.20	0.21	88.50	0.28	0.00	0.140		89.33

SMPL#	Ti	Al	Fe	Mn	Mg	Ca	Cr	O	Xilm'	Xusp'
1064	0.007	0.066	2.857	0.011	0.003	0.007	0.003	4.000	0.846	0.007
1065	0.006	0.005	2.958	0.011	0.000	0.005	0.003	4.000	0.953	0.006
1176	0.006	0.021	2.928	0.011	0.000	0.007	0.003	4.000	0.915	0.006
1178	0.007	0.014	2.921	0.012	0.002	0.008	0.002	4.000	0.880	0.007
1179	0.673	0.007	1.175	0.130	0.002	0.003	0.003	3.000	0.515	0.641
1180	1.555	0.019	0.402	0.006	0.000	0.003	0.005	3.000	not	calc.
1181	0.910	0.004	0.711	0.356	0.002	0.003	0.003	3.000	0.515	0.875
1186	0.008	0.012	2.937	0.011	0.002	0.006	0.002	4.000	0.923	0.008
1187	0.006	0.006	2.962	0.011	0.000	0.005	0.002	4.000	0.967	0.006
1188	0.006	0.010	2.945	0.009	0.000	0.006	0.004	4.000	0.932	0.006

APPENDIX 4: FE-TI OXIDES (3 or 4 Oxygens) BW84-18 RSgd

SMPL#	TiO2	Al2O3	FeO	MnO	MgO	CaO	Cr3O4	TOTAL
1085	0.21	0.14	92.37	0.43	0.00	0.130		93.28
1086	0.22	0.09	89.97	0.24	0.00	0.120		90.64
1041	0.22	0.16	92.45	0.84	0.00	0.130		93.80
1045	0.27	0.40	90.51	0.93	0.01	0.140		92.26

SMPL#	Ti	Al	Fe	Mn	Mg	Ca	Cr	O	Xilm'	Xusp'
1085	0.006	0.006	2.954	0.014	0.000	0.005	0.002	4.000	0.951	0.006
1086	0.007	0.004	2.959	0.008	0.000	0.005	0.002	4.000	0.948	0.006
1041	0.006	0.007	2.940	0.027	0.000	0.005	0.005	4.000	0.944	0.006
1045	0.008	0.018	2.923	0.030	0.001	0.006	0.002	4.000	0.932	0.008

APPENDIX 4: FE-TI OXIDES (3 or 4 Oxygens) CA84-46 gap

SMPL#	TiO2	Al2O3	FeO	MnO	MgO	CaO	Cr3O4	TOTAL
3487	28.71	0.11	49.68	19.23	0.12	0.400	0.11	98.36
3489	0.23	0.41	90.24	0.41	0.12	0.100	0.12	91.63
3490	11.83	0.09	74.88	7.61	0.13	0.110	0.13	94.78
3491	12.15	0.10	73.84	8.42	0.11	0.130	0.11	94.86
3492	0.25	0.18	89.73	0.51	0.13	0.110	0.13	91.04
3493	26.60	0.13	51.66	17.37	0.11	0.220	0.08	96.17
3494	52.94	0.02	11.47	39.78	0.11	0.110	0.07	104.50
3495	0.13	0.15	90.92	0.61	0.12	0.110	0.17	92.21
3496	32.73	0.19	42.17	23.20	0.15	0.410	0.11	98.96
3497	0.15	0.13	91.57	0.63	0.10	0.130	0.14	92.85
3498	0.15	0.12	91.57	0.75	0.10	0.130	0.14	92.96
3499	0.11	0.08	91.43	0.64	0.10	0.130	0.15	92.64

SMPL#	Ti	Al	Fe	Mn	Mg	Ca	Cr	O	Xilm'	Xusp'
3487	0.533	0.003	1.025	0.402	0.004	0.011	0.002	3.000	0.057	0.265
3489	0.007	0.019	2.931	0.013	0.007	0.004	0.002	4.000	0.931	0.007
3490	0.226	0.003	1.588	0.163	0.005	0.003	0.002	3.000	0.024	0.087
3491	0.231	0.003	1.563	0.181	0.004	0.004	0.003	3.000	0.010	0.057
3492	0.007	0.008	2.935	0.017	0.008	0.005	0.002	4.000	0.924	0.007
3493	0.502	0.004	1.084	0.369	0.004	0.006	0.003	3.000	0.037	0.206
3494	0.949	0.001	0.229	0.803	0.004	0.003	0.003	3.000	0.113	0.850
3495	0.004	0.007	2.938	0.020	0.007	0.005	0.003	4.000	0.922	0.004
3496	0.605	0.006	0.866	0.483	0.005	0.011	0.003	3.000	0.041	0.277
3497	0.004	0.006	2.941	0.020	0.006	0.005	0.002	4.000	0.929	0.004
3498	0.004	0.005	2.939	0.024	0.006	0.005	0.002	4.000	0.927	0.004
3499	0.499	0.003	2.940	0.021	0.006	0.005	0.003	4.000	0.914	0.003

APPENDIX 4: FE-TI OXIDES (3 or 4 Oxygens) CA85-111 RSgr

SMPL#	TiO2	Al2O3	FeO	MnO	MgO	CaO	Cr3O4	TOTAL
3125	1.01	3.73	82.79	0.41	0.12	0.160	0.12	88.34
3126	0.16	4.08	82.88	0.39	0.17	0.250	0.11	88.04
3127	0.27	0.98	84.58	0.34	0.14	0.170	0.09	86.57
3128	0.25	0.80	87.05	0.39	0.11	0.140	0.11	88.85
3148	0.22	4.18	83.99	0.31	0.19	0.170	0.11	89.17
3149	0.22	1.16	87.21	0.37	0.13	0.150	0.13	89.37

SMPL#	Ti	Al	Fe	Mn	Mg	Ca	Cr	O	Xilm'	Xusp'
3125	0.030	0.173	2.722	0.014	0.007	0.007	0.002	4.000	0.867	0.033
3126	0.005	0.189	2.723	0.013	0.010	0.011	0.003	4.000	0.831	0.005
3127	0.008	0.047	2.862	0.012	0.008	0.007	0.003	4.000	0.822	0.008
3128	0.007	0.037	2.894	0.013	0.007	0.006	0.003	4.000	0.883	0.007
3148	0.006	0.192	2.732	0.010	0.011	0.007	0.002	4.000	0.861	0.007
3149	0.007	0.054	2.876	0.012	0.008	0.006	0.002	4.000	0.875	0.006

APPENDIX 4: FE-TI OXIDES (3 or 4 Oxygens) CA85-18 RSgr

SMPL#	TiO2	Al2O3	FeO	MnO	MgO	CaO	Cr3O4	TOTAL
3255	0.22	23.63	70.97	0.28	0.09	0.180	0.12	95.49
3256	0.33	1.04	84.27	0.34	0.18	0.210	0.06	86.43
3257	0.15	1.19	86.61	0.31	0.15	0.150	0.09	88.65
3258	0.23	0.42	88.20	0.00	0.34	0.100	0.11	89.41
3279	0.27	0.45	86.77	0.28	0.10	0.110	0.06	88.04

SMPL#	Ti	Al	Fe	Mn	Mg	Ca	Cr	O	Xilm'	Xusp'
3255	0.004	0.624	1.331	0.005	0.003	0.004	0.001	3.000		
3256	0.010	0.050	2.861	0.012	0.011	0.009	0.003	4.000	0.846	0.010
3257	0.004	0.056	2.879	0.010	0.009	0.006	0.002	4.000	0.881	0.004
3258	0.007	0.020	2.924	0.000	0.020	0.004	0.002	4.000	0.915	0.007
3279	0.008	0.021	2.935	0.010	0.006	0.005	0.003	4.000	0.951	0.008

APPENDIX 4: EQUANT APATITE ANALYSES (13 Oxygen) BW84-20a RSgr

SMPL#	SiO2	P2O5	FeO	MnO	CaO	F	TOTAL	Si	P	Fe	Mn	Ca	F
7028	0.40	39.89	0.13	0.42	55.09	2.85	98.78	0.03	2.82	0.01	0.03	4.93	0.75
7030	0.35	39.34	0.28	0.40	55.21	2.88	98.46	0.03	2.80	0.02	0.03	4.98	0.77
7031	0.39	39.77	0.39	0.50	54.83	3.14	99.02	0.03	2.81	0.03	0.04	4.91	0.83
7032	0.15	39.66	0.09	0.57	54.53	3.84	98.84	0.01	2.81	0.01	0.04	4.89	1.02
7033	0.12	38.46	0.12	0.49	54.84	3.99	98.02	0.01	2.76	0.01	0.04	4.98	1.07
7034	0.14	39.55	0.18	0.46	54.60	3.83	98.76	0.01	2.80	0.01	0.03	4.90	1.01
7035	0.16	39.20	0.26	0.31	54.90	3.92	98.75	0.01	2.79	0.02	0.02	4.94	1.04
7036	0.17	39.41	0.36	0.49	54.23	3.82	98.48	0.01	2.80	0.03	0.04	4.87	1.01
7037	0.16	38.49	0.47	0.27	55.52	3.72	98.63	0.01	2.75	0.03	0.02	5.02	0.99
7039	0.52	38.00	0.08	0.53	53.10	2.94	95.17	0.05	2.79	0.01	0.04	4.94	0.81
7040	0.30	40.64	0.11	0.60	54.42	2.73	98.80	0.03	2.86	0.01	0.04	4.85	0.72
7041	0.27	40.30	0.13	0.50	55.15	2.70	99.05	0.02	2.84	0.01	0.04	4.92	0.71
7042	0.22	40.71	0.17	0.50	55.13	2.90	99.63	0.02	2.85	0.01	0.04	4.88	0.76
7043	0.23	40.66	0.29	0.56	54.71	2.89	99.34	0.02	2.85	0.02	0.04	4.86	0.76
7044	0.09	39.33	0.05	0.38	54.65	3.43	97.93	0.01	2.82	0.00	0.03	4.95	0.92
7045	0.15	40.67	0.10	0.45	55.02	3.50	99.89	0.01	2.84	0.01	0.03	4.86	0.91
7046	0.12	40.54	0.15	0.48	54.25	3.58	99.12	0.01	2.85	0.01	0.03	4.82	0.94
7047	0.17	40.15	0.27	0.41	54.65	3.58	99.23	0.01	2.82	0.02	0.03	4.86	0.94
7048	0.18	39.93	0.51	0.45	54.25	3.78	99.10	0.02	2.82	0.04	0.03	4.84	1.00
7049	0.19	40.86	0.87	0.38	54.04	3.67	100.01	0.02	2.85	0.06	0.03	4.76	0.96
7053	0.37	39.08	0.22	0.49	54.05	3.76	97.97	0.03	2.79	0.02	0.04	4.88	1.00
7054	0.28	39.41	0.21	0.50	53.88	3.93	98.21	0.02	2.80	0.02	0.04	4.84	1.04
7056	0.28	40.22	0.27	0.46	54.02	4.01	99.26	0.02	2.82	0.02	0.03	4.79	1.05
7057	0.23	40.67	0.33	0.51	53.98	3.71	99.43	0.02	2.84	0.02	0.04	4.78	0.97
7061	0.24	40.50	0.05	0.45	51.41	3.99	96.64	0.02	2.89	0.00	0.03	4.64	1.06
AVG	0.24	39.82	0.24	0.46	54.42	3.48	98.66	0.02	2.82	0.02	0.03	4.87	0.92
STD	0.10	0.77	0.18	0.07	0.81	0.44	0.99	0.01	0.03	0.01	0.01	0.08	0.12

APPENDIX 4: ACICULAR APATITE ANALYSES (13 Oxygen) BW84-20a RSgr

SMPL#	SiO2	P2O5	FeO	MnO	CaO	F	TOTAL	Si	P	Fe	Mn	Ca	F
7178	0.34	41.41	0.14	0.52	53.41	2.86	98.68	0.03	2.90	0.01	0.04	4.74	0.75
7179	0.40	40.47	0.10	0.58	53.05	3.48	98.08	0.03	2.86	0.01	0.04	4.74	0.92
7180	0.25	40.31	0.36	0.51	53.39	3.06	97.88	0.02	2.86	0.03	0.04	4.80	0.81
7182	0.15	40.95	0.13	0.42	50.13	3.82	95.60	0.01	2.94	0.01	0.03	4.55	1.02
7183	0.17	40.60	0.08	0.46	51.23	3.71	96.25	0.01	2.91	0.01	0.03	4.64	0.99
7184	0.19	40.74	0.32	0.17	54.12	3.70	99.24	0.02	2.85	0.02	0.01	4.79	0.97
7185	0.20	40.65	0.41	0.42	54.44	2.75	98.87	0.02	2.87	0.03	0.03	4.87	0.73
7186	0.14	42.12	0.35	0.29	52.90	3.60	99.40	0.01	2.93	0.02	0.02	4.65	0.93
7187	0.39	38.49	0.33	0.36	54.46	2.94	96.97	0.03	2.79	0.02	0.03	5.00	0.80
7188	0.30	41.66	0.64	0.28	53.59	2.41	98.88	0.03	2.92	0.04	0.02	4.76	0.63
7189	0.35	41.92	0.52	0.42	53.91	2.71	99.83	0.03	2.91	0.04	0.03	4.74	0.70
7190	0.18	42.10	0.41	0.28	54.77	2.34	100.08	0.02	2.92	0.03	0.02	4.81	0.61
7191	0.24	42.02	0.50	0.39	53.44	2.78	99.37	0.02	2.93	0.03	0.03	4.71	0.72
7234	0.28	40.36	0.24	0.50	51.64	2.92	95.94	0.02	2.91	0.02	0.04	4.72	0.79
7235	0.28	40.08	0.20	0.51	52.53	3.65	97.25	0.02	2.87	0.01	0.04	4.75	0.98
AVG	0.26	40.93	0.32	0.41	53.13	3.12	98.15	0.02	2.89	0.02	0.03	4.75	0.82
STD	0.08	0.95	0.16	0.11	1.25	0.48	3.04	0.01	0.04	0.01	0.01	0.10	0.13

APPENDIX 4: ACICULAR APATITE ANALYSES (13 Oxygen) BW84-20a RSencl

SMPL#	SiO2	P2O5	FeO	MnO	CaO	F	TOTAL	Si	P	Fe	Mn	Ca	F
7074	0.71	36.98	0.02	0.24	54.91	3.23	96.09	0.06	2.71	0.00	0.02	5.10	0.89
7075	0.92	36.58	0.18	0.17	54.28	4.10	96.23	0.08	2.68	0.01	0.01	5.03	1.12
7082	0.21	33.40	0.75	0.56	57.89	3.49	96.30	0.02	2.52	0.06	0.04	5.53	0.98
7148	0.40	42.67	0.49	0.45	52.19	2.42	98.62	0.03	2.97	0.03	0.03	4.60	0.63
7149	0.27	44.61	0.30	0.34	52.48	2.59	100.59	0.02	3.02	0.02	0.02	4.50	0.66
7153	0.71	43.29	0.04	0.26	52.98	2.06	99.34	0.06	2.98	0.00	0.02	4.62	0.53
7154	0.73	42.92	0.11	0.23	52.20	2.56	98.75	0.06	2.97	0.01	0.02	4.57	0.66
7155	0.28	44.19	0.50	0.37	52.98	2.29	100.61	0.02	3.01	0.03	0.03	4.56	0.58
7156	0.33	44.41	0.36	0.36	52.41	2.58	100.45	0.03	3.02	0.02	0.02	4.50	0.65
7158	0.41	43.08	0.62	0.11	51.00	3.39	98.61	0.03	2.98	0.04	0.01	4.47	0.88
7159	0.38	44.47	0.06	0.24	52.57	2.19	99.91	0.03	3.03	0.00	0.02	4.53	0.56
7160	0.32	44.18	0.48	0.21	52.76	2.37	100.32	0.03	3.01	0.03	0.01	4.55	0.60
7161	0.46	43.97	0.06	0.36	51.78	2.43	99.06	0.04	3.02	0.00	0.03	4.50	0.62
7162	0.27	44.76	0.05	0.14	52.40	2.67	100.29	0.02	3.03	0.00	0.01	4.50	0.68
AVG	0.46	42.11	0.29	0.29	53.06	2.74	98.94	0.04	2.92	0.02	0.02	4.68	0.72
STD	0.21	3.51	0.24	0.12	1.63	0.56	1.59	0.02	0.16	0.02	0.01	0.30	0.17

APPENDIX 4: EQUANT APATITE ANALYSES (13 Oxygen) BW84-23 RSgd

SMPL#	SiO2	P2O5	FeO	MnO	CaO	F	TOTAL	Si	P	Fe	Mn	Ca	F
7144	0.23	43.09	0.07	0.50	50.84	3.30	98.03	0.02	2.99	0.01	0.04	4.47	0.86
7146	0.26	43.59	0.05	0.47	51.73	3.23	99.33	0.02	2.99	0.00	0.03	4.50	0.83
7147	0.20	44.26	0.06	0.49	51.73	3.28	100.02	0.02	3.01	0.00	0.03	4.45	0.83
AVG	0.23	43.65	0.06	0.49	51.43	3.27	99.13	0.02	3.00	0.00	0.03	4.47	0.84
STD	0.02	0.48	0.01	0.01	0.42	0.03	0.97	0.00	0.01	0.00	0.00	0.02	0.01

APPENDIX 4: ACICULAR APATITE ANALYSES (13 Oxygen) BW84-29 m encl

SMPL#	SiO2	P2O5	FeO	MnO	CaO	F	TOTAL	Si	P	Fe	Mn	Ca	F
7111	0.77	41.74	0.07	0.06	54.05	2.27	98.96	0.06	2.91	0.01	0.00	4.77	0.59
7112	0.74	42.29	0.07	0.10	54.79	1.58	99.57	0.06	2.93	0.01	0.01	4.81	0.41
7113	0.64	43.16	0.10	0.06	54.53	1.96	100.45	0.05	2.96	0.01	0.00	4.73	0.50
7114	0.89	42.27	0.04	0.08	54.12	1.82	99.22	0.07	2.93	0.00	0.01	4.75	0.47
7115	0.23	43.67	0.06	0.04	54.78	2.06	100.84	0.02	2.98	0.00	0.00	4.73	0.53
7116	0.82	42.26	0.09	0.09	53.64	2.02	98.92	0.07	2.94	0.01	0.01	4.72	0.53
7117	0.74	41.57	0.12	0.07	54.81	2.04	99.35	0.06	2.90	0.01	0.01	4.83	0.53
7118	0.59	42.64	0.06	0.11	54.60	1.75	99.75	0.05	2.95	0.00	0.01	4.78	0.45
7119	0.31	43.69	0.06	0.06	54.67	2.01	100.80	0.03	2.98	0.00	0.00	4.72	0.51
7120	1.69	41.80	0.51	0.09	53.45	1.91	99.45	0.14	2.90	0.04	0.01	4.69	0.50
7121	0.91	43.56	0.50	0.09	55.48	1.60	102.14	0.07	2.94	0.03	0.01	4.74	0.40
7122	0.24	43.45	0.41	0.13	54.51	1.99	100.73	0.02	2.98	0.03	0.01	4.72	0.51
7123	0.32	44.04	0.05	0.10	53.95	1.29	99.75	0.03	3.03	0.00	0.01	4.69	0.33
7124	0.35	43.40	0.20	0.11	54.39	1.80	100.25	0.03	2.98	0.01	0.01	4.73	0.46
AVG	0.66	42.82	0.17	0.09	54.41	1.86	100.01	0.05	2.95	0.01	0.01	4.74	0.48
STD	0.37	0.80	0.17	0.02	0.51	0.24	2.12	0.03	0.04	0.01	0.00	0.04	0.06

APPENDIX 4: ACICULAR APATITE ANALYSES (13 Oxygen) CA84-65A mdike

SMPL#	SiO2	P2O5	FeO	MnO	CaO	F	TOTAL	Si	P	Fe	Mn	Ca	F
7192	0.30	42.20	0.03	0.06	54.81	2.01	99.41	0.03	2.94	0.00	0.00	4.83	0.52
7193	0.70	40.79	0.02	0.13	54.23	1.75	97.62	0.06	2.90	0.00	0.01	4.88	0.46
7194	0.86	40.65	0.02	0.09	53.36	1.62	96.60	0.07	2.91	0.00	0.01	4.84	0.43
7195	0.33	41.35	0.22	0.05	53.98	1.93	97.86	0.03	2.93	0.02	0.00	4.84	0.51
7196	0.17	42.41	0.00	0.07	53.66	1.64	97.95	0.01	2.98	0.00	0.01	4.78	0.43
AVG	0.47	41.48	0.06	0.08	54.01	1.79	97.89	0.04	2.93	0.00	0.01	4.83	0.47
STD	0.26	0.72	0.08	0.03	0.50	0.16	1.74	0.02	0.03	0.01	0.00	0.03	0.04

The vita has been removed from
the scanned document

GEOLOGIC MAP OF THE TURTLE PLUTON SAN BERNARDINO COUNTY, CALIFORNIA

by C.M. ALLEN 1989

CORRELATION OF MAP UNITS

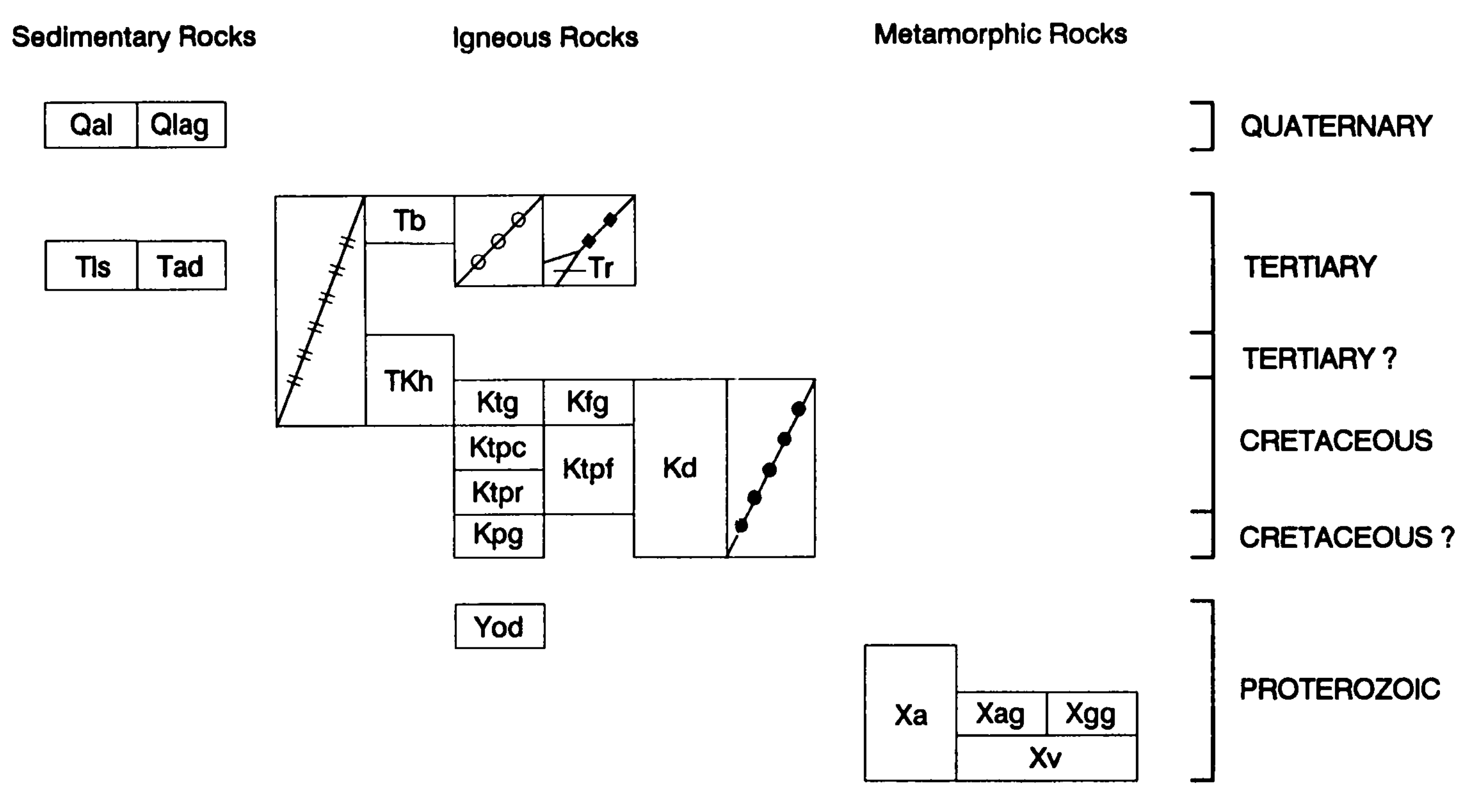

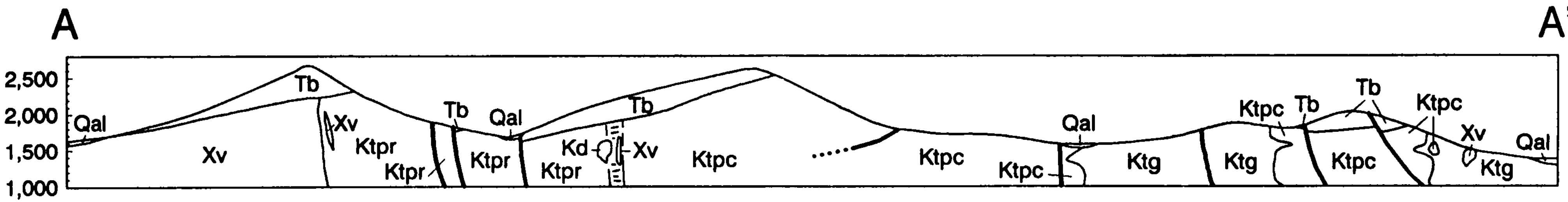

No vertical exaggeration
Elevation in feet above sea level

METAMORPHIC ROCKS

Xa

Amphibolite (Early Proterozoic)--Amphibolite gneiss composed of hornblende and plagioclase with lesser biotite, chlorite, epidote and quartz. This unit generally occurs in association with the gneiss of the Virginia May Mine (Xv), and contains foliations partially or fully transposed into parallelism with the surrounding gneisses. A tabular body of amphibolite whose margins truncate foliation in augen gneiss (Xag) suggests a second, younger generation of amphibolite

Xag

Augen Gneiss (Early Proterozoic)--Mafic augen gneiss containing prominant, pink potassium feldspars to 4 cm in length that are commonly lineated. Biotite composes about 30% of the rock. This unit cuts gneiss of Virginia May mine (Xv) and amphibolites (Xa). Rb-Sr whole rock isotopic analysis suggests a minimum age of 1.77+/-0.04 Ga (see text)

Xgg

Granite Gneiss (Early Proterozoic)--Light colored gneissic granite with large pink potassium feldspar phenocrysts up to 2.5 cm in length. The feldspars are brittlely deformed. Mafic minerals (biotite and hematite) compose less than 5% of the rock. Trace minerals include apatite, zircon, and unusually abundant allanite. This rock type is restricted to the southern-most portion of the map area and is seen to cut the gneiss of Virginia May mine (Xv) and amphibolites (Xa). Rb-Sr whole rock isotopic analysis suggests a minimum age of 1.77+/-0.04 Ga (see text)

Xv

Gneiss of Virginia May Mine (Early Proterozoic)--Well-foliated, fine-to medium-grained, light to dark gray, biotite quartzofeldspathic gneiss. This unit is described and informally named in Howard et al. (1982). Associated with the gneiss are leucocratic dikes that are folded and boudinaged within the gneiss. Rb-Sr whole rock geochronology suggests a minimum age of 1.77+/-0.04 Ga (see text)

SYMBOLS

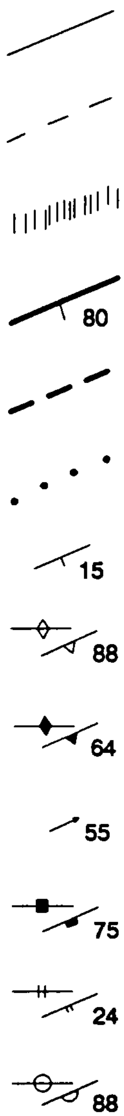

- Contact
- Approximate contact
- Gradational contact at the Schlieren Zone
- Fault showing dip of fault surface
- Approximately located fault
- Buried fault
- Strike and dip of bedding
- Strike and dip of igneous foliation, vertical and inclined
- Strike and dip of metamorphic foliation, vertical and inclined
- Trend and plunge of metamorphic lineation
- Vertical and inclined rhyolite dike
- Vertical and inclined basalt dike
- Vertical and inclined aplite or pegmatite

DESCRIPTION OF MAP UNITS

SEDIMENTARY ROCKS

Qal

Alluvium (Quaternary)--Undivided alluvium, colluvium and talus deposits

Qlag

Lag deposits (Quaternary)--Boulders of Tertiary basalt and andesite probably not far from original location of deposition

Tls

Landslide breccia (Tertiary)--Unconsolidated breccia composed of clasts ranging in size from 10 meter boulders to sand-sized particles. Dominant clast lithology is muscovite granite mylonite with lesser mafic mylonite which contains potassium feldspar porphyroblasts to 3 cm in length. This unit forms light colored hills which are cut by Tertiary basaltic dikes and travertine veins. The landslide intertongues with Tertiary alluvium (Tad)

Tad

Alluvial deposits (Tertiary)--Conglomerate, sandstone, and mudstone of primarily arkosic derivation. The lower portion of the unit is consolidated interbeds of gravels and monomineralic angular sands composed of feldspar or quartz or less common mafic grains. The upper portion is poorly sorted and composed of unconsolidated muds, sands and gravels which contain rock fragments of amphibolite and granite

IGNEOUS ROCKS

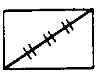

Basalt dikes (Tertiary and Cretaceous)--Primarily fine-grained greenish black basalt dikes to 3 meters in width with finer-grained margins. Hematized olivine, pyroxene and plagioclase phenocrysts are commonly visible, and these dikes are considered Tertiary. Distinct dikes found only in the Turtle pluton, are black, fine-grained, and contain hornblende, biotite, and plagioclase, and are similar to microgranitoid enclaves found in the pluton. These dikes are considered Cretaceous in age

Tb

Basalt and andesite (Tertiary)--Flows that comprise erosional remnants of larger outcrops that covered older rocks in the map area. These remnants are onlap sequences of tens of flows that were deposited over rugged topography. Layers of oxidized spatter and bombs suggest centers for local derivation. The lower flows are red-gray, green-gray, and black andesite and basalt that contain plagioclase sprays to 3 cm in length, and green clinopyroxene phenocrysts to 4 mm. These rocks are similar to the clinopyroxene-andesite and minor alkali-olivine basalt lavas of the lower sequence of Hazlett (1986). The higher flows are black fine-grained basalt with phenocrysts of hematized olivine and/or pyroxene in a groundmass of plagioclase, clinopyroxene and opaque minerals. This unit is like the "capping sequence" of Hazlett (1986) though K-Ar geochronology suggests a somewhat greater age (20 Ma, Howard et al., 1986)

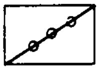

Andesite dikes (Tertiary)--Light gray to dark gray dikes up to 3 meters thick that contain phenocrysts of quartz, acicular hornblende, and biotite

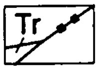

Rhyolite dikes (Tertiary)--Light gray to greenish white dikes up to 10 meters thick. Varies from aphanitic dikes to quartz porphyry dikes with phenocrysts of chloritized biotite and embayed quartz to 6 mm across

TKh

Hornblendite (Tertiary or Cretaceous)--This plagioclase-bearing pyroxene hornblendite occurs as a single tabular body in the southern portion of the map area. The body has a dike-like morphology, is about 10 meters thick, has a very coarse-grained core, and a coarse-grained margin. The finer grained borders suggest a chilled margin though its intrusive relationship with the surrounding granodiorite is not diffinitive. This rock contains euhedral and broken hornblende to 2 cm in greatest dimension in a groundmass of clinopyroxene, smaller hornblende, and oikocrystic plagioclase

Ktg

Target Granite (Cretaceous)--Light colored, equigranular, medium-grained, biotite leucogranite to granodiorite. Contains pink potassium feldspar. Near fault zones, oxidation and ductile deformation are conspicuous. Few microgranitoid enclaves were observed. This unit contains stoped blocks derived from the Core Facies of the Turtle pluton (Ktpc) and Proterozoic rocks.
In thin section, xenocrysts of resorbed and altered hornblende, sphene and feldspar cores are apparent. U-Pb geochronology on zircon suggests an intrusive age of 100+/-3 Ma (see text)

Kfg

Fortification Granodiorite (Cretaceous)--Fine-grained biotite granite to granodiorite that is light gray in outcrop, contains stoped blocks derived from the Rim Sequence of the Turtle pluton (Ktpr) and Patton Granite (Kpg) but very few microgranitoid enclaves. In thin section, the following trace minerals were observed: allanite, magnetite, and zircon

Ktpc

Core Facies of the Turtle pluton (Cretaceous)--Composed of seriate granodiorites and quartz monzodiorites with a maximum grain size of about 1 cm. Mafic minerals compose 15 to 27 percent of the rock, and include conspicuous euhedral hornblende (up to 1 cm in length) and biotite books (to 0.4 cm), with hornblende more abundant than biotite. Plagioclase and potassium feldspar phenocrysts are rare. Most K-feldspar occurs in interstitial patches. Medium brown or green, euhedral sphene may be seen with a hand lens. In thin section, trace minerals include sphene, allanite, apatite, zircon and magnetite. Secondary phases are sericite, epidote, chlorite, and calcite. This unit has a weak to moderate igneous foliation except near contact with the Rim Sequence of the Turtle pluton (Ktpr), called the Schlieren Zone, where a well-developed subvertical igneous foliation and subvertical lineation are defined by mineral alignment, and by shape and alignment of microgranitoid enclaves and screens of Precambrian gneiss. Elsewhere microgranitioid enclaves are common, are equidimensional, and generally show little preferred orientation. Total volume of these enclaves is less than 1% (see text). This unit dikes the Rim Sequence (Ktpr) at one location. U-Pb geochronology on sphene suggest a 130+/-1 Ma intrusive age (see text)

Ktpr

Rim Sequence of the Turtle pluton (Cretaceous)--Varies from fine-grained, equigranular, biotite granite at the country rock contact to coarse-grained, K-feldspar porphyritic, biotite-hornblende granodiorite toward the core of the pluton. A common igneous foliation is defined by aligned K-feldspar phenocrysts, mafic minerals, and micro-granitoid enclaves (about 1% by volume of the unit, see text). In thin section, apatite and zircon were observed in all rocks, ilmenite+/-muscovite in granites, and sphene and magnetite in all hornblende-bearing granodiorites. U-Pb geochronology on zircon indicates an inherited component, and coupled with sphene geochronology on the Core Facies, suggests a 130+/-1 Ma intrusive age which is further supported by a Rb-Sr mineral isochron age of 124+/-2 Ma (see text)

Ktpf

Four Deuce Hills facies of the Turtle pluton (Cretaceous)--Granite and granodiorite. Ranges in mineralogy and texture from equigranular biotite granite to K-feldspar porphyritic biotite hornblende granodiorite. Some rocks are very similar to the rim sequence (Ktpr) but others contain white, oikocrystic potassium feldspar. Intrusive relationships to the other facies of the Turtle pluton are unknown. This facies appears to be bounded on the west by a westward-dipping low angle fault zone. K-Ar geochronology yields ages of 97 Ma from biotite and 106 Ma from hornblende (Howard et al., 1982)

Kpg

Patton Granite (Cretaceous?)--Coarse-grained, pink, biotite granite. Occurs in the western portion of the mapped area. Feldspar and quartz are commonly 1 cm in greatest dimension. Euhedral hornblende crystals are rare. Rock is oxidized and altered. Rare microgranitiod enclaves are medium gray in color, and a few centimeters in greatest dimension. This unit is intruded by the Rim Sequence of the Turtle pluton (Ktpr) and by Fortification Granodiorite (Kfg)

Kd

Diorites (Cretaceous and Cretaceous?)--Ovoid bodies of greater than 1 meter dimensions of medium- to coarse-grained hornblende diorite and hornblendite found within the Turtle pluton. Minor mineral phases include biotite, sphene, and magnetite. Mafic pegmatoids composed of large acicular "hollow" hornblende to 7 cm in length and coarse plagioclase are common. Intrusive relationships of diorite and host granitoids are unknown, and this diorite may be contemporaneous with its hosts, or may be xenoliths

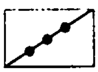

Aplite and pegmatite (Cretaceous and Cretaceous?)--Granitic aplites and pegmatites up to 4 meters thick. Except for garnet-bearing facies, these dikes intrude all Cretaceous igneous units. Ferromagnesian silicates include biotite, muscovite, opaque minerals, +/- garnet. Aplites which contain conspicuous, red poikilitic garnets were not observed to intrude the Target Granite (Ktg). Rb-Sr whole rock ages from garnet-bearing aplites suggest an intrusive age of 96+/-4 Ma (see text). Garnet-bearing dikes intrude Turtle pluton, Patton Granite, and Fortification Granodiorite, but is absent in the Target Granite

Yod

Ophitic Diabase (Middle Proterozoic)--Lenses of hornblende diabase that cut the gneiss of the Virginia May Mine (Xv). The rock lacks penetrative fabric but discontinuous outcrops may suggest tectonic disruption. Sprays of plagioclase to 1 cm in length lie in a matrix of hornblende, pyroxene and smaller plagioclase grains, with minor epidote, opaque minerals, and biotite. K-Ar age of 439 Ma from hornblende collected in the northern Turtle Mountains has been interpreted as a partially reset Proterozoic age (Howard et al., 1982)